



Hashemite Kingdom of Jordan



Jordan Journal of



Biological Sciences

An International Peer-Reviewed Scientific Journal

Financed by the Scientific Research and Innovation Support Fund



<http://jjbs.hu.edu.jo/>

Jordan Journal of Biological Sciences (JJBS) (ISSN: 1995–6673 (Print); 2307-7166 (Online)): An International Peer- Reviewed Open Access Research Journal financed by the Scientific Research and Innovation Support Fund, Ministry of Higher Education and Scientific Research, Jordan and published quarterly by the Deanship of Scientific Research , The Hashemite University, Jordan.

Editor-in-Chief

Professor Wedyan, Mohammed A.
Environmental Biochemistry,
The Hashemite University

Assistant Editor

Professor Muhannad, Massadeh I.
Microbial Biotechnology,
The Hashemite University

Editorial Board (Arranged alphabetically)

Professor Al-Eitan, Laith
Biotechnology and Genetic Engineering
Jordan University of Science and Technology

Professor Al-Khateeb , Wesam M.
Plant Genetics and Biotechnology
Yarmouk University

Professor Al-Ghzawi , Abdul Latief A.
Plant biotechnology
The Hashemite University

Professor Al-Najjar , Tariq Hasan Ahmad.
Marine Biology
The University of Jordan/ Aqaba

Professor Khleifat, Khaled M.
Microbiology and Biotechnology
Mutah University

Professor Odat , Nidal
Plant biodiversity
Al Balqa Applied University

Associate Editorial Board

Professor Al-Hindi, Adnan I.
Parasitology
The Islamic University of Gaza, Faculty of Health
Sciences, Palestine

Dr Gammoh, Noor
Tumor Virology
Cancer Research UK Edinburgh Centre, University of
Edinburgh, U.K.

Professor Kasperek, Max
Natural Sciences
Editor-in-Chief, Journal Zoology in the Middle East,
Germany

Professor Krystufek, Boris
Conservation Biology
Slovenian Museum of Natural History,
Slovenia

Dr Rabei, Sami H.
Plant Ecology and Taxonomy
Botany and Microbiology Department,
Faculty of Science, Damietta University, Egypt

Professor Simerly, Calvin R.
Reproductive Biology
Department of Obstetrics/Gynecology and
Reproductive Sciences, University of
Pittsburgh, USA

Editorial Board Support Team

Language Editor
Professor Shadi Neimneh

Publishing Layout
Eng. Mohannad Oqdeh

Submission Address

Professor Wedyan, Mohammed A.
The Hashemite University
P.O. Box 330127, Zarqa, 13115, Jordan
Phone: +962-5-3903333 ext.4147
E-Mail: jjbs@hu.edu.jo

المجلة الاردنية للعلوم الحياتية
Jordan Journal of Biological Sciences (JJBS)
<http://jjbs.hu.edu.jo>

International Advisory Board (Arranged alphabetically)

Professor Abdelaziz M. Hussein
Mansoura University, Egypt

Professor Adnan Bashir Al- Iahham
German Jordanian University, Jordan

Professor Ahmed Amri
genetic resources ICARDA in Morocco, Morocco

Professor Amir Menwer Al-Hroob
Al-Hussein Bin Talal University, Jordan

Professor Elif Demirkan
Bursa Uludag University Turkey, Turkey

Professor Erhan Nurettin ÜNLÜ
Turkey Dicle University, Turkey

Professor Hassan Mohammed M. Abd El-Rahman Awad
National Research Centre, Egypt

Professor Khalid M. Al-Batayneh
Yarmouk University, Jordan

Professor Laith Abd Jalil Jawad
School of Environmental and Animal Sciences, Unitec Institute of
Technology Auckland, New Zealand

Professor Maroof A. Khalaf
Jordan University/ Aqaba, Jordan

Professor Mohammed H. Abu-Dieyeh
Biological and Environmental Sciences, Qatar University, Qatar

Professor Nour Shafik Emam El-Gendy
Egyptian Petroleum Research Institute, Egypt

Professor Omar F. Khabour
Jordan University of Science and Technology, Jordan

Professor Saleem Hmood Aladaileh
Al-Hussein Bin Talal University, Jordan

Professor Walid Al Zyoud
German Jordanian University, Jordan

Professor Abhik Gupta
School of Environmental Sciences, Assam University, India

Professor Ahmed Deaf Allah Telfah
Leibniz-Institut für Analytische Wissenschaften-, Germany

Dr. Amalia A Tsiami
University of West London, London

Professor David Modry
Masaryk University, Science Department, Czech

Professor Emad Hussein Malkawi
Yarmouk University, Jordan

Professor Gottfried Hartmut Richard Jetschke
Friedrich-Schiller-University of Jena, Germany

Professor Ihsan Ali Mahasneh
Al al-Bayt University, Jordan

Professor Khalid Majid Hameed
Dept. of Biological Sciences, Duke University, USA

Dr Maizirwan Bin Muhammad Mel
International Islamic University Malaysia, Malaysia

Professor Mohamed Emara
Chartered Management Institute, UK

Professor Nabil Joseph Awadalla Girgis
King Khalid University, Saudi Arabia

Professor Olga Anne
Marine Technology and Natural Sciences of Klaipėda University,
Lithuania

Dr Roy Hendroko Setyobudi
University of Muhammadiyah, Indonesia

Dr. Salem M Akel
St. Jude's Children's Research Hospital, USA

Professor Yacob Hassan Yacob
Al al-Bayt University, Jordan

Instructions to Authors

Scopes

Study areas include cell biology, genomics, microbiology, immunology, molecular biology, biochemistry, embryology, immunogenetics, cell and tissue culture, molecular ecology, genetic engineering and biological engineering, bioremediation and biodegradation, bioinformatics, biotechnology regulations, gene therapy, organismal biology, microbial and environmental biotechnology, marine sciences. The JJBS welcomes the submission of manuscript that meets the general criteria of significance and academic excellence. All articles published in JJBS are peer-reviewed. Papers will be published approximately one to two months after acceptance.

Type of Papers

The journal publishes high-quality original scientific papers, short communications, correspondence and case studies. Review articles are usually by invitation only. However, Review articles of current interest and high standard will be considered.

Submission of Manuscript

Manuscript, or the essence of their content, must be previously unpublished and should not be under simultaneous consideration by another journal. The authors should also declare if any similar work has been submitted to or published by another journal. They should also declare that it has not been submitted/ published elsewhere in the same form, in English or in any other language, without the written consent of the Publisher. The authors should also declare that the paper is the original work of the author(s) and not copied (in whole or in part) from any other work. All papers will be automatically checked for duplicate publication and plagiarism. If detected, appropriate action will be taken in accordance with International Ethical Guideline. By virtue of the submitted manuscript, the corresponding author acknowledges that all the co-authors have seen and approved the final version of the manuscript. The corresponding author should provide all co-authors with information regarding the manuscript, and obtain their approval before submitting any revisions. Electronic submission of manuscripts is strongly recommended, provided that the text, tables and figures are included in a single Microsoft Word file. Submit manuscript as e-mail attachment to the Editorial Office at: JJBS@hu.edu.jo. After submission, a manuscript number will be communicated to the corresponding author within 48 hours.

Peer-review Process

It is requested to submit, with the manuscript, the names, addresses and e-mail addresses of at least 4 potential reviewers. It is the sole right of the editor to decide whether or not the suggested reviewers to be used. The reviewers' comments will be sent to authors within 6-8 weeks after submission. Manuscripts and figures for review will not be returned to authors whether the editorial decision is to accept, revise, or reject. All Case Reports and Short Communication must include at least one table and/ or one figure.

Preparation of Manuscript

The manuscript should be written in English with simple lay out. The text should be prepared in single column format. Bold face, italics, subscripts, superscripts etc. can be used. Pages should be numbered consecutively, beginning with the title page and continuing through the last page of typewritten material.

The text can be divided into numbered sections with brief headings. Starting from introduction with section 1. Subsections should be numbered (for example 2.1 (then 2.1.1, 2.1.2, 2.2, etc.), up to three levels. Manuscripts in general should be organized in the following manner:

Title Page

The title page should contain a brief title, correct first name, middle initial and family name of each author and name and address of the department(s) and institution(s) from where the research was carried out for each author. The title should be without any abbreviations and it should enlighten the contents of the paper. All affiliations should be provided with a lower-case superscript number just after the author's name and in front of the appropriate address.

The name of the corresponding author should be indicated along with telephone and fax numbers (with country and area code) along with full postal address and e-mail address.

Abstract

The abstract should be concise and informative. It should not exceed **350 words** in length for full manuscript and Review article and **150 words** in case of Case Report and/ or Short Communication. It should briefly describe the purpose of the work, techniques and methods used, major findings with important data and conclusions. No references should be cited in this part. Generally non-standard abbreviations should not be used, if necessary they should be clearly defined in the abstract, at first use.

Keywords

Immediately after the abstract, **about 4-8 keywords** should be given. Use of abbreviations should be avoided, only standard abbreviations, well known in the established area may be used, if appropriate. These keywords will be used for indexing.

Abbreviations

Non-standard abbreviations should be listed and full form of each abbreviation should be given in parentheses at first use in the text.

Introduction

Provide a factual background, clearly defined problem, proposed solution, a brief literature survey and the scope and justification of the work done.

Materials and Methods

Give adequate information to allow the experiment to be reproduced. Already published methods should be mentioned with references. Significant modifications of published methods and new methods should be described in detail. Capitalize trade names and include the manufacturer's name and address. Subheading should be used.

Results

Results should be clearly described in a concise manner. Results for different parameters should be described under subheadings or in separate paragraph. Results should be explained, but largely without referring to the literature. Table or figure numbers should be mentioned in parentheses for better understanding.

Discussion

The discussion should not repeat the results, but provide detailed interpretation of data. This should interpret the significance of the findings of the work. Citations should be given in support of the findings. The results and discussion part can also be described as separate, if appropriate. The Results and Discussion sections can include subheadings, and when appropriate, both sections can be combined

Conclusions

This should briefly state the major findings of the study.

Acknowledgment

A brief acknowledgment section may be given after the conclusion section just before the references. The acknowledgment of people who provided assistance in manuscript preparation, funding for research, etc. should be listed in this section.

Tables and Figures

Tables and figures should be presented as per their appearance in the text. It is suggested that the discussion about the tables and figures should appear in the text before the appearance of the respective tables and figures. No tables or figures should be given without discussion or reference inside the text.

Tables should be explanatory enough to be understandable without any text reference. Double spacing should be maintained throughout the table, including table headings and footnotes. Table headings should be placed above the table. Footnotes should be placed below the table with superscript lowercase letters. Each table should be on a separate page, numbered consecutively in Arabic numerals.

Each figure should have a caption. The caption should be concise and typed separately, not on the figure area. Figures should be self-explanatory. Information presented in the figure should not be repeated in the table. All symbols and abbreviations used in the illustrations should be defined clearly. Figure legends should be given below the figures.

References

References should be listed alphabetically at the end of the manuscript. Every reference referred in the text must be also present in the reference list and vice versa. In the text, a reference identified by means of an author's name should be followed by the year of publication in parentheses (e.g.(Brown,2009)). For two authors, both authors' names followed by the year of publication (e.g.(Nelson and Brown, 2007)). When there are more than two authors, only the first author's name followed by "et al." and the year of publication (e.g. (Abu-Elteen *et al.*, 2010)). When two or more works of an author has been published during the same year, the reference should be identified by the letters "a", "b", "c", etc., placed after the year of publication. This should be followed both in the text and reference list. e.g., Hilly, (2002a, 2002b); Hilly, and Nelson, (2004). Articles in preparation or submitted for publication, unpublished observations, personal communications, etc. should not be included in the reference list but should only be mentioned in the article text (e.g., Shtyawy,A., University of Jordan, personal communication). Journal titles should be abbreviated according to the system adopted in Biological Abstract and Index Medicus, if not included in Biological Abstract or Index Medicus journal title should be given in full. The author is responsible for the scuracy and completeness of the references and for their correct textual citation. Failure to do so may result in the paper being withdraw from the evaluation process. Example of correct reference form is given as follows:-

Reference to a journal publication:

Bloch BK. 2002. Econazole nitrate in the treatment of *Candida vaginitis*. *S Afr Med J.* , **58**:314-323.

Ogunseitan OA and Ndoye IL. 2006. Protein method for investigating mercuric reductase gene expression in aquatic environments. *Appl Environ Microbiol.* , **64**: 695-702.

Hilly MO, Adams MN and Nelson SC. 2009. Potential fly-ash utilization in agriculture. *Progress in Natural Sci.*, **19**: 1173-1186.

Reference to a book:

Brown WY and White SR.1985. **The Elements of Style**, third ed. MacMillan, New York.

Reference to a chapter in an edited book:

Mettam GR and Adams LB. 2010. How to prepare an electronic version of your article. In: Jones BS and Smith RZ (Eds.), **Introduction to the Electronic Age**. Kluwer Academic Publishers, Netherlands, pp. 281–304.

Conferences and Meetings:

Embabi NS. 1990. Environmental aspects of distribution of mangrove in the United Arab Emirates. Proceedings of the First ASWAS Conference. University of the United Arab Emirates. Al-Ain, United Arab Emirates.

Theses and Dissertations:

El-Labadi SN. 2002. Intestinal digenetic trematodes of some marine fishes from the Gulf of Aqaba. MSc dissertation, The Hashemite University, Zarqa, Jordan.

Nomenclature and Units

Internationally accepted rules and the international system of units (SI) should be used. If other units are mentioned, please give their equivalent in SI.

For biological nomenclature, the conventions of the *International Code of Botanical Nomenclature*, the *International Code of Nomenclature of Bacteria*, and the *International Code of Zoological Nomenclature* should be followed.

Scientific names of all biological creatures (crops, plants, insects, birds, mammals, etc.) should be mentioned in parentheses at first use of their English term.

Chemical nomenclature, as laid down in the *International Union of Pure and Applied Chemistry* and the official recommendations of the *IUPAC-IUB Combined Commission on Biochemical Nomenclature* should be followed. All biocides and other organic compounds must be identified by their Geneva names when first used in the text. Active ingredients of all formulations should be likewise identified.

Math formulae

All equations referred to in the text should be numbered serially at the right-hand side in parentheses. Meaning of all symbols should be given immediately after the equation at first use. Instead of root signs fractional powers should be used. Subscripts and superscripts should be presented clearly. Variables should be presented in italics. Greek letters and non-Roman symbols should be described in the margin at their first use.

To avoid any misunderstanding zero (0) and the letter O, and one (1) and the letter l should be clearly differentiated. For simple fractions use of the solidus (/) instead of a horizontal line is recommended. Levels of statistical significance such as: * $P < 0.05$, ** $P < 0.01$ and *** $P < 0.001$ do not require any further explanation.

Copyright

Submission of a manuscript clearly indicates that: the study has not been published before or is not under consideration for publication elsewhere (except as an abstract or as part of a published lecture or academic thesis); its publication is permitted by all authors and after accepted for publication it will not be submitted for publication anywhere else, in English or in any other language, without the written approval of the copyright-holder. The journal may consider manuscripts that are translations of articles originally published in another language. In this case, the consent of the journal in which the article was originally published must be obtained and the fact that the article has already been published must be made clear on submission and stated in the abstract. It is compulsory for the authors to ensure that no material submitted as part of a manuscript infringes existing copyrights, or the rights of a third party.

Ethical Consent

All manuscripts reporting the results of experimental investigation involving human subjects should include a statement confirming that each subject or subject's guardian obtains an informed consent, after the approval of the experimental protocol by a local human ethics committee or IRB. When reporting experiments on animals, authors should indicate whether the institutional and national guide for the care and use of laboratory animals was followed.

Plagiarism

The JJBS hold no responsibility for plagiarism. If a published paper is found later to be extensively plagiarized and is found to be a duplicate or redundant publication, a note of retraction will be published, and copies of the correspondence will be sent to the authors' head of institute.

Galley Proofs

The Editorial Office will send proofs of the manuscript to the corresponding author as an e-mail attachment for final proof reading and it will be the responsibility of the corresponding author to return the galley proof materials appropriately corrected within the stipulated time. Authors will be asked to check any typographical or minor clerical errors in the manuscript at this stage. No other major alteration in the manuscript is allowed. After publication authors can freely access the full text of the article as well as can download and print the PDF file.

Publication Charges

There are no page charges for publication in Jordan Journal of Biological Sciences, except for color illustrations,

Reprints

Ten (10) reprints are provided to corresponding author free of charge within two weeks after the printed journal date. For orders of more reprints, a reprint order form and prices will be sent with article proofs, which should be returned directly to the Editor for processing.

Disclaimer

Articles, communication, or editorials published by JJBS represent the sole opinions of the authors. The publisher shoulders no responsibility or liability what so ever for the use or misuse of the information published by JJBS.

Indexing

JJBS is indexed and abstracted by:

DOAJ (Directory of Open Access Journals)

Google Scholar

Journal Seek

HINARI

Index Copernicus

NDL Japanese Periodicals Index

SCIRUS

OAJSE

ISC (Islamic World Science Citation Center)

Directory of Research Journal Indexing
(DRJI)

Ulrich's

CABI

EBSCO

CAS (Chemical Abstract Service)

ETH- Citations

Open J-Gat

SCImago

Clarivate Analytics (Zoological Abstract)

Scopus

AGORA (United Nation's FAO database)

SHERPA/RoMEO (UK)

المجلة الأردنية للعلوم الحياتية
Jordan Journal of Biological Sciences (JJBS)
ISSN 1995- 6673 (Print), 2307- 7166 (Online)

<http://jjbs.hu.edu.jo>

The Hashemite University
Deanship of Scientific Research
TRANSFER OF COPYRIGHT AGREEMENT

Journal publishers and authors share a common interest in the protection of copyright: authors principally because they want their creative works to be protected from plagiarism and other unlawful uses, publishers because they need to protect their work and investment in the production, marketing and distribution of the published version of the article. In order to do so effectively, publishers request a formal written transfer of copyright from the author(s) for each article published. Publishers and authors are also concerned that the integrity of the official record of publication of an article (once refereed and published) be maintained, and in order to protect that reference value and validation process, we ask that authors recognize that distribution (including through the Internet/WWW or other on-line means) of the authoritative version of the article as published is best administered by the Publisher.

To avoid any delay in the publication of your article, please read the terms of this agreement, sign in the space provided and return the complete form to us at the address below as quickly as possible.

Article entitled:-----

Corresponding author: -----

To be published in the journal: Jordan Journal of Biological Sciences (JJBS)

I hereby assign to the Hashemite University the copyright in the manuscript identified above and any supplemental tables, illustrations or other information submitted therewith (the "article") in all forms and media (whether now known or hereafter developed), throughout the world, in all languages, for the full term of copyright and all extensions and renewals thereof, effective when and if the article is accepted for publication. This transfer includes the right to adapt the presentation of the article for use in conjunction with computer systems and programs, including reproduction or publication in machine-readable form and incorporation in electronic retrieval systems.

Authors retain or are hereby granted (without the need to obtain further permission) rights to use the article for traditional scholarship communications, for teaching, and for distribution within their institution.

- I am the sole author of the manuscript
- I am signing on behalf of all co-authors of the manuscript
- The article is a 'work made for hire' and I am signing as an authorized representative of the employing company/institution

Please mark one or more of the above boxes (as appropriate) and then sign and date the document in black ink.

Signed: _____ Name printed: _____

Title and Company (if employer representative) : _____

Date: _____

Data Protection: By submitting this form you are consenting that the personal information provided herein may be used by the Hashemite University and its affiliated institutions worldwide to contact you concerning the publishing of your article.

Please return the completed and signed original of this form by mail or fax, or a scanned copy of the signed original by e-mail, retaining a copy for your files, to:

Hashemite University
Jordan Journal of Biological Sciences
Zarqa 13115 Jordan
Fax: +962 5 3903338
Email: jjbs@hu.edu.jo

EDITORIAL PREFACE

Jordan Journal of Biological Sciences (JJBS) is a refereed, quarterly international journal financed by the Scientific Research and Innovation Support Fund, Ministry of Higher Education and Scientific Research in cooperation with the Hashemite University, Jordan. JJBS celebrated its 12th commencement this past January, 2020. JJBS was founded in 2008 to create a peer-reviewed journal that publishes high-quality research articles, reviews and short communications on novel and innovative aspects of a wide variety of biological sciences such as cell biology, developmental biology, structural biology, microbiology, entomology, molecular biology, biochemistry, medical biotechnology, biodiversity, ecology, marine biology, plant and animal biology, plant and animal physiology, genomics and bioinformatics.

We have watched the growth and success of JJBS over the years. JJBS has published 14 volumes, 60 issues and 800 articles. JJBS has been indexed by SCOPUS, CABI's Full-Text Repository, EBSCO, Clarivate Analytics- Zoological Record and recently has been included in the UGC India approved journals. JJBS Cite Score has improved from 0.7 in 2019 to 1.4 in 2021 (Last updated on 6 March, 2022) and with Scimago Institution Ranking (SJR) 0.22 (Q3) in 2021.

A group of highly valuable scholars have agreed to serve on the editorial board and this places JJBS in a position of most authoritative on biological sciences. I am honored to have six eminent associate editors from various countries. I am also delighted with our group of international advisory board members coming from 15 countries worldwide for their continuous support of JJBS. With our editorial board's cumulative experience in various fields of biological sciences, this journal brings a substantial representation of biological sciences in different disciplines. Without the service and dedication of our editorial; associate editorial and international advisory board members, JJBS would have never existed.

In the coming year, we hope that JJBS will be indexed in Clarivate Analytics and MEDLINE (the U.S. National Library of Medicine database) and others. As you read throughout this volume of JJBS, I would like to remind you that the success of our journal depends on the number of quality articles submitted for review. Accordingly, I would like to request your participation and colleagues by submitting quality manuscripts for review. One of the great benefits we can provide to our prospective authors, regardless of acceptance of their manuscripts or not, is the feedback of our review process. JJBS provides authors with high quality, helpful reviews to improve their manuscripts.

Finally, JJBS would not have succeeded without the collaboration of authors and referees. Their work is greatly appreciated. Furthermore, my thanks are also extended to The Hashemite University and the Scientific Research and Innovation Support Fund, Ministry of Higher Education and Scientific Research for their continuous financial and administrative support to JJBS.

Professor Y gf {cp."O qj co o gf "C0
....."Ugr vgo dgt."4245"

CONTENTS

Original Articles

- 379 – 387 Extraction, Characterization, Amino Acid Profile of Halal Gelatin from Kampong and Broiler Chicken Feet Skin
Noor Harini, Manar Fayiz Mousa Atoum, Swastika Tri Aji Wulandari, Vritta Amroini Wahyudi, Asad Jan, and Irum Iqrar
- 389 – 401 Molecular Simulations of *Moringa oleifera* Phytochemicals as Potential Antagonists of the Proinflammatory NF- κ B p50 Transcription Factor
Kathleen Cole C. Tung, Romeric F. Pobre, Glenn G. Oyong
- 403 – 412 Diversity and Seasonal Variation of Fish Assemblages of Dingapota Haor an Eutrophic Wetland of Northeastern Bangladesh
Md. Nahiduzzaman, Ehsanul Karim, Md. Nazmul Hossen, Nazia Naheen Nisheeth and Yahia Mahmud
- 413 – 424 Moderately Thermophilic Bacteria from Jordanian Hot Springs as Possible Sources of Thermostable Enzymes and Leukemia Cytotoxic Agents
Maher Obeidat, Belal Al-Shomali
- 425 – 430 First Record of the Scorpion *Vachoniolus globimanus* (Scorpiones: Buthidae) from Jordan
Bassam Abu Afifeh, Mohammad Al-Sarairoh and Zuhair S. Amr
- 431 – 437 GC-MS Analysis of Various Crude Extracts from the Leaves, Flowers, and Stems of *Datura metel* Linnaeus 1753 and the Potential Activity as Anesthetic Agents on Fish
Rindhira Humairani, Nanda Rizki Purnama, Herpandi Herpandi, Mochamad Syaifudin, Ilham Zulfahmi, Yusrizal Akmal, Muliari Muliari, Agung Setia Batubara
- 439 – 443 The Effect of 17 β -Estradiol and Genistein on the Prostate Gland and Testes of Aged Rats
Falah Shidaifat, Mohammed Khalifeh and Yousef Yasin
- 445 – 454 Immunomodulatory Properties of *Citrus limon* Extracts on BALB/c Mouse Lymphoid and Myeloid Lineage Cells
Wira Eka Putra, Ken Retno Puspaningrum, Arief Hidayatullah, Muhaimin Rifa'i
- 455 – 465 Heavy Metals Effect on the Rat Uterus and Effectiveness of Vitamin E Treatment
Sikora K, Lyndin M, Sikora V, Hyriavenko N, Piddubnyi A, Lyndina Y, Awuah WA, Abdul-Rahman T, Korobchanska A, Alexiou A, Romaniuk A
- 467 – 475 Heavy metal contamination and potential health risk assessment associated with selected farmed fish in Rajshahi, Bangladesh
Jibon Kumar Ghosh, Md. Shahidul Islam, Md. Tariqul Islam, Md. Mahedul Islam Murad and Md. Mahabubur Rahman
- 477 – 502 Comparative Analysis of Cichorieae Tribe (Asteraceae) Chloroplast Genomes: Insight to Structure, Repetitive DNA, and Phylogeny.
Rubar Hussein M. Salih
- 503 – 511 Biochemical Profile of Five Species of Cultured Marine Microalgae¹
Teja. Gurugubelli, Yedukondala Rao. Poturaju and Rukmini Sirisha. Imandi
- 513 – 518 A Histological Examination of the Sublethal Effects of Methyl Parathion on the Liver, Gills and Gonads of *Alburnus tarichi* (Güldenstädt, 1814)
Ertuğrul KANKAYA and Güler ÜNAL
- 519 – 527 Formulated Hand Sanitizer Utilizing Passion Fruit (*Passiflora edulis*) Leaf Extract as an Active Ingredient
Cabral, Daisy Anne M., Hernandez, Marianne D., Martinez, Leslie Ann B. and Sangalang, Reygan H.
- 529 – 536 Telmisartan Enhances the Accumulation of Doxorubicin as a Combination Therapy for the Management of Triple Negative Breast Cancer
Wala'a Al.Safadi, Belal Omar Al-Najjar, Moath Alqaraleh, Anas Ibrahim Abed, Walhan Alshaer, Dana Alqudah, Fadwa Daoud, Razan Mohammad Obeidat, Obada Abdulmalek Sibai, Zainab Zaki Zakaraya
- 537 – 564 *Streptomyces*–Alginate Beads Formula Promote Maize Plant Growth and Modify the Rhizosphere Microbiome
Okto Asriatno, Abdjad Asih Nawangsih, Rika Indri Astuti, Aris Tri Wahyudi

Extraction, Characterization, Amino Acid Profile of Halal Gelatin from Kampong and Broiler Chicken Feet Skin

Noor Harini¹, Manar Fayiz Mousa Atoum^{2,3}, Swastika Tri Aji Wulandari¹,
Vritta Amroini Wahyudi^{1,*}, Asad Jan⁴, and Irum Iqar⁵

¹Department of Food Technology, Faculty of Agriculture and Animal Science, University of Muhammadiyah Malang, Jl. Raya Tlogomas No 246, Malang 65144, East Java, Indonesia; ²Molecular Biology and Genetics, The Hashemite University, PO Box 330127, 13133 Zarqa, Jordan; ³Department of Medical Laboratory Sciences, The Hashemite University, Zarqa, Jordan; ⁴Institute of Biotechnology & Genetic Engineering, The University of Agriculture, Peshawar, 25130 Khyber Pakhtunkhwa, Pakistan; ⁵Office of Research, Innovation and Commercialization (ORIC), The University of Lahore, 1-Km Defence Road, 54000 Lahore, Pakistan

Received: Nov 20, 2022; Revised: Apr 2, 2023; Accepted Apr 3, 2023

Abstract

Gelatin is one of the food additives where the issue of halal is interesting to study. Several previous studies have explored alternatives to halal gelatin. This study analyzes gelatin's chemical and physical properties from kampong and broiler chicken feet skin. The results obtained can be utilized to develop a halal alternative to gelatin. The study used a nested randomized design consisting of two factors: variations in the chicken origin and the concentration of the acid solvent. The first factor, the kind of chicken, had two levels, kampong and broiler chickens. The second factor was acetic acid concentration (CH₃COOH) with 2 %, 4 %, 6 %, and 8 % (v v⁻¹). Gelatin from the skin of kampong chicken feet skin with 4 % (v v⁻¹) acetic acid reached a yield of 12.67 %, a moisture content of 10.29 %, an ash content of 1.58 %, a protein content of 82.52 %, a pH 4.53, a viscosity of 4.78 cp, and a gel strength of 66.29 g cm⁻². Gelatin from broiler chicken leg skin with 4 % acetic acid reached a yield of 10.90 %, a moisture content of 7.95 %, an ash content of 7.95 %, a protein content of 82.48 %, a pH of 4.76, a viscosity of 5.4 cp, and a gel strength of 70.13 g cm⁻². Kampong and broiler chicken feet skin gelatin were similar to commercial gelatin concerning the glycine percentage. Glycine has more than 50 % gelatin from all amino acids. Glycine from kampong chicken feet skin gelatin was 53.37 %, broiler chicken feet skin gelatin had 51.95 %, and commercial gelatin was 54.33 %. The meatballs using kampong and broiler chicken feet skin gelatin (acetic acid 4 %) meet all the requirements of NSA (National Standardization Agency of Republic of Indonesia -*Standar Nasional Indonesia*: 3818-2014) for moisture, ash, protein, and lipid content variables.

Keywords: Acetic acid hydrolysis, Collagen, Environmentally friendly, *Gallus gallus domesticus* L., Organic acid hydrolysis, Poultry waste, Waste to halal food, Waste utilization

1. Introduction

The poultry processing industry is rapidly developing along with the food industry. Annually, about 69 × 10⁶ t of chicken meat is produced worldwide. FAO data shows that 3 900 × 10³ t chicken feet were produced from the poultry processing industry (FAO Statistics, 2020). In some countries, chicken feet are thrown away without any further processing, which causes environmental hazards (Dhakal *et al.*, 2020; Radhakrishnan *et al.*, 2020). Several researchers (Karuppanan *et al.*, 2021; Lasekan *et al.*, 2013) suggest implementing zero waste in the poultry industry; in addition, the poultry processing industry produces side products such as liver, gizzard, feet, and other innards, and researchers recommend processing this waste into renewable energy, livestock feed, fertilizers, and pet foods. Haghghi *et al.* (2021); Janarthanam *et al.* (2020) have reported using chicken slaughter waste as a source of biodiesel. Some researchers (Adinurani *et al.*, 2017; Abdullah *et al.*, 2021; Latifi *et al.*, 2019;

Setyobudi *et al.*, 2021a) recycle poultry waste into sustainable clean energy, namely biogas.

Lachenmeier *et al.* (2022) show –with a pyramid model for waste utilization—that food is a primary priority. Gelatin is one of the hydrocolloids obtained from the hydrolysis of collagen from skin, bones, or another animal's part. The gelatin extraction from collagen can be done by chemical and biochemical hydrolysis. Collagen is the main protein in the skin, with a high content of fibrous protein (Liu *et al.*, 2015; Mariod and Fadul, 2013). Gelatin is widely used in food, pharmaceuticals, and cosmetics to add nutrients and functional properties, generally derived from porcine or bovine sources. Gelatin, therefore, mainly originates from porcine skin (46 %), bovine skin (29.4 %), and porcine or bovine bone (23.1 %) (Gómez-Guillén *et al.*, 2011).

Research on gelatin is currently focusing on finding alternative sources over pig sources due to the Halal issue for Muslims (Rakhmanova *et al.*, 2018; Shah and Yusuf, 2014). The demand for halal gelatin is reflected by the total number of Muslims worldwide. The Muslim

* Corresponding author. e-mail: vritta@umm.ac.id.

population amounts to 23.4 % of the global world population (Jamaludin *et al.*, 2011). There are various alternative sources of gelatin that several researchers have developed, such as seaweed (Nderitu *et al.*, 2011), other mammals (Al-Saidi *et al.*, 2012; Nitsuwat *et al.*, 2021; Sarbon *et al.*, 2013; Tümerkan, 2021), fish (Alfaro *et al.*, 2015; Zhang *et al.*, 2015), insect (Mariod and Fadul, 2013), and also poultry (Chakka *et al.*, 2017; Widyasari and Rawdkuen, 2014).

Research from poultry on gelatin has been performed on bird feet (Lin and Liu, 2007), silky fowl feet (Martínez-Ortiz *et al.*, 2015), chicken meat residues (Ramaya *et al.*, 2022), chicken skin (Silva *et al.*, 2021), and chicken feet (Chakka *et al.*, 2017; Hlaing *et al.*, 2020; Widyasari and Rawdkuen, 2014). The use of chicken feet, thus, is a considerable alternative raw material for halal gelatin. In addition, previous research stated that there is 18 % protein in chicken feet (Suparno and Prasetyo, 2019), showing sufficient potential as an alternative raw material for halal gelatin.

The most frequently consumed chickens in Indonesia are broilers and kampongs (native) chicken (*Gallus gallus domesticus* L.). Broiler chickens are pure-bred chickens having fast growth rates. In broilers, reaching a finishing weight of 1.5 kg takes a shorter time of 5 wk to 7 wk only, while kampung chicken requires a longer time of 30 wk to obtain a weight of 1.5 kg. Broiler chickens, thus, have a shorter economically relevant lifespan than kampung chickens. When slaughtered at an old age and take part of the muscle to take the collagen, we will get more collagen protein content because muscle tissue mainly consists of collagen (Cahyono, 2011). Differences in muscle tissue composition and collagen content in livestock relate to quality differences in gelatin because gelatin is obtained from the hydrolysis of collagen.

Gelatin is thus obtained by extraction, a chemical hydrolysis process with acids or bases (Das *et al.*, 2017). An acidic extraction process can change the basic structure of collagen from a triple helix into a single helix structure through a different extraction process than the one in an alkaline environment. It can only change the basic structure from a triple helix into a double helix, so the extraction of gelatin using acidic hydrolysis takes a shorter time than alkaline hydrolysis. The type of acid used in this study is an organic acid, namely acetic acid (CH_3COOH). Using inorganic acids such as hydrochloric acid (HCl) produces a very pungent odor, and the resulting gelatin is also darker in color (Liu *et al.*, 2015).

A previous study producing gelatin from the extraction of chicken feet using acetic acid (CH_3COOH), citric acid ($\text{C}_6\text{H}_8\text{O}_7$), and lactic acid ($\text{C}_3\text{H}_6\text{O}_3$) from different concentrations also evaluated its physicochemical properties (Chakka *et al.*, 2015). Other studies have produced physicochemical comparisons between gelatin made from chicken feet and gelatin made from bovine (Rahman and Jamalulail, 2012; Sarbon *et al.*, 2013). The present study aims to extract the gelatin from chicken feet skin from two chicken types, broiler chicken and kampung chicken, using acetic acid (CH_3COOH) in 2 %, 4 %, 6 %, and 8 % (v w^{-1}). The authors used acidic extraction to obtain gelatin and then analyzed the yield, moisture content, protein content, viscosity, and gel strength. The results could be used as a reference for producing gelatin from halal ingredients. The amino acid from the extracted

gelatin compared to commercially available gelatin was analyzed using High-Performance Liquid Chromatography (HPLC). The best product from the extracted gelatin samples was also used to make meatballs.

2. Materials and Methods

2.1. Materials

Fresh chicken feet were obtained from Malang, East Java, Indonesia. Chemicals for this study include acetic acid (CH_3COOH), sulfuric acid (H_2SO_4) 98 %, Na_2SO_4 -HgO catalyst, sodium hydroxide (NaOH) 50 %, boric acid (HBrO_3) 4 %, hydrochloric acid (HCl) 0.02 N, and petroleum benzene. All chemicals in this study used Pro Analytic, Merck.

2.2. Methods

First, chicken feet were washed to remove impurities and then boiled at 80 °C for 10 min. Next, chicken feet that had been sliced were rewashed to remove the remaining fat. Chicken feet were then skinned, cut into 2 cm-sized pieces, and weighed as much as 60 g. The skin was soaked with a solution of acetic acid (CH_3COOH), concentration 2 %, 4 %, 6 %, and 8 % (v w^{-1}) for 24 h. The immersion process brought up ossein. Ossein was then washed with distilled water until the pH was between 5 to 6. Ossein was extracted with distilled water (1:2) at 70 °C (Biobase WD-AD5, China) for 4 h to produce the gelatin solution. The gelatin solution was filtered (IKEME, type IKEM-5, China) and poured into a baking pan (Maspion, Indonesia). The baking sheet was put in the refrigerator (Hitachi R-VX40PGD9, Japan) at 5 °C for 24 h to concentrate the gelatin solution until the formation of the gel. The gelatin gel was dried in a cabinet dryer (Aneka Mesin, AM-TD24, Indonesia) at 60 °C for 78 h. Dry gelatin was mashed to powder (Santana *et al.*, 2020).

2.3. Characterization of gelatin

The extracted gelatin was analyzed for its amino acid composition using HPLC at the IPB (*Institut Pertanian Bogor*) University Laboratory, Indonesia. Samples of gelatin were injected into the HPLC column. HPLC column details: 150 mm × 4.6 mm ODS-2 Hypercell column and fluorescence detectors were used (Shimadzu, LP-32-IDN, Japan). Characterization of gelatin was carried out by separation through the conditions were set at a flow rate of 1 mL min^{-1} with separation using an eluent gradient system. The mobile phase uses eluent A, a mixture of sodium acetate pH 6.5, sodium ethylenediamine tetraacetate (Na-EDTA), methanol, and tetrahydrofuran (THF), and eluent B, which is a mixture of 95 % methanol and ion-free water (Setyobudi *et al.*, 2021b). Result of characterization of gelatin in the form of quantity (%) of amino acids: Aspartic acid, Threonine, Serine, Glutamate, Proline, Glycine, Alanine, Valine, Methionine, Isoleucine, Leucine, Tyrosine, Phenylalanine, Histidine, Lysine, Arginine.

2.4. Application of gelatin

Forming meatballs began with the preparation of ingredients, namely, fresh chicken meat (1 kg), tapioca flour (150 g), garlic (25 g), salt (20 g), pepper (8 g), ice cube (200 g) and gelatin powder (7.5 g). The chicken meat was ground by adding salt and ice cubes. Spices such as

garlic, shallot pepper, gelatin powder, and tapioca flour were used during the grinding process. The dough was then printed round and immediately boiled at a temperature of 60 °C to 80 °C. The cooked meatballs floated for about 10 min (Kilic *et al.*, 2021).

2.5. Gelatin and meatball analysis

Broiler and kampong chicken feet skin samples were analyzed as raw materials. The analyses of raw materials included protein, moisture, and ash content. The extracted gelatin was investigated for chemical and physical composition. The proximate analyses consisted of moisture (thermogravimetry, oven, Roman, Switzerland), ash (thermogravimetry, oven, Roman, Switzerland), and protein (Kjeldahl, Genhadet, German) content. The physical analyses consisted of pH (pH meter, SI Lab, United States), viscosity (viscometer, Nesco, Shanghai), and gel strength (texture analyzer, Shimadzu, Japan). A chemical analysis of the meatballs was conducted to test product quality concerning the extracted gelatin. As control samples were used, meatballs with commercially available gelatin and meatballs without adding gelatin. The meatball was analyzed for moisture, ash, protein, fat, texture (NSA-RI, 2019), and organoleptic properties (Damat *et al.*, 2021a; NSA-RI, 2006).

As an organoleptic analysis, this study performed a hedonic analysis which was carried out using untrained student panelists to identify consumer preferences for food ingredients. The panel used for the organoleptic test consisted of 24 untrained panelists (Damat *et al.*, 2021b; NSA-RI, 2006). The organoleptic properties assessment scores are presented in Table 1.

Table 1. Assessment score on organoleptic analyses of chicken meatballs

Score	Aroma	Taste	Texture	Appearance
1	Strong distaste	Strong distaste	Strong distaste	Strong distaste
2	Distaste	Distaste	Distaste moderately	Distaste moderately
3	Weak distaste	Weak distaste	Light distaste	Light distaste
4	Neither like nor dislike			
5	Enjoy slightly	Enjoy slightly	Enjoy slightly	Enjoy slightly
6	Enjoy moderately	Enjoy moderately	Enjoy moderately	Enjoy moderately
7	strong preference	strong preference	strong preference	strong preference

2.6. Research design

The study covered the extraction of chicken feet skin gelatin with various types of chicken and different concentrations of acetic acid solvents. The first stage of the

experimental design had a randomized design with two factors and three replications. The first factor was the chicken type with two levels, broiler chicken and kampong chicken. The second factor used was the concentration of acetic acid (CH₃COOH) with four levels of 2 %, 4 %, 6 %, and 8 % (v w⁻¹). Duncan's new multiple-range tests were used to determine the means, and $P \leq 0.05$ was considered statistically significant. Processing data using formulas in excel (Adinurani 2016, 2022).

3. Results and Discussion

3.1. Raw material analysis

Raw material analysis was used to pre-screen the protein and moisture content of the raw material. It is important because this study used different chicken types, differences in feed, and finally, differences in slaughtering age, which may have affected the chemical content (Cahyono, 2011). Table 2 shows that the protein and ash content of kampong chicken feet skin were higher than the equivalent numbers in broiler chicken. Similarly, the moisture content of kampong chicken feet skin was lower than that of broilers.

Table 2. Analysis results of raw material for chicken feet skin

Component	Kampong chicken feet skin	Broiler chicken feet skin	Chicken feet (Suparno and Prasetyo, 2019)
Protein (%)	22.73	22.00	18.09
Moisture (%)	63.01	64.00	64.00
Ash (%)	3.50	3.37	3.50

3.2. Yield and characterization of gelatin

Based on the analysis of variance, both the chicken type and acidic concentration significantly affected the yield of the gelatin produced ($\alpha = 5\%$). The highest gelatin yield was obtained through 4 % acetic acid at extraction (Table 3). The highest yield from kampong chicken feet skin gelatin was 12.67 %, while broiler chicken feet skin was 10.0 %. The results might be explained as the raw material (collagen protein in the skin) was higher in kampong chicken feet than in broiler chicken (Table 1). This yield is even higher than in a previous study using 1.5 % acetic acid (6.59 %), 3 % acetic acid (8.51 %), and 4.5 % acetic acid (10.16 %) (Chakka *et al.*, 2017). However, this present study achieved lower results than the previous study, which used alkaline-based sodium hydroxide (NaOH 0.15 %), resulting in 16 % (Sarbon *et al.*, 2013). Extraction with acid solvents effectively hydrolyses collagen through peptide bonds (Sarbon *et al.*, 2013). The acid solvent is even capable of dissolving non-cross collagen and of breaking down some cross bonds between strands in collagen, leading to higher solubility (Liu *et al.*, 2015).

Table 3. Detailed analysis of chicken feet skin gelatin

Chicken type	Treatment Concentration of acetic acid (%)	Dry based				Gel based		
		Yield (%)	Moisture (%)	Ash (%)	Protein (%)	pH	Viscosity (cp)	Gel strength (g cm ⁻²)
Kampong chicken feet skin	2	10.01 ± 0.04 ^{bc}	11.98 ± 0.47 ^d	1.67 ± 0.31 ^b	80.25 ± 0.33 ^b	5.49 ± 0.03 ^d	4.56 ± 0.04 ^b	63.47 ± 0.30 ^b
	4	12.67 ± 0.27 ^d	10.29 ± 0.14 ^c	1.58 ± 0.27 ^b	82.52 ± 0.75 ^{ab}	4.53 ± 0.08 ^c	4.78 ± 0.09 ^{bc}	66.29 ± 0.43 ^c
	6	11.36 ± 0.33 ^c	8.76 ± 0.98 ^{bc}	1.54 ± 0.31 ^b	77.21 ± 0.07 ^{ab}	4.14 ± 0.01 ^b	4.21 ± 0.02 ^{ab}	61.43 ± 0.28 ^b
	8	10.44 ± 0.63 ^c	7.54 ± 0.50 ^b	1.37 ± 0.60 ^b	76.28 ± 0.59 ^a	3.33 ± 0.06 ^a	4.02 ± 0.02 ^a	59.61 ± 0.05 ^a
Broiler Chicken Feet Skin	2	7.05 ± 0.10 ^a	9.48 ± 0.49 ^c	0.87 ± 0.01 ^{ab}	81.29 ± 0.26 ^b	5.64 ± 0.03 ^d	5.23 ± 0.02 ^{cd}	67.49 ± 0.22 ^{bc}
	4	10.90 ± 0.10 ^c	7.95 ± 0.40 ^{bc}	0.58 ± 0.19 ^{ab}	82.48 ± 0.96 ^b	4.76 ± 0.09 ^c	5.44 ± 0.02 ^d	70.13 ± 0.48 ^c
	6	9.10 ± 0.11 ^b	6.80 ± 0.12 ^{ab}	0.47 ± 0.13 ^{ab}	79.07 ± 0.95 ^{ab}	4.25 ± 0.01 ^{bc}	4.98 ± 0.05 ^c	64.95 ± 0.12 ^b
	8	9.42 ± 0.77 ^{bc}	5.52 ± 0.04 ^a	0.27 ± 0.21 ^a	77.63 ± 0.62 ^{ab}	4.02 ± 0.08 ^b	4.72 ± 0.08 ^{bc}	62.02 ± 0.74 ^{ab}

The average value followed by the same letter indicates no significant effect according to Duncan's test $\alpha = 5\%$

3.2.1. Moisture content

The analysis of variance showed that the chicken type and treatment had a very significant effect ($\alpha = 5\%$). The concentration of acetic acid substantially affected the moisture content of chicken feet skin gelatin. Table 3 shows that the mean moisture content of chicken feet skin gelatin produced in this study ranged between 5.52% and 11.99%. The moisture content of chicken feet skin gelatin obtained in the study met the GMIA (2012) and requirements, a maximum of 16%. The average moisture content of broiler chicken feet gelatin was lower than in kampong chicken. The moisture content range in kampong chicken gelatin was between 7.54% and 11.98%, while that of broiler chicken feet skin gelatin was between 5.52% and 9.48%. The range relates to the protein content in the raw material (Table 2). Chicken feet skin from broilers had a lower protein content than kampong chicken. Broiler chicken feet skin had a protein content of 22.00%, which amounted to 22.73% in kampong chicken. The protein content in chicken feet skin could bind water and the added water from the processing process. That figure is called the water-holding capacity (WHC) (Bowker and Zhuang, 2015).

3.2.2. Ash content

The analysis of variance also revealed that the chicken type related very significantly ($\alpha = 1\%$) to the ash content of the feet skin gelatin. Manipulating the acetic acid concentration did not substantially affect the gelatin ash content of chicken feet skin. The average ash content range of chicken feet skin gelatin produced in this study was 0.55% to 1.54%. The ash content of chicken feet skin gelatin obtained in this study has met the GMIA requirements, as the maximum allowed ash content in gelatin is 3.35%. A demineralization process with acetic acid at a concentration of 2% to 8% for 24 h can liberate minerals from raw materials to produce gelatin with low ash content. The mean gelatin ash content from broiler chicken feet skin (0.55%) was lower than that of kampong chicken (1.54%). Therefore, the concentration of acetic acid had no significant effect on the gelatin ash content of chicken feet skin. Still, the average ash content of chicken feet skin gelatin decreased with increasing acetic acid concentration (Weng *et al.*, 2014). Ash content in gelatin indicates the presence of minerals present in it. Gelatin from chicken feet is known for containing several macro-

(Na, Ca, K, Mg, P, S) and microminerals (Cu, Fe, Mn) (Santana *et al.*, 2020).

3.2.3. Protein content

Analyses of variance showed that chicken types and acetic acid concentration had a very significant effect ($\alpha = 5\%$) on the protein content of chicken feet skin gelatin. The average protein content of chicken feet skin gelatin in both chicken types and the concentration of acetic acid are presented in Table 2. The mean percentage of kampong chicken gelatin protein content ranged between 82.28% and 80.25%, while broiler chicken feet skin ranged between 82.48% and 77.63%. The highest protein content in the study was found when 4% acetic acid was used with village chickens' skin (82.52%) and broilers (82.48%). Using the acid extraction method, the protein content in gelatin produced from the chicken feet skin and broilers was similar to previous studies (Chakka *et al.*, 2017). Acid extraction resulted in higher protein contents than in alkaline environments and beef samples. The protein content of gelatin from chicken feet with alkaline extraction amounted to 80.76%, while gelatin from cows contained 81.75% (Sarbon *et al.*, 2013). The low protein content of kampong chicken feet skin gelatin compared to broiler chicken feet skin gelatin was most likely caused by the relatively high ash content. The high ash was considered a mineral residue that might inhibit protein binding to reactive groups in gelatin such as -OH, -COOH, and -NH₂ so that the intermolecular binding of gelatin proteins becomes weak (Gómez-Guillén *et al.*, 2011).

3.2.4. pH

The chicken type had no significant effect ($\alpha = 5\%$) on chicken feet skin gelatin's pH (acidity). However, the acetic acid concentration significantly affected chicken feet skin gelatin's pH (degree of acidity). Although the average pH was not much different between boiler chicken feet skin gelatin and kampong chicken, boiler chicken feet skin gelatin had a slightly higher pH of 4.35, while kampong chicken feet skin gelatin was 4.33.

3.2.5. Viscosity

Chicken type and acetic concentration had a very significant effect ($\alpha = 5\%$) on the viscosity of chicken feet skin gelatin. Table 2 shows that the mean viscosity of chicken feet skin produced in this study ranged between 4.02 cp and 5.44 cp. The viscosity of chicken feet skin gelatin met the requirements of GMIA (2012), requiring a

viscosity in gelatin between 1.5 cp and 7.5 cp. The protein in gelatin had a high water binding power to protein or was hydrophilic. Broiler chicken skin gelatin had a higher protein content, so its ability to bind water was also higher (Table 2) to reduce moisture and increase gelatin viscosity. Based on the Duncan test ($\alpha = 5\%$), the acetic acid concentration significantly affected the resulting chicken feet skin gelatin viscosity. The viscosity of gelatin in chicken feet skin decreased with increasing concentration of the acetic acid solution. The lowest viscosity was found at an acetic acid concentration of 8% in the gelatin of kampong and broiler chicken feet and amounted to 4.02 cp and 4.72 cp, respectively. Acetic acid can break the peptide bonds of amino acids into shorter molecular chains to decrease their viscosity. The number of amino acid chains and their molecular weight are directly proportional to viscosity (Sompie *et al.*, 2015, Sompie and Triasih, 2018).

3.2.6. Gel strength

This study observed a very significant effect ($\alpha = 5\%$) of chicken species on gelatin strength from chicken feet skin. Changing the concentration of acetic acid substantially affected the gelatin gel's strength. The average strength of chicken feet skin gel produced in this study was (59.61 to 70.13) g cm⁻². The power of gelatin from chicken feet skin in this study met the requirements of GMIA since the strength of the gel in gelatin has to be in the range of (50 to 300) g cm⁻². Based on the Duncan test ($\alpha = 5\%$), the chicken species had a powerful effect on gelatin gel strength. Table 2 shows that the average gelatin strength of broiler chicken feet skin was higher than that of kampong chickens. The average power of gelatin from

broiler chicken feet skin produced in this study was (62.02 to 70.13) g cm⁻², while the kampong chicken was between 59.61 g cm⁻² and 66.29 g cm⁻². Gel strength and gel viscosity are directly proportional to each other. As observed in this study, broiler chicken skin gelatin had a higher viscosity and also a higher gel strength. Glycine, hydroxyproline, and proline are amino acids responsible for maintaining the stability of the gelatin structure. Hydrolysis reactions break down proteins into amino acids and thus increase the distribution of molecules and gel strength (Sompie *et al.*, 2015).

3.3. Amino acid profile

Table 4 details the gelatin amino acid composition of kampong chicken feet skin gelatin from broiler chicken feet skin gelatin and commercially produced (bovine) gelatin. Kampong and broiler chicken feet skin gelatin had a similar percentage of glycine as the commercial gelatin. Glycine makes up more than 50% of all the amino acids in gelatin. This study observed 53.37% glycine in kampong chicken feet skin gelatin and 51.95% in broiler chicken feet skin gelatin compared to 54.33% in commercial (bovine) gelatin. The second-highest amino acid after glycine was alanine (Table 4). Although the percentages differed significantly, that finding corresponds to previous studies. Alanine in kampong chicken feet skin gelatin was 8.48%; in broiler chicken feet skin gelatin; it was 8.39%, and in (bovine) commercial gelatin, it was 7.72%. Glycine and alanine influence the structure of gelatin and the functional properties of gelatin as an emulsifier (Chakka *et al.*, 2017).

Table 4. HPLC analysis of amino acid from kampong, broiler, and commercial gelatin

No.	Amino acid	Kampong chicken feet skin gelatin		Broiler chicken feet skin gelatin		Commercial gelatin (Bovine)	
		RT	% Area	RT	% Area	RT	% Area
1	Aspartic acid	5.78	2.77	7.16	2.73	7.167	2.77
2	Threonine	2.02	2.64	8.73	2.72	8.738	2.31
3	Serine	2.53	2.96	9.37	2.93	9.369	3.75
4	Glutamate	11.90	5.95	10.54	5.81	10.542	5.58
5	Proline	11.881	3.83	12.00	3.82	12.007	3.87
6	Glycine	32.91	53.37	15.86	51.95	15.871	54.33
7	Alanine	11.16	8.48	17.19	8.39	17.194	7.72
8	Valine	1.81	2.30	22.13	2.36	22.117	2.76
9	Methionine	0.77	0.46	23.35	0.42	23.344	0.32
10	Ileusine	1.23	1.24	25.53	1.22	25.526	1.51
11	Leusine	3.03	1.86	26.26	1.84	26.248	1.82
12	Tyrosine	0.42	0.11	27.73	0.10	27.727	0.07
13	Phenylalanine	2.54	1.39	28.84	1.33	28.831	1.17
14	Histidine	0.90	0.94	30.42	1.00	30.410	0.98
15	Lysine	4.08	4.29	32.30	4.24	32.293	3.74
16	Arginine	8.02	5.32	35.84	7.09	35.823	5.41

3.4. Determination and best treatment

The best treatment was determined by comparing the products with the GMIA standard (Table 5). It can be seen in Table 5, the use of acetic acid at a concentration of 4% gave the highest yield in kampong (12.67% ± 0.27%) and broilers chicken feet skin gelatin (10.90% ± 0.10%).

Besides that, gelatin that used 4% acetic acid shows moisture, ash, pH, viscosity, gel strength, colour, aroma, and also taste that according to the GMIA standard. Meanwhile, protein of gelatin from 4% acetic acid kampong and broiler chicken feet skin closest to the standard value.

Table 5. Comparison of obtained gelatin characteristics with GMIA (standard)

Treatment	Concentration of acetic acid (%)	Dry based					Gel based			
		Yield (%)	Moisture (%)	Ash (%)	Protein (%)	pH	Viscosity (cp)	Gel strength (g cm ⁻²)	Colour	Aroma, taste
Kampong chicken feet skin	2	10.01 ± 0.04 ^{bc}	11.98 ± 0.47 ^d	1.67 ± 0.31 ^b	80,25 ± 0.33 ^b	5.49 ± 0.03 ^d	4.56 ± 0.04 ^b	63.47 ± 0.30 ^b	Yellowish	Normal
	4	12.67 ± 0.27 ^d	10.29 ± 0.14 ^c	1.58 ± 0.27 ^b	82,52 ± 0.75 ^{ab}	4.53 ± 0.08 ^c	4.78 ± 0.09 ^{bc}	66.29 ± 0.43 ^c	Yellowish	Normal
	6	11.36 ± 0.33 ^c	8.76 ± 0.98 ^{bc}	1.54 ± 0.31 ^b	77,21 ± 0.07 ^{ab}	4.14 ± 0.01 ^b	4.21 ± 0.02 ^{ab}	61.43 ± 0.28 ^b	Yellowish	Normal
	8	10.44 ± 0.63 ^c	7.54 ± 0.50 ^b	1.37 ± 0.60 ^b	76,28 ± 0.59 ^a	3.33 ± 0.06 ^a	4.02 ± 0.02 ^a	59.61 ± 0.05 ^a	Yellowish	Normal
Broiler Chicken Feet Skin	2	7.05 ± 0.10 ^a	9.48 ± 0.49 ^c	0.87 ± 0.01 ^{ab}	81,29 ± 0.26 ^b	5.64 ± 0.03 ^d	5.23 ± 0.02 ^{cd}	67.49 ± 0.22 ^{bc}	Yellowish	Normal
	4	10.90 ± 0.10 ^c	7.95 ± 0.40 ^{bc}	0.58 ± 0.19 ^{ab}	82,48 ± 0.96 ^b	4.76 ± 0.09 ^c	5.44 ± 0.02 ^d	70.13 ± 0.48 ^c	Yellowish	Normal
	6	9.10 ± 0.11 ^b	6.80 ± 0.12 ^{ab}	0.47 ± 0.13 ^{ab}	79,07 ± 0.95 ^{ab}	4.25 ± 0.01 ^{bc}	4.98 ± 0.05 ^c	64.95 ± 0.12 ^b	Yellowish	Normal
	8	9.42 ± 0.77 ^{bc}	5.52 ± 0.04 ^a	0.27 ± 0.21 ^a	77,63 ± 0.62 ^{ab}	4.02 ± 0.08 ^b	4.72 ± 0.08 ^{bc}	62.02 ± 0.74 ^{ab}	Yellowish	Normal
GMIA (standard)	-	Max 16	Max 16	87.26	4.5 to 6.5	1.5 to 7.5	50 to 300	Yellowish	Normal	

Gelatin from kampong and broiler chicken feet skin (acetic acid 4 %) was used to produce meatballs and compare them with control meatballs consisting of commercial gelatin and meatballs without any gelatin (Table 6). Gelatin is recognized as a food additive that acts as a thickening agent. Therefore, gelatin quality can affect the meatball quality, especially the texture (Hafid *et al.*, 2020). This study's results on moisture, ash, protein, fat, and texture can be seen in Table 6. In addition, the

organoleptic (aroma, taste, texture, appearance) variables can be obtained from Table 7. Based on the data in Table 6, it can be interpreted that the meatballs using kampong and broiler chicken feet skin gelatin (acetic acid 4 %) were meeting the NSA (National Standardization Agency of Republic of Indonesia-*Standar Nasional Indonesia*: 3818-2014 (NSA – RI, 2019) on all variables including moisture, ash, protein, and lipids.

Table 6. Results of meatball composition

Meatball type	Proximate analysis				
	Moisture content (%)	Ash content (%)	Protein content (%)	Lipid content (%)	Texture (N mm ⁻²)
Using kampong chicken feet skin gelatin (Acetic acid 4 %)	68.08±0.02 ^c	1.91±0.03 ^d	9.43±0.02 ^b	2.80±0.02 ^d	19.80±0.01 ^b
Using broiler chicken feet skin gelatin (Acetic acid 4 %)	66.93±0.03 ^b	1.42±0.04 ^c	10.40±0.02 ^c	2.09±0.02 ^b	25.27±0.02 ^d
Commercial gelatin (bovine)	65.93±0.02 ^a	1.28±0.02 ^b	10.83±0.02 ^{cd}	2.41±0.02 ^c	24.88±0.02 ^c
Without gelatin	69.52±0.04 ^d	0.80±0.04 ^a	8.95±0.02 ^a	1.35±0.02 ^a	18.07±0.01 ^a
NSA (National Standardization Agency of Republic of Indonesia -Standar Nasional Indonesia: 3818-2014)	max. 70.0	max. 3.0	min. 8.0	max. 10.0	-

The mean value followed by the same letter indicates no significant effect according to Duncan's test $\alpha = 5\%$

Table 7. Test results from organoleptics of meatballs

Meatball type	Organoleptic test			
	Aroma	Taste	Texture	Appearance
Using kampong chicken feet skin gelatin (Acetic acid 4 %)	5.74 ^a	5.27 ^{ab}	5.04 ^b	3.19 ^b
Using broiler chicken feet skin gelatin (Acetic acid 4 %)	5.75 ^a	5.27 ^{ab}	6.09 ^c	4.16 ^c
Commercial gelatin (bovine)	5.74 ^a	5.28 ^{ab}	6.10 ^c	5.06 ^d
Without gelatin	5.74 ^a	5.23 ^a	4.01 ^a	2.33 ^a

The mean value followed by the same letter indicates no significant effect according to Duncan's test $\alpha = 5\%$

Based on Table 6, the meatball moisture content using commercial gelatin was lower than that of meatballs using broiler chicken feet gelatin (65.93 % versus 66.93 %), and meatballs using kampong chicken feet skin gelatin were lower than meatballs without gelatin (68.08 % versus 69.52 %). However, meatballs using broiler chicken had a similar result as those containing commercial gelatin. Thus, it can be concluded that the water binding capacity of both gelatin types was almost the same. Gelatin can form hydrogen with water in foodstuffs. When gelatin binds to water, the gelation rate increases, thereby increasing the chewy texture of the meat (Mariod and Fadul, 2013).

The mineral content data sequentially from lowest to highest were as follows: meatballs without gelatin (0.80 %), meatballs with commercial gelatin (1.28 %), meatballs using broiler chicken feet skin gelatin (1.42 %), and meatballs using kampong chicken feet skin gelatin (1.91 %). The ash content of the meatballs using kampong and broiler chicken feet skin gelatin followed NSA (National Standardization Agency of Republic of Indonesia -Standar Nasional Indonesia).

Like moisture, protein contents showed that meatballs with gelatin using broiler chicken feet skin gelatin (10.40 %) had almost the same value as meatballs with commercial gelatin 10.83 %). That percentage has overcome the minimum required protein standard of NSA (National Standardization Agency of Republic of Indonesia - *Standar Nasional Indonesia*, (minimum 8.0 %). The meatballs using kampong chicken feet skin gelatin (9.43 %) still met NSA standards. The lipid content shown in the meatballs using kampong and broiler chicken feet skin gelatin followed the standard because it did not exceed 10 %.

Aroma and taste (*i.e.*, organoleptic) results from meatballs using kampong and broiler chicken feet skin gelatin showed similar results compared to meatballs using commercial gelatin and meatballs without gelatin. Thus, the use of gelatin did not affect the aroma and taste of the meatball itself. However, the results of the organoleptic tests differed in texture and appearance. The use of gelatin affects the texture and appearance of the meatballs perceived by the panelists. Panelists preferred meatball texture and appearance of meatballs using broiler chicken feet skin gelatin and commercial gelatin over meatballs using kampong chicken feet skin gelatin and meatballs without gelatin.

4. Conclusion

This research paper shows that the feet skin of kampong and broiler chickens has a high potential to become a halal alternative to gelatin. Both chemical and physical variables derived from the GMIA standard

support this claim. Using 4 % acetic acid provided the best results in raw materials from the feet skin of kampong and broiler chickens. Gelatin from the skin of kampong chicken feet skin with 4 % acetic acid yielded 12.67 %, moisture content of 10.29 %, ash content of 1.58 %, protein content of 82.52 %, pH 4.53, a viscosity of 4.78 cp, and gel strength of 66.29 g cm⁻². Gelatin from broiler chicken feet skin with 4 % acetic acid yielded 10.90 %, a moisture content of 7.95 %, an ash content of 7.95 %, a protein content of 82.48 %, a pH of 4.76, a viscosity of 5.4 cp, and a gel strength of 70.13 g cm⁻². In addition, kampong and broiler chicken feet skin gelatin provided similar percentages of glycine as commercial gelatin. Glycine makes up more than 50 % of all amino acids in gelatin. Glycine from kampong chicken feet skin gelatin was 53.37 %, broiler chicken feet skin gelatin 51.95 %, and commercial gelatin (bovine) was 54.33 %. Meatballs using Kampong and broiler chicken feet skin gelatin (acetic acid 4 %) met the requirements of NSA (National Standardization Agency of Republic of Indonesia -*Standar Nasional Indonesia*: 3818-2014) on moisture, ash, protein variables, and lipids. Organoleptic test showed that aroma and taste from meatballs using kampong and broiler chicken feet skin gelatin showed similar results compared to meatballs using commercial gelatin and meatballs without gelatin; panelists preferred meatball texture and appearance of meatballs using broiler chicken feet skin gelatin and commercial gelatin over meatballs using kampong chicken feet skin gelatin and meatballs without gelatin.

Acknowledgments

The authors would like to thank the Faculty of Agriculture and Animal Science, University of Muhammadiyah Malang.

References

- Abdullah K, Saepul UA, Soengeng R, Suherman E, Susanto H, Setyobudi RH, Burlakovs J and Vincēviča-Gaile Z. 2020. Renewable energy technologies for economic development. *E3S Web Conf.*, **188(00016)**:1–8. <https://doi.org/10.1051/e3sconf/202018800016>
- Adinurani PG. 2016. **Design and Analysis of Agrotorial Data: Manual and SPSS.**Plantaxia, Yogyakarta, Indonesia
- Adinurani PG, Setyobudi RH, Wahono SK, Mel M, Nindita A, Purbajanti E, Harsono SS, Malala AR, Nelwan LO, and Sasmito A. 2017. Ballast weight review of capsule husk *Jatropha curcas* Linn. on acid fermentation first stage in two-phase anaerobic digestion. *Proc. Pakistan Acad. Sci. B Life Environ. Sci.* **54(1)**: 47–57

- Adinurani, PG. 2022. **Agrotechnology Applied Statistics** (compiled according to the semester learning plan). Deepublish, Yogyakarta, Indonesia.
- Al-Saidi GS, Al-Alawi A, Rahman MS and Guizani N. 2012. Fourier transform infrared (FTIR) spectroscopic study of extracted gelatin from shaari (*Lithrinus microdon*) skin: Effects of extraction conditions. *Int. Food Res. J.*, **19(3)**: 1167–1173.
- Alfaro ADT, Balbinot E, Weber CI, Tonial IB and Machado-Lunkes A. 2015. Fish gelatin: Characteristics, functional properties, applications and future potentials. *Food Eng. Rev.*, **7(1)**: 33–44. <https://doi.org/10.1007/s12393-014-9096-5>
- Bowker B and Zhuang H. 2015. Relationship between water-holding capacity and protein denaturation in broiler breast meat. *Poult. Sci.*, **94(1)**: 1657–1664. <https://doi.org/10.3382/ps/pev120>
- Cahyono IB. 2011. **Broiler Kampung Chiken**. Penebar Swadaya Grup, Jakarta, Indonesia.
- Chakka AK, Muhammed A, Sakhare PZ and Bhaskar N. 2017. Poultry processing waste as an alternative source for mammalian gelatin: Extraction and characterization of gelatin from chicken feet using food grade acids. *Waste Biomass Valorization*, **8(1)**: 2583–2593. <https://doi.org/10.1007/s12649-016-9756-1>
- Dhakal D, Koomsap P, Lamichhane A, Sadiq MB and Anal AK. 2018. Optimization of collagen extraction from chicken feet by papain hydrolysis and synthesis of chicken feet collagen based biopolymeric fibres. *Food Biosci.*, **23**:23–30. <https://doi.org/10.1016/j.fbio.2018.03.003>
- Damat D, Setyobudi RH, Utomo JS, Vincevica-Gaile Z, Tain A and Siskawardani DD. 2021a. The characteristics and predicted of glycemic index of rice analogue from modified arrowroot starch (*Maranta arundinaceae* L.). *Jordan J. Biol. Sci.*, **14(3)**:389–393. <http://jjbs.hu.edu.jo/vol14.htm>
- Damat D, Setyobudi RH, Burlakovs J, Vincevica-Gaile Z, Siskawardani DD, Anggriani R and Tain A. 2021b. Characterization properties of extruded analog rice developed from arrowroot starch with addition of seaweed and spices. *Sarhad J. Agric.*, **37 (Special issue 1)**:159–170
- Das MP, Suguna PR, Prasad K, Vijaylakshmi JV and Renuka M. 2017. Extraction and characterization of gelatin: A functional biopolymer. *Int. J. Pharm. Pharm. Sci.*, **9(9)**: 239–242. <https://doi.org/10.22159/ijpps.2017v9i9.17618>
- FAO Statistic. 2020. **Publication Statistical**. <https://www.fao.org/food-agriculture-statistics/resources/publications/statistical-yearbook-and-pocketbook/en/>
- GMIA. 2012 (Gelatin Manufacturers Institute of America). **Gelatin Handbook**. https://nitta-gelatin.com/wp-content/uploads/2018/02/GMIA_Gelatin-Handbook.pdf
- Gómez-Guillén MC, Giménez B, López-Caballero ME and Montero MP. 2011. Functional and bioactive properties of collagen and gelatin from alternative sources: A review. *Food Hydrocoll.*, **25(1)**: 1813–1827. <https://doi.org/10.1016/j.foodhyd.2011.02.007>
- Hafid H, Napirah A and Efendi A. Organoleptic characteristics of chicken meatballs that using gelatin as a gelling agent. 2020. *IOP Conf. Ser.: Earth Environ. Sci.* **465 (012013)**: 1–7. <https://doi.org/10.1088/1755-1315/465/1/012013>
- Haghighi SFM, Parvasi P, Jokar SM and Basile A. 2021. Investigating the effects of ultrasonic frequency and membrane technology on biodiesel production from chicken waste. *Energies*, **14(2133)**: 1–21. <https://doi.org/10.3390/en14082133>
- Hlaing SAA, Sadiq MB and Anal AK. 2020. Enhanced yield of *Scenedesmus obliquus* biomacromolecules through medium optimization and development of microalgae based functional chocolate. *J. Food Sci. Technol.*, **57(1)**: 1090–1099. <https://doi.org/10.1007/s13197-019-04144-3>
- Jamaludin MA, Zaki NNM, Ramli MA, Hashim DM and Rahman SA. 2011. Istihalah: Analysis on the utilization of gelatin in food products, 2nd International Conference on Humanities, Historical and Social Sciences. IPEDR vol.17 IACSIT Press, Singapore.
- Janarthanam H, Subbiah G, Raja KSS, Gnanamani S, Roy A and Chougale V. 2020. Experimental and synthesis of chicken slaughter waste biodiesel in DI diesel engine. *AIP Conf. Proc.* **2311**, 020014. <https://doi.org/10.1063/5.0034144>
- Karuppannan SK, Dowlath MJH, Raiyaan GID, Rajadesingu S, Arunachalam KD. 2021. Application of poultry industry waste in producing value-added products—A review. In: Hussain CM. (Ed.). **Chapter five, Concepts of Advanced Zero Waste Tools. Present and Emerging Waste Management Practices**. Elsevier Inc. The Netherlands, pp. 91–121. <https://doi.org/10.1016/B978-0-12-822183-9.00005-2>
- Kilic S, Oz E and Oz F. 2021. Effect of turmeric on the reduction of heterocyclic aromatic amines and quality of chicken meatballs. *Food Control* **128**, 108189. <https://doi.org/10.1016/j.foodcont.2021.108189>
- Lachenmeier DW, Schwarz S, Rieke-Zapp J, Cantergiani E, Rawel H, Martín-Cabrejas, MA, Martuscelli M, Gottstein V and Angeloni S. 2022. Coffee by-products as sustainable novel foods: Report of the 2nd International Electronic Conference on Foods—“future foods and food technologies for a sustainable world”. *Foods* **11(3)**: 1–16. <https://doi.org/10.3390/foods11010003>
- Lasekan A, Bakar FA and Hashim D. 2013. Potential of chicken by-products as sources of useful biological resources. *Waste Manage.*, **33(3)**:552–565. <https://doi.org/10.1016/j.wasman.2012.08.001>
- Latifi P, Karrabi M and Danes S. 2019 Anaerobic co-digestion of poultry slaughterhouse wastes with sewage sludge in batch-mode bioreactors (effect of inoculum-substrate ratio and total solids). *Renewable Sustainable Energy Rev.*, **107**: 288–296. <https://doi.org/10.1016/j.rser.2019.03.015>
- Lin YK and Liu DC. 2007. Studies of novel hyaluronic acid-collagen sponge materials composed of two different species of type I collagen. *J. Biomater. Appl.*, **21(1)**: 265–281. <https://doi.org/10.1177/0885328206063502>
- Liu D, Nikoo M, Boran G, Zhou P and Regenstein JM. 2015. Collagen and gelatin. *Annu. Rev. Food Sci.* **6(1)**: 527–557. <https://doi.org/10.1146/annurev-food-031414-111800>
- Mariod AA and Fadul H. 2013. Gelatin, source, extraction and industrial applications. *Acta Sci. Pol. Technol. Aliment.*, **12(1)**:135–147.
- Martínez-Ortiz MA, Hernández-Fuentes AD, Pimentel-González DJ, Campos-Montiel RG, Vargas-Torres A and Aguirre-Álvarez G. 2015. Extraction and characterization of collagen from rabbit skin: Partial characterization. *CYTA. J. Food*, **13(1)**: 253–258. <https://doi.org/10.1080/19476337.2014.946451>
- NSA – RI. 2006. (National Standardization Agency of Republic of Indonesia -Standar Nasional Indonesia). SNI 01-2346-2006. Instructions for organoleptic and or sensory testing. https://www.academia.edu/42337013/Standar_Nasional_Indonesia_a_Petunjuk_pengujian_organoleptik_dan_atau_sensori_67_240_B_adan_Standarisasi_Nasional
- NSA – RI. 2019. (National Standardization Agency of Republic of Indonesia -Standar Nasional Indonesia). Regulation of the national standardization agency - Republic of Indonesia, number 6 of 2019 about standard conformity assessment scheme Indonesia national food sector: Technical instructions for meatball product certification scheme (<https://bsn.go.id/uploads/download>)

- Sarboon N, Badii F and Howell NK. 2013. Preparation and characterisation of chicken skin gelatin as an alternative to mammalian gelatin. *Food Hydrocoll.*, **30(1)**: 143–151. <https://doi.org/10.1016/j.foodhyd.2012.05.009>
- Melanie H, Susilowati A, Iskandar JM and Laelatunur M. 2015. Fat reduction in improving the quality of chicken feet gelatine for functional food application. *Jurnal Kimia Valensi* **1(1)**:12–19. <https://doi.org/10.15406/jkv.v0i0.3149>
- Nderitu JH, Kayumbo HY and Mueke JM. 2011. Beanfly infestation on common beans (*Phaseolus vulgaris* L.) in Kenya. *Int. J. Trop. Insect Sci.*, **11(1)**: 35–41. <https://doi.org/10.1017/S1742758400019810>
- Nitsuwat S, Zhang P and Fang Z. 2021. Fish gelatin as an alternative to mammalian gelatin for food industry: A meta-analysis. *Lwt*, **141(1)**: 110899. <https://doi.org/10.1016/j.lwt.2021.110899>
- Radhakrishnan R, Ghosh P, Selvakumar TA, Shanmugavel M and Gnanamani A. 2020. Poultry spent wastes: An emerging trend in collagen mining. *Adv Tissue Eng Regen Med.***6(2)**:26–35. <https://doi.org/10.15406/atroa.2020.06.00113>
- Rakhmanova A, Khan ZA, Sharif R and Lv X. 2018. Meeting the requirements of halal gelatin: A mini review. *Moj Food Proc. Technol.*, **6(1)**: 477–482. <https://doi.org/10.15406/mojfpt.2018.06.00209>
- Ramaya K, Shukri KS, Yin VQ and Babji AS. 2012. Mechanically deboned chicken meat residue (MDCMR) as a new raw material for gelatin extraction. The 2nd International Seminar on Food & Agricultural Sciences, Puri Pujangga, Universiti Kebangsaan Malaysia
- Santana JCC, Gardim RB, Almeida PF, Borini GB, Quispe APB, Llanos SAV, Heredia JA, Zamuner S, Gamarra F and Farias T. 2020. Valorization of chicken feet by-product of the poultry industry: high qualities of gelatin and biofilm from extraction of collagen. *Polymers*, **12(1)**: 529–532. <https://doi.org/10.3390/polym12030529>
- Sarboon NM, Badii F and Howell NK. 2013. Preparation and characterisation of chicken skin gelatin as an alternative to mammalian gelatin. *Food Hydrocoll.*, **30(1)**: 143–151. <https://doi.org/10.1016/j.foodhyd.2012.05.009>
- Setyobudi RH, Yandri E, Atoum MFM, Nur SM, Zekker I, Idroes R, Tallei TE, Adinurani PG, Vincēviča-Gaile Z, Widodo W, Zalizar L, Van Minh N, Susanto H, Mahaswa RK, Nugroho YA, Wahono SK, and Zahriah Z. 2021a. Healthy-smart concept as standard design of kitchen waste biogas digester for urban households. *Jordan J. Biol. Sci.*, **14(3)**: 613–620. <https://doi.org/10.54319/jjbs/140331>
- Setyobudi RH, Yandri E, Nugroho YA, Susanti MS, Wahono SK, Widodo W, Zalizar L, Saati EA, Maftuchah M, Atoum MFM, Massadeh MI, Yono D, Mahaswa RK, Susanto H, Damat D, Roeswitawati D, Adinurani PG and Mindarti S. 2021b. Assessment on coffee cherry flour of Mengani Arabica Coffee, Bali, Indonesia as iron non-heme source. *Sarhad J. Agric.*, **37(Special issue 1)**: 171–183. <https://dx.doi.org/10.17582/journal.sja/2022.37.s1.171.183>
- Shah H and Yusof F. 2014. Gelatin as an ingredient in food and pharmaceutical products: An Islamic perspective. *Adv. Environ. Biol.*, **8(1)**: 774–780.
- Silva OA, Pellá MCG, Friedrich JCC, Pellá MG, Beneton AG, Faria MGI, Colauto GAL, Caetano J, Simões MRR and Dragunski DC. 2021. Effects of a native cassava starch, chitosan, and gelatin-based edible coating over guavas (*Psidium guajava* L.). *Acs Food Science & Technology*, **1(1)**: 1247–1253. <https://doi.org/10.1021/acsfoodscitech.1c00131>
- Sompie M, Surtijono SE, Pontoh JHW and Lontaan NN. 2015. The effects of acetic acid concentration and extraction temperature on physical and chemical properties of pigskin gelatin. *Procedia Food Sci.*, **3(1)**: 383–388. <https://doi.org/10.1016/j.profoo.2015.01.042>
- Sompie M and Triasih A. 2018. Effect of extraction temperature on characteristics of chicken legskin gelatin. *IOP Conf. Ser.: Earth Environ. Sci.*, **102(012089)**:1–5. <https://doi.org/10.1088/1755-1315/102/1/012089>
- Suparno O and Prasetyo NB. 2019. Isolation of collagen from chicken feet with hydro-extraction method and its physico-chemical characterisation. 2019. *IOP Conf. Ser.: Earth Environ. Sci.*, **335(012018)**:1–11. <https://doi.org/10.1088/1755-1315/335/1/012018>
- Tümerkan ETA. 2021. Sustainable utilization of gelatin from animal-based agri-food waste for the food industry and pharmacology. *Valorization of Agri-Food Wastes and By-Products*, **1(1)**: 425–442. <https://doi.org/10.1016/B978-0-12-824044-1.00041-6>
- Weng W, Zheng H and Su W. 2014. Characterization of edible films based on tilapia (*Tilapia zillii*) scale gelatin with different extraction pH. *Food Hydrocoll.*, **41(1)**: 19–26. <https://doi.org/10.1016/j.foodhyd.2014.03.026>
- Widyasari R and Rawdkuen S. 2014. Extraction and characterization of gelatin from chicken feet by acid and ultrasound assisted extraction. *Food Appl. Biosci. J.*, **2(1)**: 85–97.
- Zhang QT, Tu ZC, Wang H, Huang XQ, Fan LL, Bao ZY and Xiao H. 2015. Functional properties and structure changes of soybean protein isolate after subcritical water treatment. *J. Food Sci. Technol.*, **52(1)**: 3412–3421. <https://doi.org/10.1007/s13197-014-1392-9>

Molecular Simulations of *Moringa oleifera* Phytochemicals as Potential Antagonists of the Proinflammatory NF- κ B p50 Transcription Factor

Kathleen Cole C. Tung¹, Romeric F. Pobre¹, Glenn G. Oyong^{2,*}

¹Department of Physics, De La Salle University, 2401 Taft Avenue, Manila 0922, Philippines; ²Molecular Science Unit Laboratory, Center for Natural Science and Environmental Research, De La Salle University, 2401 Taft Avenue, Manila 0922, Philippines

Received: July 16, 2022; Revised: January 2, 2023; Accepted: January 25, 2023

Abstract

This study conducted an *in silico* approach to determine which among the known *Moringa oleifera* phytochemicals demonstrate the most comparable anti-inflammatory activity compared to dexamethasone. Initial screening for druglikeness was performed using Lipinski's rule of five while the ADMET (Absorption, Distribution, Metabolism, Excretion, and Toxicity) properties were investigated. Molecular docking analysis via AutoDock Vina revealed that pterygospermin demonstrated the strongest binding affinity to the target NF- κ B p50 (–5.0 kcal/mol), higher than dexamethasone (–4.8 kcal/mol). PharmaGist also provided an overview of the structural features of pterygospermin that could ascertain binding interaction with NF- κ B p50. Molecular dynamics simulation using CABS-flex strongly suggested that pterygospermin can stably bind to NF- κ B p50 as evidenced by the minimal root mean square fluctuations between the apo and bound structures ($p = 0.4595$). These results suggest that pterygospermin can be a candidate inhibitor of NF- κ B p50. Screening for the anti-inflammatory activity of *M. oleifera* leaves, pod, and seed aqueous extract on lipopolysaccharide-induced human THP-1 macrophage cells afforded significant downregulation of proinflammatory *IL1- β* and *TNF- α* transcripts via qRT-PCR ($p < 0.0001$) when compared to non-induced controls. Results from *in silico* studies revealed that *Moringa oleifera* can be a potential source of novel phytochemicals capable of targeting NF- κ B and thus impede inflammation.

Keywords: anti-inflammatory, *Moringa oleifera*, *in silico*, NF- κ B p50, phytochemicals

1. Introduction

The ideal, rapid, and short-lived inflammatory response can be classified as acute inflammation; one of two types of inflammation that ultimately allows tissues to return to a state of balance and, consequently, the dissipation of signs and symptoms (Panigrahy *et al.*, 2021). However, the presence of certain social, psychological, environmental, and biological factors can prevent the resolution of acute inflammation, thereby promoting progression to low-grade, non-infective, systemic chronic inflammation (Furman *et al.*, 2019). This condition may entail several months to years riddled with pain, chronic fatigue, insomnia, mood disorders, gastrointestinal complications, and/or frequent infections (Pahwa *et al.*, 2020). Most of the common triggers for low-grade, systemic chronic inflammation are well-integrated into the lifestyle of most individuals (Thompson *et al.*, 2015; Walker *et al.*, 2020).

Systemic chronic inflammation (SCI) has been linked to a wide array of disability-causing diseases, including type 2 diabetes mellitus (DM2), cardiovascular disease (CVD), cancer, hypertension, chronic kidney disease, chronic fatty liver disease, sarcopenia, osteoporosis, neurodegenerative diseases, and autoimmune diseases (Furman *et al.*, 2019). Over time, SCI ultimately causes

fatalities in tissues and organs, including oxidative stress (Ferrucci and Fabbri, 2018), as well as elevated levels of high-sensitivity C-reactive protein (CRP) inflammatory marker in the blood (Ridker, 2016). SCI consistently triggers the immune cells to either leak out and interfere with insulin in DM2 or induce the cascade to cause fats, cholesterol, and wastes to form plaques that can clog blood vessels in CVD (Lesica, 2017). Prevention is a much better option than cure. However, certain reports implicate that lifestyle interventions in developing countries are plausible only in dietary changes but not substantial for physical inactivity (Sarrafzadegan *et al.*, 2009). In addition, occupational hazards which promote consistent exposure to xenobiotics (e.g. mining companies, factory workers) and disrupted circadian rhythms (e.g. call center agents, healthcare workers, college students) can cause chronic stress that weakens the immune system.

Acute and chronic inflammation are often managed with non-steroidal anti-inflammatory drugs (NSAIDs) or corticosteroids. However, these conventional drugs are associated with many adverse effects, especially with long-term use. Moreover, some of these drugs are expensive and not accessible in rural areas which constitute the majority of the population anywhere (Ma *et al.*, 2020). This is the reason why around 80% of the population in developing countries has utilized plants as traditional

* Corresponding author. e-mail: glenn.oyong@dlsu.edu.ph.

medicine for health (Adedapo *et al.*, 2015). In the Philippines, the Department of Health (DOH) endorses the use of safe, effective, and scientifically validated medicinal plants through the Philippine Institute of Traditional Alternative Health Care (PITAHC) as mandated by Republic Act No. 8423 that was passed in 1997 (Pangalangan, 2013).

Moringa, also called drumstick tree, is a medicinal plant indigenous to South Asia, mainly in the Himalayas, and is now widely distributed in Afghanistan, Nepal, Bangladesh, Sri Lanka, South and Central America, West Indies, the Philippines, and Cambodia (Bhattacharya *et al.*, 2018). *Moringa oleifera* is the most well-studied among the thirteen species of the family Moringaceae. It is believed that *M. oleifera* was first introduced in the Philippines by seamen traveling along the Nao de China route from Manila to Acapulco (Velázquez-Zavala *et al.*, 2016). This fast-growing, drought-resistant tree has been deemed “miraculous” as all of its parts, from the leaves to the roots, have been used for food and medicinal purposes (Velázquez-Zavala *et al.*, 2016; Olson *et al.*, 2016). Its diverse bioactivity is commonly attributed to the phytochemicals that these plants produce to protect themselves from bacteria, viruses, and fungi. Furthermore, traditional medicine asserts *Moringa oleifera* is beneficial for asthma, headaches, digestive disorders, fevers, rheumatism, and inflammation in addition to its nutritional content. Healing properties are mainly due to the presence of several phytochemicals that have antioxidant, antihypertensive, diuretic, analgesic, anticancer, anti-diabetic, antimicrobial, and anti-inflammatory properties (Gopalakrishnan *et al.*, 2016; Padayachee and Bajinath, 2020).

A number of *in vivo* and *in vitro* studies indicate that *M. oleifera* has an inhibitory effect on inflammation. A number of *in vivo* and *in vitro* studies indicate that *M. oleifera* has an inhibitory effect on inflammation. Studies conducted *in vivo* to treat induced conditions in mouse and rat models explored the anti-inflammatory and antinociceptive spectrum of *M. oleifera* extracts (Jaja-Chimedza *et al.*, 2017; Martínez-González *et al.*, 2017; Cretella *et al.*, 2020). Meanwhile, *in vitro* studies have examined the anti-inflammatory activity of *M. oleifera* extracts by quantifying proinflammatory cytokines and measuring nitric oxide production in RAW 264.7 or J774A.1 murine macrophage cells in culture (Coppin *et al.*, 2013; Arulseivan *et al.*, 2016; Avilés-Gaxiola *et al.*, 2021). In general, these studies demonstrated that NF- κ B signaling was suppressed through the effective inhibition of inflammatory mediators like cyclooxygenase-2, nitric oxide synthase, and NF- κ B expression as well as the upregulated expression of I κ B α , the inhibitor of κ B, which prevented NF- κ B from translocating into the nucleus. These studies conducted consistent efforts in developing an NF- κ B signaling inhibitor with therapeutic benefits that would far outweigh its risks. Thus, computer-aided drug design is a practical and cost-effective tool that could predict the potential of different phytochemicals to be developed as potential drugs for clinical use. This study, therefore, proposed an *in silico* approach to analyzing and identifying the major phytochemicals of *M. oleifera* that can potentially be used as an alternative drug for the treatment of inflammation.

2. Materials and Methods

2.1. Retrieval and Preparation of the NF- κ B p50 Target Protein

The three-dimensional (3D) structure of the NF- κ B p50 homodimer bound to DNA (PDB ID: 1SVC) was downloaded from the Protein Data Bank (RCSB PDB, <https://www.rcsb.org/>, accessed on 6 June 2022) and saved as a pdb file (Müller *et al.*, 1995). The 3D structure was modified via BIOVIA Discovery Studio Visualizer v21.1.0.20298 (Dassault Systèmes, Waltham, CA, USA) by removing the heteroatoms and water molecules surrounding the structure. The ligand binding site was defined using the DNA interacting with the NF- κ B p50 protein by incorporating a structure-based design (SBD) site sphere which consisted of grid parameters set as center-x-coordinate = 27.79, center-y-coordinate = 30.85, center-z-coordinate = 27.70, and x-, y-, z- size = 20. Lastly, the DNA molecule was deleted from the complex, and the resulting apo (unbound) structure of NF- κ B p50 was saved as a pdb file.

Further modifications including the addition of polar hydrogen, Kollman charges, and AutoDock4 atom types on the structure of the protein were done using AutoDock Tools (ADT) v.1.5.6 (Scripps Research, CA, USA) and the resulting structure was saved as a pdbqt file (Morris *et al.*, 2009). Finally, the modified NF- κ B p50 structure was verified for structural integrity using ERRAT (MacArthur *et al.*, 1994) and Verify3D (Bowie *et al.*, 1991; Lüthy *et al.*, 1992) via SAVES v.6.0 server (UCLA-DOE, Los Angeles, CA, USA, <https://saves.mbi.ucla.edu/>, accessed on 6 June 2022), and Ramachandran plot (Anderson *et al.*, 2005) via ZLAB (UMass Chan Medical School, Worcester, MA, USA, <https://zlab.umassmed.edu/bu/rama/>, accessed on 6 June 2022).

2.2. Retrieval and Preparation of Ligands

The phytochemicals of *M. oleifera* were retrieved from the curated database, Indian Medicinal Plants, Phytochemistry, and Therapeutics (IMPPAT 1.0) – a non-redundant *in silico* library with over 9000 phytochemicals identified from medicinal plants. IMPPAT also introduces 960 druggable phytochemicals that are great candidates for prospective drugs and has no similarities to existing FDA-approved drugs (Mohanraj *et al.*, 2018). A total of 15 compounds were available for *M. oleifera* in the Phytochemical Composition section with curated identifiers, names, and references. All 15 structures were downloaded as pdb files from the Phytochemical Identifier section of the database. Dexamethasone (DEX) served as the positive ligand control (Nandeesh *et al.*, 2018). The sdf structure (CID: 5743) was retrieved from PubChem (<https://pubchem.ncbi.nlm.nih.gov/>, accessed on 6 June 2022) as an sdf file.

2.3. Druglikeness and ADMET Prediction

All 15 phytochemicals of *M. oleifera* were evaluated based on their druglikeness via ADMETlab 2.0 (Computational Biology & Drug Design Group, Central South University, Hunan, China, <https://admet.scbdd.com/>, accessed on 7 June 2022) (Dong *et al.*, 2018). Screening criteria is based on Lipinski's rule of five, i.e. a phytochemical is only considered a potential drug

candidate for molecular docking analysis if it does not violate more than one of the following criteria: (1) number of hydrogen bond donors ≤ 5 ; (2) number of hydrogen bond acceptors ≤ 10 ; (3) molecular weight is ≤ 500 Da; and (4) $\text{Log } P \leq 5$ (Lipinski *et al.*, 2001). Veber *et al.* (2002) also introduced (5) $\text{TPSA} \leq 140 \text{ \AA}^2$ as the fifth rule that should be considered when assessing the druglikeness of a compound. The isomeric simplified molecular input line entry system (SMILES) of each phytochemical was obtained from PubChem by searching for the provided identifier on IMPPAT. These SMILES structures are submitted to the ADMETlab server. Similarly, further screening was conducted on these phytochemicals by submitting their isomeric SMILES for systematic absorption, distribution, metabolism, excretion, and toxicity (ADMET) assessment. The results were visualized and analyzed via a heatmap created with GraphPad Prism v.9.0.0 for Windows GraphPad Software, San Diego, CA, USA, www.graphpad.com.

2.4. Conversion of Ligands to Dockable Format

The phytochemicals of *M. oleifera* that passed the druglikeness evaluation and ADMET analysis, as well as the reference drug DEX, were checked for stereochemical properties and converted from pdb and sdf to pdbqt using Open Babel GUI v.2.4.1 (GPL v2, SourceForge, San Diego, CA, USA, <https://sourceforge.net/projects/openbabel/>), accessed on 6 June 2022 (O'Boyle *et al.*, 2011). Their structural validity was also checked using BIOVIA Discovery Studio Visualizer.

2.5. Molecular Docking Analysis

Each of the dockable ligands that passed the druglikeness evaluation was individually paired with NF- κ B p50. Using AutoDock Vina v.1.2.0. (Scripps Research, CA, USA) (Trott *et al.*, 2010), docking was performed by applying the previously determined binding site configuration defined as the center ($x = 27.79$, $y = 30.85$, $z = 27.70$) and size ($x = 20$, $y = 20$, $z = 20$) coordinates. The exhaustiveness was left at a default level of 8. After running the command, AutoDock Vina performed an exhaustive series of docking calculations based on the defined binding site by allowing flexibility for the ligands but keeping the NF- κ B p50 rigid. Results from the molecular docking analysis were presented as a cluster based on the spatial overlapping of the resulting poses. In each cluster, the pose with the lowest binding energy was selected as its representative. These docking calculations were then repeated thrice (a total of three trials) to obtain the most recurring value for binding energy. These values were then tabulated and ranked. The compound which afforded the lowest binding energy than the positive control DEX was selected for further visualization and analysis using BIOVIA Discovery Studio Visualizer.

2.6. Pharmacophore Modeling

The best binding compound and the positive control were uploaded as a mol2 file to the PharmaGist web server (<https://bioinfo3d.cs.tau.ac.il/PharmaGist/php.php>, accessed on 8 June 2022) (Inbar *et al.*, 2007; Schneidman-Duhovny *et al.*, 2008), which determined their pharmacophore features including hydrogen bond donors, hydrogen bond acceptors, hydrophobic atoms, aromatic rings, positively ionizable groups, and negatively ionizable

groups. These were visualized with location constraints and vector aromatic ring features using BIOVIA Discovery Studio Visualizer. PharmaGist also provided a score for each pairwise alignment depending on which molecule is considered the key or pivot. The pivot can be set as the ligand with the highest affinity to the receptor (Dror *et al.*, 2009). In this case, DEX was the pivot since it is the reference inhibitor.

2.7. Molecular Dynamics Simulation

Due to the known limitations of molecular docking, molecular dynamics simulation was performed to validate the stability of the complex and evaluate the conformational changes in the protein. The pdb files for the bound NF- κ B p50-ligand complex and unbound (apo) structures were individually uploaded to the CABS-flex v.2.0 server (<http://biocomp.chem.uw.edu.pl/CABSflex2>, accessed on 8 June 2022) (Kuriata *et al.*, 2018; Jamroz *et al.*, 2014). Several models representing the conformational changes occurring in the structure within 0 to 10 nanoseconds were generated. The conformational changes of the apo and bound structures were visualized using BIOVIA Discovery Studio Visualizer by superimposing the different models captured at each nanosecond. To further visualize the differences after ligand binding, the model of the apo structure at 0 nanoseconds was superimposed with the model of the bound structure at 10 nanoseconds. In addition to that, CABS-flex also provided a root mean square fluctuation (RMSF) plot from each amino acid residue before (apo structure) and after binding (bound structure). Paired t-test analysis was applied using GraphPad Prism to determine statistical differences between the models with a significance value set at 0.05.

2.8. Anti-inflammatory Assay against LPS-activated THP-1 Macrophage

2.8.1. Collection and Preparation of Plant Material

The leaves and fruits of *M. oleifera* were collected from the Bureau of Plant Industry, Malate, Manila, Philippines, with the taxonomic identity verified by a resident botanist. A collection of specimens was obtained from and taxonomically identified by the Bureau of Plant Industry, Manila, and was deposited to the Center for Natural Science and Environmental Research at De La Salle University in Manila, Philippines, under voucher number MSUL-XX1902. The leaves and fruits were carefully washed with distilled deionized water three times and air-dried for an hour before carefully removing the leaves from stalks, and separately dissecting the fruit into seeds and pods. The leaves, seeds, and pods were separately ground using liquid nitrogen and the powdered samples were resuspended in complete DMEM cell culture media (described below) to a final of 100 $\mu\text{g/mL}$ concentrations. The aqueous working solutions were filter-sterilized using 0.2 μm syringe filters (Acrodisc, Pall Corp., Port Washington, NY, USA) before further experimentations described below.

2.8.2. Culture of THP-1 monocytes

THP-1 monocytes (ATCC, Manassas, VA, USA) were cultured in 50 mL T-flasks containing complete Dulbecco's Modified Eagle Medium (cDMEM) composed of DMEM with 10% fetal bovine serum and 1X antibiotic antimycotic. All incubation processes were achieved at

37°C with 5% CO₂ in a humidified chamber (Shyu *et al.*, 2014). All cell culture reagents were purchased from Invitrogen (Thermo Fisher Scientific, Waltham, MA, USA).

2.8.3. RT-qPCR of Pro-inflammatory *IL1-β* and *TNF-α* Transcripts

When 90% confluence was reached, THP-1 cells were harvested and subjected to 0.4% Trypan Blue (Thermo Fisher Scientific, Waltham, MA, USA) exclusion for counting and viability staining. A total of 1 x 10⁵ viable cells/mL were seeded in 100 μL volumes into the wells of a 96-well culture plate. THP-1 differentiation into macrophages was performed by the addition of 160 nM phorbol myristate acetate (PMA) (Sigma-Aldrich, St. Louis, MO, USA) followed by 48 hours incubation. Subsequently, the PMA-induced THP-1 cells (macrophages or Mφ) were stimulated with 100 ng/mL lipopolysaccharide (LPS) (*Escherichia coli* O111:B4, Sigma-Aldrich, St. Louis, MO, USA) for one hour (Shyu *et al.*, 2014).

The assay set-up consisted of the following controls: (A) five negative controls – (1) THP-1 cells only (non-differentiated); (2) PMA-induced THP-1 cells (Mφ); and (3–5) PMA-induced THP-1 cells (Mφ) treated with *M. oleifera* leaves, seed, and pod aqueous extracts, respectively; and (B) positive control which consisted of PMA-induced THP-1 cells (Mφ) stimulated with LPS. The treatment set-up was composed of (1–3) PMA-induced THP-1 cells activated by LPS and treated with *M. oleifera* leaves, seed and pod aqueous extracts, and (4) the anti-inflammatory drug DEX. Treatments were done for 30 minutes of incubation. The treatment concentrations of *M. oleifera* extract used were less than the IC₅₀ (μg/mL), more precisely IC₄₀, as determined by a previous cytotoxicity test on THP-1 cells (data not shown). The IC₅₀ values for the leaf, seed, and pod extracts were 4.65, 7.32, and 8.47 μg/mL, respectively. These IC₅₀ values were used to compute the final IC₄₀ (sub-IC₅₀) treatment concentrations, yielding values of 3.10, 4.88, and 5.65 μg/mL, respectively. In order to obtain enough cells for gene expression investigation, IC₄₀ values were used to maximize the number of viable cells remaining after treatment exposure (Shyu *et al.*, 2014). The treatment concentration of DEX was set at 10 μM (~3.925 μg/mL) (Gao *et al.*, 2022). All set-ups were accomplished in three replicates. After 30 minutes, 30 μL of RNAlater reagent (Thermo Fisher Scientific, Waltham, MA, USA) was added into each well followed by total RNA extraction using TRIzol kit (Thermo Fisher Scientific, Waltham, MA, USA) following the manufacturer's instructions.

RT-qPCR reactions were performed using Rotor-Gene Q (Qiagen, Germantown, MD, USA) in 20 μL volumes containing: 1X KAPA SYBR FAST One-Step reagent (1X KAPA RT and 1X KAPA SYBR qPCR Master Mix) (Sigma-Aldrich, St. Louis, MO, USA), 10 μM each of forward and reverse primers, nuclease-free water, and 1.0 μL RNA template (50 μg/mL). The primer pair sequences

for *IL1-β* were 5'-ATG AAG TGC TCC TTC CAG GAC CTG-3' (forward) and 5'-CCT GGA GTG GAG AGC TTC AGT T-3' (reverse); while for *TNF-α* were 5'-GGA CGT GGA GCT GGC CGA GG-3' (forward) and 5'-TGG GAG TAG ATG AGG TAC AGG CCC-3' (reverse) (Bjorkbacka *et al.*, 2004). The PCR profile conditions were as follows: preliminary cDNA synthesis at 50°C for 3 minutes, followed by cDNA amplification of 40 cycles set at 95°C for 20 seconds, 50°C for 40 seconds, and 72°C for 20 seconds. Confirmation of amplified signals was double-checked after high-resolution melting curve analysis set at increments of 72°C to 95°C. Quantification was interpreted as relative fold gene expression ($2^{-\Delta\Delta C_t}$) normalized using the human GAPDH housekeeping control.

2.8.4. Statistical Analysis

Fold gene expression values were presented as mean ± SD. To ascertain the differences between the different treatments, one-way ANOVA with Dunnett's multiple comparisons test integrated within GraphPad Prism was applied, with the level of significance set at 0.05.

3. Results

3.1. Druglikeness and ADMET Evaluation

All 15 *M. oleifera* phytochemicals retrieved from the IMPPAT 1.0 database are presented in Table 1 including their most abundant organ distribution (Abd Rani *et al.*, 2018).

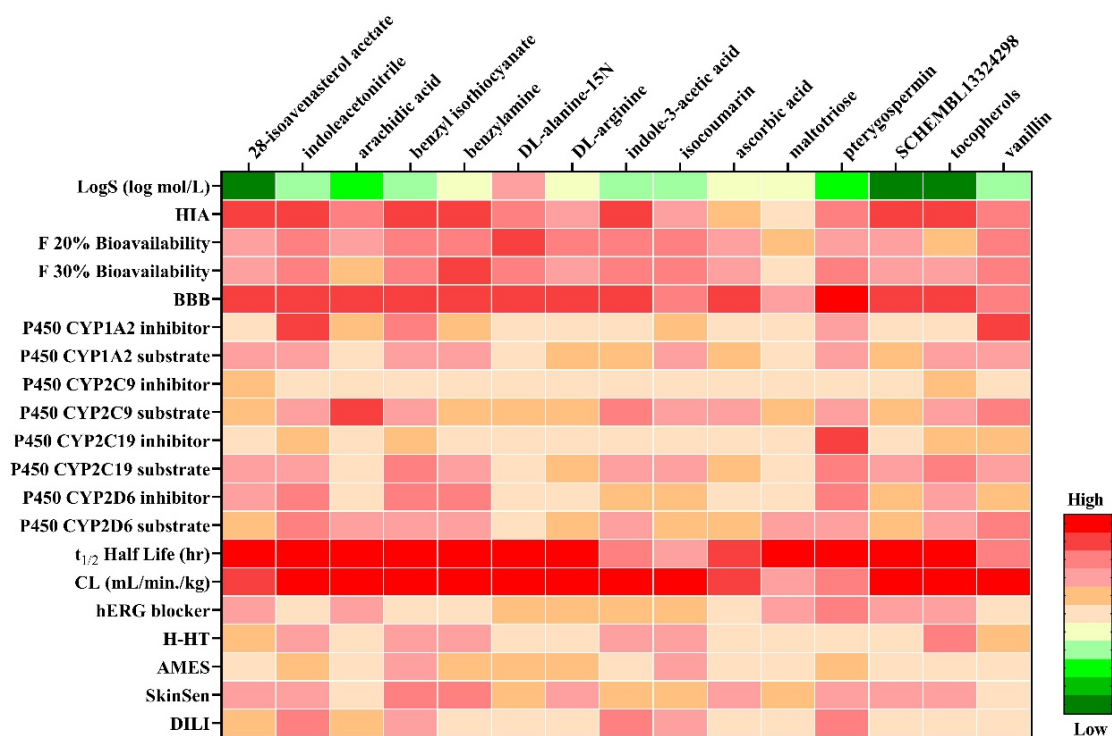
Table 1. List of fifteen *M. oleifera* phytochemicals retrieved from the IMPPAT 1.0 database.

No.	Phytochemical Name	Plant Part Abundance
1	28-isoavenasterol acetate	Seed
2	indole acetonitrile	Not listed
3	arachidic acid	Roots
4	benzyl isothiocyanate	Leaves, seeds
5	benzylamine	Aerial
6	DL-alanine-15N	Leaves
7	DL-arginine	Leaves
8	indole-3-acetic acid	Not listed
9	isocoumarin	Not listed
10	ascorbic acid	Leaves, Seeds, Pods
11	maltotriose	Leaves
12	pterygospermin	Seeds
13	SCHEMBL13324298	Not listed
14	tocopherols	Leaves
15	vanillin	Leaves, fruits, seeds

All phytochemicals passed Lipinski's rule of five (RO5) except maltotriose which violated four conditions (Table 2). Meanwhile, results for ADMET were presented as heatmap property distribution depicted in Figure 1.

Table 2. Druglikeness properties of *M. oleifera* phytochemicals based on Lipinski's rule of five: MW = molecular weight; HBD = hydrogen bond donor; HBA = hydrogen bond acceptor; LogP = lipophilicity TPSA = topological polar surface area). Shaded values correspond to violations of the rule.

No.	Phytochemical	MW (g/mol) ≤ 500	HBD ≤ 5	HBA ≤ 10	LogP ≤ 5	TPSA (Å ²) ≤ 140	Druggability
1	28-isoavenasterol acetate	468.766	0	2	8.906	26.30	Pass
2	indole acetonitrile	156.188	1	1	2.234	39.58	Pass
3	arachidic acid	312.538	1	1	7.113	37.30	Pass
4	benzyl isothiocyanate	149.218	0	2	2.289	12.36	Pass
5	benzylamine	107.156	1	1	1.145	26.02	Pass
6	DL-alanine-15N	90.087	2	2	-0.582	63.32	Pass
7	DL-arginine	175.212	4	2	-5.519	133.78	Pass
8	indole-3-acetic acid	175.187	2	1	1.795	53.09	Pass
9	isocoumarin	194.186	2	4	0.984	66.76	Pass
10	ascorbic acid	176.124	4	6	-1.407	107.22	Pass
11	maltotriose	504.438	11	16	-7.573	268.68	Fail
12	pterygospermin	406.532	0	4	4.14	24.94	Pass
13	SCHEMBL13324298	398.675	1	1	7.555	20.23	Pass
14	tocopherols	416.69	1	2	8.532	29.46	Pass
15	vanillin	152.149	1	3	1.213	46.53	Pass

**Figure 1.** Heatmap for the ADMET property distribution of *M. oleifera* phytochemicals. LogS = solubility; HIA = Human Intestinal Absorption; BBB = Blood-Brain Barrier; CL = Clearance Rate; H-HT = Human Hepatotoxicity; AMES = Ames Mutagenicity; SkinSen = Skin Sensitization; DILI = Drug-Induced Liver Injury). LogS, HIA, bioavailability, and BBB are predictive properties of a drug's absorption; cytochrome P450 inhibitors and substrates are predictive properties of metabolism; half-life and CL are predictive properties of excretion; and hERG blocker, H-HT, AMES, SkinSen, and DILI are predictive properties of toxicity.

3.2. Structural Validity of Prepared NF- κ B p50 Protein

The prepared structure of NF- κ B p50 was verified for structural validity via Ramachandran plot, ERRAT, and Verify3D (Figure 2A-2C). Results from the Ramachandran Plot Zlab server showed that 251 amino acid residues (94.361%) were in the highly preferred observations (Figure 2A). It also showed that 13 amino acid residues (4.887%) were in the preferred observations while only 2 amino acid residues (0.752%), Tyr90 and Ser81, were in the questionable observations. This confirmed that the

prepared protein possesses a good model structure since over 90% of the protein residues are in the most favored or core regions in the Ramachandran plot (Balaji *et al.*, 2006). The 3D folding of the prepared NF- κ B p50 protein was assessed by VERIFY3D using the protein's own amino acid sequence to test the accuracy of the 3D model, also known as the 3D-1D profile (AboMeireles *et al.*, 1992). According to Figure 2B, 99.04% of the residues afforded an averaged 3D-1D score ≥ 0.2 and at least 80% of the amino acids scored ≥ 0.2 in the 3D/1D profile. ERRAT differentiates between correctly and incorrectly

determined regions of protein structures based on characteristic atomic interaction and is expressed as the percentage of the protein for which the calculated error value falls below the 95% rejection limit. As shown in

Figure 2C, the overall quality factor of the modified NF- κ B p50 protein is 80.537%. Thus, the prepared NF- κ B p50 protein has passed all verification methods of structural validity for molecular docking analysis.

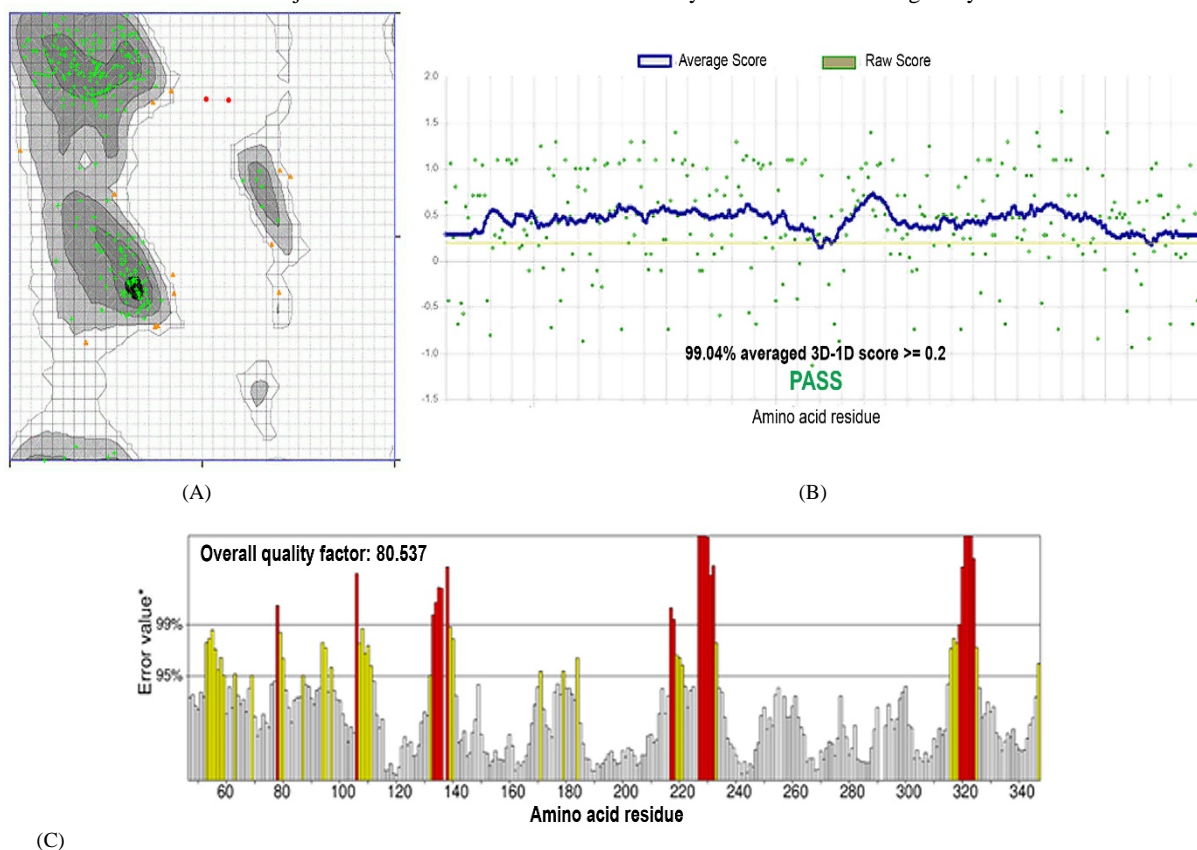


Figure 2. (A) Ramachandran plot of the modified NF- κ B p50 protein with highly preferred observations (green), preferred observations (orange), and questionable observations (red). (B) VERIFY3D showing the averaged 3D-1D score ≥ 2.0 and 99.04 % pass score. (C) ERRAT which shows that the overall quality factor falls below the 95% rejection limit.

3.3. Molecular Docking Results

Based on the results of the druglikeness evaluation (Table 2), 14 out of 15 *M. oleifera* phytochemicals from the IMPPAT database were subjected to docking analysis. DEX was also used as a reference inhibitor of the target

protein NF- κ B p50. For each pair (protein and ligand), AutoDock Vina performed docking calculations to determine the binding energy of the protein-ligand complex. Results from these docking calculations are shown in Table 3.

Table 3. Binding energies of the 14 phytochemicals and dexamethasone reference compound to the NF- κ B p50 binding site.

Compound	PubChem CID	Phytochemistry	Binding Energy (kcal/mol)
Dexamethasone (control)	5743	corticosteroid	-4.8
Pterygospermin	72201063	benzenoid (benzene/substituted derivative)	-5.0
28-isoavenasterol acetate	91746804	lipid and lipid-like (triterpenoid)	-4.7
isocoumarin, 3,4-dihydro-4,8-dihydroxy-3-methyl-	169539	organoheterocyclic compound (2-benzopyran)	-4.4
SCHEMBL13324298	23724573	lipid and lipid-like molecules (ergostane steroid)	-4.4
2-(1H-indol-2-yl)acetone nitrile	169731	organoheterocyclic compound (indole)	-4.2
indole-3-acetic acid	802	organoheterocyclic (indolyl carboxylic acid derivative)	-4.1
DL-arginine	1549073	amino acid	-4.0
Tocopherols	14986	lipid and lipid-like (Quinone/Hydroquinone)	-3.9
arachidic acid	10467	lipid and lipid-like (fatty acid)	-3.6
Vanillin	1183	benzenoid (methoxy phenol)	-3.6
ascorbic acid	54670067	organoheterocyclic (furanone)	-3.5
benzyl isothiocyanate	2346	benzenoid (benzene/substituted derivative)	-3.4
Benzylamine	7504	benzenoid (phenylmethylamine)	-3.2
DL-alanine-15N	51283	amino acid	-2.9

Pterygospermin topped the lowest score (-5.0 kcal/mol) for binding energy (highest affinity) and the docked configuration with NF- κ B p50 is shown in Figure 3A-3F.

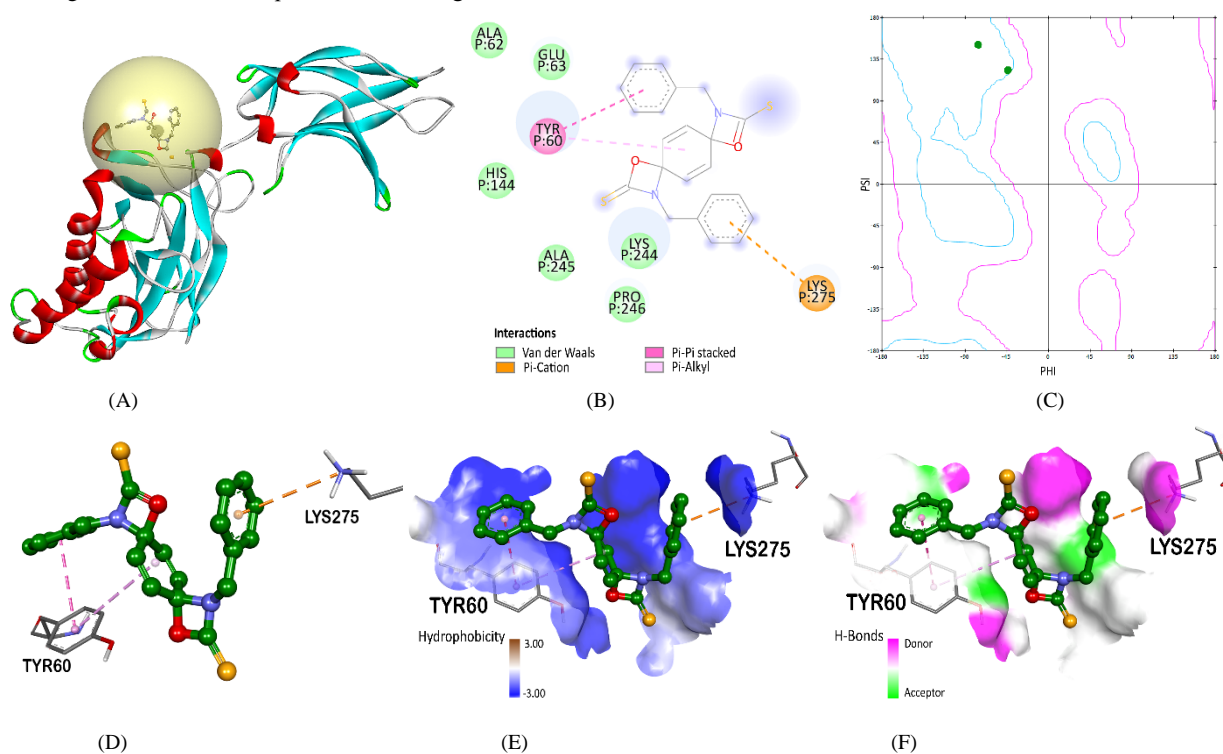


Figure 3. Binding interactions of NF- κ B p50 and pterygospermin: (A) 3D visualization of pterygospermin docked in NF- κ B p50 within the ligand binding site (yellow sphere); (B) 2D display of pterygospermin-NF- κ B p50 interactions; (C) Ramachandran plot of ligand-interacting amino acid residues; (D) 3D display of pterygospermin-NF- κ B p50 interactions; (E) hydrogen bond surface of binding pocket; and (F) hydrophobicity surface of the binding pocket.

3.4. Pharmacophore Features and Pairwise Alignment Score

Pharmacophore analysis (Table 4) confirmed that pterygospermin has four acceptors (two oxygen and two sulfur atoms) and two aromatic rings that can form hydrogen bonds and non-covalent π -system interactions with NF- κ B p50, respectively (Figure 4A). On the other

hand, dexamethasone has eleven hydrophobic groups and four acceptors (oxygen atoms) that can interact with NF- κ B p50 (Figure 4B). Despite having a pairwise alignment score of 4.51428 which is most likely the result of the shared hydrogen-bond acceptor features, pterygospermin and dexamethasone have been shown to snugly fit in the NF- κ B p50 binding pocket (Figure 4C).

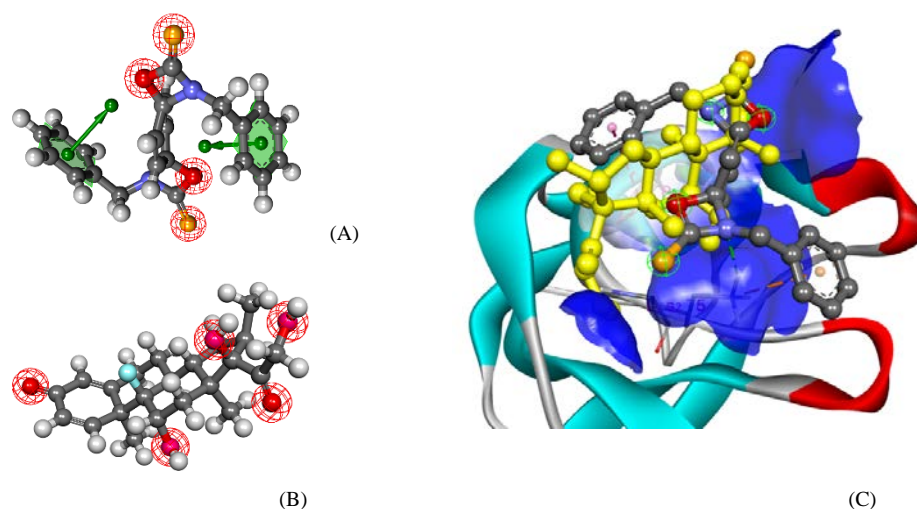


Figure 4. Comparison of 3D models showing the pharmacophore features of (A) pterygospermin and (B) dexamethasone. Each color corresponds to the hydrogen bond donors (orange), hydrogen bond acceptors (red), and aromatic rings (green). Note that some oxygen atoms in dexamethasone act as both hydrogen bond donors and acceptors. (C) Superimposed structures of pterygospermin (gray) and dexamethasone (yellow) showing both compounds fitting inside the NF- κ B p50 binding pocket.

Table 4. Pharmacophore physico-chemical features of dexamethasone and pterygospermin.

Molecule	Atoms	Features	Aromatic	Hydrophobic	Donors	Acceptors
dexamethasone	57	19	0	11	3	5
pterygospermin	46	6	2	0	0	4

3.5. Molecular Dynamics Simulation

Minimal fluctuations ($0\text{--}7.2\text{\AA}$) were observed between the pterygospermin-bound NF- κ B p50 compared with the apo (non-bound) structure (Figure 5A). The superimposed multimodel MDS structures across 0 to 10 nanosecond trajectories also affirmed insignificant structural variations

when the apo (Figure 5B) is compared with the pterygospermin-bound structure (Figure 5C) which can also be seen with the overlaid structures of the apo at 0 nanoseconds and the bound structure at 10 nanoseconds (Figure 5D).

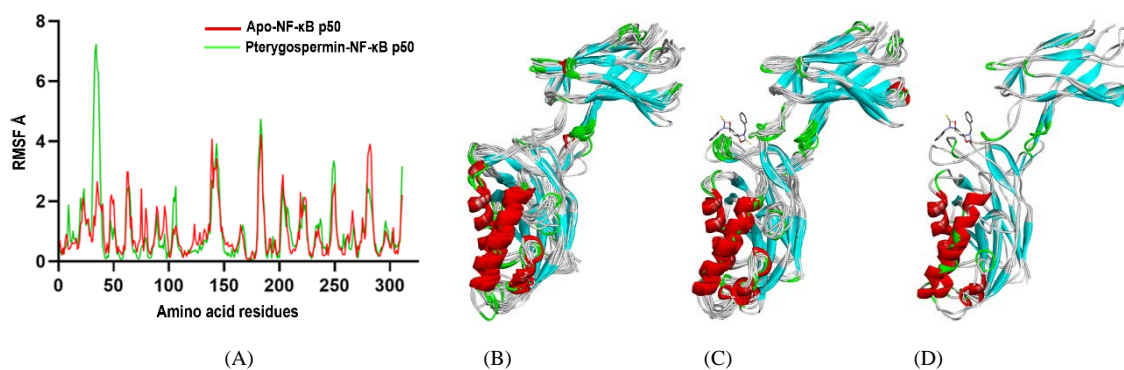


Figure 5. Molecular dynamics simulation (MDS) comparing the apo and pterygospermin-bound structures of NF- κ B p50. (A) RMSF profiles of the amino acid residues of the apo (red) and bound structures (green). Trajectory model superimposition of: (B) apo-NF- κ B structures from 0–10 nanoseconds; (C) pterygospermin-NF- κ B p50 complexes from 0–10 nanoseconds; and (D) apo structure at 0 nanosecond and pterygospermin-NF- κ B p50 at 10 nanoseconds.

3.6. Anti-inflammatory Assay against LPS-activated THP-1 Macrophage

THP-1 cells transformed into macrophages and induced by LPS bacterial antigen were assayed for the expression of *IL1- β* and *TNF- α* transcripts (Figure 6). Figure 7 shows

the downregulation of the expression of both proinflammatory cytokine genes brought about by treatment with *M. oleifera* leaves, seed, and pod aqueous extracts.

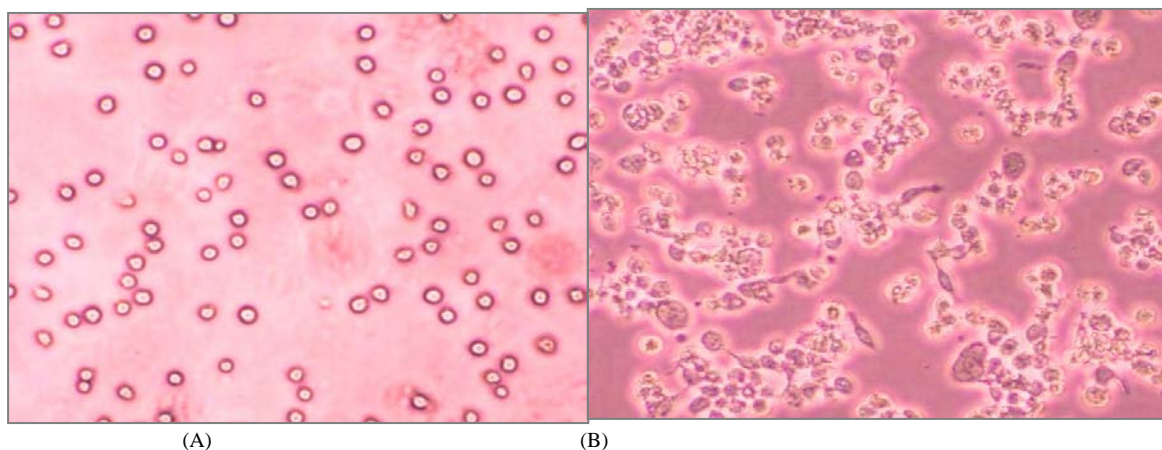


Figure 6. Phase contrast photomicrographs (200X) of (A) floating THP-1 monocytes and (B) differentiated macrophages which appear enlarged and attached 48 hours after PMA treatment.

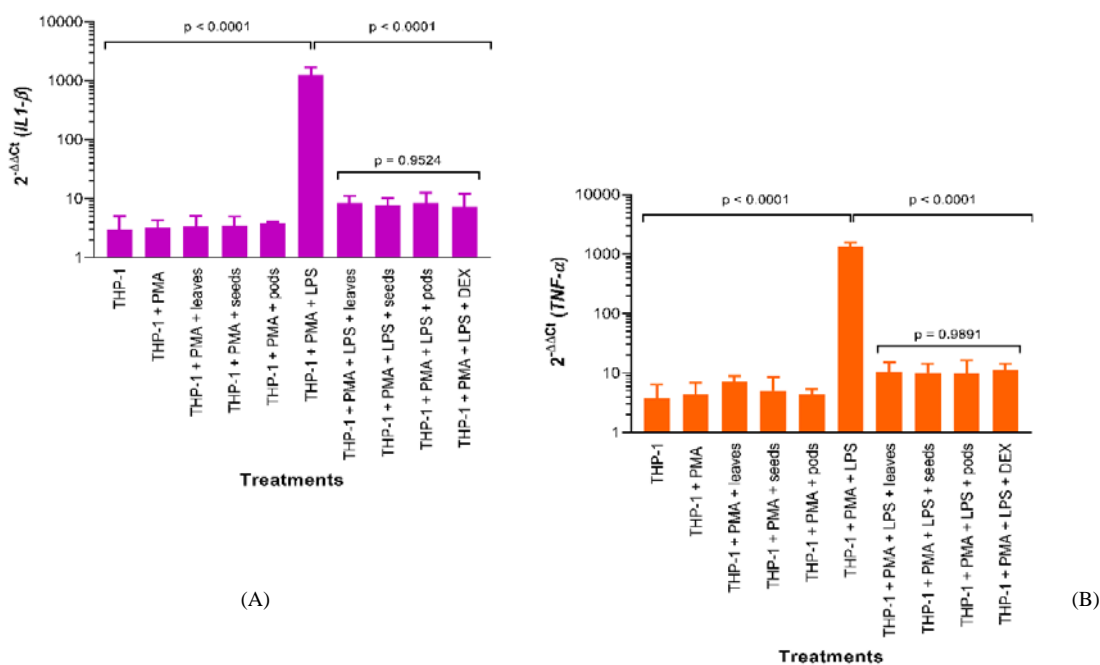


Figure 7. Relative gene expression ($2^{-\Delta\Delta C_t}$) profiles of (A) *IL-1β* and (B) *TNF-α* cytokine gene transcripts. Significant difference from the control group positive for inflammation afforded an F test of $F(9, 20) = 24.60$, $p < 0.0001$ for *IL-1β*, and $F(9, 20) = 90.34$, $p < 0.0001$ for *TNF-α*.

4. Discussion

Druglikeness analysis using Lipinski's rule of five (RO5) resulted in all *M. oleifera* phytochemicals passing the criteria except for maltotriose. According to the rule, this could indicate that maltotriose would perform poorly as a drug because of its suboptimal permeability and absorption. More specifically, its molecular weight could mean that the molecule is too large to pass through the cell membrane. It also exceeded the acceptable number of hydrogen bond donors and acceptors which contribute to its enhanced solubility in the blood thereby decreasing its bioavailability and time to effectively permeate membranes and cross the blood-brain barrier. Maltotriose also exceeded the cut-off value for TPSA, which implies that it may be poorly distributed and transported in the

body. Despite these, it is important to note that this rule is not a strong indication that maltotriose would perform poorly as a drug during actual in vivo clinical settings. Moreover, ADMET analysis also showed that maltotriose has relatively high solubility and low blood-brain barrier permeability compared to the other phytochemicals (Figure 1). Considering these probabilities, maltotriose was eliminated from the list of phytochemicals that were subjected to subsequent molecular docking simulations with the NF-κB p50 protein.

ADMET analysis of the 14 compounds which showed no RO5 violations deduced high intestinal absorption (HIA), cross the blood-brain barrier (BBB), and high bioavailability (F20%, F30%) properties (Figure 1). However, alanine solely appeared to be highly soluble (LogS). All 14 compounds also indicated a medium-to-high probability of either inhibitors or substrates for P450

CYP-aided drug metabolism. Further analysis also suggested that these compounds may exhibit an average likelihood of exhibiting toxicity albeit with a short half-life and high systemic clearance (CT).

Subsequent Autodock Vina analysis ranked the phytochemicals from the lowest to highest binding energies (Table 3). Note that the values for the binding energy represent the most recurring values after three runs of docking calculations. Results from these calculations revealed that the reference inhibitor DEX had a binding energy of -4.8 kcal/mol. The phytochemicals of *M. oleifera* produced binding energies that ranged from -2.9 kcal/mol to -5.0 kcal/mol. Out of all the phytochemicals, pterygospermin demonstrated the strongest affinity (the lowest binding energy) to NF- κ B p50 (-5.0 kcal/mol), whereas DL-alanine-15N showed the weakest (-2.9 kcal/mol). Pterygospermin also displayed a stronger affinity for NF- κ B p50 at the DNA binding site than the reference inhibitor DEX which suggests that it could be a possible drug candidate for p50 inhibition, and therefore, potentially ameliorate inflammation. Further analysis of the interactions between pterygospermin and the NF- κ B p50 binding site showed only Tyr60 and Lys275 directly interacting with the ligand (Figures 3B, 3D). The Ramachandran plot indicates that Tyr60 and Lys275 are located in the β -sheet structures of NF- κ B p50 (Figure 3C). Tyr60 has an aromatic ring that can form hydrophobic interactions with the aromatic ring of pterygospermin via pi (π) stacking. This π - π interaction occurs at a distance of 4.261\AA . This is a notable type of non-covalent interaction because it reportedly plays a vital role in the biological recognition and organization of biomolecular structures (Brylinski, 2018). Pi stacking can occur in three different ways: perpendicular, parallel, or eclipsed. A pi-alkyl hydrophobic interaction (5.38\AA) between the aromatic ring of Tyr60 and the alkyl group of the non-aromatic ring structure in pterygospermin is also present. There is also a pi-cation electrostatic interaction (4.38\AA) between the nitrogen of Lys275 and the second aromatic ring in pterygospermin (Figure 3D).

It is clearly shown that the active pocket amino acids are mostly hydrophilic based on the generated hydrophobicity and H-bond surfaces (Figure 3E, 3F). Further analysis revealed that the formal positively charged nitrogen from Lys275 is the reason for the electrostatic interaction with the negatively charged center of the aromatic ring in pterygospermin. Pi interactions between the protein and the ligand depicted by the pi-alkyl interaction have an edge-to-face configuration. Additionally, the aromatic rings of tyrosine and pterygospermin demonstrated a face-to-face or parallel configuration which is theorized to "correspond to energy minima of comparable depth" (Brylinski, 2018). Paired t-test analysis confirmed that there is no significant difference in the fluctuation of amino acid residues from both unbound NF- κ B p50 and pterygospermin-bound NF- κ B p50 complex ($p = 0.4595$) after molecular dynamics simulation. These results strongly suggest that pterygospermin can form a stable complex with NF- κ B

p50 and, therefore, has considerable potential to serve as an anti-inflammatory drug.

This study also investigated the anti-inflammatory activity of *M. oleifera* leaves, seed, and pod aqueous extracts in LPS-stimulated human macrophages. Figure 7 shows the downregulation of the expression of both proinflammatory cytokine genes brought about by treatment with the *M. oleifera* extracts. There was a significant decrease or downregulation in the expression of the levels of *IL1- β* ($p < 0.0001$) and *TNF- α* ($p < 0.0001$) proinflammatory cytokine genes in cells exposed to any of the three *M. oleifera* extracts compared to the positive control set-up composed of macrophages stimulated with LPS. Several studies have recently investigated the anti-inflammatory potential of *M. oleifera*. The leaves were discovered to control *TNF- α* and *INF- γ* production in natural killer cells from type 1 diabetes mice models (Lestari *et al.*, 2022). The ethanolic leaf extract was also found to promote the ameliorative effects against oxidative stress, inflammation, and apoptosis in CCl_4 -induced hepatic encephalopathy (Mahmoud *et al.*, 2022) and bisphenol-induced gastric ulcer in mice (Abo-Elsoud *et al.*, 2022). The seeds were discovered to contain bioactive compounds with antiviral activity against H1N1 and anti-inflammatory properties by decreasing the levels of *TNF- α* , *IL-6*, and *IL-1 β* , in hosts with H1N1 infection (Xiong *et al.*, 2022). Additionally, antibacterial and anti-inflammatory activity against *Helicobacter pylori* infections was also ascertained in *M. oleifera* seeds (Sayed *et al.*, 2022). Meanwhile, *M. oleifera* pods, together with leaves and seeds, were reported to exhibit medicinal properties including anti-inflammatory, antidiabetic, antineoplastic, antibacterial, and antifungal activities (Anwar *et al.*, 2007; Mbikay, 2012; Meireles, *et al.*, 2020).

Research that investigated the anti-inflammatory property of *M. oleifera* commonly involved the detection of proinflammatory cytokines in mice models (Sharma *et al.*, 2012; Lestari *et al.*, 2022; Mahmoud *et al.*, 2022; Abo-Elsoud *et al.*, 2022). By extensive literature search, this study is the first to report the application of human macrophage cells derived from PMA-transformed THP-1 monocytes for determining the anti-inflammatory activity of *M. oleifera* leaves, pod, and seed aqueous extracts. Furthermore, the significant decrease in the relative gene expression of *IL1- β* and *TNF- α* is directly due to transcriptional level downregulation which can be directly linked to the inactivation of NF- κ B. A proposed mechanism is presented in Figure 8. Pterygospermin and other phytochemicals present in *M. oleifera* may have consequentially played pivotal roles in the inhibition of the NF- κ B p50 transcription factor domain which may have blocked its binding to the promoter regions of genes specifically coding for proinflammatory cytokines such as *IL1- β* and *TNF- α* . However, this putative mechanism has to be tested and confirmed further by isolating the phytochemicals from the extracts and subjecting them to anti-inflammatory bioassays.

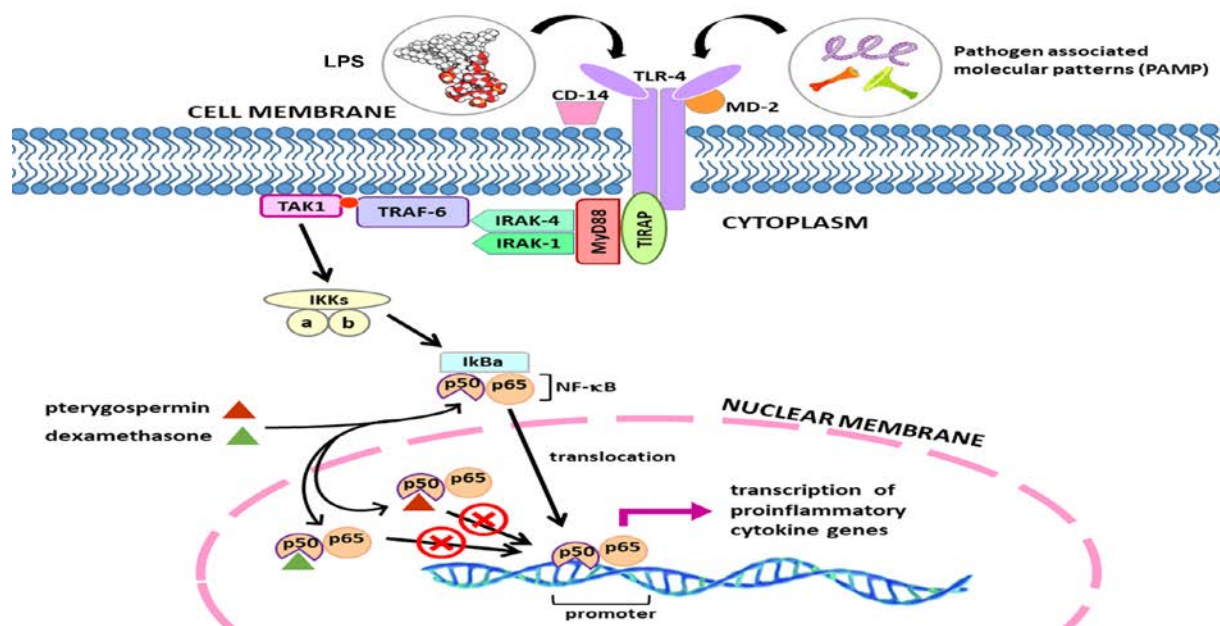


Figure 8. Proposed mechanism of NF- κ B p50 antagonism by pterygospermin. The binding of either LPS or PAMP on TLR-4 activates the NF- κ B signaling system to promote the transcriptional activation of proinflammatory cytokine gene expression. Pterygospermin is proposed to block the NF- κ B p50 DNA binding domain inhibiting downstream cytokine expression.

5. Conclusions

Researchers are prompted to develop a safe and effective drug that can alleviate the signs and symptoms of inflammation. One particular research area of interest is the inhibition of NF- κ B – a transcription factor that is widely accepted as a major inflammatory mediator. Most of the drugs in development for NF- κ B inhibition are still in their clinical stages. Simultaneously, there is an increasing wealth of research on the anti-inflammatory activity of *M. oleifera*. Its biological activity has been attributed to the numerous phytochemicals that can be extracted and can be potential drug candidates. This study utilized an in silico approach to identify a lead compound among the phytochemicals of *M. oleifera* for potential use as an inhibitory drug against the homodimer NF- κ B p50.

Pterygospermin passed the druggability criteria characterized by good absorption properties, moderately high metabolic stability, and median to low toxicity but with high half-life and clearance. Docking analysis on the NF- κ B p50 binding pocket afforded the highest binding affinity surpassing dexamethasone, a known anti-inflammatory drug. This suggests the potential of pterygospermin to block the p50 transcription factor from recognizing the promoter regions of proinflammatory cytokine genes. This has been proven in part by the effective downregulation of expression of *IL1- β* and *TNF- α* transcripts after the treatment of LPS-activated macrophages with *M. oleifera* extracts. In conclusion, *M. oleifera* can be a good potential source of pharmaceutical leads capable of inhibiting the NF- κ B p50 protein. However, the eventual prevention of the expression of cytokine genes at the transcriptional, and subsequently at the protein levels, warrants further investigation and additional experiments to firmly establish the inhibition of the NF- κ B pathway.

Acknowledgments

The authors wish to express thanks to the Department of Physics and the Molecular Science Unit Laboratory–Center for Natural Science and Environmental Research, De La Salle University, Manila.

References

- Abd Rani NZ, Hisain K and Kumolosasi E. 2018. *Moringa* genus: A review of phytochemistry and pharmacology. *Front Pharmacol.*, **9(108)**: 1-26.
- Abo-Elsoud RAEA, Abdelaziz SAM, Eldaim MAA and Hazzaa SM. 2022. *Moringa oleifera* alcoholic extract protected stomach from bisphenol A-induced gastric ulcer in rats via its anti-oxidant and anti-inflammatory activities. *Environ Sci Pollut Res.*, **29(45)**: 68830-68841.
- Adedapo AA, Falayi OO and Oyagbemi AA. 2015. Evaluation of the analgesic, anti-inflammatory, anti-oxidant, phytochemical and toxicological properties of the methanolic leaf extract of commercially processed *Moringa oleifera* in some laboratory animals. *J Basic Clin Physiol Pharmacol.*, **26(5)**: 491-499.
- Anderson RJ, Weng Z, Campbell RK and Jiang X. 2005. Main-chain conformational tendencies of amino acids. *Proteins.*, **60(4)**: 679-689.
- Anwar F, Latif S, Ashraf M and Gilani AH. 2007. *Moringa oleifera*: A food plant with multiple medicinal uses. *Phytother Res.*, **21(1)**: 17–25.
- Arulselvan P, Tan WS, Gothai S, Muniandy K, Fakurazi S, Esa NM, Alarfaj AA and Kumar SS. 2016. Anti-inflammatory potential of ethyl acetate fraction of *Moringa oleifera* in downregulating the NF- κ B signaling pathway in lipopolysaccharide-stimulated macrophages. *Molecules.*, **21(11)**: 1-13.
- Avilés-Gaxiola S, León-Félix J, Jiménez-Nevárez YB, Angulo-Escalante MA, Ramos-Payán R, Colado-Velázquez JI and Heredia JB. 2021. Antioxidant and anti-inflammatory properties of novel peptides from *Moringa oleifera* Lam. leaves. *S Afr J Bot.*, **141**: 466-473.

- Balaji S, Kalpana R and Shapshak P. 2006. Paradigm development: comparative and predictive 3D modeling of HIV-1 Virion Infectivity Factor (VIF). *Bioinformation.*, **1(8)**: 290-309.
- Bhattacharya A, Tiwari P, Sahu PR and Kumar S. 2018. A review of the phytochemical and pharmacological characteristics of *Moringa oleifera*. *J Pharm Bioallied Sci.*, **10(4)**: 181-191.
- Bjorkbacka H, Fitzgerald KA, Huet F, Li X, Gregory JA, Lee MA, Ordija CM, Dowley NE, Golenbock DT and Freeman MW. 2004. The induction of macrophage gene expression by LPS predominantly utilizes Myd88-independent signaling cascades. *Physiol Genomics.*, **19(3)**: 319-330.
- Bowie JU, Lüthy R and Eisenberg D. 1991. A method to identify protein sequences that fold into a known three-dimensional structure. *Science.*, **253(5016)**: 164-170.
- Brylinski M. 2018. Aromatic interactions at the ligand-protein interface: Implications for the development of docking scoring functions. *Chem Biol Drug Des.*, **91(2)**: 380-390.
- Coppin JP, Xu Y, Chen H, Pan M, Ho C, Juliani R, Simon JE and Wu Q. 2013. Determination of flavonoids by LC/MS and anti-inflammatory activity in *Moringa oleifera*. *J Funct Foods.*, **5(4)**: 1892-1899.
- Cretella ABM, Soley BDS, Pawloski PL, Ruziska RM, Scharf DR, Ascari J, Cabrini DA and Otuki MF. 2020. Expanding the anti-inflammatory potential of *Moringa oleifera*: topical effect of seed oil on skin inflammation and hyperproliferation. *J Ethnopharmacol.*, **23(254)**: 1-12.
- Dong J, Wang NN, Yao ZJ, Zhang L, Cheng Y, Ouyang D, Lu AP and Cao DS. 2018. ADMETlab: a platform for systematic ADMET evaluation based on a comprehensively collected ADMET database. *J Cheminform.*, **10(1)**: 1-29.
- Dror O, Schneidman-Duhovny D, Inbar Y, Nussinov and Wolfson HJ. 2009. Novel approach for efficient pharmacophore-based virtual screening: method and applications. *J Chem Inf Model.*, **49(10)**: 2333-2343.
- Ferrucci L and Fabbri E. 2018. Inflammageing: chronic inflammation in ageing, cardiovascular disease, and frailty. *Nat Rev Cardiol.*, **15(9)**: 505-522.
- Furman D, Campisi J, Verdin E, Carrera-Bastos P, Targ S, Franceschi C, Ferrucci L, Gilroy DW, Fasano A, Miller GW, Miller AH, Mantovani A, Weyand CM, Barzilai N, Goronzy JJ, Rando TA, Effros RB, Lucia A, Kleinsteuber N and Slavich GM. 2019. Chronic inflammation in the etiology of disease across the life span. *Nat Med.*, **25(12)**: 1822-1832.
- Gao M, Lee SB, Lee J-E, Kim GJ, Moon J, Nam J-W, Bae J-S, Chin J, Jeon YH and Choi H. 2022. Anti-Inflammatory butenolides from a marine-derived *Streptomyces* sp. 13G036. *Appl Sci.*, **12(9)**: 1-11.
- Gopalakrishnan LH, Doriya K and Kumar DS. 2016. *Moringa oleifera*: A review on nutritive importance and its medicinal application. *Food Sci Hum Wellness.*, **5(2)**: 49-56.
- Inbar Y, Schneidman-Duhovny D, Dror O, Nussinov R and Wolfson HJ. 2007. Deterministic pharmacophore detection via multiple flexible alignment of drug-like molecules. Proceedings of Research in Computational Molecular Biology, Lecture Notes in Computer Science. Springer Verlag, Germany.
- Jaja-Chimedza A, Graf BL, Simmler C, Kim Y, Kuhn P, Pauli GF and Raskin I. 2017. Biochemical characterization and anti-inflammatory properties of an isothiocyanate-enriched moringa (*Moringa oleifera*) seed extract. *PLoS One.*, **12(8)**: 1-21.
- Jamroz M, Kolinski A and Kmiecik S. 2014. CABS-flex predictions of protein flexibility compared with NMR ensembles. *Bioinformatics.*, **30(15)**: 2150-2154.
- Kuriata A, Gierut AM, Oleniecki T, Ciemny MP, Kolinski A, Kurcinski M and Kmiecik S. 2018. CABS-flex 2.0: a web server for fast simulations of flexibility of protein structures. *Nucleic Acids Res.*, **46(W1)**: W338-W343.
- Lesica NA. 2017. Inflammation. In: **Conversation about Healthy Eating**. UCL Press, London, England, pp. 26-38.
- Lipinski CA, Lombardo F, Dominy BW and Feeney PJ. 2001. Experimental and computational approaches to estimate solubility and permeability in drug discovery and development settings. *Adv Drug Deliv Rev.*, **46(1-3)**: 3-26.
- Lüthy R, Bowie JU and Eisenberg D. 1992. Assessment of protein models with three-dimensional profiles. *Nature.*, **356(6364)**: 83-85.
- Ma ZF, Ahmad J, Zhang H, Khan I and Muhammad. 2020. Evaluation of phytochemical and medicinal properties of *Moringa oleifera* as a potential functional food. *S Afr J Bot.*, **129**: 40-46.
- Mahmoud MS, El-Kott AF, AlGwaiz HIM and Fathy SM. 2022. Protective effect of *Moringa oleifera* Lam. leaf extract against oxidative stress, inflammation, depression, and apoptosis in a mouse model of hepatic encephalopathy. *Environ Sci Pollut Res Int.*, **29(55)**: 83783-83796.
- MacArthur MW, Laskowski RA and Thornton J M. 1994. Knowledge-based validation of protein structure coordinates derived by X-ray crystallography and NMR spectroscopy. *Curr Opin Struct Biol.*, **4(5)**: 731-737.
- Martínez-González CL, Martínez L, Martínez-Ortiz EJ, González-Trujano ME, Déciga-Campos M, Ventura-Martínez R and Díaz-Reval I. 2017. *Moringa oleifera*, a species with potential analgesic and anti-inflammatory activities. *Biomed Pharmacother.*, **87**: 482-488.
- Mbikay, M. 2012. Therapeutic potential of *Moringa oleifera* leaves in chronic hyperglycemia and dyslipidemia: A review. *Front Pharmacol.*, **3**: 1-24.
- Meireles D, Gomes J, Lopes L, Hinzmann M and Machado J. 2020. A review of properties, nutritional and pharmaceutical applications of *Moringa oleifera*: integrative approach on conventional and traditional Asian medicine. *Adv Tradit Med.*, **20(4)**: 495-515.
- Mohanraj K, Karthikeyan BS, Vivek-Ananth RP, Chand RPB, Aparna SR, Mangalapandi P and Samal A. 2018. IMPPAT: A curated database of Indian Medicinal Plants, Phytochemistry and Therapeutics. *Sci Rep.*, **8(1)**: 1-17.
- Müller CW, Rey FA, Sodeoka M, Verdine GL and Harrison SC. 1995. Structure of the NF-kappa B p50 homodimer bound to DNA. *Nature.*, **373(6512)**: 311-317.
- Nandeesh R, Vijayakumar S, Munnolli A, Alreddy A, Veerapur VP, Chandramohan V and Manjunatha E. 2018. Bioactive phenolic fraction of *Citrus maxima* abate lipopolysaccharide-induced sickness behaviour and anorexia in mice: In-silico molecular docking and dynamic studies of biomarkers against NF-κB. *Biomed Pharmacother.*, **108**: 1535-1545.
- Lestari ND, Rahmah AC, Adharini WI, Nilamsari RV, Jatmiko NW, Yoga D, Rahayu S and Rifa'i M. 2022. Bioactivity of *Moringa oleifera* and albumin formulation in controlling TNF-α and IFN-γ production by NK cells in mice model type 1 diabetes. *Jordan J Biol Sci.*, **15(2)**: 205-208.
- O'Boyle NM, Banck M, James CA, Morley C, Vandermeersch T and Hutchison GR. 2011. Open Babel: An open chemical toolbox. *J Cheminform.*, **3(33)**: 1-14.
- Olson ME, Sankaran RP, Fahey JW, Grusak MA, Odee D and Nouman W. 2016. Leaf protein and mineral concentrations across the 'miracle tree' genus *Moringa*. *PLoS One.*, **11(7)**: 1-17.

- Padayachee B and Baijnath H. 2020. An updated comprehensive review of the medicinal, phytochemical and pharmacological properties of *Moringa oleifera*. *S Afr J Bot.*, **129**: 304-316.
- Panigrahy D, Gilligan MM, Serhan CN and Kashfi K. 2021. Resolution of inflammation: an organizing principle in biology and medicine. *Pharmacol Ther.*, **227**: 1-16.
- Pangalangan, RC. 2013. The domestic implementation of the international right to health: the Philippine experience. In: Zuniga JM, Marks AP and Gostin LO (eds.), **Advancing the Human Right to Health**. Oxford University Press, Oxford, England, pp.143.
- Ridker PM. 2016. A test in context: high-sensitivity C-reactive protein. *J Am Coll Cardiol.*, **67(6)**: 712-723.
- Sarrafadegan N, Kelishadi R, Esmailzadeh A, Mohammadifard N, Rabiei K, Roohafza H, Azadbakht L, Bahonar A, Sadri G, Amani A, Heidari S and Malekafzali H. 2009. Do lifestyle interventions work in developing countries? Findings from the Isfahan Healthy Heart Program in the Islamic Republic of Iran. *Bull World Health Organ.*, **87(1)**: 39-50.
- Sayed AME, Omar FA, Emam MMA and Farag MA. 2022. UPLC-MS/MS and GC-MS based metabolites profiling of *Moringa oleifera* seed with its anti-*Helicobacter pylori* and anti-inflammatory activities. *Nat Prod Res.*, **36(24)**: 6433-6438.
- Schneidman-Duhovny D, Dror O, Inbar Y, Nussinov R and Wolfson HJ. 2008. PharmaGist: a webserver for ligand-based pharmacophore detection. *Nucleic Acids Res.*, **36**: W223-W228.
- Sharma V, Paliwal R, Janmeda P and Sharma S. 2012. Chemopreventive efficacy of *Moringa oleifera* pods against 7, 12-dimethylbenz[a]anthracene induced hepatic carcinogenesis in mice. *Asian Pac J Cancer Prev.*, **13(6)**: 2563-2569.
- Shyu PT, Oyong GG and Cabrera EC. 2014. Cytotoxicity of probiotics from Philippine commercial dairy products on cancer cells and the effect on expression of *cfos* and *cjun* early apoptotic-promoting genes and Interleukin-1 β and Tumor Necrosis Factor- α proinflammatory cytokine genes. *Biomed Res Int.*, **491740**: 1-9.
- Thompson PA, Khatami M, Baglolle CJ, Sun J, Harris SA, Moon EY, Al-Mulla F, Al-Temaimi R, Brown DG, Colacci A, Mondello C, Raju J, Ryan EP, Woodrick J, Scovassi AI, Singh N, Vaccari M, Roy R, Forte S, Memeo L, Salem HK, Amedei A, Hamid RA, Lowe L, Guarnieri T and Bisson WH. 2015. Environmental immune disruptors, inflammation and cancer risk. *Carcinogenesis.*, **36(Suppl 1)**: S232-S253.
- Trott O and Olson AJ. 2010. AutoDock Vina: improving the speed and accuracy of docking with a new scoring function, efficient optimization, and multithreading. *J Comput Chem.*, **31(2)**: 455-461.
- Walker WH 2nd, Walton JC, DeVries AC and Nelson RJ. 2020. Circadian rhythm disruption and mental health. *Transl Psychiatry.*, **10(1)**: 1-13.
- Veber DF, Johnson SR, Cheng HY, Smith BR, Ward KW and Kopple KD. 2002. Molecular properties that influence the oral bioavailability of drug candidates. *J Med Chem.*, **45(12)**: 2615-2623.
- Velázquez-Zavala M, Peón-Escalante IE, Zepeda-Bautista R and Jiménez-Arellanes MA. 2016. *Moringa (Moringa oleifera Lam.)*: potential uses in agriculture, industry and medicine. *Rev Chapingo Ser Hortíc.*, **22(2)**: 95-116.
- Xiong Y, Riaz Rajoka MS, Zhang M and He Z. 2022. Isolation and identification of two new compounds from the seeds of *Moringa oleifera* and their antiviral and anti-inflammatory activities. *Nat Prod Res.*, **36(4)**: 974-983.

Diversity and Seasonal Variation of Fish Assemblages of Dingapota Haor an Eutrophic Wetland of Northeastern Bangladesh

Md. Nahiduzzaman^{*}, Ehsanul Karim, Md. Nazmul Hossen, Nazia Naheen Nisheeth and Yahia Mahmud

Bangladesh Fisheries Research Institute, Mymensingh-2201

Received: October 18, 2022; Revised: December 12, 2022; Accepted: January 25, 2023

Abstract

Wetlands are considered as the heart of natural feeding and breeding grounds of many indigenous fishes of Bangladesh. These are also the most diversified habitat in the world. However, the wetlands of Bangladesh are in danger of extinction due to various manmade and natural causes. Therefore, wetlands need special attention to conserve this unique ecosystem of Bangladesh. As a part of the conservation measures needed for wetland ecosystem, the present study was undertaken to describe the abundance and diversity status of fish in Dingapota wetland of Bangladesh and to identify the key environmental factors influencing the fish community assemblage. A total of 52 fish species were recorded from 7 orders during the study period. Cypriniformes comprises the most abundant order (47.91%) followed by Perciformes (20.71%) and Clupeiformes (20.22%). Higher number of species was recorded in post-monsoon season. Fish community assemblage was significantly differentiated among the three seasons (ANOSIM, Global R = 0.803, P < 0.05), while the overall average differences in the period of three seasons was estimated as 39.92% and similarity percentage analysis (SIMPER) revealed the greater contribution of *Osteobrama cotio*, *Esomus danricus*, *Nandus nandus*, *Gudusia chapra* and *Chanda nama* to ascertain this dissimilarity. Multivariate analysis based on non-metric multidimensional scaling (nMDS) generated three separate groups of each seasonal samplings and cluster analysis to find out natural grouping of samples according to their abundance. Diversity indices (Shannon-Weiner diversity (*H*), Margalef's richness (*D*) and Pielou's evenness (*e*)) were found to vary significantly among the seasons. Canonical correspondence analysis (CCA) revealed the significant roles of temperature, depth, transparency, pH, dissolved oxygen and alkalinity for structuring the community assemblage of fish in Dingapota wetland. Essential baseline information generated by this study will help the respective authority to formulate sustainable conservation measures for Dingapota wetland.

Keywords: diversity indices, environmental parameters, fish community, Canonical correspondence analysis, similarity percentage analysis

1. Introduction

Haor (bowl-shaped massive geological depression in wetland) is the most diverse habitat in Bangladesh. These special ecosystems are considered as the sixth hotspot in the Delta Plan 2100 of Bangladesh. Haors are typically submerged during the rainy season and merge with riverine flood waters. Therefore, seasonal flooding in these haors mostly controls the variety and number of fish species. Owing to the increase in water areas, fish are not typically present in large numbers during the monsoon. There are about 373 haors, or roughly 43% of the entire area of the haor region, spread across the districts of Netrokona, Kishoreganj, Sunamganj, Habiganj, Sylhet, Maulvibazar and Brahmanbaria, (Ahmed, 2013; Islam *et al.*, 2010; Master Plan of Haor Areas, 2012). They encompass an area of about 858,000 ha. Numerous freshwater fin fish species as well as several prawn species, including 143 indigenous and 12 exotic species,

are found in these haors (Mustafa *et al.*, 2019; Islam *et al.*, 2012; MoW, 2005; Muzaffar, 2004).

Since the turn of the century, there has been significant human meddling in the natural world, leading to overexploitation, loss of natural habitats, and terrible conditions for aquatic ecosystems. For this reason, many fish species are currently in danger of going extinct. Bangladesh is now facing a serious problem with the ongoing aquatic biodiversity declining from natural water bodies (Galib *et al.*, 2009 and 2013; Mohsin *et al.*, 2013 and 2014). The decline in fish biodiversity in inland water bodies serves as an example of the need for an extensive study, which is necessary for evaluating the present situation and ensure the effective management approach of a water body (Imteazzaman and Galib, 2013).

Dingapota Haor is One of the significant inland freshwater wetland ecosystems, which is situated at Mohonganj Upazila of Netrokona District at 24°52'00"N 90°58'00"E / 24.8667°N 90.9667°E (Fig. 1) covering the surface area of 8000 ha. To the authors' knowledge, several research projects on the fish faunal biodiversity of

^{*} Corresponding author. e-mail: nahid.bfri83@gmail.com.

various water of diverse water bodies in Bangladesh have been carried out; however, there has only been one study on the aquatic fish faunal biodiversity of the Dingapota Haor, Netrokona. In this case, study is necessary to comprehend the wetland's overall state and maintain the appropriate management practices. The diversity of fish in the water must be known before implementing any fisheries management technique, but no report on the fish diversity and ecological status of the water has been released (Huda *et al.* 2009). Therefore, the current study examines seasonal variation in environmental variables as well as changes in various freshwater fish species diversity indices at Dingapota Haor (Mohanganj Upazilla) Netrokona, Bangladesh.

2. Materials and methods

2.1. Study area and duration

From July 2020 to June 2021, the study was carried

out over a 12-month period at three sampling sites (Karchapur, 24°77'72" N, 91°05'10"E; Mollikipur, 24°80'23" N, 91°03'57"E; Khurshimul, 24°88'66" N, 91°01'99"E) in the Dingapota haor, a wetland at Mohanganj Upazila (Sub-district) in Netrokona District, Bangladesh (Fig. 1). It is an important ecosystem that supports many different fish species and is regarded as an essential breeding and feeding habitat for inland freshwater fish species. Additionally, this region provides small-scale fishermen and nearby residents with a means of subsistence. Fish and environmental factors were sampled throughout each month, which was further divided into three distinct seasons; a) From July to October is monsoon season; b) from November to February is post-monsoon; and c) from March to June is pre-monsoon

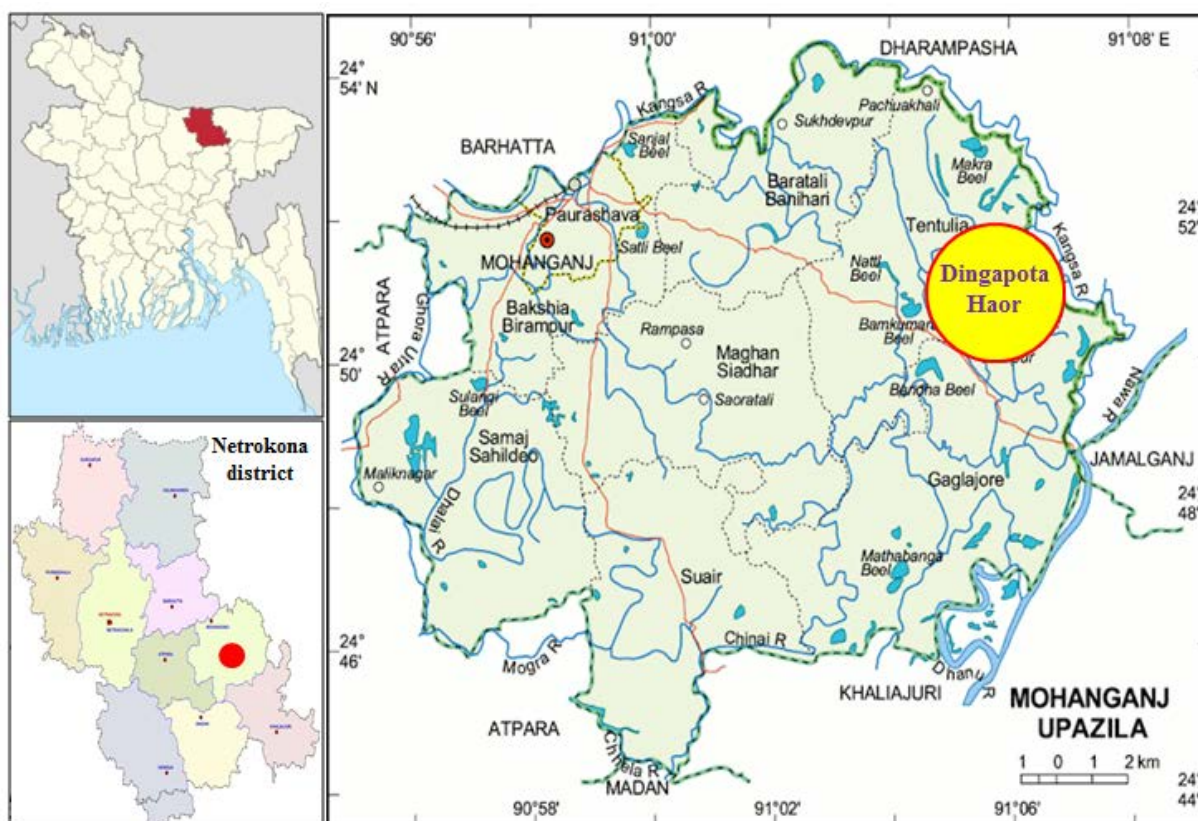


Figure 1. Map of the Dingapota haor at Mohanganj Upazila of Netrokona district, Bangladesh.

2.2. Measurement of water quality parameters

Temperature, transparency, depth, dissolved oxygen, pH, NO₃-N, PO₄-P, alkalinity, and TDS were the water quality parameters measured each month and documented. Water quality parameters were measured between 9:00 am and 12:00 pm throughout every sampling month. On the sampling date, 500ml of surface water from each study locations were collected in black colored coded bottles. A highly advanced Multi-Parameter Water Quality Meter (HANNA, HI 98194, pH/EC/DO multi-parameter) was used to measure the water's temperature (°C), pH, DO, and TDS. Water depth was measured with a measuring tape. A Secchi disk was used to measure the water's transparency

(in cm). A spectrophotometer (DR-1900) was used to measure alkalinity (mg/l), NO₃-N, and PO₄-P.

2.3. Species collection and identification

Fish samples were collected from the specified sampling site with the assistance of experienced fishermen on each sampling date. A seine net with a length, width and mesh size of 100 m, 5 m and 1-2 mm, respectively, was used for sampling of fishes. After collecting, the fishes were identified and enumerated. Fishes which were difficult to identify were kept in 10% buffered formalin solution and transported to the laboratory of the Bangladesh Fisheries Research Institute, Mymensingh. Subsequently, morphometric and meristic data were used

to identify the fishes up to species level followed by the keys of (Rahman *et al.* 2009). Identified fishes were categorized into taxonomic groups following Nelson *et al.* (2006).

2.4. Diversity indices

Shannon-Weiner diversity, Margalef's richness and Pielou's evenness were calculated by using the following formula-

Shannon-Weiner diversity, $H = -\sum_i \frac{n_i}{N} \ln \frac{n_i}{N}$ (Shannon and Weiner, 1949)

Where, S is the number of individuals for each species, N is the total number of individuals, n_i is the relative abundance (S/N) H represents the diversity index,

Margalef's richness, $D = \frac{S-1}{\ln N}$ (Margalef 1968)

Where, N is the total number of distinct species in the sample, S is the different species in the sample; D is Margalef's richness index.

Pielou's evenness, $J_e = \frac{H}{\ln S}$ [\ln = the natural logarithm] (Poulet's, 1966)

Where, S indicates the number of distinct species in the sample and H is the Shannon-Weiner index.

2.5. Statistical analyses

One-way analysis of variance (ANOVA) was used to assess seasonal fluctuation in water quality parameters using Statistical Package for Social Sciences (version 20.0) software. Seasonal distribution of water quality parameters was analyzed by principal component analysis (PCA). Species abundance and diversity indices were also analyzed by ANOVA. Mean differences among the seasons were determined by Duncan's multiple range test (DMRT) at 5% level of significance. Community assemblage pattern of fish species among the seasons was tested by multivariate analysis. Before analyzing the data, water quality parameters were square root transformed, and the fish abundance data was $\log_{10}(x+1)$ transformed for the normalization. Analysis of similarity (ANOSIM) was conducted to assess the differences in fish community assemblage among the seasons. Similarity percentage analysis (SIMPER) was also used to determine the most contributory species causing differences among the seasons (Clarke and Warwick 1994). The distribution pattern of the fishes among the season was visualized using non-metric multi-dimensional scaling (nMDS), and the species was categorized using a cluster analysis based on Bray-Curtis similarity matrix. The potential correlations between fish species and water quality parameters were determined by canonical corresponding analysis (CCA) using PAST (Paleontological Statistics, Version 4.10) program.

3. Results

3.1. Seasonal variation of water quality parameters

Table 1 provides an overview of the water quality metrics that were noticed and noted during the investigation. All the water quality measures showed a significant variation across the seasons ($P < 0.05$). Pre-monsoon had the greatest water temperature ($29.89 \pm 0.65^\circ\text{C}$), while post-monsoon had the lowest ($22.36 \pm 3.98^\circ\text{C}$). Observed transparency was ranged between

$39.59 \pm 4.41\text{cm}$ (Post-monsoon) to $24.66 \pm 0.81\text{ cm}$ (Monsoon). The highest water depth was observed during the Monsoon ($5.96 \pm 1.61\text{ m}$) and the lowest during pre-monsoon ($1.66 \pm 0.82\text{ m}$) whereas pH was ranged between 7.00 ± 0.78 (post-monsoon) to 6.38 ± 0.60 (pre-monsoon). In addition, DO was between $6.63 \pm 0.74\text{ mg/l}$ (post-monsoon) to $4.56 \pm 0.53\text{ mg/l}$ (pre-monsoon). In case of $\text{NO}_3\text{-N}$ and $\text{PO}_4\text{-P}$, pre-monsoon showed the greatest levels of (0.33 0.04 and 1.34 0.11 mg/l), while monsoon had the lowest levels (0.13 0.01 mg/l and 1.16 0.02 mg/l). The total alkalinity was $126.89 \pm 7.47\text{ mg/l}$ during pre-monsoon and $103.38 \pm 4.44\text{ mg/l}$ during monsoon while TDS was also the highest during pre-monsoon ($135.73 \pm 5.50\text{ mg/l}$) and the lowest during monsoon ($100.97 \pm 5.16\text{ mg/l}$). PCA was also used to explain the seasonal variation of water quality measures, with its first two axes accounting for 85.94% of the variability in the data (Fig. 2). PCA demonstrated a distinct seasonal separation of the samples, whereas the monsoon samples are related with water depth and the post-monsoon samples are associated with transparency, DO, $\text{NO}_3\text{-N}$ and $\text{PO}_4\text{-P}$. Furthermore, pre-monsoon samples are correlated with alkalinity and TDS.

Table 1. Water quality parameters (Mean \pm SD) in different seasons

Variables	Monsoon	Post-monsoon	Pre-monsoon
Temperature ($^\circ\text{C}$)	28.70 ± 0.62^a	22.36 ± 3.98^b	29.89 ± 0.65^a
Transparency (cm)	24.66 ± 0.81^c	38.02 ± 3.29^b	39.59 ± 4.41^a
Depth (m)	5.96 ± 1.61^a	1.93 ± 0.41^b	1.66 ± 0.82^c
pH	6.99 ± 0.85^a	7.00 ± 0.78^a	6.38 ± 0.60^b
DO (mg/l)	5.72 ± 0.52^b	6.63 ± 0.74^a	4.56 ± 0.53^c
$\text{NO}_3\text{-N}$ (mg/l)	0.13 ± 0.01^c	0.21 ± 0.11^b	0.33 ± 0.04^a
$\text{PO}_4\text{-P}$ (mg/l)	1.16 ± 0.02^c	1.28 ± 0.09^b	1.34 ± 0.11^a
Total alkalinity (mg/l)	103.38 ± 4.44^c	112.79 ± 2.00^b	126.89 ± 7.47^a
TDS (mg/l)	100.97 ± 5.16^c	116.92 ± 7.38^b	135.73 ± 5.50^a

Mean values in the same row having difference superscript letters indicate significant ($P < 0.05$) differences.

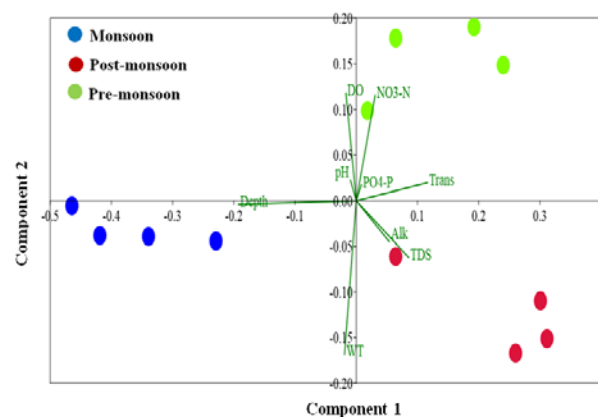


Figure 2. Water quality parameters during the monsoon, post-monsoon, and pre-monsoon seasons were analyzed using the principle component method (Wt = water temperature, Trans = transparency, Depth, DO = dissolved oxygen, pH, $\text{NO}_3\text{-N}$ = nitrate-nitrite, $\text{PO}_4\text{-P}$ = phosphate-phosphorus, Alka = total alkalinity, TDS = total dissolved solids).

3.2. Catch composition

During the study period, 52 fish species from 17 families and 7 orders were recorded. Figure 3 demonstrates that the most abundant order was the cypriniformes followed by the perciformes (20.71%) and the clupeiformes (20.22%). A total of 1242 individual of fishes was collected during the study period (Table 2) which consists of 52 species. The total abundance was

significantly higher during post-monsoon season (725) and the lowest in pre-monsoon season (107). Similarly, total number of species was significantly higher during post-monsoon season (47) and the lowest in pre-monsoon season (34). *Amblypharyngodon mola* (11.03%) was the most dominant species followed by *Gudusia chapra* (10.03%) and *Osteobrama cotio* (8.01%).

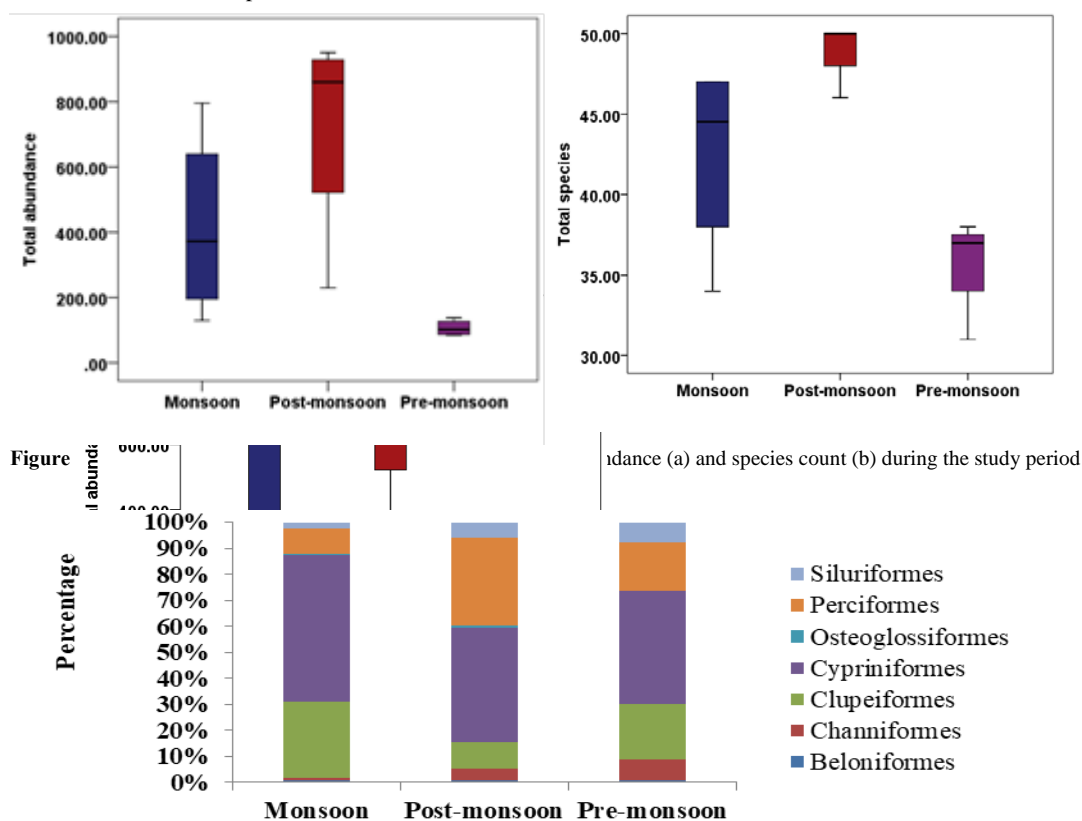


Figure 4. Percentage composition of different fish taxonomic orders in the studied wetland

Table 2. List of species with number of individuals and their contribution (%) in each season

Sl. No.	Species Name	Code	Total	Overall contribution (%)	Seasonal contribution (%)		
					Monsoon	Post-monsoon	Pre-monsoon
1	<i>Xenentodon cancila</i>	Xc	9	0.73	0.54	0.82	0.89
2	<i>Hyporhamphus limbatus</i>	Hl	1	0.07	0.21	0.00	0.00
3	<i>Channa punctatus</i>	Cp	21	1.65	0.61	1.85	4.35
4	<i>Channa striatus</i>	Cs	19	1.56	0.28	2.23	1.94
5	<i>Channa orientalis</i>	Co	6	0.52	0.32	0.50	1.36
6	<i>Channa marulius</i>	Cm	5	0.42	0.13	0.50	1.02
7	<i>Corica soborna</i>	Cso	114	9.20	18.49	3.15	14.24
8	<i>Gudusia chapra</i>	Gc	131	10.52	15.60	7.79	9.39
9	<i>Gibelion catla</i>	Gca	2	0.16	0.16	0.18	0.00
10	<i>Labeo rohita</i>	Lr	1	0.05	0.16	0.00	0.00
11	<i>Labeo bata</i>	Lb	11	0.90	0.33	0.66	4.69
12	<i>Labeo calbasu</i>	Lc	6	0.47	0.18	0.30	2.70
13	<i>Labeo gonius</i>	Lg	10	0.81	0.38	0.87	2.05
14	<i>Cirrhinus cirrhosus</i>	Cci	5	0.39	0.27	0.39	0.84
15	<i>Amblypharyngodon Mola</i>	Am	137	11.03	21.14	4.98	13.03
16	<i>Chela Laubuca</i>	Cl	64	5.19	5.06	5.10	6.35
17	<i>Osteobrama cotio</i>	Oc	99	8.01	11.11	7.24	1.26

Table 2. cont

18	<i>Pontius sarana</i>	Ps	10	0.77	0.77	0.57	2.18
19	<i>Puntius sophore</i>	Pso	65	5.21	1.09	8.02	2.05
20	<i>Pethia ticto</i>	Pt	18	1.43	0.67	1.74	2.28
21	<i>Salmostoma Bacaila</i>	Sb	2	0.13	0.11	0.17	0.00
22	<i>Esomus danricus</i>	Ed	85	6.84	7.12	7.51	1.15
23	<i>Botia dario</i>	Bd	2	0.18	0.31	0.13	0.00
24	<i>Lepidocephalichthys Guntea</i>	Leg	17	1.38	1.15	1.71	0.00
25	<i>Notopterus chitala</i>	Nc	4	0.35	0.09	0.55	0.00
26	<i>Notopterus notopterus</i>	Nn	0	0.04	0.06	0.03	0.00
27	<i>Anabas testudineus</i>	At	16	1.30	0.08	1.82	2.49
28	<i>Chanda nama</i>	Cn	47	3.79	1.44	5.53	1.02
29	<i>Pseudambassis ranga</i>	Pr	13	1.04	0.40	1.56	0.00
30	<i>Glossogobius giuris</i>	Gg	12	0.95	0.39	1.40	0.00
31	<i>Glossogobius chuno</i>	Goc	49	3.91	1.32	5.68	1.91
32	<i>Macrognathus aculeatus</i>	Ma	30	2.45	1.43	3.05	2.28
33	<i>Macrognathus pancalus</i>	Mp	37	2.96	1.31	4.05	1.97
34	<i>Mastacembelus armatus</i>	Maa	11	0.89	0.30	1.13	1.57
35	<i>Nandus nandus</i>	Nan	28	2.22	0.17	3.38	2.25
36	<i>Colisa fasciata</i>	Cf	21	1.65	0.37	2.33	2.05
37	<i>Badis badis</i>	Bad	0	0.04	0.00	0.07	0.00
38	<i>Mystus aor</i>	Mao	10	0.83	0.11	1.21	1.02
39	<i>Mystus cavassius</i>	Mc	37	2.96	2.49	3.40	1.76
40	<i>Mystus vittatus</i>	Mv	18	1.43	0.83	1.74	1.57
41	<i>Rita rita</i>	Rr	1	0.09	0.08	0.10	0.00
42	<i>Ompok bimaculata</i>	Ob	6	0.45	0.18	0.49	1.21
43	<i>Ompok pabda</i>	Opa	8	0.62	0.42	0.63	1.36
44	<i>Wallago attu</i>	Wa	8	0.68	0.32	0.83	1.08
45	<i>Ailia coila</i>	Ac	8	0.63	0.54	0.78	0.00
46	<i>Clupisoma garua</i>	Clug	9	0.73	0.61	0.91	0.00
47	<i>Eutropiichthys vacha</i>	Eucv	1	0.05	0.16	0.00	0.00
48	<i>Bagarius bagarius</i>	Bb	2	0.16	0.11	0.22	0.00
49	<i>Clarias batrachus</i>	Cb	4	0.33	0.14	0.28	1.39
50	<i>Heteropneustes fossilis</i>	Hfo	5	0.41	0.12	0.39	1.65
51	<i>Chaca chaca</i>	Cch	3	0.26	0.00	0.21	1.65
52	<i>Neotropius atherinoides</i>	NA	14	1.16	0.32	1.80	0.00

3.3. Species diversity

The seasonal values of the Pielou's evenness, Margalef's richness, and Shannon-Wiener diversity indices are presented in Fig. 6. The studied haor is more diverse in post-monsoon season with the Shannon–Wiener diversity

value of 3.27 ± 0.17 . Furthermore, fish species of the studied haor were more evenly distributed for the period of post-monsoon season (Pielou's evenness value 0.89 ± 0.08). Species richness was also higher in post-monsoon season with the Margalef's richness value 7.97 ± 0.24 .

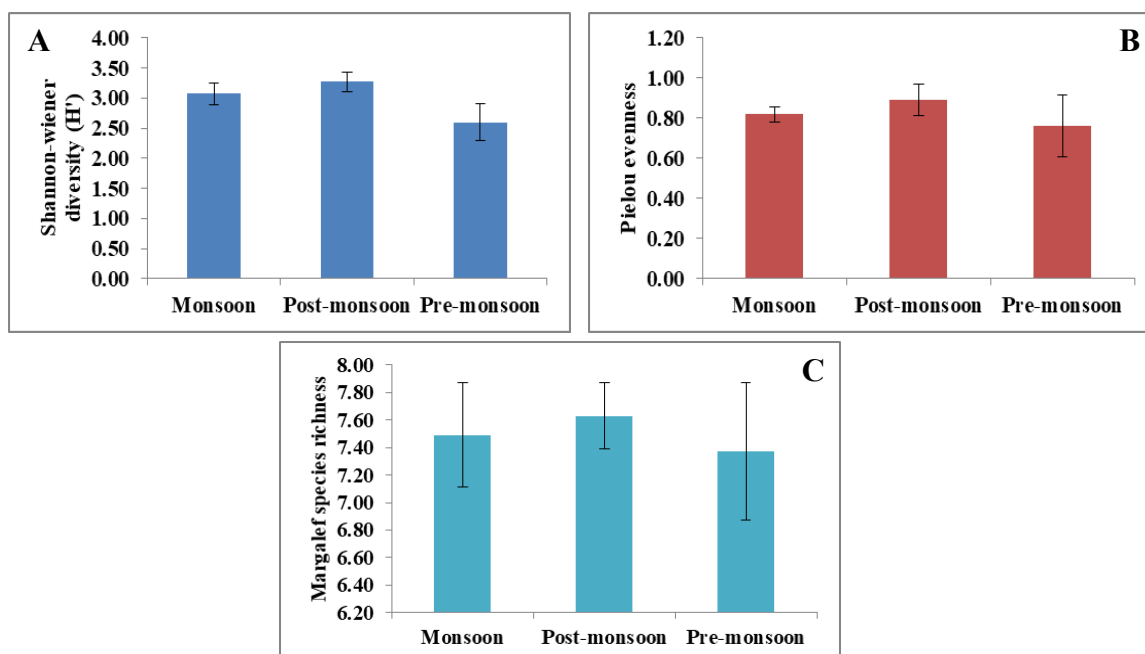


Figure 5. Seasonal variation of species diversity indices. (A) Shnnon-wiener, (B) Pielou evenness, (C) Magalef richness.

3.4. Species assemblage

According to analysis of similarity (ANOSIM), the species assemblage varied significantly among each of the seasonal groups (Table 3), with global R values of 0.5313, 0.08646, and 0.9063 and P values of 0.0477, 0.0293, and 0.0323. According to SIMPER analysis, there is an average dissimilarity of 36.61, 39.89, and 43.25 % between monsoon and post-monsoon, monsoon and pre-monsoon, and post-monsoon and pre-monsoon, respectively, whereas the most contributory species from

Table 3. ANOSIM and SIMPER analysis of fish species assemblage

Groups	ANOSIM		Dissimilarity index from SIMPER		% contribution
	R	P	Ave. Diss. (%)	Typical species	
Monsoon vs. Post-monsoon	0.5313	0.0477	36.61	<i>Nandus nandus</i>	5.55
				<i>Gudusia chapra</i>	4.17
				<i>Channa striatus</i>	3.83
				<i>Chanda nama</i>	3.57
				<i>Puntius sophore</i>	3.36
				<i>Esomus danricus</i>	5.53
Monsoon vs. pre-monsoon	0.08646	0.0293	39.89	<i>Osteobrama cotio</i>	5.35
				<i>Gudusia chapra</i>	4.18
				<i>Lepidocephalichthys guntea</i>	3.80
				<i>Amblypharyngodon mola</i>	3.65
				<i>Gudusia chapra</i>	4.34
Post-monsoon vs. Pre-monsoon	0.9063	0.0323	43.25	<i>Chanda nama</i>	4.15
				<i>Osteobrama cotio</i>	4.07
				<i>Neotropius atherinoides</i>	3.76
				<i>Glossogobius giuris</i>	3.59
				<i>Osteobrama cotio</i>	4.04
				<i>Esomus danricus</i>	3.96
overall or pool all groups	0.8032	0.0007	39.92	<i>Nandus nandus</i>	3.90
				<i>Gudusia chapra</i>	3.36
				<i>Chanda nama</i>	3.30

According to the Bray-Curtis similarity index (stress 0.043), three distinct seasonal groupings of fish assemblage were found by nMDS. (Fig. 6) which is

each group were *Nandus nandus* (5.55%), *Esomus danricus* (5.53%) and *Gudusia chapra* (4.34%). ANOSIM ($P < 0.0007$, $R = 0.8032$) has revealed significant variation in species assemblage among the seasons with an overall average dissimilarity of 39.92% determined by SIMPER analysis. Five most contributory fish species responsible for these seasonal variations are *Osteobrama cotio* (4.04%), *Esomus danricus* (3.96%), *Nandus nandus* (3.90%), *Gudusia chapra* (3.36%) and *Chanda nama* (3.30%).

indicating dissimilarity of fish samples among the three seasons. The fish samples collected from different sites of Dingapota haor are grouped separately indicating their

similarity. Samples within a group are more similar compared to the other groups.

Cluster analysis also separated the collected fish species into three distinct groups at 50.00% similarity (Fig. 7), whereas the first cluster (from the left side of the Fig. 7) consists of the species which had lower abundance during the study period. However, fish species with a moderate abundance are classified into the second cluster, and the fish species with the greatest abundance are represented by the third cluster.

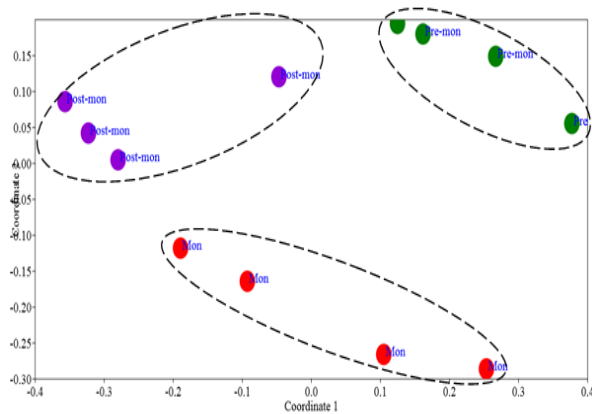


Figure 6. Non-metric multidimensional scaling (NMDS) of fish species

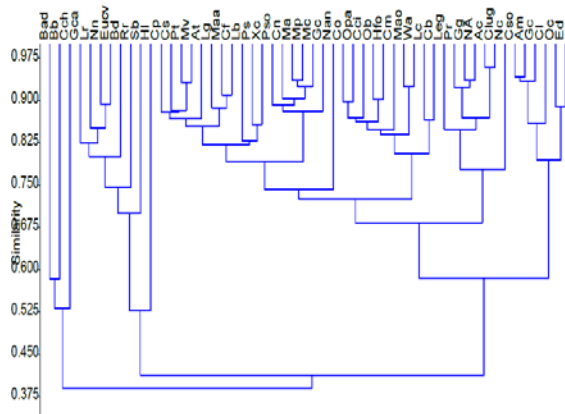


Figure 7. Dendrogram demonstrating 2D ordination of a cluster analysis of fish species using the Bray-Curtis similarity matrix.

3.5. Canonical correspondence analysis (CCA)

Results obtained from CCA were plotted in Fig. 8 whereas the species placed nearer the vector were more closely related to them. The length and direction of the arrows show the relative significance of the water quality parameters. The CCA ordination directs that transparency, depth, DO and TDS are the most influential water quality parameters shaping fish species accumulation in the studied wetland. Water temperature and depth have close affinity with *Esomus danricus*, *Gudusia chapra* and *Amblypharyngodon mola* which are describing the monsoonal abundance of these species. *Osteobrama cotio*, *Chanda nama* and *Macragnathus pancalus* are found to be influenced mainly by DO, pH, $\text{NO}_3\text{-N}$ and $\text{PO}_4\text{-P}$, and this interaction is highlighting the post monsoonal species abundance. Transparency, alkalinity and TDS showed their highest value during pre-monsoon season and the fish species *Glossogobius chuno*, *Channa striatus*, *Chela*

laubuca and *Puntius sophore* are found to be influenced mostly by these parameters

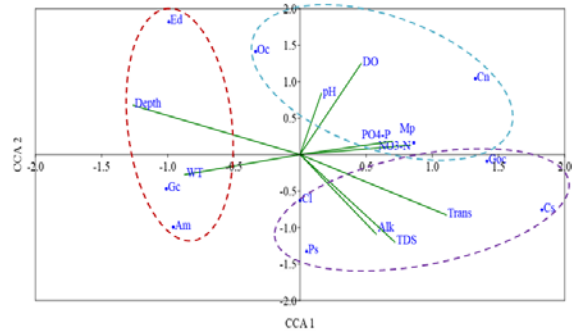


Figure 8. Biplot for canonical correspondence analysis. Wt = Water temperature, Trans = Transparency, Depth, DO = Dissolved oxygen, pH, $\text{NO}_3\text{-N}$ = Nitrate-nitrite, $\text{PO}_4\text{-P}$ = Phosphate-phosphorus, Alk = Total alkalinity, TDS = Total dissolved solids. Species codes are shown in Table 2.

4. Discussion

The maximum average temperature was 29.89 ± 0.65 °C in pre-monsoon, and the minimum temperature was 22.36 ± 3.98 °C in post-monsoon. The temperature in Ashulia beel ranged between 28.7 to 31.7°C and 22.4 to 25.6°C during wet and dry season, respectively (Islam *et al.* 2010). During the study period, transparency was fluctuated from 39.59 ± 4.41 cm (Post-monsoon) to 24.66 ± 0.81 cm (Monsoon). Chowdhury and Mazumder (1981) reported the instances of excessive turbidity during the monsoon season. Productive water body should contain transparency of less than 40 cm (Salaudhin and Islam 2011). The Water depth was found to range between 5.96 ± 1.61 m in Monsoon to 1.66 ± 0.82 m during pre-monsoon. The water level in the haor area becomes lowest during February, reaching its peak during July and declining again from August onward (Salaudhin and Islam 2011). The maximum pH was noted 7.00 ± 0.78 in post-monsoon and the lowermost was 6.38 ± 0.60 in pre-monsoon. pH ranged between 7.15 and 7.45 was recorded by (Islam *et al.* 2017) at Karimganj haor in Kishoreganj, which is more or less similar to the present study. The DO contents ranged from 6.63 ± 0.74 mg/L in post-monsoon to 4.56 ± 0.53 mg/L in pre-monsoon. DO in Hakaluki haor and Karimganj haor (Aker *et al.* 2017) ranged between 3.1 to 7.0 and 6.4 to 6.8 mg/L, respectively, which are mostly similar to the current investigation. $\text{NO}_3\text{-N}$ was the highest during pre-monsoon (0.33 ± 0.04 mg/L), and the lowest during monsoon (0.13 ± 0.01 mg/L). Nitrate-N ($\text{NO}_3\text{-N}$) concentrations ranged from 0.01 to 0.33 mg/L at different locations in Chalan Beel, and in Kaptai Lake (Halder *et al.* 1992) of Bangladesh. The $\text{PO}_4\text{-P}$ was 1.34 ± 0.11 mg/L in pre-monsoon to 1.16 ± 0.02 mg/L in monsoon. The $\text{PO}_4\text{-P}$ in the Kaptai Lake ranged from 0.32 to 0.41 mg/L with an average of 0.367 mg/L. Khan *et al.* (1996) also revealed a higher level of $\text{PO}_4\text{-P}$ in dry season compared to rainy season in their study location. Total alkalinity was 126.89 ± 7.47 mg/L in pre-monsoon to 103.38 ± 4.44 mg/L during monsoon season which is more or less similar to the findings of Ahatun *et al.* (2020) in Korotoa River (122.05 mg/L). The peak TDS content of the haor was 135.73 ± 5.50 mg/L throughout pre-monsoon mg/L, and the lowermost was 100.97 ± 5.16 mg/L in monsoon season. The TDS at various sampling locations of Hakaluki haor ranged

between 80.75 to 184.0 mg/L with the mean value of 132.38 mg/L (Akter *et al.*, 2017), which was comparable to the present study.

Fifty-two fish species were incurred during the study period which was abundantly belonging to 17 families, and the Cypriniformes was the most dominant (47.91%) group. Previous study conducted by Hasan *et al.* (2017) reported 17 families from Kishorgonj haor in Bangladesh, while slightly higher number of families was recorded by Islam *et al.* (2021) and Pandit *et al.* (2015) from Dekhar haor, Bangladesh. Freshwater bodies of Bangladesh are mainly dominated by Cypriniformes as was stated by Maria *et al.* (2016), Chowdhury *et al.* (2019), Akhi *et al.* (2020), Mazumder *et al.* (2016), Sunny *et al.* (2020), and Jannatul *et al.* (2015). Therefore, the current results supported the previous investigations. A total of 52 fish species obtained during the present work, which was supported by the findings of Islam *et al.* (2021) who described 57 species of fishes in their study. Seasonal fluctuation in the total species abundance was significant, whereas the maximum abundance was found in post-monsoon and the lowest in pre-monsoon season. *Amblypharyngodon mola* (11.03%) was the most dominant species followed by *G. chapra* (10.03%) and *O. cotio* (8.01%) which were mainly influenced by water temperature and depth. Small indigenous fishes are the main and inexpensive form of indispensable vitamin and mineral in the diet of people in Bangladesh (Bogard *et al.*, 2015). Therefore, market value of these fish species is increasing day by day. As a result, fishermen are currently enhancing their fishing effort in the haor to catch them.

Seasonal changes in diversity of the present study were depicted by several diversity indices such as the number of species in an assemblage (Gotelli and Chao, 2013), evenness (Jost, 2010) and richness (Delang and Li, 2013). Diversity indices in the present study were found to increase significantly in post-monsoon season and decrease for the period of monsoon season. Higher diversity index during post-monsoon indicates the increase in fish species by reproducing, feeding and sheltering themselves successfully (Aziz *et al.*, 2021). Similar findings were also made by Nath and Deka (2012) and Iqbal *et al.* (2015), who observed the highest diversity of fish during the post-monsoon season. However, lower species diversity during monsoon can be described by the higher water depth which reduced the effectiveness of fishing gear to catch fish. On the other hand, comparatively lower diversity indices during pre-monsoon season are possibly because of the stress caused by overfishing and scarcity of water (Aziz *et al.*, 2021). Increased water temperature is also causing higher evaporation rate and decreased surface water area. As a result, intensive rice production and irrigation activities are affecting the ecological process of haor. Reduced transparency caused by silt particle inhibits the light penetration into the water. As a result reduced the primary and secondary productivity of water, which might be responsible for declining fish diversity in the present study. However, the diversity index recorded during the present study (2.60-3.27) was within the range (2.90-3.12) reported by Iqbal *et al.* (2015), higher (1.22-1.36) than the findings of Hossain and Rabby (2020) and lower (3.76-3.81) than the findings of Aziz *et al.* (2021). According to

Biligrami (1988) improved status of an aquatic habitat for fish diversity is indicated by Shannon-Wiener index of 3.0-4.5. That means studied haor is light to slightly polluted during monsoon season and this might be due to the domestic discharge, poor water quality and the uses of different insecticides and pesticides. Evenness and richness of fish species was also peak in post-monsoon season. Evenness is the degree of relative diversity which can be higher when the entire habitat supports similar density and richness is the range of relative abundance of fish species. In an even population, all species are assumed to be distributed identically into the habitat. As observed in the present study, decreased water level during post-monsoon season leads to more fish species caught by fishing activities causing a homogenous catches of the fishes. On the contrary, higher water depth during monsoon season causes irregular distribution of fish species, and the majority of fishes were caught using selective fishing gears which have low evenness and richness indices. Similar patterns of seasonal variation of fishes are also observed in various aquatic habitat of Bangladesh (Jewel *et al.*, 2018; Joadder *et al.*, 2015; Akhi *et al.*, 2020).

5. Conclusion

Along with 52 species, Dingapota haor is the most species-rich haor in Bangladesh. However, water depth and heavy post-monsoonal fishing pressure were the main causes of the seasonal variation in species diversity in this area. To protect the remaining fish species, control over the perennial water regions during post-monsoon season needs to be maintained. The present study recommends designation of the perennial water areas as a sanctuary for the survival of matured fish in the post-monsoon season.

Acknowledgement

The research was supported by Bangladesh Fisheries Research Institute through the project entitled "Ecological assessment of inland open water fisheries population with bio-physicochemical properties to frame EBFM approach (Comp-A)."

Reference

- Ahatun S, Islam MS, Kabir MH, Rehnema M and Hoq ME. 2020. Water quality and fish diversity in Korotoa River of Bogura, Bangladesh. *Bangladesh J. Fish.*, **32**(1): 61-72.
- Ahmed A. 2013. Bangladesh: Environmental and Climate Change Assessment. International Fund for Agricultural Development: Rome, Italy.
- Ahmed K KU, Hasan RR, Ahamed SU, Ahmed T and Mustafa G. 2004. Ecology of Shakla beel (Brahmanbaria), Bangladesh. *Bang J. Fish. Res.*, **8**(2): 101-111.
- Akhi MM, Jewel MAS, Haque MA, Sarker BK, Khatun MS, Paul AK, Islam MS and Das SK. 2020. Multivariate approaches to determine the relationship between fish assemblage structure and environmental variables in Karatoya River, Bangladesh. *Community Ecol.*, **21**(2): 171-181.
- Akter S, Saha SK, Kabir MH, Mamun SA, Islam MS. 2017. Fluctuations in water quality at Hakaluki Haor of Bangladesh. *Bangladesh J. Environ. Sci.*, **32**: 35-40.

- Alam MS, Quayum MA and Islam MA. 2010. Crop Production in the Haor Areas of Bangladesh: Insights from Farm Level Survey. *The Agriculturists*, **8**(2): 88-97.
- Aquatic Research Group (ARG).1986.Hydrobiology of the Kaptai reservoir. University of Chittagong, FAO /UNDP Final Report No. DP /BGD /79 /015-4/Fl. 192 pp.
- Aziz MSB, Hasan NA, Mondol MMR, Alam MM and Haque MM. 2021. Decline in fish species diversity due to climatic and anthropogenic factors in Hakaluki Haor, an ecologically critical wetland in northeast Bangladesh. *Heliyon*, **7**(1):e05861.
- Bhuiyan AL. 1964. Fishes of Dacca. Dacca: Asiatic Society of Pakistan.
- Biligrani KS. 1988. Biological monitoring of rivers, problems and prospect in India. *Aqua. Ecotoxicol.*: 245–250.
- Bogard JR, Thilsted SH, Marks GC, Wahab MA, Hossain MAR, Jokobesen J and Stangoulis J. 2015. Nutrient composition of important fish species in Bangladesh and potential contribution to recommended nutrient intakes. *J. Food Compos. Anal.*, **42**: 120–156.
- Bray JR and Curtis JC. 1957. An ordination of the upland forest communities of southern Wisconsin. *Ecological Monographs*, **27**, 325–349.
- Chowdhury MA, Karim MA, Rahman MT, Shefat SHT, Rahman A and, Hossain MA. 2019. Biodiversity assessment of indigenous fish species in the Surma river of Sylhet Sadar, Bangladesh. *Punjab Uni. J. Zool.*, **34**(1): 73-77
- Chowdhury SH and Mazumder A. 1981. Limnology of lake Kaptai I. Physicochemical features. *Bangladesh J. Zool.*, **9**(1): 59-72.
- Clarke KR and Warwick WM. 1994. Similarity-based testing for community pattern: The 2-way layout with no replication. *Mar. Biol.*, **118**: 167–176.
- Delang, Claudio O and Wing Man Li. 2013. Species richness and diversity. *Ecological Succession on Fallowed Shifting Cultivation Fields*. 39-66.
- Froese R and Pauly D. 2015. List of freshwater fishes reported from Bangladesh. Fish Base, World Wide Web electronic publication. Retrieved October, 2015, from www.Fishbase.Org,version.
- Galib SM, Naser SMA, Mohsin ABM, Chaki N and Hassan F. 2013. Fish diversity of the River Choto Jamuna , Bangladesh : Present status and conservation needs. *Int. J. Biodivers. Conserv.*, **5**: 389-395.
- Galib SM, Samad MA, Mohsin ABM, Flowra FA and Alam MT. 2009. Present Status of Fishes in the Chalan Beel- the Largest Beel (Wetland) of Bangladesh. *Int. J. Ani. Fish. Sci.*, **2**(3): 214-218.
- Gotelli Nicholas J and Chao Anne. 2013. Measuring and Estimating Species Richness, Species Diversity, and Biotic Similarity from Sampling Data. In: Levin S.A. (ed.) *Encyclopedia of Biodiversity*, second edition, Volume 5, pp. 195-211.
- Haldar GC, Mazid MA and Ahmed K. 1992. Limnology and primary production of Kaptai lake, Bangladesh. In: *Reservoir Fisheries of Asia* (ed. S.S. De Silva). Proceedings of the 2nd Asian reservoir fisheries workshop held in Hangzhou, People's Republic of China, 15-19 October, 1990. IDRC, Ottawa, ON, Canada. IDRC- 291e. pp. 2-11.
- Hasan M, Hasan AS and Bhuyan MS. 2017. Fish diversity assessment of the haor region in Kishoreganj district, Bangladesh. *Res. J. Environ. Sci.*, **11**(1), 29-35.
- Hossain MA and Rabby AF. 2020. Seasonality of physicochemical parameters and fin fish diversity at Hakaluki Haor (Fenchungonj Upazilla), Sylhet, Bangladesh. *Marine Life Sci.*, **2**(2): 113-119.
- Huda ATMN, Shah MS, Hasanuzzaman AFM and Azam MR. 2009. An Investigation on the Ichthyofauna of the Gorai-Modhumati River System. *Bang J. Zool.*, **37**(1):11-24.
- Imteazzaman AM and, Galib SM. 2013. Fish Fauna of Haldi Beel, Bangladesh. *Inter. J. Curr. Res.*, **5**(1): 287-290.
- Iqbal MM, Nasren S and Mosarof Hossain M. 2015. Fish assemblage including threatened species in Hakaluki Haor, Sylhet, Bangladesh. *J. Aqua. Trop.*, **30**(3–4): 223-246.
- Islam J, Anisuzzaman, Minar MH and, Sarker J, “Fish Biodiversity of Dingaputa Haor and its Surrounding Area of Mohanganj Upazila, Netrakona District.2013. *J. Ocean Res.*, **1**(1): 1-5.
- Islam MS, Jahan J, Mou MA, Kabir MH and Uddin MJ. 2017. Investigation of water quality and fish status of Karimganj Haor area in Kishoreganj. *J. Environ. Sci. Nat. Reso*, **10**(2): 19-27.
- Islam MS, Suravi and Meghla NT. 2010. Investigation on water quality in the Ashulia Beel, Dhaka. *Bangladesh J. Fish. Res.*, **14**(1-2): 55-64.
- Islam SM, Haque SA, Islam F, Rahman M, Rahman M, Das PS and Karmakar M. 2021. Diversity assemblages of fish genetic resources and conservation necessities in Hakaluki Haor, an ecologically sensitive natural wetland in north-eastern Bangladesh. *J. South Pacific Agri.*, **24**: 1-11.
- Jannatul F M, Rashidul K, Amzad M and Arifur R. 2015. Fin fish assemblage and biodiversity status of carps on halda river. *Annals Vet. Ani. Sci.*, **2**(6): 151-161.
- Jewel MAS, Haque MA, Khatun R and Rahman MS. (2018). A comparative study of fish assemblage and diversity indices in two different aquatic habitats in Bangladesh: Lakhandaha Wetland and Atari River. *Jordan J. Biol. Sci.*, **11**(4): 427-434.
- Joadder MAR, Galib SM, Haque SMM and Chaki N. 2015. Fishes of the river Padma, Bangladesh: Current trend and conservation status. *J. Fish.*, **3**: 259–266.
- Jost L. (2010). The Relation between Evenness and Diversity. *Diversity*, **2**: 207–232.
- Khan MAG, Chowdhury SH and Paul JC. 1996. Community structure and ecology of microbenthic invertebrate fauna of Lake Kaptai, Bangladesh. *Trop. Ecol.*, **37**(2): 229-245.
- Khan MAI, Hossain AMM, Huda ME, Islam MS and Elahi SF. 2007. Physicochemical and biological aspects of monsoon waters of Ashulia for economic and aesthetic applications: preliminary studies. *Bangladesh J. Scien. Industr. Res.*, **42**(4): 377-396.
- Khan MS, Haq E, Huq S, Rahman A, Rashid SMA and Ahmed H. 1990. Wetland of Bangladesh: A report. 1-79.
- Margalef R. 1968. *Perspectives in ecological theory*. Chicago: University of Chicago Press.
- Maria AB, Iqbal MM, Hossain MAR, Rahman MA Uddin S, Hossain MA and Javed MN. 2016. Present status of endangered fish species in Sylhet Sadar, Bangladesh. *Int. J. Nat. Sci.*, **6**(2): 104-110.
- Mazumder SK, Das SK, Ghaffar MA, Rahman MH, Majumder MK and Basak LR. 2016. Role of co-management in wetland productivity: A case study from Hail haor in Bangladesh. *AACL Bioflux*, **9**(3): 466-482.
- Mohsin ABM, Haque SkM, Galib SM, Hassan F, Chaki N, Islam N and Rahman M. 2013. Seasonal Abundance of Fin Fishes in the Padma River at Rajshahi District, Bangladesh. *World J. Fish Mar. Sci.*, **5**(6): 680-685.
- MoW. 2005. Government of the People's Republic of Bangladesh.

- Mustafa MG, Sarker GC, Anwar SN, Ahsanuzzaman M, Rahman S, Azher S and Morshed RM. 2019. Analysis of pond fisheries in climate change scenario in the Haor region of Bangladesh. *Adv. Res.*, 1-14.
- Muzaffar S. 2004. Diurnal time-activity budgets in wintering Ferruginous Pochard *Aythya nyroca* in Tanguar Haor, Bangladesh. *Forktail*, **20**(2): 25-27.
- Nath B and Deca C. 2012. A Study on Fish Diversity, Conservation Status and Anthropogenic Stress of Chandubi Tectonic Lake, Assam, India. *J. Bio. Innov.*, **1**(6):148-155.
- Nelson JS. (2006). *Fishes of the world* (4th ed.). London: Wiley.
- Pandit D, Kunda M, Harun-al-rashid A, Sufian MA and Mazumder SK. 2015. Present status of fish biodiversity in Dekhar Haor, Bangladesh : a case study. *World J. Fish Mar. Sci.*, **7**(4): 278-287.
- Pielou EC. 1966. Species diversity and pattern diversity in the study of ecological succession. *J. Theor. Biol.*, **3**: 131-144.
- Poffenberger M. 2000. Communities and forest management in South Asia: a regional profile of the Working Group on Community Involvement in Forest Management. *Communities and forest management*
- Quddus MMA and Shafi M. 1983. *Bangaposagar Matsya Sampad* (The Fisheries Resources of the Bay of Bengal). Dhaka: Kabir Publications.
- Quddus MMA, Sarker MN and Banerjee AK.1988. Studies of the chondrichthyes Fauna (Sharks, Skates and Rays) of the Bay of Bengal. *The Journal of Noami.*, **5**: 19-39.
- Rahman AKA, Kabir SMH, Ahmad M, Ahmed ATA , Ahmed ZU and, Begum ZNT. 2009. Encyclopedia of Flora and Fauna of Bangladesh. *J. Asiatic Soci. Bangladesh.* **24**: 2-57.
- Rahman AKA.1989. *Freshwater fishes of Bangladesh* (1st ed., p. 364). Dhaka: Zoological Society of Bangladesh, University of Dhaka.
- Rahman AKA.2005. *Freshwater fishes of Bangladesh* (2nd ed.). Dhaka: Zoological Society of Bangladesh, Department of Zoology, University of Dhaka.
- Rahman MS.1992. *Water quality management in aquaculture*. Bangladesh: BRAC Prokashana, pp. 84.
- Roy BJ, Dey MP, Alamand MF and Singh NK. 2007. Present status of shark fishing in the marine water of Bangladesh. UNEP/CMS/MS/Inf/10.17p. Retrieved March 15, 2009, from [Sharks/pdf-docs/Inf-10-Bangladesh-Presentation-on-Shark-Fishing.pdf](#).
- Saha BK and Hossain MA. 2002. Saldu Beel fishery of Tangail. *Bang. J. Zool.*, **30**(2): 187-194.
- Salauddin M and Islam AKMS. 2011. Identification of land cover changes of the haor area of Bangladesh using modis images.In: 3rd international conference on water and flood management (ICWFM-2011).
- Shannon CE and Wiener W. (1949). *The mathematical theory of communication* (p. 117). Urbana, IL: University of Illinois Press.
- Sunny AR, Alam R, Sadia MA, Miah Y and Hossain S. 2020. Factors affecting the biodiversity and human well-being of an ecologically sensitive wetland of North Eastern Bangladesh. *J. Coastal Zone Manag.*, **23**(1): 1-8.
- Talwar PK and Jhingran AG. 1991. *Inland fishes of India and adjacent countries* (Vol. 1 and 2). New Delhi: Oxford and IBH Publishing Company Pvt. Ltd.
- Thompson P, Das AK, Deppertand DL and Chouhury SN. 2007. Changes in biodiversity with wetland restoration and fish reintroduction, MACH technical paper 5. Dhaka: Winrock International.

Moderately Thermophilic Bacteria from Jordanian Hot Springs as Possible Sources of Thermostable Enzymes and Leukemia Cytotoxic Agents

Maher Obeidat^{1,*}, Belal Al-Shomali²

¹Department of Medical Laboratory Sciences, Faculty of Science, Al-Balqa Applied University, Al-Salt, Jordan; ²Department of Biotechnology, Faculty of Agricultural Sciences, Al-Balqa Applied University, Al-Salt, Jordan.

Received: December 8, 2022; Revised: January 22, 2023; Accepted: January 28, 2023

Abstract

This study was conducted to isolate and identify thermophilic and thermotolerant bacteria from Jordanian hot springs and to determine hydrolytic, antimicrobial, and anticancer activities of the isolates. Thirty bacterial isolates were recovered from water samples of five main local hot springs. Nineteen of the isolated colonies were light yellow and circular to rhizoid on nutrient agar; cells were Gram-positive, endospore-forming, and rod-shaped. Eleven isolates were Gram-negative non-spore forming rods. It was found that 21 isolates met the criteria of moderate thermophiles; all isolates were grown aerobically (JA5 was facultative anaerobes) at 40-60 °C, pH 6-9, and 0-4% salt concentration and most of these isolates were reacted positively with catalase and oxidase. The remaining nine isolates were thermotolerant. Depending on the 16S rRNA gene sequences of the isolates, it was found that 19 thermophilic isolates have 97-100% sequence homology to the genus *Bacillus*; eight isolates were closely related to the thermophilic genus *Geobacillus* showing 97-100% homology to *G. stearothermophilus* ATCC 7953. The isolate JM2 shares 99% sequence homology with *Thermomonas hydrothermalis*. Remarkably, it was found that the 16S rDNA sequence of isolate JZ9 were highly similar (99% identity) to the thermophilic bacterium *Caldimonas hydrothermale*. To our knowledge, this is the first record of *Caldimonas* isolation from Jordanian hot springs. A wide spectrum of hydrolytic activities for protease, lipase, xylanase, cellulase, amylase, and pectinase was detected from the obtained isolates. It was found that JM1, JS3, and JZ11 isolates produced all tested enzymatic activities. Antimicrobial activities were only exhibited by three isolates (thermophilic JH1 and JM11 and thermotolerant JS3). Results indicated that three thermophilic *Bacillus* isolates (JA2, JM11, and JM12) produced selective cytotoxicity against human leukemia cell line K562. Therefore, many of the obtained isolates in this study can be considered as a promising source of effective agents that may be used for medical, pharmaceutical, and industrial purposes.

Keywords: Hot spring; Thermophilic; Thermotolerant; *Caldimonas*; Enzymatic; Leukemia

1. Introduction

Thermophiles can live and reproduce in hot environments where they have been able to grow at high temperature and they have been isolated from many geothermal sites such as hot springs. They are classified into moderate (40 to 70 °C), extreme (55 to 85 °C), and hyperthermophiles (75 to 113 °C) based on their growth temperatures (Baker *et al.*, 2001). Generally, moderate thermophiles are primarily bacteria (Baker *et al.*, 2001). Interest in thermophilic bacteria has come from their significant potential for production of valuable compounds such as thermostable enzymes, antibiotics, and hormones (Maugeri *et al.*, 2001; Singh, 2006).

Hot springs are fairly distributed in Jordan and formed due to volcanic activity or movement of the Earth's crust which form a pressure leads to the upward mobilization of heated water (Simoneit *et al.*, 2000). Different microbial communities have been successfully colonized in hot springs predominantly thermophilic bacteria such as

Bacillus and thermophilic archaea, for example *Methanococcus* and *Sulfolobus* (Chen and Roberts, 1999; Lengeler *et al.*, 1999; Saul *et al.*, 1999). The genus *Bacillus* is highly diverse and includes many important thermophilic and thermotolerant species that have biotechnological significance as a sources of thermostable enzymes were industrially important such as proteases, lipases, xylanases, amylases, cellulases, pectinases, and DNA restriction endonucleases as well as DNA polymerases including *Taq* DNA polymerase that used for polymerase chain reaction (PCR) (Maugeri *et al.*, 2001).

Thermophilic bacteria have been adapted to hot environments by often having high G+C content in their DNA, more H-bonds, and having reverse DNA gyrase (producing positive supercoils in the DNA) which rise the melting point of DNA (Galtier and Lobry, 1997). In addition, thermophilic bacteria adapt to high temperatures by increased electrostatic, disulphide, and hydrophobic interactions in their proteins. The membrane fatty acids of thermophilic bacteria are highly saturated to remain stable and functional at high temperatures (Galtier and

* Corresponding author. e-mail: obeidat@bau.edu.jo.

Lobry, 1997). Compared with their mesophilic counterparts, the structural and functional proteins of thermophiles are very heat stable due to dehydration and more hydrophobic amino acids and salt bridges (Karlin, *et al.*, 2002).

Jordan has a unique ecological location with extreme environments including hot springs. There are about 200 thermal springs in Jordan distributed in three territories (Swariéh, 2000). Interest in isolation and identification of thermophilic organisms from hot springs in Jordan has been growing in recent years. Most of the isolated bacteria in such springs were found to belong to the genus *Bacillus* (Khalil, 2002; Malkawi and Al-Omari, 2010; Fandi *et al.*, 2012; Obeidat *et al.* 2012; Mohammad *et al.* 2017). Moreover, the ability of the isolated thermophilic *Bacillus* species to produce thermostable enzymes that have importance in industrial and biotechnological applications was also investigated (Al-Qodah, 2006; Obeidat *et al.*, 2012; Mohammad *et al.* 2017). Therefore, this study was conducted to isolate and identify thermophilic bacteria from Jordanian hot springs and to determine their extracellular enzymatic activity as well as their antimicrobial activity. Furthermore, because all current treatments for cancer have not until now adequate and have not been conducted on the level of medical community satisfaction, this research was also aimed to evaluate the possible anticancer effect of isolated bacteria from local hot springs.

2. Materials and Methods

2.1. Collection of samples and isolation of bacteria

Fifty water samples (10 from each selected hot spring) were collected during summer/ 2011 from five main Jordan hot springs (Hammat Afra, Jordan Himma, Shuna-North, Zara-Bani Hamida, and Ma'in-Roman Bath). The samples were collected in 500 ml sterile containers from 20-40 cm below the surface away from the margin. After filtration of water samples through 0.45 µm membrane filter, the remaining residues on membrane filter were resuspended in 10 ml of sterile water. A 100 µl aliquot from each sample was plated by spreading on nutrient agar (NA) plates (five replicates) and incubated, aerobically and anaerobically, for 48 hr at 40°C. The developing colonies were selected and subcultured on NA medium.

2.2. Phenotypic and physiological characterization of isolates

Phenotypic characteristics including colony and cell morphology, Gram and endospore stainings along with catalase and oxidase activity were performed for each isolate according to the standard protocols. To determine the cardinal temperatures and pH ranges for the growth of each isolate, the isolates were incubated in NB medium at 20°C to 80°C with an interval of 5 units and at pH in the range 4.0-12.0 in NB medium with an interval of 0.5 unit using hydrochloridric acid (HCl) or sodium hydroxide (NaOH). Growth was checked after 24 hr of incubation. The effect of sodium chloride (NaCl) concentration on the growth of isolates was studied by incubating the bacterial isolates at 40°C for 24 hr in 10 ml NB medium containing 0.0 to 10% NaCl with 0.5% interval. Growth was checked after 24 hr of incubation.

2.3. PCR amplification, sequencing, and phylogenetic analysis of the 16S rRNA gene

Luria Bertani (LB) broth cultures of bacterial isolates and the reference strain *Geobacillus stearothermophilus* ATCC 7953 were incubated overnight with shaking at 150 rpm at 40°C. After centrifugation of LB cultures at 14000 rpm for 5 min, cell pellets were washed two times with distilled water, then the genomic DNA was extracted, using Wizard Genomic DNA purification kit (Promega, USA, part no. A1120), according to the manufacturer's instructions.

The 16S rRNA gene from purified genomic DNA was amplified by PCR according to Belduz *et al.* (2003) using the forward primer UNI16S-L (5'-ATTCTAGAGTTTGATCATGGCTCA- 3') and the reverse primer UNI16S-R (5'-ATGGTACCGTGTGACGGGCGGTGTGTA- 3'). The PCR products with predicted size of ~1400 bp were analyzed by 1.5% agarose gel electrophoresis using 10 µl of each PCR sample. The 1 kb DNA ladder marker (Genedirex, USA) was used and the generated bands were digitally photographed under UV light.

Using the ABI PRISM cycle sequencing kit (Macrogen, Korea), the 16S rRNA gene sequences from the isolates and the reference strain *G. stearothermophilus* ATCC 7953 were determined. They were then compared with those found in GenBank using BLAST search. Then, the phylogenetic tree was created by DNAMAN software for the closely related sequences that were retrieved from the database.

2.4. Extracellular enzymatic activity

Six enzymatic activities were assessed for each bacterial isolate; protease, lipase, xylanase, cellulase, amylase, and pectinase activities were detected using the diffusion agar method on skim milk agar medium, lipase test medium, xylanase test medium, carboxymethylcellulose (CMC) medium, starch medium, and polygalacturonase (PGase) test medium, respectively. Sterile cork borer (6 mm i.d.) was used to make wells in each medium and 50 µl from bacterial NB-culture (about 10⁶ CFU / ml) was added into each well and left for 1 hr for proper diffusion (Gessner, 1980; Priest *et al.*, 1988; Bragger *et al.*, 1989; Kobayashi *et al.*, 1999; Habá *et al.*, 2000; Ten *et al.*, 2004).

For protease and lipase tests, after incubation at 40°C for 48 hr, the development of clear zones around wells indicated the presence of proteolytic activity (Priest *et al.* 1988) and the appearance of opaque halos around the wells demonstrated a positive lipase activity (Habá *et al.*, 2000). For xylanase and cellulase activities, after incubation for 3 days at 40 °C, 0.1% Congo red solution was poured onto the plates and left for 30 minutes at room temperature. Then, the plates were washed with 1 M NaCl solution. Clear zones around the wells on a red background were taken as the evidence for the xylanase and cellulase activities (Bragger *et al.*, 1989; Ten *et al.*, 2004). After incubation for 48 hr at 40 °C, starch plates were flooded with 1% iodine solution to determine amylase activity. The development of yellow clear zones around the wells against a blue background was interpreted as an indication of positive α-amylase activity (Gessner, 1980; Bragger *et al.*, 1989). After incubation of PGase medium for 3 days at 40 °C, pectinase activity was determined by pouring 1%

cetyltrimethylammoniumbromide (CTAB) solution onto the surface of the plates and left for 10 min at room temperature. The formation of clear zones around wells was taken as an indication of positive pectinase activity (Kobayashi *et al.*, 1999).

2.5. Preparation of bacteria for antimicrobial and anticancer activities

To examine the antimicrobial and anticancer activities, cultures of isolated bacteria from hot springs were grown in 25 ml NB at 40°C for one week and centrifuged at 13,000 rpm for 10 min. The supernatant was evaporated after being filtered through a 0.45 µm membrane filter. To get a concentration of 200 mg/ml, the leftover residues were resuspended in a suitable amount of phosphate buffer saline (PBS).

2.6. Antimicrobial activity

To research an isolate's antibacterial and antifungal properties, 11 reference bacterial species (*Staphylococcus aureus* ATCC 25923 and Methicillin resistant *S. aureus* ATCC 95047 (MRSA), *Escherichia coli* ATCC 8739 and ATCC 25922, *Klebsiella pneumonia* ATCC 7700 and *K. oxytoca* ATCC 13182, *Proteus vulgaris* ATCC 33420 and *P. mirabilis* ATCC 12453, *Pseudomonas aeruginosa* ATCC 27253, *Salmonella typhimurium* ATCC 14028 and *Enterobacter aerogenes* ATCC 35029) were cultured in NB at 37°C for 24 hr to achieve 2×10^6 CFU/ml and two fungal species (*Candida albicans* ATCC 10231 and *Aspergillus brasiliensis* ATCC 16404) were cultured in sabouraud dextrose broth (SDB) at 28 °C for 48 hr that adjusted to achieve 2×10^5 spore/ml for fungi (Ceylan *et al.*, 2008).

Resuspended crudes of each bacterial isolate were screened for antimicrobial activities using the agar-well diffusion method. A 50 µl aliquot from each test microorganism was swabbed on NA medium for bacteria and sabouraud dextrose agar for fungi. A sterile cork borer (6 mm i.d.) was used to create three wells in the medium. Following that, 50 µl of the crude (10 mg) from each isolate was carefully poured to each well and incubated at 40°C for 48 hours after being let to stand on the bench for 1 hr. The antibacterial and the antifungal activities were measured by assessment of the diameter of generated inhibition zones in mm (Ceylan *et al.*, 2008). Data were expressed as the mean ± standard deviation (SD).

2.7. Hemolytic and anticancer activities

The type of hemolysis for bacterial crudes was verified by inoculating 50 µl of crude into each well (6 mm i.d.) prepared on blood agar plates and incubating the plates at 40°C for 48 h (Carillo *et al.*, 1996).

Normal mammalian Vero cells and human leukemia cancer cell line K562 were used to investigate the anticancer activities of non-hemolytic bacterial crudes. The K562 cells and Vero cells were cultured in Roswell Park Memorial Institute (RPMI) 1640 medium and in Dulbecco's Modified Eagle Medium (DMEM) medium, respectively, and incubated at 37°C in a humidified 5% CO₂ incubator according to Freshney (1987). The cells were harvested, subcultured, and reseeded in fresh medium every 48 h.

To determine the selective cytotoxicity of non-hemolytic bacterial crudes, 200 µl of non-hemolytic

bacterial crude (2 mg/well) was added to 200 µl of freshly harvested cells and 100 µl medium in each 96 well micro test plate. Then, the plates were incubated at 37°C in a humidified 5% CO₂ incubator for 48 hr. The viability of cells was determined by MTT assay as previously demonstrated by Mosmann (1983) and Heiss *et al.* (1997) using ELISA microplate reader at 450 nm with 630 nm reference wavelength. Each treatment was performed in triplicate and repeated five times.

2.8. Statistical Analysis

The cytotoxicity of non-hemolytic bacterial crudes was calculated according to Obeidat (2017), and the median inhibitory concentration (IC₅₀) was determined by comparing the average of mortality values with control by using the most fit non-linear regression analysis software.

3. Results

3.1. Isolation of bacteria from Jordanian hot springs

In the current study, the existence of thermophilic bacteria in hot water was investigated in five main hot springs distributed through the three territories of Jordan (Table 1), including Jordan-Himma and Shuna-North in North territory, Ma'in-Romman Bath and Zara-Bani Hamida in Middle territory, and Hammat Afra in South territory. The water temperatures and pH of thermal vents are approximately 40-65 °C and 6.0-7.0, respectively. Table 1 demonstrated that a total of 30 diverse bacterial isolates were obtained from the screened water samples.

Table 1. Diversity of moderately thermophilic and thermotolerant bacteria from five main Jordanian hot springs

Territory	Thermal Vent	Water Temperature (°C)	Water pH	No. of Selected Isolates
North	Jordan Himma	42.1	7.0	7
	Shuna-North	54.5	6.6	2
Middle	Ma'in-Roman Bath	62.3	6.0	8
	Zara-Bani Hamida	54.1	6.3	8
South	Hammat Afra	48.2	6.5	5
Total				30

3.2. Phenotypic and physiological characterization of isolates

Regarding morphological, physiological, and some biochemical properties, 21 bacterial isolates obtained from hot springs were unable to grow below 40 °C and met the criteria of thermophilic bacteria (Table 2 and 3). Out of them, 19 were Gram-positive, rod-shaped, endospore-forming, and most of their developed colonies on nutrient agar were light yellow circular to rhizoid (Table 2), whereas the remaining thermophilic isolates JM2 and JZ9 were Gram-negative non-spore forming rods and produced light brown and transparent colonies, respectively (Table 3). On the other hand, nine isolates (JA4, JH7, JH8, JM13, JM14, JS3, JZ11, JZ12, JZ14) were found thermotolerant (can grow below 40 °C) Gram-negative non-spore forming rods (Table 3). As shown in Tables 2 and 3, all isolates were able to grow aerobically (JA4, JA5, JH8, JM14 and

JS3 were facultative anaerobes) and exhibited positive-catalase and positive-oxidase for 13 thermophilic isolates (JA2, JA5, JH4, JM1, JM2, JM5, JM7, JM11, JM12, JS1, JZ1, JZ5, JZ9, and JZ13) and for two thermotolerant isolates (JH7 and JZ14).

All thermophilic isolates were capable to grow at 40 to 60 °C (optimum growth temperature at 50 °C; except JA5 has 55 °C optimum temperature). However, most thermotolerant isolates were able to grow between 30 to 60 °C and the optimum growth temperature was in the range of 30-40 °C (Table 2 and 3). Moreover, all isolates were able to grow at pH 6 to 9 and in 0-4% salt concentration; six thermophilic isolates (JA2, JA3, JH3, JH4, JH6, and JM5) and one thermotolerant isolate (JM13) were found tolerant to 10% NaCl concentration.

For further identification of Gram-negative non-spore forming rod-shaped bacteria, some biochemical tests were

investigated (Table 3). All isolates were negative for indole and methyl red (MR). JZ9 was the only isolate that exhibited urease activity. It was found that four isolates (JM13, JM14, JZ11, and JZ12) were non-motile, catalase-positive, oxidase-negative, and reacted negatively for Voges-Proskauer (VP), citrate, nitrate, and triple sugar iron (TSI) tests (Table 3), three isolates (JA4, JH8, and JS3) were motile, catalase-positive, oxidase-negative, and were reacted positively for VP, citrate, nitrate, and TSI (ferment glucose, lactose and/or sucrose, and give gas bubbles). Isolates JH7 and JZ14 were found motile, catalase-positive, oxidase-positive, utilize citrate, do not reduce nitrate, and give negative TSI (Table 3). The thermophilic isolates JM2 and JZ9 were non-motile and positive for catalase, oxidase, and citrate tests. JM2 was negative for the other tests, while JZ9 was positive for the urease and nitrate tests.

Table 2. Phenotypic and growth characteristics of thermophilic Gram-positive bacterial isolates obtained from Jordanian hot springs

Hot Spring	Isolate	Colony Morphology	Catalase / Oxidase	Gram Stain	Cell Shape	Spore former	O ₂ ^a	Temperature (optimum) ^b	pH	NaCl %
Hammat Afra	JA1	Light yellow, rhizoid, rigid	+ / -	+	Rod	+	+	40-60 (50)	5-11	0-4
	JA2	Light yellow, Flat, circular	+ / +	+	Rod	+	+	40-60 (50)	4-10	0-10
	JA3	Light yellow, circular, convex	+ / -	+	Rod	+	+	40-60 (50)	4-10	0-10
	JA5	Light yellow, rhizoid, mucoid	+ / +	+	Rod	+	±	40-65 (55)	5-10	0-4
Jordan Himma	JH1	Light yellow, circular	+ / -	+	Rod	+	+	40-60 (50)	6-9	0-4
	JH3	Transparent, irregular	+ / -	+	Rod	+	+	40-60 (50)	4-10	0-10
	JH4	Light yellow, irregular	+ / +	+	Rod	+	+	40-60 (50)	4-10	0-10
	JH5	Light yellow, irregular, mucoid	+ / -	+	Rod	+	+	40-60 (50)	5-10	0-5
	JH6	Light yellow, flat, circular	+ / -	+	Rod	+	+	40-60 (50)	5-10	0-10
Ma'in-Roman Bath	JM1	Paige, rhizoid, mucoid	+ / +	+	Rod	+	+	40-60 (50)	6-9	0-4
	JM5	Paige, circular	+ / +	+	Rod	+	+	40-60 (50)	4-11	0-10
	JM7	Light yellow, rhizoid, rigid	+ / +	+	Rod	+	+	40-60 (50)	5-11	0-8
	JM11	Milky, undulate margins	+ / +	+	Rod	+	+	40-60 (50)	4-10	0-5
	JM12	Yellow, rhizoid	+ / +	+	Rod	+	+	40-60 (50)	4-10	0-5
Shuna-North	JS1	Light yellow, circular	+ / +	+	Rod	+	+	40-60 (50)	6-9	0-5
Zara-Bani Hamida	JZ1	Light yellow, rhizoid, rigid	+ / +	+	Rod	+	+	40-60 (50)	6-11	0-7
	JZ5	Light yellow, rhizoid, mucoid	+ / +	+	Rod	+	+	40-60 (50)	6-9	0-5
	JZ10	Dull gray, undulate margins	+ / -	+	Rod	+	+	40-60 (50)	4-10	0-5
	JZ13	Light yellow, Flat, circular with undulate margin	+ / +	+	Rod	+	+	40-60 (50)	4-10	0-5

^aO₂ Requirement: +; aerobic, ±; facultative anaerobes. ^bTemperature is measured in °C.

Table 3. Phenotypic and growth characteristics of thermotolerant and thermophilic Gram-negative bacterial isolates obtained from Jordanian hot springs

Isolate	JA4	JH7	JH8	JM2	JM13	JM14	JS3	JZ9	JZ11	JZ12	JZ14
Colony Morphology	Gray, moist, smooth	Yellow, circular	Translucent, circular	Light brown, circular	Opaque yellow, mucoid	milky, mucoid, smooth	Light yellow, circular	Transparent circular	Gray, domed, mucoid, smooth	pale, mucoid	Yellow, circle
Catalase	+	+	+	+	+	+	+	+	+	+	+
Oxidase	-	+	-	+	-	-	-	+	-	-	+
Gram Stain	-	-	-	-	-	-	-	-	-	-	-
Cell Shape	Rod	Rod	Rod	Rod	Coccobacilli	Rod	Rod	Rod	Coccobacilli	Coccobacilli	Rod
Sporulation	-	-	-	-	-	-	-	-	-	-	-
Motility	+	+	+	-	-	-	+	+	-	-	+
O ₂ ^a	±	+	±	+	+	±	±	+	+	+	+
Temperature (optimum) ^b	20-65 (35)	20-60 (40)	20-65 (35)	40-60 (50)	30-60 (40)	30-60 (40)	20-55 (40)	40-65 (50)	30-60 (40)	35-60 (40)	30-60 (40)
pH	5-10	5-10	5-11	6-9	4-10	5-10	5-9	8-9	4-10	4-10	5-10
NaCl %	0-4	0-5	0-4	0-4	0-10	0-4	0-4	0-6	0-5	0-5	0-5
Indole	-	-	-	-	-	-	-	-	-	-	-
Methyl red	-	-	-	-	-	-	-	-	-	-	-
Voges Proskauer	+	-	+	-	-	-	+	-	-	-	-
Citrate	+	+	+	-	-	-	+	+	-	-	+
Urease	-	-	-	-	-	-	-	+	-	-	-
Nitrate	+	-	+	-	-	-	+	+	-	-	-
TSI ^c	A/A,+,-	K/K,-,-	A/A,+,-	K/K,-,-	K/K,-,-	K/K,-,-	A/A,+,-	ND	K/K,-,-	K/K,-,-	K/K,-,-

^aO₂ Requirement: +; aerobic, ±; facultative anaerobes.

^bTemperature is measured in °C.

^cTSI: Triple Sugar Iron; A/A,+,-: glucose, lactose and/or sucrose fermentation, gas bubbles production but no H₂S production; K/K,-,-: no fermentation, no gas bubbles and no H₂S production.

3.3. Molecular characterization and sequence alignment

To confirm the conventional methods of classification of the bacterial isolates, the 16S rRNA gene sequence of the isolates and *G. stearothermophilus* ATCC 7953 was investigated by amplification with UNI16S-L and UNI16S-R primers and production of PCR band with about 1400 bp in size (Figure 1). Based on the 16S rDNA sequences' BLAST matching to GenBank sequences, 19 thermophilic isolates from all examined hot springs were found to belong to the genus *Bacillus/Geobacillus* with 97-100% identity and the thermophilic Gram-negative bacterial isolates JM2 and JZ9 showed 99% homology to the genera *Thermomonas* and *Caldimonas*, respectively (Table 4). For thermotolerant Gram-negative bacterial isolates, BLAST alignment of GenBank sequences demonstrated that four isolates (JM13, JM14, JZ11 and JZ12) were closely related to the genus *Acinetobacter* with 96-99% identity. Isolates JA4 and JH8 were shown 98% identity to the genus *Enterobacter*. Isolates JH7 and JZ14

were found closely related, with 97% and 99% identity respectively, to the genus *Pseudomonas*. The remaining isolate JS3 was found closely related, with 96% identity, to the genus *Cronobacter* (Table 4).

Based on the obtained sequences, a homology matrix and a phylogeny tree were created as shown in Figure 2. The phylogenetic analysis of the 16S rDNA sequences illustrated that Gram-positive and Gram-negative isolates were allocated into two separate clades and reflected the affiliation of eight thermophilic isolates (JA1, JH1, JH5, JM1, JM5, JS1, JZ1, and JZ5) to *Geobacillus* with 97-100% sequence homology to the reference strain *G. stearothermophilus* ATCC 7953; the 16S rRNA gene sequence of isolates JA1, JH1, and JM1 had 100% identity to *G. stearothermophilus* ATCC 7953. Moreover, it was observed that the 16S rDNA sequence of nine thermophilic isolates had 97 to 100% identity to the thermophilic bacteria *Bacillus licheniformis* (Table 4).

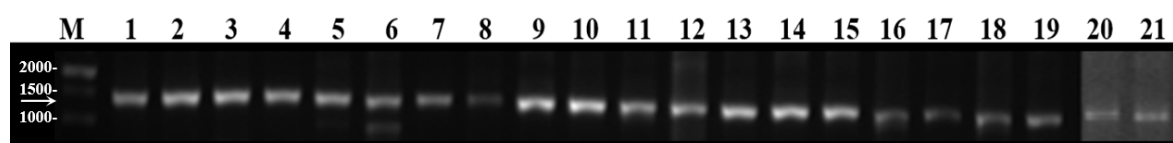


Figure 1. Electrophoresis of PCR amplification of 16S rRNA gene fragments with forward primer UNI16S_L and reverse primer UNI16S_L of thermophilic isolates on 1.5% agarose gel. Lanes 1-21: isolates JA1, JA2, JA3, JA5, JH1, JH3, JH4, JH5, JH6, JM1, JM2, JM5, JM7, JM11, JM12, JS1, JZ1, JZ5, JZ9, JZ10, and JZ13, respectively. Lane M: 1 kb DNA ladder marker (Genedirex, USA); the molecular size of DNA bands is in base pairs (bp). The left arrow indicated 1400 bp band.

Table 4. Comparing the 16S rRNA gene sequences of the 30 isolates to those at GenBank

Thermal Vent	Isolate	Sequence		
		No. of aligned nucleotides	Closest phylogenetic relative (GenBank accession No.)	% identity ^a
Thermophilic Isolates				
Hammat Afra	JA1	1308	<i>Geobacillus stearothermophilus</i> (HQ143640)	99
	JA2	1359	<i>Bacillus licheniformis</i> (CP022477)	98
	JA3	1356	<i>Bacillus licheniformis</i> (DQ071568)	97
	JA5	1394	<i>Bacillus licheniformis</i> (JX847115)	97
Jordan Himma	JH1	1369	<i>Geobacillus stearothermophilus</i> (HQ143640)	100
	JH3	1237	<i>Bacillus</i> sp.(C4KC310834)	98
	JH4	1252	<i>Bacillus licheniformis</i> (FJ614258)	97
	JH5	1381	<i>Geobacillus</i> sp. RSNPB7 (HM588147)	97
	JH6	1311	<i>Bacillus licheniformis</i> (KP050497)	97
Ma`in-Roman Bath	JM1	1237	<i>Geobacillus stearothermophilus</i> (HQ143640)	99
	JM2	1284	<i>Thermomona hydrothermalis</i> (AF542054)	99
	JM5	1271	<i>Geobacillus</i> sp. RSNPB7 (HM588147)	99
	JM7	1082	<i>Bacillus licheniformis</i> (DQ071560)	99
	JM11	1341	<i>Bacillus</i> sp.(C4KC310834)	97
	JM12	1370	<i>Bacillus licheniformis</i> (FJ614258)	100
Shuna-North	JS1	1134	<i>Geobacillus</i> sp. RSNPB7 (HM588147)	97
Zara-Bani Hamida	JZ1	1240	<i>Geobacillus kaustophilus</i> (NC006510)	99
	JZ5	1373	<i>Geobacillus</i> sp. RSNPB7 (HM588147)	97
	JZ9	1291	<i>Caldimonas hydrothermale</i> (HE798193)	99
	JZ10	1391	<i>Bacillus licheniformis</i> (KC443100)	97
	JZ13	1398	<i>Bacillus licheniformis</i> (JQ411812)	100
Thermotolerant Gram-negative Isolates				
Hammat Afra	JA4	1438	<i>Enterobacter</i> sp. (GQ418085)	98
Jordan Himma	JH7	1291	<i>Pseudomonas</i> sp. (DQ205301)	97
	JH8	1300	<i>Enterobacter</i> sp. (JN697628)	98
Ma`in-Roman Bath	JM13	1365	<i>Acinetobacter calcoaceticus</i> (JN700142)	99
	JM14	1356	<i>Acinetobacter baumannii</i> (JN668579)	97
Shuna-North	JS3	1099	<i>Cronobacter sakazakii</i> (HQ880366)	96
Zara-Bani Hamida	JZ11	1372	<i>Acinetobacter baumannii</i> (JX966428)	97
	JZ12	1399	<i>Acinetobacter baumannii</i> (JN669235)	96
	JZ14	1345	<i>Pseudomonas</i> sp. (DQ205301)	99

^aThe percentage identity with the 16S rRNA gene sequence of the closest phylogenetic relative of bacteria.

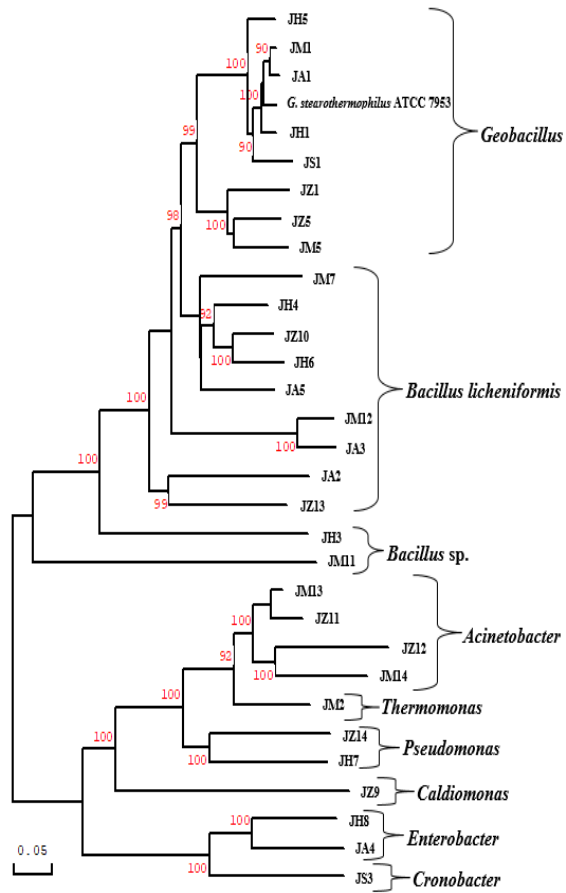


Figure 2. Phylogenetic analysis of 16S rDNA sequences of 21 thermophilic isolates, 9 thermotolerant isolates, and *G. stearothermophilus* ATCC 7953. The phylogenetic tree is based on the maximum likelihood parameter analysis. The bootstrap confidence values are shown at the nodes and expressed as percentages of 1000 replications.

3.4. Hydrolytic Activities

Figure 3 illustrates the distribution of hydrolytic activities among 30 bacterial isolates obtained from thermal water of five hot springs investigated in this study.

It was found that Jordanian hot springs were rich in bacteria producing protease (27 isolates), lipase (20 isolates), xylanase (22 isolates), cellulase (18 isolates), amylase (20 isolates), and pectinolytic/polygalacturonase (16 isolates).

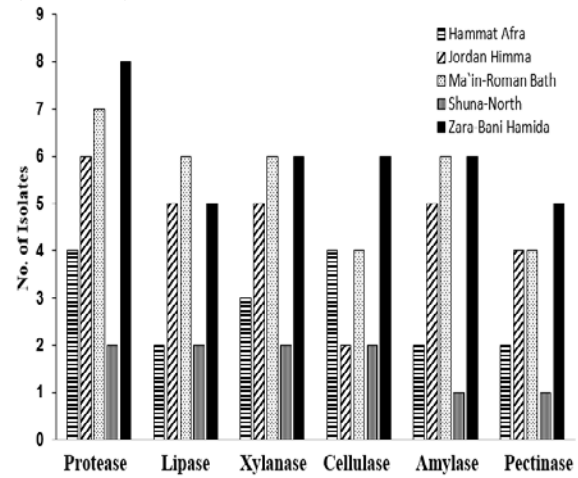


Figure 3. Hydrolytic activities of the obtained 30 bacterial isolates from five Jordanian hot springs.

Results of hydrolytic activities produced from tested thermophilic and thermotolerant bacterial isolates obtained from local hot springs indicated that most isolates produced wide spectrum of enzymes (Table 5). Interestingly, it was found that one thermophilic isolate (JM1) and two thermotolerant isolates (JS3 and JZ11) produced all enzymatic activities tested in this study. All isolates produced protease activity except JA4, JH6, and JM14. The degree of protease activity in most isolates was high. Lipase and amylase activities, ranged from low to very high, were observed in two-third of the isolates. More than 50% of the isolates had polygalacturonase activity ranged from low to high. It was noticed that the degree of enzymatic activities was low to moderate in all isolates producing xylanase or cellulase.

Table 5. Enzymatic activities of bacterial isolates obtained from Jordanian hot springs

Hot Spring	Isolate	Protease	Lipase	Xylanase	Cellulase	Amylase	Polygalacturonase
Hammat Afra	JA1	+	++	++	++	-	+++
	JA2	++++	-	-	+	++	+
	JA3	++	-	+	++	-	-
	JA4	-	-	+	+	-	-
	JA5	++++	++	-	-	++	-
Jordan Himma	JH1	++++	+	+	-	-	+++
	JH3	++	+++	++	-	+++	-
	JH4	+++	++	-	-	+++	+
	JH5	+++	-	-	-	-	++
	JH6	-	+++	++	-	+	-
	JH7	+++	+++	+	++	+++	-
	JH8	++	-	+	+	++	++
	Ma'in-Roman Bath	JM1	++	+++	++	+	++++
JM2		+++	+	-	+	+++	-
JM5		+++	++	++	+	+++	-
JM7		++	++	+	-	++++	-
JM11		+++	++	+	-	-	+
JM12		++	++	+	-	++	+
JM13		++++	-	+	-	++	+
JM14		-	-	-	+	-	-
Shuna-North	JS1	+++	++	++	+	-	-
	JS3	++	+	+	+	+++	+
Zara-Bani Hamida	JZ1	++	++	-	+	+++	++
	JZ5	+	++	+	-	++++	-
	JZ9	+	++	+	+	-	+
	JZ10	++++	-	++	++	+++	-
	JZ11	++	++	+	+	+++	++
	JZ12	+++	++	+	+	-	-
	JZ13	+++	-	-	-	+++	+
	JZ14	+++	-	++	+	++++	+

The degree of enzymatic activity was graded on the basis of the inhibition zone diameter (millimeter): +++++, very high (≥ 31); +++, high (21 to 30); ++, moderate (11 to 20); +, low (7 to 10); \pm , very low (1 to 6); -, no inhibition

3.5. Antimicrobial activities

The inhibitory effects of thermophilic and thermotolerant bacterial crudes were screened against 11 reference bacterial species and two fungal species. It was found that only three isolates (two thermophilic (JH1 and JM11) and one thermotolerant (JS3) isolated from Jordan Himma, Ma'in-Roman Bath, and Shuna-North, respectively) produced antimicrobial effect (Figure 4). Isolates JH1 and JS3 (allocated to genera *Bacillus* and *Coronobacter*, respectively) exhibited antibacterial activity against *K. pneumonia* ATCC 7700, whereas the *Bacillus* isolate JM11 showed anticandidal activity against *C. albicans* ATCC 10231. The remaining isolates exhibited neither antibacterial activity nor antifungal activity.

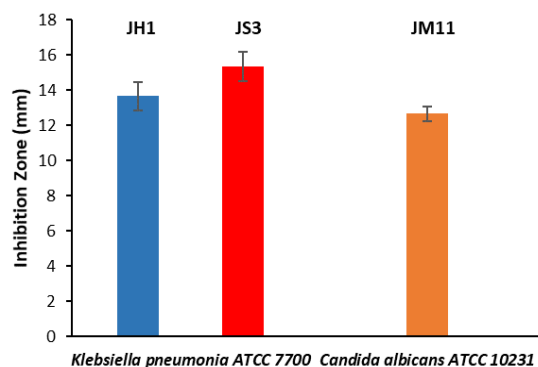


Figure 4. Antimicrobial activity of thermophilic and thermotolerant isolates against test microorganisms. Inhibition zone diameters are expressed as Means \pm SD of triplicate.

3.6. Hemolytic and anticancer activities

The crudes of six thermophilic *Bacillus* isolates (JA1, JA2, JA3, JA5, JM11, and JM12) and five thermotolerant Gram-negative isolates (JA4, JM13, JM14, JZ12, and JZ14) were non-hemolytic (γ -type), whereas the remaining isolates displayed either α - or β -hemolysis against human erythrocytes (Data are not shown).

Non-hemolytic bacterial crudes were selected and screened for their ability to induce cytotoxic effect against normal Vero cells and leukemic K562 cell line (Figure 5). The viability of cells was determined by MTT assay. A total of three non-hemolytic thermophilic isolates obtained from Hammat Afra and Ma'in-Roman Bath (JA2, JM11, and JM12) exhibited very low to low cytotoxicity against Vero cells and very high (Inhibition is greater than 90%) selective cytotoxicity against K562 leukemic cells (Figure 5); selective cytotoxicity of an isolate is when the isolate crude had no to low cytotoxicity against Vero cells and had moderate to very high cytotoxicity against K562 leukemia cells. These cytotoxic isolates JA2, JM11, and JM12 were found to belong to the genus *Bacillus*. Isolate JM11 was the only selective cytotoxic isolate which had antimicrobial activity. As shown in Table 6, the IC₅₀ values of the three cytotoxic bacterial crudes against K562 cells ranged from 1.48 to 1.93 mg, and the highest cytotoxic effect was obtained from JM12.

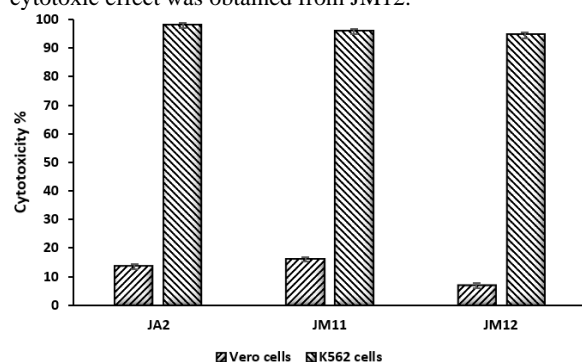


Figure 5. Cytotoxicity screening of non-hemolytic thermophilic and thermotolerant isolates against Vero cells and leukemic cell line K562. The degree of cytotoxicity was expressed as Mean \pm SD and graded on the basis of the relative value of absorbance to the vehicle (Absorbance; Inhibition%): "very high (<0.1; >90%); high (0.1 to <0.4; >60% to 90%); moderate (0.4 to <0.7; >30% to 60%); low (0.7 to <0.9; >10% to 30%); very low (0.9 to <0.95; >5% to 10%); non-toxic (\geq 0.95, \leq 5%)".

Table 6. Cytotoxicity of non-hemolytic thermophilic isolates against leukemic K562 cells

Thermal Vent	Isolate	IC ₅₀ ^a (mg)	R ^{2b}	Regression equation ^c
Hammat Afra	JA2	1.93	0.99	y = 25.713Ln(x) + 33.138
Ma'in-Roman Bath	JM11	1.66	0.98	y = 29.518Ln(x) + 34.988
	JM12	1.48	0.99	y = 32.465Ln(x) + 37.186

^aIC₅₀: the median inhibitory concentration.

^bR²: correlation coefficient.

^cY; inhibition percentage, X; inhibitory concentration at Y (X = IC_Y).

4. Discussion

Due to their potential value in biotechnological and industrial applications, extremophiles have been the focus of substantial and intensive research efforts over the past few decades. The discovery of new chemicals and pathways, the isolation of novel microbial strains, and the molecular and biochemical characterisation of cellular components has been raising these research efforts tremendously. Furthermore, the importance of thermostable biomolecules in the growing field of biotechnology has encouraged research into organisms capable of growth at high temperatures. Thus, the isolation of novel thermophilic organisms, from both the domains archaea and bacteria, has received attention for their potential in the production of thermostable enzymes. For example, DNA polymerases have been obtained from thermophilic bacteria for application in PCR technology. Therefore, the main goals of this study were to isolate thermophilic bacteria from local hot springs and to identify them by phenotypic and molecular tools. Furthermore, this study was initiated to determine the hydrolytic, antimicrobial, and anticancer activities of isolated bacteria in attempt to determine isolates with unique or promising activity. The present study was the first to examine the anticancer activity of moderately thermophilic bacteria detected in water from Jordan hot springs.

Thirty bacterial isolates were isolated from five hot springs in Jordan. Out of them, 19 isolates appeared to belong to moderate thermophiles of the genus *Bacillus* or *Geobacillus* in terms of phenotypic and physiological properties. This result, based on morphological and physiological characteristics, is in agreement with the findings of several preceding studies (Ezeji *et al.*, 2005; Fortina *et al.*, 2001; Nazina *et al.*, 2001, 2004; Romano *et al.*, 2005), whereas the remaining 11 isolates were not related to *Bacillus* because they were Gram-negative, did not produce endospores, and their 16S rRNA gene sequences were allocated into other genera.

To confirm the conventional identification of the bacterial isolates, 16S rDNAs of the 30 isolates along with the *G. stearothermophilus* ATCC 7953 were sequenced and compared with those in the GenBank. Consequently, the sequences of isolates, which were phenotypically and physiologically *Bacillus*, revealed 97-100% sequence homology to the genus *Bacillus*. Eight *Bacillus* isolates were found closely related to the genus *Geobacillus* (Figure 2) and showed 97-100% identity to *G. stearothermophilus* ATCC 7953. Nazina *et al.* (2001) reported that different *Geobacillus* species have more than 96% sequence homology. As a result, these isolates can be allocated into the genus *Geobacillus*. Furthermore, the phylogenetic analysis of the 16S rDNA sequences of three *Geobacillus* isolates (JA1, JH1, and JM1) illustrated that these isolates can be grouped in the species *stearothermophilus* with 100% homology. However, further analysis is required, it was clearly noticed that the investigated Jordanian hot springs were rich in *Geobacillus*. The results of this study were consistent with findings of Obeidat *et al.* (2012).

In conclusion, the results presented in this study indicated that thermophilic bacilli were ubiquitous and diverse in thermal water of Jordanian hot springs. The

dominance of thermophilic *Bacillus* species in waters obtained from hot springs of Jordan was reported previously by several Jordanian researchers (Khalil, 2002; Malkawi and Al-Omari, 2010; Fandi *et al.*, 2012; Obeidat *et al.*, 2012; Mohammad *et al.*, 2017). In several previous studies (Al-Qodah, 2006; Elnasser *et al.*, 2007; Obeidat *et al.*, 2012), it was reported that thermal waters of Jordanian hot springs were rich in the thermophilic bacillus *G. stearothermophilus*. This study showed that thermophilic *B. licheniformis* seems to be abundant in Jordanian hot springs. This is in agreement with Mohammad *et al.* (2017) who demonstrated that thermophilic *B. licheniformis* were prevalent in the Jordanian hot springs.

Geobacillus isolates were found to exhibit a wide array of enzymatic activities. All isolates were protease and lipase producers. Isolate JA1 was produced high pectinolytic activity. Isolates JH1 and JM5 produced very high and high protease activity, respectively, while isolates JM1, JM5, JZ1, and JZ5 were able to give high to very high amylolytic activity. Only one *Geobacillus* isolate (JZ1) did not give activity of xylanase enzyme. Four isolates (JA1, JM1, JM5, and JZ1) showed cellulase activity. These findings were consistent with that reported previously (Obeidat *et al.*, 2012). Al-Qodah (2006) isolated amylolytic *Geobacillus* isolate from Ma`in-Roman Bath. In consistence, two amylolytic *Geobacillus* isolates (JM1 and JM5) were obtained from Ma`in-Romman Bath in the present study.

Interestingly, it was found that the 16S rDNA sequence of Zara isolate JZ9 was highly related (99% identity) to that of the thermophilic bacterium *Caldimonas hydrothermale*. This isolate was thermophilic (grew between 40 to 60 °C, at pH 8-9, and at 0-6% NaCl) with rod cells, strictly aerobic, stained Gram-negative, non-spore forming, and positive to catalase and oxidase tests. Moreover, isolate JZ9 produced different important enzymatic activities which have been used in biotechnological and industrial applications, including; proteolytic, lipolytic, xylanolytic, celluolytic, and pectinolytic activities. To our knowledge, no previous work reported the isolation of *Caldimonas* from Jordanian hot springs. Moreover, this is the second study after Bouraoui *et al.*, (2010) which demonstrated the isolation of *Caldimonas* that may be allocated to the species *hydrothermale*.

The 16S rDNA sequence of JM2, which was isolated in 2011 from Ma`in-Roman Bath, shares 99% sequence similarity with the thermophilic bacterium *Thermomonas hydrothermalis*. This bacterium species had been repeatedly detected in 2017 and isolated from different Jordanian hot spring called Jordan Himma or Al- Hemma (Mohammad *et al.*, 2017) and furtherly analyzed for biotechnological and medical purposes by Al-Daghistani *et al.*, 2021. The enzyme profiles detected for *Thermomonas* by Mohammad *et al.* (2017) were positive for cellulase and amylase activity which is in agreement with the finding of this study, but it is negative for lipase activity which is contrary to the result obtained in this study.

It was found that a total of nine Gram-negative thermotolerant bacterial isolates were allocated, based on 16S rDNA sequences, into *Acinetobacter* (JM13, JM14, JZ11, and JZ12), *Cronobacter* (JS3), *Enterobacter* (JA4 and JH8), and *Pseudomonas* (JH7 and JZ14). Since these

isolates are human pathogens, they might be present as contaminants from patients who visited hot springs for physiotherapy purposes.

While these results are important for further taxonomic work, positive results on several enzymes including protease, lipase, xylanase, cellulase, amylase, and pectinase (polygalacturonase) of most isolates are indicative of probable applications in industry and biotechnology. It was found that three isolates (thermophilic JM1, thermotolerant JS3 and JZ11) produced all hydrolytic activities which tested in the current study. Therefore, those isolates might draw a lot of attention largely because they produce vital enzymes for industry.

In the beginning of this century, many serious bacterial infections have developed resistance to commonly used antibiotics and become a major worldwide healthcare issue (Alanis, 2005). On the other hand, fungal pathogens cause serious problems worldwide in agriculture and food industry and many fungal pathogens produce mycotoxins, which are harmful to humans and livestock (Augustine *et al.*, 2005). Finding new natural sources, such as thermophilic bacteria, of antibacterial and antifungal drugs is therefore urgently needed. Only three isolates (JH1 and JM11 were thermophilic and JS3 was thermotolerant) produced a narrow range of antimicrobial activity against test microorganisms (Figure 4). Results indicated that two isolates JH1 and JS3 exhibited antibacterial activity against *K. pneumonia* and isolate JM11 produced antifungal activity against *C. albicans*. This result is in agreement with preceding studies (Venugopalan *et al.*, 2008; Muhammad *et al.*, 2009; Sethy and Behera 2012). Crudes of these three isolates can be developed for the use in drugs industry. Remarkably, these isolates were protease, lipase, xylanase, and polgalacturonase producers. As a result, the antimicrobial activity of those isolates toward Gram-negative bacteria might be correlated to their ability to produce protease activity. This is in agreement with Farouk (1982) who demonstrated that proteolytic enzymes such as protease exhibited higher killing effect against Gram-negative bacteria than Gram-positive bacteria. Furthermore, this result implies that the produced antimicrobial agents are cationic and effectively interacting with the negatively charged surface of the outer lipopolysaccharide (LPS) of Gram-negative cell wall to cause membrane instability and rupturing, which ultimately leads to cell death.

After cardiovascular illnesses, cancer was the second leading cause of death worldwide and in Jordan (Heron *et al.*, 2009; Al-Tarawneh *et al.*, 2010). So, finding new sources of anticancer agents, such as bacterial byproducts, is urgently needed. No previous studies demonstrated the ability of thermophilic bacteria to produce anticancer agents. The results showed that crudes of three *Bacillus* isolates (JA2, JM11, and JM12) showed non-hemolytic activity against human erythrocytes and displayed selective *in vitro* cytotoxicity against human leukemic cell line K562 (Figure 5). These cytotoxic isolates were found to produce low pectinolytic activity and moderate to very high proteolytic activity. So, protease activity could be responsible for cytotoxic effect against leukemic cells. Given that the cytotoxic isolates exhibited no hemolytic activity against human erythrocytes, the anticancer activity in such isolates was not attributed to the induced

hemolysis. Because of their ability to discriminate between cancer cells (K562) and healthy Vero cells by killing cancer cells only, these isolates are considered to produce promising bioactive chemicals with selective *in vitro* cytotoxicity against leukemia cells. This finding clearly suggests that thermophilic bacteria, which naturally make selective substances against cancer, could be used for medical and pharmaceutical therapies of some cancer types.

5. Conclusion

In terms of phenotypic and physiological properties as well as 16S rDNA sequences, the majority of the thermophilic isolates obtained from thermal water of local hot springs belonged to the genus *Bacillus/Geobacillus*. This study was considered the first that described the isolation of *Caldimonas* bacterium from local hot springs in addition to the isolation of *Thermomonas*. Most of the isolates were found to produce protease, lipase, xylanase, cellulase, amylase, and pectinase. As an achievement of this study, three isolates exhibited selective *in vitro* cytotoxicity against human leukemia cells. To our knowledge, this is the first study that examined the anticancer activity of thermophilic bacteria crudes against leukemia cancer cells. Therefore, hot springs of Jordan are rich sources for the isolation of different thermophilic bacterial species producing hydrolyzing enzymes and anticancer agents that may be used in medical, biotechnological, and industrial applications.

Acknowledgment

The authors are grateful to “Ministry of Higher Education of Jordan; grant no. M-Ph/2/14/2008” for financial support and to “Dr. Saeid Ismaeil, Faculty of Medicine, University of Jordan” for providing cell lines used in this work.

References

- Alanis, AJ. 2005. Resistance to antibiotics: are we in the post-antibiotic era? *Arch Med Res*, **36** (6): 697-705.
- Al-Daghistani, HI, Mohammad, BT, Kurniawan, TA, Singh, D, Rabadi, AD, Xue, W, Avtar, R, Othman, MHD and Shirazian S. 2021. Characterization and applications of *Thermomonas hydrothermalis* isolated from Jordan's hot springs for biotechnological and medical purposes. *Process Biochem*, **104**: 171-181.
- Al-Qodah, Z. 2006. Production and characterization of thermostable α -amylase by thermophilic *Geobacillus stearothermophilus*. *Biotechnol J*, **1**: 850-857.
- Al-Tarawneh, M, Khatib, S and Arqub, K. 2010. Cancer incidence in Jordan, 1996-2005. *East Mediterr Health J*, **16**(8): 837-845.
- Augustine, SK, Bhavsar, SP and Kapadnis, BP. 2005. A non-polyene antifungal antibiotic from *Streptomyces albidoflavus* PU 23. *J. Biosci*, **30**(2): 201-11.
- Baker, G, Gaffar, S, Cowan, DA and Suharto, ARI. 2001. Bacterial Community Analysis of Indonesian Hotsprings. *FEMS Microbiol Lett*, **200** (1): 103-109.
- Belduz, AO, Dulger, S and Demirbag, Z. 2003. *Anoxybacillus gonensis* sp. nov., a moderately thermophilic, xylose-utilizing, endospore-forming bacterium. *Int J Syst Evol Microbiol*, **53**: 1315-1320.
- Bouraoui, H, Boukari, I, Touzel, JP, O'Donohue, M and Manai, M. 2010. *Caldimonas hydrothermale* sp. nov., a novel thermophilic bacterium isolated from Roman hot bath in south Tunisia. *Arch Microbiol*, **192**(6): 485-491.
- Bragger, J.M, Daniel, RM, Coolbear, T and Morgan, HW. 1989. Very stable enzymes from extremely thermophilic archaeobacteria and eubacteria. *Appl Microbiol Biotechnol*, **31**(5-6): 556-561.
- Carrillo, PG, C Mardaraz, SI, Alvarez, P and Giulietti, AM. 1996. Isolation and selection of biosurfactant producing bacteria. *World J Microbiol Biotechnol*, **12** (1): 82-84.
- Ceylan, O, Okmen, G and Ugur, A. 2008. Isolation of soil *Streptomyces* as source antibiotics active against antibiotic-resistant bacteria. *Eurasia J Biosci*, **2**: 73-82.
- Chen, L and Roberts, MF. 1999. Characterization of a tetrameric inositol monophosphatase from the hyperthermophilic bacterium *Thermotoga maritima*. *Appl Environ Microbiol*, **65** (10): 4559-4567.
- Elnasser, Z, Maraqa, A, Owais, W and Khraisat, A. 2007: Isolation and Characterization of New Thermophilic Bacteria in Jordan. *Internet J Microbiol*, **3**(2): 1-10.
- Ezeji TC, Wolf A and Bahl H. 2005. Isolation, characterization, and identification of *Geobacillus thermodenitrificans* HRO10, an α -amylase and α -glucosidase producing thermophile. *Can J Microbiol*, **51**(8): 685-693.
- Fandi K, Massadeh M and Laatsch, H. 2012. LC-MS/MS Profiling-based metabolite screening of thermophilic bacteria from Jordanian hot springs. International Conference on Applied Chemistry and Pharmaceutical Sciences (ICACPS'2012), May 19-20, 2012 Penang (Malaysia).
- Farouk, A. 1982. Antibacterial activity of proteolytic enzymes. *Int J Pharm*, **12**(4): 295-298.
- Fortina, MG, Mora, D, Schumann, P, Parini, C, Manachini, PL and Stackebrandt, E. 2001. Reclassification of *Saccharococcus caldoxylosilyticus* as *Geobacillus caldoxylosilyticus*. *Int J Syst Evol Microbiol*, **5**: 2063-2071.
- Freshney, RI. 1987. Culture of Animal Cells: A Manual of Basic Techniques, 2a ed., Alan R. Liss, Inc., New York.
- Galtier, N and Lobry, JR. 1997. Relationships between genomic G+C content, RNA secondary structures, and optimal growth temperature in prokaryotes. *J Mol Evol*, **44**(6): 632-636.
- Gessner, RV. 1980. Degradative enzyme production by salt march fungi. *Bot Mar*, **23**: 133-139.
- Haba, E, Bresco, O, Ferrer, C, Marques, A, Basquets, M and Manresa, A. 2000. Isolation of lipase secreting bacteria by deploying used frying oil as selective substrate. *Enzyme Microb Technol*, **26**: 40-44.
- Heiss, P, Bernatz, S, Bruchelt, G and Schmidtke, SR. 1997. Cytotoxic effect of immunoconjugate composed of glucose-oxidase coupled to an anti-ganglioside (GD2) antibody on spheroids. *Anticancer Res*, **17** (4B): 3177-3178.
- Heron, M, Hoyert, DL, Murphy, SL, Xu, J, Kochanek KD and Tejada-Vera, B. 2009. Deaths: Final Data for 2006. *Natl Vital Stat Rep*, **57**(14): 1-135.
- Karlin, S, Brocchieri, L, Trent, J, Blaisdell, BD and Mra'zek, J. 2002. Heterogeneity of Genome and Proteome Content in Bacteria, Archaea, and Eukaryotes. *Theor Popul Biol*, **61** (4): 367-390.
- Khalil, AB. 2002. Isolation and characterization of thermophilic *Bacillus* species from thermal ponds in Jordan. *Pak J Biol Sci*, **5**(11): 1272-1273.

- Kobayashi, T, Koike, K, Yoshimatsu, T, Higaki N, Suzumatsu A and Ozawa, T. 1999. Purification and properties of a low-molecular weight, high-alkaline pectate lyase from an alkaliphilic strain of *Bacillus*. *Biosci Biotechnol Biochem*, **63** (1): 72-75.
- Lengeler, JW, Drews, G and Schlegel, HG. 1999. *Biology of the Prokaryotes*: Blackwell Science Inc., pp. 652-915.
- Malkawi, HI and Al-Omari, MN. 2010. Culture-dependent and culture-independent approaches to study the bacterial and archaeal diversity from Jordanian hot springs. *Afr J Microbiol Res*, **4**(10): 923-932.
- Maugeri, LT, Gugliandolo, C, Caccamo, D and Stackebrandt, E. 2001. A polyphasic taxonomic study of thermophilic Bacilli from shallow, marine vents. *Syst Appl Microbiol*, **24** (4): 572-587.
- Mohammad BT, Al Daghistani HI, Jaouani A, Abdel-Latif S and Kennes C. 2017. Isolation and characterization of thermophilic bacteria from Jordanian hot springs: *Bacillus licheniformis* and *Thermomonas hydrothermalis* isolates as potential producers of thermostable enzymes. *Int J Microbiol*, **2017**: 6943952.
- Mosmann, T. 1983. Rapid colorimetric assay for cellular growth and survival: application to proliferation and cytotoxicity assays. *J Immunol Methods*, **65** (1-2): 55-63.
- Muhammad, SA, Ahmad, S and Hameed, A. 2009. Antibiotic production by thermophilic *Bacillus specie* SAT-4. *Pak J Pharm Sci*, **22**(3): 339-345.
- Nazina, TN, Lebedeva, EV, Poltarau, AB, Tourova, TP, Grigoryan, AA, Sokolova, DS, Lysenko, AM and Osipov, GA. 2004. *Geobacillus gargensis* sp. nov., a novel thermophile from a hot spring, and the reclassification of *Bacillus vulcani* as *Geobacillus vulcani* comb. Nov. *Int J Syst Evol Microbiol*, **54** (6): 2019-2024.
- Nazina, TN, Tourova, TP, Poltarau, AB, Novikova, EV, Grigoryan, AA, Ivanova, AE, Lysenko, AM, Petrunyaka, VV, Osipov GA, Belyaev, SS and Ivanov, MV. 2001. Taxonomic study of aerobic thermophilic bacilli: descriptions of *Geobacillus subterraneus* gen. nov., sp. nov., and *Geobacillus uzenensis* sp. nov. from petroleum reservoirs and transfer of *Bacillus stearothermophilus*, *Bacillus thermocatenulatus*, *Bacillus thermoleovorans*, *Bacillus kaustophilus*, *Bacillus thermoglucosidasius* and *Bacillus thermodenitrificans* to *Geobacillus* as the new combinations *G. stearothermophilus*, *G. thermocatenulatus*, *G. thermoleovorans*, *G. kaustophilus*, *G. thermoglucosidasius* and *G. thermodenitrificans*. *Int J Syst Evol Microbiol*, **51** (2): 433-446.
- Obeidat, M. 2017. Cytotoxicity of n-butanol extracts of *Streptomyces* against human breast cancer cells. *Int J Pharm*, **13**(8): 969-979.
- Obeidat, M, Khyami-Horani, H, Al-Zoubi A and Otri, I. 2012. Isolation, characterization, and hydrolytic activities of *Geobacillus* species from Jordanian hot springs. *Afr J Biotechnol*, **11**(25): 6763-6768.
- Priest, GF, Goodfellow, M and Todd, CA. 1988. Numerical Classification of the genus *Bacillus*. *J Gen Microbiol*, **134**: 1847-1882.
- Romano, I, Poli, A, Lama, L, Gambacorta, A and Nicolaus B. 2005. *Geobacillus thermoleovorans* subsp. *stromboliensis* subsp. nov., isolated from the geothermal volcanic environment. *J Gen Appl Microbiol*, **51**(3): 183-189.
- Saul, DJ, Reeves, RA, Morgan, HW and Bergquist, PL. 1999. *Thermus* diversity and strain loss during enrichment. *FEMS Microbiol Ecol*, **30**(2): 157-162.
- Sethy, K and Behera, N. 2012. Antimicrobial activity of thermotolerant bacterial isolate from coal mine spoil. *African Journal of Microbiology Research*, **6**(26): 5459-5463.
- Simoneit, TRB, Aboul-Kassim, TAT and Tiercelin, JJ. 2000. Hydrothermal petroleum from lacustrine sedimentary organic matter in the East African Rift. *Appl Geochem*, **15**: 355-368.
- Singh, SP. 2006. *Extreme Environments and Extremophiles*. National Science Digital Library (CSIR): E- Book on Environmental Microbiology, pp. 1-35.
- Swarieh, A. 2000. Geothermal energy resources in Jordan, country update report. *Proceedings World Geothermal Congress*. pp. 469-474.
- Ten, LN, Im, WT, Kim, MK, Kang, MS and Lee, ST. 2004. Development of a plate technique for screening of polysaccharide-degrading microorganisms by using a mixture of insoluble chromogenic substrates. *J Microbiol Methods*, **56**(3): 375-382.
- Venugopalan, V, Singh, B, Verma, N, Nahar, P, Bora, TC, Das, RH and Gautam, HK. 2008. Screening of thermophiles from municipal solid waste and their selective antimicrobial profile. *Curr Res Bacteriol*, **1**(1): 17-22.

First Record of the Scorpion *Vachoniolus globimanus* (Scorpiones: Buthidae) from Jordan

Bassam Abu Afifeh¹, Mohammad Al-Saraireh² and Zuhair S. Amr^{3,*}

¹Al Rumman Secondary School, Ministry of Education, Amman, Jordan; ²Oncology Department, Royal Medical Services, Amman, Jordan;

³Department of Biology, Jordan University of Science & Technology, Irbid, Jordan.

Received: October 28, 2022; Revised: January 19, 2023; Accepted: January 28, 2023

Abstract

Four species of the genus *Vachoniolus* have been described from Iran, Oman, Saudi Arabia and the United Arab Emirates. The scorpion *Vachoniolus globimanus* Levy, Amitai and Shulov, 1973 is recorded from Jordan for the first time. Specimens of this species have been collected from Wadi Rum, southern Jordan. Morphological analysis, morphometric values, and taxonomic features were used to identify the collected specimens. This record extends the known distribution range of the genus *Vachoniolus* from central, western and southern Arabian Peninsula and Iran to the northwest in southern Jordan. The aim of the present study is to identify and describe the newly collected scorpion species from Wadi Rum desert in Jordan with additional ecological notes on their habitat.

Keywords: *Vachoniolus globimanus*, WadiRum, scorpions, Jordan.

1. Introduction

Despite recent extensive fieldwork and description of five new species from Jordan in the past two years (Lourenço *et al.*, 2021a & b; Al-Saraireh *et al.*, 2021; Abu Afifeh *et al.*, 2022; Al-Saraireh *et al.*, 2023), the fauna of the scorpion in Jordan is still to be explored, particularly in southern and eastern deserts with different and varied habitats including sand and rock-covered deserts.

In Jordan, family Buthidae includes nine genera (*Androctonus* Ehrenberg, 1828, *Birulatus* Vachon, 1974, *Buthacus* Birula, 1908, *Buthus* Leach, 1815, *Compsobuthus* Vachon, 1949, *Hottentotta* Birula, 1908, *Leiurus* Ehrenberg, 1828, *Orthochirus* Karsch, 1891, and *Trypanothacus* Lowe, Kovařík, Stockmann and Štáhlavský, 2019 (Amr *et al.*, 1988; Amr and Al-Oran 1994; Lourenço *et al.*, 2002 and 2010).

The southern and eastern deserts such as Wadi Rum and parts of Wadi Araba are suitable habitats for sand dwelling scorpions. These scorpions are stenotopic and adapted to live in sandy desert environments (Fet *et al.*, 1998; Prendini, 2001). Several scorpion genera are considered psammophilous (e.g. *Apistobuthus*, *Buthacus*, *Buthiscus*, *Trypanothacus* and *Vachoniolus*) and known to occur in the deserts of North Africa and Middle East (Levy *et al.*, 1973; Lowe *et al.*, 2019).

The genus *Vachoniolus* was originally created by Levy *et al.* (1973) based on a single male specimen found in the collection of British Museum, collected from Oman in 1950. It was closely related to genus *Buthacus* by having reduced carapacial and mesosomal carination in addition to the presence of bristle combs, but the new genus is

mainly characterized by grossly swollen pedipalp chela, and the absence of tibial spurs. *Vachoniolus globimanus* Levy, Amitai and Shulov, 1973, was described as the type species for this genus. Until now, four species of the genus *Vachoniolus* have been described from the Middle East; *Vachoniolus iranensis* Navidpour, Kovařík, Sologlad and Fet, 2008 from Iran, *Vachoniolus batinahensis* Lowe, 2010, *Vachoniolus gallagheri* Lowe, 2010 and *Vachoniolus globimanus* from Oman. *Vachoniolus globimanus* has a wide range of distribution and was recorded from Oman, Saudi Arabia and the United Arab Emirates (El-Hennawy, 1992; Lowe, 2010; Alqahtani and Badry, 2021). So far, this genus has not yet been recorded from Jordan.

Vachon (1974) reported that the trichobothrial pattern of *V. globimanus* (male type, swollen chela) was similar in neobothriotaxy to that of *Buthacus minipectinibus* (female type, non-swollen chela), and suggested that these two taxa might belong to the same genus. However, he delayed a formal taxonomic action until a later study. Later, Vachon (1979) transferred *B. minipectinibus* to *Vachoniolus* and reported on sexual dimorphism. Hendrixson (2006) studied additional specimens of *Vachoniolus* from Saudi Arabia and United Arab Emirates and placed *V. minipectenibus* as a synonymy to *V. globimanus*.

Here, to the best of our knowledge, this is the first record of *V. globimanus* in Jordan with accurate and integrated information about its distribution across the desert environment.

* Corresponding author. e-mail: amrz@just.edu.jo.

2. Material and methods

2.1. Systematics

***Vachoniolus globimanus* Levy, Amitai et Shulov, 1973**
Vachoniolus globimanus Levy, Amitai and Shulov, 1973: 113–140, figs. 42–48; Vachon 1974: 910, 948, fig. 49; Vachon, 1979: 42–44, figs. 18–25, 28, 31, 34–36; Vachon and Kinzelbach, 1987: 100; El-Hennawy, 1992: 102, 133; Tigar and Osborne, 1997: 552, tab. 2; Tigar and Osborne, 1999: 174, 180, tab.2; Fet and Lowe, 2000: 278; Fet, Soleglad and Lowe, 2005: 13; Hendrixson, 2006: 36, 100–102, figs. 23–24, pl. 18; Kaltsas, Stathi and Mylonas, 2008: 525; Navidpour et al., 2008: 24–26; Lourenço and Duhem, 2009: 47, fig. 29; Lowe, 2010: 17–23, 37, figs. 57–83, 94–96, 104–111, 137–141, 146–148, tab. 1; Alqahtani and Badry, 2021: 8, 12, figs. 3, 7, tab. 1; Aloufi *et al.*, 2022: 16–17, figs. 3. = *Buthacus minipectenibus* Levy, Amitai and Shulov, 1973: 128–130, figs. 27–31. *Vachoniolus minipectinibus* (incorrect subsequent spelling): Vachon, 1974: 948; Vachon, 1979: 49, figs. 12–17, 27, 30, 33, 36. *Vachoniolus minipectenibus*: Kinzelbach, 1985: III; Vachon and Kinzelbach, 1987: 101; El-Hennawy, 1992: 102, 133; Tigar and Osborne, 1997: 552, tab. 2; Acosta and Fet 2005: 5–6; Fet, Soleglad and Lowe, 2005: 13. *Buthacus minipectenibus* (incorrect subsequent spelling): Vachon and Kinzelbach, 1987: 100. *Vachoniolus minipectinatus* (unjustified emendation): Fet and Lowe, 2000: 278; Hendrixson, 2006: 99–100.

2.2. Collection sites and diagnosis:

The specimens were collected at night around 21:00 hr in 15 July 2022. Scorpions were collected by ultraviolet (UV) detection and preserved in the field by standard methods (Williams, 1968; Stahnke, 1972; Sissom, Polis and Watt, 1990). Specimens were transferred to Biology Department, Jordan University. Specimens of *V. globimanus* collected from Saudi Arabia were used as comparative materials.

Illustrations and measurements were made with the aid of stereoscopic microscope with a camera and an ocular micrometer (efix). Measurements follow Stahnke (1970) and are given in mm, with the following exceptions: carinal terminology is after Francke (1977). Trichobothrial notations follow Vachon (1974 and 1975) and morphological terminology mostly follows Vachon (1952) and Hjelle (1990).

Examined material: 2 adults ♂♂, 1 adult ♀, Wadi Rum, 13 km SE Al Ghal (29° 26' 00.1" N, 35° 40' 56.8" E), 890 m asl., 15.VII.2022, leg. B. Abu Afifeh and R. Abu Afifeh.

Comparative material of *V. globimanus* from Saudi Arabia: Adult ♂, Al Qarnaen, Uruq Bani M'arid Protected Area (19° 07' 58.45"N, 45° 08' 27.06"E), 5.V.2019, leg. A. Aloufi. 1 adult ♀, Al Makhrameah, Al Wabari Farm, Tabuk Province (28° 53' 43.08"N, 36° 07' 28.94"E), 23.VII.2017, leg. A. Aloufi.

All materials were deposited in the collections of the University of Jordan, Amman, Jordan.

3. Results

3.1. Taxonomy and systematics

Family Buthidae C. L. Koch, 1837

Genus *Vachoniolus* Levy, Amitai and Shulov, 1973

Vachoniolus globimanus Levy, Amitai and Shulov, 1973, Figs.1-4, Tab. 1

3.2. Characteristics of *V. globimanus*

Medium to large buthid scorpion 45–65 mm; base color yellow to orange-yellow with or without melanic pigmentation on metasoma IV–V and telson; Carapace smooth to shagreened, without distinct carinae; tergites smooth to finely granular, weak median carina on tergites I–VI, 5 carinae on tergite VII; pedipalp chela of males distinctly swollen; aculeus long; external surface of pedipalp patella with eight or nine trichobothria; pedipalp femoral trichobothrium d_5 distal to e_2 , femur and patella shorter than carapace; metasomal segments relatively slender; pectine teeth for females 10–18, for males 16–25; legs with or without tibial spurs (Hendrixson, 2006; Lowe, 2010).

3.3. Description of *Vachoniolus globimanus* collected from Wadi Rum

Large size buthid scorpions, male 64 mm, and female 52 mm in total length.

Coloration: male has uniform pale-yellow body with faint fuscosity on tergites and marked melanic pigmentation on telson and metasoma V. Female's segment V with light grey pigmentation (Fig. 1 A & B, Fig. 2 & 3).

Prosoma: carapace smooth devoid of carinae; surface of carapace shagreened with minute granules anteriorly; anterior margin of carapace slightly convex, median eyes relatively large and located on the anterior one-half of carapace, four pairs of small size lateral eyes.

Mesosoma: Tergites smooth to shagreened, Tergite I smooth, lacking carinae; Tergites II–VI with single median obsolete carina, tergite VII with weak median protuberance and two pairs of weak lateral carinae, Sternites III–VI smooth; sternite VII with obsolete to smooth two pairs of median and lateral carinae. Pectinal tooth counts 17–21 in males, 14–14 in the female; males pectines long, extending beyond middle of trochanter of leg IV, female pectines short, not reaching beyond coxa of leg IV, pectines with fulcra.

Metasoma: All segments longer than wide, becoming more narrow and slender posteriorly; L/W ratios: I=1.40–1.42, II=1.73–1.74, III=1.86–1.87, IV=2.24–2.35, V=2.75–2.91, (Table 1), 10 complete carinae on segment 1, 8 complete carinae on segments II and III, 4 carinae on segment IV, segment V with 3 carinae. **Telson:** Vesicle slim, narrower than metasomal segment V, long aculeus, without subaculear tubercule.

Legs: tibial spurs present on legs III–IV; vestigial and reduced on III; moderate on IV, retrolateral and prolateral pedal spurs present on all legs; tibiae I–III with retrosuperior bristle combs; basitarsi I–III with bristle combs.

Pedipalps: Manus of male swollen; slender in female; the ratios between manus width of male to manus width of

female is 2.29; the ratios between manus depth of male to manus depth of female is 2.47. Smooth manus and movable finger; fixed and movable fingers with 6-9 rows of denticles. Trichobothrial pattern: neobothriotaxic (Fig. 4), type A-beta (Vachon, 1974 and 1975), with supernumerary *esb*₃ on external surface of patella (Fig. 4D and J); femoral trichobothrium *d*₅ located distally relative to trichobothrium *e*₂ on the external surface of femur (Fig. 4B and I), *d*₂ of dorsal surface of both femur and patella, chela external *Eb*₃, *Est* and *esb* petite.

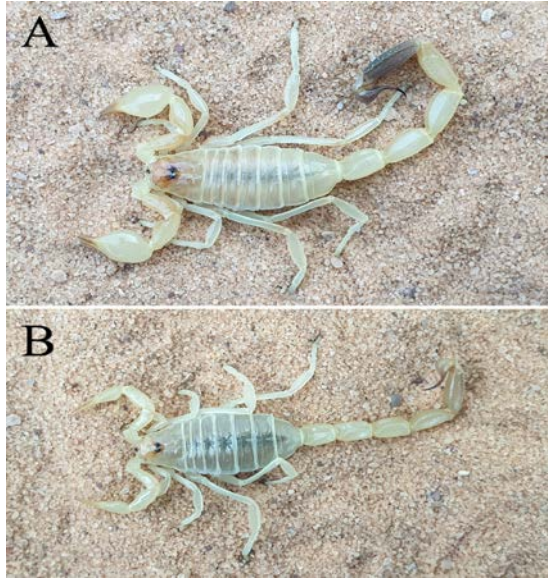


Figure 1: Habitus of *Vachoniolus globimanus* from Wadi Rum. A. Adult male. B. Adult female.

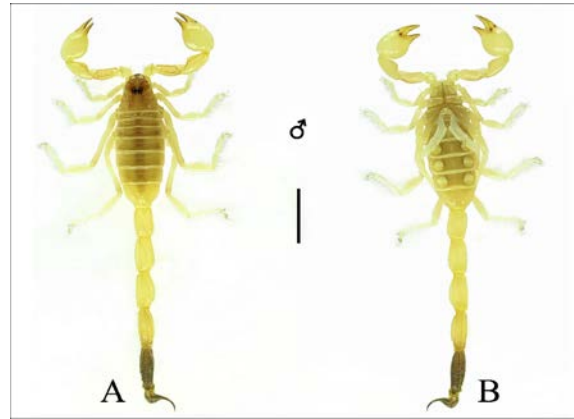


Figure 2: Male *Vachoniolus globimanus* from Wadi Rum. A. Dorsal aspect. B. ventral aspect. Scale bar = 10 mm.

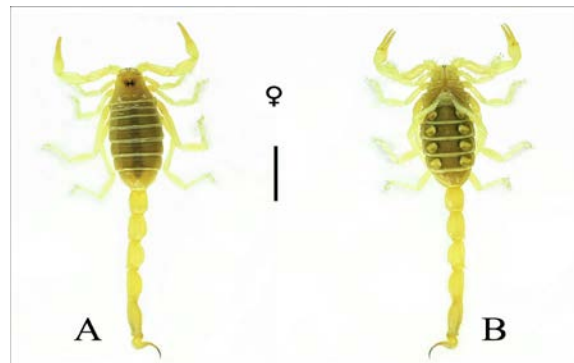


Figure 3: Female *Vachoniolus globimanus* from Wadi Rum. A. Dorsal aspect. B. ventral aspect. Scale bar = 10 mm.

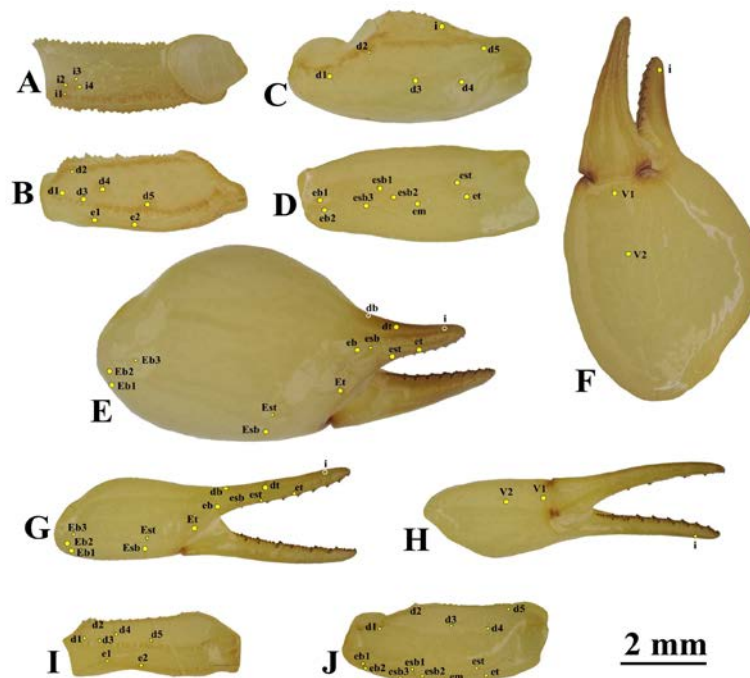


Figure 4: *Vachoniolus globimanus* from Wadi Rum, 13 km SE Al Ghal. (A-F: male). A. Femur of right pedipalp, internal aspect, B. Femur of right pedipalp, dorsal aspect, C. Patella of right pedipalp, dorsal aspect, D. Patella of right pedipalp, external aspect, E. Chela of right pedipalp, external aspect, F. Chela of right pedipalp, ventral aspect. (G-J: female). G. Chela of right pedipalp, external aspect, H. Chela of right pedipalp, ventral aspect, I. Femur of right pedipalp, dorsoexternal aspect, J. Patella of right pedipalp, dorsoexternal aspect. Scale bar = 2 mm.

** **Abbreviations for trichobothria:** b: basal, d: dorsal, db: dorsal basal, dt: dorsal terminal, e: external, eb: external basal, esb: external suprabasalem: external median, et: external terminal, i: internal, m: median, sb: suprabasal, sd: supradistal, st: subterminal, t: terminal v: ventral. For the hand: E: external, Eb: external basal, Est: external subterminal, V: ventral.

Table 1. Measurements for males and females of *V. globimanus* from Wadi Rum in Jordan and Saudi Arabia.

	Jordan		Saudi Arabia	
	Male	Female	Male	Female
Morphometric values in mm				
Total length (Including telson)	64.23	52.82	50.70	63.92
Carapace: Length / Anterior width / Posterior width	6.24 / 3.60 / 7.32	5.64 / 3.24 / 6.60	5.28 / 3.18 / 5.76	6.90 / 3.96 / 7.80
Mesosoma length	17.53	15.13	10.32	14.90
Metasomal segment I: Length / Width	5.28 / 3.72	4.20 / 3.00	4.38 / 3.12	5.40 / 3.84
Metasomal segment I: L/W ratio	1.42	1.40	1.40	1.41
Metasomal segment II: Length / Width	6.24 / 3.60	4.80 / 2.76	5.16 / 3.00	6.00 / 3.54
Metasomal segment II: L/W ratio	1.73	1.74	1.72	1.69
Metasomal segment III: Length / Width	6.48 / 3.48	5.04 / 2.70	5.52 / 2.94	6.24 / 3.48
Metasomal segment III: L/W ratio	1.86	1.87	1.88	1.79
Metasomal segment IV: Length / Width	7.32 / 3.12	5.64 / 2.52	6.12 / 2.64	7.20 / 3.24
Metasomal segment IV: L/W ratio	2.35	2.24	2.32	2.22
Metasomal segment V: Length / Width / Depth	8.04 / 2.76 / 2.52	6.60 / 2.40 / 2.28	6.96 / 2.52 / 2.18	8.16 / 3.12 / 2.88
Metasomal segment V: L/W ratio	2.91	2.75	2.76	2.62
Telson:				
Length / Width / Depth	6.00 / 1.80 / 1.86	5.16 / 1.68 / 1.56	5.76 / 1.68 / 1.68	6.96 / 2.04 / 2.04
Pedipalp femur: Length / Width	4.80 / 1.92	4.08 / 1.56	4.32 / 1.50	4.92 / 1.92
Pedipalp patella: Length / Width	5.52 / 2.64	4.80 / 1.92	5.04 / 2.16	6.00 / 2.40
Pedipalp chela:				
Length / Width / Depth	8.28 / 3.84 / 5.04	6.84 / 1.68 / 2.04	7.92 / 3.36 / 3.72	8.40 / 1.95 / 2.28
Movable finger: Length	3.96	4.32	3.60	5.04

3.4. Habitats

Al Ghal is located within the vast Wadi Rum escarpment (Fig. 5). It is surrounded by precipitous, sandstone and granite mountains, isolated from each other by flat corridors covered with mobile sand-dunes and sand sheets. Small patches of trees (e.g. *Acacia radiana*) and bushes such as *Haloxylon persicum* and *Retama raetam* are the typical plants of this sandy habitat, with a rainfall less than 200 mm annually (Abu Baker *et al.*, 2004). The sand of Wadi Rum massifs originated from the wind erosion of the Paleozoic sandstone rocks, and the sedimentation continued during the Ordovician and Silurian periods (Abed, 2002).



Figure 5: Habitat of Al Ghal area Wadi Rum, southern Jordan.

Specimens were collected by UV detection after 9-11 pm. Scorpions were found near the edge between sand dunes and rocky terrain with scattered vegetation. They were not observed in sand dunes devoid of vegetation. *Buthacus* sp. was found about 500 m from the site in more cohesive flat sandy soil, *Leiurus jordanensis* Lourenço, Modrý and Amr, 2002 and *Orthochirus* sp. were also found near rocky areas surrounded by sand dunes. Within the area, the Urchin Beetle, *Prionothea coronate* (Olivier, 1795), was very common.

4. Discussion

The original description of *Vachoniolus globimanus* matched with the specimens examined in this study (Levy *et al.*, 1973; Vachon, 1974 and 1979; Hendrixson, 2006; Lowe, 2010). L/W ratios for the metasomal segments of *V. globimanus* were as follows: I=1.37-1.60, II=1.64-1.95, III=1.76-2.09, IV=2.20-2.62, V=2.46-3.05 (Lowe, 2010). The collected specimens from Wadi Rum in this study as well as the comparative materials from Saudi Arabia were within this range.

The closest record comes from Al Makhrameah, Tabuk Province, in northwestern Saudi Arabia, some 75 km far from the present locality (Aloufi *et al.*, 2022). This record extends the known distribution range of *V. globimanus* from central, western and southern Arabian Peninsula to the northwest in southern Jordan. All known species of this genus are confined to southeastern and southwestern Arabia (Lowe, 2010) and eastern Iran (Navidpour *et al.*, 2008). It shares similar habitat that consists of soft sand deserts (Fig. 6).

The presence of *V. globimanus* in southern Jordan draws the attention for the possible presence of other psammophilous species known from Saudi Arabia such as *Parabuthus liosoma* (Ehrenberg, 1828) and *Apistobuthus pterygocercus* Finnegan, 1932 in southwestern Jordan, as well as further north along the sand crescents that extend from southern Jordan reaching as far as Al Hazim area near Azraq (Disi *et al.*, 1999).

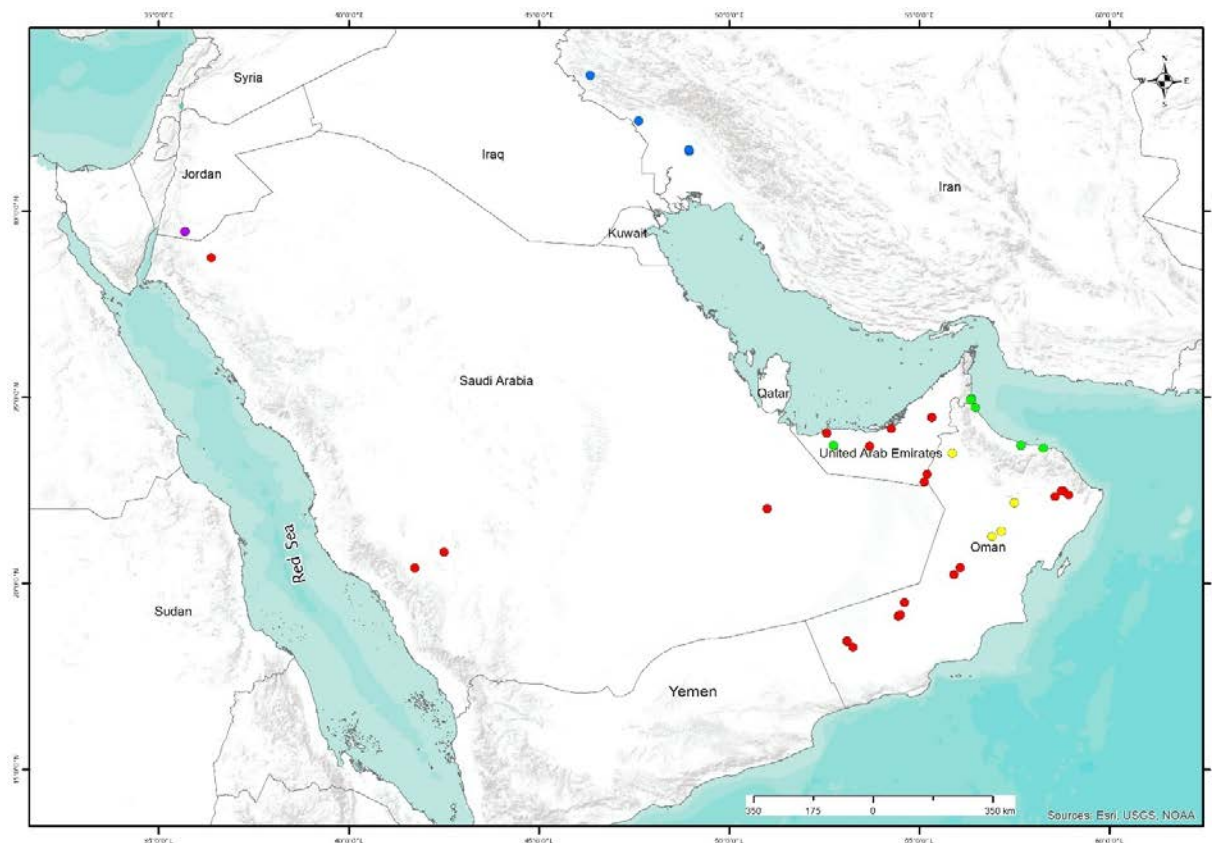


Figure 6: Distribution of species of the genus *Vachoniolus* in the Middle East. *Vachoniolus batinahensis* (Green circle). *Vachoniolus gallagheri* (Yellow circle). *Vachoniolus globimanus* (Red circle), Wadi Rum new locality (Purple circle). *Vachoniolus iranus* (Blue circle). Localities are based on Hendrixson (2006), Navidpour *et al.* (2008), Lowe (2010), Alqahtani and Badry (2021), Navidpour (2021), and Aloufi *et al.* (2022).

Acknowledgement

Special thanks are extended to Mrs. Laya Majid (GIS unit, Royal Society for the Conservation of Nature, Jordan) for map preparation. Our thanks also extended to Mr. Rami Abu Afifeh for his invaluable assistance in the field and collecting scorpions.

References

- Abed AM. 2002. An overview of the geology of Jordan. In: Disi A (Ed.). *Jordan Country Study on Biological Diversity: The Herpetofauna of Jordan*. United Nations Environment Programme, Amman. Pp. 21–24.
- Abu Afifeh AB, Al-Saraireh M, Abu Baker M, Amr Z and Lourenço WR. 2022. The genus *Buthacus* Birula, 1908 in Jordan: description of a new species and comments on possible micro-endemic populations (Scorpiones: Buthidae). *Arthropoda Sel.*, **31**: 51–62.
- Abu Baker M, Qarqaz M, Rifai L, Hamidan N, Al Omari K, Modrý D and Amr Z. 2004. Results of herpetofaunal inventory of Wadi Ramm Protected Area, with notes on some relict species. *Russ. J. Herpetol.*, **11**:1-5.
- Aloufi A, Abu Afifeh B and Amr ZS. 2022. Further collection of scorpions from Saudi Arabia. *Jordan Journal of Natural History*, **9**:11-20.
- Alqahtani A and Badry A. 2021. A contribution to the scorpion fauna of Saudi Arabia, with an identification key (Arachnida: Scorpiones). *J. King Saud Univ. Sci.*, **33**:1–13. No. 101396.
- Al-Saraireh M, Abu Afifeh B, Aloufi A, Amr ZS and Lourenço WR. 2021. First record of the genus *Trypanothacus* Lowe, Kovařík, Stockmann & Šťáhlavský, 2019 in Jordan and description of a new species (Scorpiones: Buthidae). *Serket*, **18**:11-21.
- Al-Saraireh, M., Yağmur, E. A., Abu Afifeh, B., & Amr, Z. 2023. A new species of *Scorpio* from Jordan (Scorpiones: Scorpionidae). *Euscorpius*, **369**: 1-17.
- Amr Z, Hyland K, Kinzelbach R, Amr S and Defosse D. 1988. Scorpion etpiques de scorpions enJordanie. *Bull. Soc. Pathol. Exot.*, **81**:369–379.
- Amr ZS and Al-Oran R. 1994. Systematics and distribution of scorpions (Arachnida, Scorpionida) in Jordan. *Boll. Zool.*, **61**:185–190.
- Disi AM, Modrý D, Bunian F, Al-Oran R and Amr Z. 1999. Amphibians and reptiles of the Badia region of Jordan. *Herpetozoa*, **12**:135-146.
- El-Hennawy HK. 1992 A catalogue of the scorpions described from the Arab countries (1758–1990) (Arachnida: Scorpionida). *Serket*, **2**:95–153
- Fet V, Polis GA and Sissom WD. 1998. Life in sandy deserts: the scorpion model. *J. Arid Environ.*, **39**:609-622
- Francke O. 1977. Scorpions of the genus *Diplocentrus* from Oaxaca, Mexico (Scorpionida, Diplocentridae). *J. Arachnol.*, **4**:145-200.
- Hendrixson BE. 2006. Buthid scorpions of Saudi Arabia, with notes on other families (Scorpiones: Buthidae, Liochelidae, Scorpionidae). *Fauna of Arabia*, **21**:33–120.
- Hjelle JT. 1990. Anatomy and morphology. In: Polis GA (Ed.), *The Biology of Scorpions*. Palo Alto (USA), Stanford University Press Pp. 9–63.

- Levy G, Amitai P and Shulov A. 1973. New scorpions from Israel, Jordan and Arabia. *Zool. J. Linn. Soc.*, **52**:113–140.
- Lourenço WR, Abu Afifeh B, Al-Saraireh M, Abu Baker M and Amr Z. 2021a. New insights on the taxonomy of the genus *Buthus* Leach, 1815 in Jordan and description of a new species (Scorpiones: Buthidae). *Zool. Middle East*, **67**: 168-176.
- Lourenço WR, Modrý D and Amr Z. 2002. Description of a new species of *Leiurus* Ehrenberg, 1828 (Scorpiones, Buthidae) from the South of Jordan. *Rev. Suisse Zool.*, **109**:635–642.
- Lourenço WR, Yağmur EA and Duhem B. 2010. A new species of *Buthus* Leach, 1815 from Jordan. *Zool. Middle East*, **49**:95–99.
- Lowe G. 2010. The genus *Vachoniolus* (Scorpiones: Buthidae) in Oman. *Euscorpius*, **100**:1-37.
- Lowe G, Kovařík F, Stockmann M and Štáhlavský F. 2019. *Trypanothacus* gen. n., a new genus of burrowing scorpion from the Arabian Peninsula (Scorpiones: Buthidae). *Euscorpius*, **277**:1-30.
- Navidpour S, Kovařík F, Soleglad ME and Fet V. 2008. Scorpions of Iran (Arachnida, Scorpiones). Part I. Khoozestan Province. *Euscorpius*, **65**:1-41.
- Navidpour SH. 2021. Psammophilic scorpions in deserts of Iran. *Global Journal of Zoology*, 001-005. 10.17352/gjz.000020.
- Prendini L. 2001. Substratum specialization and speciation in southern African scorpions: the effect hypothesis revisited. Pp. 113–138. In: Fet V & Selden PA (Eds.), **Scorpions 2001. In Memoriam Gary A. Polis**. British Arachnological Society, Burnham Beeches, Buckinghamshire, UK.
- Stahnke HL. 1970. Scorpion nomenclature and mensuration. *Entomological News*, **81**:297–316.
- Vachon M. 1952. **Etudes sur les scorpions**. Alger: Publications de l'Institut Pasteur d'Algérie.
- Vachon M. 1974. Etude des caractères utilisés pour classer les familles et les genres de Scorpions (Arachnides). 1. La trichobothriotaxie en arachnologie. Sigles trichobothriotaxiques et types de trichobothriotaxie chez les Scorpions. *Bull. Mus. natl. hist. 3e sér.*, **104**:857–958.
- Vachon M. 1975. Sur l'utilisation de la trichobothriotaxie du bras des pédipalpes des Scorpions (Arachnides) dans le classement des genres de la famille des Buthidae Simon. *Comptes Rendus des Séances de l'Académie de Sciences*, **281(D)**:1597–1599.
- Vachon M. 1979. Arachnids of Saudi Arabia Scorpiones. *Fauna of Saudi Arabia*, **1**:30-66.

GC-MS Analysis of Various Crude Extracts from the Leaves, Flowers, and Stems of *Datura metel* Linnaeus 1753 and the Potential Activity as Anesthetic Agents on Fish

Rindhira Humairani^{1,*}, Nanda Rizki Purnama¹, Herpandi Herpandi², Mochamad Syaifudin³, Ilham Zulfahmi⁴, Yusrizal Akmal¹, Muliari Muliari⁵, Agung Setia Batubara⁶

¹Department of Aquaculture, Faculty of Agriculture, Universitas Almuslim, Bireuen 24261, Indonesia; ²Department of Fisheries Products Technology, Faculty of Agriculture, Universitas Sriwijaya, Indralaya Ogan Ilir, South Sumatera 30662, Indonesia; ³Department of Aquaculture, Faculty of Agriculture, Universitas Sriwijaya, Indralaya Ogan Ilir, South Sumatera 30662, Indonesia; ⁴Department of Fisheries Resources Utilization, Faculty of Marine and Fisheries, Universitas Syiah Kuala, Banda Aceh, Indonesia; ⁵Department of Marine Science, Faculty of Agriculture, Universitas Malikussaleh, Aceh Utara, Indonesia; ⁶Department of Biology, Faculty of Mathematics and Natural Sciences, Universitas Negeri Medan, Medan, Indonesia.

Received: August 16, 2022; Revised: January 24, 2023; Accepted: January 29, 2023

Abstract

Anesthesia made from the *Datura metel* (locally known as kecubung) has high potential as an alternative to synthetic fish anesthetics. This study aimed to identify the active compound in leaves, stems and flowers of *D. metel* and describe its potency as a fish anaesthetic agent. Samples of *D. metel* were collected from Takengon City, Aceh Tengah Regency, Indonesia. The phytochemical and fractionation tests were carried out at the Microbiology and Biotechnology Laboratory as well as the Chemistry and Biochemistry Laboratory, Department of Fisheries, Faculty of Agriculture, Sriwijaya University, Indonesia. Maceration technique using n-hexan solvent for 24 hours at a ratio of 1:2 v/v. GC-MS analysis was carried out to identify the chemical compounds in the extracts. The results showed that, as many as eleven compounds in leaves, seven compounds in flowers, and two compounds in stems of *D. Metel* were potential as fish anesthetics agent. In leaves, several compounds that have the potential as anesthetics agent of fish include: seychellene; trans-caryophyllene; α -guaiene; 1h-3a,7-methanoazulene,2,3,6,7,8,8a-hexa; alloaromadendrene; δ -guaiene; (-)-caryophyllene oxide; epiglobulol; 2-pentadecanone,6,10,14-trimethyl-; phytol. In the flower, include: trans-caryophyllene; α -guaiene; seychellene; alloaromadendrene; (-)-caryophyllene oxide; phytol. While, in stems include: α -guaiene and seychellene. These substances have reportedly been utilized as anaesthetic agents for several fish, including *Collossoma macropomum*, *Rhamdia quelen*, and *Oreochromis niloticus*.

Keywords: α -guaiene, phytol, seychellene, anesthetics

1. Introduction

The use of synthetic anesthetics in fish has several risks, such as residues that have an impact on fish, consumers and the environment. Synthetic anesthetics commonly used in fish include 2-phenoxyethanol, benzocaine (etil paraaminobenzoate), carbon dioxide, eetomidate, and tricaine methanesulfonate (MA-222) (Purbosari *et al.*, 2019). The risk of using synthetic anesthetics in fish causes hypoxemia, hypercapnia, hypoglycaemia, increased levels of lactic acid, erythrocyte swelling, elevated haematocrit and changes in blood electrolytes, hormones, cholesterol, urea and inter-renal ascorbic acid (Martins *et al.*, 2019). Therefore, an inventory of natural anesthetics continues to be carried out to avoid residues. The advantages of natural anesthetics include low impact on the environment, no residue, cheaper, and effective at low concentrations compared to

synthetic anesthetics (Purbosari *et al.*, 2019). There are several herbal plants that have bioactive components as anesthetic agents that have been identified, where *Datura metel* (local name is kecubung) is one of them that has high potential as an anesthetic compound (Adebayo and Olufayo, 2017; Hariyanto *et al.*, 2009; Palmi *et al.*, 2019; Akbar *et al.*, 2021; Saputra *et al.*, 2021).

All parts of *D. metel* including roots, stems, leaves, flowers, fruits and seeds are reported to contain bioactive compounds including alkaloids, saponins, flavonoids, and phenols (Kuganathan and Ganeshalingam, 2011; Alabri, 2014). The concentration of alkaloids in the roots and seeds reached 0.4-0.9%, while in the leaves and flowers it reached 0.2-0.3%. High concentrations of alkaloids in *D. metel* can cause anticholinergic activity in the body, resulting in several cases such as hallucinations, delirium and convulsions. Based on BNN (National Anti-Narcotics Agency of Indonesia) (2014) data, *D. metel* is often used as a narcotic, where hallucinogenic compounds reach 3%.

* Corresponding author. e-mail: humairanirindhira@gmail.com.

D. metel originated from Central America and southeastern Mexico which was then cultivated and spread widely because of the beauty of the flower and its medicinal benefits (Monira and Munan, 2012). *D. metel* has the same name for all races although it actually has chromosomal differences and produces different flower colors (Bergner, 1943). In the Gayo highlands (Aceh Tengah Regency, Indonesia), this plant is widely cultivated and used as an ornamental plant in the yard for the treatment of asthma. *D. metel* which grows in the Gayo highlands has stems that can grow tall and have reddish yellow flowers. *D. metel* has been used as a medicinal ingredient for centuries as an anti-bacterial, antiseptic, narcotic, and sedative (Ganesh *et al.*, 2015; Alam *et al.*, 2021). The people of Aceh use *D. metel* to mix hernia ingredients, treat toothache, rheumatism and fungal infections (Ristoja, 2012).

Studies on extraction solutions, chemical compositions of extracts from various parts of the plant genus *Datura* have been analyzed and their anesthetic activity tested on various types of fish such as *Cyprinus carpio* (Rahanandeh *et al.*, 2022), *Epinephelus* sp. (Saputra *et al.*, 2021), *Heterobranchus bidorsalis* (Adebayo and Olufayo, 2017), *Oreochromis niloticus* (Palmi *et al.*, 2019), and *Osphronemus gourami* (Mashuda *et al.*, 2020). In addition, the effectiveness of this plant anesthetic has also been tested on dogs (Bbalola *et al.*, 2014) and rabbits (Elsa *et al.*, 2001). Previous research by Kiruthika and Sornaraj (2011) revealed that there are four active compounds in *D. metel* flower extract including 1,4-cyclohexadiene, 1-methyl; acetic acid, trifluoro-, 2,2-dimethylpropylester; 4-trifluoroacetoxyoctane; cis-2-nitro-4-tbutylcyclohexanone. However, information regarding the content of active compounds (including stems, leaves and flowers) that have the potential as anesthetic in *D. metel* has not been reported completely. Therefore, identification is needed to obtain complete information to support the use of *D. metel* extract as a natural anesthetic that is safe and does not leave negative effects on fish, people, and the environment.

2. Material and methods

2.1. Site and Time

This research was carried out from September 2021 to January 2022. Sample preparation and extraction were carried out in the MIPA Laboratory of Almuslim University, Indonesia. The phytochemical and fractionation tests were carried out at the Microbiology and Biotechnology Laboratory as well as the Chemistry and Biochemistry Laboratory, Department of Fisheries, Faculty of Agriculture, Sriwijaya University, Indonesia.

2.2. Sample Collection

Samples of *D. metel* were collected from Takengon City, Aceh Tengah Regency, Indonesia. The samples were then sorted between stems, leaves and flowers, then air-dried. The dried sample was then crushed with a waring blender to obtain the required sample size. The resulting yield was calculated based on weight percent extract/dry weight (w/w) and stored in a sample bottle at -4°C (Silva *et al.*, 2012). The ingredients were then identified by comparing mass spectrum value based on the NIST (2005)

and Adams (2001) mass spectrum literature. Fractionation and isolation of essential oils were carried out according to the method of Benovit *et al.* (2015).

2.3. Extraction of Phytochemical Components

The leaves, stems and flowers that have been air-dried and crushed were then extracted by maceration technique using n-hexan solvent for 24 hours at a ratio of 1:2 v/v. The extract solution was filtered using Whatman paper no.1. A thick extract was generated by combining the maceration filtrates and vaporizing the solvent in a vacuum rotary evaporator at a temperature close to the solvent's boiling point (n-hexane 69°C).

2.4. GC-MS Analysis

GC-MS analysis was performed using a Shimadzu GC-MS-QP2010 Ultra equipped with a 30 m × 0.25 mm × 0.25 µm Rxi-1MS column (Restek), and the initial temperature of the 100°C column was heated for 5 minutes, then the temperature was gradually increased up to 250°C at a rate of 10°C min⁻¹. The split injector and the GC-MS interface were each at a temperature of 250°C. The detectors used were mass-selective and electron-impact mass ionization spectrometry programmed at 70 eV and a temperature of 250°C. The carrier gas used was helium with a flow rate of 2.0 mL min⁻¹, and an injection volume of 2 L. Data was recorded using GC-MS Solution Software (Shimadzu).

2.5. Chemical Identification

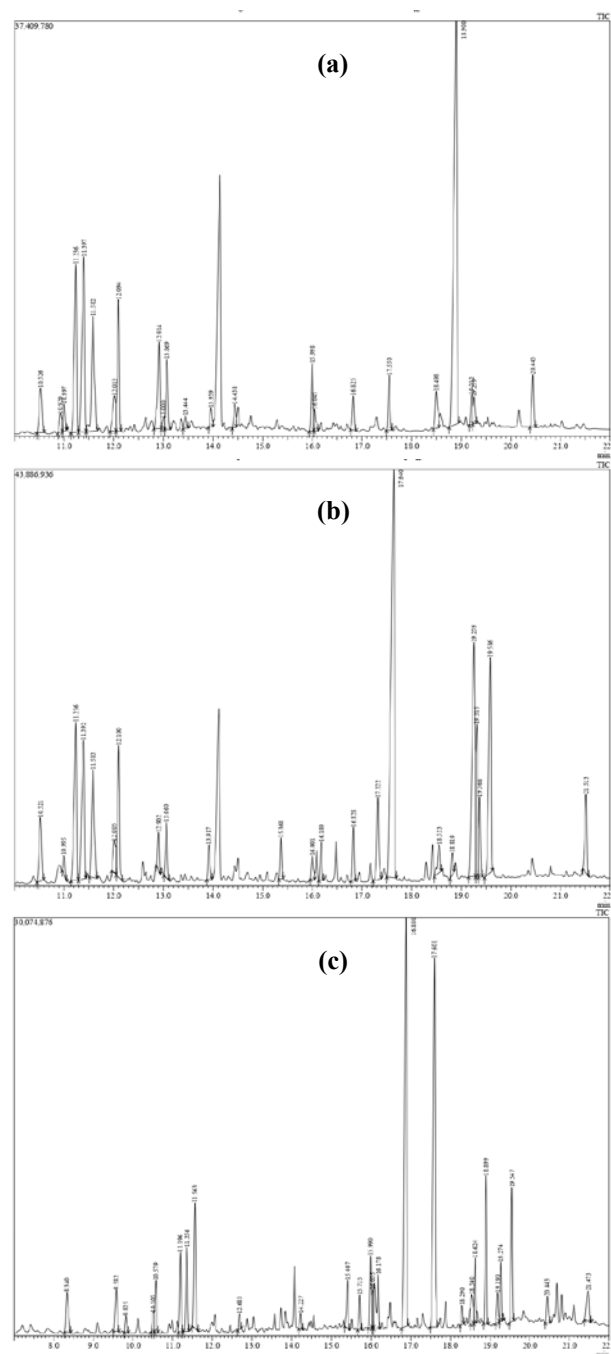
Chemical compounds in the extracts from the leaves, stems and flowers of *D. metel* were identified based on the retention time of GC on the column. Chromatograms were interpreted based on the NIST (2005) library consisting of two hundred thousand compounds. The name, molecular weight and percentage of the unknown compound were evaluated by Mass Spectrometry. The compounds were identified by comparing the results of Mass spectrometry measurements with data obtained from the literature and the NIST database.

3. Results

About 23-26 (a total of 52) compounds were identified in the hexane extract of *D. metel* from the leaves, flowers and stems (Table 1 and Figure 1). Based on the results of the GC-MS analysis and literature studies, the compounds that have the potential as anesthetics in *D. metel* are 11 compounds in the leaf, 7 compounds in the flower, and 2 compounds in the stem. Compounds that have the potential as anesthetics in *D. metel* are 11 compounds in the leaves, 7 compounds in the flowers, and 2 compounds in the stems. In the hexane extract of the *D. metel* leaves, compounds that have the potential to be anesthetics include seychellene; trans-caryophyllene; α-guaiene; 1h-3a,7-methanoazulene,2,3,6,7,8,8a-hexa; alloaromadendrene; δ-guaiene; (-)-caryophyllene oxide; epiglobulol; 2-pentadecanone,6,10,14-trimethyl-; phytol. In the hexane extract of the flowers of *D. metel*, compounds that have the potential to be anesthetics include trans-caryophyllene; α-guaiene; seychellene; alloaromadendrene; (-)-caryophyllene oxide; phytol. In the hexane extract of the stem of *D. metel*, compounds that have the potential to be anesthetics include α-guaiene dan seychellene.

Table 1. Compounds detected in leaves, flowers and stems of *Datura metel* with hexane solvent using GC-MS analysis

No	Compounds	Leaves		Flowers		Stems	
		Retention Time (minute)	Area (%)	Retention Time (minute)	Area (%)	Retention Time (minute)	Area (%)
1	Guaia-1(10),11-diene	10.526	2.96	10.521	2.92	-	-
2	Seychellene	10.920	1.14	-	-	-	-
3	trans-Caryophyllene	10.997	1.39	10.995	0.65	-	-
4	α -Guaiene	11.236	9.41	11.236	6.90	11.196	3.13
5	Seychellene	11.397	11.20	11.392	6.84	11.356	3.82
6	1H-3a,7-Methanoazulene, 2,3,6,7,8,8a-hexa	11.582	7.98	-	-	-	-
7	Alloaromadendrene	12.013	2.60	12.005	1.62	-	-
8	δ -Guaiene	12.094	5.88	12.100	4.73	-	-
9	Ledol	12.914	4.83	-	-	-	-
10	1H-Cycloprop[e]azulen-4-ol, decahydro-1,	13.000	0.57	12.902	1.09	-	-
11	(-)-Caryophyllene oxide	13.069	3.38	-	-	-	-
12	Kauran-18-al, 17-(acetyloxy)-, (4-beta.)- (C	13.444	0.65	-	-	-	-
13	Epiglobulol	13.959	0.94	-	-	-	-
14	6-ISOPROPENYL-4,8A-DIMETHYL-3,5,	14.438	1.20	-	-	-	-
15	2-Pentadecanone, 6,10,14-trimethyl-	15.998	3.01	-	-	15.990	2.89
16	NEOPHYTADIENE	16.045	0.96	16.001	0.96	16.035	1.51
17	Palmitic acid, Hexadecanoic acid, methyl e	16.825	1.51	-	-	-	-
18	Hexadecanoic acid, ethyl ester (CAS) Ethyl	17.550	2.25	-	-	-	-
19	1-Octadecanol (CAS) Stenol	18.498	2.29	-	-	-	-
20	Phytol	18.900	31.07	18.819	0.69	-	-
21	Ethyl linoleate	19.212	1.26	19.259	13.10	-	-
22	ETHYL LINOLEOLATE	19.259	1.17	-	-	-	-
23	1-Octadecanol (CAS) Stenol	20.445	2.36	-	-	-	-
24	α -Patchoulene	-	-	11.583	5.27	-	-
25	(-)-Caryophyllene oxide	-	-	13.060	1.84	-	-
26	Decanedioic acid, diethyl ester (CAS) Bisof	-	-	13.917	1.18	-	-
27	Tetradecanoic acid, ethyl ester (CAS) Ethyl	-	-	15.368	1.16	-	-
28	Pentadecanoic acid, ethyl ester	-	-	16.180	1.11	-	-
29	Hexadecanoic acid, methyl ester (CAS) Me	-	-	16.828	1.61	-	-
30	Ethyl 9-hexadecenoate	-	-	17.322	3.08	-	-
31	Hexadecanoic acid, ethyl ester (CAS) Ethyl	-	-	17.640	24.57	17.601	20.58
32	Octadecanoic acid, ethyl ester (CAS) Ethyl	-	-	18.553	1.34	18.290	0.70
33	ETHYL OCTADEC-9-ENOATE	-	-	19.315	5.03	-	-
34	(E)-9-Octadecenoic acid ethyl ester	-	-	19.368	2.36	19.274	2.14
35	Octadecanoic acid, ethyl ester	-	-	19.586	9.07	19.547	5.01
36	Eicosanoic acid, ethyl ester	-	-	21.513	2.89	21.473	2.28
37	2-Decenal, (Z)-	-	-	-	-	8.340	2.48
38	2(3H)-Furanone, dihydro-5-pentyl- (CAS)	-	-	-	-	9.582	2.25
39	2-Undecenal, E-	-	-	-	-	9.825	0.70
40	4,7-Methanoazulene, 1,2,3,4,5,6,7,8-octahy	-	-	-	-	10.505	1.08
41	Nonanoic acid, 9-oxo-, methyl ester	-	-	-	-	10.579	2.19
42	Nonanoic acid, 9-oxo-, ethyl ester (CAS)	-	-	-	-	11.563	6.08
43	9-Octadecenoic acid, methyl ester, (E)- (C	-	-	-	-	12.683	0.58
44	Nitrobenzene, 3,4,5-trimethoxy-	-	-	-	-	14.227	0.59
45	Tridecanoic acid, 12-methyl-, methyl ester	-	-	-	-	15.407	1.93
45	Pentadecanoic acid, methyl ester (CAS) Me	-	-	-	-	15.715	1.28
46	Heptadecanoic acid, ethyl ester (CAS) Ethy	-	-	-	-	16.178	4.23
47	Pentadecanoic acid, 14-methyl-, methyl est	-	-	-	-	16.880	22.27
46	Linoleic acid, 9,12-Octadecadienoic acid (Z	-	-	-	-	18.540	1.72
49	9-Octadecenoic acid, methyl ester, (E)-	-	-	-	-	18.624	2.42
50	Methyl stearate	-	-	-	-	18.899	5.57
51	9,12-Octadecadienoic acid (Z,Z)-	-	-	-	-	19.190	1.30
52	N-HENTRIACONTANOL-1	-	-	-	-	20.443	1.28



2018), δ -guaiene (Silva *et al.*, 2015; Uritu *et al.*, 2018; Jugran *et al.*, 2019), (-)-caryophyllene oxide (Silva *et al.*, 2015; Almeida *et al.*, 2018; Benovit *et al.*, 2015; Sharif *et al.*, 2020), and phytol (Sharif *et al.*, 2020). In the seven compounds, the percentage of chromatogram area indicated by α -guaiene and seychellene was the highest, reaching 6.90% and 6.84%, respectively.

The hexane extract of the stem of *D. metel* showed compounds that have the potential to have anesthetic activity including α -guaiene (Silva *et al.*, 2015; Jugran *et al.*, 2019) and seychellene (Lu *et al.*, 2011; Swamy and Sinniah, 2015) with the percentage of the chromatogram area is 3.13% and 3.82%. This percentage is smaller than that contained in flowers and leaves. The dominating compounds in the hexane extract are fatty acid ester compounds, namely pentadecanoic acid, 14-methyl-, methyl ester, and hexadecanoic acid, ethyl ester with a chromatogram area of 22.27% and 20.58%, respectively. Similar with the research conducted by Hossain *et al.* (2013) that the hexane extract from *D. metel* was dominated by fatty acid groups and their derivatives, but the presence of several types of sesquiterpene compounds in the hexane extract of leaves, flowers and stems of *D.*

metel identified was slightly different from previous studies. The molecular configurations read from the mass spectra of α -guaiene, seychellene and phytol compounds can be seen in Figure 2.

Various studies have been conducted to identify fish anaesthetic agents derived from natural substances. Inoue *et al.* (2003) revealed that clove oil was an effective anaesthetic for *Brycon cephalus* fish. It has also been reported that extracts from the plants *Lippia alba*, *Spilanthes acmella*, and *Nicotiana tabacum* have the potential to serve as anaesthetic agents for several species of fish (Cunha *et al.*, 2011; Barbas *et al.*, 2016; Agokei and Adebisi, 2010; Zulfahmi *et al.*, 2019). Several secondary metabolic compounds found in *datura metel*, such as guaiene; seychellene; trans-caryophyllene; α -guaiene; 1h-3a,7-methanoazulene,2,3,6,7,8,8a-hexa; alloaromadendrene; δ -guaiene; (-)-caryophyllene oxide; epiglobulol; 2-pentadecanone,6,10,14-trimethyl-; phytol. Phytol was also observed in other plants (*Lippia alba* and *Colossoma macropomum*) that have been demonstrated to be effective as natural anesthetics for fish (Barbas *et al.*, 2016; dos Santos Maia *et al.*, 2019).

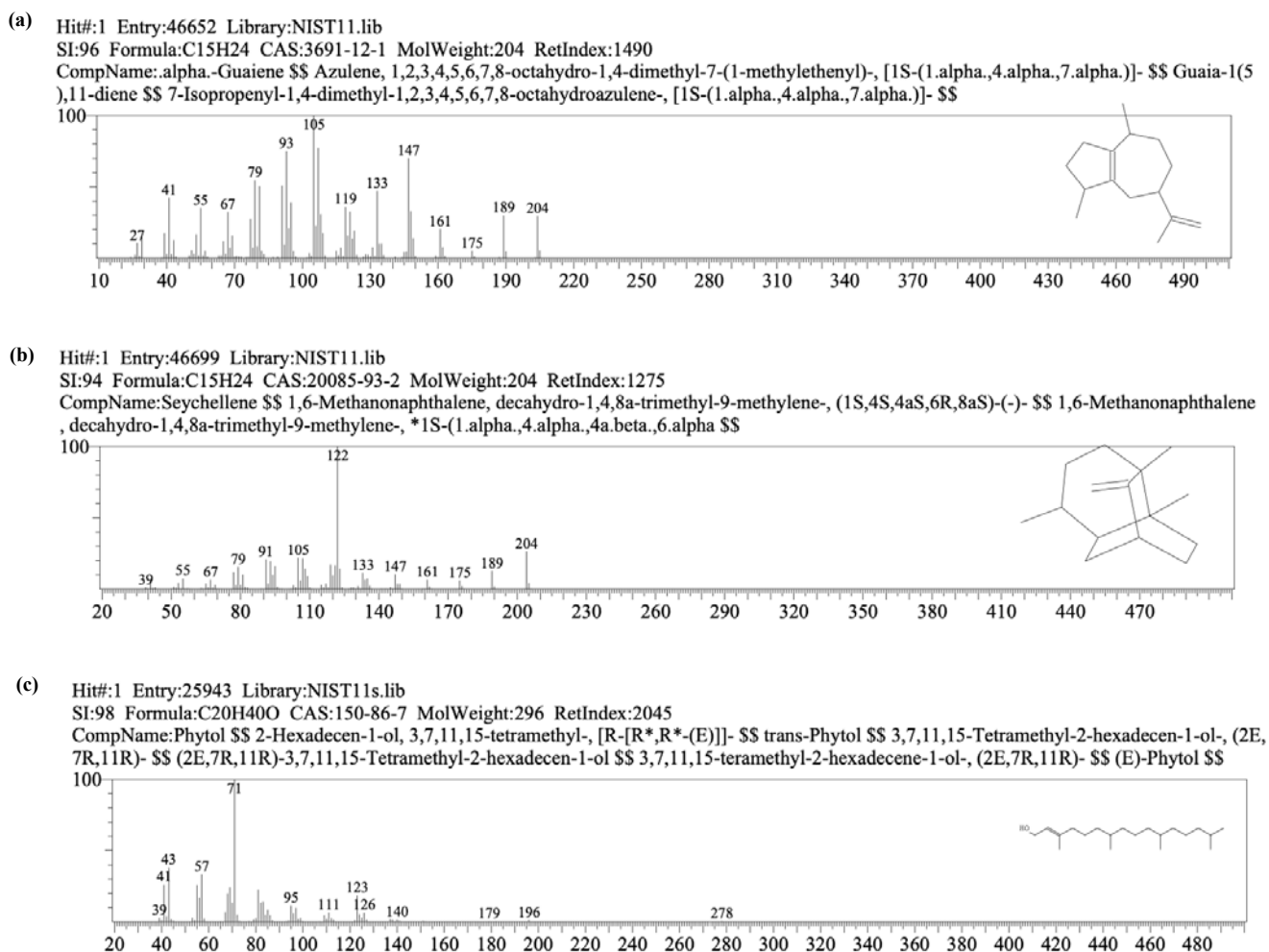


Figure 2. Mass spectra of α -guaiene (a), Seychellene (b) and Phytol (c) according to the NIST library.

5. Conclusion

Compounds that have the potential as anesthetics in *D. metel* are 11 compounds in the leaves, 7 compounds in the flowers, and 2 compounds in the stems. In the hexane extract of the leaves of *D. metel*, compounds that have the potential to be anesthetics include seychellene; trans-caryophyllene; α -guaiene; 1h-3a,7-methanoazulene,2,3,6,7,8,8a-hexa; alloaromadendrene; δ -guaiene; (-)-caryophyllene oxide; epiglobulol; 2-pentadecanone,6,10,14-trimethyl-; phytol. In the hexane extract of the flowers of *D. metel*, compounds that have the potential to be anesthetics include trans-caryophyllene; α -guaiene; seychellene; alloaromadendrene; (-)-caryophyllene oxide; phytol. In the hexane extract of the stem of *D. metel*, compounds that have the potential to be anesthetics include α -guaiene dan seychellene. The leaves of *D. metel* have the best anesthetic potential because they have the most anesthetic components, so their use and testing are important to do in fish in future studies.

Conflict of interest

None.

Acknowledgments

We would like to thank the Directorate of Research and Community Service of RISTEK-BRIN which has funded this research, the Laboratory of Mathematics and Natural Sciences (MIPA) of Almuslim University and the Laboratory of the Faculty of Agriculture, Sriwijaya University for facilitating the implementation of this research, as well as the Research and Community Service (LPPM) of Almuslim University.

References

- Adams RP. 2001. Identification of essential oil components by gas chromatography/quadrupole mass spectroscopy. Allured Publishing Corporation, Illinois.
- Adebayo SF and Olufayo MO. 2017. Anaesthetic effects of *Datura stramonium* leaf on *Heterobranchus bidorsalis* Juveniles. *Int J Fish Aqua Stud.*, **5**: 590-593.
- Agokei OE and Adebisi AA. 2010. Tobacco as an anesthetic for fish handling procedures. *J Med Pla Res.*, **4**: 1396-1399.
- Akbar R, Jumsurizal J and Putri RMS. 2021. Teknik imotilisasi ikan kerapu cantang (*Epinephelus* sp.) menggunakan ekstrak daun kecubung (*Datura Metel* L.). *Marinade*, **4**: 40-49. (in Indonesian)
- Alabri THA, Al-Musalami AHS, Hossain MA, Weli AM and Al-Riyami Q. 2014. Comparative study of phytochemical screening, antioxidant and antimicrobial capacities of fresh and dry leaves crude plant extracts of *Datura metel* L. *J King Saud UnivSci.*, **26**: 237-243.
- Alam W, Khan H, Khan SA, Nazir S and Akkol EK. 2021. *Datura metel*: A review on chemical constituents, traditional uses and pharmacological activities. *Curr Pharmac Des.*, **27**: 2545-2557.
- Almeida APG, Maria HB, Val AL and Baldissarroto B. 2018. Essential oils and eugenol as anesthetics for *Serrasalmus rhombeus*. *Bol Inst Pesc Sao Paulo*, **44**: 44-50.
- Astuti P, Khairan K, Marthoenis M and Hasballah K. 2022. Antidepressant-like activity of patchouli oil var. Tapak Tuan (*Pogostemon cablin* Benth) via elevated dopamine level: a study using rat model. *Pharmaceuticals*, **15**: 608.
- Barbas LAL, Hamoy M, Mello VJ, Barbosa RPM, Lima HST, Torres MF, Nascimento LAS, Silva JKR, Andrade EHA and Gomes MRF. 2017. Essential oil of citronella modulates electrophysiological responses in tambaqui *Colossoma macropomum*: A new anaesthetic for use in fish. *Aqua.*, **479**: 60-68.
- Bbalola SA, Suleiman MM, Hassan AZ and Adawa DAY. 2014. Evaluation of the crude methanolic seed extract of *Datura metel* L. as a potential oral anaesthetic in dogs. *Glob J Pharmacol.*, **8**: 154-159.
- Benovit SC, Silva LL, Salbego J, Loro VL, Mallmann CA, Baldissarroto B, Flores EMM and Heinzmann BM. 2015. Anesthetic activity and bio-guided fractionation of the essential oil of *Aloysiagrattissima* (Gillies & Hook) tronc. in silver catfish *Rhamdiaquelen*. *An Acad Brasil Cien.*, **87**: 1675-1689.
- Bergner AD. 1943. Geographical distribution of chromosomal types in *Datura metel*. *Am J Bot.*, **30**: 222-230.
- BNN (National Anti Narcotics Agency of Indonesia). 2014. Jurnal data pencegahan dan pemberantasan penyalahgunaan dan peredaran gelap narkoba (P4GN) 24 Tahun 2013 Edisi 2014. National Anti Narcotics Agency of Indonesia, Jakarta. (in Indonesian)
- Cunha MA, Silva BF, Delunardo FAC, Benovit SC, Gomes LC, Heinzmann BM and Baldissarroto B. 2011. Anesthetic induction and recovery of *Hippocampus reidi* exposed to the essential oil of *Lippia alba*. *Neotrop Ichthyol.*, **9**: 683-688.
- Durugbo EU, Ogah JO, Chukwuemeka N, Sename PG, Olukanni AT, Yusuf KO, Awuzie IC, Olukanni OD and Aboaba SO. 2021. Phytochemical, chemical and biomedical characterization of crude extracts of *Macrosphyra longistyla* (DC.) Hiern. *Jordan J Biol Sci.*, **14**: 453-461.
- Dahan A, Sarton E, Teppema L, Olievier C, Nieuwenhuijs D, Matthes HW and Kieffer BL. 2001. Anesthetic potency and influence of morphine and sevoflurane on respiration in μ -opioid receptor knockout mice. *J Am Soc Anesthesiol.*, **94**: 824-832.
- dos Santos Maia JL, de Oliveira Sousa EM, da Silva HNP, Pinheiro MTL, Mourão RHV, Maia JGS and da Silva LVF. 2019. Hydrolate toxicity of *Lippia alba* (Mill.) NE Brown (Verbenaceae) in juvenile tambaqui (*Colossoma macropomum*) and its potential anaesthetic properties. *Aquac.*, **503**: 367-372.
- Elsa AT, Ayika WG, Rabi I, Osunkwo UA and Onyeyili PA. 2001. Preliminary studies on the effects of *Datura metel* seed extract on amylobarbitone anaesthesia in rabbits. *Sokoto J Vet Sci.*, **3**: 39-43.
- Ganesh S, Radha R and Jayshree N. 2015. A review on phytochemical and pharmacological status of *Datura fastuosa* Linn. *Int J Multidisc Res Dev.*, **2**: 602-605.
- Hariyanto SE, Pranata FS and Aida Y. 2009. Pemanfaatan ekstrak daun kecubung (*Datura metel* L.) sebagai pembius ikan koi (*Cyprinus carpio* L.) pada saat pengangkutan. *Biota*, **13**: 24-30. (in Indonesian)
- Hossain MA, Alsabari KM, Weli AM, and Al-Riyami Q. 2013. Gas chromatography-mass spectrometry analysis and total phenolic contents of various crude extracts from the fruits of *Datura metel* L. *J Taibah Univ Sci.*, **7**: 209-215.
- Ibrahim HA, El-Morsy ESM, Amer MS, Farhat AZ and Mohesien MT. 2022. Suppression of *Aspergillus* and *Penicillium* species by organic extracts of common soft corals and sponge species habitated in Hurghada, Red Sea, Egypt. *Jordan J. Biol Sci.*, **15**: 43-57.

- Islam MT, Ali ES, Uddin SJ, Shaw S, Islam MA, Ahmed MI and Atanasov AG. 2018. Phytol: A review of biomedical activities. *Food Chem Toxicol.*, **121**: 82-94.
- Jain PL, Patel SR and Desai MA. 2022. Patchouli oil: an overview on extraction method, composition and biological activities. *J Ess Oil Res.*, **34**: 1-11.
- Jash SK and Gorai D. 2015. Sugar derivatives of morphine: A new window for the development of potent anesthetic drugs. *Nat Prod Biopros.*, **5**: 111-127.
- Jugran AK, Rawat S, Bhatt ID and Rawal RS. 2019. *Valeriana jatamansi*: An herbaceous plant with multiple medicinal uses. *Phytoth Res.*, **33**: 482-503.
- Junren C, Xiaofang X, Mengting L, Qiuyun X, Gangmin L, Huiqiong Z and Cheng P. 2021. Pharmacological activities and mechanisms of action of *Pogostemon cablin* Benth: a review. *Chinese Med.*, **16**: 1-20.
- Kartal M, Kaya S and Kurucu S. 2002. GC-MS analysis of propolis samples from two different regions of Turkey. *Zeitschrift für Naturforschung*, **57**: 905-909.
- Kiruthika KA and Sornaraj R. 2011. Screening of bioactive components of the flower *Datura metel* using the GC-MS technology. *Int J Pharm Technol Res.*, **3**: 2025-2028.
- Kuganathan N and Ganeshalingam S. 2011. Chemical analysis of *Datura metel* leaves and investigation of the acute toxicity on grasshoppers and red ants. *E-J Chem.*, **8**: 107-112.
- Lu TC, Liao JC, Huang TH, Lin YC, Liu CY, Chiu YJ and Peng WH. 2011. Analgesic and anti-inflammatory activities of the methanol extract from *Pogostemon cablin*. *Evid Bas Compl Altern Med.*, **2011**: 1-9.
- Martins T, Valentim A, Pereira N and Antunes LM. 2019. Anaesthetics and analgesics used in adult fish for research: A review. *Lab Anim.*, **53**: 325-341.
- Mashuda MM, Triastuti J and Pursetyo KT. 2020. Activity test of anti-stress from extract of *Datura metel* seeds with ethanol solvent towards blood glucose levels and survival rate of *Osphronemus gouramy* seed in closed system transportation. *IOP Conf Ser: Earth Envir Sci.*, **441**: 012145.
- Monira KM and Munan SM. 2012. Review on *Datura metel*: A potential medicinal plant. *Glob J Res Med Plant Indig Med.*, **1**: 123-132.
- NIST (National Institute of Standards and Technology). 2005. Mass spectral library and search/analysis programs. John Wiley & Sons Hoboken, New Jersey.
- Palmi RS, Yudha IG and Wardiyanto W. 2019. The effects of amethyst *Datura metel* (Linn, 1753) leaves extract as an anesthetic agent on haematological condition of tilapia *Oreochromis niloticus* (Linn, 1758) fry. *E-J Rek Tekn Bud Per.*, **8**: 897-908.
- Pinho-Da-Silva L, Mendes-Maia PV, Teófilo TMDNG, Barbosa R, Ceccatto VM, Coelho-De-Souza AN and Leal-Cardoso JH. 2012. Trans-caryophyllene, a natural sesquiterpene, causes tracheal smooth muscle relaxation through blockade of voltage-dependent Ca²⁺ channels. *Molecules*, **17**: 11965-11977.
- Purbosari N, Warsiki E, Syamsu K and Santoso J. 2019. Natural versus synthetic anesthetic for transport of live fish: A review. *Aqua Fish.*, **4**: 129-133.
- Rahanandeh M, Tizkar B and Rahanandeh M. 2022. The effects of *Datura stramonium* L seed extract on anesthesia of farmed *Cyprinus carpio* in Guilan province. *Iran J Aqua Anim Health*, **8**: 16-25.
- Ristoja T. 2012. Laporan riset tumbuhan obat dan jamu (RISTOJA) Provinsi Aceh. Universitas Syiah Kuala, Aceh. (in Indonesian)
- Santos CCDMP, Salvadori MS, Mota VG, Costa LM, De-Almeida AAC, De-Oliveira GAL and De-Almeida RN. 2013. Antinociceptive and antioxidant activities of phytol in vivo and in vitro models. *Neurosci J.*, **2013**: 1-9.
- Saputra A, Putri MS and Apriandi A. 2021. Grouper imotilization technique *Epinephelus* sp. using *Datura Metel* L. seed extract. *J Mar Coas Sci.*, **10**: 105-117.
- Sharif M, Najafizadeh P, Asgarpanah J and Mousavi Z. 2020. In vivo analgesic and anti-inflammatory effects of the essential oil from *Tanacetum balsamita* L. *Brazil J Pharmac Sci.*, **56**: e18357.
- Silva LL, Parodi TV, Reckziegel P, Garcia VO, Bureger ME, Baldisserotto B, Malmann CA, Pereira AMS and Heinzmann BM. 2012. Essential oil of *Ocimum gratissimum* L.: Anesthetic effects, mechanism of action and tolerance in silver catfish *Rhamdia quelen*. *Aquacul.*, **350**: 91-97.
- Silva LDL, Garlet QI, Koakoski G, Abreu MSD, Mallmann CA, Baldisserotto B and Heinzmann BM. 2015. Anesthetic activity of the essential oil of *Ocimum americanum* in *Rhamdia quelen* (Quoy & Gaimard, 1824) and its effects on stress parameters. *NeotropIchthyol.*, **13**: 715-722.
- Swamy MK and Sinniah UR. 2015. A comprehensive review on the phytochemical constituents and pharmacological activities of *Pogostemon cablin* Benth.: An aromatic medicinal plant of industrial importance. *Molecules*, **20**: 8521-8547.
- Taj T, Sultana R, Shahin HDH, Chakraborty M and Ahmed MG. 2021. Phytol a phytoconstituent, its chemistry and pharmacological actions. *GIS Sci J.*, **8**: 395-406.
- Uritu CM, Mihai CT, Stanciu GD, Dodi G, Alexa-Stratulat T, Luca A and Tamba BI. 2018. Medicinal plants of the family Lamiaceae in pain therapy: A review. *Pain Res Manag.*, **2018**: 1-44.
- Wang X, Liu Y, Niu Y, Wang N and Gu W. 2018. The chemical composition and functional properties of essential oils from four species of *Schisandra* growing wild in the Qinling Mountains, China. *Molecules*, **23**: 1645.
- Wang LM, Zhang Z, Yao RZ and Wang GL. 2021. The role of intrathecal morphine for postoperative analgesia in primary total joint arthroplasty under spinal anesthesia: A systematic review and meta-analysis. *Pain Med.*, **22**: 1473-1484.
- Zulfahmi I, Humairani R and Akmal Y. 2019. Hemp leaf (*Cannabis sativa* Linn) extract as anesthetic agents on Koi (*Cyprinus carpio* Koi). *J Agroqua*, **16**: 100-108.

The Effect of 17 β -Estradiol and Genistein on the Prostate Gland and Testes of Aged Rats

Falah Shidaifat^{*}, Mohammed Khalifeh and Yousef Yasin

Department of Basic Veterinary Medical Sciences, Faculty of Veterinary Medicine, Jordan University of Science and Technology, Irbid, Jordan.

Received: November 10, 2022; Revised: January 29, 2023; Accepted: February 6, 2023

Abstract

This experiment was carried out to investigate the effect of 17 β -estradiol and genistein, a phytoestrogen, on the primary and the secondary male organs of aged male rats and related reproductive hormones. The effect of each chemical was evaluated using several tests. The effect of 17 β -estradiol and genistein on the histological structures of the testes and the prostate gland was evaluated by Hematoxylin and Eosin staining. The ability of 17 β -estradiol and genistein to affect the proliferation capacity of the prostatic cells was determined by the immunolocalization of the proliferating cell nuclear antigen (PCNA). Finally, the pituitary-gonadal hormonal interplay was evaluated by ELISA which was used to determine the changes that occurred in the blood hormone levels of testosterone, follicle stimulating hormone (FSH), and luteinizing hormone (LH). The results showed that the 17 β -estradiol significantly reduced the gross weights of the prostate and testes. This reduction of the weight was accompanied by a prominent degeneration of the secretory epithelial cells of the prostate and the seminiferous tubules of the testes. In addition, 17 β -estradiol acts to inhibit the proliferation of the prostatic cells as evident by a significant reduction of the PCNA proliferation index. Although 17 β -estradiol treatment was associated with significant decrease of blood testosterone level, it exerts no significant effect on either LH or FSH levels. On the other hand, genistein did not show any effect on the prostate, testes or blood hormone levels when compared to the control group. These results indicated that 17 β -estradiol exerts a deleterious effect on the structure of the prostate, testes, and testosterone production without any appreciable effect on the pituitary hormones.

Keywords: Prostate, Testes, 17 β -estradiol, Genistein, Testosterone, Proliferation Index

1. Introduction

Exposure of animals to a naturally occurring and synthetic estrogenic compounds, such as 17 β -estradiol have been shown to affect male reproduction by interfering with the testicular structure and function (Gill-Sharma *et al.*, 2001). These estrogenic compounds are also implicated in the disruption of normal endocrine functions of the hypothalamic-pituitary-gonadal axis, therefore posing a potentially serious male fertility problem (Gill-Sharma *et al.*, 2001). Of particular concern is the effect of the estrogenic compounds on the testicular androgen production (Jones *et al.*, 1978), which might influence the prostate gland growth, as its growth and maturity depend on the continuous supply of testosterone (Shidaifat *et al.*, 2007). Indeed, it has been shown that estrogen treatment of neonatal rodents acts to decrease the number of estrogen receptors and alter prostatic cell proliferation (Un-No *et al.*, 2007), and differentiation (Putz *et al.*, 2001).

Benign Prostatic Hyperplasia (BPH) is a spontaneously occurring condition of aged males (Oesterling, 1996) with hormones being the major role players of such progression (Nicholson *et al.*, 2013; Nicholson and Rieke, 2011). Although androgens are the primary hormones that cause such a condition, estrogen also has its contribution by

targeting the estrogen receptor alpha (ER α) and beta (ER β) (Gallardo *et al.*, 2009). While estrogenic effect mediated by ER α contributes to the pathogenesis of BPH (Shi *et al.*, 2017), estrogenic effects mediated by ER β act to suppress prostatic cells proliferation, and support their differentiation (Christoforou *et al.*, 2014; Prins and Korach, 2008). Therefore, it is reasonable to assume that activation of ER β with its antiproliferative feature has the potential to play a suppressive role, and thus could be used to control BPH.

Genistein, a non-steroidal chemical derived from soybeans, exerts an estrogen like activity on vertebrates' tissues. It has been reported that genistein consumption is associated with lower risk of many cancers, including the prostate cancer (Jaiswal *et al.*, 2019). Genistein appears to reduce the incidence of prostate adenocarcinoma through a mechanism that involves, at least, the down regulation of ER α (Lamartiniere *et al.*, 2002), and modulation of its activation (Kostelac *et al.*, 2003). Together, these findings suggest a suppressive role of genistein on the growth, and development of the prostate gland, as well as providing a potential therapeutic value to treat prostate gland modalities. This study was conducted to compare the effect of estradiol and genistein on the testes, the prostate gland, and the associated endocrinological interplay of the pituitary-gonadal axes in aged rats.

^{*} Corresponding author. e-mail: falah@just.edu.jo.

2. Materials and Methods

2.1. Animals

Fifteen male Wistar rats, aged between 10 – 12 months were used in this study. They were housed in the Animal House at the Jordan University of Science and Technology. The rats were randomly assigned to one of three groups (n=5). The first group served as a control and rats of this group received a daily injection of 0.1 ml of dimethyl sulfoxide (DMSO) for 26 days. The rats of the second group were treated daily with Genistein (10mg/0.1ml) for 26 days. The rats of the third group received treatment of estrogen (1mg/0.1ml) for 26 days. At the end of the treatment period, all rats were euthanized in a jar that contained ether-soaked cotton. Samples were then collected from each rat and included the prostate gland, testes, and blood. All procedures of animal handling, and sample collection were approved by the Animal care and use committee of the Jordan University of Science and Technology.

2.2. Preparation of tissue and blood samples

Upon euthanasia of rats, the prostate glands, and the testes were collected and weighed. The prostate glands and testes were then fixed in a 4% buffered formaldehyde for 4 hours, after which the samples were processed and embedded in paraffin. The blood samples were centrifuged at 2500 rpm for 10 minutes, then serum was collected from each sample and stored for subsequent hormonal assay by Enzyme-linked Immunosorbent Assay (ELISA).

2.3. Hematoxylin & Eosin staining

Five μm thick sections were cut and mounted on microscopic glass slides. Sections were deparaffinized and hydrated and were then stained in Hematoxylin and Eosin.

2.4. PCNA Index

The proliferation rate of prostatic cells was determined as previously described (Shidaifat *et al.*, 2013). Briefly, nonspecific binding was blocked by with Power Block® (BioGenex, CA) and polyclonal antibody against PCNA (MyBioSource, San Diego, CA) was added. Sections were then covered with horseradish peroxidase, Mach 3 Rabbit HRP-Polymer® (BioCare, Concord, CA) in the humidified chamber and after washing the DAB (DakoCytomotion, Glostrup Denmark) was added. Finally, tissues were counter stained with Mayer's Hematoxylin, and then visualized under light microscope. The PCNA index was determined by counting 500 epithelial cells in a random field from each sample, and then the percentage of positive cells among the 500 cells was calculated.

2.5. ELISA

Serum sample were used to measure the concentration of hormones according to the manufacture's instructions provided with the ELISA kit. Testosterone was measured using the kit supplied by BioCheck (Foster city, CA), whereas LH and FSH were measured using kits supplied by MyBioSource (San Diego, CA).

2.6. Statistical Analysis

Statistical analysis was performed using one-way analysis (ANOVA). Results were presented as the mean \pm SEM. Differences were statistically significant at $p < 0.05$.

3. Results

The results show that 17β -estradiol exerted a prominent effect on the testes and the prostate gland structures. Estradiol treatment induced a significant decrease in the weight of the testes (Figure 1), and its testosterone production (Figure 2) when compared to the control group. However, genistein treatment exerted no significant effect on the weight of the testes or its testosterone production.

The decrease in the weight of the testes, caused by estradiol treatment, was associated with prominent change in the histological structure. While the testes of a control (Figure 3A) and genistein treated rats (Figure 3B) appear to have a normally rounded circumference of seminiferous tubules containing germ cells at different stages of development, the seminiferous tubules of the estradiol treated rats appeared collapsed, shrunken, and contained disorganized cells (Figure 3C).

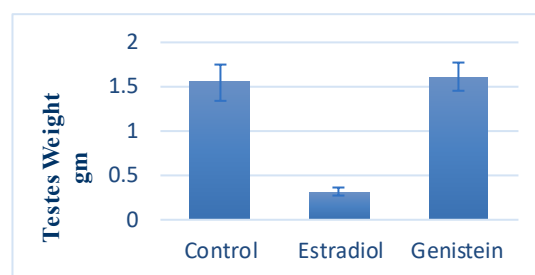


Figure 1. Comparison between the weights of testes of rats treated with estradiol and genistein for 26 days with the control group. Estradiol treatments caused a significantly ($P < 0.05$) decrease of testes weight as compared to control.

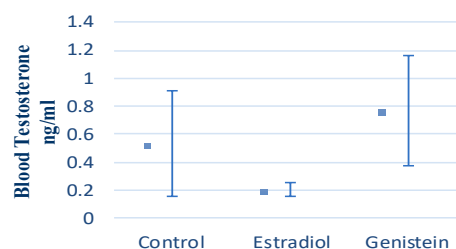


Figure 2. Concentration of serum testosterone of rats treated with estradiol and genistein for 26 days and the control group. Estradiol treatment causes a significantly ($P < 0.05$) decrease of testosterone as compared to control and genistein treated rats.

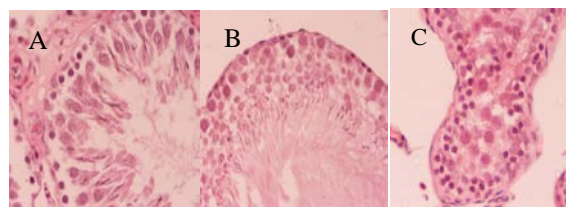


Figure 3: Testicular structure of rats treated with genistein and estradiol for 26 days and the control group. A) The seminiferous tubules of the control group appear normal with a rounded exterior along with the presence of cells developing from the basal layer towards the lumen. B) Represents the seminiferous tubules of testes from genistein treated rats, which appear similar to that of the control. C) Represents the seminiferous tubules of rats treated with estradiol. The seminiferous tubules are collapsed and contain disorganized cells.

Similarly, estradiol treatment caused a significant decrease in the weight of the prostate gland when compared to the control group (Figure 4). The histological evaluation revealed that the prostate gland from the estradiol-treated rats suffered prominent structural changes. While the acini of the prostate glands from the control (Figure 5A) and genistein treated rats (Figure 5B) appeared to contain a tall cuboidal secretory cell, the acini of the prostate gland from estradiol-treated rats appeared to contain atrophied cells with scant cytoplasm and prominent nuclei (Figure 5C).

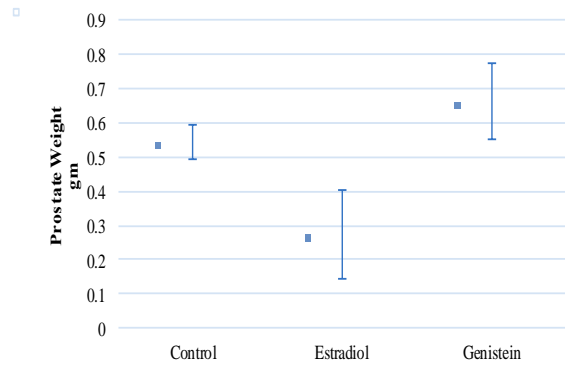


Figure 4. Comparison of weights of the prostate gland of rats treated with estradiol and genistein for 26 days and the control group. Estradiol causes a significant ($P < 0.05$) decrease of prostate weight as compared to control.

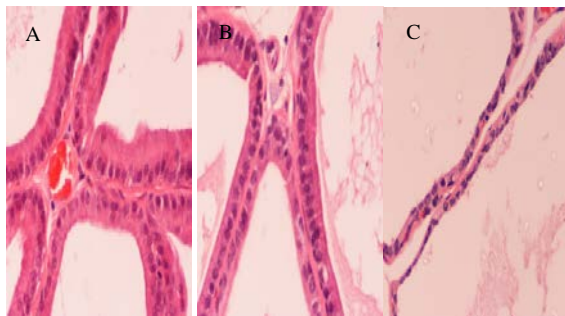


Figure 5. Comparison of the histological structures of the prostate treated for 26 days. (A) Prostate gland of control rat. Note that the glandular acini contain tall cuboidal epithelial cells. (B) Prostate gland from genistein-treated rats. The glandular acini retain similar structure to that of the control. (C) Prostate gland of estradiol treated rats. The acini contain atrophied cells with scant cytoplasm.

These structural changes of the prostate gland from estradiol-treated rats are paralleled with a significant decrease in the active proliferating cells. Estradiol treatment was associated with a significant reduction in the percent of cells that are expressing PCNA as evident by the PCNA proliferation index (Figure 6).

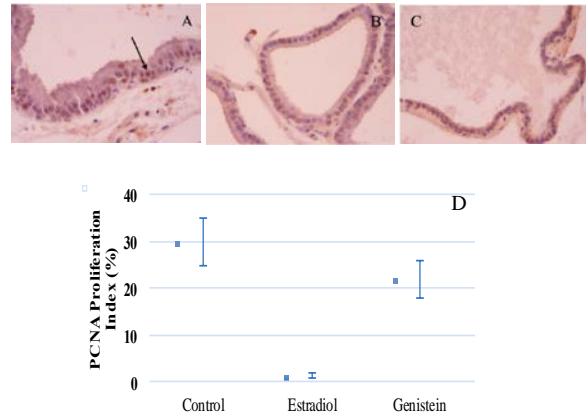


Figure 6. Expression of PCNA by the prostatic cells of rats treated for 26 days with genistein or estradiol. The arrow points to stained nuclei of actively proliferating cells. A) Control group, B) Genistein treated rats, and C) Estradiol treated rats. PCNA Proliferation index of rats treated with estradiol or genistein for 26 days (D). Estradiol treatment induced a significant ($P < 0.05$) decrease in the percent of proliferating cells.

On the other hand, estradiol and genistein treatment exerted no significant effect on the serum level of FSH and LH (Figure 7 and 8 respectively).

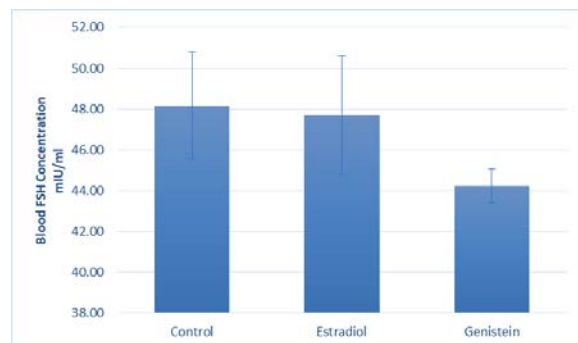


Figure 7. Blood concentration of FSH of rats treated with estradiol and genistein for 26 days as compared to the control group. There is no significant difference ($P < 0.05$).

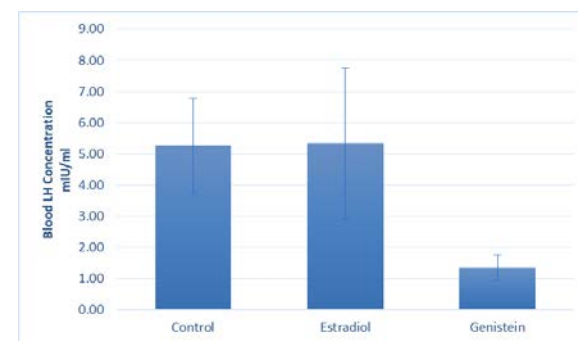


Figure 8. Blood concentrations of LH from rats treated with estradiol and genistein for 26 days compared with the control group. There is no significant difference ($P < 0.05$).

4. Discussion

The findings of this study indicate that estradiol treatment induced a significant decrease in the weight of the testes, which appeared to contain collapsed and shrunken seminiferous tubules with disorganized cells. The damage caused to the testicular structure by 17 β -estradiol is like that induced by zeranol, a non-steroidal estrogenic derivative of the myco-estrogen zearalenone (Shidaifat *et al.*, 2013). In addition, it has been shown that elevated levels of estradiol alter the seminiferous tubules morphology (Gill-Sharma *et al.*, 2001) and impaired spermatogenesis (Leavy *et al.*, 2017), sperm count and motility (Mohammadzadeh *et al.*, 2021).

Interestingly, the effect estradiol on the testicular structure was accompanied by a significant reduction in testosterone production without any appreciable effect on FSH and LH levels. These results suggest a direct effect of estradiol on the testicular cells. In fact, it has been reported that estradiol exerts a direct effect on leydig cells steroidogenesis without interrupting the hypothalamus-pituitary-gonadal axis (Jones *et al.*, 1978).

The deleterious effect of estradiol was extended to the prostate gland, which appeared to be significantly smaller and suffered a prominent histological alteration of its glandular compartment. These structural changes of the prostate gland obtained from the estradiol-treated rats were accompanied with a significant reduction of the proliferation potential of the prostatic cells. Previously, we have demonstrated that testosterone is the only hormonal factor that is required to drive prostate gland development to maturity (Shidaifat *et al.*, 2007), and its deprivation is associated with a dramatic regression of the gland (Shidaifat *et al.*, 2004). Therefore, the ability of estradiol to significantly decrease serum testosterone levels (as shown in this study), and to impair testicular steroidogenesis (Adibnia *et al.*, 2016) implicates a potential indirect effect of estradiol on the structural, and functional integrity of the prostate gland through its effect on the testicular androgen.

On the other hand, genistein as a naturally occurring substance related to the isoflavonoids with an estrogenic potency less than that of 17 β -estradiol (Leffers *et al.*, 2001) has been shown to inhibit the growth of both BPH, and prostate cancer (Bektic *et al.*, 2005; Geller *et al.*, 1998). Despite the evidence shown for such activity of genistein, this study revealed that animals treated with genistein had unchanged levels of LH or FSH, hence, unchanged levels of testosterone. As a result, the gross mass, structure of prostate gland and the cellular proliferation showed no significant changes. Although there is evidence that males ingesting genistein as part of their diet are less exposed to BPH (Bektic *et al.*, 2005), aged rats used in this study were only exposed to genistein injections for 26 days, a period that may have been insufficient to induce any visible effect.

5. Conclusion

The results of this study supported and extended the existing evidence of the 17 β -estradiol effects on the growth of the primary and the secondary sex organs. The effect of 17 β -estradiol on the prostate gland appears to be

indirect and probably mediated by disruption of the testicular androgen production. In contrast, genistein at a dosage and duration used in this study appears to exhibit no significant role on the structures of the male reproductive system, particularly the prostate gland. Although the results of this study cast doubt on the therapeutic potential of genistein for treating prostate gland modalities, further studies using different genistein treatment regimens and protocols are warranted.

Acknowledgment

This study was supported by the Deanship of Scientific Research at the Jordan University of Science and Technology.

References

- Adibnia E, Razi M and Malekinejad H. 2016. Zearalenone and 17 β -estradiol induced damages in male rats reproduction potential; evidence for ER α and ER β receptors expression and steroidogenesis. *Toxicol*, **120**: 133–146.
- Bektic J, Guggenberger R, Eder I E, Pelzer A E, Berger A P, Bartsch G and Klocker H. 2005. Molecular Effects of the Isoflavonoid Genistein in Prostate Cancer. *Clin Prostate Cancer*, **4(2)**: 124–129.
- Christoforou P, Christopoulos P F and Koutsilieris M. 2014. The role of estrogen receptor β in prostate cancer. *Mol Med.*, **20(1)**: 427–434.
- Gallardo F, Lloreta J, García F, Moll X, Baró T, González L A, Morote J, Reventos J and Mogas T. 2009. Immunolocalization of androgen receptors, estrogen α receptors, and estrogen β receptors in experimentally induced canine prostatic hyperplasia. *J Androl.*, **30(3)**: 240–247.
- Geller J, Sionit L, Partido C, Li L, Tan X, Youngkin T, Nachtsheim D and Hoffman R M. 1998. Genistein inhibits the growth of human-patient BPH and prostate cancer in histoculture. *Prostate*, **34(2)**: 75–79.
- Gill-Sharma M K, Dsouza S, Padwal V, Balasinar N, Aleem M, Parte P and Juneja H S. 2001. Antifertility effects of estradiol in adult male rats. *J Endocrinol Invest.*, **24(8)**: 598–607.
- Jaiswal N, Akhtar J, Singh S P and Ahsan F. 2019. An Overview on Genistein and its Various Formulations. *Drug Res.*, **69(6)**: 305–313.
- Jones T M, Fang VS, Landau R L and Rosenfield R. 1978. Direct inhibition of Leydig cell function by estradiol. *J Clin Endocrinol Metab.*, **47(6)**: 1368–1373.
- Kostelac D, Rechkemmer G and Briviba K. 2003. Phytoestrogens Modulate Binding Response of Estrogen Receptors α and β to the Estrogen Response Element. *J Agric Food Chem.*, **51(26)**: 7632–7635.
- Lamartiniere C A, Cotroneo MS, Fritz W A, Wang J, Mentor-marcel R and Elgavish A. 2002. Genistein Chemoprevention: Timing and Mechanisms of Action in Murine Mammary and Prostate. *J Nutr.*, **132(3)**: 552–558.
- Leavy M, Trottmann M, Liedl B, Reese S, Stief C, Freitag B, Baugh J, Spagnoli G and Kölle S. 2017. Effects of Elevated β -Estradiol Levels on the Functional Morphology of the Testis - New Insights. *Sci Rep.*, **7**: 39931.
- Leffers H, Naesby M, Vendelbo B, Skakkebaek NE and Jørgensen M. 2001. Oestrogenic potencies of Zeranol, oestradiol, diethylstilboestrol, Bisphenol-A and genistein: implications for exposure assessment of potential endocrine disrupters. *Hum Reprod.*, **16(5)**: 1037–1045.

- Mohammadzadeh M, Pourentezari M, Zare-Zardini H, Nabi A, Ghasemi Esmailabad S, Khodadadian A and Talebi AR. 2021. The effects of sesame oil and different doses of estradiol on testicular structure, sperm parameters, and chromatin integrity in old mice. *Clin. Exp. Reprod Med.*, **48 (1)**: 34-42.
- Nicholson T M and Ricke W A. 2011. Androgens and estrogens in benign prostatic hyperplasia: past, present and future. *Differentiation*, **82(4-5)**: 184-199.
- Nicholson T M, Sehgal P D, Drew SA, Huang W and Ricke W A. 2013. Sex steroid receptor expression and localization in benign prostatic hyperplasia varies with tissue compartment. *Differentiation*, **85(4-5)**: 140-149.
- Oesterling J E. 1996. Benign prostatic hyperplasia: a review of its histogenesis and natural history. *Prostate. Suppl.*, **6**: 67-73.
- Prins G S and Korach K S. 2008. The role of estrogens and estrogen receptors in normal prostate growth and disease. *Steroids*, **73(3)**: 233-244.
- Putz O, Schwartz C B, Kim S, LeBlanc G A, Cooper R L and Prins G S. 2001. Neonatal Low- and High-Dose Exposure to Estradiol Benzoate in the Male Rat: I. Effects on the Prostate Gland. *Biol of Reprod.*, **65(5)**: 1496-1505.
- Shi X, Peng Y, Du X, Liu H, Klocker H, Lin Q, Shi J and Zhang J. 2017. Estradiol promotes epithelial-to-mesenchymal transition in human benign prostatic epithelial cells. *The Prostate*, **77(14)**: 1424-1437.
- Shidaifat F, AL-Trad B and AL-Omari R. 2007. Testosterone effect on immature prostate gland development associated with suppression of transforming growth factor- β . *Life Sci.*, **80(9)**: 829-834.
- Shidaifat F, Daradka M and Al-Omari R. 2004. Effect of androgen ablation on prostatic cell differentiation in dogs. *Endocr Res.*, **30(3)**: 327-334.
- Shidaifat F, Kulp S K and Lin Y C. 2013. Zeranol Induces Deleterious Effects on the Testes and the Prostate Gland of Mature Rats. *Endocr Res.*, **38(4)**: 232-241.
- Un-No T, Hayami S, Nobata S, Sudoko H, Honma S, Fujita K and Ozono S. 2007. Neonatal Exposure to Estrogen in the Wistar Rat Decreases Estrogen Receptor-Beta and Induces Epithelial Proliferation of the Prostate in the Adult. *Urol Int.*, **79(4)**: 345-351.

Immunomodulatory Properties of *Citrus limon* Extracts on BALB/c Mouse Lymphoid and Myeloid Lineage Cells

Wira Eka Putra¹, Ken Retno Puspaningrum², Arief Hidayatullah³, Muhaimin Rifa'i^{2*}

¹Biotechnology Study Program, Department of Applied Sciences, Faculty of Mathematics and Natural Sciences, Universitas Negeri Malang, East Java, Indonesia; ²Department of Biology, Faculty of Mathematics and Natural Sciences, Brawijaya University, East Java, Indonesia; ³Health Governance Initiative, United Nations Development Programme Indonesia, Eijkman-RSCM Building, Jakarta, Indonesia

Received: November 17, 2022; Revised: January 24, 2023; Accepted: February 6, 2023

Abstract

To maintain or restore immunological homeostasis, life forms frequently rely on immunomodulators, also known by many terms such as biological response modifiers, immunostimulants, and immune restoratives. Lemon (*Citrus limon* (L.) Burm) is another well-known source of micronutrients and bioactive phytochemicals that serve as antioxidant against oxidative stress. In this present study, we aimed to examine the immunomodulatory properties of *Citrus limon* extracts (CLE) on lymphoid and myeloid lineage cells from BALB/c mouse. Six-weeks-old mice were treated by four different doses of CLE, 0, 200, 400, and 800 mg/kg BW for 14 days. Several markers of immune cells were investigated including CD8, CD62L, CD4, B220, VLA-4, TER119, CD55, Gr1, and CD11b antibodies which cover the population of lymphoid and myeloid lineage cells. Flow cytometry analysis was used to identify the specific subset of studied cell population. The results showed that CLE significantly increased the number of Gr1⁺ granulocyte cells but did not affect other cell types. As a result, we surmised that the components of CLE might have a particular impact on granulocyte cells. Importantly, more investigation is needed to learn how CLE boosts granulocyte cell production.

Keywords: *Citrus limon*, granulocyte, immunomodulator, lymphoid, myeloid

1. Introduction

The immune system is undoubtedly one of the human body's most complex and dynamic systems (Huntington and Graym, 2018). Immune system comprises a network of innate and adaptive immune cells that continuously monitor their respective microenvironment by constantly recognizing and distinguishing between self and non-self-antigens while maintaining communication (Cao *et al.* 2019; Horwitz *et al.* 2019; Netea *et al.* 2020). Those responses are carried out by specific immune cell types, which are generally further categorized into two main groups, the effector and regulatory cells (Mezheyeuski *et al.* 2018; Zemmour *et al.* 2018). The alteration of these delicate balances could lead to an autoimmune problem when the effector cells become aberrantly reactive to self-antigens or their responses become exaggerated. Also, the amplitude of particular immune responses is highly influenced by the amount of pro-inflammatory and anti-inflammatory cells activated during the event. Maintaining immune homeostasis is critical to maintaining a normal and sufficient immune response (Cicchese *et al.* 2018; Sozzani *et al.* 2017).

On the other hand, the immune responses could also be compromised due to primary or secondary immune deficiency. Genetic factors often cause the first one, while the latter is caused by various environmental stress and diseases, such as actively taking cancer therapy, including

radiation and chemotherapy, malnutrition, alcohol consumption, and smoking. These conditions significantly reduce the ability of the immune cells to fight any potential threat, causing longer and more severe infections and worsening the disease's prognosis. They interfere with MAPK and NF- κ B signaling pathways, reducing pro-inflammatory cytokines synthesis such as IFN- γ , TNF- α , and IL-1 β , hampering MHC II expression in APCs, increasing TLRs expression, decreasing anti-inflammatory cell counts such as Th2 and Tregs, reducing the number of CD4⁺ and CD8⁺ T cells, and also lowering IgG expression and avidity (Bourke *et al.* 2016; Qiu *et al.* 2016; Romeo *et al.* 2007).

To maintain or recover immunological homeostasis, we often depend on various immunomodulators, which are referred to by various names, including biological response modifiers, immunostimulants, and immune restoratives (Ogbue *et al.* 2022; Sapkota *et al.* 2022; Shamliyan and Dospinescu 2017). Its mechanism of action might involve the augmentation of anti-infective immunity of immune system cells such as lymphocytes, macrophages, dendritic cells, and natural killer cells. Other processes may occur, including activating or restoring immunological effector activity (Ferrari *et al.* 2020; Machado *et al.* 2020; Riaz *et al.* 2019). Some of the most often used immunomodulators include drugs produced from natural or synthetic components and microbial compounds. For instance, one of the most intensively studied herbal extracts, the extract of ginseng significantly reduces the ROS-induced IL-6 and

* Corresponding author. e-mail: rifa123@ub.ac.id.

IL-8 expression preventing pro-inflammatory hypercytokinemia while also increasing the ratio of CD4⁺/CD8⁺ T cells, NK cell cytolytic activity, as well as increasing serum level of IgA, IgG and IgM (Hong *et al.* 2012; Lee *et al.* 2014; Predy *et al.* 2005; Riaz *et al.* 2019; Zhou *et al.* 2014).

Another highly capitalized source for its micronutrients and bioactive phytochemicals is lemon. It contains a wide variety of natural antioxidants, including vitamin C. It also contains bioflavonoids, a group of antioxidants that help protect the body from oxidative stress. In our previous study, we found that *C. limon* extract have ameliorative effect on breast cancer mouse model (Putra *et al.* 2023). Some studies suggested that it could lower the concentration of C-reactive protein in the blood plasma, soluble vascular cell adhesion molecule-1 (sVCAM-1), and the soluble endothelial leukocyte adhesion molecule-1 (sE-selectin), both in normal individuals and persons with metabolic-disorder (Alhabeeb *et al.* 2022; Asgary *et al.* 2014; Buscemi *et al.* 2012). The highly dominant bioflavonoids identified on it are hesperidin and its aglycone variant, hesperetin (Miles and Calder 2021; Pyrzynska 2022; Zanwar *et al.* 2014). Interestingly, both hesperidin and hesperetin showed immunomodulatory effects through reducing the expression of TNF- α , IL-1 β , and ICAM-1. Furthermore, these compounds also increasing the phosphorylation rate of the p38 MAPK and activating c-Jun-N-terminal kinase pathway (Choi and Lee 2010; Karthikeyan *et al.* 2021; Miles and Calder 2021).

On the other hand, vitamin C could optimize the phagocytosis capability of various phagocytic cells in the innate immune system (Gombart *et al.* 2020; Leal *et al.* 2017), as well as increase T cell proliferation and the concentration of various Ig in the blood serum (Miles and Calder 2021). Besides, the high content of flavonoids, terpenoids, fibers, and minerals in lemon has an essential function in preventing several severe diseases like obesity, diabetes, hypertension, cardiovascular disease, and certain malignancies (Asgary *et al.* 2018; Mahmoud *et al.* 2019; Saini *et al.* 2022), making it one of the best sources of various bioactive compounds which could be studied further particularly as immunomodulator compounds. As a result, the lemon extract is hypothesized to have immunomodulatory properties that affect both lymphoid and myeloid lineage cells.

2. Materials and Methods

2.1. Research Design

We applied a completely randomized design approach in this study by altering the treatment to examine the effect of the intervention by varying the variables used. This study was done in vivo on healthy BALB/c mice weighing about 20-25g, using four treatment groups: negative control (no lemon extract), lemon extract dosage 1 (200 mg/kg BW), dose 2 (400 mg/kg BW), and dose 3 (800 mg/kg BW). Each treatment had five replicates. The spleen was then examined to see how every treatment affected it.

2.2. The Lemon Extraction

The extraction mechanism we applied during this study was the crude extraction mechanism. About 100 g of lemons was blended until homogenous and then filtered. The filtrate of the crude lemon extract was then freeze-

dried until it became a paste that was kept at 4°C until usage. Before the oral admission, we dissolved the crude extract paste that had been weighed before with distilled water into several working dosages. They are dose 1 (200 mg/kg BW), dose 2 (400 mg/kg BW), and dose 3 (800 mg/kg BW).

2.3. Oral Administration of CLE to BALB/C Mice Model

Mice about six-weeks-old were kept in cages in the Animal Physiology Laboratory of the Department of Biology, Faculty of Mathematics and Natural Sciences, Brawijaya University, Malang, for ten days to allow the mice to adjust to their new environment. Five mice were placed in each cage. They were kept at room temperature with food and water daily, *ad libitum*. The cages were cleaned every two days. The acclimatized mice were then orally administered lemon extract in three doses. The following were the treatment doses: dose 1 (200 mg/kg BW), dose 2 (400 mg/kg BW), and dose 3 (800 mg/kg BW). The oral administration of lemon extract was carried out for 14 days.

2.4. Sacrificing and Isolation of the BALB/c Mice Model

All mice models were sacrificed by neck-dislocating method, then sprayed with 70% alcohol before surgery to retrieve the mouse's spleen conducted from the left dorsal to ventral. The spleen of each treated mouse was washed with PBS solution and homogenized with 10-ml PBS. The homogenized spleen were placed into a 15-ml propylene tube. The acquired cell suspension was placed in a propylene tube. The cell suspension in the propylene tube was then centrifuged for 5 minutes at a speed of 2500 rpm and a temperature of 10°C. After discarding the supernatant, the pellet was resuspended in 1 ml of PBS. All animal treatments in this study have been approved by Ethical Board Commission of Brawijaya University with ethical approval number 779-KEP-UB.

2.5. Antibody Staining and Flow Cytometry Analysis

The isolated cells were resuspended, and 80 μ l was transferred to a microtube. Then, 400 μ l of PBS was added to the sample microtube and centrifuged for 5 minutes at a speed of 2500 rpm and a temperature of 10°C. The combination staining used for the flow cytometry analysis including PE-CD8, PE-Cy5-CD62L, PE-CD4, PE-Cy5-B220, PE-VLA-4, PE-Cy5-TER119, PE-CD55, FITC-Gr1, and FITC-CD11b antibodies (Figure 1) is as described below: The pellets were removed from the supernatant and stained with 50 μ l of extracellular antibody (1 μ l stock solution of antibody diluted with 50 μ l of PBS and 10% FBS) before being incubated on ice for 20 minutes. The cell suspension was washed with 500 μ l of washperm and resuspended to clean the fixative solution. The suspension was then centrifuged for 5 minutes at a speed of 2500 rpm at a temperature of 10°C. The pellets were then separated from the supernatant. After extracellular antibody staining, the cells were incubated in 300-500 μ l of PBS before being transferred to a cuvette for flow cytometry analysis as our previous protocols (Putra *et al.* 2016; Putra *et al.* 2015).

2.6. Data Analysis

The BD Cellquest ProTM software was used to analyze the flow cytometry results. Then, we analyzed the data using a One-way ANOVA parametric analysis ($p \leq 0.05$), followed by Tukey's posthoc test to determine the

significance between treatment groups. We used SPSS version 16 for Windows for all statistical analyses mentioned.

3. Results and Discussion

3.1. The Effect of CLE Administration on Memory T Cells

Flow cytometry analysis revealed that the relative number of effector memory T cells ($CD8^+CD62L^-$) in the first dosage treatment, was 68.14%. Meanwhile, the relative number in the negative control, dose 2, and dose 3 treatments was 58.72%, 55.39%, and 66.07%, respectively (Figure 2). Compared to other treatment groups, dose 1 was the most efficacious in increasing the relative number of $CD8^+CD62L^-$. Previously, we also found that chloramphenicol induce the $CD8^+CD62L^-$ T cells (Putra *et al.* 2020; Putra and Rifa'i 2019). However, there were no significant statistical differences among all treatment groups in this present study.

The T cells that have matured and been released from the thymus have not yet encountered their appropriate antigen, expressing the CD62 protein (L-selectin) and C-C Chemokine receptor type 7 (CCR7) on their surface and are known as naïve T cells (Horna *et al.* 2019; Hunter *et al.* 2016). To transform into activated T cells, they migrate to secondary lymphoid organs such as the spleen, lymph nodes, tonsils, Peyer's patches, and other mucosal tissues, interacting with antigen, antigen-presenting cells, other lymphocytes through their respective cell receptors (Farber *et al.* 2014; Krummel *et al.* 2016). Because effector memory T cells circulate in the periphery and have direct effector activities when they encounter antigens, they do not express L-selectin (Watson *et al.* 2019). This subtype of memory T cells has a high cytotoxicity level yet lower proliferation ability (Martin and Badovinac 2018; Meryk *et al.* 2020). Without previous challenge from antigens, it is suggested that the improved number of memory T cells in lemon extract-treated groups is because vitamin C in the extract indirectly promotes memory T cells proliferation by enhancing phosphorylation of MAPK and ERK1/2, as well as increasing the activation of NF- κ B in the dendritic cells. This phenomenon increases the synthesis of IL-15, promoting survival and proliferation of memory T cells through activating MAPK/PI3K-AKT pathway (Hong *et al.* 2016; Van Gorkom *et al.* 2018; Watkinson *et al.* 2021).

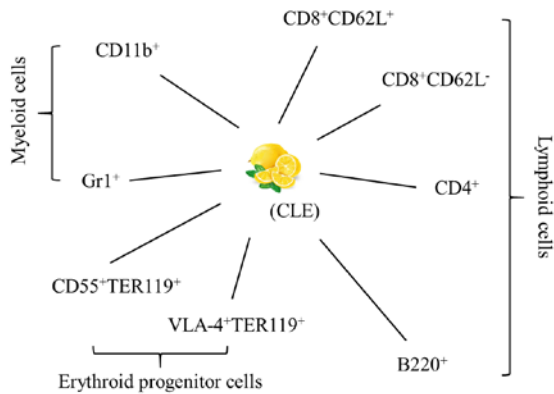


Figure 1. Different subsets of major immune cells evaluated after CLE administration.

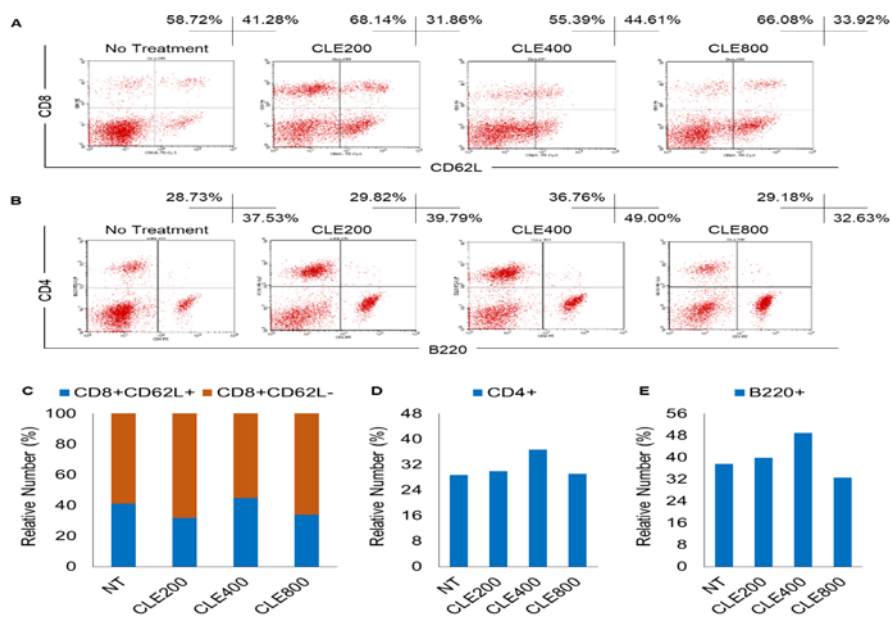


Figure 2. Immunomodulatory evaluation of CLE on $CD8^+CD62L^+$, $CD8^+CD62L^-$, $CD4^+$, and $B220^+$ subsets. (A). Flow cytometry graph of $CD8^+CD62L^+$ and $CD8^+CD62L^-$; (B). Flow cytometry graph of $CD4^+$ and $B220^+$; (C). Bar graph of $CD8^+CD62L^+$ and $CD8^+CD62L^-$; (D). Bar graph of $CD4^+$; and (E). Bar graph of $B220^+$.

The direct mechanism of vitamin C in the lemon extract that could stimulate memory T cell proliferation is still unknown. However, it is suggested that the memory T cells' immediate effect of vitamin C intake through sodium-dependent vitamin C transporters (SVCT) reduces apoptosis and induces more proliferation in a limited dose, known as the physiological dose (Van Gorkom *et al.* 2018). Folate in the extract could also have a similar effect in the T cells population, but with a far less known mechanism; it is predicted to influence the transcription process needed for proliferation and protein synthesis (Duthie *et al.* 2010; Miles and Calder 2021). Based on the results, dose 1 administration is the most effective dose to stimulate memory T cell proliferation without prior antigen exposure.

The ROS, which is involved in triggering cell death and terminating the immunological response, modulates naïve T cell activation because it is accumulated immediately upon activation (Hong *et al.* 2016). T cell differentiation is also influenced by ROS, but not their activation or proliferation. A proper T-cell response occurs under physiological conditions when there is an equilibrium between ROS and antioxidants in the tissue microenvironment and intracellular compartment (Belikov *et al.* 2015). Compared to memory and effector CD8⁺ T cells, activated CD8⁺ T cells have a distinct genetic signature. Chronically infected mice models and chronically infected people with HIV, EBV, or CMV do not express or re-express CD62L or CCR7, rendering them dysfunctional in their route and lymph node localization (Nolz *et al.*, 2011).

3.2. The Effect of CLE Administration on B cells

According to the flow cytometry data, the relative number of B cells, also known as B220⁺ cells, in the dose 2 treatment was 49.00%, while the negative control, dose 1, and dose 3 had a relative number of B cells of 37.53%,

39.79%, and 32.63%, respectively (Figure 2). We suggest that the dose 2 treatment was the most effective in increasing the relative number of B lymphocytes (B220) among other dosages. However, in this present study we found there were no statistically significant differences between these treatment dosages.

A particular compound in the lemon extract, naringenin, stimulates the proliferation of B cells in the spleen. (Maatouk *et al.* 2016). Vitamin C is also thought to increase the percentage of B cells and retain their viability. However, the result is still inconsistent among studies, and the molecular mechanism for both compounds remains unclear (Carr and Maggini 2017; Maatouk *et al.* 2016; Van Gorkom *et al.* 2018). For instance, a human-based study suggests that vitamin C intake positively correlates to the level of antibodies in the blood plasma, particularly IgM, IgA, and IgG, while others suggest the contrary results (Carr and Maggini 2017; Van Gorkom *et al.* 2018). A study that may explain these phenomena suggests that vitamin C is an important cofactor to ten-eleven translocation enzyme (TET) type 2 and 3 and promotes cytosine demethylation at Blimp1, which later triggers the activation mechanism of B cells towards plasma cells lineage, later increasing the concentration of antibodies (Qi *et al.* 2020).

The increasing number of mature B cells in the spleen without prior antigen challenge could be due to three main factors: increasing proliferation of B cell progenitor in the bone marrow, increasing proliferation capacity of B cells in the spleen, and increasing viability of mature or naïve B cells in the spleen during the selection mechanism (Ruiz-Iglesias *et al.* 2020; Shahaf *et al.* 2016; Van Gorkom *et al.* 2018). The second one is suggested as the main action mechanism of hesperidin, a major flavonoid in the extract, to increase the number of B cells in the spleen (Ruiz-Iglesias *et al.* 2020; Sassi *et al.* 2017).

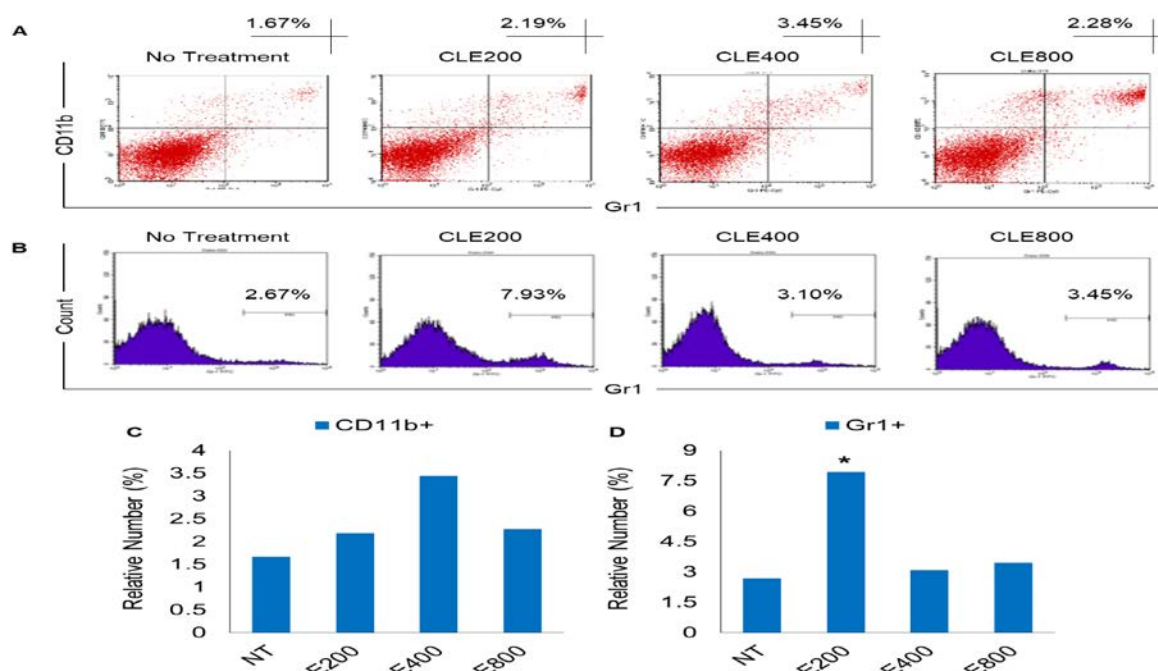


Figure 3. Immunomodulatory evaluation of CLE on CD11b⁺ and Gr1⁺ subsets. (A). Flow cytometry graph of CD11b⁺; (B). Flow cytometry graph of Gr1⁺; (C). Bar graph of CD11b⁺; and (D). Bar graph of Gr1⁺. The asterisk indicates the statistical significance compared to the other groups with p-values < 0.05.

On the other hand, research suggests that polysaccharide content in the extract could increase the viability of mature B cells in the spleen. The polysaccharide increases the viability of B cells by interacting with Toll-like receptor 4 (TLR4) and activating the MAPK signaling pathway (Xie *et al.* 2020). Pectin, furthermore could also increase the number of mature B cells in the spleen by increasing the production of IL-4 in the spleen, subsequently stimulating the B cells' differentiation and proliferation, as well as inhibit BCR-mediated apoptosis towards the mature B cells (Granato *et al.* 2014; Merheb *et al.* 2019; Zhou *et al.* 2020).

3.3. The Effect of CLE Administration on Helper T cells

According to the flow cytometry results, the relative number of helper T cells (CD4⁺) in the dosage 2 treatment was 36.76%, whereas the relative number of the helper T cells in the negative control, dose 1, and dose 3 treatments was 28.73%, 29.82%, and 29.18%, respectively (Figure 2). Among the different treatment doses, it was clear that dose 2 was the most efficient in boosting the relative proportion of helper T cells. But the results of these treatments did not differ in a way that was statistically important.

Although there is no significant difference between groups, we suggest that lymphocytes, particularly T cells, have been known to accumulate a certain amount of vitamin C using sodium-dependent vitamin C transporter protein type 2 (SVCT2) (Hong *et al.* 2016; Oyarce *et al.* 2018). However, the results involving vitamin C and T cells primarily resulted in conflicting and inconsistent results. All of the previous research agrees that the cells tend to accumulate intracellular ROS after activation as a byproduct of mitochondrial activity as well as the vitamin C mentioned before, but at some point, it did not behave as an antioxidant as most predicted. Primarily, vitamin C is suggested to act as a cofactor for epigenetic regulation through interaction with Jumonji C histone-lysine demethylase, which acts as primary hydroxylate agent for methylcytosine residues specifically in Cd4 and Cd8 genes, as well as histone demethylation (Manning *et al.* 2013). It is also suggested that it triggers the continuation of the developmental stage of T cells from double-negative to double-positive stage, which is highly needed to begin the functional TCR $\alpha\beta$ selection process (Manning *et al.* 2013). These exact mechanisms also drive the polarization of naïve helper T cells into subsequent subsets (Song *et al.* 2017; Van Gorkom *et al.* 2018).

The higher number of CD4⁺ T helper cells in the spleen could be attributed to their higher viability caused by vitamin C intake. It significantly decreases the T cell apoptosis rate and increases their proliferation (Carr and Maggini 2017; Miles and Calder 2021; Van Gorkom *et al.* 2018). As an antioxidant, it denies the promotion of activation-induced cell death by ROS through activation of the NF- κ B pathway by lowering the concentration of the ROS (Carr and Maggini 2017; Hong *et al.* 2016; Kawashima *et al.* 2015). However, a study's results proved the opposite conclusion by stating that it exerts a toxic effect after some point. Unfortunately, the exact mechanism remains unclear, but they predict that it nullified the ROS amount and role as an important control mechanism during differentiation and functional stages

(Belikov *et al.* 2015; Hong *et al.* 2016; Yarosz and Chang 2018).

Apart from vitamin C, other sources mentioned that the effect of *Citrus limon's* flavonoids on the population of helper T cells is much more limited. Hesperidin in the citrus extract could also influence the increasing number of CD4⁺ T helper cells by influencing the lymphoid tissue. However, the exact mechanism still needs to be figured out (Ruiz-Iglesias *et al.* 2020). A study suggests that hesperidin intake in healthy people had no notable effect (Perche *et al.* 2014). Its aglycone counterpart, hesperetin, is thought to have immunostimulatory characteristics by promoting T cell proliferation. Unfortunately, its exact mechanisms also remain unclear (Sassi *et al.* 2017). Polysaccharides such as pectin could also increase the number of splenic CD4⁺ cells, particularly in IL-10 deficient mice, by downregulating pro-inflammatory cytokine expression (Beukema *et al.* 2022; Ye and Lim 2010). We still need further investigation to clearly picture why both lymphocytes' numbers peaked at the intermediate dose rather than the highest one.

3.4. The Effect of CLE Administration on Macrophages

The relative number of macrophage cells (CD11b⁺) in the dosage 2 treatment was 3.45%, whereas the lowest relative number of macrophage cells was in the negative control group with 1.67%. The rest of the treatment doses had a relative number of macrophages around 2%, with dose 1 and dose 3 numbers being 2.19% and 2.28%, respectively (Figure 3). Among the several treatment dosages, dose 2 has the highest ability to increase the relative number of macrophage cells. Those results showed no statistically significant changes.

Other studies suggest that administering flavonoids or other bioactive compounds lowers the cell count and inhibits the maturation process of macrophages by inhibiting LPS-induced inflammatory response (Carr and Maggini 2017; Han *et al.* 2022; Zhang *et al.* 2014). Instead, we found that the number of macrophages increased without statistical significance. We cannot find any sufficient explanation for why this phenomenon occurs. A study in traumatic ulcer rats showed that the number of macrophages increased after the administration of *Citrus limon* peel oil and suggested that fumarate acid and d-limonene could act as a free radical scavenger which suppresses the production of ROS and iNOS, protecting macrophages from oxidative damage and prevent them from undergoing apoptosis, hence promoting their proliferation (Surboyo *et al.* 2019).

Another study using *Citrus limon* peel essential oil on guinea pig suggests that the induction of it causes type IV hypersensitivity, which triggers the antigen recognition mechanism by APCs, introduced to T-helper cells and initiating the synthesis of IFN- γ , promoting macrophage activation and proliferation. These inflammatory responses, however, did not show any sign of inflammation. They suggest that the increasing number of macrophages may not be fully driven towards pro-inflammatory response but also contribute to anti-inflammatory responses because some flavonoids like d-limonene and linalool drive the macrophage polarization towards M2 phenotype and induce the synthesis of IL-10, inhibiting the inflammatory responses and minimizing the

effect (Sulaiman *et al.*, 2022; Mahdani *et al.* 2020). Rutin, another flavonoid, also stimulates the CD11b⁺ cells toward the M2 phenotype (Ferraz *et al.* 2020).

3.5. The Effect of CLE Administration on Myeloid Cells Quantity

Flow cytometry results show that all treatment groups have a higher relative number of Gr-1 cells than the negative control at 2.67%. It was significantly higher in the dose 1 group, with 7.93%, while the other dosages were consistent at around 3%, with dose 2 at 3.1% and dose 3 at 3.45% (Figure 3). The dose 1 treatment was the most effective in inducing Gr-1 myeloid cell differentiation. The relative number of Gr-1 neutrophils in the dose 1 group increased by 5.26% but remained within acceptable limits. If the relative number exceeds the acceptable limit, it is considered neutrophilia, defined as an increased number of neutrophils beyond the average threshold caused by inflammation, stress, the corticosteroid reaction, excessive exercise, and the epinephrine response (Goldman and Schafer 2020). It also developed due to physiological events such as corticosteroid induction, inflammation, and neoplasia.

Granulocytes are white blood cell subgroups distinguished by granules' presence in their cytoplasm. Because of the different forms of the nucleus, which generally contains a three-segment gap, granulocytes, also known as polymorphonuclear leukocytes (PMNs), consist of three types of cells: neutrophils, basophils, and eosinophils (Breedveld *et al.* 2017). Neutrophils are white blood cells with the highest population among PMNs cells, accounting for over 70% of the total number of cells. It has an extremely crucial role in innate immune responses because of its phagocytic nature in circulation (Rosales 2018). It is one of the first cells to migrate toward the site of inflammation during the early acute inflammatory phase, generally caused by bacterial infection, environmental exposure, or malignancy by following chemical signals such as IL-8, C5a, fMLP, leukotriene B₄, and H₂O₂ (Kraus and Gruber 2021; Selders *et al.* 2017).

One of the few compounds in the extract thought to have a critical effect on myeloid cells is coumarin. It has a vital function in the immune system by regulating the activity of white blood cells, particularly the granulocytes, making them, particularly the neutrophils, work more efficiently because it prevents extensive and potentially dangerous activation of neutrophils has been proposed as a critical injury-limiting way by acting as scavengers for ROS generated by the neutrophils (Chen *et al.* 2015). Conversely, vitamin C acts as an antioxidant by scavenging free radicals in activated leukocytes due to lipid oxidation, preserving normal membrane fluidity and motility (Miles and Calder 2021). It also influences immune function by regulating redox-sensitive cell communication pathways. Another distinctive bioactive compound in lemon is auraptene, which has immunomodulatory properties by increasing the activities of β -glucuronidase and acid phosphatase in macrophages (Genovese and Epifano 2011), as well as stimulating the production of IL-1 β and TNF- α (Hsia *et al.* 2021).

As mentioned previously, vitamin C is highly critical for various immune cells, including myeloid cell lineage, so normally they maintain it at an adequate intracellular level (Ang *et al.* 2018; Liugan and Carr 2019). A study in

septic patients suggests that vitamin C could prevent the peripheral neutrophils from undergoing apoptosis by increasing the level of Bcl-2 while simultaneously lowering apoptosis-promoting factors such as caspase-3 and poly-ADP-ribose polymerase in the downstream (Liugan and Carr 2019), as well as the upstream by inhibiting caspase-8 activation induced by Fas-ligand interaction, and Fas-induced apoptosis as general primarily as a consequence of its properties as antioxidant (Ang *et al.* 2018). On the other hand, hesperidin also had a similar effect on inhibiting granulocyte apoptosis by acting as an antioxidant in the ROS-induced apoptosis pathway (Adefegha *et al.* 2017). These mechanisms could be the factor behind the higher number of granulocytes we found in this study.

3.6. The Effect of CLE Administration on Erythroid Cells Quantity

Flow cytometry analysis revealed that the relative proportion of TER119⁺VLA-4⁺ cells in dose 2 was 73.31% and 65.65% in dose 3. The relative number of erythroid cells in both dosages dropped from the negative control of 75.27%. In contrast, the relative number of TER119⁺VLA-4⁺ cells in the dose 1 group grows by 9.68% compared to the normal group, to 84.95%, although the increase is not statistically significant (Figure 4). These findings suggest that the dose 1 treatment is the most efficient in stimulating the differentiation process in erythrocytes. The results also showed that the relative number of TER119⁺CD55⁺ cells dropped to 23.78%, 18.49%, and 24.19%, respectively, for those three dosages, compared to the normal control group, 28.96%. However, the declining number in these three treatments was not statistically significant compared to each other. It is suggested that the dose 1 treatment is the most effective in preventing cell lysis.

Iron ion is a necessary precursor in the synthesis of hemoglobin in erythrocytes. In contrast, vitamin C is an exogenous antioxidant that plays a vital role in erythrocyte synthesis because it acts as an enzyme cofactor and promotes the mobilization of the ferrous form of iron to transferrin, increasing its bioavailability (Cimmino *et al.* 2018; Imam *et al.* 2017). It can reduce oxidative stress and prevent free radical damage to erythrocyte cells (Milošević *et al.* 2018; Suleman *et al.* 2019). Consequently, the vitamin C concentration of lemon extract, particularly in dose 1, may have a substantial role in erythrocyte precursor synthesis, although there is no statistical significance compared to other doses. Nevertheless, the high concentration of vitamin C in the other two dosages did not increase the number of red blood cell precursors because it may trap superoxide anions and have the ability to interrupt the cycle of radical reactions caused by the lipid peroxidation process exclusively in low concentration, but not in high concentration (Juan *et al.* 2021; Kaźmierczak-Barańska *et al.* 2020). In this study, the administration of lemon juice from the three doses did not significantly differ, presumably caused by the lipid peroxidation process. The lipid peroxidation on the erythrocyte membrane could reduce the membrane fluidity and enhance the fragility of the erythrocyte membrane, leading to a higher rate of hemolysis (Duchnowicz *et al.* 2021; Maćczak *et al.* 2017). Suppose the body does not have an adequate number of antioxidants. In that case, it is

conceivable that the number of erythrocytes and hemoglobin levels may drop, resulting in anemia because the erythrocyte membrane is the most vulnerable part of

erythrocyte to lipid peroxidation due to direct and continual exposure to high oxygen partial pressure and saturated fatty acids (Pisoschi *et al.* 2021).

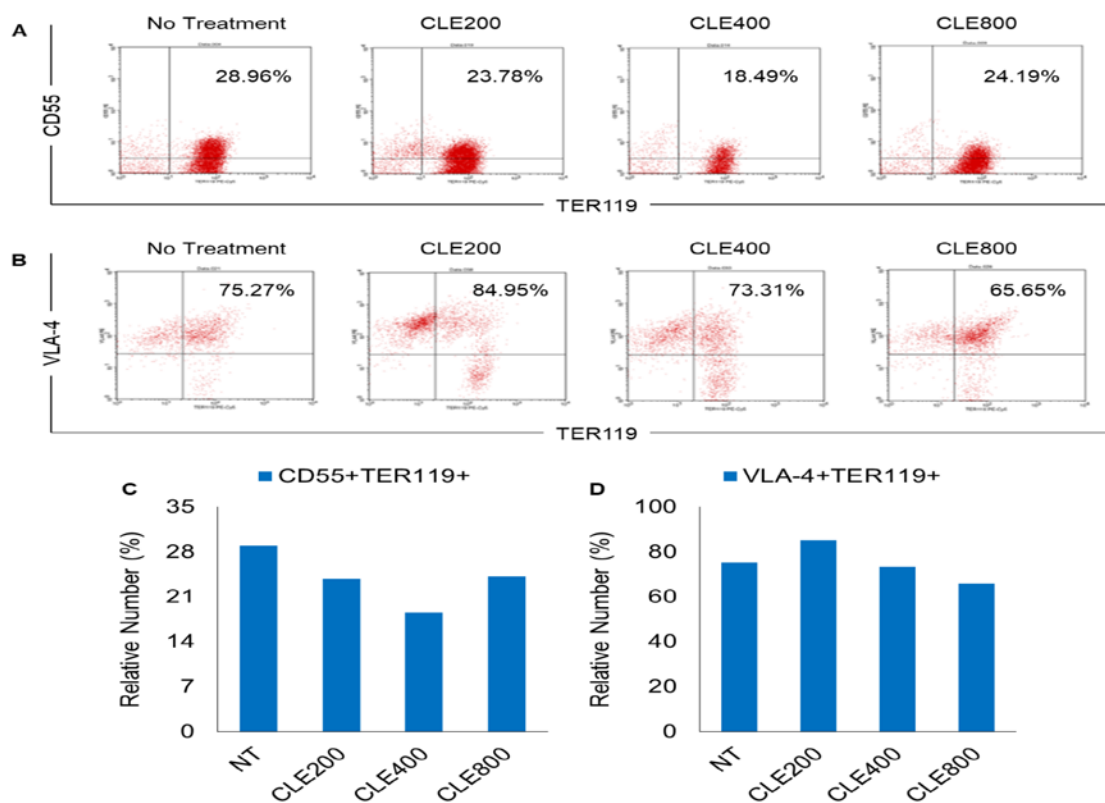


Figure 4. Immunomodulatory evaluation of CLE on CD55⁺TER119⁺ and VLA-4⁺TER119⁺ subsets. (A). Flow cytometry graph of CD55⁺TER119⁺; (B). Flow cytometry graph of VLA-4⁺TER119⁺; (C). Bar graph of CD55⁺TER119⁺; and (D). Bar graph of VLA-4⁺TER119⁺.

On the other hand, erythrocytes use both enzymatic and non-enzymatic antioxidants to combat free radicals generated by lipid peroxidation. Those two ideas stated that the quantity of adult red blood cells should be at least equivalent to or even higher than the normal group of the presence of vitamin C, which reduces hemolysis, supported by CD55, which further protects the cells from lysis. However, the statistical analysis suggests that all treatment groups had a lower relative number of erythroid cells, probably due to the high degree of lipid peroxidation in mice models.

4. Conclusion

In the present investigation, numerous subsets of lymphoid and myeloid immune cells were examined. According to our findings, CLE has a considerable effect in increasing the number of Gr1⁺ granulocyte cells, but not other cell types. Thus, we hypothesized that the chemicals in CLE could have a specific effect on granulocyte cells. Importantly, additional research must be conducted to determine how CLE increases the number of granulocyte cells.

Acknowledgement

Authors thank Universitas Brawijaya for supporting this study. Each author pays respect to late Arfan Tri Kusuma Ramadhan who was involved in this study.

Conflict of Interest

No conflict of interest

References

- Adefegha SA, Leal DBR, Doleski PH, Ledur PC, and Ecker A. 2017. Peripheral blood mononuclear cells from rat model of pleurisy: The effects of hesperidin on ectoenzymes activity, apoptosis, cell cycle and reactive oxygen species production. *Biomed. Pharmacother.*, **91**: 278–286.
- Alhabeeb H, Sohoul MH, Lari A, Fatahi S, Shidfar F, Alomar O, Salem H, Al-Badawi IA, and Abu-Zaid A. 2022. Impact of orange juice consumption on cardiovascular disease risk factors: a systematic review and meta-analysis of randomized-controlled trials. *Crit. Rev. Food Sci. Nutr.*, **62**(12): 3389–3402.
- Ang A, Pullar JM, Currie MJ, and Vissers MCM. 2018. Vitamin C and immune cell function in inflammation and cancer. *Biochem Soc Trans.*, **46**(5): 1147–1159.
- Asgary S, Keshvari M, Afshani MR, Amiri M, Laher I, and Javanmard SH. 2014. Effect of fresh orange juice intake on physiological characteristics in healthy volunteers. *Int. sch. res. notices*, **2014**: 1–8.
- Asgary S, Rastqar A, and Keshvari M. 2018. Functional food and cardiovascular disease prevention and treatment: A review. *J. Am. Coll. Nutr.*, **37**(5): 429–455.
- Belikov AV, Schraven B, and Simeoni L. 2015. T cells and reactive oxygen species. *J. Biomed. Sci.*, **22**(1): 1–11.

- Beukema M, Jermendi É, Oerlemans MMP, Logtenberg MJ, Akkerman R, An R, van den Berg MA, Zoetendal EG, Koster T, Kong C, Faas MM, Schols HA, and de Vos P. 2022. The level and distribution of methyl-esters influence the impact of pectin on intestinal T cells, microbiota, and Ahr activation. *Carbohydr. Polym.*, **286**: 1–12.
- Bourke CD, Berkley JA, and Prendergast AJ. 2016. Immune Dysfunction as a Cause and Consequence of Malnutrition. *Trends Immunol.*, **37**(6): 386–398.
- Breedveld A, Groot Kormelink T, van Egmond M, and de Jong EC. 2017. Granulocytes as modulators of dendritic cell function. *J. Leukoc. Biol.*, **102**(4): 1003–1016.
- Buscemi S, Rosafio G, Arcoleo G, Mattina A, Canino B, Montana M, Verga S, and Rini G. 2012. Effects of red orange juice intake on endothelial function and inflammatory markers in adult subjects with increased cardiovascular risk. *Am. J. Clin. Nutr.*, **95**(5): 1089–1095.
- Cao T, Shao S, Fang H, Li B, and Wang G. 2019. Role of regulatory immune cells and molecules in autoimmune bullous dermatoses. *Front. Immunol.*, **10**: 1–11.
- Carr AC, and Maggini S. 2017. Vitamin C and immune function. *Nutrients*, **9**(11): 1–25.
- Chen J-J, Yang C-K, Kuo Y-H, Hwang T-L, Kuo W-L, Lim Y-P, Sung P-J, Chang T-H, and Cheng M-J. 2015. New coumarin derivatives and other constituents from the stem bark of *Zanthoxylum avicennae*: Effects on neutrophil pro-inflammatory responses. *Int. J. Mol. Sci.*, **16**(5): 9719–9731.
- Choi EM, and Lee YS. 2010. Effects of hesperetin on the production of inflammatory mediators in IL-1 β treated human synovial cells. *Cell. Immunol.*, **264** (1): 1–3.
- Cicchese JM, Evans S, Hult C, Joslyn LR, Wessler T, Millar JA, Marino S, Cilfone NA, Mattila JT, Linderman JJ, and Kirschner DE. 2018. Dynamic balance of pro- and anti-inflammatory signals controls disease and limits pathology. *Immunol. Rev.*, **285**(1): 147–167.
- Cimmino L, Neel BG, and Aifantis I. 2018. Vitamin C in stem cell reprogramming and cancer. *Trends Cell Biol.*, **28**(9): 698–708.
- Duchnowicz P, Pilarski R, Michałowicz J, and Bukowska B. 2021. Changes in human erythrocyte membrane exposed to aqueous and ethanolic extracts from *Uncaria tomentosa*. *Molecules*, **26**(11): 1–15.
- Duthie SJ, Horgan G, de Roos B, Rucklidge G, Reid M, Duncan G, Pirie L, Basten GP, and Powers HJ. 2010. Blood folate status and expression of proteins involved in immune function, inflammation, and coagulation: Biochemical and proteomic changes in the plasma of humans in response to long-term synthetic folic acid supplementation. *J. Proteome Res.*, **9**(4): 1941–1950.
- Farber DL, Yudanin NA, and Restifo NP. 2014. Human memory T cells: Generation, compartmentalization and homeostasis. *Nat. Rev. Immunol.*, **14**(1): 24–35.
- Ferrari L, Martelli P, Saleri R, De Angelis E, Ferrarini G, Cavalli V, Passeri B, Bazzoli G, Ogno G, Magliani W, and Borghetti P. 2020. An engineered anti-idiotypic antibody-derived killer peptide (KP) early activates swine inflammatory monocytes. CD3+CD16+ natural killer T cells and CD4+CD8 α + double positive CD8 β + cytotoxic T lymphocytes associated with TNF- α and IFN- γ secretion. *Comp. Immunol. Microbiol. Infect. Dis.*, **72**: 1–15.
- Ferraz CR, Carvalho TT, Manchope MF, Artero NA, Rasquel-Oliveira FS, Fattori V, Casagrande R, and Verri WA. 2020. Therapeutic potential of flavonoids in pain and inflammation: mechanisms of action, pre-clinical and clinical data, and pharmaceutical development. *Molecules*, **25**(3): 1–35.
- Genovese S, and Epifano F. 2011. Auraptene: A natural biologically active compound with multiple targets. *Curr. Drug Targets*, **12**(3): 381–386.
- Goldman L, and Schafer AI (Eds.). 2020. **Goldman-Cecil medicine, 26th edition**. ed. Elsevier, Philadelphia, USA.
- Gombart AF, Pierre A, and Maggini S. 2020. A review of micronutrients and the immune system—working in harmony to reduce the risk of infection. *Nutrients*, **12**(1): 1–41.
- Granato A, Hayashi EA, Baptista BJA, Bellio M, and Nobrega A. 2014. IL-4 regulates Bim expression and promotes B cell maturation in synergy with baf conferring resistance to cell death at negative selection checkpoints. *J. Immunol.*, **192**(12): 5761–5775.
- Han L, Fu Q, Deng C, Luo L, Xiang T, and Zhao H. 2022. Immunomodulatory potential of flavonoids for the treatment of autoimmune diseases and tumour. *Scand. J. Immunol.*, **95**(1): 1–19.
- Hong J-M, Kim J-H, Kang JS, Lee WJ, and Hwang Y. 2016. Vitamin C is taken up by human T cells via sodium-dependent vitamin C transporter 2 (SVCT2) and exerts inhibitory effects on the activation of these cells in vitro. *Anat. Cell Biol.*, **49**(2): 88–98.
- Hong YJ, Kim N, Lee K, Hee Sonn C, Eun Lee J, Tae Kim S, Ho Baeg I, and Lee KM. 2012. Korean red ginseng (*Panax ginseng*) ameliorates type 1 diabetes and restores immune cell compartments. *J. Ethnopharmacol.*, **144**(2): 225–233.
- Horna P, Moscinski LC, Sokol L, and Shao H. 2019. Naïve/memory T-cell phenotypes in leukemic cutaneous T-cell lymphoma: Putative cell of origin overlaps disease classification. *Cytom. B - Clin. Cytom.*, **96**(3): 234–241.
- Horwitz DA, Fahmy TM, Piccirillo CA, and Cava AL. 2019. Rebalancing immune homeostasis to treat autoimmune diseases. *Trends Immunol.*, **40**(10): 888–908.
- Hsia CH, Jayakumar T, Lu WJ, Sheu JR, Hsia CW, Manubolu M, Huang WC, Chang Y, and Saravana BP. 2021. Auraptene, a monoterpene coumarin, inhibits LTA-induced inflammatory mediators via modulating NF- κ B/MAPKs signaling pathways. *Evid. Based Complement Alternat. Med.*, **2021**: 1–11.
- Hunter MC, Teijeira A, and Halin C. 2016. T cell trafficking through lymphatic vessels. *Front. Immunol.*, **7**: 1–14.
- Huntington ND, and Gray DH. 2018. Immune homeostasis in health and disease. *Immunol. Cell Biol.*, **96**(5): 451–452.
- Imam MU, Zhang S, Ma J, Wang H, and Wang F. 2017. Antioxidants mediate both iron homeostasis and oxidative stress. *Nutrients*, **9**(7): 1–19.
- Juan CA, Pérez de la Lastra JM, Plou FJ, and Pérez-Lebeña E. 2021. The chemistry of reactive oxygen species (ROS) Revisited: outlining their role in biological macromolecules (DNA, lipids and proteins) and induced pathologies. *Int. J. Mol. Sci.*, **22**(9): 1–21.
- Karthikeyan A, Kim HH, Preethi V, Moniruzzaman M, Lee KH, Kalaiselvi S, Kim GS, and Min T. 2021. Assessment of anti-inflammatory and antioxidant effects of *Citrus unshiu* peel (CUP) flavonoids on LPS-stimulated RAW 264.7 Cells. *Plants (Basel)*, **10**(10): 1–15.
- Kawashima A, Sekizawa A, Koide K, Hasegawa J, Satoh K, Arakaki T, Takenaka S, and Matsuoka R. 2015. Vitamin C induces the reduction of oxidative stress and paradoxically stimulates the apoptotic gene expression in extravillous trophoblasts derived from first-trimester tissue. *Reprod. Sci.*, **22**(7): 783–790.
- Każmierczak-Barańska J, Boguszewska K, Adamus-Grabicka A, and Karwowski BT. 2020. Two faces of vitamin C—antioxidative and pro-oxidative agent. *Nutrients*, **12**(5): 1–19.

- Kraus RF, and Gruber MA. 2021. Neutrophils—from bone marrow to first-line defense of the innate immune system. *Front. Immunol.*, **12**: 1-10.
- Krummel MF, Bartumeus F, and Gérard A. 2016. T-cell migration, search strategies and mechanisms. *Nat. Rev. Immunol.*, **16**(3): 193–201.
- Leal E, Zarza C, and Tafalla C. 2017. Effect of vitamin C on innate immune responses of rainbow trout (*Oncorhynchus mykiss*) leukocytes. *Fish Shellfish Immunol.*, **67**: 179–188.
- Lee JS, Hwang HS, Ko E-J, Lee Y-N, Kwon Y-M, Kim M-C, and Kang S-M. 2014. Immunomodulatory activity of red ginseng against influenza A virus infection. *Nutrients.*, **6**(2): 517–529.
- Liu J, Geng X, Hou J, and Wu G. 2021. New insights into M1/M2 macrophages: Key modulators in cancer progression. *Cancer Cell Int.*, **21**(1): 1–7.
- Liugan M, and Carr AC. 2019. Vitamin C and neutrophil function: Findings from Randomized Controlled Trials. *Nutrients.*, **11**(9): 1-35.
- Maatouk M, Elgueder D, Mustapha N, Chaaban H, Bzéouich IM, Loannou I, Kilani S, Ghoul M, Ghedira K, and Chekir-Ghedira L. 2016. Effect of heated naringenin on immunomodulatory properties and cellular antioxidant activity. *Cell Stress and Chaperones.*, **21**(6): 1101–1109.
- Maćczak A, Duchnowicz P, Sicińska P, Koter-Michalak M, Bukowska B, and Michałowicz J. 2017. The in vitro comparative study of the effect of BPA, BPS, BPF and BPAF on human erythrocyte membrane; perturbations in membrane fluidity, alterations in conformational state and damage to proteins, changes in ATP level and Na⁺/K⁺ ATPase and AChE activities. *Food Chem. Toxicol.*, **110**: 351–359.
- Machado FC, Girola N, Maia VSC, Bergami-Santos PC, Morais AS, Azevedo RA, Figueiredo CR, Barbutto JAM, and Travassos LR. 2020. Immunomodulatory protective effects of Rb9 cyclic-peptide in a metastatic melanoma setting and the involvement of dendritic cells. *Front. Immunol.*, **10**: 1–20.
- Mahdani FY, Parmadiati AE, Ernawati DS, Husain H, Ekaperdana SAP, Rachmaningayu U, Hadi P, Hendarti HT, and Surboyo MDC. 2020. *Citrus limon* peel essential oil-induced type IV hypersensitivity reaction. *J. Exp. Pharmacol.*, **12**: 213–220.
- Mahmoud AM, Hernández Bautista RJ, Sandhu MA, and Hussein OE. 2019. Beneficial effects of citrus flavonoids on cardiovascular and metabolic health. *Oxid. Med. Cell Longev.*, **2019**: 1–19.
- Manning J, Mitchell B, Appadurai DA, Shakya A, Pierce LJ, Wang H, Nganga V, Swanson PC, May JM, Tantin D, and Spangrude GJ. 2013. Vitamin C promotes maturation of T-cells. *Antioxid. Redox. Signal.*, **19**(7): 2054–2067.
- Martin MD, and Badovinac VP. 2018. Defining memory CD8 T cell. *Front. Immunol.*, **9**: 1–10.
- Merheb R, Abdel-Massih RM, and Karam MC. 2019. Immunomodulatory effect of natural and modified *Citrus pectin* on cytokine levels in the spleen of BALB/c mice. *Int. J. Biol. Macromol.*, **121**: 1–5.
- Meryk A, Grasse M, Balasco L, Kapferer W, Grubeck-Loebenstien B, and Pangrazzi L. 2020. Antioxidants N-acetylcysteine and vitamin c improve T cell commitment to memory and long-term maintenance of immunological memory in old mice. *Antioxidants (Basel).*, **9**(11): 1–14.
- Mezhzeyuski A, Bergsland CH, Backman M, Djureinovic D, Sjöblom T, Bruun J, and Micke P. 2018. Multispectral imaging for quantitative and compartment-specific immune infiltrates reveals distinct immune profiles that classify lung cancer patients. *J. Pathol.*, **244**(4): 421–431.
- Miles EA, and Calder PC. 2021. Effects of Citrus Fruit Juices and Their Bioactive Components on Inflammation and Immunity: A Narrative Review. *Front. Immunol.*, **12**: 1–18.
- Milošević MD, Paunović MG, Matić MM, Ognjanović BI, and Saičić ZS. 2018. Role of selenium and vitamin C in mitigating oxidative stress induced by fenitrothion in rat liver. *Biomed. Pharmacother.*, **106**: 232–238.
- Netea MG, Domínguez-Andrés J, Barreiro LB, Chavakis T, Divangahi M, Fuchs E, Joosten LAB, van der Meer JWM, Mhlanga MM, Mulder WJM, Riksen NP, Schlitzer A, Schultze JL, Stabell Benn C, Sun JC, Xavier RJ, and Latz E. 2020. Defining trained immunity and its role in health and disease. *Nat. Rev. Immunol.*, **20**(6): 375–388.
- Ogbue CO, Onyegbule FA, Ezugwu CO, Nchekwube IHM, and Ajaghaku AA. 2022. Immunostimulatory and immunorestorative effects of leaf extract and fractions of *Musanga cecropioides* on immunocompetent and experimentally induced immunocompromised mice. *CCMP.*, **100075**: 1-9.
- Oyarce K, Campos-Mora M, Gajardo-Carrasco T, and Pino-Lagos K. 2018. Vitamin C Fosters the In Vivo Differentiation of Peripheral CD4⁺ Foxp3⁻ T Cells into CD4⁺ Foxp3⁺ Regulatory T Cells but Impairs Their Ability to Prolong Skin Allograft Survival. *Front. Immunol.*, **9**: 1–13.
- Perche O, Vergnaud-Gauduchon J, Morand C, Dubray C, Mazur A, and Vasson M-P. 2014. Orange juice and its major polyphenol hesperidin consumption do not induce immunomodulation in healthy well-nourished humans. *Clin. Nutr.*, **33**(1): 130–135.
- Pisoschi AM, Pop A, Iordache F, Stanca L, Predoi G, and Serban AI. 2021. Oxidative stress mitigation by antioxidants—an overview on their chemistry and influences on health status. *Eur. J. Med. Chem.*, **209**: 1–52.
- Putra WE, Agusinta AK, Ashar MSAA, Manullang VA, Rifa'i M. 2023. Immunomodulatory and ameliorative effect of *Citrus limon* extract on DMBA-induced breast cancer in mouse. *Karbala Int. J. Mod. Sci.*, **9**(2): 1-14.
- Putra WE and Rifa'i M. 2020. Assessing the immunomodulatory activity of ethanol extract of *Sambucus javanica* berries and leaves in chloramphenicol-induced aplastic anemia mouse model. *Trop. Life Sci. Res.*, **31**(2): 175–185.
- Putra WE, and Rifa'i M. 2019. Hematopoiesis activity of *Sambucus javanica* on chloramphenicol-induced aplastic anemia mouse model. *Nat. Prod. Sci.*, **25**(1): 59-63.
- Putra WE, Soewondo A, and Rifa'i M. 2016. Effect of dexamethasone administration toward hematopoietic stem cells and blood progenitor cells expression on BALB/c mice. *JPACR.*, **4**(3): 100-108.
- Putra WE, Soewondo A, and Rifa'i M. 2015. Expression of erythroid progenitor cells and erythrocytes on dexamethasone induced-mice. *Biotropika*, **3**(1): 42-45.
- Predy GN, Goel V, Lovlin R, Donner A, Stitt L, and Basu TK. 2005. Efficacy of an extract of North American ginseng containing poly-furanosyl-pyranosyl-saccharides for preventing upper respiratory tract infections: a randomized controlled trial. *CMAJ.*, **173**: 1043–1048.
- Pyrzynska K. 2022. Hesperidin: A review on extraction methods, stability and biological activities. *Nutrients.*, **14**(12): 1–11.
- Qi T, Sun M, Zhang C, Chen P, Xiao C, and Chang X. 2020. Ascorbic acid promotes plasma cell differentiation through enhancing TET2/3-mediated DNA demethylation. *Cell Rep.*, **33**(9): 1–19.
- Qiu F, Liang C-L, Liu H, Zeng Y-Q, Hou S, Huang S, Lai X, and Dai Z. 2016. Impacts of cigarette smoking on immune responsiveness: Up and down or upside down? *Oncotarget.*, **8**(1): 268–284.

- Riaz M, Rahman NU, Zia-Ul-Haq M, Jaffar HZE, and Manea R. 2019. Ginseng: A dietary supplement as immune-modulator in various diseases. *Trends Food Sci. Technol.*, **83**: 12–30.
- Romeo J, Wärnberg J, Nova E, Díaz LE, Gómez-Martínez S, and Marcos A. 2007. Moderate alcohol consumption and the immune system: A review. *Br. J. Nutr.*, **98**(1): 111–115.
- Rosales C. 2018. Neutrophil: A cell with many roles in inflammation or several cell types? *Front. Physiol.*, **9**: 1–17.
- Ruiz-Iglesias P, Estruel-Amades S, Camps-Bossacoma M, Massot-Cladera M, Franch À, Pérez-Cano FJ, and Castell M. 2020. Influence of hesperidin on systemic immunity of rats following an intensive training and exhausting exercise. *Nutrients.*, **12**(5): 1–18.
- Saini RK, Ranjit A, Sharma K, Prasad P, Shang X, Gowda KGM, and Keum Y-S. 2022. Bioactive compounds of citrus fruits: A review of composition and health benefits of carotenoids, flavonoids, limonoids, and terpenes. *Antioxidants.*, **11**(2): 1–27.
- Sapkota B, Makandar SN, and Acharya S. 2022. **Biologic Response Modifiers (BRMs)**, in: StatPearls. StatPearls Publishing, Treasure Island (FL).
- Sassi A, Mokdad Bzécouich I, Mustapha N, Maatouk M, Ghedira K, and Chekir-Ghedira L. 2017. Immunomodulatory potential of hesperetin and chrysin through the cellular and humoral response. *Eur. J. Pharmacol.*, **812**: 91–96.
- Selders GS, Fetz AE, Radic MZ, and Bowlin GL. 2017. An overview of the role of neutrophils in innate immunity, inflammation and host-biomaterial integration. *Regen. Biomater.*, **4**(1): 55–68.
- Shahaf G, Zisman-Rozen S, Benhamou D, Melamed D, and Mehr R. 2016. B Cell Development in the Bone Marrow Is Regulated by Homeostatic Feedback Exerted by Mature B Cells. *Front. Immunol.*, **7**: 1–13.
- Shamliyan TA, and Dospinescu P. 2017. Additional improvements in clinical response from adjuvant biologic response modifiers in adults with moderate to severe systemic lupus erythematosus despite immunosuppressive agents: A systematic review and meta-analysis. *Clin. Ther.*, **39**(7): 1479–1506.
- Song MH, Nair VS, and Oh KI. 2017. Vitamin C enhances the expression of IL17 in a Jmjd2-dependent manner. *BMB Rep.*, **50**(1): 49–54.
- Sozzani S, Del Prete A, and Bosio D. 2017. Dendritic cell recruitment and activation in autoimmunity. *J. Autoimmun.*, **85**: 126–140.
- Suleman M, Khan A, Baqi A, Kakar MS, and Ayub M. 2019. 2. Antioxidants, its role in preventing free radicals and infectious diseases in human body. *Pure Appl. Biol.*, **8**(1): 380–388.
- Surboyo MDC, Mahdani FY, Ernawati DS, Hadi P, Hendarti HT, Parmadiati AE, Radithia D, Mardiyana SD, and Syarifah IM. 2019. Number of macrophages and transforming growth factor β expression in *Citrus limon* L. Tlekung peel oil-treated traumatic ulcers in diabetic rats. *Trop. J. Pharm. Res.*, **18**(7): 1427–1433.
- Van Gorkom GNY, Klein Wolterink RGJ, Van Elssen CHMJ, Wieten L, Germeraad WTV, and Bos GMJ. 2018. Influence of Vitamin C on Lymphocytes: An Overview. *Antioxidants.*, **7**(3): 1–14.
- Watkinson F, Nayar SK, Rani A, Sakellariou CA, Elhage O, Papaevangelou E, Dasgupta P, and Galustian C. 2021. IL-15 upregulates telomerase expression and potently increases proliferative capacity of NK, NKT-like, and CD8 T cells. *Front. Immunol.*, **11**: 1–14.
- Watson HA, Durairaj RRP, Ohme J, Alatsianos M, Almutairi H, Mohammed RN, Vigar M, Reed SG, Paisey SJ, Marshall C, Gallimore A, and Ager A. 2019. L-selectin enhanced T cells improve the efficacy of cancer immunotherapy. *Front. Immunol.*, **10**: 1–20.
- Xie Y, Wang L, Sun H, Shang Q, Wang Y, Zhang G, Yang W, and Jiang S. 2020. A polysaccharide extracted from alfalfa activates splenic B cells by TLR4 and acts primarily via the MAPK/p38 pathway. *Food Funct.*, **11**(10): 9035–9047.
- Yarosz EL, and Chang C-H. 2018. The role of reactive oxygen species in regulating T cell-mediated immunity and disease. *Immune Netw.*, **18**(1): 1–15.
- Ye MB, and Lim BO. 2010. Dietary pectin regulates the levels of inflammatory cytokines and immunoglobulins in interleukin-10 knockout mice. *J. Agric. Food Chem.*, **58**(21): 11281–11286.
- Zanwar AA, Badole SL, Shende PS, Hegde MV, and Bodhankar SL. 2014. Chapter 76 - Cardiovascular effects of hesperidin: A Flavanone Glycoside, in: Watson, R.R., Preedy, V.R., Zibadi, S. (Eds.), Polyphenols in Human Health and Disease. Academic Press, San Diego, pp. 989–992.
- Zemmour D, Zilionis R, Kiner E, Klein AM, Mathis D, and Benoist C. 2018. Single-cell gene expression reveals a landscape of regulatory T cell phenotypes shaped by the TCR. *Nat. Immunol.*, **19**(3): 291–301.
- Zhang X, Wang G, Gurley EC, and Zhou H. 2014. Flavonoid apigenin inhibits lipopolysaccharide-induced inflammatory response through multiple mechanisms in macrophages. *PLoS One.*, **9**(9): 1–18.
- Zhou X, Shi H, Jiang G, Zhou Y, and Xu J. 2014. Antitumor activities of ginseng polysaccharide in C57BL/6 mice with Lewis lung carcinoma. *Tumor Biol.*, **35**(12): 12561–12566.
- Zhou Y, Zhang Y, Han J, Yang M, Zhu J, and Jin T. 2020. Transitional B cells involved in autoimmunity and their impact on neuroimmunological diseases. *J. Transl. Med.*, **18**(1): 1–12.

Heavy Metals Effect on the Rat Uterus and Effectiveness of Vitamin E Treatment

Sikora K^{1,*}, Lyndin M^{1,2}, Sikora V^{3,1}, Hyriavenko N¹, Piddubnyi A^{1,4,5}, Lyndina Y¹, Awuah WA¹, Abdul-Rahman T¹, Korobchanska A⁶, Alexiou A^{8,9}, Romaniuk A¹.

¹ Sumy State University, Sumy, Ukraine; ² University of Duisburg-Essen, Essen, Germany; ³ University of Foggia, Foggia, Italy; ⁴ Umeå University, Umeå, Sweden; ⁵ Ukrainian-Swedish research center SUMEYA, Sumy, Ukraine; ⁶ Kharkiv National Medical University, Kharkiv, Ukraine; ⁷ Novel Global Community Educational Foundation, Hebersham, Australia; ⁸ AFNP Med Austria, Wien, Austria

Received: November 29, 2022; Revised: January 26, 2023; Accepted: February 7, 2023

Author Contributions: Conceptualization, K.S. and A.R.; methodology, K.S., M.L., A.W., T.A.R., A.K. and N.H.; software, K.S., V.S. and A.P.; formal analysis, K.S., M.L., A.A. and Y.L.; investigation, K.S., M.L., V.S., A.W., T.A.R., N.H., and Y.L.; resources, K.S., V.S., M.L. and A.A.; data curation, K.S., M.L., V.S., A.P., A.A. and A.R.; writing—original draft preparation, K.S., M.L., V.S., N.H., Y.L., A.W., T.A.R., A.K. and A.P.; writing—review and editing, K.S., M.L., V.S., A.A. and A.R.; visualization, K.S., M.L., V.S. and A.P.; supervision, A.R.; project administration, K.S., M.L., V.S., A.A. and A.R.. All authors have read and agreed to the published version of the manuscript.

Acknowledgments: This research has been supported by the Ministry of Education and Science of Ukraine [Grant № 0121U100472 and Grant № 123U100111] and research theme of the Department of Pathological anatomy of Sumy State University [№ 0119U100887].

Institutional Review Board Statement: The study was approved by the Bioethics Committee of the Medical Institute of Sumy State University (protocol No. 2/10 from 10.10.2019).

Compliance with Ethical Standards

Disclosure of potential conflicts of interest: The authors report no conflict of interest. The authors declare that the research was conducted in the absence of any commercial or financial relationships that could be construed as a potential conflict of interest.

Research involving Human Participants and/or Animals: All applicable international, national, and/or institutional ethical guidelines for the care and use of animals were followed.

Data availability: All data generated and analyzed during this study are included in this published article and its supplementary information files.

Abstract

Environmental pollution by heavy metals (HMs) is an increasingly critical problem that is posing a growing threat to reproductive health. Consequently, the aim of the current research was to study changes in rat uterus under 90 days of HMs exposure and estimate the efficacy and benefits of vitamin E treatment.

Female rats were randomly divided into three groups: untreated animals (control group); animals orally treated with the HMs mixture (HM group); and animals treated simultaneously with HMs and vitamin E (HM+E group). The toxic effects of the HMs (comprising Zn, Cu, Mn, Fe, Pb, and Cr) on the uterus of rats were investigated by histological, morphometrical, spectrophotometrical, and statistical methods.

Long-term HMs exposure triggered pathological (degenerative, inflammation, and atrophic) changes in the rat uterus together with a significant reduction of the uterine-wall thickness (37.99%, $p < 0.0001$) compared to the control. In contrast, there was a lower intensity of morphological lesions and wall thickness decrease (26.03%, $p < 0.0001$) in the uterus, in rats that underwent treatment with vitamin E. A substantial bioaccumulation of zinc, copper, manganese, iron, lead, and chromium general levels in the rat uterus was demonstrated in both the HM group (74.46%, $p < 0.0001$) and the HM+E group (49.81%, $p < 0.0001$), as compared to the control group. The lowest accumulative potential belonged to Zn and the highest to Pb. The results obtained showed a significant decline in the weight of animals treated by HMs in both HM (18,21%, $p < 0.01$) and HM+E (13,09%; $p < 0.05$) groups compared to the control. Our findings have demonstrated that treatment with vitamin E in HM-induced intoxication has a significant restrain of HMs accumulation (up to 16.46%, $p < 0.0001$) together with morphometric variations (less on 16.17%, $p < 0.01$).

In summary, long-term exposure to the HMs mixture had a pernicious toxic effect on the morphology and chemical content of the uterus of rats (strong negative correlations). Treatment with vitamin E significantly reversed the HMs impact on the uterus but did not demonstrate absolute protection.

* Corresponding author. e-mail: k.sikora@med.sumdu.edu.ua.

Keywords: uterus; heavy metals; reproductive health; vitamin E; antioxidant; detox treatment

1. Introduction

In recent years, significant insights have been gained in understanding the roles of the uterus in menstruation, fertility, and pregnancy together with orchestrating the development, differentiation, and maturation of the reproductive system. However, in the context of the deterioration of reproductive health and infertility increase (up to 21.9%), the study of uterus pathology became relevant (Cedars *et al.*, 2017; Ho *et al.*, 2017; Nik Hazlina *et al.*, 2022). Indeed, certain conditions and diseases of the uterus can cause reproductive-health disorders and dysfunction of the synergistic action of the procreative system, disrupting the reproduction and survival of species (Peters *et al.*, 2016; Cedars *et al.*, 2017; Hanson *et al.*, 2017). Any disturbance of estrogenic/anti-androgenic endocrine activity and enzyme mechanisms that can act by mimicking or inhibiting the actions of endogenous hormones may be accompanied by uterus lesions (e.g., benign and malignant tumors, congenital uterine malformation, infertility, ectopic gestation, pregnancies abort and poor pregnancy outcomes). Moreover, such damage of the uterus can be manifested in subsequent generations (Newbold *et al.*, 2006; Gore *et al.*, 2015; Rosenfeld, 2015; Katz *et al.*, 2016; Hanson *et al.*, 2017; Ho *et al.*, 2017). In addition, uterus macroscopic and microscopic lesions (atrophic and hyperplastic) can be caused by the development of pathological processes in this organ (e.g., endometritis, endometriosis, reproductive tract infection (about 33% in females), microflora imbalance, and benign and malignant tumors) or in other organs (e.g., diabetes, obesity, cardiovascular disease, oxidative stress, chronic stress, reproductive tract obstruction, and neurological disorders) (Gore *et al.*, 2015; Peters *et al.*, 2016; Katz *et al.*, 2016; Cedars *et al.*, 2017; Chen *et al.*, 2017; Hanson *et al.*, 2017; Lin *et al.*, 2018; Vannuccini and Petraglia, 2019). It is important to note that uterine lesions can also be provoked by factors with exogenous origins, such as viruses, bacteria, parasites, ionizing/non-ionizing radiation, and pollutants (Newbold *et al.*, 2006; Gore *et al.*, 2015; Cedars *et al.*, 2017; Chen *et al.*, 2017; Hanson *et al.*, 2017; Ho *et al.*, 2017; Lytvynenko *et al.*, 2017; Lin *et al.*, 2018; Nwosu *et al.*, 2018). It is known that long-term exposure of the organism to exogenous pollutants can contribute to epigenetic modifications that are reflected in subsequent generations (i.e., transgenerational epigenetic inheritance). The effects of various chemicals (e.g., heavy metals (HMs), bisphenol A, genistein, phytoestrogens, diethylstilbestrol, phthalates, and polyaromatic hydrocarbons) can simulate the impact of sex hormones and morphogens (Romaniuk *et al.*, 2015; Katz *et al.*, 2016; Ho *et al.*, 2017; Mohammad Hosseini *et al.*, 2019).

The increased morbidity risk due to xenobiotic contamination of the environment has encouraged the study of their effects. Among the most common pollutants that have a detrimental effect on organisms are HMs (Romaniuk *et al.*, 2015; Hamid *et al.*, 2016; Romaniuk *et al.*, 2017; Mohammad Hosseini *et al.*, 2019). However, HMs are not always toxic — most of them are essential trace elements. They are involved in numerous enzymatic, hormonal, redox, and other processes at all developmental

stages. However, exceeding the threshold level in the body results in their accumulation in tissues, and they can acquire toxic properties (Singh *et al.*, 2011; Hamid *et al.*, 2016; Nwosu *et al.*, 2018). In addition, some metals are always toxic (Pb, Cd, Cr, Ti, Si, Rb, Sr, Al, As, and Sn). The HMs effect depends on their properties, concentration, type, density, duration of exposure, molecular stability, partition coefficient, polarity, the interaction between metals, distribution, and transport into the ecosystem (Singh *et al.*, 2011; Jaishankar *et al.*, 2014; Nakade *et al.*, 2015; Hamid *et al.*, 2016; Nwosu *et al.*, 2018; Mohammad Hosseini *et al.*, 2019).

It is important to note that the long-term effects of various HMs are reflected in the abnormal variability of biochemical, functional (inhibition of menstruation, decrease in the frequency of implanted ova and of pregnancies, intrauterine growth restriction, preterm delivery, and spontaneous abortions), morphological (histopathological changes in the endometrium, myometrium and perimetrium; inflammation; reduction in the uterine gland, and decrease in the height of columnar cells, etc.), and molecular genetic (degeneration of hormones receptors and decrease of their sensitivity, oxidative stress, altering enzymes, growth factors, proliferation activities, tumor suppressor genes, cytokines, lymphokines, transport proteins and proteases, etc.) parameters of the uterus (Jaishankar *et al.*, 2014; Nakade *et al.*, 2015; Hamid *et al.*, 2016; Katz *et al.*, 2016; Hanson *et al.*, 2017; Ho *et al.*, 2017; Mohammad Hosseini *et al.*, 2019). However, some recent data revealed discrepancies regarding these changes due to the effect of the most common HMs and their accumulation (Nakade *et al.*, 2015; Mohammad Hosseini *et al.*, 2019; Lee *et al.*, 2021). On the one hand, this might have been due to the one or several effects of HMs. On the other hand, these changes might have depended on the variability of the xenobiotic concentrations (Singh *et al.*, 2011; Jaishankar *et al.*, 2014; Hamid *et al.*, 2016; Su *et al.*, 2017; Mohammad Hosseini *et al.*, 2019; Lee *et al.*, 2021). In addition, most previous research has considered pollutants and their concentrations in specific geographic locations. HMs accumulation in the organism differs globally depending on the pollution source and the ways of environmental spread (Singh *et al.*, 2011; Jaishankar *et al.*, 2014; Romaniuk *et al.*, 2015; Nakade *et al.*, 2015; Hamid *et al.*, 2016; Romaniuk *et al.*, 2017; Su *et al.*, 2017; Lee *et al.*, 2021). Consequently, the HMs effects on the body are extremely unpredictable and may negatively affect reproductive health (such as breast, endometrial, fallopian tubes or ovarian cancers, endometriosis, endometritis, menstrual disorders, infertility and spontaneous abortions, as well as pre-term deliveries, stillbirths) (Jaishankar *et al.*, 2014; Peters *et al.*, 2016; Hamid *et al.*, 2016; Cedars *et al.*, 2017; Doncova *et al.*, 2019; Dutta S *et al.*, 2022).

Nevertheless, there have been increasing numbers of reports of the successful use of various (natural or artificial compounds) supplementation, which can withstand the adverse impact of HMs. These agents have detoxifying and antioxidant properties and can reduce the intensity of xenobiotics' effects as prophylactics and for the treatment of HMs-related disorders. Most of these protective substances have a direct antagonistic relationship with

HMs and have high efficiency (Al-Attar, 2011; Jaishankar *et al.*, 2014; Romaniuk *et al.*, 2018; Sahiti *et al.*, 2020). However, multiple mechanisms of action of each trace element (especially in combination) can complicate the search for universal natural compounds that will neutralize the accumulation of HMs in body tissues and/or completely block their effect.

One of the most discovered naturally occurring supplementation is vitamin E (α -tocopherol) which consists of tocopherols and tocotrienols. This effective lipid-soluble non-enzymatic antioxidant can reduce radical-induced peroxidation in biological membranes and blood, stimulate the activation of antioxidant enzymes, suppress inflammation, accelerate structural recovery, protect cellular membranes and reduce the intensity of oxidative stress caused by HMs-induced toxicity. This enables free radicals to acquire a hydrogen atom from antioxidant molecules, effectively countering lipid peroxidation and safeguarding unsaturated membrane lipids due to its oxygen-scavenging capability. (Al-Attar, 2011; Mohd Mutalip *et al.*, 2018; Sahiti *et al.*, 2020). Moreover, various studies have shown that adequate intake of vitamin E solves reproductive health problems (an essential dietary factor required to maintain normal reproduction), such as enhancing term delivery, sustaining the endometrial membrane, preventing breast cancer growth, decreasing the level of fetal death and spontaneous abortion, etc. (Al-Attar, 2011; Mohd Mutalip *et al.*, 2018; Sahiti *et al.*, 2020). Based on these, vitamin E is often used in researches that describe its effectiveness and protective effects from oxidative stress specifically caused by the impact of various HMs (Al-Attar, 2011; Romaniuk *et al.*, 2018; Sahiti *et al.*, 2020). However, till today, there is no clear information regarding the beneficial effect of vitamin E on the uterus induced by HMs exposure.

Summarizing all the above, the *aim* of our current research was to study the changes in rats' uterus under 90 days of HMs exposure and estimate the efficacy and benefits of vitamin E treatment.

2. Materials and Methods

2.1. Animals

For this study, we used 12-week-old healthy Wistar female rats with an average weight of 221.7 ± 17.1 g, which were purchased from the Animal Experimental Unit of the Medical Institute, Sumy, Ukraine. The rats were selected after physical and behavioral examinations (body weight and health state, posture, and response to handling). The animals were acclimated for 7 days before any experimental procedures. All animals were housed in same-sex sub-groups (4 animals in 1 cage) in polypropylene cages with individual ventilation and were maintained under environmentally controlled laboratory conditions of temperature $22^\circ\text{C} \pm 1^\circ\text{C}$, relative humidity $55 \pm 5\%$, and 12 hours light/dark cycle. During the experiment, the animals had *ad libitum* access to standard pellets and water. Cage cleaning was performed daily. Individual animal bodyweights were recorded at weekly intervals. All necessary procedures were adopted to keep the rodents free from stress. Nulliparous and non-pregnant female rats were used in the study. The estrous-cycle monitoring was performed by daily vaginal smears. These

were collected every morning at 9.00 and were analyzed by light microscopy (Sikora *et al.*, 2021). The results before and during experiments were presented according to four phases (proestrus, estrus, metestrus, and diestrus). However, we used data only from the estrus phase to avoid the cyclic hormonal changes in female rats that could be associated with the estrous cycle and confound the results.

2.2. Experimental design

The female rodents were randomly assigned to three groups (eight rats per group). Group I (Control) comprised normal (untreated) rats that received ordinary food and drinking water. Group II (HM) comprised rodents that were orally treated with HMs substances for 90 days. Group III (HM+E) comprised animals that received water with HMs and vitamin E within 90 days. The experimental animals were euthanized by CO_2 inhalation followed by cervical dislocation and their uteruses were immediately exposed by low abdominal midline incision. The uteruses were then collected and trimmed of fascia and fat. From each rat, the uterine wall of 1.0 cm in length was excised from each uterine horn (proximal part) in the direction from the partial caudal fusion to the ovaries. One random uterine horn was assigned to atomic absorption spectrometry and the other horn was fixed in formaldehyde for later use. A total of 48 uterine horns from 24 rats were assigned to the investigation.

2.3. Experimental substances

The experimental model comprised six of the most common (dangerous and potentially dangerous) HMs (Jaishankar *et al.*, 2014; Nakade *et al.*, 2015; Romaniuk *et al.*, 2017; Su *et al.*, 2017; Romaniuk *et al.*, 2018; Lee *et al.*, 2021) at the following concentrations: zinc ($\text{ZnSO}_4 \times 7\text{H}_2\text{O}$) – 5 mg/l, copper ($\text{CuSO}_4 \times 5\text{H}_2\text{O}$) – 1 mg/l, iron (FeSO_4) – 10 mg/l, manganese ($\text{MnSO}_4 \times 5\text{H}_2\text{O}$) – 0.1 mg/l, lead ($\text{Pb}(\text{NO}_3)_2$) – 0.1 mg/l, and chromium ($\text{K}_2\text{Cr}_2\text{O}_7$) – 0.1 mg/l. The concentrations of mentioned above HMs were comparable to those found in the environment according to the results of the epidemiological examination of the environment of the Northern regions of Ukraine and in accordance with preliminary reports (Romaniuk *et al.*, 2015; Romaniuk *et al.*, 2017). The list of chemical elements and their concentrations were confirmed and approved by the Bioethics Committee of the Medical Institute of Sumy State University (No. 2/10 from 10.10.2019). The HMs mixture was dissolved in ordinary water and prepared each three days. Contaminated water was supplied in a drinking bottle in *ad libitum* access for oral administration annually within 90 days.

As antagonist supplementation, we used alpha-tocopherol (vitamin E) due to its antioxidant properties at an average daily prophylactic dose (9.1 mg/kg to rats' bodyweight considering species' characteristics). Conversion of human doses to rat doses was as following: Animal equivalent dose (mg/kg) = Human dose (mg/kg) \times Km ratio (Nair and Jacob, 2016). Based on this, considered the coefficient of species characteristics of rats (6.0) and humans (37.0) with average human body weight (70 kg), the dose for rats was followed: $37.0/6.0 = 6.2$; $1,47 \text{ mg/kg} \times 6.2 = 9.1 \text{ mg/kg}$. The average weight of animals was 221.7 ± 17.1 g. Therefore, animals received vitamin E at an average dose of 2.02 mg per rat bodyweight. Animals

were administered vitamin E via the oral gavage technique (daily at 10.00 am) for 90 days. Selected antioxidant was estimated based on the literature and manufacturer's recommendations (Al-Attar, 2011; Nair and Jacob, 2016; Romaniuk *et al.*, 2018; Sahiti *et al.*, 2020).

2.4. Tissue processing, histology, and morphometric scoring of the uterus

The fresh rat uterine horns were fixed in 10% neutral buffered formaldehyde for 24 hours, dehydrated in ethanol (70–96%), and embedded in paraffin wax blocks. Formalin-fixed paraffin-embedded tissue blocks were sectioned using a rotational microtome Shandon Finesse 325 (Thermo Scientific, USA). Transverse sections of uterine horns with a thickness of 5 μm were placed on SuperFrost Plus™ Adhesion slides (Thermo Scientific, USA) and dried overnight. The next day, the samples were submerged in xylene (dewaxing – 2 times per 5 minutes each), descending grades of ethanol (rehydration – 100% (1 time per 5 minutes), 95% (1 time per 5 minutes), 70% (1 time per 5 minutes)) and washed in running tap water (2 times per 5 minutes each). Immediately after, samples were immersed in hematoxylin solution for 4 min and followed by immersion in eosin solution for 2 min. The sample were washed in running tap water (2 times per 10 minutes each) after incubation of both hematoxylin and eosin solutions. Finally, sections were dipped in 96% (2 times per 5 minutes) and 100% (1 time per 5 minutes) ethanol, cleared up with xylene (1 time per 5 minutes), and mounted on Histomount Mounting Solution (Thermo Scientific, USA). Two independent pathologists additionally evaluated the histopathological examination. In case, two pathologists did not reach a consensus regarding the results, we sought the help of a third pathologist. The microscopy and morphometric scoring of the rats' uteruses were performed with the Zeiss Axio Primo Star microscope, Zeiss AxioCam ERc 5s digital camera, and ZEN 2 (blue edition) software package (Germany).

2.5. Atomic absorption spectrometry of uterine tissues

The atomic absorption spectrometry of uterine tissues was performed according to the following protocol. Tissue samples were scaled, weighed on an analytical balance, dried (at 105°C), and burnt in porcelain crucibles at 450°C (48 h). Ash was dissolved into hydrochloric and nitric acids at 50°C overnight. After dilution with distilled water, the samples were measured. The sample solution was evaporated with the flame atomizer. Thereafter, the electrothermal atomic absorption spectrophotometer C-115M1 (Ukraine) with the analytic software package AAS SPEKTR (Ukraine) was used to determine the number of chemical elements according to their wavelength as follows: zinc (213.9 nm), copper (324.7 nm), iron (248.3 nm), manganese (279.4 nm), lead (283.3 nm), and chromium (357.9 nm).

2.6. Statistical analysis

All results are expressed as the mean \pm standard deviation ($M \pm SD$). Distribution type was estimated with the Shapiro–Wilk test. The differences between groups for normally distributed datasets were determined by the

independent student's t-test. The one-way analysis of variance (ANOVA) followed by Bonferroni's post-hoc comparisons test was performed to compare variables among groups. Analysis of the strength and direction of the relationships between two variables was performed using the Pearson's (r) correlation coefficient. Differences in values were considered significant at $p < 0.05$. Data analysis and graphs were prepared with GraphPad Prism® 6.0.

2.7. Ethics approval

All animals handling and experimental procedures fully adhere to the Animal Research: Reporting of In Vivo Experiments (ARRIVE) guidelines 2.0 (Percie *et al.*, 2020). The experiment has been conducted in the European Community Guide for the Care and Use of Laboratory Animals guidelines, ethical and responsible manner, and is in full compliance with all relevant codes of experimentation (institutional and national) and legislation. This study was approved by the Bioethics Committee of the Medical Institute of Sumy State University (No. 2/10 from 10.10.2019).

3. Results

3.1. Liveweight, histopathologic and morphometric changes in rat uterus caused by HMs

HMs administration induced body weight loss in both experimental groups. Indeed, the liveweight proportion of female rats was less in HM group (HMs exposure only) (decrease of 18,21%; $p < 0.01$) and in HM+E group (HMs exposure with vitamin E treatment) (decrease of 13,09%; $p < 0.05$) than in the Control group. There was no significant difference between HM group and HM+E group. A difference in body weight was first noticed in the third week of the experiment and it increased in the following weeks. Other visual changes were not detected.

Long-term HMs exposure (HM group) contributed to pathological changes in the initial part of the uterine horn and reduction of the organ's wall thickness (see Figure 1 and Figure 2). However, these changes were found in both the endometrium and the myometrium. Detailed morphological analysis indicated a nonspecific versatility of these changes: dystrophy of the prismatic (vacuolar degeneration) and exocrine cells (cystic transformation of goblet cells) of the mucous membrane and myometrial myocytes. Atrophic changes in the epithelium were also observed — that are, reduced and uneven height of the superficial (cylindrical epithelium changes to cubic) and glandular epithelium due to a reduction of cytoplasm volume; reduction of endometrial gland number, size, and lumen; and cystic enlargement of single glands. The uterine mucosa had a decreased number of folds and a significantly increased intrauterine lumen. Focal inflammatory infiltration was found mainly in the endometrium. However, the myometrium was also locally involved in the inflammatory process. This was accompanied by connective tissue disorganization, microcirculatory disorders, and slight edema along the entire wall of the uterine horn.

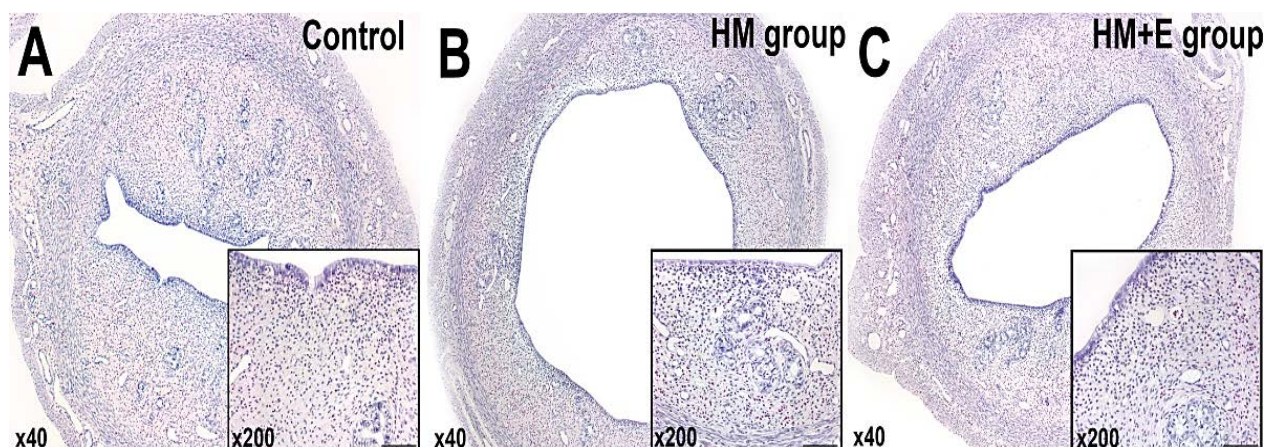


Figure 1. The HMs (Zn, Cu, Mn, Fe, Pb, and Cr) effect on the histopathologic changes in rats uterine horns: control group (A), HM group (B), and HM+E group (C). Staining with hematoxylin and eosin. Magnification: $\times 40$ and $\times 200$. Scale bar – 50 μm .

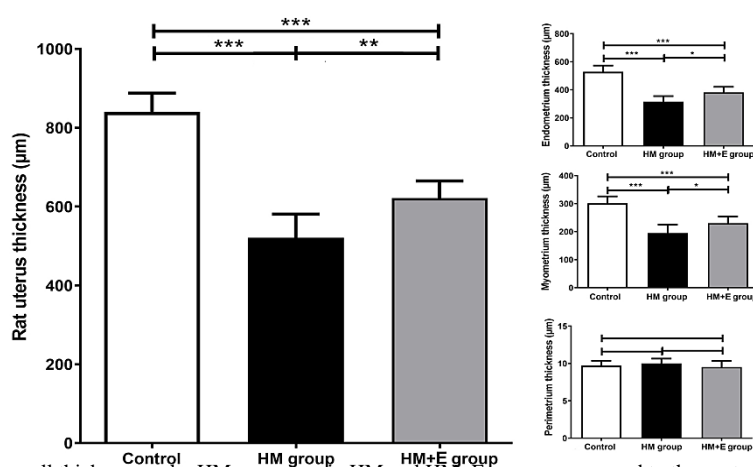


Figure 2. Variability of rat uterus wall thickness under HMs exposure in HM and HM+E groups, compared to the control. Data are expressed as Mean \pm SD (Bars – T style with above direction). Values were analyzed by One-way ANOVA followed by Bonferroni's post-hoc comparisons test (n=24): *p < 0.05; **p < 0.01; ***p < 0.001.

Additionally, compared to the control group, the morphometric analysis revealed a significant reduction of the uterine-wall thickness (37.99%, $p < 0.0001$) under HMs long-term exposure. Among all of the uterine layers, the endometrium had the highest reduction of the thickness (40.28%, $p < 0.0001$), followed by the myometrium (35.28%, $p < 0.0001$), and the perimetrium (2.88%, $p > 0.05$).

In contrast, we detected moderate degenerative and atrophic changes in the rat uteruses of the HM+E group. On the one hand, the intensity of pathological transformations and morphometric variations (less on 16.17%, $p < 0.01$) of the uterus wall were lower than those in the HM group. On the other hand, the morphometric scoring showed a reduction of rat uterine thickness (26.03%, $p < 0.0001$) in the HM+E group due to a decrease of the endometrium and myometrium sizes by 27.88% and 23.56% ($p < 0.0001$), respectively, compared to the control group. The difference in perimetrium thickness was not statistically significant (1.95%, $p > 0.05$).

3.2. Imbalance of chemical contents in rat uterus tissues caused by HMs

The detection limits, distribution, and variability of the HMs concentration levels in rat uteruses are shown in

Figure 3 and Table 1. The HM and HM+E groups had a wide range of variations of HMs accumulation in uterus tissues. According to atomic absorption spectrometry, the mean concentration of each element (Zn, Cu, Fe, Mn, Pb, and Cr) differed significantly (74.46%, $p < 0.0001$) from the control values, even in the group with treatment by vitamin E (49.81%, $p < 0.0001$). The highest concentration was estimated for Fe and the lowest for Pb. However, we detected a tendency for a general increase of HMs in rat uterus tissues as follows (listed in descending order): Pb (88.11%, $p < 0.0001$) > Fe (86.26%, $p < 0.0001$) > Cr (73.09%, $p < 0.0001$) > Mn (63.6%, $p < 0.0001$) > Cu (61.8%, $p < 0.0001$) > Zn (49.34%, $p < 0.0001$) for HM group vs Pb (62.24%, $p < 0.0001$) > Fe (58.81%, $p < 0.0001$) > Cr (55.58%, $p < 0.0001$) > Cu (46.17%, $p < 0.0001$) > Mn (44.77%, $p < 0.0001$) > Zn (29.4%, $p < 0.0001$) for the HM+E group relative to the control group. Therefore, the HMs bioaccumulation in the HM+E group was lower than that in the HM group (16.46%, $p < 0.0001$).

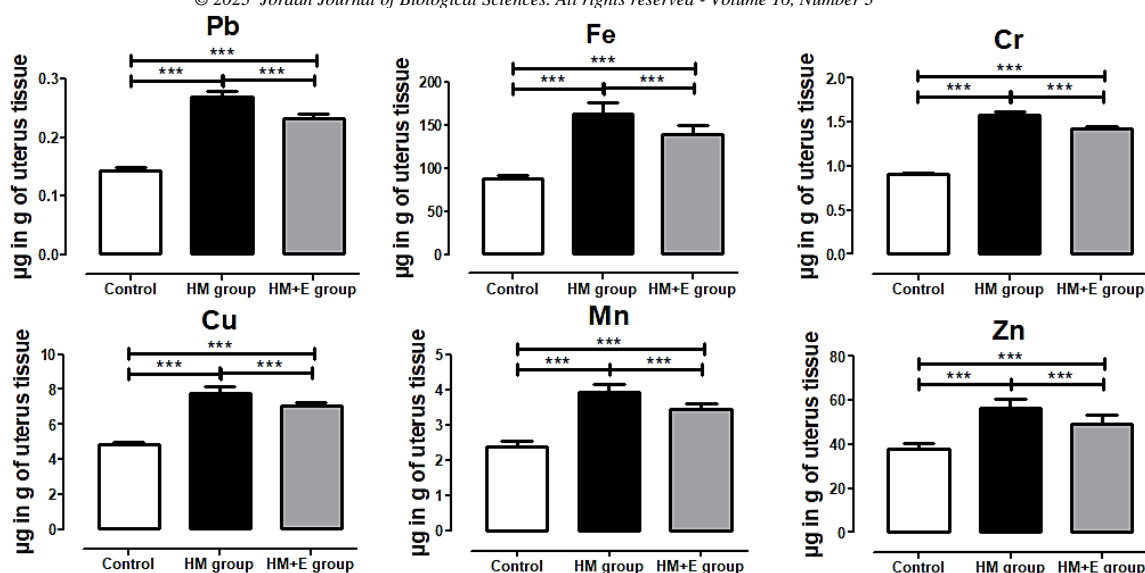


Figure 3. The imbalance of HMs concentration in rat uterine tissues in HM and HM+E groups. The Zn, Cu, Mn, Fe, Pb, and Cr concentrations were significantly higher in the HM group than in the control and HM+E group. The HMs concentration in the HM+E group was significantly higher than in the control group. Data are expressed as Mean \pm SD (Bars – T style with above direction). Values were analyzed by One-way ANOVA followed by Bonferroni's post-hoc comparisons test (n=24): *p < 0.05; **p < 0.01; ***p < 0.001.

Table 1. Variability of HMs concentration ($\mu\text{g/g}$) in rats uterine tissues.

	HM group	HM+E group	Control group
Pb	0.269 \pm 0.009*** ¹ / ²	0.232 \pm 0.009*** ¹	0.143 \pm 0.006
Fe	163.18 \pm 12.650*** ¹ / ²	139.13 \pm 10.37*** ¹	87.61 \pm 4.38
Cr	1.582 \pm 0.037*** ¹ / ²	1.422 \pm 0.034*** ¹	0.914 \pm 0.01
Mn	3.91 \pm 0.23*** ¹ / ²	3.46 \pm 0.15*** ¹	2.39 \pm 0.15
Cu	7.78 \pm 0.35*** ¹ / ²	7.06 \pm 0.21*** ¹	4.83 \pm 0.15
Zn	56.69 \pm 3.8*** ¹ / ²	49.74 \pm 4.01*** ¹	37.96 \pm 2.45
Total	233.41 \pm 8.84*** ¹ / ²	200.42 \pm 9.86*** ¹	133.83 \pm 5.5

Note: ¹ – compared to control group. ² – compared to HM+E group. *p < 0.05; **p < 0.01; ***p < 0.001.

3.3. Correlation analysis

There were strong negative correlations between rats' uterine thickness and HMs accumulation in both experimental groups — HM and HM+E (see Table 2). Thus, each individual metal had a different strength of influence as follows: Zn (r=−0.89), Cu (r=−0.93), Mn (r=−0.91), Fe (r=−0.95), Pb (r=−0.93), Cr (r=−0.95) vs Zn (r=−0.77), Cu (r=−0.95), Mn (r=−0.87), Fe (r=−0.97), Pb

(r=−0.91), Cr (r=−0.93) (p<0.0001), respectively. It is important to note that the strength of these relationships was different in the endometrium, myometrium, and perimetrium. The correlation between the uterus membranes thickness and the HMs concentration was slightly lower in the HM+E group (r=−0.91, p<0.0001), compared to the HM group (r=−0.96, p<0.0001).

Table 2. The strength of Pearson's correlations (r) between HMs accumulation and uterus thickness.

	Endometrium		Myometrium		Perimetrium	
	HM group	HM+E group	HM group	HM+E group	HM group	HM+E group
Pb	-0.92***	-0.85***	-0.87***	-0.84***	0.16	-0.21
Fe	-0.94***	-0.85***	-0.9***	-0.83***	0.38	-0.19
Cr	-0.93***	-0.87***	-0.9***	-0.84***	0.24	-0.14
Mn	-0.9***	-0.8**	-0.85***	-0.82***	0.14	-0.18
Cu	-0.91***	-0.9***	-0.87***	-0.84***	0.25	-0.05
Zn	-0.88***	-0.74**	-0.81***	-0.65***	0.13	-0.05
Total	-0.95***	-0.86***	-0.9***	-0.82***	0.33	-0.17

Note: *p < 0.05; **p < 0.01; ***p < 0.001 – compared to the control group.

4. Discussion

Industrialization and urbanization have affected many organisms' natural lifestyles, violating the evolutionarily programmed organism existence and corresponding complex (genetic) diseases (Saeb and Al-Naqeb, 2016). The progressive accumulation of pollutants in the environment poses a great threat. Therefore, humanity should focus on mitigating (degassing and deactivation) existing and preventing future pollution (Jaishankar *et al.*, 2014; Hamid *et al.*, 2016; Ho *et al.*, 2017; Zhang *et al.*, 2019; Sahiti *et al.*, 2020). Many previous studies have shown the effects of chemical toxins on organisms. Such 'coexistence' may depend on the origin, ways of pollutants influence, individual characteristics of each species, the effectiveness of individual protection or prevention, social behavior, health outcomes, social and demographic features (Saeb and Al-Naqeb, 2016). In general, four factors can contribute to the violation of physiological homeostasis in the body: genetic, hormonal, ontogenetic, and life/health factors (Jaishankar *et al.*, 2014; Saeb and Al-Naqeb, 2016; Ho *et al.*, 2017; Su *et al.*, 2017; Zhang *et al.*, 2019; Lee *et al.*, 2021).

HMs are among the top exogenous pollutants worldwide that can spread and bioaccumulate in terrestrial, aquatic, and airborne environments. In such natural conditions, essential and toxic trace elements have a long half-life, and they can accumulate and change their nature (Singh *et al.*, 2011; Jaishankar *et al.*, 2014; Romaniuk *et al.*, 2015; Nakade *et al.*, 2015; Hamid *et al.*, 2016; Romaniuk *et al.*, 2017; Nwosu *et al.*, 2018; Mohammad Hosseini *et al.*, 2019; Zhang *et al.*, 2019; Sahiti *et al.*, 2020). It should be noted that the geochemical cycling of HMs on the planet has both artificial and natural compounds (weathering of metal-bearing rocks and volcanic eruptions, etc.). This increases their spread even in regions with low urbanization and technological progress levels (Singh *et al.*, 2011; Jaishankar *et al.*, 2014; Nakade *et al.*, 2015; Hamid *et al.*, 2016; Ali *et al.*, 2019; Zhang *et al.*, 2019; Lee *et al.*, 2021). Moreover, polyelemental additive metal contamination can contribute to the suppression and/or stimulation of each compound or even change its properties (Lodovici and Bigagli, 2011; Singh *et al.*, 2011; Jaishankar *et al.*, 2014; Nwosu *et al.*, 2018; Ali *et al.*, 2019).

The main effects of HMs on the body are the development of oxidative stress (hyperproduction of free radicals, reactive oxygen and nitrogen forms and lipid peroxidation, and inhibition of antioxidant mechanisms), inhibition of enzymatic activity, hormonal disorders, disruption of cell integrity, imbalance of cell division and apoptosis, impaired gene expression (blocking of signal pathways), chromosomal aberrations, pathological methylation and accumulation of damaged DNA, etc. (Singh *et al.*, 2011; Jaishankar *et al.*, 2014; Romaniuk *et al.*, 2015; Hamid *et al.*, 2016; Romaniuk *et al.*, 2017; Chen *et al.*, 2019). However, the mechanisms of HMs effect on the reproductive system are not fully understood. On the one hand, the toxicity at low exposure concentrations of metals such as cadmium, lead, aluminum, metalloid arsenic is more or less clear (cytotoxic, carcinogenic, and genotoxic effects). On the other hand, the excessive concentrations of essential elements (such as copper, zinc, manganese, nickel, iron, etc.) can act through complex

direct and indirect pathways (Fenton-type reaction, or depletion of antioxidant systems). It is related to their mandatory physiological participation in antioxidant protection (Bielen *et al.*, 2013; Jaishankar *et al.*, 2014; Hamid *et al.*, 2016; Romaniuk *et al.*, 2017; Chen *et al.*, 2019).

Antioxidant deficiency, chronic diseases, or toxicants exposure are accompanied by an increased free radical concentration. It contributes to the violation of redox regulation and the development of oxidative stress, damage to the integrity of lipids, proteins, and DNA. On the one hand, the imbalance of redox systems occurs by direct inhibition of enzymatic protective (antioxidant) mechanisms (superoxide dismutase, ascorbate peroxidase, catalase, and glutathione peroxidase), non-enzymatic metabolic antioxidants (lipoic acid, glutathione, L-arginine, coenzyme Q10, melatonin, uric acid, bilirubin, metal-chelating proteins, transferrin, etc.) and nutrient non-enzymatic antioxidants (vitamin E, vitamin C, carotenoids, trace metals (selenium, manganese, zinc), flavonoids, omega-3 and omega-6 fatty acids, etc.). On the other hand, it is achieved by stimulation of enzymes that produce free radicals (hydroxyl (OH•), superoxide (O²•-), nitric oxide (NO•), nitrogen dioxide (NO₂•), peroxy (ROO•) and lipid peroxy (LOO•)) and other non-radical reactive derivatives (hydrogen peroxide (H₂O₂), ozone (O₃), singlet oxygen (¹O₂), hypochlorous acid (HOCl), nitrous acid (HNO₂), peroxy nitrite (ONOO⁻), dinitrogen trioxide (N₂O₃), lipid peroxide (LOOH)) (Shao *et al.*, 2007; Pham-Huy *et al.*, 2008; Bielen *et al.*, 2013; Phaniendra *et al.*, 2015).

Vitamins and trace metals co-factors have an essential role in the non-enzymatic antioxidant mechanisms (Singh *et al.*, 2011; Bielen *et al.*, 2013; Phaniendra *et al.*, 2015; Su *et al.*, 2017). Artificial induction of non-enzymatic antioxidants leads to the counteraction of free radicals by direct and/or indirect ways (Bielen *et al.*, 2013; Hamid *et al.*, 2016; Mohammad Hosseini *et al.*, 2019; Sahiti *et al.*, 2020). Antioxidants can block the action of free radicals on the cell surface and in the blood. Tocopherol locates on the biological membrane of cells reduces the risk of free radicals entering the cell. Also, when combined with other antioxidants, vitamin E promotes faster cell "cleansing" and protection. They are also able to neutralize free radicals by transferring them positively charged atoms. Based on this, in our study, we used vitamin E for treatment because it is considered as the most powerful exogenous antioxidant and free-radical scavenger (Pham-Huy *et al.*, 2008; Al-Attar, 2011; Sahiti *et al.*, 2020). It is also known that stabilization of one antioxidant can lead to exhibiting cooperative behavior and enhance other's antioxidant mechanisms (Al-Attar, 2011; Bielen *et al.*, 2013; Sahiti *et al.*, 2020). For example, vitamin C has a regenerative effect on vitamin E from α -tocopherol radicals damage to membranes, zeaxanthin synthesis in the xanthophyll cycle, and inhibits activation of the caspase cascade and DNA damage, etc. (Shao *et al.*, 2007; Al-Attar, 2011; Bielen *et al.*, 2013; Sahiti *et al.*, 2020).

The results of our study indicated a pernicious toxic effect of HMs on the rat uterus. Histopathological studies on uteri of different exposure groups in the present study revealed its dose-dependent deleterious effects in all structural elements. Thus, the heterogeneity of uterine transformation was represented mainly by degenerative

and atrophic changes (degeneration and decrease in the height of luminal and glandular epithelium, decrease in the number of glands, their size and lumen), interstitial edema, inflammatory cells infiltration, microcirculatory disorder, connective tissue disorganization, and uterus wall thinning. Simultaneously, there was a decrease of the uterus thickness on the 37.99 % ($p < 0.0001$) vs 26.03 % ($p < 0.0001$), HM vs HM+E groups compared to the control. The reduction of the uterine wall (37.99%, $p < 0.0001$) was caused by thinning of mucous and muscular membranes, respectively. It resulted in an increased intrauterine lumen and a decreased number of endometrial folds. This can complicate the movement of sperm and oocyte fixation (Höfer *et al.*, 2009; Lukacinova *et al.*, 2012; Nakade *et al.*, 2015; Hamid *et al.*, 2016; Cedars *et al.*, 2017; Hanson *et al.*, 2017; Chen *et al.*, 2019; Doncova *et al.*, 2019; Mohammad Hosseini *et al.*, 2019). It seems that this reaction of the uterus was caused by an increased concentration of Zn, Cu, Fe, Mn, Pb, and Cr in the organ tissue. It was also confirmed by the correlation between spectrophotometric and morphometric values imbalance.

Similar morphological and morphometric changes in the uterus have been described in other studies (Höfer *et al.*, 2009; Lukacinova *et al.*, 2012; Nakade *et al.*, 2015; Nasiadek *et al.*, 2018; Doncova *et al.*, 2019). However, different HMs combinations (mono- and/or polyelemental), their concentrations, and exposure time were used. In contrast, it was reported about the opposite effect of pollutants on the uterus, which was manifested by hyperplasia and dystrophy of the uterine mucosa (Höfer *et al.*, 2009; Nasiadek *et al.*, 2018). Authors indicate that HMs accumulation in the body can both stimulate and inhibit the activity of sex hormones and their effect on receptors in the uterus (Höfer *et al.*, 2009; Chatterjee and Chatterji, 2010; Katz *et al.*, 2016; Hanson *et al.*, 2017). Moreover, we have previously found an HMs effect on developing dystrophic/atrophic and/or oncological changes in other organs (the bladder, bone marrow, breast, and others) (Romaniuk *et al.*, 2015; Romaniuk *et al.*, 2017; Romaniuk *et al.*, 2018).

Our results point out that in contrast to HMs exposure of rats in HM group, the less significant histopathological lesions were identified in the rats' uterus after vitamin E treatment (HM+E group). Thus, after vitamin E treatment, moderate atrophy (decrease in height of columnar cells and fibrosis) and inflammation in the uterus were observed. Moreover, treatment in HM+E group caused the less pronounced reduction of rat uterine thickness (less on 16.17%, $p < 0.01$) against the background of suppression of the accumulation of the metal in the uterus tissue, compared to HM group. Based on this, a vitamin E supplement may be beneficial in slowing progressive uterus damage. Such morphological results coincide with the data on the effectiveness and importance of the natural or artificial compounds with detoxifying and antioxidant properties (Pham-Huy *et al.*, 2008; Bielen *et al.*, 2013; Yadav *et al.*, 2016; Romaniuk *et al.*, 2019; Romaniuk *et al.*, 2018; Sahiti *et al.*, 2020). Unfortunately, a definitive defense mechanism against the impact of pollutants on the organism has not been identified or reported.

HMs exposure (both short- and long-term) leads to their accumulation in the organs (Hamid *et al.*, 2016; Romaniuk *et al.*, 2017; Su *et al.*, 2017; Nwosu *et al.*, 2018; Ali *et al.*, 2019; Mohammad Hosseini *et al.*, 2019).

However, the imbalance of their concentrations in the uterus and other organs differed among reports (Höfer *et al.*, 2009; Lukacinova *et al.*, 2012; Rzymiski *et al.*, 2016; Nasiadek *et al.*, 2018). Our study showed an increase of HMs accumulation ($p < 0.001$) in rats' uterus. Moreover, the concentration and intensity of their accumulation differed in each case. Thus, the lowest relative bioaccumulation in both groups (HM and HM+E groups) belonged to Zn and the maximum to Pb (Pb>Fe>Cr>Mn>Cu>Zn for HM group and Pb>Fe>Cr>Cu>Mn>Zn for the HM+E group in descending order). It should be noted that corrector treatment caused the change in Mn and Cu accumulation order. In the HM+E group, the HMs levels were higher than control levels but were significantly lower (for Zn, Cu, Fe, Mn, Pb, and Cr; $p < 0.0001$) compared to the HM group. This difference may be due to several factors, such as the properties of each individual metal, competition bonds (synergistic and antagonistic) both between metals and between metals with vitamin E, accumulative characteristics of HMs and bioaccumulative characteristics of the uterus, and others (Jaishankar *et al.*, 2014; Nakade *et al.*, 2015; Hamid *et al.*, 2016; Rzymiski *et al.*, 2016; Romaniuk *et al.*, 2018; Mohammad Hosseini *et al.*, 2019; Sahiti *et al.*, 2020; Wang *et al.*, 2020). In addition, we demonstrated the relationship between the excess concentration of HMs in uterine tissue and the variability of morphometric values of the uterine wall. Strong negative correlations were found between organ thickness and HMs accumulation in the uterine tissues in both groups (HM group ($r = -0.96$, $p < 0.0001$) and HM+E group ($r = -0.91$, $p < 0.0001$)). In this case, the greatest influence on uterine wall thickness had Pb and Cr. On the other hand, the lowest influence had Zn and Cu. The essential HMs are prone to lower accumulation in the uterus on the background of detoxification by vitamin E. At the same moment, toxic or potentially dangerous metals have bigger accumulative properties. The lower HMs accumulation and reduced morphological changes in uterine tissue (HM+E group compared to HM group) validated the feasibility of the use of natural supplementation with antioxidant and detoxifying properties.

Based on our results and analysis of the literature, as a general concept, it has become clear that rats' uterus changes depending on the HMs influence. The long-term intake of low HMs doses and their accumulation in the uterus (as in other organs) led to the gradual imbalance of intracellular homeostasis, atrophy, inflammation, suppression of cellular transduction mechanisms, disruption of compensatory defense mechanisms, redox imbalance, and oxidative stress (decrease of the cellular antioxidants and increased oxidative DNA damage, lipid peroxidation, and reactive oxygen species) (Lodovici and Bigagli, 2011; Jaishankar *et al.*, 2014; Hamid *et al.*, 2016; Diantin *et al.*, 2018). The inflammation, provoked by the HMs action on the background of already existing pathological changes, also increased the free radical generation. Under the influence of chronic stress, adaptive mechanisms were exhausted and led to the development of atrophic changes of uterus cells. The aggravated cellular hypoxia leads to the progression of periglandular and perivascular fibrosis. Most likely, oxidative stress appeared to be one of the main mechanisms of the HMs effect on the body, which led to morphological transformations in the uterus. It was confirmed by reports

on the long-term adverse effects of free radicals under oxidative stress on the background of antioxidant capacity depletion (Shao *et al.*, 2007; Pham-Huy *et al.*, 2008; Phaniendra *et al.*, 2015; Yadav *et al.*, 2016; Romaniuk *et al.*, 2017; Romaniuk *et al.*, 2019). Vitamin E allows free radicals to abstract a hydrogen atom from the antioxidant molecule rather than from polyunsaturated fatty acids, thus breaking the chain of free radical reactions, the resulting antioxidant radicals being a relatively unreactive species. At the same time, the prolongation of the experimental conditions caused activation of adaptive mechanisms and the subsequent start of the recovery processes (Al-Attar, 2011; Yadav *et al.*, 2016; Romaniuk *et al.*, 2018; Mohammad Hosseini *et al.*, 2019; Albishtue *et al.*, 2020; Sahiti *et al.*, 2020; Tahtamouni *et al.*, 2020).

Such histopathological transformations of the uterine wall can disrupt the estrous cycle, cause hormonal imbalance, and reduce fertility (Höfer *et al.*, 2009; Lukacinova *et al.*, 2011; Doncova *et al.*, 2019). Moreover, it has been shown that low doses of various metals (lead, mercury, and cadmium) are associated with metal-specific reproductive system lesions (Doncova *et al.*, 2019). However, long-term HMs exposure activates epigenetic and adaptive mechanisms as evidenced by an increase in the total number of litters and neonates (i.e., vulnerable groups showed increased reproductive activity). HMs can impair reproductive function by affecting other organs in both female and male rats. Moreover, the HMs accumulation in different organs is much higher than that in the uterus (Höfer *et al.*, 2009; Lukacinova *et al.*, 2012; Sahiti *et al.*, 2020; Wang *et al.*, 2020; Shraideh *et al.*, 2021). In addition, the proven reprotoxic properties of HMs have been manifested as deteriorations of physical and reproductive health parameters in subsequent generations (Lukacinova *et al.*, 2011; Doncova *et al.*, 2019; Mohammad Hosseini *et al.*, 2019;). Also, from the results of this study, there was group-dependent body weight loss. The most pronounced weight loss was observed in the HM group. Such results can be explained by chronic HM intoxication, which is accompanied by endocrine disorders of the thyroid gland, atrophic changes in internal organs, alteration of electrolyte balance and lipid metabolism, injury of hepatic function and the induction of neurobehavioral function (Su *et al.*, 2017; Fiati Kenston *et al.*, 2018).

Increased environmental pollution is reflected in increased risks of deterioration of plants, animals, and humans. This has been confirmed by links between HMs excesses in the organs (including the uterus) of wild animals (from potentially contaminated areas) and human population density, age, season, and extent of territory contamination (Wirth *et al.*, 2010; Jaishankar *et al.*, 2014; Hamid *et al.*, 2016; Ljungvall *et al.*, 2017; Romaniuk *et al.*, 2017; Avilova *et al.*, 2018; Shah *et al.*, 2020; Lytvynenko *et al.*, 2021). Based on the variability of the consequences of pollutants, the prediction of the development of pathological changes is a complex process. This requires a consideration of HMs combinations and concentrations, their exposure time, the intake way, the features of local environmental pollution, the presence of concomitant pathologies and so on.

5. Conclusions

Long-term exposure (within 90 days) to the HMs combination had a pernicious toxic effect on the rats' uterus. A strong negative correlation between the accumulation of HMs (zinc, copper, iron, manganese, lead, and chromium) in uterus tissue with morphological (degenerative and atrophic) and morphometric (reduced uterine-wall thickness) changes was detected. Uncontrolled exposure to HMs was found to lead to serious complications and adverse reproductive health risks. The HMs exposure combined with vitamin E treatment was accompanied by significantly lower accumulation of chemical elements in the uterine wall and restraint of morphological lesions in the rats' uterus. This could be an important step towards the development of preventive and protective approaches to addressing toxic pollutants.

References

- Al-Attar AM. 2011. Antioxidant effect of vitamin E treatment on some heavy metals-induced renal and testicular injuries in male mice. *Saudi J Biol Sci.*, **18(1)**: 63-72. doi: 10.1016/j.sjbs.2010.10.004
- Albishtue AA, Almhanna HK, Yimer N, Zakaria ZA, Haron AW and Almhanaw BH. 2020. Effect of edible bird's nest supplement on hepato-renal histomorphology of rats exposed to lead acetate toxicity. *JJBS.*, **13(2)**: 213-218.
- Ali H, Khan E and Ilahi I. 2019. Environmental chemistry and ecotoxicology of hazardous heavy metals: environmental persistence, toxicity, and bioaccumulation. *J Chem.*, **2019**: 6730305. doi: 10.1155/2019/6730305.
- Avilova O, Shyian D, Marakushin D, Erokhina V and Gargin V. 2018. Ultrastructural changes in the organs of the immune system under the influence of xenobiotics. *Georgian Med News.*, **279**: 132-7.
- Bielen A, Remans T, Vangronsveld J and Cuypers A. 2013. The influence of metal stress on the availability and redox state of ascorbate, and possible interference with its cellular functions. *Int J Mol Sci.*, **14(3)**: 6382-413. doi: 10.3390/ijms14036382.
- Cedars MI, Taymans SE, DePaolo LV, Warner L, Moss SB and Eisenberg ML. 2017. The sixth vital sign: what reproduction tells us about overall health. Proceedings from a NICHD/CDC workshop. *Hum Reprod Open.*, **2017(2)**: hox008. doi: 10.1093/hropen/hox008.
- Chatterjee A and Chatterji U. 2010. Arsenic abrogates the estrogen-signaling pathway in the rat uterus. *Reprod Biol Endocrinol.*, **8**: 80. doi: 10.1186/1477-7827-8-80
- Chen C, Song X, Wei W, Zhong H, Dai J, Lan Z, Li F, Yu X, Feng Q, Wang Z, Xie H, Chen X, Zeng C, Wen B, Zeng L, Du H, Tang H, Xu C, Xia Y, Xia H, Yang H, Wang J, Wang J, Madsen L, Brix S, Kristiansen K, Xu X, Li J, Wu R and Jia H. 2017. The microbiota continuum along the female reproductive tract and its relation to uterine-related diseases. *Nat Commun.*, **8(1)**: 875. doi: 10.1038/s41467-017-00901-0.
- Chen QY, DesMarais T and Costa M. 2019. Metals and mechanisms of carcinogenesis. *Annu Rev Pharmacol Toxicol.*, **59**: 537-554. doi: 10.1146/annurev-pharmtox-010818-021031.
- Diantini NSE, Soeharto S and Wiyasa WA. 2018. The effect of lead acetate administration to the uterine malondialdehyde level and endometrial thickness in albino rats (*Rattus norvegicus*). *Med J Indones.*, **27**: 150-4. doi: 10.13181/mji.v27i3.2031.

- Doncova V, Lukacinova A, Benacka R and Nistiar F. 2019. Effect of low-dose exposure to toxic heavy metals on the reproductive health of rats a multigenerational study. *Folia Veterinaria.*, **63(1)**: 64–71. doi: 10.2478/fv-2019-0010.
- Dutta S, Gorain B, Choudhury H, Roychoudhury S, Sengupta P. 2022. Environmental and occupational exposure of metals and female reproductive health. *Environ Sci Pollut Res Int.*, **29(41)**:62067-62092. doi: 10.1007/s11356-021-16581-9.
- Fiati Kenston SS, Su H, Li Z, Kong L, Wang Y, Song X, Gu Y, Barber T, Aldinger J, Hua Q, Li Z, Ding M, Zhao J, Lin X. 2018. The systemic toxicity of heavy metal mixtures in rats. *Toxicol Res (Camb).*, **7(3)**:396-407. doi: 10.1039/c7tx00260b.
- Gore AC, Chappell VA, Fenton SE, Flaws JA, Nadal A, Prins GS, Toppari J and Zoeller RT. 2015. EDC-2: The endocrine society's second scientific statement on endocrine-disrupting chemicals. *Endocr Rev.*, **36(6)**: E1-E150. doi: 10.1210/er.2015-1010.
- Guyot E, Solovyova Y, Tomkiewicz C, Leblanc A, Pierre S, El Balkhi S, Le Frère-Belda MA, Lecuru F, Poupon J, Barouki R, Aggerbeck M and Coumoul X. 2015. Determination of heavy metal concentrations in normal and pathological human endometrial biopsies and in vitro regulation of gene expression by metals in the ishikawa and Hec-1b endometrial cell line. *PLoS One.*, **10(11)**: e0142590. doi: 10.1371/journal.pone.0142590.
- Hamid A, Riaz H, Akhtar S and Ahmad SR. 2016. Heavy metal contamination in vegetables, soil and water and potential health risk assessment. *Am-Euras J Agric & Environ Sci.*, **16(4)**: 786–94. doi: 10.5829/idosi.ajeaes.2016.16.4.103149.
- Hanson B, Johnstone E, Dorais J, Silver B, Peterson CM and Hotaling J. 2017. Female infertility, infertility-associated diagnoses, and comorbidities: a review. *J Assist Reprod Genet.*, **34(2)**: 167-177. doi: 10.1007/s10815-016-0836-8.
- Ho SM, Cheong A, Adgent MA, Veevers J, Suen AA, Tam NNC, Leung YK, Jefferson WN and Williams CJ. 2017. Environmental factors, epigenetics, and developmental origin of reproductive disorders. *Reprod Toxicol.*, **68**: 85-104. doi: 10.1016/j.reprotox.2016.07.011.
- Höfer N, Diel P, Wittsiepe J, Wilhelm M and Degen GH. 2009. Dose- and route-dependent hormonal activity of the metalloestrogen cadmium in the rat uterus. *Toxicol Lett.*, **191(2-3)**: 123-31. doi: 10.1016/j.toxlet.2009.08.014.
- Jaishankar M, Tseten T, Anbalagan N, Mathew BB and Beeregowda KN. 2014. Toxicity, mechanism and health effects of some heavy metals. *Interdiscip Toxicol.*, **7(2)**: 60-72. doi: 10.2478/intox-2014-0009.
- Katz TA, Yang Q, Treviño LS, Walker CL and Al-Hendy A. 2016. Endocrine-disrupting chemicals and uterine fibroids. *Fertil Steril.*, **106(4)**: 967-77. doi: 10.1016/j.fertnstert.2016.08.023.
- Lee AC, Idrus FA and Aziz F. 2021. Cadmium and Lead concentrations in water, sediment, fish and prawn as indicators of ecological and human health risk in Santubong Estuary, Malaysia. *JJBS.*, **14(2)**: 317-325. doi: 10.54319/jjbs/140218
- Lin YH, Chen YH, Chang HY, Au HK, Tzeng CR and Huang YH. 2018. Chronic niche inflammation in endometriosis-associated infertility: current understanding and future therapeutic strategies. *Int J Mol Sci.*, **19(8)**: 2385. doi: 10.3390/ijms19082385.
- Ljungvall K, Magnusson U, Korvela M, Norrby M, Bergquist J and Persson S. 2017. Heavy metal concentrations in female wild mink (Neovison vison) in Sweden: Sources of variation and associations with internal organ weights. *Environ Toxicol Chem.*, **36(8)**: 2030-2035. doi: 10.1002/etc.3717.
- Lodovici M and Bigagli E. 2011. Oxidative stress and air pollution exposure. *J Toxicol.*, **2011**: 487074. doi: 10.1155/2011/487074.
- Lukacinova A, Benacka R, Sedlakova E, Lovasova E and Nistiar F. 2012. Multigenerational lifetime low-dose exposure to heavy metals on selected reproductive parameters in rats. *J Environ Sci Health A Tox Hazard Subst Environ Eng.*, **47(9)**: 1280-7. doi: 10.1080/10934529.2012.672132.
- Lukačínová A, Rác O, Lovásová E and Ništiar F. 2011. Effect of lifetime low dose exposure to heavy metals on selected serum proteins of Wistar rats during three subsequent generations. *Ecotoxicol Environ Saf.*, **74(6)**: 1747-55. doi: 10.1016/j.ecoenv.2011.04.017.
- Lytvynenko M, Narbutova T, Vasylyev V, Bondarenko A and Gargin V. 2021. Morpho-functional changes in endometrium under the influence of chronic alcoholism. *Georgian Med News.*, **315**: 160-164.
- Lytvynenko M, Shkolnikov V, Bocharova T, Sychova L and Gargin V. 2017. Peculiarities of proliferative activity of cervical squamous cancer in HIV infection. *Georgian Med News.*, **270**:10–5.
- Mohammad Hosseini S, Hossein Moshrefi A, Amani R, Vahid Razavimehr S, Hasan Aghajanihah M, Sokouti Z and Babaei Holari B. 2019. Subchronic effects of different doses of Zinc oxide nanoparticle on reproductive organs of female rats: An experimental study. *Int J Reprod Biomed.*, **17(2)**: 107–18. doi: 10.18502/ijrm.v17i2.3988.
- Mohd Mutalip SS, Ab-Rahim S and Rajikin MH. 2018. Vitamin E as an antioxidant in female reproductive health. *Antioxidants (Basel).*, **7(2)**: 22. doi: 10.3390/antiox7020022.
- Nair AB and Jacob S. 2016. A simple practice guide for dose conversion between animals and human. *J Basic Clin Pharm.*, **7(2)**: 27-31. doi: 10.4103/0976-0105.177703.
- Nakade UP, Garg SK, Sharma A, Choudhury S, Yadav RS, Gupta K and Sood N. 2015. Lead-induced adverse effects on the reproductive system of rats with particular reference to histopathological changes in uterus. *Indian J Pharmacol.*, **47(1)**: 22-6. doi: 10.4103/0253-7613.150317.
- Nasiadek M, Danilewicz M, Sitarek K, Świątkowska E, Daragó A, Stragierowicz J and Kilanowicz A. 2018. The effect of repeated cadmium oral exposure on the level of sex hormones, estrous cyclicity, and endometrium morphology in female rats. *Environ Sci Pollut Res Int.*, **25(28)**: 28025-28038. doi: 10.1007/s11356-018-2821-5.
- Newbold RR, Padilla-Banks E and Jefferson WN. 2006. Adverse effects of the model environmental estrogen diethylstilbestrol are transmitted to subsequent generations. *Endocrinology.*, **147(6 Suppl)**: S11-7. doi: 10.1210/en.2005-1164.
- Nik Hazlina NH, Norhayati MN, Shaiful Bahari I, Nik Muhammad Arif NA. 2022. Worldwide prevalence, risk factors and psychological impact of infertility among women: a systematic review and meta-analysis. *BMJ Open.*, **12(3)**:e057132. doi: 10.1136/bmjopen-2021-057132.
- Nwosu LC, Zakka U, China BO and Ugagu GM. 2018. Arsenic exposure from bean seeds consumed in owerri municipal, imo state, nigeria: can insect pest detoxify the metalloid during infestation? *JJBS.*, **11(1)**: 113-116.
- Percie du Sert N, Hurst V, Ahluwalia A, Alam S, Avey MT, Baker M, Browne WJ, Clark A, Cuthill IC, Dirnagl U, Emerson M, Garner P, Holgate ST, Howells DW, Karp NA, Lázic SE, Lidster K, MacCallum CJ, Macleod M, Pearl EJ, Petersen O, Rawle F, Peynolds P, Rooney K, Sena ES, Silberberg SD, Steckler T and Wurbel H. 2020. The ARRIVE guidelines 2.0: updated guidelines for reporting animal research. *PLoS Biol.*, **18(7)**: e3000410. doi: 10.1371/journal.pbio.3000410
- Peters SAE, Woodward M, Jha V, Kennedy S and Norton R. 2016. Women's health: a new global agenda. *BMJ Glob Health.*, **1(3)**: e000080. doi: 10.1136/bmjgh-2016-000080.

- Pham-Huy LA, He H and Pham-Huy C. 2008. Free radicals, antioxidants in disease and health. *Int J Biomed Sci.*, **4(2)**: 89-96. PMID: 23675073; PMCID: PMC3614697.
- Phaniendra A, Jestadi DB and Periyasamy L. 2015. Free radicals: properties, sources, targets, and their implication in various diseases. *Indian J Clin Biochem.*, **30(1)**: 11-26. doi: 10.1007/s12291-014-0446-0.
- Romaniuk A, Lyndin M, Lyndina Y, Sikora V, Hrintsova N, Timakova O, Gudymenko O and Gladchenko O. 2018. Changes in the hematopoietic system and blood under the influence of heavy metal salts can be reduced with vitamin E. *Turk Patoloji Derg.*, **34(1)**: 73-81. doi: 10.5146/tjpath.2017.01412.
- Romaniuk A, Lyndin M, Moskalenko R, Kuzenko Y, Gladchenko O and Lyndina Y. 2015. Pathogenetic mechanisms of heavy metals effect on proapoptotic and proliferative potential of breast cancer. *Interv Med Appl Sci.*, **7(2)**: 63-8. doi: 10.1556/1646.7.2015.2.4.
- Romaniuk A, Sikora V, Lyndin M, Smiyarov V, Sikora V, Lyndina Y, Piddubnyi A, Gyryavenko N and Korobchanska A. 2017. The features of morphological changes in the urinary bladder under combined effect of heavy metal salts. *Interv Med Appl Sci.*, **9(2)**: 105-111. doi: 10.1556/1646.9.2017.2.09.
- Romaniuk A, Sikora V, Lyndina Yu, Lyndin M, Hyriavenko N, Sikora V, Karpenko L, Piddubnyi A and Miroshnichenko M. 2019. Effect of heavy metals on the readaptive processes in the urinary bladder. *Bangladesh Journal of Medical Science.*, **18**: 100-6. doi: 10.3329/bjms.v18i1.39558.
- Rosenfeld CS. 2015. Sex-specific placental responses in fetal development. *Endocrinology.*, **156(10)**: 3422-34. doi: 10.1210/en.2015-1227.
- Rzyski P, Niedzielski P, Rzyski P, Tomczyk K, Kozak L and Poniedziałek B. 2016. Metal accumulation in the human uterus varies by pathology and smoking status. *Fertil Steril.*, **105(6)**: 1511-1518.e3. doi: 10.1016/j.fertnstert.2016.02.006.
- Saeb AT and Al-Naqeb D. 2016. The impact of evolutionary driving forces on human complex diseases: a population genetics approach. *Scientifica (Cairo).*, **2016**: 2079704. doi: 10.1155/2016/2079704
- Sahiti H, Bislimi K, Rexhepi A and Dalo E. 2020. Metal accumulation and effect of vitamin C and E in accumulated heavy metals in different tissues in common carp (*Cyprinus carpio*) treated with heavy metals. *Polish Journal of Environmental Studies.*, **29(1)**: 799-805. doi: 10.15244/pjoes/103354.
- Shah N, Khan A, Ali R, Marimuthu K, Uddin MN, Rizwan M, Rahman K, Alam M, Adnan M, Muhammad, Jawad SM, Hussain S and Khisroon M. 2020. Monitoring bioaccumulation (in gills and muscle tissues), hematology, and genotoxic alteration in ctenopharyngodon idella exposed to selected heavy metals. *Biomed Res Int.*, **2020**: 6185231. doi: 10.1155/2020/6185231.
- Shao HB, Chu LY, Lu ZH and Kang CM. 2007. Primary antioxidant free radical scavenging and redox signaling pathways in higher plant cells. *Int J Biol Sci.*, **4(1)**: 8-14. doi: 10.7150/ijbs.4.8. PMID: 18167531; PMCID: PMC2140154.
- Shraideh Z, Badran D, Alzbeede A, Alqattan D, Alzbeede A and Friehtat K. 2021. Effect of garlic, vitamin C, vitamin E-selenium against bioaccumulated organolead-induced cellular injury in liver and spleen of albino rats: pilot study. *JJBS.*, **14(2)**: 285-290. doi: 10.54319/ijbs/140213
- Sikora K, Lyndin M, Hyriavenko N, Lyndina Yu, Sikora V and Romaniuk A. 2021. Morphological features of the rat uterus. *Pol Merkur Lekarski.*, **XLIX(294)**: 420-5.
- Singh R, Gautam N, Mishra A and Gupta R. 2011. Heavy metals and living systems: An overview. *Indian J Pharmacol.*, **43(3)**: 246-53. doi: 10.4103/0253-7613.81505.
- Su H, Li Z, Fiati Kenston SS, Shi H, Wang Y, Song X, Gu Y, Barber T, Aldinger J, Zou B, Ding M, Zhao J and Lin X. 2017. Joint toxicity of different heavy metal mixtures after a short-term oral repeated-administration in rats. *Int J Environ Res Public Health.*, **14(10)**: 1164. doi: 10.3390/ijerph14101164.
- Tahtamouni RW, Shibli RAA, Younes LS, Abu-Mallouh S and Al-Qudah TS. 2020. Responses of Lantana Camara Linn. Callus cultures to heavy metals added to the culture media. *JJBS.*, **13(4)**: 551-557.
- Vannuccini S and Petraglia F. 2019. Recent advances in understanding and managing adenomyosis. *F1000Res.*, **8**: F1000 Faculty Rev-283. doi: 10.12688/f1000research.17242.1.
- Wang Y, Tang Y, Li Z, Hua Q, Wang L, Song X, Zou B, Ding M, Zhao J and Tang C. 2020. Joint toxicity of a multi-heavy metal mixture and chemoprevention in sprague dawley rats. *Int J Environ Res Public Health.*, **17(4)**: 1451. doi: 10.3390/ijerph17041451.
- Wirth JJ and Mijal RS. 2010. Adverse effects of low level heavy metal exposure on male reproductive function. *Syst Biol Reprod Med.*, **56(2)**: 147-67. doi: 10.3109/19396360903582216.
- Yadav S, Jan R, Roy R and Satsangi PG. 2016. Role of metals in free radical generation and genotoxicity induced by airborne particulate matter (PM2.5) from Pune (India). *Environ Sci Pollut Res Int.*, **23(23)**: 23854-23866. doi: 10.1007/s11356-016-7494-3.
- Zhang JJ, Adcock IM, Bai Z, Chung KF, Duan X, Fang Z, Gong J, Li F, Miller RK, Qiu X, Rich DQ, Wang B, Wei Y, Xu D, Xue T, Zhang Y, Zheng M and Zhu T. 2019. Health effects of air pollution: what we need to know and to do in the next decade. *J Thorac Dis.*, **11(4)**: 1727-1730. doi: 10.21037/jtd.2019.03.65.

Heavy metal contamination and potential health risk assessment associated with selected farmed fish in Rajshahi, Bangladesh

Jibon Kumar Ghosh, Md. Shahidul Islam, Md. Tariqul Islam, Md. Mahedul Islam
Murad and Md. Mahabubur Rahman*

Department of Fisheries, University of Rajshahi, Rajshahi-6205, Bangladesh

Received: November 10, 2022; Revised: January 29, 2023; Accepted: February 11, 2023

Abstract

The present investigation was conducted with a view to evaluating heavy metal contamination of four selected fish species (*Labeo rohita*, *Catla catla*, *Cirrhinus cirrhosus*, and *Hypophthalmichthys molitrix*) and the potential health risks of its consumers in Rajshahi, Bangladesh. Twenty-one feed samples and eighty-four fish specimens were collected from seven different farms scattered across the Rajshahi district and subsequent screening of heavy metal was conducted through atomic absorption spectrophotometer (AAS). The heavy metal concentration of Pb, Co, Cr, Cd and Ni was found beyond the permissible limits in fish feed and raw fish with a strong correlative association of heavy metals between them. Metal pollution index revealed that *C. cirrhosus* was the most polluted species while *L. rohita* was the least. Health risk assessment was conducted by evaluating estimated daily intake (EDI), health risk index (HRI), target hazard quotient (THQ), hazard index (HI) and target carcinogenic risk (TR). EDI of metal was higher in children, and according to HRI, they were at two to three times more risk compared to the adults. THQ of all the heavy metals across the selected species was found to be less than 1 demonstrating the absence of non-carcinogenic hazard for individual heavy metal intake. However, HI values indicated that the cumulative effect of those heavy metals might impart some degree of non-carcinogenic effect over lifelong exposure. TR values suggested that the carcinogenic effect of Pb remained negligible while Cr, Cd and Ni had low to moderate risk of developing cancer with a greater probability of its occurrence in women than men.

Keywords: Heavy metals, Fish Feed, Carp, Health Hazard, Carcinogenic and Non-carcinogenic risk

1. Introduction

Aquaculture has played an integral part in the recent economic development of Bangladesh. Owing to the expanding aquaculture operation in concurrent times, Bangladesh has become self-sufficient in producing fish and met its required per capita consumption rate (Shamsuzzaman *et al.*, 2020). Providing for the livelihoods of millions of people, fish is Bangladesh's second-most crucial agricultural commodity (Mannan *et al.*, 2018). It is also one of the principal sources of animal protein and micronutrients and plays an important role in assuring nationwide nutritional security (DoF, 2020). However, intense fish farming has presented a number of concerns regarding environmental impact and human health hazards for consumers (Cole *et al.*, 2009). Pollution caused by heavy metals is a widely acknowledged concern that poses serious health risks for humans and animals. Heavy metals have become more prevalent in the environment in recent years in comparison to their natural abundance (Tchounwou *et al.*, 2014). This predicament has emerged due to fast population growth, growing urbanization, increased industrialization, discovery and extraction of environmental resources, the spread of other contemporary agrarian methods, and the absence of environmental policies and regulations (Mannan *et al.*, 2018). Fishes are

aquatic inhabitants who can absorb heavy metals from various sources like food, water, and bottom sediments (Ayas *et al.*, 2007). It is well-acknowledged that fish feed is the most significant source of heavy metal contamination in aquaculture systems (Anhwange *et al.*, 2012). Along with various plant-based feed ingredients, solid tannery wastes are being used during fish feed manufacturing in Bangladesh, which acts as a prominent source of harmful heavy metals (Hossain *et al.*, 2007). As a result, both naturally occurring and anthropogenic origins are exerting an impact on the surrounding aquatic systems, causing environmental destruction (Ogundele and Ayeku, 2020). The accumulation of heavy metals in the human body through diet is associated with a wide range of health complications (Jaishankar *et al.*, 2014). Metals discharged in the aquatic systems may find their way within the food web due to biomagnification and have carcinogenic and other negative implications (Malik *et al.*, 2009). Trace elements are required for humans in minute quantities, but on the contrary heavy metals are carcinogenic or poisonous, damaging the neurological and osmoregulatory system, as well as the skin, bones, and teeth (Bhattacharya *et al.*, 2007). Certain heavy metals have consistently exhibited detrimental effects on neural development of children in many scientific studies (Heng *et al.*, 2022). In the Rajshahi district, intensive to semi-intensive carp polyculture is widely practiced for its high

* Corresponding author. e-mail: : mratan1980@gmail.com.

profitability and market demand. The fish farms in Rajshahi largely contribute to the nationwide supply of animal protein. There is reason to be concerned over the possibility of heavy metals being concentrated in fish raised in captivity to levels that are high enough to be potentially hazardous to human health. As a result, the current investigation was carried out to measure the concentrations of potentially harmful heavy metals found in fish feed and farmed fish, as well as to determine the extent of any associated risks to human health.

2. Methodology

2.1. Study Duration, Site, and Sample Collection

The investigation was performed over the course of one year, from March 2019 to February 2020. Fish feed and raw fish specimens were obtained from seven distinct fish farms located at the Goharia, Parila Bazar, Naohata, and Paba under Paba Upazila, Mougachi under Mohanpur Upazila and Matikata under Godagari Upazila of Rajshahi district (Figure 1) as these regions were the top contributors to fish production of the region (DoF, 2019). Available secondary data also suggested that *Labeo rohita*, *Catla Catla*, *Cirrhinus cirrhosus* and *Hypophthalmichthys*

molitrix were the top most produced fish species in the studied district (DoF, 2019), which led to the selection of these species for sampling and subsequent analysis for heavy metals. For the assessment of heavy metals, a total of eighty-four fish samples and twenty-one fish feed samples were analyzed. A culture duration of at least one year from fingerling stocking and a weight range of 1.5 to 2.5 kg were established as the selection criteria for collecting fish samples from polyculture systems in which all fish species were concurrently raised. Three live specimens of each species were collected from each of the seven ponds that met the selection criteria for sampling (Table 1). All the fish farms used commercial fish feeds for rearing purposes and seven different feed samples, each with three replicates, were also collected from the respective farms to determine their levels of heavy metals.

Table 1. Mean weight and sample size of the studied fish

Parameters	<i>L. rohita</i>	<i>C. catla</i>	<i>C. cirrhosus</i>	<i>H. molitrix</i>
Mean Weight (kg)	1.88±0.29	1.93±0.25	1.76±0.21	2.02±0.36
Sample Size (n)	21	21	21	21

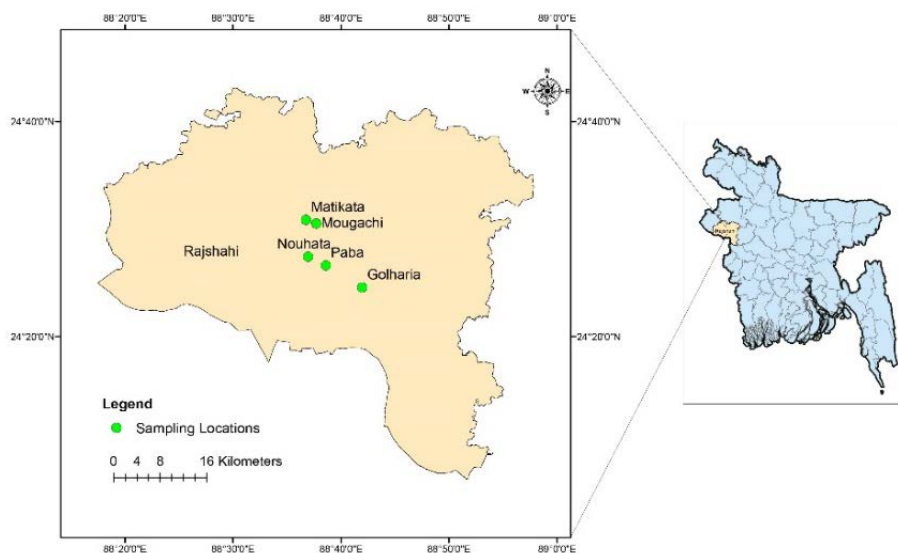


Figure 1. Locations of sample collection

2.2. Sample Preparation and Digestion

The collected feed samples were desiccated in a hot air oven and then stored at normal temperature. After the collection of fish specimens from the study ponds, they were washed with deionized water and weighed and following the removal of the fish's skin, the muscle was removed with a knife. For further laboratory analysis, the materials were fragmented, homogenized, placed in polybags, and chilled at 4°C. The preserved fish muscle was heated in an oven at 120°C for 48 hours. The samples were then cooled in a desiccator and consequently powdered and homogenized using a grinder machine. Finally, the powdered sample was placed in a dry plastic bottle that had been previously cleaned, and it was desiccated for 24 hours before further investigation. The digested feed and fish samples were analyzed quantitatively for heavy metals. Each sample was held in a

separate crucible in a muffle furnace at 600°C to obtain ash. After six hours in the muffle furnace, samples were removed, cooled, and combined with 20 ml of 1N HCl acid and enough distilled water to make 100 ml of solution in a 500 ml beaker. A filter paper was used to remove any solids from this solution.

2.3. Determination of Heavy Metal Concentrations

The heavy metal concentrations of lead (Pb), cobalt (Co), chromium (Cr), cadmium (Cd), and nickel (Ni) from digested feed and raw fish samples were determined in the central lab of the University of Rajshahi. A flame atomic absorption spectrophotometer with acetylene gas and air serving as the instrument's fuel, and oxidizer, was used to determine the concentrations of heavy metals found in the collected samples. The metal concentrations in digested samples were measured using calibration curves produced from standard solutions after they were aspirated into

the air acetylene flame. Each measurement was carried out using the mean of three replicate samples. The absorption wavelengths and detection thresholds were 217.0 nm and 0.001 ppm for Pb, 247.7 nm and 0.02 ppm for Co, 357.9 nm and 0.01 ppm for Cr, 228.8 nm and 0.002 ppm for Cd, and 232.0 nm and 0.01 ppm for Ni. Blinding of the experimenter was ensured by labelling the samples with unique codes to prevent any observation bias.

2.4. Calibration of the Instrument

Establishing a connection between the signal response and a predetermined set of standards is necessary for calibration. In atomic absorption spectrometry, the terms "standards" and "working standards" denote the creation of a set of liquid solutions with different concentrations of the target analyte. Quantifying the signals for a number of solutions with known standard concentrations yielded an appropriate measurement graph. Then, by exposing the instrument to a solution with an unknown concentration, a signal was generated that could be decoded from the graph, allowing the element concentrations in the sample solution to be calculated. The specific amount of each metal present in feed and fish samples was calculated using the following formula.

Actual concentration of metal in sample (mg/kg) = R × dilution factor
Where R = AAS Reading of digest
Dilution Factor = Volume of digest used / Weight of digested sample.

2.5. Health Risk Assessment

The human health risk assessment from consuming the selected fish species in this study was conducted using the following methods.

2.5.1. Metal Pollution Index (MPI)

The metal pollution index (MPI) was used to express the cumulative heavy metal concentration in raw fish and was calculated as a geometric mean using the following equation (Usero *et al.*, 1997).

$$MPI \frac{mg}{kg} = \sqrt[n]{(cf_1 \times cf_2 \times cf_3 \times \dots \times cf_n)}$$

Here, Cfn = the quantity of each heavy metal in sample "n" in mg per kg.

2.5.2. Daily Intake of Metal (DIM)

The following equation by Islam *et al.* (2017) was implied to estimate the daily exposure to heavy metals through the consumption of the selected fish species in human individuals (adults and children).

$$DIM = \frac{CM \times FIR \times K}{B_{mean}}$$

Here, CM is the metal content in fishes (mg/kg), FIR is the average daily fish consumption rate measuring 62.58g/persons/day (DoF, 2020), B_{mean} is the average body weight measuring 52.3 kg for adults (WHO, 2011) and 19.15 kg for children of the age group 5-10 (Ferdous *et al.*, 2015). The dry weight of fish samples was converted to fresh weight using the estimated conversion factor K = 0.249 based on the average moisture levels of the fish samples.

2.5.3. Health Risk Index (HRI)

The health risk index (HRI) is an indicator that compares the daily intake of a particular substance to its recommended daily dose (Rf_D) and is expressed as their

ratio. Rf_D is an estimate of the daily oral exposure to the human population that is anticipated to not exert any substantial risk of adverse effects over the course of their lifetimes (USEPA-IRIS, 2006). The values of Rf_D for Pb, Co, Cr, Cd and Ni are presented in Table 2. The HRI for human adults and children due to consumption of the studied fish containing heavy metals was calculated using the following equation (Cui *et al.*, 2004).

$$HRI = \frac{DIM}{Rf_D}$$

An HRI > 1 indicates the possible detrimental effect of that component on human health.

2.5.4. Non-carcinogenic Health Effect

Using the following equation provided by USEPA (2011), the target hazard quotient (THQ) was derived to estimate the potential non-carcinogenic health risks associated with the consumption of heavy metal contaminated fish in adult men and women.

$$THQ = \frac{EF \times ED \times FIR \times CF \times CM}{WAB \times ATn \times Rf_d} \times 10^{-3}$$

Here, EF = frequency of exposure in days (365 days), ED = the exposure duration, which is the estimated life expectancy of 71.2 years for men and 74.5 years for women in Bangladesh (BBS, 2020), WAB = the average body weight which is 55.2 kg for adult men and 49.8 kg for adult women in Bangladesh (WHO, 2011). ATn = the average exposure duration for non-carcinogens (EF × ED) as used in depicting non-carcinogenic risk (USEPA, 2011). The remaining parameters are described earlier.

Food substances are usually polluted with more than one heavy metal and estimation of hazard index (HI) is a holistic method to quantify the degree of non-carcinogenic risk. It is expressed through the following equation as the summation of THQ of all heavy metals (n) present in a fish sample (USEPA, 2011).

$$\sum_{i=1}^n THQ$$

The maximum acceptable limit for both THQ and HI index is 1, and values beyond this limit are considered to be unsafe for humans (USEPA, 2011).

2.5.5. Carcinogenic Health Effect

Target cancer risk (TR) was determined in order to assess the carcinogenic risk to adult men and women posed by the lifelong ingestion of the studied fish species in accordance with the model proposed by the USEPA (2011).

$$TR = \frac{EF \times ED \times FIR \times CF \times CM \times CPSo}{WAB \times ATc} \times 10^{-3}$$

Here, ATc = the average exposure time for carcinogens (EF × ED), and CPSo is the carcinogenic potency slope. TR categories are described as if $TR \leq 10^{-6}$ = Low; 10^{-4} to 10^{-3} = moderate; 10^{-3} to 10^{-1} = high; $\geq 10^{-1}$ = very high (NYSDOH, 2007). Additionally, a TR value within the range of 10^{-4} to 10^{-6} is considered acceptable (USEPA, 2011). USEPA (2011) also regards cobalt as non-carcinogenic for humans; therefore, TR was estimated for the rest of the heavy metals. The CPSo values for the studied heavy metals are presented in Table 2.

Table 2. RfD and CPSo values of different heavy metals regarding human exposure (mg/kg body weight/day)

Heavy Metals	Rf _D	CPSo	Reference
Pb	0.0035	0.0085	
Co	0.003	-	USEPA (2010); USEPA (2011); USEPA IRIS (2006); Aendo <i>et al.</i> , (2022)
Cr	0.003	0.5	
Cd	0.001	0.5	
Ni	0.02	1.7	

2.6. Statistical Analysis

Statistical analysis of the collected data and development of graphs was carried out using Microsoft Excel 2016. Mean, standard deviation, and standard error of data were carried out and presented in tables where necessary. After confirming the homogeneity of the data using Levene's test, a one-way ANOVA was performed to assess if there was any significant difference ($P < 0.05$) among the studied fish species for each particular heavy metal. The Correlation matrix of heavy metal levels in fish and fish feed was constructed in SPSS 21, and the measured correlations were highlighted with two distinct levels of significance ($P < 0.01$ and $P < 0.05$).

3. Results

3.1. Heavy Metal Concentration in Fish Feed

The heavy metal content in the collected fish feeds was estimated to determine any possible correlation it may display with the metal deposition in fish muscle. The collected feed samples exhibited a wide range of variation in heavy metal concentration in most cases which is apparent from the minimum and maximum values (Table 3). The concentration of Pb was recorded to be the highest among the tested heavy metals, followed by Co, Ni, Cr and Cd, respectively. Although heavy metals in a few feed

Table 4. Heavy metal concentrations in fish (mg/kg) in dry weight

Heavy Metals	Heavy metal concentrations in fish (mg/kg) in dry weight				MPL	
	<i>L. rohita</i>	<i>C. catla</i>	<i>C. cirrhosus</i>	<i>H. molitrix</i>	FAO (1983)	EU(2001)
Pb	5.63±1.02 ^a	5.74±1.14 ^a	6.94±1.58 ^a	5.97±1.12 ^a	2.5	0.1
Co	3.67±0.81 ^a	2.38±0.29 ^a	3.71±0.42 ^a	3.66±0.74 ^a	-	-
Cr	1.83±0.24 ^a	2.09±0.57 ^a	1.80±0.21 ^a	1.66±0.39 ^a	1.0	1.0
Cd	1.84±0.58 ^a	2.01±0.17 ^a	1.82±0.36 ^a	1.75±0.41 ^a	0.2	0.05
Ni	1.88±0.33 ^a	2.31±0.22 ^a	2.31±0.49 ^a	2.26±0.20 ^a	0.2	-

3.3. Correlation of Heavy Metals Between Fish Feed and Fish

To estimate the degree of correlative association of heavy metals within and between fish feed and fish, a Pearson correlation matrix was constructed and presented in Table 5. A statistically significant positive correlation was found between each of the tested heavy metals in the collected feeds and their corresponding levels in the fish samples. This finding led to the assumption that fish feed acted as a potential source for heavy metal accumulation in

samples were within the acceptable level, the overall mean values of the heavy metals were well beyond the maximum permissible limit (MPL) proposed by FAO and EU.

Table 3. Heavy metal concentrations in fish feed (mg/kg) in dry weight

Heavy Metals	Heavy metal concentrations in fish feed (mg/kg) in dry weight					MPL	
	Min.	Mean	Max.	SE	SD	FAO/WHO (1984)	EU (2003)
Pb	1.04	9.36	13.96	1.02	3.82	2.0	5.0
Co	1.06	5.74	11.77	1.06	3.95	1.0	1.0-1.5
Cr	1.90	2.79	4.23	0.18	0.69	1.0-2.0	1.0
Cd	0.99	2.60	3.65	0.24	0.89	2.2	2.0
Ni	2.17	4.00	7.35	0.42	1.56	2.0	0.1-8.0

Abbreviation: Min. = Minimum, Max. = Maximum, SE = Standard Error, SD = Standard Deviation

3.2. Heavy Metal Concentration in Fish

Heavy metal levels in the selected four carp species were estimated in order to quantify their impact on human health due to fish consumption. The measured concentration of heavy metals is shown in Table 4. Similar to the feed samples, Pb was the most abundant heavy metal in fish muscle, followed by Co, Ni, Cr, and Cd. The highest amount of Pb, Co, and Ni were found to be deposited in *C. cirrhosus*, whereas the highest amount of Cr and Cd deposition was recorded in *C. catla*. Alarmingly, every heavy metal concentration present in the studied fish species was found to be exceeding the MPL suggested by FAO and EU in this investigation. Additionally, no statistically significant difference ($P < 0.05$) was observed when comparing particular heavy metal levels across the studied fish species.

studied fish species. Within the feed samples, Ni showed a significant positive correlation with Co, Cr, and Cd suggesting that these elements might be originating from a similar biochemical source in the feeds. However, Pb and Co were the only two metals which demonstrated a significant negative correlation both within the feed and the fish samples. In case of fish samples, a significant positive correlation was also found among Co, Cr and Cd, whereas Pb, Cr, and Cd also showed a significant positive correlation with Ni.

Table 5. Pearson correlation matrix of heavy metals in fish (f) and fish feed (ff) samples

	Pb (f)	Co (f)	Cr (f)	Cd (f)	Ni (f)	Pb (ff)	Co (ff)	Cr (ff)	Cd (ff)	Ni (ff)
Pb (f)	1									
Co (f)	-0.435**	1								
Cr (f)	0.213	0.356**	1							
Cd (f)	0.149	0.404**	0.787**	1						
Ni (f)	0.402**	0.216	0.528**	0.508**	1					
Pb (ff)	0.850**	-0.599**	0.113	0.038	0.215	1				
Co (ff)	-0.435**	0.850**	0.360**	0.477**	0.267*	-0.696**	1			
Cr (ff)	0.207	0.399**	0.775**	0.684**	0.399**	0.090	0.317*	1		
Cd (ff)	0.182	0.456**	0.580**	0.649**	0.595**	0.113	0.479**	0.354**	1	
Ni (ff)	0.037	0.625**	0.687**	0.764**	0.412**	-0.089	0.589**	0.740**	0.685**	1

** . Correlation is significant at the 0.01 level (2-tailed); * . Correlation is significant at the 0.05 level (2-tailed).

3.4. MPI of the Selected Fish Species

MPI index was calculated to measure the degree of contamination of the studied fish species owing to the presence of different heavy metals and is illustrated in figure 2. The higher the MPI value is, the more health risk is expected to be associated with it. The highest MPI value was found in *C. cirrhosus* (2.43 mg/kg) while, the lowest was recorded in *L. rohita* (2.29 mg/kg). MPI values for *C. catla* and *H. molitrix* were 2.40 and 2.31 mg/kg, respectively.

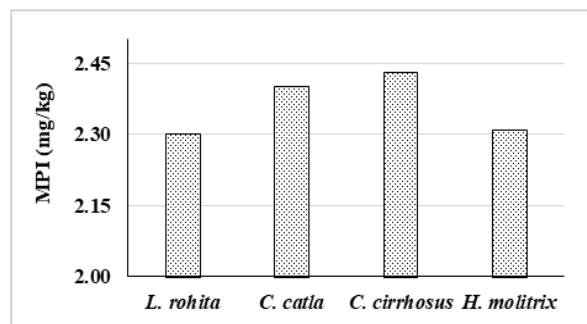


Figure 2. Estimated metal pollution index (MPI) of the selected fish species (mg/kg)

Table 6. Estimated DIM in adults and children due to fish consumption (mg/kg body weight/day)

Heavy Metals	<i>L. rohita</i>		<i>C. catla</i>		<i>C. cirrhosus</i>		<i>H. molitrix</i>	
	Adult	Children	Adult	Children	Adult	Children	Adult	Children
Pb	16.8×10^{-04}	45.8×10^{-04}	17.1×10^{-04}	46.7×10^{-04}	20.7×10^{-04}	56.5×10^{-04}	17.8×10^{-04}	48.6×10^{-04}
Co	10.9×10^{-04}	29.9×10^{-04}	7.09×10^{-04}	19.4×10^{-04}	11.1×10^{-04}	30.2×10^{-04}	10.9×10^{-04}	29.8×10^{-04}
Cr	5.45×10^{-04}	14.9×10^{-04}	6.24×10^{-04}	17.0×10^{-04}	5.37×10^{-04}	14.7×10^{-04}	4.96×10^{-04}	13.5×10^{-04}
Cd	5.47×10^{-04}	14.9×10^{-04}	6.01×10^{-04}	16.4×10^{-04}	5.45×10^{-04}	14.9×10^{-04}	5.24×10^{-04}	14.3×10^{-04}
Ni	5.60×10^{-04}	15.3×10^{-04}	6.89×10^{-04}	18.8×10^{-04}	6.89×10^{-04}	18.8×10^{-04}	6.74×10^{-04}	18.4×10^{-04}

3.6. HRI Associated with Fish Consumption in Adults and Children

HRI in this investigation was estimated to quantify the potential health risks in humans caused by daily exposure to hazardous heavy metals. The HRI for adults and children due to the consumption of the studied fish is shown in Table 7. HRI value associated with individual heavy metals was found to be less than 1 for each of the

3.5. DIM in Adults and Children due to fish consumption

In this study, the daily intake of heavy metals was estimated for adults and children to assess the potential health risk to its consumers. In all cases, DIM for children were found to be higher than the adults (Table 6). The highest daily intake of Pb and Co was associated with the consumption of *C. cirrhosus*, whereas the corresponding levels for Cr and Cd were found in *C. catla*. Furthermore, both *C. cirrhosus* and *C. catla* were found to be the leading source of Ni when consumed by adults and children. In contrast, the lowest daily intake of Pb and Ni was associated with the consumption of *L. rohita* whereas the lowest Cr and Cd intake was linked with consuming *H. molitrix*.

experimental fish when consumed by adults. However, in case of children, the HRI values for the heavy metals were two to three folds greater than those of adults. Additionally, in children, the HRI for Pb and Cd exceeds the acceptable limit in all the studied fish species suggesting they were at a greater health risk than adults owing to the toxic effects of these two metals.

Table 7. HRI values for adult and children due to fish consumption

Heavy Metals	<i>L. rohita</i>		<i>C. catla</i>		<i>C. cirrhosus</i>		<i>H. molitrix</i>	
	Adult	Children	Adult	Children	Adult	Children	Adult	Children
Pb	0.48	1.31	0.49	1.33	0.59	1.62	0.51	1.39
Co	0.36	1.00	0.24	0.65	0.37	1.00	0.36	0.99
Cr	0.18	0.50	0.21	0.57	0.18	0.49	0.17	0.45
Cd	0.55	1.49	0.60	1.64	0.54	1.49	0.52	1.43
Ni	0.03	0.08	0.03	0.09	0.03	0.09	0.03	0.09

3.7. Non-carcinogenic Health Effect of the Studied Fish on Men and Women

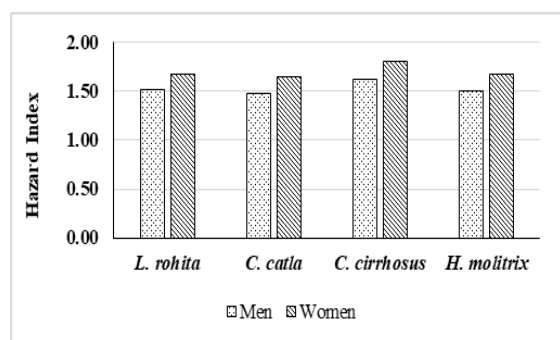
THQ and HI indices were estimated in this study to evaluate the non-carcinogenic effect to human health due to prolonged consumption of toxic heavy metals. THQ for

the consumption of each fish species in adult men and women are shown in Table 8. All the heavy metals in this study exhibited THQ values of less than 1 for both men and women indicating no potential health hazard for individual heavy metal intake.

Table 8. THQ values for men and women due to fish consumption

Heavy Metals	<i>L. rohita</i>		<i>C. catla</i>		<i>C. cirrhosus</i>		<i>H. molitrix</i>	
	Men	Women	Men	Women	Men	Women	Men	Women
Pb	0.45	0.50	0.46	0.51	0.56	0.62	0.48	0.53
Co	0.35	0.38	0.22	0.25	0.35	0.39	0.34	0.38
Cr	0.17	0.19	0.20	0.22	0.17	0.19	0.16	0.17
Cd	0.52	0.57	0.57	0.63	0.52	0.57	0.50	0.55
Ni	0.03	0.03	0.03	0.04	0.03	0.04	0.03	0.04

However, fish contains more than one heavy metal in its edible parts and, therefore, a cumulative THQ value for all the heavy metals known as hazard index (HI) should be taken into account while estimating non-carcinogenic health risks. The HI value shown in figure 3 indicates that the consumers were at risk of a health hazard as the aggregated THQ values for each of the five heavy metals in all four species exceeded 1. The highest HI for men and women were found to be associated with the consumption of *C. cirrhosus* (1.63 and 1.81) and the lowest with *C. catla* (1.49 and 1.65).

**Figure 3.** Estimated values of hazard index (HI) in men and women due to fish consumption**Table 9.** TR values for adult men and women due to fish consumption

Heavy Metals	<i>L. rohita</i>		<i>C. catla</i>		<i>C. cirrhosus</i>		<i>H. molitrix</i>	
	Men	Women	Men	Women	Men	Women	Men	Women
Pb	1.35×10^{-05}	1.50×10^{-05}	1.38×10^{-05}	1.53×10^{-05}	1.67×10^{-05}	1.85×10^{-05}	1.43×10^{-05}	1.59×10^{-05}
Cr	2.58×10^{-04}	2.86×10^{-04}	2.96×10^{-04}	3.28×10^{-04}	2.55×10^{-04}	2.82×10^{-04}	2.35×10^{-04}	2.60×10^{-04}
Cd	2.59×10^{-04}	2.87×10^{-04}	2.85×10^{-04}	3.15×10^{-04}	2.58×10^{-04}	2.86×10^{-04}	2.48×10^{-04}	2.75×10^{-04}
Ni	9.02×10^{-04}	1.00×10^{-03}	1.11×10^{-03}	1.23×10^{-03}	1.11×10^{-03}	1.23×10^{-03}	1.09×10^{-03}	1.20×10^{-03}

4. Discussion

Heavy metal pollution is one of Bangladesh's top environmental concerns, where most farmland, field crops,

3.8. Carcinogenic Health Effect of the Studied Fish on Men and Women

In order to estimate the degree of carcinogenic risk due to consumption of heavy metal polluted fish, the TR levels were determined and are presented in Table 9. The findings showed that the estimated cancer risk of Pb in this study was very low and considered to be negligible across all four fish species. However, TR for Cr, Cd, and Ni were within the low to moderate range and indicated some degree of risk of contracting cancer for the consumers. The TR values also indicated that Ni had the highest probability of being carcinogenic in the studied fish followed by Cd and Cr. Similar to the non-carcinogenic health hazards, women were more likely to develop cancer than men.

and freshwater outflows are heavily contaminated (Islam *et al.*, 2018). Fish feeds are regarded to be the most significant reason for heavy metal pollution in aqua farms where no other anthropogenic source of contamination is in action (Ali and Khan, 2018; Sabbir *et al.*, 2018). The

mean heavy metal (Pb, Co, Cr, Cd and Ni) concentration in fish feed was found to be exceeding the maximum permissible limit of FAO and EU, thus raising concerns regarding its effect on fish biology and ultimately human health. An unacceptable limit of Pb and Cd in numerous commercial fish feeds has been reported by Kundu *et al.* (2017) in tilapia farms in Bangladesh. An extensive feed evaluation study by Sarkar *et al.* (2021) also confirmed the presence of Cd and Cr in several types of fish feeds (starter, grower, finisher, and mixed) beyond the permissible limit with respect to national and international standards. The findings of this study are also in accordance with Saha *et al.* (2018) who reported that concentrations of Pb, Co and Cr are exceeding the maximum permissible limit in different brands of fish feed. An unsafe level of Ni is also documented by Fatema *et al.* (2019) in different commercial feeds used in the culture of *Anabas testudineus* in Bangladesh. Heavy metal pollution in fish feed can be attributed to the use of trace metal feed additives like tannery waste without performing a proper decontamination process (Sarker *et al.*, 2017; Sarker *et al.*, 2022). The strong correlative association among Co, Cr, Cd, and Ni in the studied feeds found in this study might be an indication of utilizing such toxic components as feed additives as these metals are the major pollutant in tannery wastes (Islam *et al.*, 2013).

All the selected fish species have exhibited heavy metal levels that are higher than the maximum allowable limit for food fish. Fish having unsafe levels of heavy metals pose a variety of health risks to people of all ages, including children. Pb is a very toxic substance, especially for children, as they have less renal excretion capabilities and greater gastrointestinal absorption (Azaman *et al.*, 2015). Pb also has nephrotoxic and neurotoxic potency and can induce cardiovascular disease (Umar *et al.*, 2001; García-lestón *et al.*, 2010). Toxic levels of Co can introduce cardiovascular, neurological, and endocrinal dysfunction (Leyssens *et al.*, 2017). Cr is a carcinogenic element and can cause disruption in nutrient metabolism (Akoto *et al.*, 2014). Chronic exposure to cadmium may result in respiratory discomfort, cancer of the lung and breasts, damage to blood vessels, and cardiac issues (Prozialeck *et al.*, 2008). Ni is another potential carcinogen that can cause inflammation of the respiratory system, fibrosis, and emphysema (Forti *et al.*, 2011).

Many studies have depicted the concerning scenario of heavy metal pollution in a broad spectrum of fish species and numerous toxic heavy metals in Bangladesh. Ghosh *et al.* (2021) have reported unacceptable levels of Co and Cr with an alarming level of Pb in farmed *Pangasius pangasius*, *Oreochromis niloticus*, *Heteropneustes fossilis*, *A. testudineus*, and *Clarias batrachus*, Mannan *et al.* (2018) have also concluded that commercial fish feed can contribute to unsafe bioaccumulation of Pb, Cd, and Ni in *L. rohita* and raise potential health risks upon consumption of such fish. Nowadays, heavy metal pollution in fish is not exclusively limited to aquaculture farms and can be detected in open-water fish species as well. Ahmed *et al.* (2019) have reported bioaccumulation of Pb, Cr, and Cd exceeding the recommended limits in five estuarine fish species. Kumar *et al.* (2020) also validated the presence of hazardous levels of Pb and Cd in *L. rohita* from Mahananda river, India. The MPI of our studied fish species was found to be ranging from 2.29 to 2.43 mg/kg.

Ghosh *et al.* (2021) also evaluated MPI values in the five fish species and reported relatively higher MPI ranging from 4.85 to 6.65 mg/kg. The MPI value estimated by Ahmed *et al.* (2019) in estuarine fish species ranging from 3.65 to 4.70 mg/kg also surpassed our current findings. In both studies, demersal and bottom dwelling fish exhibited higher MPI which is in accordance with the result of this investigation where *C. cirrhosus* demonstrated the highest MPI value.

The DIM values of heavy metals in this study showed that *C. cirrhosus* and *C. catla* are the top contributors to heavy metals in daily diets. The findings also indicate Pb as the most and Cd as the least consumed among the studied heavy metals which agree with the findings of Ullah *et al.* (2017) and Saha and Zaman (2013). Consistent with the results of Ghosh *et al.*, (2021) the HRI in this study implies that children are more at risk than adults from consuming heavy metal contaminated fish. The THQ value indicates the potential non-carcinogenic risk of heavy metal consumption, and it is desired to be less than 1. The THQ values for Pb, Co, Cr, Cd, and Ni in this study were within this acceptable limit and posed no serious non-carcinogenic health upon consumption of individual heavy metals and in accordance with earlier studies (Ahmed *et al.*, 2019; Akter *et al.*, 2021). However, a number of heavy metals are simultaneously contained within the fish muscle; therefore, HI values should be taken into consideration while estimating non-carcinogenic risk as it is more representative of the actual scenario of heavy metal consumption. The HI values for all fish species for each heavy metal surpassed the suggested threshold of 1, indicating possible non-carcinogenic health risks similar to previously reported findings (Ahmed *et al.*, 2019; Ullah *et al.*, 2017; Saha and Zaman, 2013). The findings of this study also indicated that in comparison to men, women were more susceptible to the non-carcinogenic impacts of heavy metals.

The TR values in this investigation imply that Cr, Cd, and Ni from the lifelong consumption of the studied fish species may have a carcinogenic impact in both men and women at some stage. It should be noted that TR is not certain estimation for the occurrence of cancer but rather an expression of the probability that the exposed individuals may develop cancer at a stage of life. Evidence of potential carcinogenic risk owing to the intake of both cultured and captured fish species has been presented in prior studies (Kundu *et al.*, 2017; Kawser *et al.*, 2016; Wahiduzzaman *et al.*, 2021). The data also suggest that women are more likely to develop cancer compared to the men population which agrees with the findings of Javed and Usmani (2016) and Vahter *et al.* (2002).

5. Conclusion

This investigation was accomplished to determine the levels of five heavy metals in four demandable fish species (*L. rohita*, *C. catla*, *C. cirrhosus*, and *H. molitrix*) of Rajshahi region and their possible implication on human health. Heavy metals from all the selected fish species exceeded the recommended international threshold. Correlative association implies that fish feed is the primary source of heavy metal accumulation in the studied fish. MPI values flagged *C. cirrhosus* as the most contaminated

species and *L. rohita* as the least. HRI values indicated greater health risks to children compared to adults. THQ values showed no substantial health risk for individual heavy metal consumption, while TR values suggested possible carcinogenic impact of Cr, Cd, and Ni on consumers. It is recommended that necessary regulations are strictly implied by the respective authorities while feed manufacturers and farmers become more careful in eliminating or controlling the sources of heavy metal in aquaculture practice.

Acknowledgement

We would like to express our gratitude to the BANBEIS, Ministry of Education (under GARE), the Government of the People's Republic of Bangladesh for providing financial support for this project. We would also like to express their gratitude to the Center Laboratory authorities at the University of Rajshahi in Rajshahi, Rajshahi, for their cooperation and laboratory support.

Ethics Approval

In compliance with the National Wildlife Protection and Conservation Act of 2012, the Rajshahi University Research Ethics Committee has exempted this investigation from the need for ethical approval on the grounds that the fish species utilized in this study are farmed and not wild or endangered. Nonetheless, all procedures in this study were conducted in conformity with the ethical criteria given by The International Council for Laboratory Animal Science (ICLAS) for researchers.

References

- Aendo P, Netvichian R, Thindedsakul P, Khaodhiar S and Tulayakul P. 2022. Carcinogenic risk of Pb, Cd, Ni, and Cr and critical ecological risk of Cd and Cu in soil and groundwater around the municipal solid waste open dump in central Thailand. *J Environ Public Health.*, **2022**: 1-12.
- Ahmed A, Sultana S, Habib A, Ullah H, Musa N, Hossain M, Rahman M and Sarker M. 2019. Bioaccumulation of heavy metals in some commercially important fishes from a tropical river estuary suggests higher potential health risk in children than adults. *PLoS One.*, **14**: e0219336.
- Akoto O, Bismark Eshun F, Darko G and Adei E. 2014. Concentrations and health risk assessments of heavy metals in fish from the Fosu lagoon. *Int J Environ. Res.*, **8(2)**: 403-410.
- Akter A, Hosen A, Hossain M, Khalil F and Mustafa T. 2021. Heavy metal concentrations and human health risk assessment of selected wild and cultured fishes of Bangladesh. *Bangladesh J. Zool.*, **49**: 189-203.
- Ali H and Khan E. 2018. Bioaccumulation of non-essential hazardous heavy metals and metalloids in freshwater fish. Risk to human health. *Environ Chem Lett.*, **16**: 903-917.
- Anhwange BA, Asemave K, Kim BC and Nyiaatagher DT. 2012. Heavy metals contents of some synthetic fish feeds found within Makurdi metropolis. *Int J Food Nutr Safe.*, **2**: 55-61.
- Ayas Z, Ekmekci G, Yerli SV and Ozmen M. 2007. Heavy metal accumulation in water, sediments and fishes of Nallihan Bird Paradise, Turkey. *J Environ Biol.*, **28(3)**: 545-549.
- Azaman F, Juahir H, Yunus K, Azid A, Kamarudin M, Toriman M, Mustafa A, Amran M, CheHasnam C and Mohd Saudi A. 2015. Heavy metal in fish: analysis and human health-a review. *J Teknol.*, **77(1)**.
- BBS. 2020. **Bangladesh sample vital statistics 2020**. Bangladesh Bureau of Statistics. Ministry of Planning, Dhaka, Bangladesh.
- Bhattacharya P, Welch AH, Stollenwerk KG, McLaughlin MJ, Bundschuh J and Panaullah G. 2007. Arsenic in the environment: biology and chemistry. *Sci Total Environ.*, **379(2-3)**: 109-120.
- Cole DW, Cole R, Gaydos SJ, Gray J, Hyland G, Jacques ML, Powell-Dunford N, Sawhney C and Au WW. 2009. Aquaculture: Environmental, toxicological, and health issues. *Int J Hyg Environ Health.*, **212**: 369-377.
- Cui YJ, Zhu YG, Zhai RH, Chen DY, Huang YZ, Qiu Y and Liang JZ. 2004. Transfer of metals from soil to vegetables in an area near a smelter in Nanning, China. *Environ Int.*, **30(6)**: 785-791.
- DoF. 2019. **Yearbook of Fisheries Statistics of Bangladesh, 2018-19**. Fisheries Resources Survey System (FRSS), Department of Fisheries, Bangladesh: Ministry of Fisheries and Livestock.
- DoF. 2020. **Yearbook of Fisheries Statistics of Bangladesh, 2019-20**. Fisheries Resources Survey System (FRSS), Department of Fisheries. Bangladesh: Ministry of Fisheries and Livestock.
- EU. 2001. **Commission Regulation as Regards Heavy metals, Directive, 2001/22/EC**, No: 466.
- EU. 2003. **Opinion of the scientific committee on animal nutrition on undesirable substances in feed**. https://food.ec.europa.eu/system/files/2020-12/sci-com_scan-old_report_out126_bis.pdf. Accessed 13 October 2022.
- FAO. 1983. **Compilation of Legal Limits for Hazardous Substances in Fish and Fishery Products**. FAO Fishery Circular No. 464, Food and Agriculture Organization.
- FAO/WHO. 1984. **List of maximum levels recommended for contaminants by the Joint FAO/WHO**. Codex Alimentarius Commission. Second Series. CAC/FAL, Rome.
- Fatema K, Sakib MN, Zahid MA, Sultana N and Hasan MR. 2019. Growth performances and bioaccumulation of heavy metals in *Anabas testudineus* (Bloch, 1792) cultured using different market feeds. *Bangladesh J Zool.*, **47(1)**: 77-88.
- Ferdous MJ, Sumon MAA, Mahamud AMN, Ara MG, Fatema J and Fatema MK. 2015. A comparative study on fish intake and nutritional status of children in different areas of Sylhet district, Bangladesh. *Int J Nat Soc.*, **2(4)**: 113-117.
- Forti E, Salovaara S, Cetin Y, Bulgheroni A, Tessadri R, Jennings P and Prieto P. 2011. In vitro evaluation of the toxicity induced by nickel soluble and particulate forms in human airway epithelial cells. *Toxicol in Vitro.*, **25(2)**: 454-461.
- García-lestón J, Mendez J, Pásaro E and Laffon B. 2010. Genotoxic effects of lead: An updated review. *Environ Int.*, **36**: 623-636.
- Ghosh P, Ahmed Z, Alam R, Begum B, Akter S and Jolly Y. 2021. Bioaccumulation of metals in selected cultured fish species and human health risk assessment: a study in Mymensingh Sadar Upazila, Bangladesh. *Stoch Environ Res Risk Assess.*, **35**: 2287-2301.
- Heng YY, Asad I, Coleman B, Menard L, Benki-Nugent S, Hussein WF, Karr CJ, McHenry MS. Heavy metals and neurodevelopment of children in low and middle-income countries: A systematic review. *PLoS One.*, **17(3)**: e0265536.
- Hossain AMMM, Monir T, Haque AMRU, Kazi ALM, Islam SM and Elahi SF. 2007. Heavy metal concentration in tannery solid wastes used as poultry feed and ecotoxicological consequences. *Bangladesh J Sci Ind Res.*, **42**: 397-426.

- Islam GMR, Habib MR, Waid JL, Rahman MS, Kabir J, Akter S and Jolly YN. 2017. Heavy metal contamination of freshwater prawn (*Macrobrachium rosenbergii*) and prawn feed in Bangladesh: A market-based study to highlight probable health risks. *Chemosphere.*, **170**: 282-289.
- Islam MM, Karim MR, Zheng X and Li X. 2018. Heavy metal and metalloid pollution of soil, water and foods in Bangladesh: a critical review. *Int J Environ Res Public Health.*, **15**(12):2825.
- Islam S, Islam F, Bakar MA, Das S and Bhuiyan HR. 2013. Heavy metals concentration at different tannery wastewater canal of Chittagong city in Bangladesh. *Int J Agric Environ Biotechnol.*, **6**(3): 355-361.
- Jaishankar M, Tseten T, Anbalagan N, Mathew BB and Beeregowda KN. 2014. Toxicity, mechanism and health effects of some heavy metals. *Interdiscip Toxicol.*, **7**: 60-72.
- Javed M and Usmani N. 2016. Accumulation of heavy metals and human health risk assessment via the consumption of freshwater fish *Mastacembelus armatus* inhabiting, thermal power plant effluent loaded canal. *Springerplus.*, **5**: 776.
- Kawser AM, Baki M, Kundu G, Saiful Islam M, Monirul Islam M and Muzammel Hossain M. 2016. Human health risks from heavy metals in fish of Buriganga river, Bangladesh. *Springerplus.*, **5**:1697.
- Kumar A, Kumar A and Jha S. 2020. Human health risk assessment of heavy metals in major carp (*Labeo rohita*) of Mahananda river in Northern India. *Emergent Life Sci Res.*, **06**: 34-49.
- Kundu GM, Alauddin M, Akter MS, Khan MS, Islam MM, Mondal G, Islam D, Mohanta LC and Haque A. 2017. Metal contamination of commercial fish feed and quality aspects of farmed tilapia (*Oreochromis niloticus*) in Bangladesh. *Biores Commun.*, **3**(1): 345-353.
- Leyssens L, Vinck B, Van Der Straeten C, Wuyts F and Maes L. 2017. Cobalt toxicity in humans-A review of the potential sources and systemic health effects. *Toxicol.*, **387**: 43-56.
- Malik N, Biswas AK, Qureshi TA, Borana K and Virha R. 2009. Bioaccumulation of heavy metals in fish tissues of a freshwater lake of Bhopal. *Environ Monit Assess.*, **160**(1-4):267-276.
- Mannan M, Hossain M, Sarker M, Hossain M, Chandra L, Haque A and Zahan M. 2018. Bioaccumulation of toxic heavy metals in fish after feeding with synthetic feed: A potential health risk in Bangladesh. *J Nutr Food Sci.*, **8**(5): 100728.
- NYSDOH. 2007. **Hopewell precision area contamination: appendix C-NYS DOH.** Procedure for evaluating potential health risks for contaminants of concern. <https://www.health.ny.gov/environmental/investigations/hopewell/appendc.htm>. Accessed 12 October 2022.
- Ogundele LT and Ayeku PO. 2020. Source apportionment and associated potential ecological risk assessment of heavy metals in coastal marine sediments samples in Ondo, Southwest, Nigeria. *Stoch Env Res Risk Assess.*, **34**: 2013-2022.
- Prozialeck WC, Edwards JR, Nebert DW, Woods JM, Barchowsky A and Atchison WD. 2008. The vascular system as a target of metal toxicity. *Toxicol Sci.*, **102**: 207-218.
- Sabbir W, Rahman Z and Halder T. 2018. Assessment of heavy metal contamination in fish feed available in three districts of South Western region of Bangladesh. *Int J Fish Aquatic Stud.*, **26**(2):100-104.
- Saha B, Mottalib MA and Al-Razee ANM. 2018. Assessment of selected heavy metals concentration in different brands of fish feed available in Bangladesh. *J Bangladesh Acad.*, **42**(2): 207-210.
- Saha N and Zaman M. 2013. Evaluation of possible health risks of heavy metals by consumption of foodstuffs available in the central market of Rajshahi City, Bangladesh. *Environ Monit Assess.*, **185**: 3867-3878.
- Sarker M, Rohani M, Hossain M and Shahjahan M. 2021. Evaluation of heavy metal contamination in some selected commercial fish feeds used in Bangladesh. *Biol Trace Elem Res.*, **200**: 844-854.
- Sarker A, Kim J, Islam A, Bilal M, Rakib M, Nandi R, Rahman M and Islam T. 2022. Heavy metals contamination and associated health risks in food webs - A review focuses on food safety and environmental sustainability in Bangladesh. *Environ Sci Pollut Res.*, **29**: 3230-3245.
- Sarker MS, Quadir QF, Zakir HM, Nazneen T and Rahman A. 2017. Evaluation of commonly used fertilizers, fish and poultry feeds as potential sources of heavy metals contamination in food. *Asian Aus J Food Safe Sec.*, **1**(1): 74-81.
- Shamsuzzaman MM, Hoque Mozumder MM, Mitu SJ, Ahamad AF and Bhyuian MS. 2020. The economic contribution of fish and fish trade in Bangladesh. *Aquac Fish.*, **5**:174-181.
- Tchounwou PB, Yedjou CG, Patlolla AK and Sutton DJ. 2012. Heavy metal toxicity and the environment. *Exp Suppl.*, **101**: 133-164.
- Ullah A, Maksud M, Khan S, Lutfu L and Quraishi S. 2017. Dietary intake of heavy metals from eight highly consumed species of cultured fish and possible human health risk implications in Bangladesh. *Toxicol Rep.*, **4**: 574-579.
- Umar A, Umar R and Ahmad MS. 2001. Hydrogeological and hydrochemical frame works of regional aquifer system in kaliganga sub-basin. *India Envir Geol.*, **40**(4-5): 602611.
- USEPA. 2010. **Risk-based concentration table**, Washington, DC, USA: United States Environment Protection Agency.
- USEPA. 2011. **Regional screening level (RSL) summary table: November 2011**. United States Environment Protection Agency, Washington, DC, USA.
- USEPA-IRIS. 2006. **Integrated Risk Information System, Washington, DC, USA**. United States Environmental Protection Agency. <http://www.epa.gov/iris>. Accessed 23 September 2019.
- Usero J, González-Regalado E, Gracia I. 1997. Trace metals in the bivalve molluscs *Ruditapes decussatus* and *Ruditapes philippinarum* from the Atlantic Coast of Southern Spain. *Environ Int.*, **23**(3):291-298.
- Vahter M, Berglund M, Åkesson A and Lidén C. 2002. Metals and women's health. *Environ Res.*, **88**: 145-155.
- Wahiduzzaman M, Islam M, Sikder A and Parveen Z. 2021. Bioaccumulation and heavy metal contamination in fish species of the Dhaleswari river of Bangladesh and related human health implications. *Biol Trace Elem Res.*, **200**: 3854-3866.
- WHO. 2011. **Non-Communicable Disease Risk Factor Survey Bangladesh 2010**. Dhaka: World Health Organization.

Comparative Analysis of Cichorieae Tribe (Asteraceae) Chloroplast Genomes: Insight to Structure, Repetitive DNA, and Phylogeny.

Rubar Hussein M. Salih*

Biotechnology and Crop Science Department, College of Agricultural Engineering Sciences, University of Sulaimani, Kurdistan Region, Iraq.

Received: August 24, 2022; Revised: December 29, 2022; Accepted: February 12, 2023

Abstract

The whole chloroplast genome has been increasingly used over the past three decades for systematic and ordered analysis of evolutionary relationships, variation within species, and developmental studies. There were several other studies on the Asteraceae family, but the studies were on the family level. This study investigates the plastomes of an important Asteraceae tribe, Cichorieae, that are widely distributed, morphologically complex, include several species reproduce apomictically. Plastomes belonging to 36 different species in 12 different genera have been studied in detail and compared. The comparisons were based on plastome structure, number of coding and noncoding genes, and number of rRNA and tRNA genes. Further, the repetitive DNA types, frequency, and their position in the chloroplast genomes have been analyzed. Moreover, SSRs types and frequency were compared and analyzed. In addition, a number of coding and noncoding regions were studied and used to construct a phylogenetic tree.

The investigation of this study indicated the distinctiveness of sequence divergence among the plastomes of Cichorieae tribe species in various aspects. The results provided excellent phylogenetic linkages that can be used for advanced comparative studies at both generic and species levels. Most noncoding and coding regions showed the least variation; however, major variations were shown by those regions that have rarely been used in chloroplast phylogenetics. Regions of coding (*clpP*, *matK*, *ndhA*, *rpoC1*, *rpoC2*, and *ycf1*) and non-coding (*ndhF-rpl32*, *petN-psbM*, *psbE-petL*, *rps4-ndhJ*, *rps15-ycf1*, *trnL-trnF*, *trnT-psbD*, and *ycf3-trnS*) are recommended to use in studying Cichorieae tribe members to achieve better phylogenetic construction, population genetic analysis, and use as a marker for accurate and automated species identification. The tandem repeat of 21-30 period size is the most variable among the Cichorieae tribe plastomes. Ttra-, penta-, and hexanucleotide SSR types were found in *Cichorium intybus*, *Crepidiastrum*, *Sonchus*, and *Taraxacum* plastomes, while, they were not found in other plastomes under study. These SSRs may be useful for identifying species, detecting hybridization, determining phylogeny, and differentiating populations.

Keywords: Whole Chloroplast genome, Plastomes, Cichorieae tribe, Phylogenetic, Repetitive DNA, SSRs.

1. Introduction

Species belonging to the tribe Cichorieae LAM. & DC. (also called Lactuceae), distributed mainly in the temperate regions of the northern hemisphere. This tribe includes ca. 93 genera, excluding mix population of apomictic and sexual reproductions of *Hieracium* L., *Pilosella* Hill., and *Taraxacum* Wigg. These three genera alone include nearly 1,400 species. The Cichorieae tribe includes many economic, cultivated, and locally important species, such as lettuce (*Lactuca* L.), chicory (*Cichorium* L.), and some invasive worldwide distributed weeds such as dandelion (*Taraxacum*) (Jeffrey, 2001; Salih *et al.*, 2017).

According to Carlquist (1976), morphological, physiological, cytological (chromosome counts), and biochemical variables were used to evaluate the variation in the Cichorieae tribe taxa at the level of intra- and inter-

specific levels. Thus, species diversity, phylogenetic relationships, and evolution of the tribe members can be studied using both phenotypic and genotypic features (Lundberg and Bremer, 2003; Kilian *et al.*, 2009).

In eukaryotic cells of autotrophic organisms, chloroplast (plastid) genomes are essential organelles. Plant chloroplast genomes (plastome, ctDNA, cpDNA), in terms of their genomes and genetic systems, are independent and are uniparentally inherited (Raubeson and Jansen, 2005; Kilian *et al.*, 2009; Gholipour and Kohnehrouz, 2017). Plastome comprises a large genomic sequence; its size in plants ranges from 85 - 218 kbp (Palmer, 1991; Daniell *et al.*, 2016), with a very low rate of recombination. Moreover, gene contents and order are highly conserved among plant chloroplast genomes. The above features all together make the chloroplast genome a valuable source for comparative analysis within the genera, tribe, and family members, and a good marker for

* Corresponding author. e-mail: rubar.salih@univsul.edu.iq.

plant phylogenetic analysis and DNA barcoding. Also, chloroplast genome provides an opportunity for analyzing the relationships between distant and closely related species, as well as the analysis of variation at the intraspecific and interspecific levels by analyzing the repetitive sequences, thereby producing a valuable investigation into plant diversity, molecular evolution, and cytogenetic relationships (Salih *et al.*, 2017; Yaradua *et al.*, 2020).

Here in this study, 36 chloroplast genomes belonging to the tribe Cichorieae were selected to compare and analyze: the characterization and structure patterns of chloroplast genomes, gene contents, phylogenetic relationships, selecting polymorphic regions for developing chloroplast marker, and intermolecular combination and microstructural variation of repetitive DNA domains in Cichorieae tribe. The result of this investigation will provide valuable information on chloroplast genome evolution among these tribe members.

2. Materials and Methods

2.1. Genome Content and Organization of plastomes

Sequences of 36 Cichorieae tribe species plastomes (complete chloroplast genome) belonging to 12 genera were obtained from National Center for Biotechnology Information (NCBI). The plastome selection was according to the plastome genome availability in the NCBI gene bank. All plastomes belonging to the Cichorieae tribe were downloaded first, and then all plastomes belonging to each genus within the Cichorieae tribe were separately analyzed by aligning them to ensure diverse plastome genomes and similar genomes were omitted, as there were several duplicated plastomes for the same species in NCBI with a different accession number. Further, only up to 8 plastomes were randomly selected for a single genus (*Taraxacum* and *Sonchus* L.).

The size and GC% of all 36 Cichorieae tribe species plastomes were compared using the GENEIOUS prime 2021 (Kearse *et al.*, 2012). Annotations of the plastome sequence were used to examine gene contents and their organization in the plastomes. Then, the transfer RNA gene prediction program tRNAscan-SE was used to confirm the number and location of tRNA genes (Table 1). Later, dot-plot analyses were used to compare each plastome with that of *Nicotiana tabacum* L. (Solanaceae - NC_001879) (Shinozaki *et al.*, 1986), to examine the gene order conservation and identify the position of the Long Single Copy (LSC), Short Single Copy (SSC), two identical Inverted Repeat (IR), and the two inversion events nested in LSC region (Inv-a, Inv-b), respectively (Kearse *et al.*, 2012).

Using the IR-plot visualization tool, which is available at (<https://irscope.shinyapps.io/irapp/>), Genome plotting was used to represent the location of the sites connecting the IRs to the SSC and LSC regions in order to show the genetic organization of 17 representative chloroplast genomes (Amiryousefi *et al.*, 2018).

2.2. Sequence variation analysis of chloroplast genomes

For comparing DNA sequences, the online program mVISTA (Frazer *et al.*, 2004) was used to identify

sequence similarities and differences. *Cichorium intybus* chloroplast genome and its annotation were used as the reference chloroplast genome with the rest of the 35 Cichorieae plastomes. The program uses Shuffle-LAGAN mode to align the sequences. The high sequence polymorphism region of the genes and spacers regions were selected to use later in phylogenetic constructions.

2.3. Phylogenetic analysis

Phylogenetic relationships were constructed using high sequence diversity of the protein-coding genes and most polymorphic intergenic regions; these regions were analyzed and selected using the mVISTA alignment. The most polymorphic regions were extracted from each of the 36 plastomes. A multi-sequence alignment tool with default parameters was used to align sequences of each regions by using GENEIOUS prime 2021 software (Kearse *et al.*, 2012). Subsequent to sequence alignments, each alignment was double-checked manually in the GENEIOUS program alignment viewer to avoid any faults or mismatches by the alignment software.

Maximum likelihood (ML) trees were constructed, using whole chloroplast genomes, LSC, SSC, and IR regions, also the most polymorphic protein-coding genes and most polymorphic intergenic regions by MEGA11 (Tamura *et al.*, 2021). To infer the best-fit substitution model for these polymorphic datasets, the best-fit evolutionary model was scored according to the Bayesian Information Criterion (BIC) by using MEGA11 with 1000 replicates bootstrap consensus tree (Felsenstein, 1985). Bootstrap replicates of the tree branches less than 50% were collapsed. For the out-group, the *N. tabacum* plastome was used (Shinozaki *et al.*, 1986).

2.4. Repeat sequence identification

Elements of repetitive DNA in chloroplast genomes of the Cichorieae tribe were investigated using three different programs. Size and location of forward, invert/palindrome, and complement repeats were analyzed using the REPuter v1.0 program (Kurtz *et al.*, 2001), using the program parameters 30 bp as a minimum repeat size, 3 kb for the hamming distance, and a 90% sequence identity threshold. Further, TRF v4.09 (Benson, 1999) was used to identify tandem repeat sequences (> 10 bp in length); program parameters were 2, 7, and 7 for matches, mismatches, and indels, respectively, and the minimum alignment score and maximum period size were set to 50 and 500, respectively. Likewise, microsatellite identification tool MISA v1.0 was used to analyze the number and type of Single Sequence Repeats -SSRs (≥ 10 bp), with thresholds of 10, 5, 4, 3, 3, and 3 repeat units for mono-, di-, tri-, tetra-, Penta-, and hexanucleotides, respectively (Thiel *et al.*, 2003).

3. Results and Discussions

3.1. Structural and organization comparison of Cichorieae tribe plastomes

The Cichorieae tribe of Asteraceae is the most taxonomically researched tribe; its members display easy identification by overall morphological characteristics. However, an extensive range of evolutionary features made it difficult to identify natural groups. Consequently, many taxonomists classified this tribe member at both generic and suprageneric levels differently. This study

provided genetic comparisons of Cichorieae tribe members by utilizing the whole chloroplast genome in order to assess genetic diversity at low taxonomic levels and systematic analyses.

Cichorieae tribe plastomes show a typical quadripartite circular structure consisting of one LSC and SSC and two IRs (IRa and IRb) as indicated by using dot blot analysis in the GENEIOUS program (Figure 1). The average genome size of the 36 Cichorieae tribe plastomes was 152 kbp, ranging from 151,173 bp (*Taraxacum erythrospermum*) up to 153,017 bp (*Ixeris repens*). Each IRs region size ranged from 24,420 (*T.erythrospermum*) to 25,174 bp (*Ixeris polycephala*). The LSC region size ranged from 82,924 bp (*Hypochaeris radicata*) to 84,386 bp (*Crepidiastrum sonchifolium*), and the SSC region with the size of about 18,150 bp (*H. radicata*) to 18,596 bp (*Lactuca sativa*) (Table 1).

The plastomes of tribe Cichorieae were with an overall average of 37.7% GC%; there was slight variation among the species with values ranging from 37.5 to 37.8 %. The *L.sativa* plastomes were the only plastomes found to have the lowest GC% content (37.5%) for their whole genomic chloroplast sequence, while each of (*Crepidiastrum denticulatum*, *Crepidiastrum lanceolatum*, *H. radicata*, *Lapsanastrum humile*, *Reichardia ligulata*) had the highest GC content (37.8%) in their plastomes (Table 1). However, the GC% contents of IR regions (43.0-43.2%) were much higher than the LSC region (35.7-36.0%) and SSC region (31.0-31.6%). This variation is certainly related to the high GC% content of ribosomal RNA (rRNA) genes (54.2-55.4%) located and distributed only within IR regions. These results show that the GC contents comparison among Cichorieae tribe plastomes showed high similarities among genera and at the species levels (Table 1).

Previous studies have shown that expansions and contractions of the IRs caused variations in the chloroplast genome size and LSC and SSC length across contrasting genera. Accordingly, the IRs and their gene contents are the most conserved regions of the plastome, while the LSC region is the least conserved (Wang *et al.*, 2008; Zhu *et al.*, 2016).

3.2. Gene contents and organization

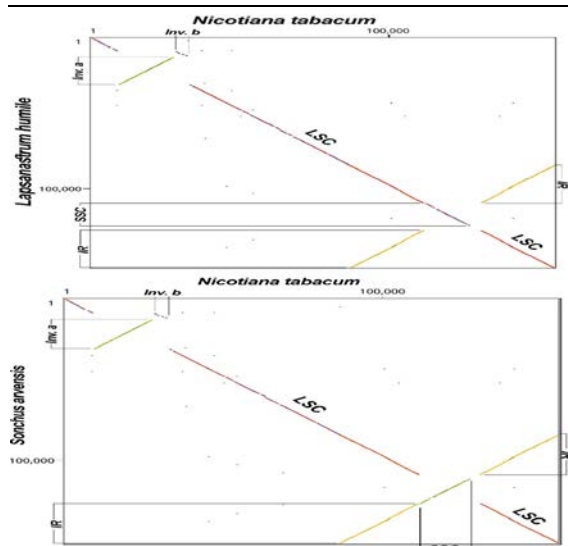
The chloroplast genomes of the tribe Cichorieae encoded a range of functional genes (Table 1). The lowest number of plastome functional genes is 126 genes recorded in *Sonchus boulosii*, and the highest number is 136 genes recorded in each of *H.radicata*, *Stebbinsia umbrella*, *Taraxacum brevicorniculatum*, and *Taraxacum kok-saghyz*. The recorded functional genes include 90 protein-coding genes in the plastome of *L.sativa*, and *S.umbrella*. Likewise, 91 protein-coding genes were recorded in *T.brevicorniculatum*, and *T.kok-saghyz* plastomes, and the rest of the plastomes of Cichorieae tribe generally comprised of 89 protein-coding genes (Table 1). These differences in coding genes number took place with the presence of the *ycf9* gene in *L.sativa*, *pbfl* in *S.umbrella*, and *ycf68* with *ihbA* genes in each of *T.brevicorniculatum*, and *T.kok-saghyz* plastomes. The above genes all were absent in the remaining Cichorieae tribe plastomes. However, according to Wicke *et al.* (2011), the angiosperm plastomes include 70 up to 88 protein-coding genes. In angiosperms, plastid genome gene number and order is conserved (Wolfe *et al.*, 1987) in comparison to nuclear genome. This is because chloroplast sequences evolve at approximately half the speed of nuclear regions (Jansen *et al.*, 2005; Walker *et al.*, 2014).

Number of genes duplicated in IRs (from rps19 to rps15) were different among plastomes, 17-21 duplicated genes have been recorded in Cichorieae tribe plastomes (Table 1). There were 17 genes duplicated in IRs of *C.intybus*, *Dendroseris* plastomes, *Sonchus* plastomes, in addition to recording 18 genes duplicated in each of *Crepidiastrum* plastomes, *Ixeris* plastomes, *R.ligulata*, *S.umbrella*, *Taraxacum* plastomes, and *Youngia japonica*, whereas each of *H.radicata*, *L.humile* plastomes included 19 genes duplicated in IRs.

rRNA genes were 3-4 different genes, all duplicated in the IRs, of which plastomes of *Dendroseris*, *Lactuca*, *Sonchus*, and *R.ligulata* contain only 3 different rRNA genes (5S-rRNA, 16S-rRNA, and 23s-rRNA), and the rest of the Cichorieae tribe in this study contains 4 different rRNA genes (4.5S- rRNA, 5S- rRNA, 16S- rRNA, and 23S-rRNA) (Table 1). However, six tRNA genes were duplicated in IRs in Cichorieae plastomes under study.

Table 1. Size, gene contents, and gene orders of complete chloroplast genome sequences of 36 Cichorieae tribe species downloaded from the National Center for Biotechnology Information (NCBI).

# Genus	Genome characteristics	Genome Size (bp)	LSC Length (bp)	SSC Length (bp)	IR Length (bp)	% GC				No. of Functional genes	No. of protein-coding genes	No. of tRNA genes	No. of rRNA genes	No. of gene duplicated by IRs	Accession No.	
						Whole Genome	LSC region	IR	rRNA in IR							
1 <i>Cichorium</i> L.	<i>C. intybus</i> L.	152,975	84,232	18,561	25,091	37.7	35.8	43.2	54.2	31.4	129	89	32	8	20	NC_043842.1
	<i>C. denticulatum</i> (Houtt.) Pak & K.	152,689	84,154	18,519	24,942	37.8	35.9	43.2	55.2	31.4	135	89	38	8	21	NC_042149.1
2 <i>Crepidiastrum</i> Nakai.	<i>C. lanceolatum</i> Nakai.	152,748	84,022	18,568	25,079	37.8	35.9	43.3	55.2	31.3	135	89	38	8	21	NC_046512.1
	<i>C. sonchifolium</i> (Bunge) Pak & K.	152,603	84,386	18,547	24,835	37.7	35.8	43.2	55.2	31.5	134	89	37	8	21	NC_046513.1
	<i>D. berteroaana</i> Hook. & Arn.	152,199	84,187	18,552	24,730	37.6	35.8	43.2	55.2	31.3	127	89	32	6	18	NC_051923.1
	<i>D. litoralis</i> Skottsb.	152,263	84,213	18,576	24,737	37.6	35.8	43.1	55.3	31.2	128	89	33	6	18	NC_051922.1
	<i>D. macrantha</i> Skottsb.	152,263	84,213	18,576	24,737	37.6	35.8	43.1	55.3	31.2	128	89	33	6	18	NC_051924.1
3 <i>Dendroseris</i> D.Don.	<i>D. marginata</i> Hook. & Arn.	152,261	84,236	18,551	24,737	37.6	35.8	43.1	55.3	31.2	128	89	33	6	18	NC_051925.1
	<i>D. micrantha</i> Hook. & Arn.	152,327	84,287	18,564	24,738	37.6	35.8	43.1	55.3	31.2	128	89	33	6	18	NC_051921.1
	<i>D. pinnata</i> Hook. & Arn.	152,290	84,258	18,568	24,732	37.6	35.8	43.1	55.4	31.2	128	89	33	6	18	NC_051926.1
	<i>D. pruinata</i> Skottsb.	152,348	84,291	18,583	24,737	37.6	35.8	43.1	55.4	31.2	128	89	33	6	18	NC_051920.1
4 <i>Hypochaeris</i> L.	<i>H. radicata</i> L.	151,330	82,924	18,150	25,128	37.8	36	43.1	54.9	31.6	136	90	38	8	21	NC_044795.1
5 <i>Ixeris</i> Cass.	<i>I. polycephala</i> Cass.	152,776	84,084	18,344	25,174	37.7	35.9	43.0	55.2	31.2	135	89	38	8	21	NC_046514.1
	<i>I. repens</i> A. Grey.	153,017	84,242	18,495	25,140	37.6	35.8	43.1	55.1	31.2	135	89	38	8	21	MW092111.1
6 <i>Lactuca</i> L.	<i>L. raddeana</i> Maxim.	152,339	83,976	18,521	24,921	37.7	35.9	43.1	54.4	31.2	132	89	35	8	21	NC_056380.1
	<i>L. sativa</i> L.	152,765	84,103	18,596	25,033	37.5	35.7	43.1	55.1	31	135	90	37	8	21	AP007232.1
7 <i>Lapsanastrum</i> P&K	<i>L. humile</i> (Thunb) Pak & K. Bremer	152,582	84,066	18,462	25,027	37.8	35.9	43.0	55.2	31.4	135	89	38	8	21	NC_046515.1
8 <i>Reichardia</i> Roth.	<i>R. ligulata</i> (Vent.) K. & Sun.	152,620	84,205	18,525	24,945	37.8	35.7	43.2	55.3	31.1	127	89	32	6	18	NC_051919.1
	<i>S. acaulis</i> Dum. Cours.	152,071	84,334	18,244	24,746	37.6	35.8	43.1	55.2	31.5	127	89	32	6	18	NC_042382.1
	<i>S. arvensis</i> L.	151,967	84,251	18,184	24,766	37.6	35.8	43.1	55.2	31.5	127	89	32	6	18	NC_054161.1
	<i>S. asper</i> (L.) Hill.	151,849	84,156	18,217	24,738	37.6	35.8	43.1	55.3	31.4	127	89	32	6	18	NC_048510.1
	<i>S. boulosii</i> Chamboul.	152,016	83,988	18,566	24,731	37.6	35.8	43.0	55.2	31.2	126	89	31	6	18	NC_042244.1
9 <i>Sonchus</i> L.	<i>S. canariensis</i> (Sch.Bip.) Boulos.	152,075	84,337	18,245	24,746	37.6	35.8	43.1	55.3	31.5	127	89	32	6	18	NC_042381.1
	<i>S. leptocephalus</i> Cass.	152,406	84,331	18,583	24,746	37.6	35.8	43.1	55.3	31.2	130	89	35	6	19	MN334533.1
	<i>S. oleraceus</i> L.	151,849	84,156	18,217	24,738	37.6	35.8	43.1	55.3	31.5	127	89	32	6	18	NC_048452.1
	<i>S. webbia</i> Sch. Bip.	152,194	84,269	18,427	24,749	37.6	35.8	43.1	55.3	31.3	127	89	32	6	18	NC_042383.1
10 <i>Stebbinsia</i> Lipsch.	<i>S. umbrella</i> (Franch.) Lipsch.	152,462	84,125	18,561	24,888	37.7	35.9	43.1	55.2	31.2	136	90	38	8	21	NC_051973.1
	<i>T. brevicorniculatum</i> Korol.	151,282	83,862	18,578	24,421	37.7	35.9	43.3	55.1	31.2	136	91	37	8	21	NC_032056.1
	<i>T. coreanum</i> Nakai.	151,451	84,019	18,500	24,466	37.7	35.8	43.3	55.1	31.2	135	89	38	8	21	MN689808.1
	<i>T. erythrosperrum</i> Resser.	151,173	83,812	18,521	24,420	37.7	35.8	43.2	55.1	31.2	135	89	38	8	21	MN689810.1
11 <i>Taraxacum</i> Wigg.	<i>T. hallaisanense</i> Nakai.	151,554	84,066	18,524	24,482	37.7	35.8	43.3	55.1	31.2	135	89	38	8	21	MW067130.1
	<i>T. kok-saghyz</i> Rodin.	151,338	83,986	18,490	24,431	37.7	35.9	43.2	55.1	31.3	136	91	37	8	21	NC_032057.1
	<i>T. mongolicum</i> Hand. Mazz.	151,451	84,052	18,541	24,429	37.7	35.8	43.3	55.1	31.2	135	89	38	8	21	NC_031396.1
	<i>T. officinale</i> Wigg.	151,324	83,895	18,567	24,431	37.7	35.9	43.3	55.1	31.2	135	89	38	8	21	NC_030772.1
12 <i>Youngia</i> Cass.	<i>T. platycarpum</i> Dahlst.	151,307	83,922	18,507	24,439	37.7	35.9	43.3	55.1	31.3	135	89	38	8	21	NC_031395.1
	<i>Y. japonica</i> (L.) DC.	152,540	84,047	18,445	25,024	37.7	35.9	43.2	55.2	31.4	135	89	38	8	21	NC_046516.1

**Figure 1.** Dot-plot analyses show the position of the LSC, SSC, IRs, and the two inversions (Inv-a, Inv-b) in the LSC region.

The tRNA gene numbers ranged from 31 tRNA in *S.boulosii* up to 38 tRNA in plastomes of *Taraxacum*, *Ixeris*, *Crepidiastrum*, *H.radicata*, *S.umbrella*, and *Y.japonica*. The tRNA genes that were present in some plastomes and absent in others include *trnfM*-CAU, *trnG*-GCC, *trnG*-UCC, *trnI*-CAU, *trnI*-GAU. They were absent in each of the *Dendroseris*, *Lactuca*, and *Sonchus* plastomes. Furthermore, there were no *trnfM*-CAU and *trnG*-UCC genes in each of the plastomes of *C.intybus*, and *R.ligulata*. And *trnI*-GAU were not recorded in each of *C.intybus* and *R.ligulata*. There is no *trnG*-GCC in *T.brevicorniculatum* or *T.kok-saghyz*. Contrarily, the plastomes of *C.intybus*, *Dendroseris berteroaana*, *Lactuca raddeana*, and *S.boulosii* lack any *trnV*-UAC annotation. Only the plastomes of *R.ligulata*, *C.intybus*, and *C.sonchifolium* lack the *trnI*-CAU gene, *trnL*-UAA, and *trnY*-GUA, respectively.

In contrast to the absence of a particular gene in some plastomes, examination of the LSC region of Cichorieae plastomes showed duplication of some genes in certain

lineages. The results showed variation in numbers of *trnF*-GAA repeated in *Taraxacum* plastomes compared to all other Cichorieae tribe plastomes. The *trnF*-GAA gene is doubled in (*Taraxacum coreanum*, *Taraxacum hallaisanense*, *Taraxacum mongolicum*, *Taraxacum officinale*, and *Taraxacum platycarpum*) plastomes and tripled in (*T.brevicorniculatum*, *T.erythrospermum*, and *T.kok-saghyz*) plastomes. As the results show, this duplication and triplication could be restricted to *Taraxacum* chloroplast genomes only and previously encountered by Salih *et al.* (2017) in comparing three *Taraxacum* plastomes with several different Asteraceae plastomes. Furthermore, Wittzell (1999) studied different *Taraxacum* taxa based on *trnL*-*trnF* region sequence diversity. The diversification in repeating *trnF*-GAA gene provides support for *Taraxacum* diversification on evolutionarily old and younger/derived taxa.

3.3. Inverted repeat regions contraction and expansion

It has been found that all land plants exhibit expansion and contraction of IR regions and junction formation (LSC/IR and IR/SSC), which is an indication of plastome evolution (Zhang *et al.*, 2013; Walker *et al.*, 2014). The border between LSC and IRs along with the border of the IR and SSC regions of the 36 Cichorieae plastomes were compared with that of the *N. tabacum* as a reference genome to study the impact of the junction formation and expansion of the IR regions. The *N.tabacum* was chosen for this comparison because none of the inversion events (the two inversions in the LSC region and SSC inversion event) occurred in its plastome (Timme *et al.*, 2007; Liu *et al.*, 2013; Zhang *et al.*, 2013). Additionally, the plastome of *N.tabacum* is regarded as an early angiosperm genome structure. Only plastomes that show variation at their junctions are represented in IR-plot in Figure 2, (*D.berteroana*, for example, stands in for the other two species in the genus. Each of *S.boulosii*, *Sonchus canariensis*, *Sonchus leptocephalus*, *Sonchus oleraceus*, and *Sonchus webbii* are represented by the *Sonchus acaulis*, while *Sonchus arvensis* shares connections with *Sonchus asper*. Each of *T.kok-saghyz* and *T.platycarpum* is represented by *T.brevicorniculatum*, whilst *T.coreanum* represents *T.erythrospermum*, *T.hallaisanense*, *T.mongolicum*, and *T.officinale*).

In all the 36 plastomes, the border between LSC and IRb starts at the location of the *rps19* gene, resulted to produce a pseudogene at the end of IRb, the length of this pseudogene is equal to the expansion of the IRb into the *rps19* gene. The IRb of *Crepidiastrum* spp., *L.humile*, and *Y.japonica* were extended lesser (about 32 bp) into the *rps19* gene, whereas *I.polycephala* and *I.repens* had extended into the *rps19* pseudogene at the end of IRb by 93 and 97 bp, respectively.

In addition, there were different events of IRb region extension into the *ycf1* gene in the 36 Cichorieae tribe plastomes. The *Dendroseris*, *I.repens*, *R.ligulata*, *S.arvensis*, *S.asper*, *T.brevicorniculatum*, and *T.kok-saghyz* there IRb region extended into the *ycf1* gene, while in the rest of the plastomes IRb region extended into the *ycf1* gene because of the re-inversion event. This extension created a pseudogene of about 462-472 bp length of the *ycf1* gene at the beginning of the IRa region.

This conserved border among Cichorieae tribe plastomes is similar to the results found among

angiosperm plastomes, which are mostly located within *rps19* or *ycf1* genes (Walker *et al.*, 2014; Downie and Jansen, 2015) (Figure 2).

Moreover, the gene *ndhF* is expanded and overlapped by 46 bp to the gene *ycf1* in the downstream of IRb/SSC region in the plastomes of *T.coreanum*, *T.erythrospermum*, *T.hallaisanense*, *T.mongolicum*, *T.officinale*, and *T.platycarpum*, while, the *ndhF* gene of the rest of Cichorieae plastomes (*Cichorium intibus*, *Crepidiastrum* plastomes, *H.radicata*, *I.polycephala*, *Lactuca* plastomes, *L.humile*, *S.acaulis*, *S.boulosii*, *S.canariensis*, *S.leptocephalus*, *S.oleraceus*, *S.webbii*, *S.umbrella*, and *Y.japonica*) was located 4 to 51 bp away from the downstream of the IRb/SSC border and did not overlap with *ndhF* gene. By contrast, *Dendroseris* plastomes, *I.repens*, *R.ligulata*, *S.arvensis*, *S.asper*, *T.brevicorniculatum*, and *T.kok-saghyz* had the *ndhF* gene located up to 16 bp from the upstream of the SSC/IRa junction without overlapping (Figure 2).

Furthermore, another junction is IRa/LSC junction, starting with the *trnH* gene located entirely within the LSC region, with various distances from the IRa/LSC junction. The plastome of *H.radicata* with 26 bp was the longest intergenic space of *trnH* genes from the border of SSC/IRa among the 36 plastomes species, while the plastomes of *Sonchus*, *R.ligulata*, and *Dendroseris* have only 2 bp spacer from the border of SSC/IRa, which is the shortest intergenic spacer of *trnH* genes from the border of SSC/IRa among the 36 plastomes species (Figure 2).

3.4. SSC and LSC inversion events

Despite the two large IRs events in the chloroplast genome, there has been another inversion event in the SSC region of the plastomes when comparing the Cichorieae tribe plastomes with that of *N.tabacum*. The inversion events in the SSC region and LSC region were investigated by dot-plot analysis using GENEIOUS program (Figure 1) and double-checked manually by visualizing the alignment of the 36 complete chloroplast genomes of the Cichorieae tribe. The gene orders in the SSC region began with the *ycf1* gene and ended with the *ndhF* gene in a completely reversed SSC. These gene orders (SSC inversion) are represented by some of the Cichorieae tribe plastomes including *Dendroseris* plastomes, *I.repens*, *R.ligulata*, *S.arvensis*, *S.asper*, *T.brevicorniculatum*, and *T.kok-saghyz* (Figure 2). The rest of the Cichorieae tribe plastomes in this study do not represent these gene order; thus, their SSC was not inverted (Figure 2). The results also showed that there were differences in occurring SSC region inversion at the species level, as indicated in plastomes of *Taraxacum*, *Ixeris*, and *Sonchus*. The inversion occurred in some species plastomes and was absent in other plastomes belonging to these three genera (Figure 2). These structural variations and sequence rearrangements of the Cichorieae chloroplast genomes are very important for providing a vital resource for molecular evolution and phylogenetic studies (Ogihara *et al.*, 1988). IR/SSC junction expansion and constriction along with the inversion of the SSC region were of interest to several researchers to study earlier in detail (Palmer, 1991; Wang *et al.*, 2008; Downie and Jansen, 2015; Walker *et al.*, 2015; Zhu *et al.*, 2016). In addition, it has been demonstrated that chloroplast DNA within individual plants exhibits a form of heteroplasmy in

which the plastome exists in two equimolar states (inversion isomers) that differ in the relative orientation of the SSC region (Palmer, 1983; Walker et al., 2015). This re-inversion is considered an ordinary phenomenon among chloroplast genomes of higher plants, and it is not a product of any evolutionary event.

Another and third inversion events in chloroplast genomes are the two inversions in the LSC region, as they are a specific feature of the Asteraceae chloroplast genomes (Salih et al., 2017). These two inversion events in the LSC region were shared among the plastome of all the 36 Cichorieae tribe plastomes under study when compared to *N.tabacum* (Figure 1). The two inversion events consist

of the large inversion of about 22 kbp inversion (Inv-a) and a smaller inversion (Inv-b) sized 2.6 kb nested within the large inversion region (Inv-a). The only differences between these two inversions in Cichorieae tribe plastomes studied compared to the same inversion present in other Asteraceae plastomes are from the size of these inversions, as it is recorded in other Asteraceae chloroplast genomes the inv-a size is about 22.8 kb and the inv-b is about 3.3 kb (Kim et al., 2005). Consequently, the results from the current study showed that the Inva and Invb size are small in comparison to same inversion in other Asteraceae plastomes.

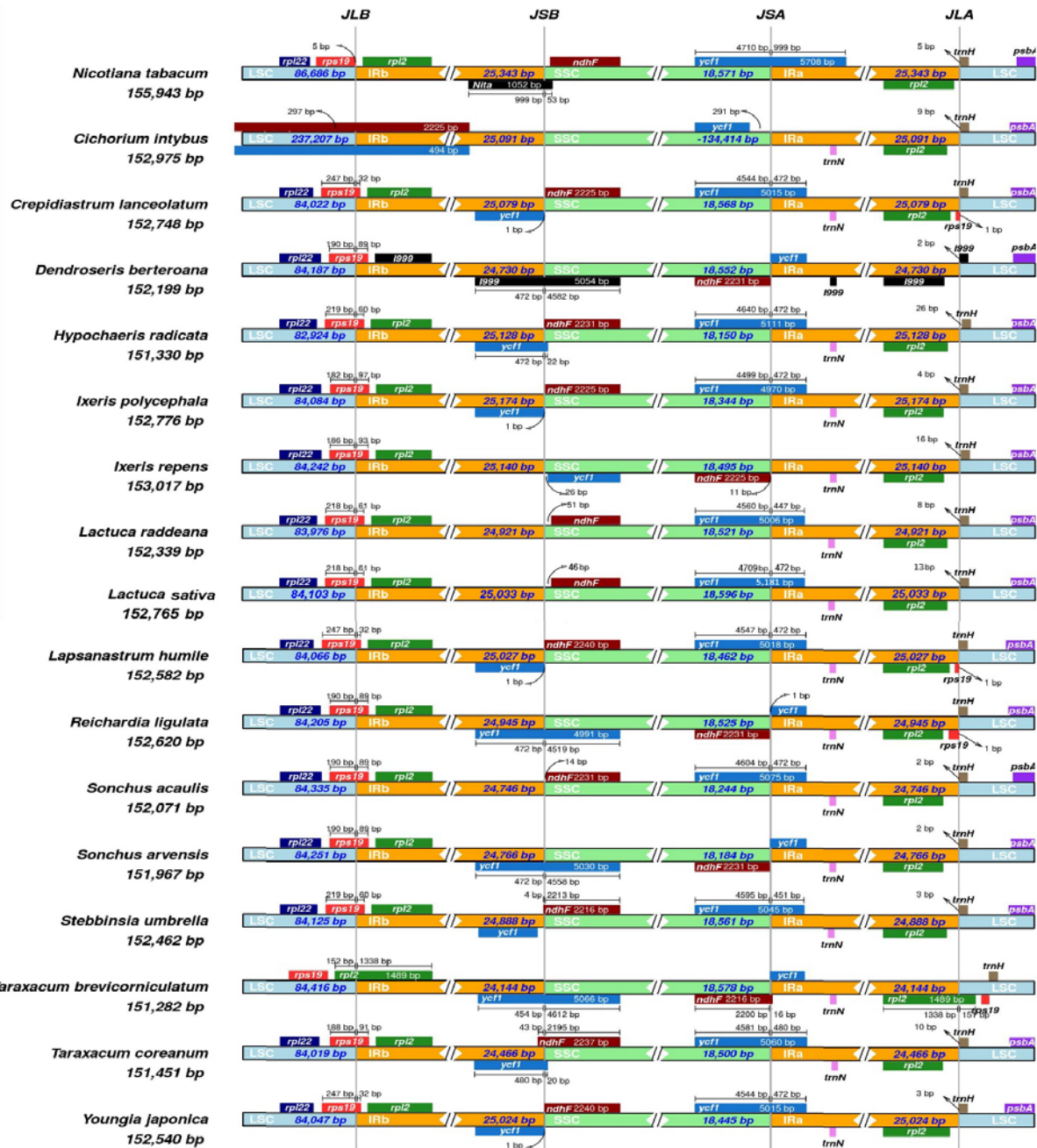


Figure 2. IR-plot of 17 plastomes. Each species and their corresponding chloroplast genome sequence length are depicted to the left of each track. Genes transcribed in positive and negative strands are presented above and below of their corresponding tracks with from right-to-left and left-to-right directions, respectively. The arrows are showing the bp distance of the start or end coordinate of a given gene from the corresponding junction site. For the genes extending from a region to another, the T bar on the top or below shows the extent of their parts with their corresponding values. The genes in the vicinity of the junctions are the realistically scaled projections of the bp distances for each

site. JLB= junction between LSC and IRb, JSB= junction between SSC and IRb, JSA= junction between SSC and IRa and JLA= junction between IRa and LSC.

3.5. Sequence divergence

Overall sequence identity and divergent regions within the Cichorieae tribe species at the plastome level were performed using mVISTA (Frazer *et al.*, 2004) programs by calculating and visualizing regions with high sequence variations among the 36 plastomes (Appendix 1). The results showed that the structure and gene order conservation in Cichorieae tribe plastomes indicate evolutionary conservation at the plastome level (Appendix 1). The non-coding regions (intergenic spacers) were more divergent than the coding regions. However, there was an exception of some coding region diversity among Cichorieae plastomes, including *ccsA*, *clpP*, *matK*, *ndhA*, *ndhF*, *rbcL*, *rpoC1*, *rpoC2*, *ycf1*, *ycf2*, and *ycf3* (Appendix 1). One of these coding genes was located in IRs, 4 of them were located in the SSC region, one (*ycf1*) in the junction of the IR/SSC region, and the rest of the 5 coding genes were located in the LSC region. There was a high level of similarity recorded in IRs sequences and a low level of similarity recorded in the LSC sequences. The differences in the level of similarity between IRs and LSC sequences possibly regarded as gene conservation resulted from the copy number variations in IR sequences (Khakhlova and Bock, 2006; Bock, 2014).

3.6. Phylogenetic tree construction and marker Identification

However, accurate phylogenetic construction can be achieved using the whole chloroplast genomes. Scientists constantly attempt to discover new and valuable plastid markers, through finding new plastome regions for investigating intra-genomic and interspecific variations in rates of molecular evolution. In the current study, the phylogenetic inference was built for the whole plastomes, each of the LSC, SSC, and IR regions separately, using *N.tabacum* as the outgroup. Furthermore, from the mVISTA analysis, a set of 37 regions with a high sequence diversity was selected (one intron is included among the 27 most polymorphic intergenic regions and the 10 most polymorphic coding genes). In order to perform a phylogenetic analysis, these regions were extracted from each plastome under study. The ML method was used based on the best-fit substitution model for such polymorphic datasets, scored according to the Bayesian information criterion (BIC). Mostly (for the coding, whole chloroplast genomes, LSC, SSC, and IR regions), the best substitution model was GTR+G., whereas T92+G was generally the best substitution model for intergenic spacers (Appendix 2). Phylogenetic analyses were conducted in MEGA11 (Tamura *et al.*, 2021). The bootstrap consensus tree was inferred from 1000 replicates. Branches corresponding to partitions reproduced in less than 50% bootstrap replicates were collapsed.

The whole chloroplast genome and LSC region have provided the phylogeny of the Cichorieae tribe with great success, and they result in the same ML tree topology (Figure 3 and Appendix 3). These data support the monophyly of the tribe Cichorieae with two clades.

Further, from the coding and noncoding regions phylogenetic inference, different genes and intergenic spacers have been identified as evolutionarily significant markers (Appendix 3); these markers have been used for

phylogenetic analysis at the species level and below (Shaw *et al.*, 2005; Kress *et al.*, 2005; Takahashi *et al.*, 2005; Daniell *et al.*, 2006; Timme *et al.*, 2007; Shaw *et al.*, 2007). In the field of evolutionary phylogeny, chloroplast genes and genomes have been major research areas (Tremetsberger *et al.*, 2013; Mandel *et al.*, 2017; 2019). The resolution of the phylogenetic tree of the tribe Cichorieae is in progress with some results from the remaining topology in the current study (Appendix 3) and in already published works (Tremetsberger *et al.*, 2013; Mandel *et al.*, 2017; 2019). Incongruence exists in gene and intergenic spacer trees from current work and that of others (Tremetsberger *et al.*, 2013; Mandel *et al.*, 2017). However, among the 10 selected coding regions, only six of them (*clpP*, *matK*, *ndhA*, *rpoC1*, *rpoC2*, and *ycf1*) were detected as hypervariable regions in the present study, and they have been shown to be useful for inferring phylogenetic relationships within Cichorieae tribe plastomes. However, they have not been widely used possibly because of a lack of universal primers and the large number of primer pairs needed to sequence the entire region. The other four coding genes (*rbcL*, *ndhF*, *ycf2*, and *ycf3*) did not show satisfactory variability to use for inferring the phylogenetic tree (Kumar *et al.*, 2009). Nevertheless, the *rbcL* coding region has been usually used in many previous studies as a phylogenetic marker for Asteraceae and many other plant families. However, using the *rbcL* coding gene in this study makes it impossible to derive a solid phylogenetic topology (Appendix 3).

In general, analysis of the sequences of non-coding regions generated a congruent phylogenetic topology with high support for most internal nodes. A high level of divergence was observed along intergenic spacers, including *ndhF-rpl32*, *petN-psbM*, *psbE-petL*, *rps4-ndhJ*, *rps15-ycf1*, *trnL-trnF*, *trnT-psbD*, and *ycf3-trnS*, and trees were fully congruent with the phylogenetic topology of the chloroplast genome. Although *ycf4-cemA*, *trnH-psbA*, and *petB-petD* spacers were frequently used to construct phylogenetic relationships among plant families (Doorduyn *et al.*, 2011), the results from this study did not show a congruent topology with high support among the Cichorieae tribe plastomes (Appendix 3). For example, the intergenic region between *trnH* and *psbA* genes has been the most preferred region for their primer amplification success and phylogenetic topology construction (Hebert *et al.* 2003; Hebert and Gregory 2005; Taberlet *et al.* 2007). In this investigation, this non-coding region does not succeed to generate a congruent phylogenetic topology for the Cichorieae tribe, possibly because these regions are short, and therefore may not yield enough variation to distinguish among closely related species (Shaw and Small, 2005). However, studies showed that some of these regions worked well when combining these short regions with other coding or noncoding region to construct a phylogenetic tree (Kumar *et al.*, 2009).

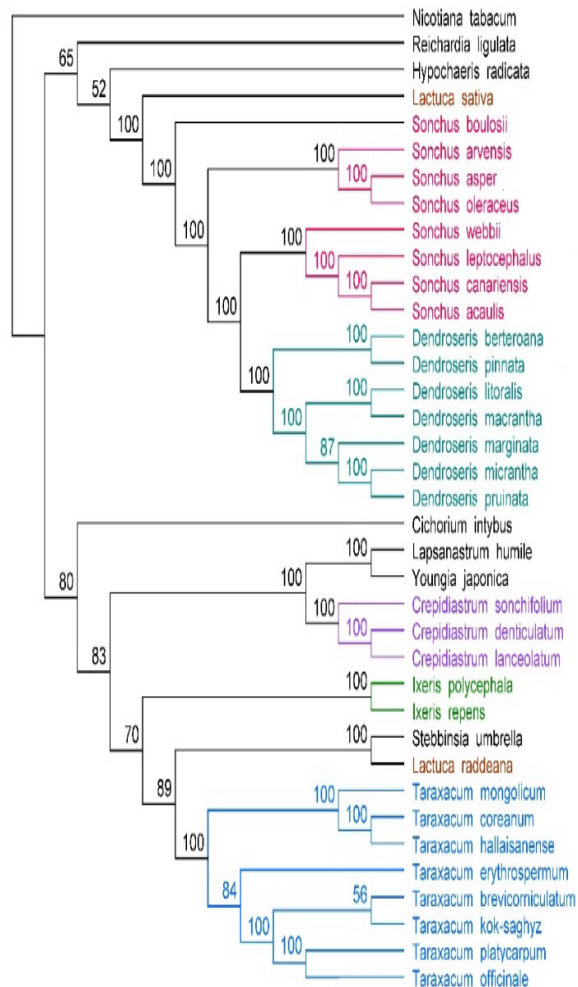


Figure 3. Molecular Phylogenetic analysis of whole chloroplast genomes of 36 plastomes of the Cichorieae tribe by Maximum Likelihood (ML) method. The percentage of trees in which the associated taxa clustered together is shown next to the branches. *N.tabacum* is used as an outgroup. Evolutionary analyses were conducted in MEGA11.

The rest of the coding regions and intergenic spacers in Appendix 3 are possibly better to use to analyze the divergence that occurs in taxa at family and generic levels as mutational hotspots but not for the interspecific level. Thus, the above investigated coding (*clpP*, *matK*, *ndhA*, *rpoC1*, *rpoC2*, and *ycf1*) and non-coding (*ndhF-rpl32*, *petN-psbM*, *psbE-petL*, *rps4-ndhJ*, *rps15-ycf1*, *trnL-trnF*, *trnT-psbD*, and *ycf3-trnS*) regions have a higher level of variability, and they are with good congruent topology and high bootstrap support. These regions, however, having rarely been used, may represent a novel combination of markers for analyzing phylogenetic relationships among the Cichorieae tribe. Thus, universal primers for these coding and intergenic regions may be valuable for the investigation of phylogenetic inference and population genetic analysis of the Cichorieae tribe plastomes at various taxonomic levels. These regions can also be used as a marker for accurate and automated species identification, providing plant taxonomists with a species-specific DNA barcode catalogue that is simple to use (Shaw *et al.*, 2005; Kress *et al.*, 2005; Takahashi *et al.*, 2005; Hughes *et al.*, 2006; Daniell *et al.*, 2006; Timme *et al.*, 2007; Shaw *et al.*, 2007).

Regarding the *Lactuca* plastome, as shown in Figure 3 and other phylogenetic topography in Appendix 3, *L.raddeana* nested in a clade including *Taraxacum* and *Ixeris* as it is the wrong place for the *Lactuca* genus, and *L.sativa* placed in the related genera of *Sonchus* and *Dendroseris* clade. So, no consistent conclusions have been reached based on the analysis of different coding and noncoding regions from this genus. However, the classification of *Lactuca* was also controversial in the previous studies (Wang *et al.* 2013; Mandel *et al.*, 2019; Jiang *et al.*, (2021).

3.7. Repeat sequence analysis

The recombination events and genome rearrangements consequently have affected on occurring different repetitive DNA sequences and regions in a genome (Ogihara *et al.*, 1988, Milligan *et al.*, 1989). Different repeat types, sizes, and locations in chloroplast genomes of the Cichorieae tribe were analyzed through using three different programs. The size and location of forwarding (F), inverted (R)/ palindromic (P), and complement (C) repeats were determined using REPuter (Kurtz *et al.*, 2001) (Figure 4). The repetitive calculations excluded the two largest palindromic repetitive DNA of IR regions for the chloroplast genome of 36 Cichorieae tribe plastomes. The Cichorieae tribe plastomes were conserved in their total number of repeats; however, there were some exceptions, as the majority of plastomes under study included 49 total number of repeats, except 45 repeats in *S.boulosii*, 48 repeats in *S.umbrella* and *T.brevicorniculatum*, 50 in *S.arvensis* and *S.canariensis*, and the highest number of repeats was 58 repeats recorded in *I.polycephala* plastome. The most abundant repeat type was forwarded repeats (11-130 bp of length) among the 36 Cichorieae tribe plastomes, ranging from 20 repeats in *Y.japonica* and 32 repeats in *I.polycephala*. Reverse repeats were the least abundant repeats, ranging from only one reversed repeat in *S.arvensis*, *S.boulosii*, *T.hallaisanense*, *T.kok-saghyz*, and 7 repeats in *I.repens*, *L.humile*, and *Y.japonica* (Figure 4).

Meanwhile, tandem repeat sequences (> 10 bp in length) were identified with tandem repeat finder (TRF) v4.09 (Benson, 1999). The most abundant tandem repeats in Cichorieae plastomes were 46 tandem repeats in *S.boulosii*, and the lowest numbers were found in *R.ligulata* and *S.umbrella* which was only 28 tandem repeats (Table 2). The tandem repeat distributed abundantly and widely in the LSC region and were around 70% of total tandem repeats recorded in the LSC region, 7% in SSC, and 23% in IR regions. The majority of tandem repeats were located in intergenic spacers and were around 74% of total repeats found in plastomes, and 26% located in coding genes (Table 2). The tandem repeats of 21-30 period size are most variable among the Cichorieae tribe plastomes.

The simple sequence repeats (SSRs) are the small unit of repetitive DNA sequence occurring in both coding and non-coding regions. SSRs are useful DNA markers to study population genetics because of their co-dominant expression, polymorphic nature (Yamane *et al.*, 2009; Redwan *et al.*, 2015), and genetic variation among plant genotypes in chloroplast genomes (Vendramin *et al.*, 1999, Deguilloux *et al.*, 2004, Piya and Nepal, 2013). The Perlscript MicroSatellite identification tool MISA v1.0 (Beier *et al.*, 2017) was used to analyse the number and

type of simple sequence repeats (SSRs) (Figure 5 and 6). The results showed that the total number of SSRs ranged from the lowest of 26 SSRs in *C. sonchifolium*, *Y. japonica*, and the most abundant is 42 SSRs in *C. denticulatum* (Figure 5). Number of each SSRs type identified in plastomes under study is 14-37 mononucleotide SSRs, 2-9 dinucleotide SSRs, 1-6 trinucleotide SSRs, 1-2 tetranucleotide SSRs in some plastomes, and in some cases 1-2 penta- and hexanucleotide chloroplast SSRs. The distribution of SSRs in the LSC region is more abundant than their distribution in SSC and IRs regions (Huotari and Korpelainen, 2012). The mononucleotide SSRs are the most abundant (Figure 5) among the SSRs repeats. In general, the intergenic SSRs are more abundant than the genic SSRs in Cichorieae tribe plastomes; this is the common result for occurring SSRs in Asteraceae plastomes as previously analyzed by Liu *et al.* (2012) and chloroplast genomes of some other plant families (Sherman-Broyles *et al.*, 2014; Dong *et al.*, 2018; Liu *et al.*, 2020), which explains the lower polymorphism of coding region in comparison to non-coding region.

The majority of mononucleotide SSRs (14–29 bp) are composed of A/T type which comprises 46 (79%) of the total SSRs in the plastomes (Figure 6). The di-nucleotide SSRs type was AC/GT and AT/AT; however, the most abundant was AT/AT type of di-nucleotide SSRs comprises the 10 (28%) of the total SSRs, yet AC/GT was recorded only one time in *C. sonchifolium* plastome among the Cichorieae plastomes (Figure 6). The tri-nucleotide SSRs types of AAG/CTT, AAT/ATT, ATC/ATG comprised 3 (15%) of the total SSRs, although ATC/ATG tri-nucleotide SSR was recorded only one time in each of *T. coreanum*, *T. hallaisanense*, *T. mongolicum* plastomes among the other plastomes (Figure 6). The tetra-nucleotide (AAAG/CTTT, AAAT/ATTT, AATC/ATTG,

AGGG/CCCT, and AGAT/ATCT) chloroplast SSRs was more abundant than tri-nucleotide SSRs, comprising 4 (20%) of the total SSRs; However, the tetra-nucleotide SSRs of the AGGG/CCCT type recorded twice in the plastomes of *C. intybus* and *Crepidiastrum*, while AGAT/ATCT only recorded once and was present in the plastomes of *Taraxacum* (Figure 6). Contrarily, pentanucleotide (AATCT/AGATT) chloroplast SSRs have only been detected in the plastome of *L. raddeana*, (AATAT/ATATT) chloroplast SSRs have only been detected in the plastome of *T. mongolicum*, and (AACCC/GGGTT) chloroplast SSRs have only been detected in the plastome of *T. platycarpum*. In addition, hexanucleotide (AATCTC/AGATTG, AATCCT/AGGATT, AAGGAT/ATCCTT, AAAATT/AATTTT, AGATAT/ATATCT) chloroplast SSRs were identified in each of *Crepidiastrum*, *Sonchus*, and *Taraxacum* plastomes only, recorded one time in each plastomes, and absent in other Cichorieae chloroplast genomes under study.

The above-mentioned SSRs types are valuable markers for species identification, hybridization, and introgression analyses, the study of plant phylogeny, and population differentiation (Yamane *et al.*, 2009; Haasl and Payseur, 2011; Sonah *et al.*, 2011; Laiadi *et al.*, 2019). The results of this study showed PCR-based analysis of tetra-, penta-, and hexanucleotide repeats is better to be used to detect diversity in the chloroplast genomes of Cichorieae tribe plastomes at the level of genera and species. Thus, the analysis of polymorphic microsatellites provides an important and not expensive experimental tool to examine several plant genetic issues such as genetic diversity, genetic structure, evolutionary history, and hybridization in native and agricultural species (Wheeler *et al.*, 2014).

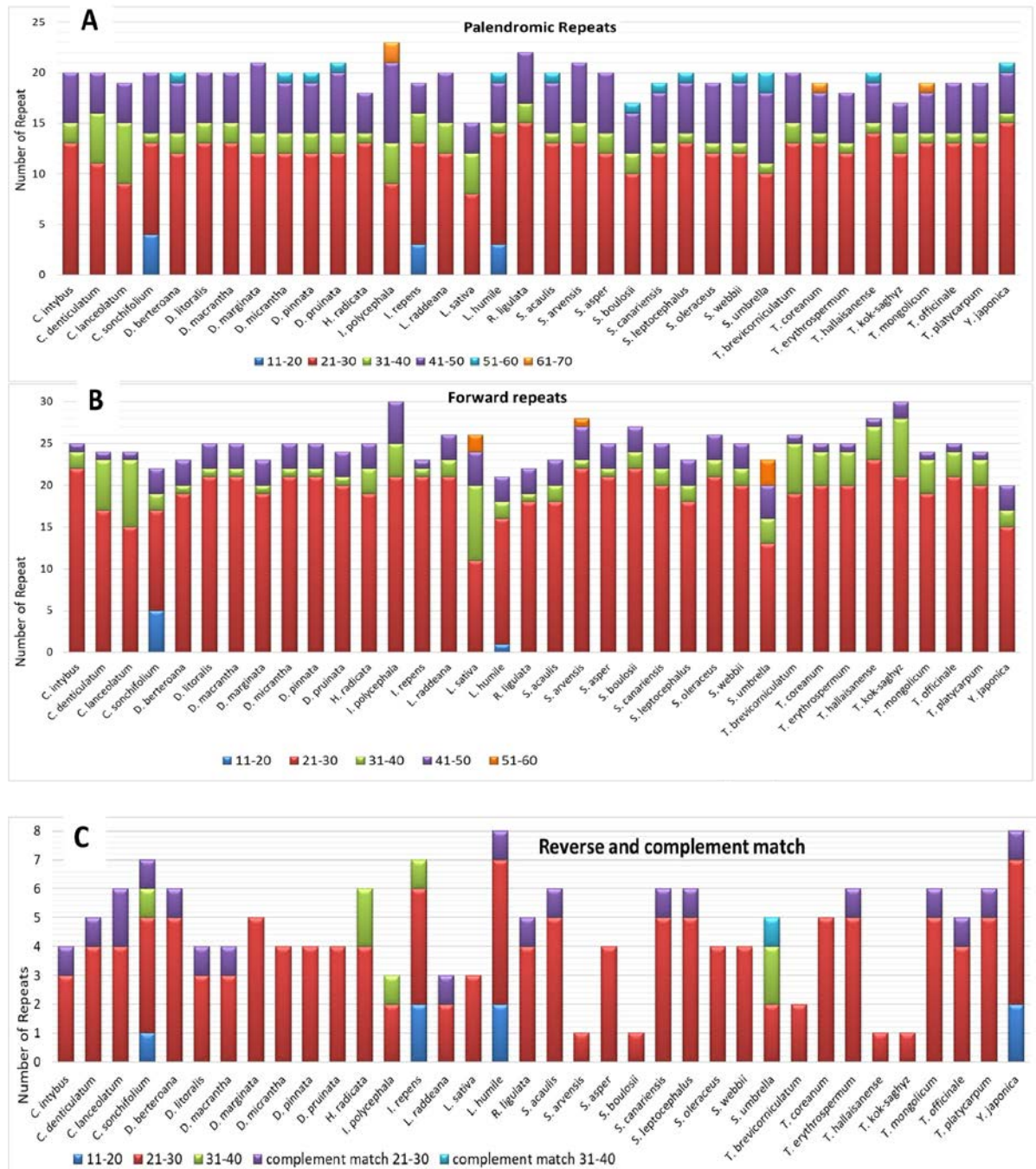


Figure 4. Comparison of the Palindromic, Forward, and reverses repeats among Chichorieae tribe plastomes.

Table 2. Shows the total number, size, location, and region of Tandem repeats (TRs) in Cichorieae tribe plastomes, identified with TRF v4.09 (Benson, 1999), with parameters of 2, 7, and 7 for matches, mismatches and indels, respectively. The minimum alignment score and maximum period size were set to 50 and 500, respectively.

#	Species	Total	TRs period size				Location		Region		
			11-20	21-30	31-40	>40	No. of tandem repeat located in spacer	No. of repeat located in gene	No. of TR in LSC	No. of TR in SSC	No. of TR in IRs
	<i>C. intybus</i> L.	40	32	4	4		31	9	27	7	6
	<i>C. denticulatum</i> (Houtt.) Pak & K.	40	26	10	4		30	10	29	3	8
	<i>C. lanceolatum</i> Nakai.	43	29	10	4		32	11	28	8	7
	<i>C. sonchifolium</i> (Bunge) Pak & K.	39	30	7	2		28	11	25	6	8
	<i>D. berteriana</i> Hook. & Arn.	32	22	6	4		24	8	22	2	8
	<i>D. litoralis</i> Skotts.	33	22	7	4		25	8	23	2	8
	<i>D. macrantha</i> Skotts.	33	22	7	4		25	8	23	2	8
	<i>D. marginata</i> Hook. & Arn.	33	22	7	4		25	8	24	1	8
	<i>D. micrantha</i> Hook. & Arn.	33	21	8	4		26	7	24	1	8
	<i>D. pinnata</i> Hook. & Arn.	34	22	8	4		26	8	24	2	8
	<i>D. pruinata</i> Skotts.	34	22	8	4		26	8	24	2	8
	<i>H. radicata</i> L.	36	27	4	5		29	7	22	2	12
	<i>I. polycephala</i> Cass. Ex DC.	38	27	7	4		32	6	29	1	8
	<i>I. repens</i> A. Grey.	32	21	9	2		25	7	23	3	6
	<i>L. raddeana</i> Maxim.	37	22	12	3		27	10	23	4	10
	<i>L. sativa</i> L.	36	21	12	3		26	10	17	5	14
	<i>L. humile</i> (Thunb) Pak & K. Bremer	33	27	4	2		23	10	22	5	6
	<i>R. ligulata</i> (Vent.) K. & Sun.	28	18	4	6		15	13	18	2	8
	<i>S. acaulis</i> Dum. Cours.	36	23	9	4		24	12	24	4	8
	<i>S. arvensis</i> L.	38	23	11	4		28	10	25	1	12
	<i>S. asper</i> (L.) Hill.	38	26	8	4		19	19	29	1	8
	<i>S. boulosii</i> Chamboul.	46	31	11	4		33	13	35	3	8
	<i>S. canariensis</i> (Sch.Bip.) Boulos.	37	24	9	4		25	12	25	4	8
	<i>S. leptocephalus</i> Cass.	36	24	8	4		24	12	27	4	5
	<i>S. oleraceus</i> L.	39	26	9	4		25	14	29	2	8
	<i>S. webbii</i> Sch. Bip.	40	25	11	4		30	10	29	3	8
	<i>S. umbrella</i> (Franch.) Lipsch.	28	21	5	2		22	6	16	3	9
	<i>T. brevicorniculatum</i> Korol.	33	19	11	2	1	26	7	22	3	8
	<i>T. coreanum</i> Nakai.	30	17	11	2		24	6	20	2	8
	<i>T. erythrospermum</i> Resser.	36	21	12	2	1	27	9	28	0	8
	<i>T. hallaisanense</i> Nakai.	36	17	17	2		30	6	24	2	10
	<i>T. kok-saghyz</i> Rodin.	37	21	13	2	1	31	6	26	3	8
	<i>T. mongolicum</i> Hand. Mazz	29	19	8	2		23	6	21	2	6
	<i>T. officinale</i> Wigg.	35	19	14	2		29	6	26	1	8
	<i>T. platycarpum</i> Dahlst.	35	19	14	2		27	8	25	0	10
	<i>Y. japonica</i> (L.) DC.	31	25	4	2		21	10	22	2	7

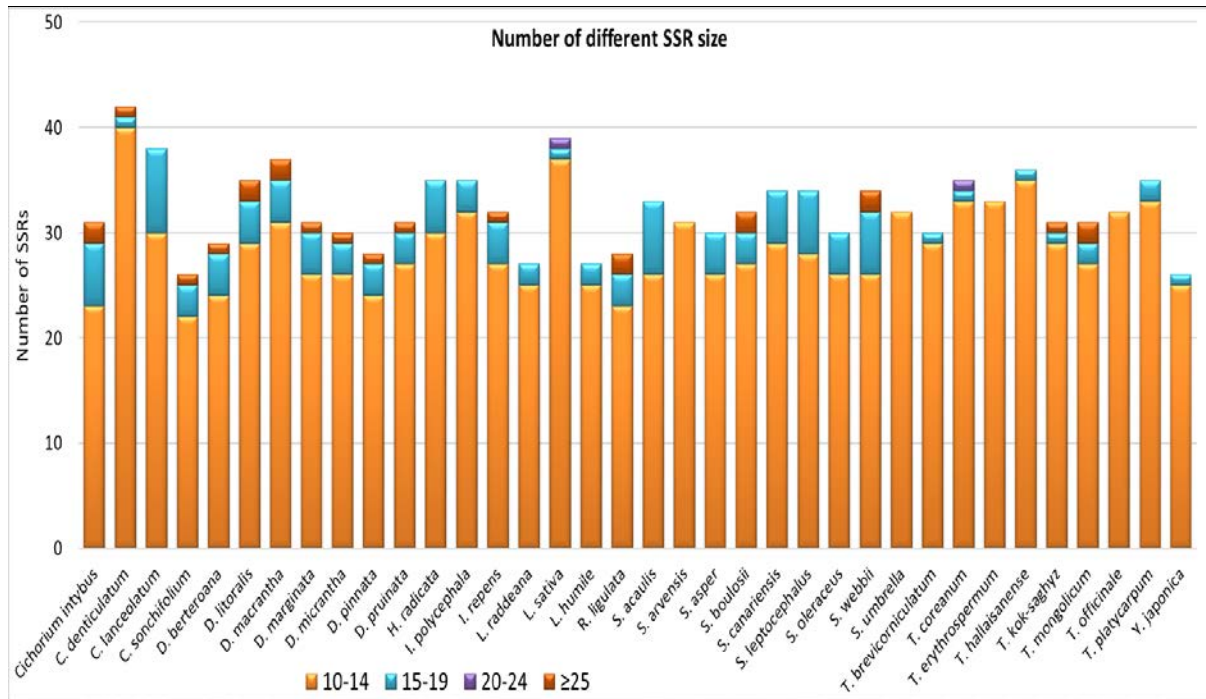


Figure 5. The number of SSRs, each repeat sequence SSRs length was screened to be ≥ 10 bp. SSRs were identified with thresholds of 10, 5, 4, 3, 3, and 3 repeat units for mono-, di-, tri-, tetra-, Penta-, and hexanucleotides, respectively using the microsatellite identification tool MISA v1.0 (Thiel *et al.*, 2003).

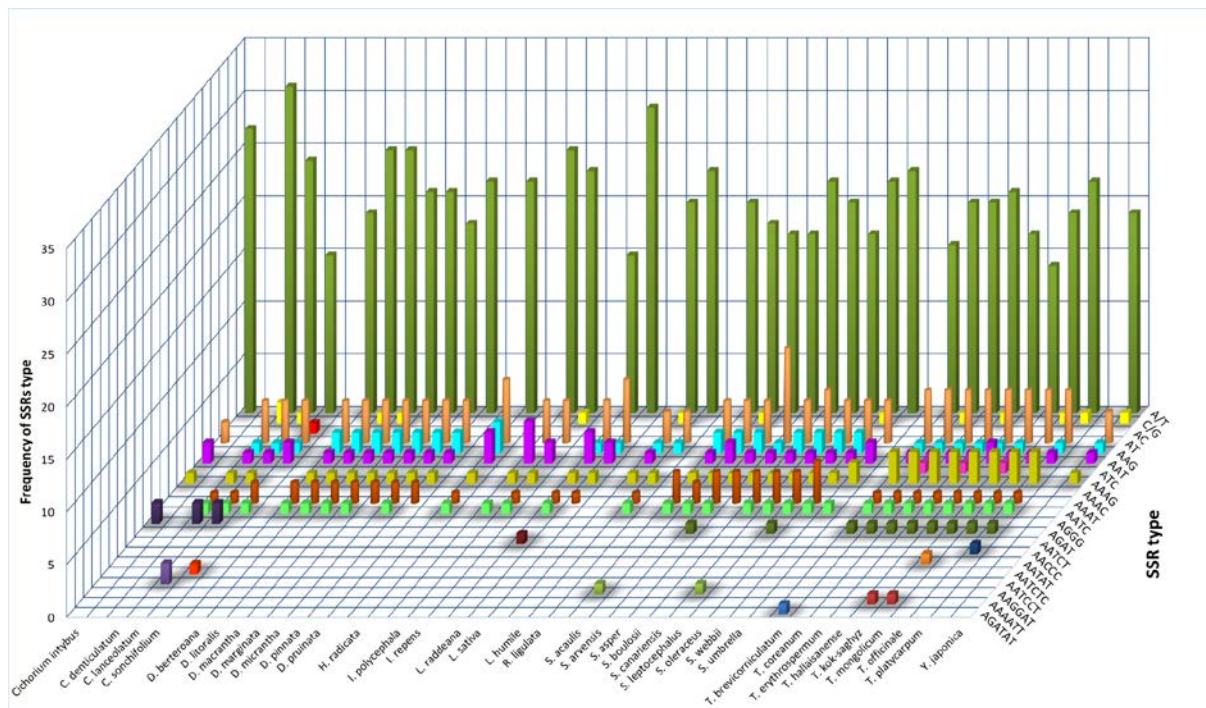


Figure 6. The type of SSRs, each repeat sequence SSRs length was screened to be ≥ 10 bp. SSRs were identified with thresholds of 10, 5, 4, 3, 3, and 3 repeat units for mono-, di-, tri-, tetra-, Penta-, and hexanucleotides, respectively using the microsatellite identification tool MISA v1.0 (Thiel *et al.*, 2003).

4. Conclusion

Characteristic comparison among 36 Cichorieae tribe plastomes showed overall similarity of its plastomes structure. There were no significant differences among representatives plastomes of the tribe, these similarity among the tribe plastomes results of the remarkable stability of chloroplast characteristics at lower taxonomic

level. However, there were some exceptions: number of rRNA genes was different among the plastomes, and there were little differences in the total number of coding, tRNA, and rRNA genes among the tribe plastomes. In addition, the large LSC region is the least conserved when all parts of the plastome are compared, including group of inversions (Inv a, Inv b), and insertions/ deletions region (*trnF-GAA* gene). The results also showed that there are differences in SSC region inversion that is occurring at the

species level, as indicated in plastomes of *Taraxacum*, *Ixeris*, and *Sonchus* plastomes, as the inversion occurred in some species plastomes and was absent in other plastomes belonging to these three genera. Furthermore, the LSC inversion (Inv-a and Inv-b) is smaller in Cichorieae plastomes in comparison with other Asteraceae plastomes; there is a 0.8 kb difference between the size of an Inv-a in Cichorieae chloroplast genomes and a 0.7 kb difference between the size of an Inv-b in Cichorieae.

The sequence alignments and phylogenetic trees highlighted six potentially concatenated coding regions include *clpP*, *matK*, *ndhA*, *rpoC1*, *rpoC2* and nine potentially concatenated non-coding regions *ycf1*, *ndhF-rpl32*, *petN-psbM*, *psbE-petL*, *rps4-ndhJ*, *rps15-ycf1*, *trnL-trnF*, *trnT-psbD*, and *ycf3-trnS*. These regions possibly are more variable than the regions used so far, at least at the level of a tribe in the Asteraceae family such as the Cichorieae tribe. These regions offer levels of variation better than the regions identified in previous studies and are therefore likely to be good choices for molecular studies at low taxonomic levels for the Cichorieae tribe members. The results also showed that most likely the sample sequence of *Lactuca sativa* in NCBI was incorrectly identified.

The most abundant repeat type was forwarded repeats among the 36 Cichorieae tribe plastomes and reverse repeats were the least abundant repeats, ranging from only one reversed repeat to 7 repeats. When it comes to tandem repetitive DNA, up to 46 repeats were documented, with the LSC area recording 70% of all tandem repeats, the SSC region 7%, and the IR regions 23%. The majority of tandem repeats were located in intergenic spacers and 26% located in coding genes. The tandem repeat of 21-30 period size is most variable among the Cichorieae tribe plastomes.

The distribution of SSRs in the LSC region is more abundant than their distribution in SSC and IRs regions. The mononucleotide SSRs are the most abundant among the SSRs repeats. In general, the intergenic SSRs are more abundant than the genic SSRs in Cichorieae tribe plastomes. The majority of mononucleotide SSRs are composed of A/T type which comprises 79% of the total SSRs in the plastomes. However, the tetra-, penta-, and hexa-nucleotide SSRs were recorded in some plastomes and absent in other plastomes of Cichorieae tribe, so these SSRs repeat could be valuable markers for species identification, hybridization, and introgression analyses, the study of plant phylogeny, and population differentiation.

References

Amiryousefi A, Jaakko H, Peter P. 2018. IRscope: an online program to visualize the junction sites of chloroplast genomes. *Bioinformatics*, **34**: 17.

Beier S, Thiel T, Münch T, Scholz U and Mascher M. 2017. Misa-Web: A Web Server For Microsatellite Prediction. *J. Bioinform.*, **33**: 2583-2585.

Benson G. 1999. Tandem Repeats Finder: a program to analyze DNA sequences. *Nucleic Acids Res.*, **27**: 573-580.

Bock R. 2014. Genetic engineering of the chloroplast: novel tools and new applications. *COBIOT*, **26**, 7-13.

Carlquist S. 1976. Tribal interrelationships and phylogeny of the Asteraceae. *ALISO*, **8**: 465-492.

Daniell H, Lee SB, Grevich J, Saski C, Quesada-Vargas T, Guda C, Tomkins J and Jansen RK. 2006. Complete chloroplast genome sequences of *Solanum bulbocastanum*, *Solanum lycopersicum* and comparative analyses with other Solanaceae genomes. *Theor. Appl. Genet.*, **112**: 1503-1518.

Daniell H, Lin CS, Yu M and Chang WJ. 2016. Chloroplast genomes: diversity, evolution, and applications in genetic engineering. *Genome Biol.*, **17**: 1-29.

Deguilloux MF, Pemonge MH and Petit RJ. 2004. Use of chloroplast microsatellites to differentiate oak populations. *Ann. For. Sci.*, **61**: 825-830.

Dong WL, Wang RN, Zhang NY, Fan WB, Fang MF and Li ZH. 2018. Molecular evolution of chloroplast genomes of orchid species: insights into phylogenetic relationship and adaptive evolution. *Int. J. Mol. Sci.*, **19**: 716.

Doorduyn L, Gravendeel B, Lammers Y, Ariyurek Y, Chin AT and Vrieling K. 2011. The complete chloroplast genome of 17 individuals of pest species *Jacobaea vulgaris*: SNPs, microsatellites and barcoding markers for population and phylogenetic studies. *DNA Res.*, **18**: 93-105.

Downie SR and Jansen RK. 2015. A comparative analysis of whole plastid genomes from the apiales: expansion and contraction of the inverted repeat, mitochondrial to plastid transfer of DNA, and identification of highly divergent noncoding regions. *Syst. Bot.*, **40**: 336-351.

Felsenstein J. 1985. Confidence limits on phylogenies: an approach using the bootstrap. *Evolution*, **39**: 783-791.

Frazer KA, Pachter L, Poliakov A, Rubin EM and Dubchak I. 2004. Vista: computational tools for comparative genomics. *Nucleic Acids Res.*, **32**: W273-W279.

Gholipour M and Kohnehrouz BB. 2017. molecular cloning and in silico analysis of rps7 gene from the Lactuca sativa. JJBS, 10(2): p.279.

Haas RJ and Payseur BA. 2011. Multi-locus Inference of population structure: a comparison between single nucleotide polymorphisms and microsatellites. *Heredity*, **106**: 158-171.

Hebert PD, Cywinska A, Ball SL and deWaard JR. 2003. Biological identifications through DNA barcodes. *Proc. Biol. Sci.*, **270**: 313-321.

Hebert PD, Gregory TR. 2005. The promise of DNA barcoding for taxonomy. *System. Biol.*, **54(5)**:852-9.

Huotari T and Korpelainen H. 2012. Complete chloroplast genome sequence of *Elodea canadensis* and comparative analyses with other monocot plastid genomes. *Gene*, **508**: 96-105.

Jeffrey C. 2001. **Compositae (Asteraceae)**. Hanelt P, Institute of plant genetics and crop plant research (Eds) Mansfeld's Encyclopedia of agricultural and horticultural Crops, 4, 2035-2145.

Jiang M, Li Y, Chen H, Wang B, Liu C. 2021. Comparative and phylogenetic analysis of the complete chloroplast genome sequences of *Lactuca raddeana* and *Lactuca sativa*. *Mitochondrial DNA Part B*, **3;6(4)**:1498-506.

Kearse M, Moir R, Wilson A, Stones-Havas S, Cheung M, Sturrock S, Buxton S, Cooper A, Markowitz S, and Duran C. 2012. Geneious basic: an integrated and extendable desktop software platform for the organization and analysis of sequence data. *J. Bioinform.*, **28**: 1647-1649.

Khakhlova O and Bock R. 2006. Elimination of deleterious mutations in plastid genomes by gene conversion. *TPJ*, **46**: 85-94.

Kilian N, Gemeinholzer B and Lack H. 2009. **Tribe Cichorieae Lam. & DC. systematics, evolution and biogeography of the compositae**. Iapt Vienna, Austria.

- Kim KJ, Choi KS and Jansen RK. 2005. Two chloroplast DNA inversions originated simultaneously during the early evolution of the sunflower family (Asteraceae). *Mol. Biol. Evol.*, **22**: 1783-1792.
- Kress WJ, Wurdack KJ, Zimmer EA, Weigt LA and Janzen DH. 2005. Use of DNA barcodes to identify flowering plants. *PNAS.*, **102**: 8369-8374.
- Kumar S, Hahn FM, McMahan CM, Cornish K and Whalen MC. 2009. Comparative analysis of the complete sequence of the plastid genome of *Parthenium argentatum* and identification of DNA barcodes to differentiate *Parthenium* species and lines. *BMC plant boil.*, **9(1)**: pp.1-12.
- Kurtz S, Choudhuri JV, Ohlebusch E, Schleiermacher C, Stoye J and Giegerich R. 2001. Reputer: the manifold applications of repeat analysis on a genomic scale. *Nucleic Acids Res.*, **29**: 4633-4642.
- Laiadi Z, Rahali M and Achour H. 2019. Molecular clarifications of grapevine identities in Algerian germplasm collections using microsatellite markers. *JJBS*, 12(3).**
- Liu J, Qi ZC, Zhao YP, Fu CX and Xiang QYJ. 2012. Complete cpDNA genome sequence of *Smilax china* and phylogenetic placement of Liliales—influences of gene partitions and taxon sampling. *Mol. Phylogenet. Evol.*, **64**: 545-562.
- Liu JX, Zhou MY, Yang GQ, Zhang YX, M PF, Guo C, Vorontsova MS and Li DZ. 2020. ddRAD analyses reveal a credible phylogenetic relationship of the four main genera of Bambusa-Dendrocalamus-Gigantochloa complex (Poaceae: Bambusoideae). *Mol. Phylogenet. Evol.*, **146**: 106758.
- Liu Y, Huo N, Dong L, Wang Y, Zhang S, Young HA, Feng X and G YQ. 2013. Complete chloroplast genome sequences of mongolia medicine *Artemisia frigida* and phylogenetic relationships with other plants. *PLoS One*, **8**: E57533.
- Lowe TM and Chan PP. 2016. Trnscan-Se on-line: integrating search and context for analysis of transfer rna genes. *Nucleic Acids Res.*, **44**: W54-W57.
- Lundberg J and Bremer K. 2003. A phylogenetic study of the order Asterales using one morphological and three molecular data sets. *IJPS*, **164**: 553-578.
- Mandel JR, Barker MS, Bayer RJ, Dikow RB, Gao TG, Jones KE, Keeley S, Kilian N, Ma H, Siniscalchi CM and Susanna A. 2017. The Compositae tree of life in the age of phylogenomics. *JSE.*, **55(4)**: pp.405-410.
- Mandel JR, Dikow RB, Siniscalchi CM, Thapa R, Watson LE and Funk VA. 2019. A fully resolved backbone phylogeny reveals numerous dispersals and explosive diversifications throughout the history of Asteraceae. *PNAS.*, **116(28)**: pp.14083-14088.
- Milligan BG, Hampton JN and Palmer JD. 1989. Dispersed repeats and structural reorganization in subclover chloroplast DNA. *Mol. Biol. Evol.*, **6**: 355-368.
- Ogihara Y, Terachi T and Sasakuma T. 1988. Intramolecular recombination of chloroplast genome mediated by short direct-repeat sequences in wheat species. *PNAS*, **85**: 8573-8577.
- Palmer D. 1983. Broken ties: Interlocking directorates and intercorporate coordination. *Adm. Sci. Q.* **1**:40-55.
- Palmer JD. 1991. Plastid chromosomes: structure and evolution. *Plant Mol. Biol.*, **7**: 5-53.
- Piya S and Nepal MP. 2013. Characterization of nuclear and chloroplast microsatellite markers for *Falcaria vulgaris* (Apiaceae). *Am. J. Plant Sci.*, **4**: 590-595.
- Raubeson LA and Jansen RK. 2005. **Chloroplast genomes of plants.** plant diversity and evolution: genotypic and phenotypic variation in higher plants. 45-68.
- Redwan R, Saidin A and Kumar S. 2015. Complete chloroplast genome sequence of MD-2 pineapple and its comparative analysis among nine other plants from the subclass Commelinidae. *Bmc Plant Biology*, **15**: 1-20.
- Salih RHM, Majeský L, Schwarzacher T, Gornall R and Heslop-Harrison P. 2017. Complete chloroplast genomes from apomictic *Taraxacum* (Asteraceae): identity and variation between three microspecies. *PLoS One*, **12**: E0168008
- Shaw J and Small RL. 2005. Chloroplast DNA phylogeny and phylogeography of the North American plums (*Prunus* subgenus *Prunus* section *Prunocerasus*, Rosaceae). *AJB.*, **92**: 2011-2030.
- Shaw J, Lickey EB, Schilling EE and Small RL. 2007. Comparison of whole chloroplast genome sequences to choose noncoding regions for phylogenetic studies in angiosperms: the tortoise and the hare III. *AJB.*, **94(3)**: pp.275-288.
- Sherman-Broyles S, Bombarely A, Grimwood J, Schmutz J and Doyle J. 2014. Complete plastome sequences from glycine syndetika and six additional perennial wild relatives of soybean. *G3*, **4**: 2023-2033.
- Shinozaki K, Ohme M, Tanaka M, Wakasugi T, Hayashida N, Matsubayashi T, Zaita N, Chunwongse J, Obokata J and Yamaguchi-Shinozaki K. 1986. The complete nucleotide sequence of the tobacco chloroplast genome: its gene organization and expression. *EMBO*, **5**: 2043-2049.
- Sonah H, Deshmukh RK, Sharma A, Singh VP, Gupta DK, Gacche RN, Rana JC, Singh NK and Sharma TR. 2011. Genome-wide distribution and organization of microsatellites in plants: an insight into marker development in brachypodium. *PLoS One*, **6**: E21298.
- Taberlet P, Coissac E, Pompanon F and Gielly L. 2007. Power and limitations of the chloroplast trnL (UAA) intron for plant DNA barcoding. *Nucleic Acids Res.* **35**: e14.
- Takahashi S, Furukawa T, Asano T, Terajima Y, Shimada H, Sugimoto A and Kadowaki K. 2005. Very close relationship of the chloroplast genomes among *Saccharum* species. *Theor. Appl. Genet.*, **110**: 1523-1529.
- Tamura K, Stecher G and Kumar S. 2021. Mega11: molecular evolutionary genetics analysis version 11. *Mol. Bio. Evol.*, **38**: 3022-3027.
- Thiel T, Michalek W and Varshney R. 2003. Exploiting EST databases for the development of cDNA derived microsatellite markers in barley (*Hordeum Vulgare* L.). *Mol. Bio. Evol.*, **4**: 411-422.
- Timme R, Kuehl EJ, Boore JL and Jansen RK. 2007. A comparative analysis of the *Lactuca* and *Helianthus* (Asteraceae) plastid genomes: identification of divergent regions and categorization of shared repeats. *AJB.*, **94**: 302-313.
- Timmis JN, Ayliffe MA, Huang CY and Martin W. 2004. Endosymbiotic gene transfer: organelle genomes forge eukaryotic chromosomes. *Nat. Rev. Genet.*, **5**: 123-135.
- Tremetsberger K, Gemeinholzer B, Zetzsche H, Blackmore S, Kilian N and Talavera S. 2013. Divergence time estimation in Cichorieae (Asteraceae) using a fossil-calibrated relaxed molecular clock. *Orga. Divers. Evol.*, **13(1)**: pp.1-13.
- Vendramin G, Degen B, Petit R, Anzidei M, Madaghiele A and Ziegenhagen B. 1999. High level of variation at abies alba chloroplast microsatellite loci. *Mol. Ecol.*, **8**: 1117-1126.
- Walker JF, Jansen RK, Zanis MJ and Emery NC. 2015. Sources of inversion variation in the small single copy (SSC) region of chloroplast genomes.
- Walker JF, Zanis MJ, Emery NC. 2014. Comparative analysis of complete chloroplast genome sequence and inversion variation in *Lasthenia burkei* (Madieae, Asteraceae). *AJB.* **101(4)**:722-9.

- Wang J, Duncan D, Shi Z, Zhang B. 2013. WEB-based gene set analysis toolkit (WebGestalt): update 2013. *Nucleic Acids Res.* **1;41(W1)**:W77-83.
- Wang RJ, Cheng CL, Chang CC, Wu CL, Su TM, Chaw SM. 2008. Dynamics and evolution of the inverted repeat-large single copy junctions in the chloroplast genomes of monocots. *BMC Evol. Biol.*, **8(1)**:1-4.
- Wang ZH, Peng H, Kilian N. 2013. Molecular phylogeny of the *Lactuca* alliance (Cichorieae subtribe Lactucinae, Asteraceae) with focus on their Chinese centre of diversity detects potential events of reticulation and chloroplast capture. *PLoS One.* **20;8(12)**:e82692.
- Wheeler GL, Dorman HE, Buchanan A, Challagundla L and Wallace LE. 2014. A review of the prevalence, utility, and caveats of using chloroplast simple sequence repeats for studies of plant biology. *APPS*, **2**: 1400059.
- Wicke S, Schneeweiss GM, Depamphilis CW, Müller KF and Quandt D. 2011. The evolution of the plastid chromosome in land plants: gene content, gene order, gene function. *Plant Mol. Biol.*, **76**: 273-297.
- Wittzell H. 1999. Chloroplast DNA variation and reticulate evolution in sexual and apomictic sections of dandelions. *Mol. Ecol.*, **8**: 2023-2035.
- Yaradua SS, Alzahrani DA, Abba A and Albokhary EJ. 2020. Characterization of the complete chloroplast genome of *Blepharis ciliaris* (Acanthoideae, Acanthaceae). *JJBS.*, **13**: 1995-6673.
- Zhang H, Li C, Miao H and Xiong S. 2013. Insights from the complete chloroplast genome into the evolution of *Sesamum indicum* L. *PLoS One*, **8**: E80508.
- Zhu A, Guo W, Gupta S, Fan W and Mower JP. 2016. Evolutionary dynamics of the plastid inverted repeat: the effects of expansion, contraction, and loss on substitution rates. *New Phytol.*, **209(4)**:1747-1756.

Cichorium-intybus

Alignment 1
Crepediastrum-denticulatum
Crepediastrum_denticulatum
9 alignments
Criteria: 70%, 100 bp
Regions: 231

Alignment 2
Crepediastrum-lanceolatum
Crepediastrum_lanceolatum
12 alignments
Criteria: 70%, 100 bp
Regions: 233

Alignment 3
Crepediastrum-sonchifolium
Crepediastrum_sonchifolium
12 alignments
Criteria: 70%, 100 bp
Regions: 235

Alignment 4
Dendroseris-berteroana
Dendroseris_berteroana
11 alignments
Criteria: 70%, 100 bp
Regions: 235

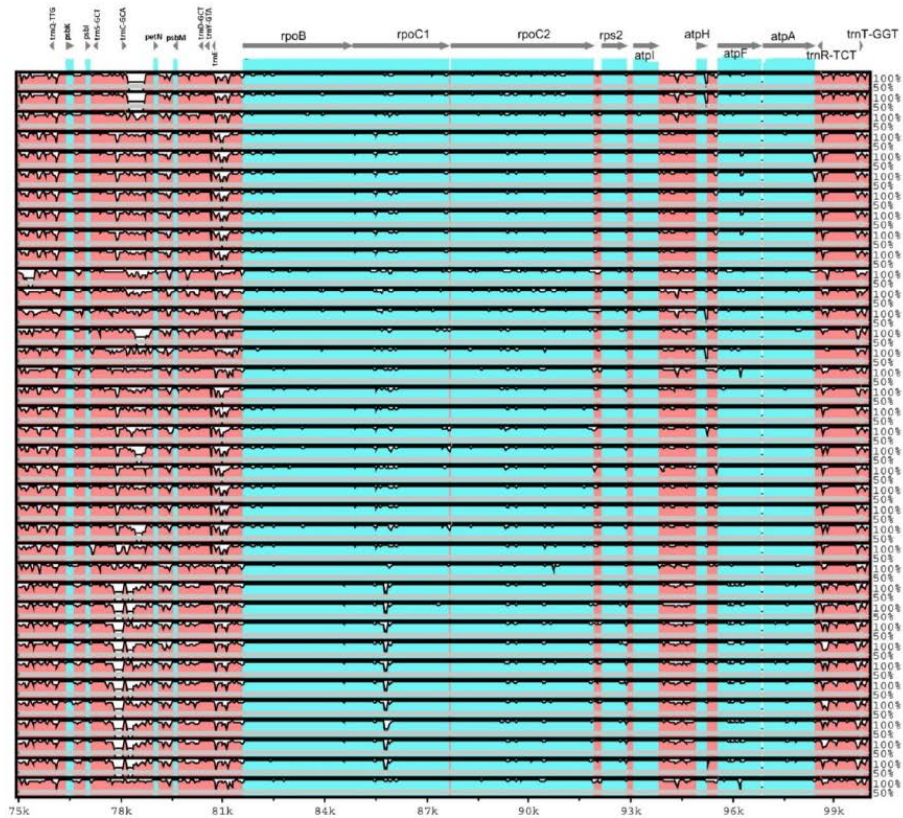
Alignment 5
Dendroseris-litoralis
Dendroseris_litoralis
11 alignments
Criteria: 70%, 100 bp
Regions: 234

Alignment 6
Dendroseris-macrantha
Dendroseris_macrantha
11 alignments
Criteria: 70%, 100 bp
Regions: 234

Alignment 7
Dendroseris-marginata
Dendroseris_marginata
11 alignments
Criteria: 70%, 100 bp
Regions: 234

Alignment 8
Dendroseris-micrantha
Dendroseris_micrantha
12 alignments
Criteria: 70%, 100 bp
Regions: 235

Alignment 9
Dendroseris-pinnata
Dendroseris_pinnata
10 alignments
Criteria: 70%, 100 bp
Regions: 234



Cichorium-intybus

Alignment 1
Crepediastrum-denticulatum
Crepediastrum_denticulatum
9 alignments
Criteria: 70%, 100 bp
Regions: 231

Alignment 2
Crepediastrum-lanceolatum
Crepediastrum_lanceolatum
12 alignments
Criteria: 70%, 100 bp
Regions: 233

Alignment 3
Crepediastrum-sonchifolium
Crepediastrum_sonchifolium
12 alignments
Criteria: 70%, 100 bp
Regions: 235

Alignment 4
Dendroseris-berteroana
Dendroseris_berteroana
11 alignments
Criteria: 70%, 100 bp
Regions: 235

Alignment 5
Dendroseris-litoralis
Dendroseris_litoralis
11 alignments
Criteria: 70%, 100 bp
Regions: 234

Alignment 6
Dendroseris-macrantha
Dendroseris_macrantha
11 alignments
Criteria: 70%, 100 bp
Regions: 234

Alignment 7
Dendroseris-marginata
Dendroseris_marginata
11 alignments
Criteria: 70%, 100 bp
Regions: 234

Alignment 8
Dendroseris-micrantha
Dendroseris_micrantha
12 alignments
Criteria: 70%, 100 bp
Regions: 235

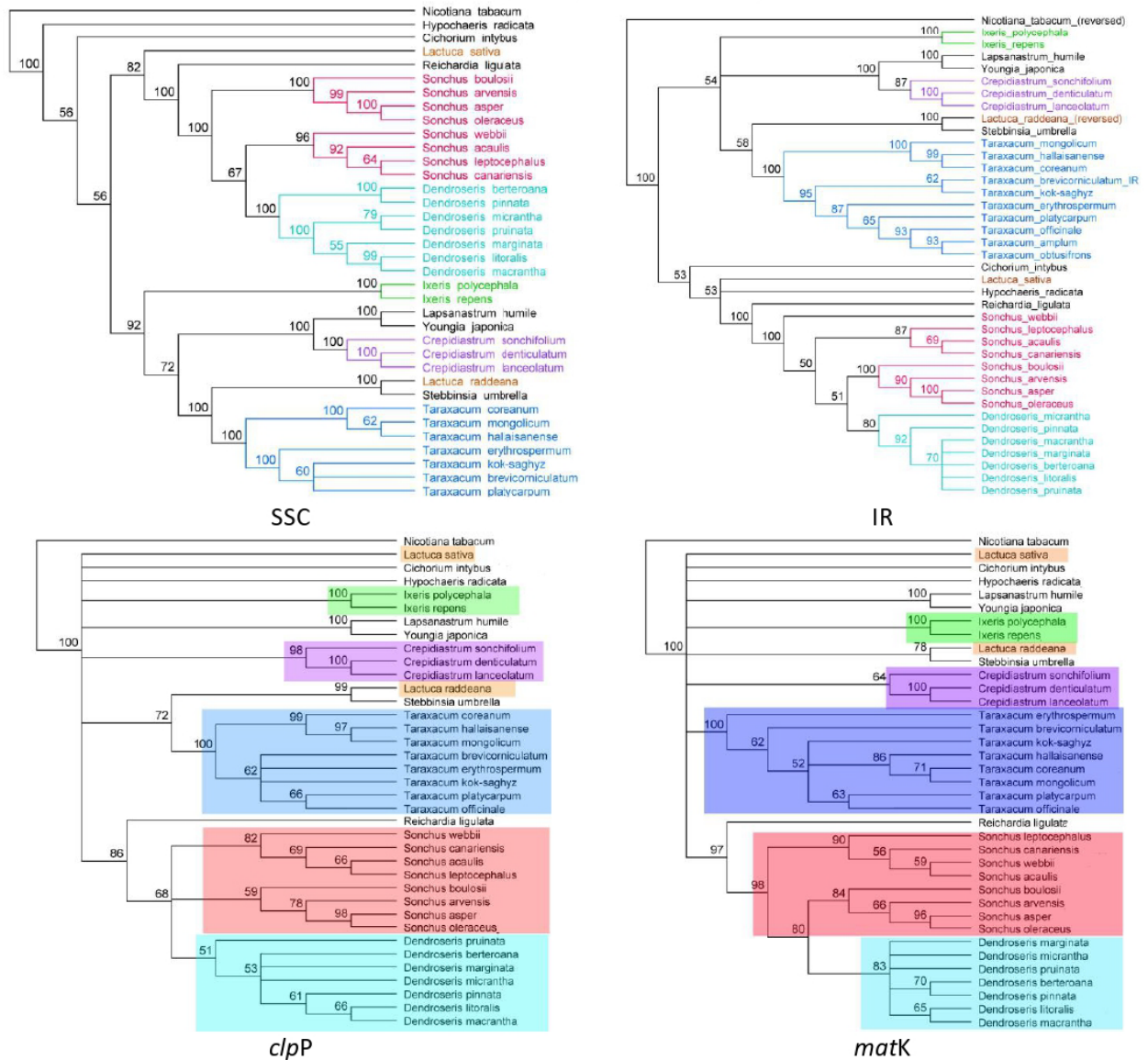
Alignment 9
Dendroseris-pinnata
Dendroseris_pinnata
10 alignments
Criteria: 70%, 100 bp
Regions: 234

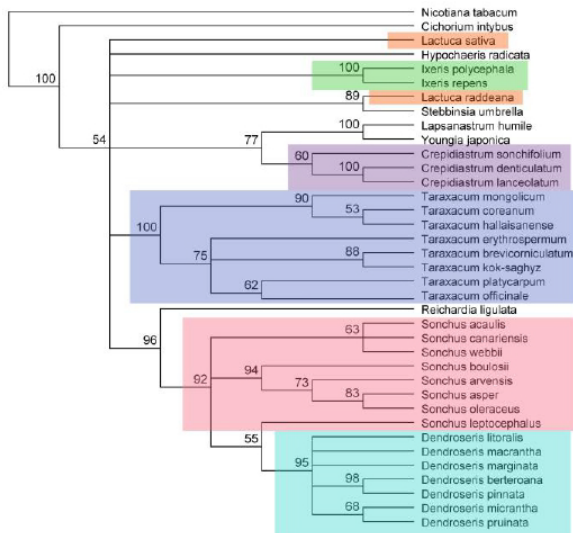


Appendix 2. The best-fitted model of evolution for the whole chloroplast genomes, LSC, SSC, IR and all polymorphic regions analyzed in this investigation. Each analysis involved 37 nucleotide sequences. The table shows the total positions in the final dataset for each model, and BIC scores (Bayesian Information Criterion) which describe the best substitution pattern for each models. Evolutionary analyses were conducted in MEGA11 (Tamura et al., 2021).

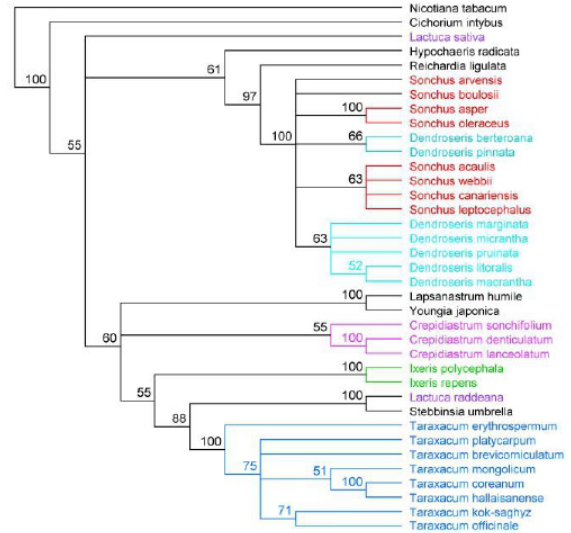
#	Region for phylogenetic analysis	Model	total number of positions in a dataset	BIC
1.	Whole genome	GTR+G	136267	1038336.106
2.	LSC	GTR+G	88267	938336.209
3.	SSC	GTR+G+I	21241	149228.126
4.	IR	GTR+G+I	26615	99146.24677
5.	clpP	T92+G	2375	16915.02854
6.	matK	GTR+G	1563	10589.44004
7.	ndhA	GTR+I	2356	14965.56373
8.	ndhF	GTR+G	2285	15021.52762
9.	rbcL	T92+G+I	1459	8143.670817
10.	rpoC1	GTR+G	2886	17048.15912
11.	rpoC2	GTR+G	4209	23413.47337
12.	ycf1	GTR+G+I	6433	53978.64294
13.	ycf2	GTR+G	7094	27720.25902
14.	ycf3	T92+G	2081	11034.21292
15.	atpI-atpH	GTR	1314	8510.050189
16.	ndhC-atpE	T92+G	153466	428169.7554
17.	ndhF-rpl32	GTR+G	1427	11827.82275
18.	petA-psbJ	T92+G	1092	8035.746059
19.	petB-petD	T92+G	2081	11034.21292
20.	petD-rps11	T92+G	1363	7936.536827
21.	petG-rpl20	T92+G	2648	14800.50839
22.	petN-psbM	GTR+G	5446	28823.03943
23.	psaA-ycf3	T92+G	895	6287.743009
24.	psaI-ycf4	T92	474	3577.660599
25.	psbA-trnK	T92+G	266	2272.706353
26.	psbE-petL	GTR+G	1514	10670.35651
27.	rpl32-trnL UAG	GTR+G	1186	10568.76413
28.	rps4-ndhJ	T92+G	3366	22221.07111
29.	rps12-clpP	T92	179	1741.680704
30.	rps15-ycf1	T92+G	574	5152.612542
31.	rps16 intron	T92+G	1268	8537.406947
32.	rps16-trnQ UUG	GTR+G	1377	11020.19351
33.	trnH GUG-psbA	HKY+G	649	6108.51606
34.	trnK-rps16	GTR+G	1102	8192.155682
35.	trnL-trnFGAA	GTR+G	761	5598.25329
36.	trnS-trnC GCA	T92+G	981	8039.29115
37.	trnT GGU-psbD	T92+G	1513	10824.81313
38.	trnT UGU-trnL	T92+G	971	7371.637396
39.	ycf3-trnS GAA	GTR+G	1042	7956.211414
40.	ycf4-cemA	T92+G	936	6352.32406
41.	ycf15-rps7	T92+G	2060	8562.738488

Appendix 3. Molecular Phylogenetic analysis by ML method. Each analysis involved 37 nucleotide sequences. Numbers on the nodes are bootstrap values based on 1000 replicates. *Nicotiana tabacum* is used as an out-group. Evolutionary analyses were conducted in MEGA11 (Tamura *et al.*, 2021).

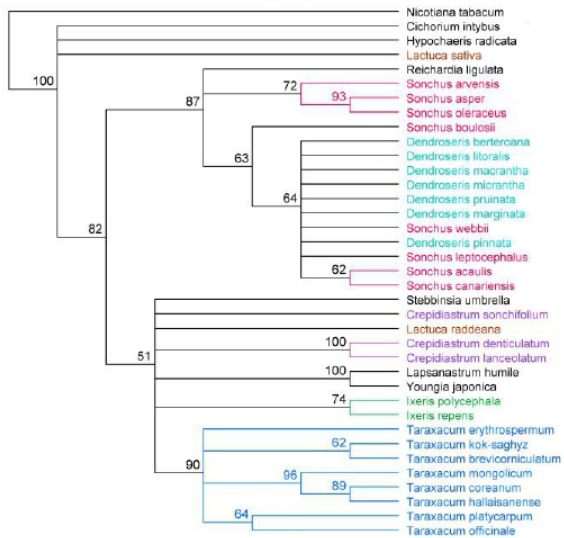




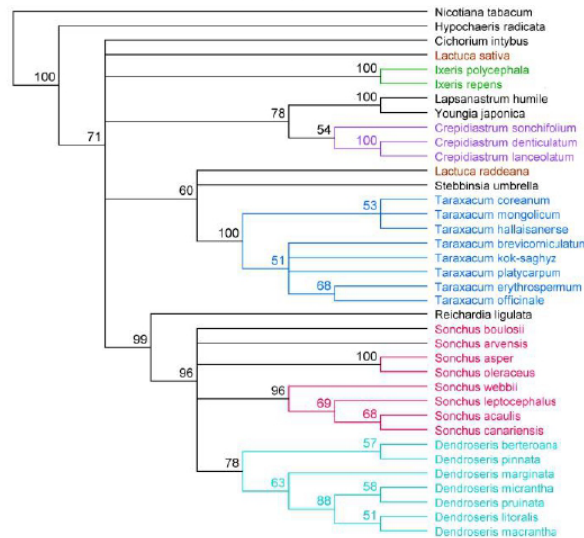
ndhA



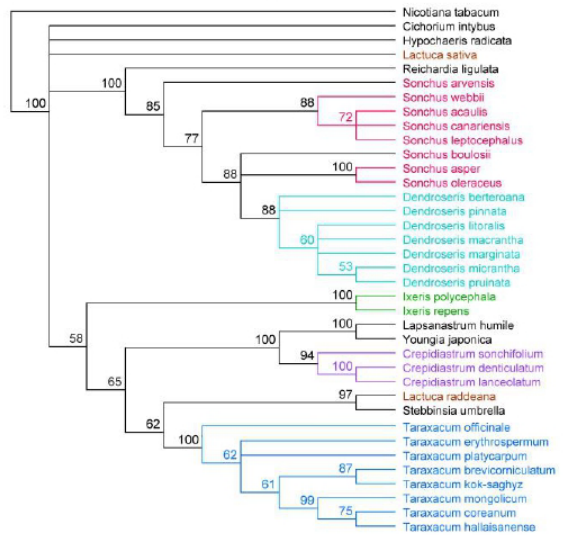
ndhF



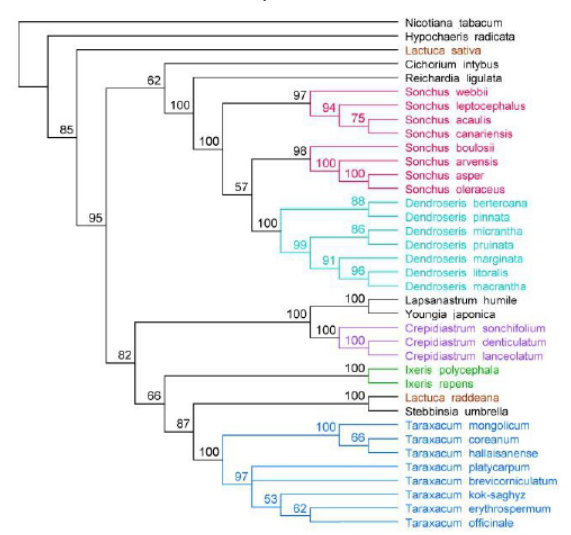
rbcL



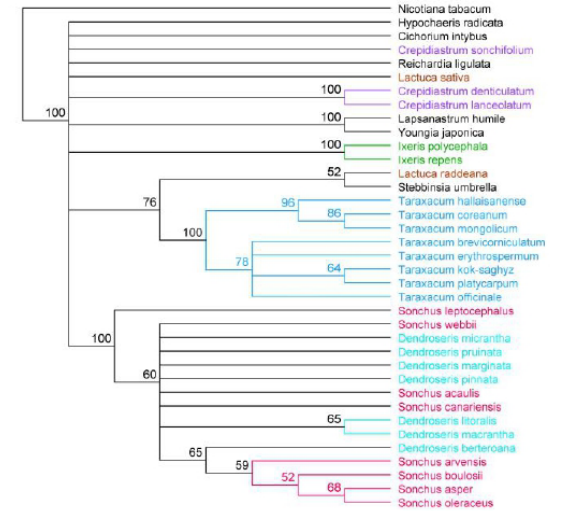
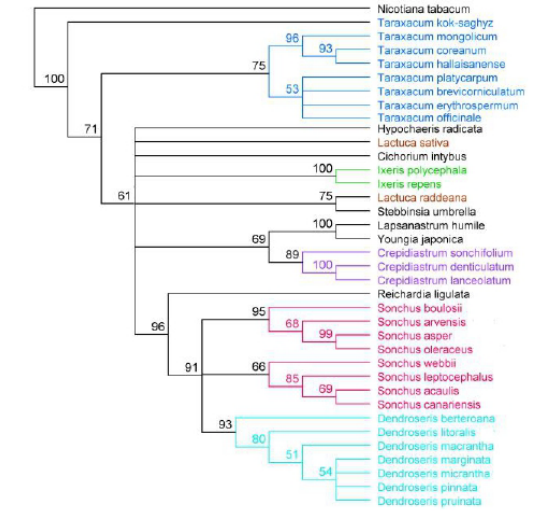
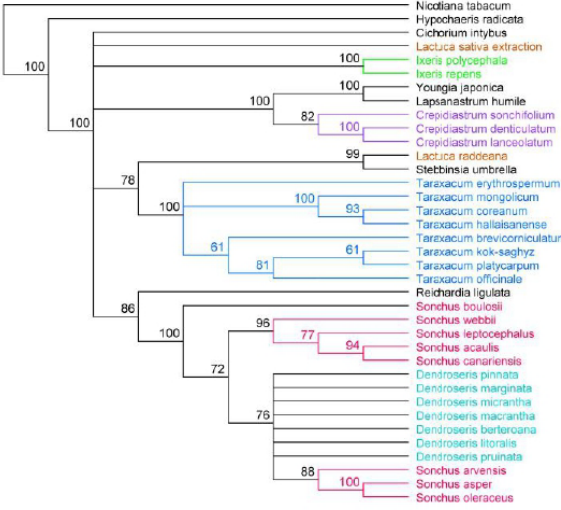
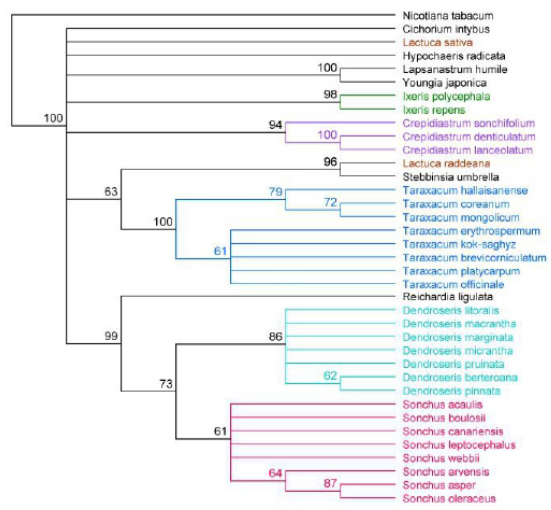
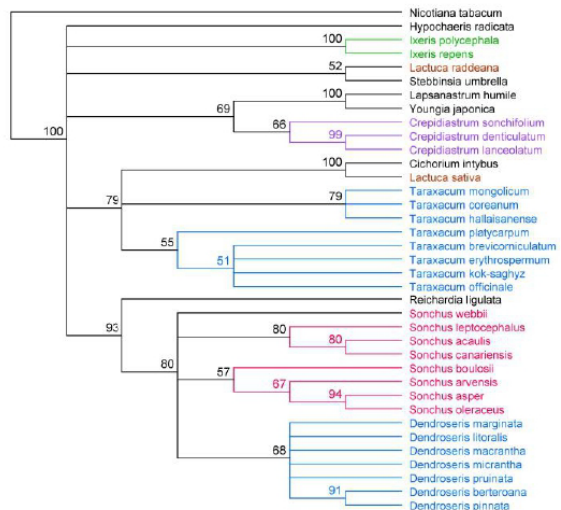
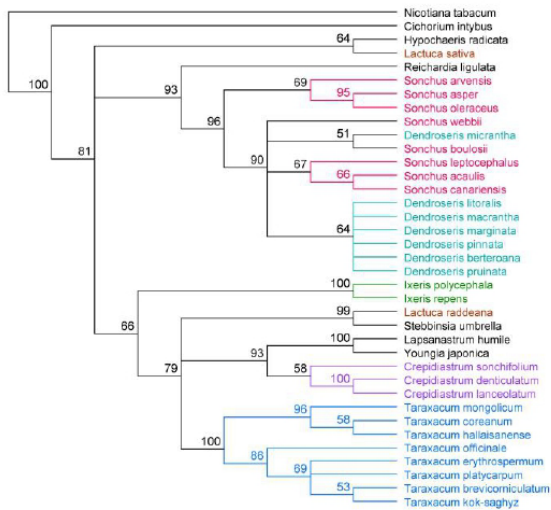
rpoC1

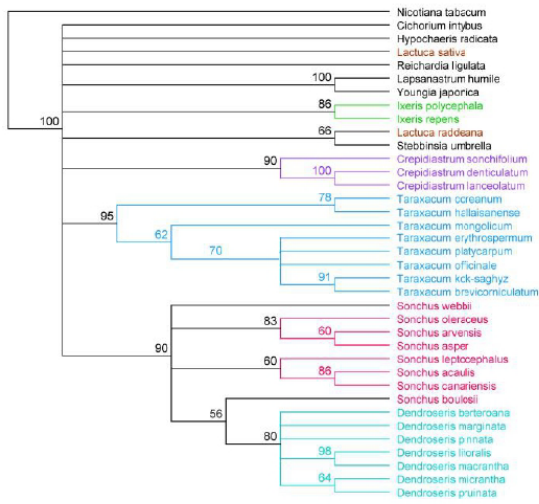


rpoC2

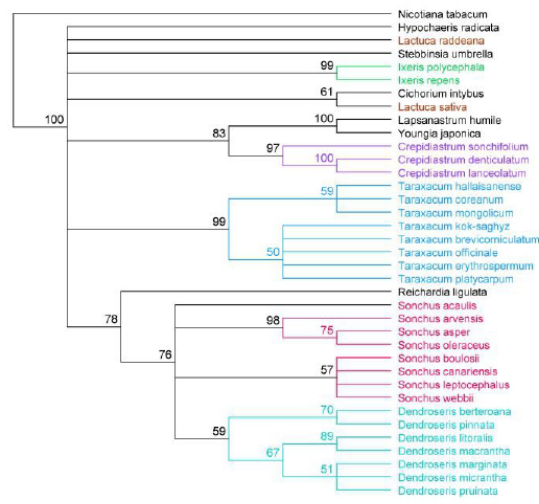


ycf1

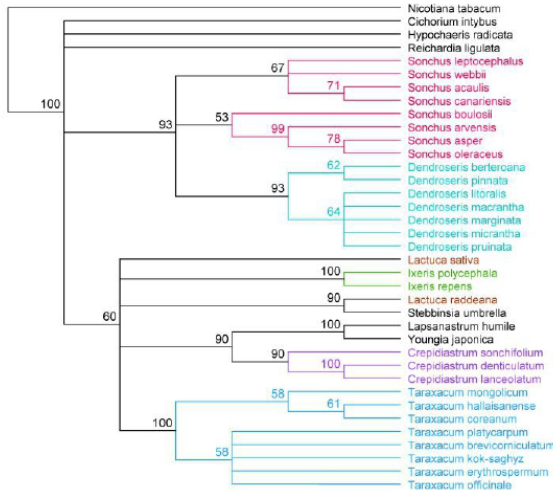




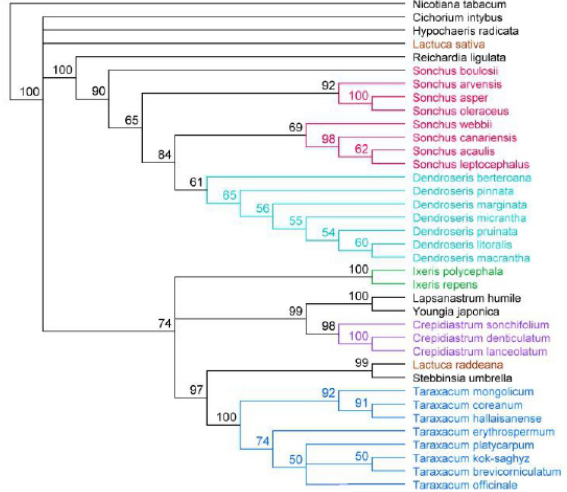
petB-petD



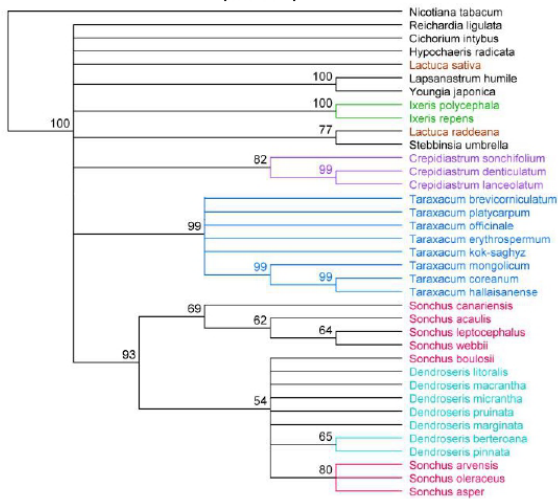
petD-rps11



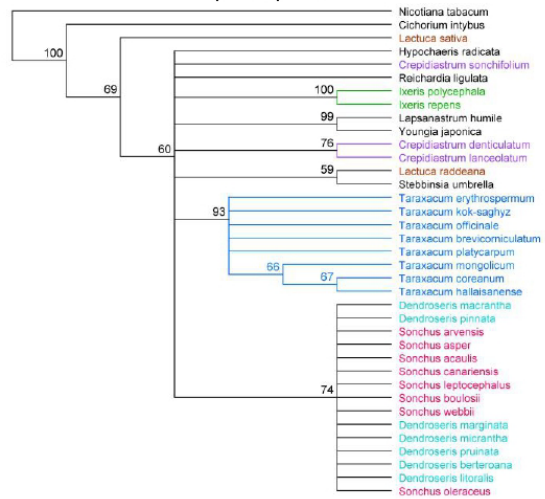
petG-rpl20



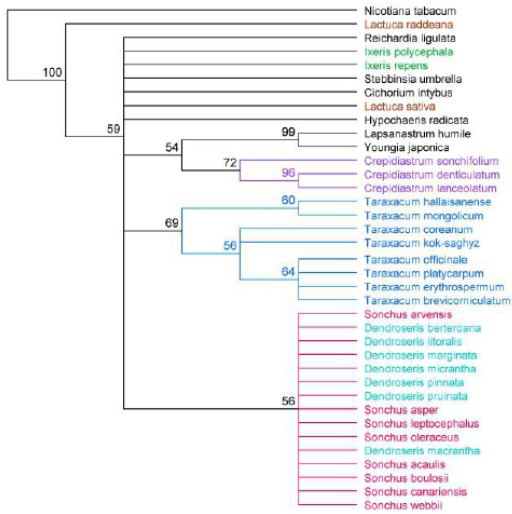
petN-psbM



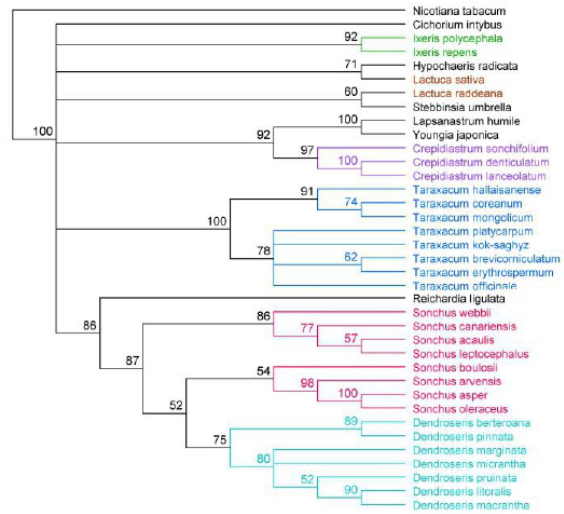
psaA-ycf3



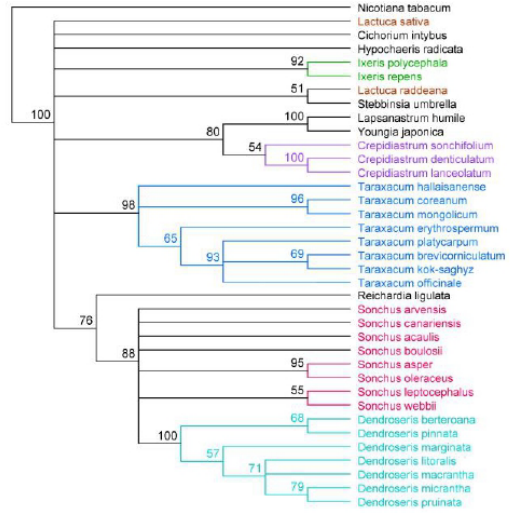
psal-ycf4



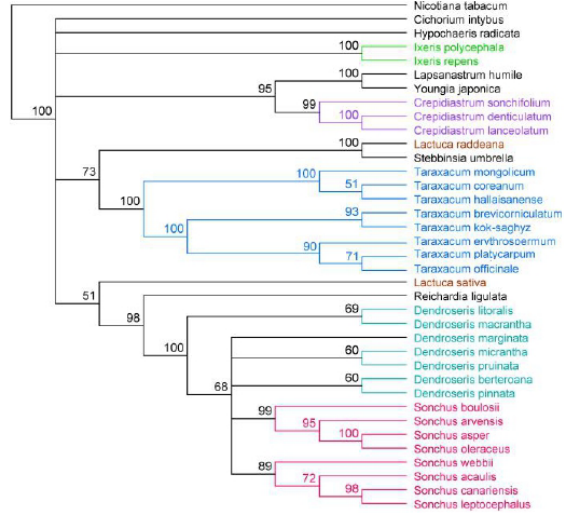
psbA-trnK



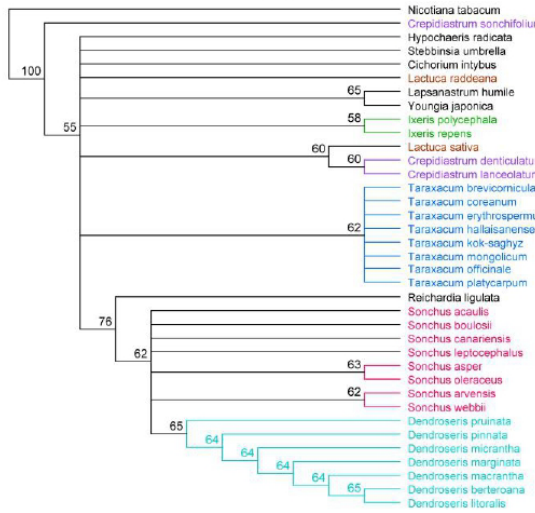
psbE-petL



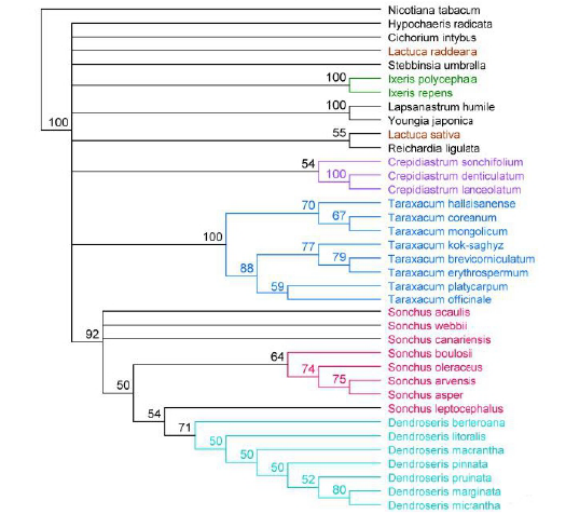
rpl32-trnL-UAG



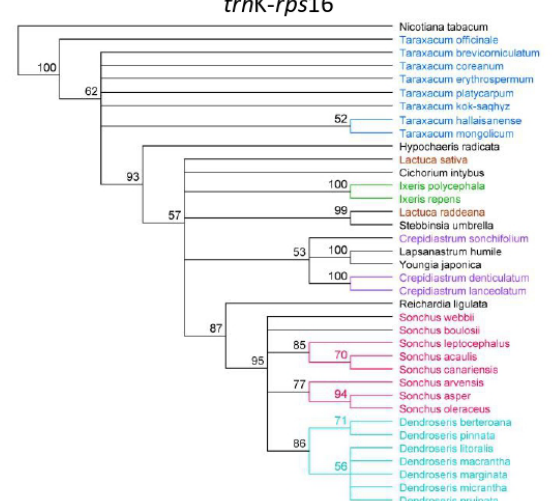
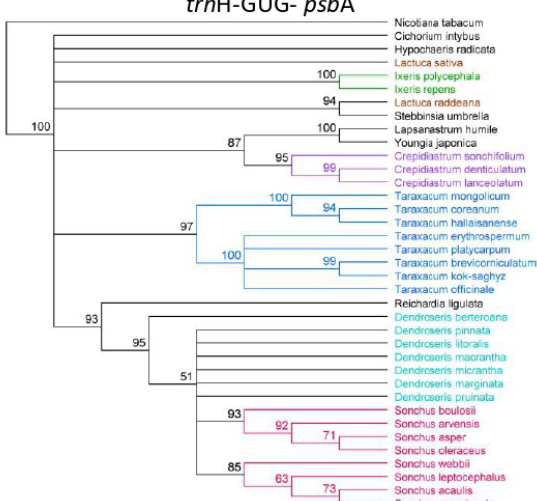
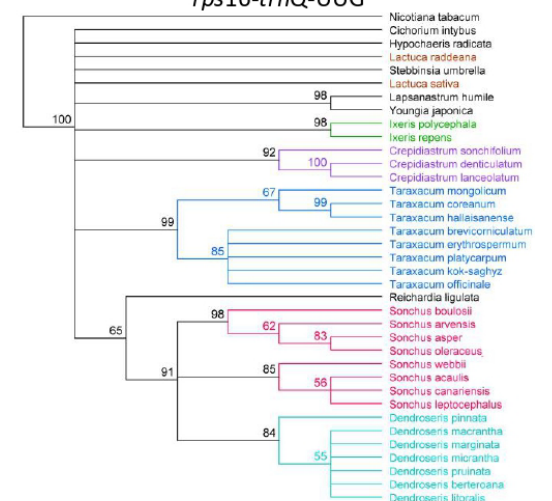
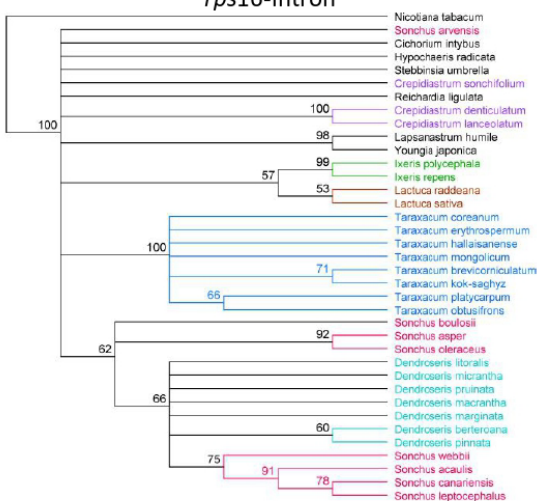
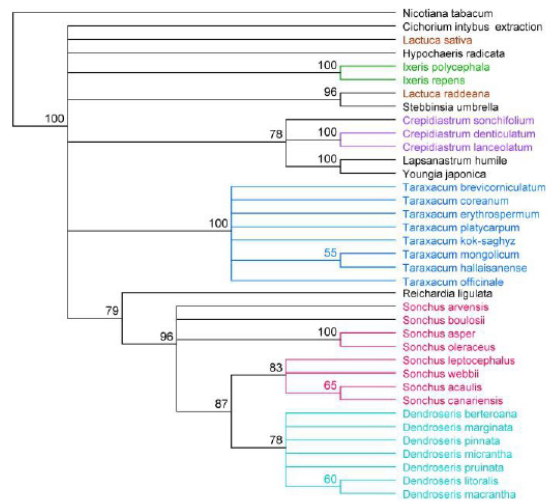
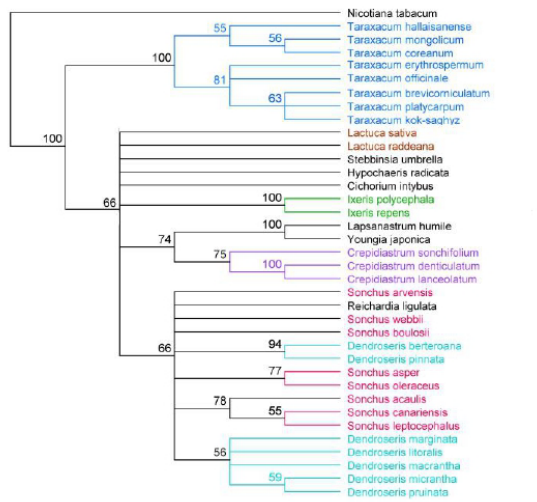
psb4-ndhJ

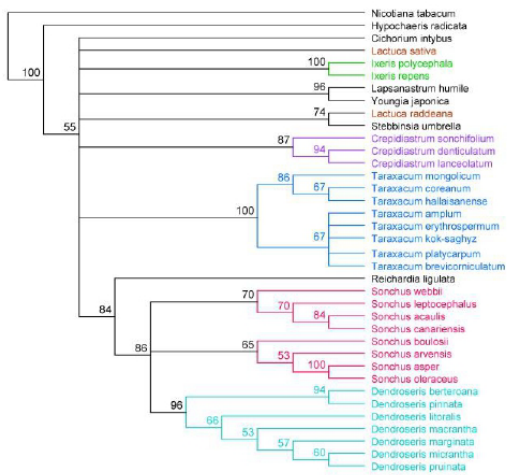


rpl12-clpP

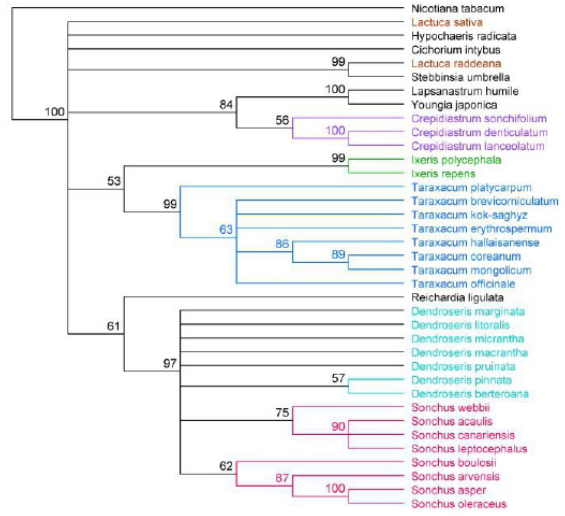


rps15-ycf1

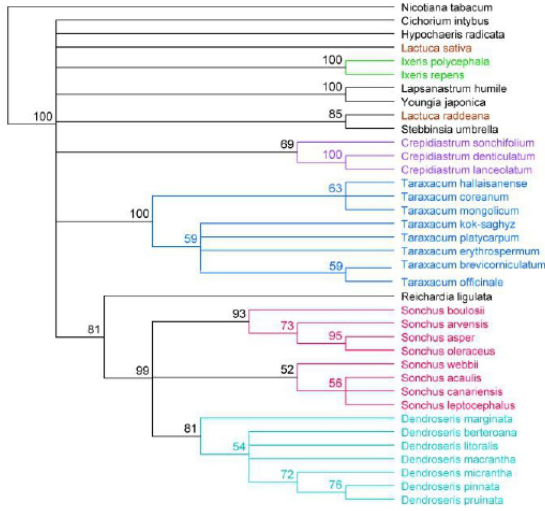




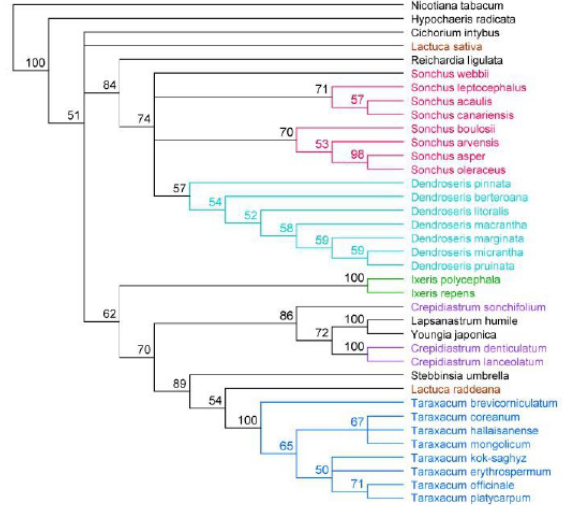
trnT-GGU-psbD



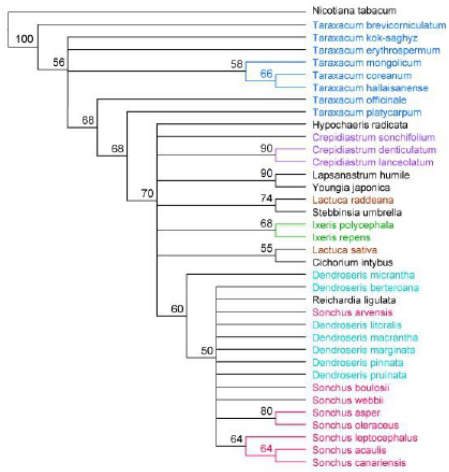
trnT-UGU-trnL-UAA



ycf3-trnS-GAA



ycf4-cemA



ycf15-rps7

Biochemical Profile of Five Species of Cultured Marine Microalgae¹

Teja. Gurugubelli*, Yedukondala Rao. Poturaju and Rukmini Sirisha. Imandi

Department of Marine Living Resources, Andhra University, Visakhapatnam, 530003, Andhra Pradesh, India

Received: December 8, 2022; Revised: February 1, 2023; Accepted: February 14, 2023

Abstract

Biochemical profile of five marine microalgae *Isochrysis galbana*, *Chaetoceros calcitrans*, *Tetraselmis suecica*, *Nannochloropsis oculata* and *Aphanocapsa* sp. was studied to understand the changes of the biochemical profile under different culture conditions, i.e. Conway and f/2 media at 20 and 30ppt salinities (‰). The microalgae culture was undertaken in the indoor facility with 24±1° C temperature, P^H 8.7±1, 24-hour illumination. Biochemical constituents of five algal species showed variations, the highest protein (26.86%) was recorded in *C. calcitrans* in f/2 medium at 30‰, lipid (32.00%) in *N. oculata* in Conway medium at 30‰, carbohydrate (32.06%) in *T. suecica* in Conway medium at 30‰ and ash (54.71%) in *C. calcitrans* in f/2 medium at 30‰. Among macro minerals, a high concentration of sodium (1.05g/100g) was recorded in *C. calcitrans* in Conway medium-20‰, potassium (4.12g/100g) in *C. calcitrans* in f/2 medium-30‰, calcium (1.57g/100g) in *C. calcitrans* in Conway medium-20‰, phosphorus (8.53g/100g) in *C. calcitrans* in Conway medium-20‰, magnesium (4.10g/100g) in *N. oculata* in f/2 medium-20‰. Among micro minerals, a high concentration of iron (1.44g/100g) was recorded in *C. calcitrans* in f/2 medium-30‰, zinc(0.95g/100g) in *I. galbana* in Conway medium-20‰, manganese(0.02g/100g) in *N. oculata* in Conway medium-30‰, copper(0.04g/100g) in *Aphanocapsa* sp. in Conway medium-30‰. Among fatty acids, C16:0 become the dominant saturated fatty acid (SFA) found in *I. galbana*, C16:1 become the dominant monounsaturated fatty acid (MUFA) found in *N. oculata* and C18:2 become the dominant polyunsaturated fatty acid (PUFA) found in *I. galbana* cultured in Conway medium-20‰. The biochemical composition of five microalgae indicated that these are potential food sources for humans, cattle and aquaculture industries.

Keywords: Marine microalgae, Biochemical profile, Fatty acids, Culture conditions, Conway and f/2 media, Different salinities.

1. Introduction

Microalgae are considered a very interesting source for the preparation of new food products and can be used to improve the nutritional value of conventional foods because of their valued biochemical composition (Niccolai *et al.*, 2019). Algal biomass is recognized as the most reliable raw source for balancing the ever-increasing global need for food, feed, biofuel and chemical production (Vandamme *et al.*, 2013; Foley *et al.*, 2011). Microalgae products that are commercially available appear to be valuable alternative food and feed products. However, because of the wide range of nutrient profiles, attention should be paid to product analytical characterization (Wild *et al.*, 2018). The utilization of microalgae and cyanobacteria as a food source and food supplement is known for centuries (Wells *et al.*, 2017). Microalgae are cultivated for human consumption in many Asian countries, Europe, USA, and Australia for several decades (Vigani *et al.*, 2015). Microalgae are also commercialized in the cosmetics industry or as animal feed (Huntley *et al.*, 2015; Ariede, 2017). Nowadays microalgal business sector is very dynamic with several new companies beginning every year; more than 150 companies of diverse scales, producing *Arthrospira*

(*spirulina*), are running in Europe and France (Verdelho Vieira, 2015).

Microalgae, being the pioneers of the food chain, are contributing to the important additives of many habitats on the earth. Algae have the potential to considerably contribute to the future nutritional pool; consequently, it is necessary to understand the chemical composition of the algal biomass. Furthermore, they have been recognized as a promising and economically valuable natural source of high-value products like as fatty acids, carotenoids and steroids in the food and aquaculture industries. (Cardozo *et al.*, 2007). In the last decade, research and the application of microalgae have increased significantly. Microalgae are a rich source of natural compounds that can be employed as functional components (Gouveia *et al.*, 2010).

There are numerous microalgae species available, but knowledge of their physicochemical characteristics and understanding their chemical composition is essential in screening because it allows researchers to target valuable compounds, pigments, antioxidants, polyunsaturated fatty acids (PUFAs) and other novel food compounds in the microalgae (Batista *et al.*, 2013). Microalgae represent a valuable source of a diverse range of lipids with a variety of applications. Polyunsaturated fatty acids, as well as the essential fatty acids linoleic acid, α -linolenic acid (ALA), g -linolenic acid (GLA), arachidonic acid (AA), and

* Corresponding author. e-mail: : tejaag@gmail.com ; drteja.gf@andhrauniversity.edu.in.

eicosapentaenoic acid (EPA), are especially interesting. Essential fatty acids are precursors to prostaglandins and their role in the pharmaceutical sector is growing (Borowitzka, 1988; Becker, 1994). Fatty acids are essential for the growth of marine organisms; hence they play a vital role in aquaculture. As a result, some microalgal species that are high in necessary PUFAs may be suggested as ideal for feeding marine animals. Micro-algae are few of the most significant feed sources in aquaculture because of their nutritional value and their ability to synthesize and store up higher quantities of ω 3-PUFAs (Patil *et al.*, 2007), like 22:6n-3 (DHA) and 20:5n-3 (EPA), two of the most vital essential fatty acids necessary for gametogenesis (Ehteshami *et al.*, 2011).

Over decades, enhancement of lipid content in microalgae by various means without altering the lipid productivity was targeted. Various changes in environmental, nutritional, and physiological conditions for the cultivation of microalgae, as well as genetic manipulations, have been attempted for enhanced lipid production (Kumar *et al.*, 2020). The microalgae chemical composition can vary with culture age, as well as variations in ambient (Fernández-Reiriz *et al.*, 1989) and culture conditions (Araújo and Garcia, 2005). The composition of the growth medium is a critical aspect in producing the biomass with specific desired features. It is well understood the relation between the nutrients added and biomass composition (Becker, 1994). The growth medium, on the other hand, has an impact on the specific growth rate and maximal level of biomass production. A nutrient deficiency in the medium can cause the algae to adapt its metabolism to new environmental conditions. A modification in the growth medium alters the biochemical profile of the biomass, primarily proteins, lipids, carbohydrates and pigments (Sánchez *et al.*, 2000). In addition, a batch culture is under continuous chemical change because of the interaction of the organisms with the growth medium. These changes can impact cell metabolism and subsequently their chemical composition (Lourenço *et al.*, 2002).

The present study was designed to evaluate the biochemical profile of five species of microalgae cultured in two different culture media at two different salinities.

2. Materials and methods

2.1. Culture conditions

The stock cultures of five marine microalgal species *I. galbana*, *C. calcitrans*, *T. suecica*, *N. oculata* and *Aphanocapsa* sp. used in this study were procured from the Central Marine Fisheries Research Institute (CMFRI), Visakhapatnam, Andhra Pradesh, India. The samples were cultured in Walne medium (Walne, 1970) and subjected to consecutive rounds of serial dilution and streaked on agar plates and test tube slants. The isolates were then maintained on agar plates and in cotton plugged test tube slants at $24 \pm 1^\circ \text{C}$, 12 h light:12h dark photoperiod with an intensity of 60-80 $\mu\text{mol photons.m}^{-2}.\text{s}^{-1}$ light. The stock cultures of microalgae were maintained in 50ml conical flasks stoppered with cotton plugs and were sub-cultured in fresh medium for every 2 weeks. The microalgal culture was undertaken in Conway (Walne, 1970) and f/2 (Guillard and Rytner 1962) media at two different

salinities (20ppt and 30ppt) to test the variations of biochemical composition under different culture conditions. The treatments (culture conditions) expressed in the table as conway-20ppt and 30ppt are for the algae cultured in Conway media at 20ppt and 30ppt salinity, respectively. Similarly, the treatments f/2-20ppt and 30ppt are for the algae cultured in f/2 media at 20ppt and 30ppt salinity, respectively. The algal biomass used for fatty acids was obtained from algae cultured in Conway medium at 20ppt salinity to test the fatty acid profile in fixed ambient conditions. The microalgae culture was undertaken in the indoor facility from initial culture volume of 100 ml, 250 ml and 2 L in conical sterilized glass conical flask then up to 20 L in a PET (Polyethylene terephthalate) jars at $24 \pm 1^\circ \text{C}$ temperature, P^{H} 8.7 ± 1 and 24-hours illumination with the intensity of 80 $\mu\text{mol photons.m}^{-2}.\text{s}^{-1}$ for about 4 days. Then indoor mass culture was carried out in 200 L round vertical Fiberglass Reinforced Plastic (FRP) transparent tank by using the 20 L culture volume as seed culture under the same conditions. The exponential growth phase of algal cultures was observed according to the cell counts using Neubauer haemocytometer under a bright-field contrast microscope (Olympus CH20i magnification 400-1000X).

2.2. Harvest of algal biomass and drying

Algal biomass was harvested when cells were at the end of their exponential phase (5days) of culture by adding 0.2g of aluminium sulphate for one litre of culture volume, based on a result obtained from the bench level experiment on this study and also the earlier experiments of Shelef *et al.* (1984) and Michael Babu *et al.* (2013). The alum added culture was aerated for 1hour. After the aeration, culture was left undisturbed for 30-60 min. for complete settlement of biomass.

The flocculated algal mass was collected, and the obtained wet biomass was rinsed thoroughly with distilled water to remove the salt and excess alum, then filtered through Whatman no.1 filter paper. The microalgal paste obtained was dried in a precision hot air oven (Kemi) at $45\text{-}50^\circ \text{C}$ temperature for 48h to get the dry biomass. This dry biomass was stored in a desiccator in a cool place and later used for the estimation of biochemical analysis.

The known weight of dried algal mass was fine powdered using agate mortar and pestle. The required quantity of powder was taken for the quantitative estimation of protein, lipid, carbohydrate, ash, minerals and fatty acids. This study was undertaken from June 2017 to 2018 in the dept. of M.L.R., A.U., Andhra Pradesh and NIN, Hyderabad, Telangana, India.

2.3. Biochemical composition

Estimation of protein was followed by the Folin Ciocalteu method of Lowry *et al.* (1951). Protein was extracted with 1N NaOH using Bovine serum albumin as standard. Lipid extraction was performed by modified Bligh and Dyer (1959) by soaking the samples in chloroform: methanol (2:1). The carbohydrate estimation was by the Anthrone method of Carroll *et al.* (1956) using 5% trichloroacetic acid. Glucose was the standard for this analysis. Ash was determined by burning the tissue powder (1g) for 12h in a silica crucible in a muffle furnace at 550°C according to the AOAC (2000) method. Then the sample residues were placed in a desiccator to cool and

then the weight was recorded. The results were expressed as a percentage of dry weight.

2.4. Sample preparation and estimation of minerals

Minerals were assayed using the Perkin Elmer ELAN 9000 ICP-MS (Inductively Coupled Plasma mass spectrometry) followed by the protocol of Rodenas de la Rocha *et al.* 2009. The microwave-assisted sample digestion was followed by Smith and Arsenault (1996).

The values were expressed in gm/100g.

2.5. FAME preparation and estimation of fatty acids

The lipid extraction was performed by the modified Bligh and Dyer method (1959). The preparation for FAME was followed by a procedure similar to that of D'Oca *et al.* (2011b). Fatty acid methyl ester (FAME) analysis was carried out by Gas Chromatography and Mass Spectrometry (GC-MS) on SUPELCO SP- 2330 chromatograph using flame ionization for detection. The fatty acid structures were validated by comparing their retention times and fragmentation patterns with gas chromatography and mass spectrometry (GC-MS) standards of their methyl esters (Figure. 1 and Table 4). The results were expressed in mg/g.

2.6. Statistical analysis:

All analyses were performed in triplicates. Protein, lipid, carbohydrate and ash data are expressed as mean \pm SD. Statistical analysis for proximate composition data was carried out by using Origin Pro 8.

3. Results and discussion

There are numerous microalgal species available, and understanding their chemical composition is essential in screening because it allows researchers to target valuable compounds, pigments, antioxidants, polyunsaturated fatty acids (PUFAs) and other compounds in the microalgae (Batista *et al.*, 2013). The synthesis and accumulation of cell constituents such as pigments, proteins, carbohydrates, amino acids, nucleic acids and lipids can be influenced by nitrogen availability (Rodriguez-Lopez *et al.*, 1980; Utting, 1985). The majority of the nitrogen in cells is in the form of proteins. As a result, nitrogen intake by the medium has a direct impact on protein synthesis. In the exponential phase of cell growth, protein synthesis is predominant over neutral lipid accumulation (Sukenic and Wahnon, 1991).

The protein content of five microalgal species cultured under different mediums and salinities showed variations. The highest protein (26.85%) was reported in *C. calcitrans* cultured in f/2 medium at 30ppt salinity, whereas the lowest value (8.5%) was reported in *Apanocapsa* sp. cultured in Conway medium at 30ppt salinity (Table 2). The protein content of five species of microalgae in the current study was almost within the range of values found in earlier studies for the different microalgal species cultured under different conditions (Coutteau, 1996; Sánchez *et al.*, 2000; Reboloso-Fuentes *et al.*, 2001; Becker, 2007; Chin Ming *et al.*, 2012; Batista *et al.*, 2013; Bi & He 2013; Eshak & Omar 2017; Niccolai *et al.*, 2019). But relatively highest content of protein was reported in previous studies on various microalgal species cultured under different conditions (Vargas *et al.*, 1998; Phatarpekar *et al.*, 2000; Lourenço *et al.*, 2002; Batista *et al.*, 2013; Bi & He 2013; Wild *et al.*, 2018; Niccolai *et al.*, 2019; Reitan *et al.*, 2021).

et al., 2013; Bi & He 2013; Wild *et al.*, 2018; Niccolai *et al.*, 2019). These variations may be attributed to the culture conditions and species specificity.

Carbohydrates are the first of the organic nutrients to be used to generate required energy (Heath, 1987). They act as precursors to the non-essential amino acids and nutrients, which are metabolic intermediates essential for growth (NRC, 1993). The carbohydrate content in five microalgal species varies from 16.44% to 32.06%. The highest carbohydrate content was reported in *T. suecica* cultured in Conway medium at 30ppt salinity, whereas the lowest was reported in *C. calcitrans* cultured in f/2 medium at 30ppt salinity (Table 2). The carbohydrate content of five microalgal species in the current study was more or less similar to that of the carbohydrate found in other microalgal species studied by earlier authors (Vargas *et al.*, 1998; Phatarpekar *et al.*, 2000; Reboloso-Fuentes *et al.*, 2001; Lourenço *et al.*, 2002; Becker, 2007; Chin Ming *et al.*, 2012; Batista *et al.*, 2013; Bi & He 2013; Eshak & Omar 2017; Wild *et al.*, 2018; Niccolai *et al.*, 2019; Reitan *et al.*, 2021).

Lipid composition and yield are affected by the growth variables such as growth phase (Xu *et al.*, 2008), culture medium composition (Valenzuela-Espinoza *et al.*, 2002), irradiance (Thompson *et al.*, 1993), and temperature (Renaud *et al.*, 2002). Under nitrogen limiting conditions, lipid content increases dramatically in all microalgal species (Hu *et al.*, 2008). Neutral lipid production was high during the stationary phase (Doan *et al.*, 2011). The lipid content of five microalgal species in the current study showed variations. The highest lipid (32.00%) was reported in *N. oculata* cultured in Conway medium at 30ppt salinity, whereas the lowest value (2.00%) was noticed in *C. calcitrans* cultured in f/2 medium at 30ppt salinity (Table 2). The values found in the present study are almost similar to that of earlier results on various cultured microalgal species (Coutteau, 1996; Vargas *et al.*, 1998; Phatarpekar *et al.*, 2000; Reboloso-Fuentes *et al.*, 2001; Lourenço *et al.*, 2002; Becker, 2007; Huerlimann *et al.*, 2010; Chin Ming *et al.*, 2012; Batista *et al.*, 2013; Wild *et al.*, 2018; Niccolai *et al.*, 2019; Reitan *et al.*, 2021). But relatively highest lipid content was found in some microalgae when compared to values obtained in the present study (Phatarpekar *et al.*, 2000; Batista *et al.*, 2013). These variations may be attributed to the culture medium, salinity and species variations.

Ash content of photosynthetic microalgae is an important criterion for determining their cultivation efficiency (Liu *et al.*, 2015). Ash indicated the mineral content of a plant/animal (Khawaja, 1966). The ash content of five microalgal species showed variations in this study. The highest ash (54.71%) was reported in *C. calcitrans* cultured in f/2 medium at 30ppt salinity, whereas the lowest (15.75%) was reported in *N. oculata* cultured in Conway medium at 30ppt salinity (Table 2). The values found in the present study almost equal values found in earlier publications (Coutteau, 1996; Batista *et al.*, 2013; Bi & He 2013; Kent *et al.*, 2015; Eshak & Omar 2017; Molino *et al.*, 2018; Niccolai *et al.*, 2019). On the contrary to the present study, relatively lower values were found in some of the microalgal species (Coutteau, 1996; Vargas *et al.*, 1998; Reboloso-Fuentes *et al.*, 2001; Kent *et al.*, 2015; Zheng *et al.*, 2017; Wild *et al.*, 2018; Molino *et al.*, 2018; Metsoviti *et al.*, 2019; Niccolai *et al.*, 2019).

These variations may be attributed to culture conditions and species variations.

3.1. Statistical analysis:

Analysis of variance (two-way) of biochemical constituents was statistically significant ($p < 0.05$) between the species, but not significant ($p > 0.05$) within the species.

Table 2. Percentage composition of biochemical constituents in five microalgae under different culture conditions

Protein					
Treatments	<i>I. galbana</i>	<i>C. Calcitrans</i>	<i>T. suecica</i>	<i>N. oculata</i>	<i>Aphanocapsa</i> sp.
Conway-20 ppt	20.53±0.8632	20.86±0.1665	8.90±0.8326	20.22±0.7400	17.94±0.2203
f/2-20 ppt	16.25±0.3780	23.52±0.5594	13.61±0.4969	18.14±0.1400	21.42±0.4046
Conway-30 ppt	17.16±0.3601	24.24±0.7076	11.88±0.5556	22.68±0.5011	8.15±0.5507
f/2-30 ppt	22.70±0.7270	26.85±0.7335	12.13±0.2203	20.80±0.5768	20.08±0.4454
Lipid					
Treatments	<i>I. galbana</i>	<i>C. Calcitrans</i>	<i>T. suecica</i>	<i>N. oculata</i>	<i>Aphanocapsa</i> sp.
Conway-20 ppt	22.50±0.6132	7.00±0.800	22.5±0.5204	24.00±0.7000	13.28±0.6050
f/2-20 ppt	19.00±0.4500	5.17±0.2052	21.67±0.72	26.00±0.4473	11.13±0.1401
Conway-30 ppt	21.85±0.9765	9.22±0.3500	25.28±0.53	32.00±0.5766	12.00±0.8500
f/2-30 ppt	18.00±0.5550	2.00±0.4895	24±0.4358	29.00±0.7211	9.00±0.8660
Carbohydrate					
Treatments	<i>I. galbana</i>	<i>C. Calcitrans</i>	<i>T. suecica</i>	<i>N. oculata</i>	<i>Aphanocapsa</i> sp.
Conway-20 ppt	29.94±0.1305	17.65±0.9073	32.02±0.0550	31.43±0.0450	29.62±0.7965
f/2-20 ppt	32.05±0.2514	23.81±0.1101	31.84±0.0251	30.52±0.7597	31.11±0.2311
Conway-30 ppt	30.73±0.0152	17.84±0.4794	32.06±0.0400	29.57±0.9814	31.56±0.10583
f/2-30 ppt	29.15±0.9901	16.44±0.4557	31.72±0.0208	31.42±0.0763	31.56±0.0300
Ash					
Treatments	<i>I. galbana</i>	<i>C. Calcitrans</i>	<i>T. suecica</i>	<i>N. oculata</i>	<i>Aphanocapsa</i> sp.
Conway-20 ppt	27.03±0.7211	54.49±0.5507	36.58±0.7402	24.35±0.7272	39.16±0.0252
f/2-20 ppt	32.70±0.5507	47.50±0.7271	32.88±0.1302	25.34±0.5507	36.34±0.7211
Conway-30 ppt	30.26±0.2313	48.70±0.8200	30.78±0.0762	15.75±0.2312	48.29±0.5507
f/2-30 ppt	30.15±0.1410	54.71±0.8632	32.15±0.5507	18.78±0.4960	39.36±0.8300

Minerals are necessary nutrients that are found in various enzymes and metabolism processes. Minerals aid as structural elements of soft tissue. The minerals are important for maintaining osmotic P^H , osmotic pressure, water balance and glucose/amino acid active transportation (Glover *et al.*, 2002). Minerals showed variations in the five species of microalgae cultured in the present study. The highest values of sodium, calcium, phosphorous and potassium were reported in *C. calcitrans* cultured in Conway medium at 20ppt salinity and f/2 medium at 20ppt salinity respectively, whereas the highest value of magnesium was recorded in *N. oculata* in f/2 medium at 20 ppt salinity (Table 3). For the micro minerals, the

highest value of Iron was noticed in *C. calcitrans* cultured in f/2 medium at 30ppt salinity. Zinc in *I. galbana* cultured in Conway medium at 20ppt salinity, Manganese in *N. oculata* cultured in Conway medium at 30ppt salinity, copper in *Aphanocapsa* sp. cultured in Conway medium at 30ppt salinity (Table 3). The results agree with the earlier works on various microalgal species (Fabregas & Herrero, 1986; Reboloso-Fuentes *et al.*, 2001; Batista *et al.*, 2013; Bi & He 2013; Wild *et al.*, 2018). On contrary to the present results, low values were noticed in some microalgal species (Moura-Junior *et al.*, 2007). These variations may be attributed to the mineral composition of media and species specificity.

Table 3. Minerals in five microalgae under different culture conditions (g/100g)

<i>a. I. galbana</i>									
Treatments	Macro minerals					Micro minerals			
	Sodium	Potassium	Calcium	Phosphorus	Magnesium	Iron	Zinc	Manganese	Copper
Conway 20 ppt	0.61	2.75	0.75	6.14	0.60	0.37	0.95	0.007	0.01
f/2 20 ppt	0.28	1.33	1.46	0.65	0.23	0.49	0.04	0.002	0.01
Conway 30 ppt	0.44	2.50	0.96	2.47	0.55	0.24	0.44	0.009	0.01
f/2 30 ppt	0.43	2.10	0.43	1.15	0.54	0.81	0.08	0.006	0.01
<i>b. C. calcitrans</i>									
Treatments	Macro minerals					Micro minerals			
	Sodium	Potassium	Calcium	Phosphorus	Magnesium	Iron	Zinc	Manganese	Copper
Conway 20 ppt	1.05	3.97	1.57	8.53	1.60	0.47	0.06	0.01	0.04
f/2 20 ppt	1.00	1.60	0.86	0.60	0.29	0.59	0.14	0.004	0.01
Conway 30 ppt	0.27	1.57	0.88	7.33	0.46	0.23	0.03	0.01	0.01
f/2 30 ppt	0.50	4.12	0.78	1.03	1.29	1.44	0.05	0.009	0.01
<i>c. T. suecica</i>									
Treatments	Macro minerals					Micro minerals			
	Sodium	Potassium	Calcium	Phosphorus	Magnesium	Iron	Zinc	Manganese	Copper
Conway 20 ppt	0.83	1.49	1.51	1.90	1.54	0.15	0.03	0.004	0.009
f/2 20 ppt	0.41	2.29	0.92	1.00	0.19	1.15	0.10	0.007	0.02
Conway 30 ppt	0.10	3.29	1.08	4.61	0.46	0.30	0.32	0.008	0.01
f/2 30 ppt	0.46	1.22	1.01	0.84	0.20	0.83	0.07	0.002	0.02
<i>d. N. oculata</i>									
Treatments	Macro minerals					Micro minerals			
	Sodium	Potassium	Calcium	Phosphorus	Magnesium	Iron	Zinc	Manganese	Copper
Conway 20 ppt	0.28	3.24	0.92	7.49	0.51	0.36	0.46	0.01	0.01
f/2 20 ppt	0.58	1.50	0.36	0.61	4.10	0.48	0.08	0.005	0.01
Conway 30 ppt	0.28	1.32	1.24	6.90	1.01	0.44	0.63	0.02	0.007
f/2 30 ppt	0.21	1.73	0.47	0.86	2.12	0.64	0.07	0.008	0.01
<i>e. Aphanocapsa sp.</i>									
Treatments	Macro minerals					Micro minerals			
	Sodium	Potassium	Calcium	Phosphorus	Magnesium	Iron	Zinc	Manganese	Copper
Conway 20 ppt	0.11	2.67	1.14	2.80	0.94	0.54	0.29	0.01	0.03
f/2 20 ppt	0.24	3.16	0.34	0.98	1.98	1.19	0.08	0.01	0.01
Conway 30 ppt	0.17	1.90	0.26	1.21	0.59	0.06	0.07	0.001	0.04
f/2 30 ppt	0.30	2.13	0.60	0.73	0.91	0.67	0.04	0.006	0.02

Fatty acids are essential for the growth of marine organisms; hence they play a vital role in aquaculture. As a result, some microalgal species that are high in essential PUFAs may be suggested as suitable for feeding marine animals. Among the saturated fatty acids, C16:0 was high in all the five microalgal species. Of the monounsaturated fatty acids, C18:1 was high in *I. galbana*, *T. suecica* and *Aphanocapsa sp.*, whereas C16:1 was found in high content in *C. calcitrans* and *N. oculata*. The high content of polyunsaturated fatty acid C18:2 was found in all the five microalgal species in the present study (Table 5).

Relatively low values of fatty acids were found in five microalgal species cultured in different conditions compared to earlier reports on various microalgal species cultured in different conditions (Lourenço *et al.*, 1997; Vargas *et al.*, 1998; Sánchez *et al.*, 2000; Reboloso-Fuentes *et al.*, 2001; Lourenço *et al.*, 2002; Durmaz *et al.*, 2009; Huerlimann *et al.*, 2010; Costard *et al.*, 2012; Chin Ming *et al.*, 2012; Batista *et al.*, 2013; Bi & He 2013; Selvakumar and Umadevi 2014; Eshak & Omar 2017; Wild *et al.*, 2018; Niccolai *et al.*, 2019; Reitan *et al.*, 2021). These variations may be attributed to culture

conditions, extraction procedure and analysis. The decrease in cellular biochemical components with increasing growth rate could be due to nutritional exhaustion and a gradual metabolites accumulation in the media (Moal *et al.*, 1987; Fernandez-Reiriz *et al.*, 1989).

The difference in chemical composition of the culture medium and the difference in salinity in the experiments induced distinct biochemical profiles of five microalgal species used in the present study. The biochemical profile of microalgae might also vary greatly depending on the measuring methods followed (Barbarino & Lourenco, 2005), physiological condition of microalgae (Fernández-Reiriz *et al.*, 1989), the experimental conditions used (Lourenço *et al.*, 2002), like temperature (Durmaz *et al.*, 2009), light intensity (Lourenço *et al.*, 2008), medium of cultivation (Huerlimann *et al.*, 2010) or in outdoor conditions (Banerjee *et al.*, 2011).

63B Standard

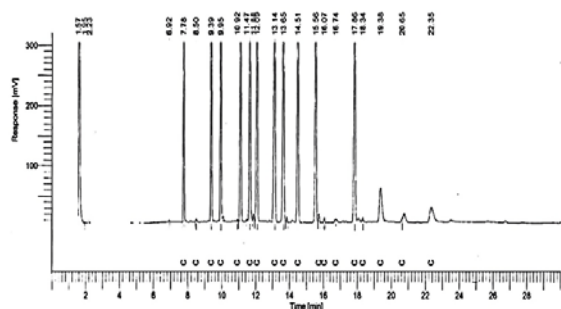
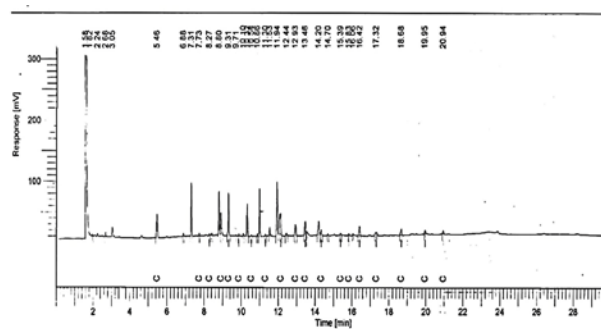


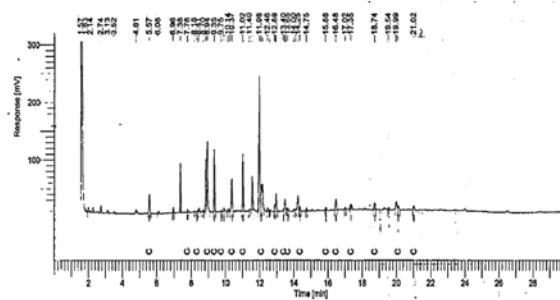
Figure 1. Chromatogram of 63B Standard

Table 4. Fatty acids of 63B Standard

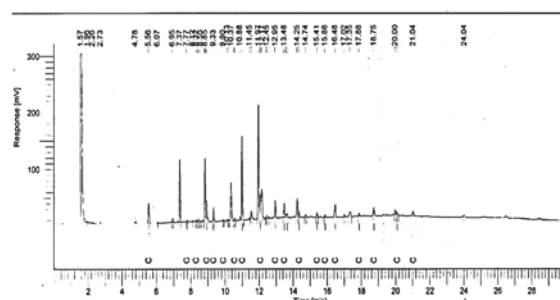
Fatty acids		63B Standard	
Common name	Empirical formula	Retention time (min)	Peak area (μ V.s)
Saturated Fatty acids			
Lauric acid – methyl ester	C 12:0	7.778	2196493.55
Myristic acid - methyl ester	C 14:0	9.387	2287731.91
Palmitic acid - methyl ester	C 16:0	11.115	2381384.38
Margaric acid - methyl ester	C 17:0	12.090	2364453.53
Stearic acid - methyl ester	C 18:0	13.138	2421943.21
Arachidic acid - methyl ester	C 20:0	17.862	2348151.41
Unsaturated Fatty acids			
Palmitoleic acid - methyl ester	C 16:1n-7	11.666	2198859.12
Oleic acid -methyl ester	C 18:1n-9	13.649	240166.16
Linoleic acid - methyl ester	C 18:2n-6	14.508	2386692.37
α - Linolenic acid - methyl ester	C 18:3n-3	15.565	2344356.67



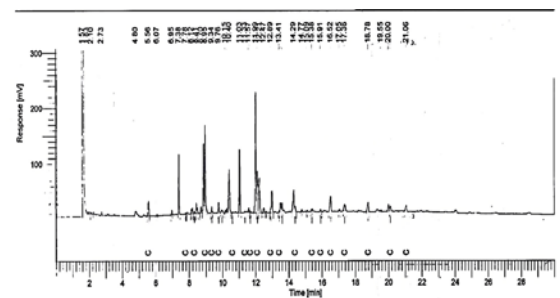
a. *I. galbana*



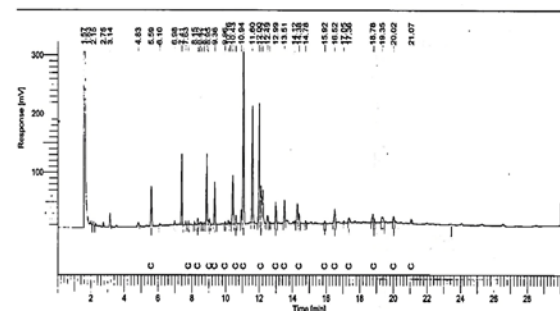
b. *C. calcitrans*



c. *T. suecica*



d. *N. oculata*



e. *Aphanocapsa sp.*

Figure 2: GC-MS Chromatograms of fatty acids in five microalgae

Table 5. Fatty acids present in five microalgae (mg/g)

	SFAs				MUFAs			PUFAs	
	C12:0	C14:0	C16:0	C18:0	C14:1	C16:1	C18:1	C18:2	C18:3
<i>I. galbana</i>	0.12	2.46	3.17	0.86	0	0.52	0.89	1.20	0.12
<i>C. calcitrans</i>	0.05	1.27	1.35	0.52	0	0.89	0.25	0.46	0
<i>T. suecica</i>	0.04	0.36	2.44	0.54	0	0.21	0.51	0.75	0.14
<i>N. oculata</i>	0.08	1.12	6.20	0.64	0	3.64	0.66	0.80	0
<i>Aphanocapsa</i> sp.	0.02	0.13	1.67	0.69	0	0.1	0.27	0.93	0

SFAs- Saturated fatty acids; MUFAs- Monounsaturated fatty acids; PUFAs- Polyunsaturated fatty acids

4. Conclusions

Microalgae are one of the most capable sources for novel functional food products and still need evaluation for usage as food and feed. They can be employed to improve the nutritional value of foods because of their well-balanced chemical composition; and it is also possible to enhance the required biochemical component of microalgae by altering the culture conditions like culture medium and salinity. The research is further needed to develop novel foods for humans as well as aquaculture industry with these microalgae.

Acknowledgment

The authors are thankful to Dr. K. Umadevi, CSIR-NMITLI laboratories, Dept. of Marine Living Resources, Andhra University for providing the algal culture lab facility and also thank Dr. P. Suryanarayana and Dr. R. Ananthan, National Institute of Nutrition, Hyderabad, India for their technical support in fatty acid analyses and mineral estimation.

Conflicts of Interest

The authors declare no conflict of interests.

Declaration of Author contributions

PYKR: study design.

GT: microalgae cultivation, biochemical composition analyses.

PYKR, GT, IRS: analysis of data, discussion of results, writing and revising the manuscript.

Funding

This research has not received any grant from funding agencies in the public, commercial, or not-for-profit sectors.

Statement of informed consent, human/animal rights

No conflicts, informed consent, or human or animal rights are applicable to this study.

References

AOAC, 2000. Official Methods of Analysis: Official Method for Ash. Method No. 936.03. *Assoc Off. Anal. Chem.*, Washington DC.

Araújo SC and Garcia VMT. 2005. Growth and biochemical composition of the diatom *Chaetoceros* cf. *wighamii* bright well under different temperature, salinity and carbon dioxide levels. I. Protein, carbohydrates and lipids. *Aquaculture*, **246**: 405-412.

Ariede MB, Candido TM, Jacome ALM, Velasco MVR, Carvalho de JCM and Baby AR. 2017. Cosmetic attributes of algae-a review, *Algal Res.*, **25**: 483-487.

[4] Banerjee S, Hew WE, Khatoun H, Shariff M and Yusoff FM. 2011. Growth and proximate composition of tropical marine *Chaetoceros calcitrans* and *Nannochloropsis oculata* cultured outdoors and under laboratory conditions. *Afr. J. Biotechnol.*, **10**: 1375-1383.

Barbarino E and Lourenço SO. 2005. An evaluation of methodologies for extraction and quantification of protein of marine macro- and microalgae. *J. Appl. Phycol.*, **17**:447-460.

Batista AP, Gouveia L, Bandarra NM, Franco JM and Raymundo A. 2013. Comparison of microalgal biomass profiles as novel functional ingredient for food products. *Algal Res.* **2** (2): 164-173.

Becker EW. 1994. *Microalgae: biotechnology and microbiology*. Cambridge, UK: Cambridge University Press.

Becker EW. 2007. Micro-algae as a source of protein. *Biotechnol. Adv.*, **25**: 207-210.

Bi Z and He BB. 2013. Characterization of microalgae for the purpose of biofuel production. *Trans. ASABE*, **56**: 1529-1539.

Bligh EG and Dyer WJ. 1959. A rapid method of lipid extraction and purification. *Can. J. Biochem. Physiol.*, **37**: 911-917.

Borowitzka MA. 1988. Algal growth media and sources of algal cultures. In: Borowitzka, M. A., and Borowitzka L. J. (eds) **Micro-algal Biotechnology**. Cambridge University Press, Cambridge, pp. 456-465.

Cardozo KHM, Guaratini T, Barros MP, Falcao VR and Tonon AP. 2007. Metabolites from algae with economical impact. *Comparative Biochem. Physiol.*, **146**: 60-78.

Carroll NVR, Longley W and Rae JH. 1956. The determination of glycogen in liver and muscle by use of Anthrone reagent. *J. Biol. Chem.*, **220**: 583-598.

Chin Ming L, Nurliyana R, Bazil Syah A, Noor Azizah M, Sim HLi and Hirzun MY. 2012. Identification and Biochemical composition of a Green Microalgae. *Asian J. Biotechnol.*, **4**(1): 38-45.

Costard GS, Machado RR, Barbarino E, Martino RC and Lourenço SO. 2012. Chemical composition of five marine microalgae that occur on the Brazilian coast, *Int. J. Fish. Aquac.*, **4**(9): 191-201.

Coutteau P. 1996. Micro-algae. In: Lavens, P., Sorgeloos, P. (Eds.), **Manual on the Production and Use of Live Food for Aquaculture**. FAO (Food and Agriculture Organization of the United Nations), Rome, pp. 7-48.

- D'oca MGM, Viêgas CV, Lemões JS, Miyasaki EK, Morón-Villarreyes JA, Primel EG and Abreu PC. 2011b. Production of FAMES from several microalgal lipidic extracts and direct transesterification of the *Chlorella pyrenoidosa*. *Biomass Bioenergy*. **35(4)**: 1533–1538.
- Doan TTY, Sivaloganathan B and Obbard JP. 2011. Screening of marine microalgae for biodiesel feedstock. *Biomass Bioenergy*. **35**: 2534–2544.
- Durmaz Y, Donato M, Monteiro M, Gouveia L, Nunes ML, Gama Pereira T, Gökpimar S. and Bandarra NM. 2009. Effect of temperature on α -tocopherol, fatty acid profile, and pigments of *Diacronema vlkianum* (Haptophyceae). *Aquac. Int.*, **17**: 391-399.
- Ehteshami F, Christianus A, Rameshi H, Harmin SA and Saad CR. 2011. The effects of dietary supplements of polyunsaturated fatty acid on pearl oyster, *Pinctada margaritifera* L., gonad composition and reproductive output. *Aquac. Res.*, **42**: 613–622.
- Eshak MB and Omar WMW. 2017. *Isochrysis maritima* Billard and Gayral Isolated from Penang National Park Coastal Waters as A Potential Microalgae for Aquaculture, *Trop. Life Sci. Res.*, **28(2)**: 163-176.
- Fabregas J and Herrero C. 1986. Marine microalgae as a potential source of minerals in fish diets, *Aquaculture*, **51**: 237-243.
- Fernández-Reiriz MJ, Perez-Camacho A, Ferreiro MJ, Blanco J, Planas M, Campos MJ and Labarta U. 1989. Biomass production and variation in the biochemical profile (total protein, carbohydrates, RNA, lipids and fatty acids) of seven marine microalgae. *Aquaculture*, **83**:17-37.
- Foley JA, Ramankutty N, Brauman KA, Cassidy ES, Gerber JS, Johnston M, Mueller ND, O'Connell C, Ray DK and West PC. 2011. Solutions for a cultivated planet. *Nature*, **478 (7369)**: 337–42.
- Glover CN and Hogstrand C. 2002. Amino acids and Minerals of in vivo intestinal zinc absorption in freshwater Rainbow trout. *J. Exp. Biol.*, **205**: 151-158.
- Gouveia L, Marques AE, Sousa JM, Moura P and Bandara NM. 2010. Microalgae-source of natural bioactive molecules as functional ingredients, **Food Science and Technology Bulletin: Functional Foods**, **7**: 21–37.
- Guillard RRL and Ryther JH. 1962. Studies of marine planktonic diatoms. I. *Cyclotella nana* Hustedt and *Detonula confervacea* (Cleve), *Can. J. Microbiol.*, **8**: 229–239,
- Heath AG. 1987. Water pollution and fish physiology. Chapter.5, **Physiological Energetics**, CRC Press, Boca Raton, FL, pp. 131-163.
- Hu Q, Sommerfeld M, Jarvis E, Ghirardi M, Posewitz M, Seibert M and Dar-zins A. 2008. Microalgal triacylglycerols as feedstocks for biofuel production: perspectives and advances. *Plant J.*, **54(4)**: 621–639.
- Huerlimann R, de Nyz R and Heimann K. 2010. Growth, lipid content, productivity, and fatty acid composition of tropical microalgae for scale-up production. *Biotechnol. Bioeng.*, **107**: 245-257.
- Huntley M, Johnson Z, Brown S, Sills D, Gerber L, Archibald I, Machesky S, Granados J, Beal C and Greene C. 2015. Demonstrated large-scale production of marine microalgae for fuels and feed, *Algal Res.*, **10**: 249–265.
- Kent M, Welladsen HM, Mangott A and Li Y. 2015. Nutritional evaluation of Australian microalgae as potential human health supplements. *PLoSOne*. 10:e0118985. 10.1371/journal.pone.0118985.
- Khawaja DK. 1966. Biochemical composition of the muscle of some freshwater fishes during prematurity phase. *Fish. Technol.*, **3**: 94-102.
- Kumar G, Shekh A, Jakhu S, Sharma Y, Kapoor R and Sharma TR. 2020. Bioengineering of Microalgae: Recent Advances, Perspectives, and Regulatory Challenges for Industrial Application. *Front. Bioeng. Biotechnol.* **8**: 914.
- Liu J, Pan Y, Yao C, Wang H, Cao X and Xue S. 2015. Determination of ash content and concomitant acquisition of cell compositions in microalgae via thermogravimetric (TG) analysis. *Algal Res.*, **12**: 149–155.
- Lourenço SO, Barbarino E, Bispo MGS, Borges DA, Coelho-Gomes C, Lavin PL and Santos F. 2008. Effects of light intensity on growth, inorganic nitrogen storage, and gross chemical composition of four marine microalgae in batch cultures. **XI Brazilian Congress of Phycology and Latin American Symposium on Harmful Algae**. National Museum Series Books, **30**: 203-214.
- Lourenço SO, Barbarino E, Mancini-Filho J and Schinke KP. 2002. Effects of different nitrogen sources on growth and biochemical profile of ten marine microalgae under batch cultures. *Phycologia*, **41**: 158-168.
- Lourenço SO, Marquez UML, Mancini-Filho J, Barbarino E and Aida E. 1997. Changes in biochemical profile of *Tetraselmis gracilis* I. Comparison of two culture media. *Aquaculture*, **148**: 153-168.
- Lowry OH, Rosebrough NJ, Farr AL. and Randall RJ. 1951. Protein measurement with the folin phenol reagent. *J. Biol. Chem.*, **193**: 265- 275.
- Metsoviti MN, Papapolymerou G, Karapanagiotidis IT and Katsoulas N. 2019. Comparison of growth rate and nutrient content of five microalgae species cultivated in greenhouses. *Plants*, **8**: 279.
- Michael Babu M, Citarasu T, Selvaraj T, Punitha SMJ, Praba T and Albin dhas S. 2013. Extraction and characterization of algal oil from selected marine microalgae and the role of associated bacteria on fatty acid profile. *Int. J. Nat. Appl. Sci.*, **2(4)**: 31-42.
- Moal J, Martin-Jezequel V, Harris RP, Samain JF and Poulet SA. 1987. Interspecific and intraspecific variability of the chemical composition of marine phytoplankton. *Oceanol. Acta.*, **10**: 339-346.
- Molino A, Iovine A, Casella P, Mehariya S, Chianese S, Cerbone A, Rimauro J and Musmarra D. 2018. Microalgae characterization for consolidated and new application in human food, animal feed and nutraceuticals. *Int. J. Environ. Res. Public Health*, **15**: 2436.
- Moura-Junior AM, Bezerra Neto E, Koenig ML and Lec,a EE. 2007. Chemical composition of three microalgae species for possible use in mariculture. *Braz. Arch. Biol. Technol.*, **50**: 461–467.
- Niccolai A, Zittelli GC, Rodolfi L, Biondi N and Tredici MR. 2019. Microalgae of interest as food source: Biochemical composition and digestibility. *Algal Res.*, **42**: 101617.
- NRC (National Research Council). 1993. **Nutrient requirements of Fish**, (p. 114). Committee on Animal Nutrition. Board on Agriculture. National Research Council. *National Academy Press*. Washington DC, USA.
- Patil V, Källqvist T, Olsen E, Vogt G and Gislefjord HR. 2007. Fatty acid composition of 12 microalgae for possible use in aquaculture feed. *Aquac. Int.*, **15**: 1-9.

- Phatarpekar PV, Sreepada RA, Pednekar C and Achuthankuty CT. 2000. A comparative study on growth performance and biochemical composition of mixed culture of *Isochrysis galbana* and *Chaetoceros calcitrans* with monocultures. *Aquaculture*, **181**: 141-155.
- Reboloso-Fuentes MM, Navarro-Pérez A, García-Camacho F, Ramos-Miras JJ and Guil-Guerrero JL. 2001. Biomass nutrient profiles of the microalga *Nannochloropsis*. *J. Agric. Food Chem.*, **49**: 2966–2972.
- Reitan KI, Oie G, Jorgensen H and Xinxin W. 2021. Chemical composition of selected marine microalgae, with emphasis on lipid and carbohydrate production for potential use as feed resources. *J. Appl. Phycol.*, **33**: 3831–3842.
- Renaud SM, Thinh LV, Lambrinidis G and Parry DL. 2002. Effect of temperature on growth, chemical composition and fatty acid composition of tropical Australian microalgae grown in batch cultures. *Aquaculture*, **211**: 195–214.
- Rodenas de la Rocha S, Sánchez-Muniz FJ, Gomez-Juaristi M and Larrea Marin MT. 2009. Trace elements determination in edible seaweeds by an optimized and validated ICP-MS method, *J. Food Compos. Anal.*, **22**: 330-336.
- Rodriguez-lopez M, Villarroya M and Munoz-calvo ML. 1980. Influence of ammonium and nitrate on protein content, amino acid pattern, storage materials and fine structure of *Chlorella* 8H recovering from N-starvation. In: Shelef, G. and C. J. Soeder (ed). **Algae biomass: Production and Use**. North-Holland Biomedical Press, Amsterdam, 723-731.
- Sánchez S, Martínez E and Espinola F. 2000. Biomass production and biochemical variability of the marine microalga *Isochrysis galbana* in relation to culture medium. *Biochem. Eng. J.*, **6**: 13-18.
- Selvakumar P and Umadevi K. 2014. Mass cultivation of marine micro alga *Nannochloropsis gaditana* KF410818 isolated from Visakhapatnam offshore and fatty acid profile analysis for biodiesel production. *J. Alga Biomass Util.*, **5**: 28-37.
- Shelef G, Sukenik A and Green M. 1984. Microalgae Harvesting and Processing: A Literature Review, Report, Solar Energy Research Institute, Golden Colorado, United States, SERI/STR-231-2396.
- Smith FE and Arsenault EA. 1996. Microwave assisted sample preparation in analytical chemistry. *Talanta*, **43**: 1207-1268.
- Sukenik A and Wannon R. 1991. Biochemical quality of marine unicellular algae with special emphasis on lipid composition. *Isochrysis galbana*. *Aquaculture*, **97**: 61-72.
- Thompson PA, Guo M and Harrison PJ. 1993. The influence of irradiance on the biochemical composition of three phytoplankton species and their nutritional value for larvae of the Pacific Oyster (*Crassostrea gigas*). *Mar. Biol.*, **117**: 259–268.
- Utting SD. 1985. Influence of nitrogen availability on the biochemical composition of three unicellular marine algae of commercial importance. *Aquac. Eng.*, **4**: 175–190.
- Valenzuela-Espinoza E, Millán-Núñez R and Núñez-Cabrero F. 2002. Protein, carbohydrate, lipid and chlorophyll a content in *Isochrysis galbana* (clone T-Iso) cultured with a low-cost alternative to the f/2 medium. *Aquac. Eng.*, **25**: 207–216.
- Vandamme D, Foubert I and Muylaert K. 2013. Flocculation as a low-cost method for harvesting microalgae for bulk biomass production. *Trends Biotechnol.*, **31**(4): 233–9.
- Vargas MA, Rodriguez H, Moreno J, Olivares H, Del Campo JA, Rivas J and Guerrero MG. 1998. Biochemical composition and fatty acid content of filamentous nitrogen fixing cyanobacteria. *J. Phycol.*, **34**: 812 - 817.
- Verdelho Vieira V. 2015. Microalgae production business in Europe 2015, *Alga. Europe Conference*, 1-3. (Lisbon, Portugal).
- Vigani M, Parisi C, Rodríguez-Cerezo E, Barbosa MJ, Sijtsma L, Ploeg M and Enzing C. 2015. Food and feed products from microalgae: market opportunities and challenges for the EU, *Trends Food Sci. Technol.*, **42**: 81–92.
- Walne PR. 1970. Studies on the food value of nineteen genera of algae to juvenile bivalves of the genera *Ostrea*, *Crassostrea*, *Mercenaria* and *Mytilus*. *Fish. Invest.*, **26**: 1-62.
- Wells ML, Potin P, Craigie JS, Raven JA, Merchant SS, Helliwell KE, Smith AG, Camire ME and Brawley SH. 2017. Algae as nutritional and functional food sources: revisiting our understanding, *J. Appl. Phycol.*, **29**: 949–982.
- Wild KJ, Steingäß H and Rodehutsord M 2018. Variability in nutrient composition and in vitro crude protein digestibility of 16 microalgae products. *J. Anim. Physiol. Anim. Nutr.*, 1-14.
- Xu ZB, Yan XJ, Pei LQ, Luo QJ and Xu JL. 2008. Changes in fatty acids and sterols during Batch growth of *Pavlova viridis* in photobioreactor. *J. Appl. Phycol.*, **20**: 237–243.
- Zheng H, Guo W, Li S, Chen Y, Wu Q, Feng X, Yin R, Ho S-H, Ren N and Chang J-S. 2017. Adsorption of p-nitrophenols (PNP) on microalgal biochar: analysis of high adsorption capacity and mechanism. *Bioresour. Technol.*, **244** (2): 1456–1464.

A Histological Examination of the Sublethal Effects of Methyl Parathion on the Liver, Gills and Gonads of *Alburnus tarichi* (Güldenstädt, 1814)

Ertuğrul KANKAYA^{1,*} and Güler ÜNAL²

¹Faculty of Fisheries, Yuzuncu Yil University, Van-65080, Türkiye; ²Department of Child Development, Faculty of Healthy Sciences, Adnan Menderes University, Aydın-09100, Türkiye

Received: December 30, 2022; Revised: February 10, 2023; Accepted: February 15, 2023

Abstract

Pesticides are chemicals used to control a wide variety of animals and plants. Methyl parathion (MP) is an organic phosphorus insecticide used in agriculture against animal organisms that damage the crop. Pesticides can reach water resources in different ways. May affect non-target organisms such as fish to varying degrees. Since fish is a valuable nutrient in human nutrition, its sustainability is very important. For this reason, sublethal effects of MP on *Alburnus tarichi*, which is economically important for the Lake Van basin, were studied. This study was carried out to determine the pathological effects of MP on the gonad, gill and liver tissues of *Alburnus tarichi*. Fish weighing 3–7 g were used in the study. The semi-static test method was applied. Fish were exposed to 4.28 mg L⁻¹ MP. The bioassay was carried out at 17.9 °C for 30 days. At the end of the test, gonad, gill and liver tissues were removed from the dissected fish for pathological evaluations. In the examinations made, cells with eosinophilic and fat accumulation in the liver, local necrosis and enlarged vessels, and yellow colored structures were determined. Thickened primary lamella, folded secondary lamella and epithelial layer separations were observed in the gills. No pathology was found in ovarian cells. Degeneration in the germ cells in the mitotic phase, interstitial tissue containing eosinophilic cell groups, enlarged follicle lumen and bleeding were observed in the testes that were not in the mitotic phase. As a result, MP is a chronic toxic substance according to histological criteria for *Alburnus tarichi*. MP should be used in agriculture in a controlled and careful way.

Keywords: Organic phosphorus, Lake Van Basin, Fish, Toxicity

1. Introduction

The increasing world population and industrial activities are polluting water resources. One of the major reasons for this pollution is contamination by chemical substances such as pesticides (Lakshmaiah, 2016a). Organophosphorus (OP) pesticides are used in agriculture in large quantities all over the world (Kwong, 2002). These uses can cause environmental contamination that will affect non-targeted organisms (Fanta *et al.*, 2003). Pesticides used to control pests in agricultural areas can be extremely toxic to non-target organisms such as fish. They affect the health of the fish causing metabolic disturbances, sometimes leading to deaths (Murthy *et al.*, 2013). It is known that OP pesticides cause structural and functional changes in fish. Histopathological studies on different tissues of exposed fish are useful tools for monitoring water pollution and toxicological studies (Banaee *et al.*, 2013; Lee *et al.*, 2021). Methyl parathion (MP) is a pesticide containing OP. It is used to control pests in a wide range of agricultural products (Rico *et al.*, 2010).

MP and OP compounds affect the histological structure of fish-like animals. It has a neurotoxic potential

(Lakshmaiah, 2016b). The histopathology of MP contamination of *Corydoras paleatus* fish via water and food (Fanta *et al.*, 2003); the histological effects on the branchial epithelium of *Metynnis roosevelti* (Machado and Fanta, 2003); the sensitivities of Amazon fish and invertebrates (Rico *et al.*, 2010); and the histopathological changes of *Catla catla* gill tissue (Selvi and Ilavazhahan, 2012) have all been studied. It was focused on the functions of gills in respiration, gonads in reproduction and liver tissue in detoxification process, which were reported to have significant effects on fish exposed to the chemical (Kankaya and Kaptaner, 2017).

Alburnus tarichi is a species endemic to the Lake Van basin in Turkey. *A. tarichi* is part of the family Cyprinidae. Settlements nearby to Lake Van usually consume them fresh and salted (Kankaya and Ünal, 2018). In May to June, the fish migrate into freshwater rivers to spawn. After laying their eggs, the fish return to the lake. The fertilization of the eggs, the incubation period, and the emergence of the larvae and their feeding for a certain period take place in these rivers (Elp and Çetinkaya, 2000). *A. tarichi* is subject to economic precautions in this region with about 10000 tons/year of fishing allowed (Tuik, 2019).

* Corresponding author. e-mail: ekankaya@yahoo.com.

MP is widely used in agricultural activities in the Van region. Therefore, *A. tarichi* is affected by the toxicity of this substance (Kankaya and Ünal, 2018). No studies on the histological examination of *A. tarichi* exposure to MP were found in literature reviews. However, micronuclei formation in *A. tarichi* erythrocytes exposed to MP (Kankaya *et al.*, 2012), increase in apoptosis in *A. tarichi* liver tissue following exposure to sublethal concentrations of MP (Kankaya and Kaptaner, 2014), the acute and chronic toxic effects of MP on *A. tarichi* (Kankaya and Ünal, 2018), and hemato-biochemical responses in *A. tarichi* exposed to cypermethrin have also been investigated (Özok *et al.*, 2018) have all been studied. Hematological and biochemical response in the blood of *A. tarichi* exposed to tebuconazole (Yeltekin *et al.*, 2020).

This study was conducted to determine the histological changes on the liver, gills and gonads of *A. tarichi* exposed to MP, which are usually associated with agricultural activities around the Lake Van basin water resources.

2. Materials and Methods

In this study, fish weighing 3 to 7 g with a fork length of 8 to 10 cm were used. Fish were collected from the natural environment by means of electrical shock. The samples were taken from the Karasu river (43°17'E, 38°39'N) pouring into Lake Van. Fish were brought to the laboratory in oxygen-supplied containers. The care and feeding of the fish were carefully followed for a month in order to remove the negative effects that may be caused by electro shock, to get used to the food, and to identify healthy individuals (Çetinkaya, 2010). Chlorine-free tap water was used in the bioassay. The fish were fed with commercial trout pellets, and the acclimatization of the fish lasted 7 days. All experimental procedures were carried out according to national animal care regulations.

Glass aquariums with a volume of 60 L were used in the bioassay. Each aquarium held 10 fish. The experiment was carried out over natural photoperiods. MP (C₈H₁₀NO₃PS) at 80% concentration was provided by a company producing agrochemicals in Turkey. MP was prepared by dissolving it in dimethyl sulfoxide (DMSO) from Sigma. The test fish were allowed to acclimation for 7 days and the tests were duplicated. Fish were exposed to a concentration of 4.28 mg L⁻¹ of MP (Kankaya and Ünal, 2018). A control and solvent control group was established. The test continued for 30 days using the semi-static test method. The semi-static test is the test in which there is no flow in the test medium, but the test solution is refreshed after a period of time (Ünsal, 1998; Çetinkaya, 2010; Audu *et al.*, 2021). The aquarium water was refreshed every two days. During the test, the fish were fed and maintained regularly. Throughout the study, the water quality criteria of aquariums were regularly monitored (pH: 8.46, dissolved oxygen: 6.04 mg L⁻¹, temperature: 17.9 °C, total hardness CaCO₃: 344 mg L⁻¹, electrical conductivity: 882 µS cm⁻¹ and total alkalinity CaCO₃: 518 mg L⁻¹) (Anonymous, 1995).

Fish were anesthetized at the end of the bioassay. The liver, gill and gonad tissues of the dissected fish were removed and fixed in the Bouin's solution. The fixed tissues were washed with 70% alcohol until the yellow color was removed, and then all tissues were passed through a series of alcohol solutions at concentrations of

80%, 96% and 100%, respectively. Subsequently, the tissues were passed through a series of xylol and paraffin solutions and embedded in paraffin blocks. Sections with a thickness of 5 µm were taken from the tissues. The sections were stained with Mayer's hematoxylin-eosin (H-E) and Mallory's trichrome (M-T) stains (Hinton, 1990; Ünal, 2010; Abdullah-Al Mamun *et al.*, 2022). M-T stains were used to detect the presence of collagen fibrils, tumor and fibrillar tissue increase (Ünal, 2010). The preparations were examined with a Nikon Eclipse E600 and Leica DMI 6000B light microscope and then photographed. The abnormalities detected in the liver, gill and gonad tissues examined histologically were evaluated qualitatively. A quantitative assessment has not been made.

3. Results

During the test, 2 fish died in the group treated with MP. No other deaths occurred in the control and MP groups throughout the bioassay. Other than stagnation, no abnormal behavior was detected in some fish in the groups from time to time. Eight fish exposed to MP were used in histological examinations. At the end of the experiment, no macroscopic abnormality was observed in the fish. No obvious abnormalities in color and size were detected in the internal organs of the fish.

3.1 Liver tissue

No histopathological findings were found in the sections taken from liver tissue in the control and solvent control group fish (Fig. 1 A, B).

It was observed that the fish exposed to MP contained fat droplets of different sizes in their hepatocytes, which combined to form large vacuole structures (Fig. 1 C). These structures were especially evident in the portal areas and around bile ducts. The existence of hypertrophic and eosinophilic cell groups among the sinusoids in the liver was seen (Fig. 1 D, E). In the liver, the sinusoids expand irregularly (Fig. 1 F). Among the hepatocyte cells, yellow droplets were present and numerous droplets were collected in cyst (Fig. 1 G, H and I).

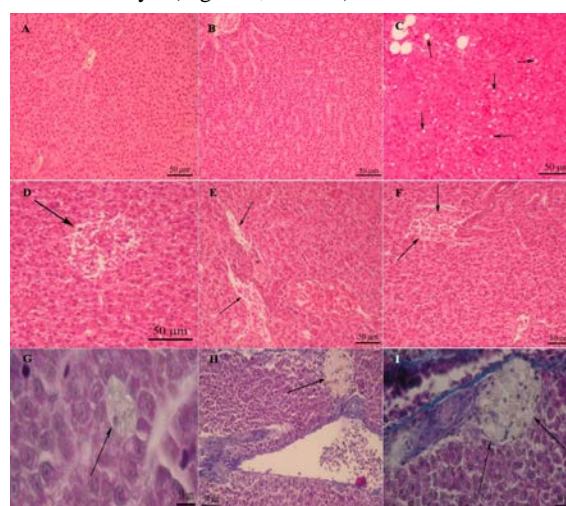


Figure 1. Images of *A. tarichi* liver tissue exposed to 4.28 mg L⁻¹ concentration of MP [A control; B solvent control group; C fat droplets (→); D groups of hypertrophied cells observed in the lobule (→); E eosinophilic cell group (*); F expanded sinusoidal (→); G, H and I overall appearance of yellow-colored structures scattered among hepatocytes (→) (H-E, M-T stain)]

3.2 Gill tissue

There was no significant difference between the control and solvent control group fish (Fig. 2 A and B). In some fish exposed to MP, it was observed that epithelial hyperplasia that causes basal fusion of secondary lamellae. This hyperplasia was observed to reach the end of the

respiratory lamellae (Fig. 2 C). In the majority of the fish, the end portions of the respiratory lamellae were curled to form hammer-like structures. In some fish, it has been determined that the epithelial layer surrounding these lamellae is separated from the sinusoid (Fig. 2 D).

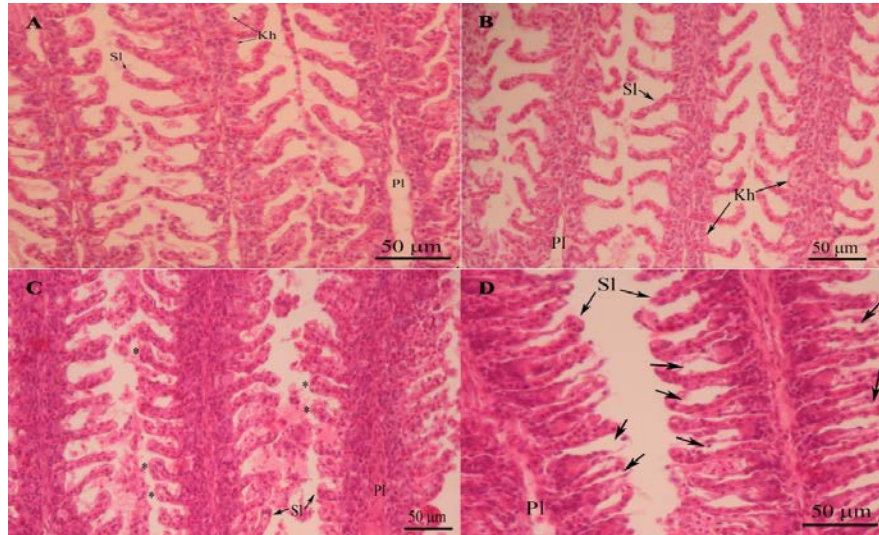


Figure 2. Sections taken from the *A. tarichi* gills exposed to a concentration of 4.28 mg L⁻¹ of MP [A control; B solvent control group; C hyperplasia of epithelial surrounding primary lamella, curtains and knobs at the ends of the secondary lamella (*); D cleavage of epithelial tissue from sinusoids in some primary lamella (→) (Pl: primary lamella; Sl: secondary lamella; Kh: chloride cell). (H-E stain)]

3.3 Ovarium tissue

There was no morphologically significant difference in the ovaries of fish exposed to the control, solvent control and MP. It was determined in all fish that the development of oocytes had recently occurred in the cortical alveolar

vessels (Fig. 3 A, B, C, D). In synchronized group development in the ovaries, young oocytes were easily distinguished in nuclear chromatin and perinuclear phases (Fig. 3 A, B, D).

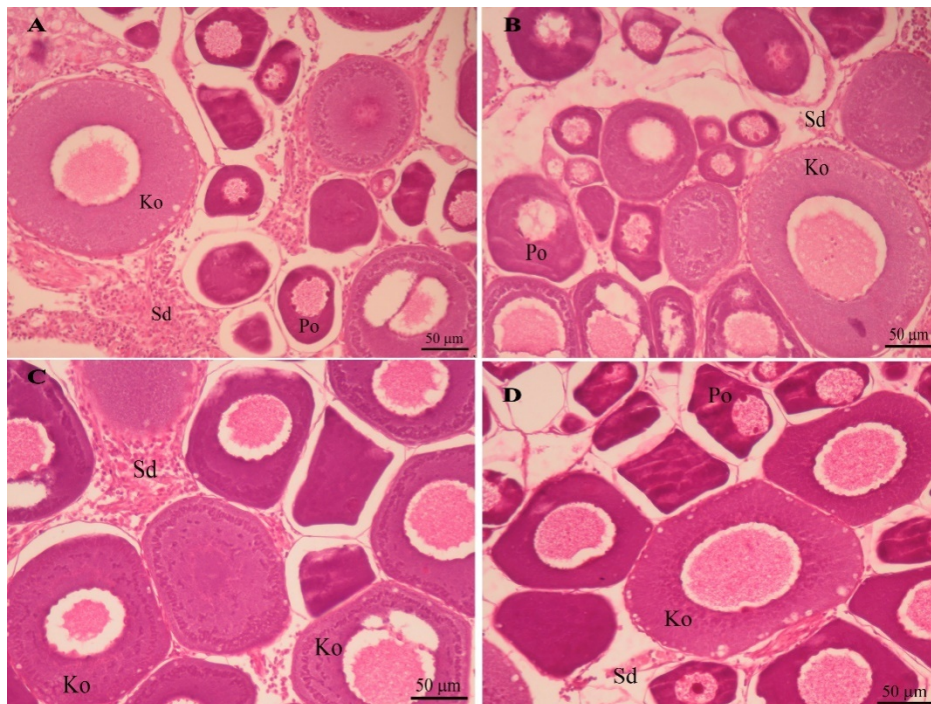


Figure 3. Sections taken from the *A. tarichi* ovarium tissue exposed to a concentration of 4.28 mg L⁻¹ of MP. [A control; B solvent control group; C, D (Ko: cortical alveolar oocyte; Po: perinuclear oocyte; Sd: stromal tissue). (H-E stain)]

3.4 Testicular tissue

In the sections taken under test from the control and solvent control group fish, some fish were found to have immature testes (Fig. 4 A). It has been determined that some fish had only just entered the mature stage, that is with primordial spermatogonial cells entering the mitotic phase (Fig. 4 B).

In some fish exposed to MP, excessive amounts of blood were found in the interstitial tissue of the testes. It was observed that the cells in the lumens of some follicles

were disrupted and the lumens expanded (Fig. 4 C). In some fish, it was seen that all the local tissue in the testes was damaged (Fig. 4 D). In some fish testes, the cells inside the seminiferous follicles were found to be empty and the follicles were filled with liquid. Some follicles combined to form large cavities (Fig. 4 E and F). The presence of a large number of eosinophilic cell populations among the follicles was observed (Fig. 4 G). In some regions of the testis tissue, it was observed that these eosinophilic structures formed into the cyst (Fig. 4 H).

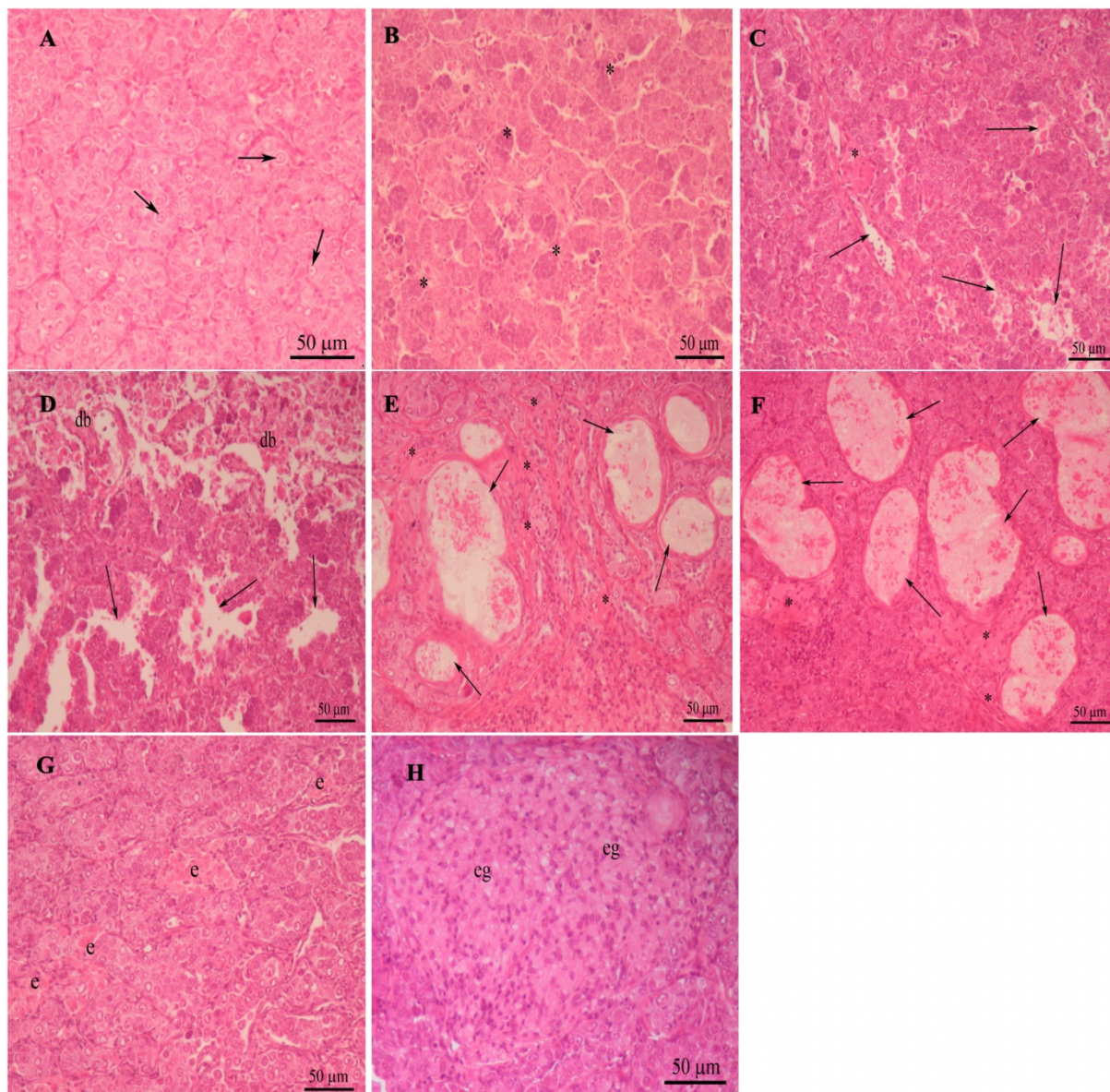


Figure 4. Sections taken from the *A. tarichi* testicular tissue exposed to a concentration of 4.28 mg L^{-1} of MP. [A control, immature stage testes, primordial germ cells (\rightarrow); B solvent control group, testes image at the stage of maturation, mitotic cell groups (*); C, D deterioration of the testes in the seminiferous follicle lumen and in the tissue (\rightarrow), eosinophilic structure (*), tissue deterioration (db); E, F expansion of the seminiferous follicle lumen and associated seminiferous follicles (\rightarrow), bleeding in interstitial tissue (*); G eosinophilic cell groups seen in the testes (e); H an eosinophilic cell group taken into the cyst (eg). (H-E stain)]

4. Discussion

4.1. Liver tissue

The pathological findings in liver tissue of different fish species exposed to pesticides with different OPs are

similar to some of the findings of this study. Balint *et al.* (1995) observed the presence of large lipid droplets and increased bile pigments in the hepatocytes of *Cyprinus carpio* fish exposed to methidathion. They reported that there were changes in the intracellular structures of hepatocytes in their electron microscopy examinations. Fanta *et al.* (2003) studied the liver and gill

histopathology of *Corydoras paleatus* fish exposed to MP. They determined cloudy swelling, bile stagnation, focal necrosis, atrophy, and vacuolization in the liver. Lakshmaiah (2016b) detected structural degeneration with increased vacuolization in the liver tissue of *Cyprinus carpio* exposed to phorate. Sunanda *et al.* (2016) determined hepatocyte hypertrophy, necrosis and fibrosis in liver tissue of *Channa punctatus* fish exposed to chlorpyrifos. In studies previously conducted, differences observed in liver tissue varied depending on the applied chemistry, the concentration of the chemical and the fish species. Studies have shown that insecticides have toxic effects on the liver of fish and cause histopathological changes in the liver. In this study, it can be said that for *A. tarichi*, MP is highly toxic to the liver tissue.

4.2. Gill tissue

As in other fish, there are four pairs of gill arches or arcs in the *A. tarichi* that are composed of cartilaginous tissue. A primary filament emerges from each arch. Secondary or respiratory lamellae emerge from both sides of the primary filaments (Fig. 2 A and B). The primary lamellae are surrounded by stratified epithelium and have chloride cells on the surface. The surface of the respiratory lamellae was surrounded by a monolayer flat epithelium. Under the epithelium were pillar cells surrounding the sinusoids (Takashima and Hibiya, 1995) (Fig. 2 A and B).

It has been reported that in *Poecilia reticulata* fish exposed to lorsban – a compound with OP – suffered shortening and loss in the secondary lamellae due to the concentration, accumulation of mucus, dysfunction of the lamellae and vacuolization in the gill tissue (De Silva and Samayawardhena, 2002). Similarly, Machado and Fanta (2003) found changes in the epithelium of the gill lamellae of *Metynnis roosevelti* exposed to mentox 600 CE, such as shrinkage, rupture, hyperplasia, necrosis, structural changes in lamellar organization and cellular morphology. Fanta *et al.* (2003) reported that epithelial hyperplasia, edema, and separation of respiratory lamellae occurred in the gills. Sunanda *et al.* (2016) reported that the gills of *Channa punctatus* fish exposed to chlorpyrifos caused edema, lamellar epithelial separation, intense enlargement of the lamellar vessel line, proliferation of the filamentous epithelium and lamellar fusion. In this study, histopathologic changes determined in the gills are similar to histopathological findings of similar chemicals in other fish. The histopathological effects of these chemicals on the gills are expected.

4.3. Ovarium tissue

Pawar and Katdare (1983) reported that mature oocytes disappeared completely in the ovaries of *Garra mullya* fish exposed to OP summertion. Ram and Sathyanesan (1987) reported that *Channa punctatus*, which had been exposed for a period of 6 months to a concentration of 2.0 mg L⁻¹ of OP cythion, showed degenerative changes in the ovaries and testes. Dutta and Maxwell (2003) reported that the microscopic anatomy of oocytes at various maturation stages was affected differently in *Lepomis macrochirus* fish exposed to diazion for varying durations. Various pesticides have been reported not to affect the initial stage of gonadal maturation in fish, which requires long-term applications (Lal, 2007). Similarly, the fact that MP has no effect on gonadal development in *A. tarichi* suggests that

young oocytes (in the perinuclear, cortical and nuclear chromatin stages) are not affected by MP.

4.4. Testicular tissue

Pandey and Shukla (1982) found that tilapia testicular elements exposed to concentrations of 2 to 4 mg L⁻¹ of OP malathion were disrupted. Saxena and Mani (1985; 1987) reported that they observed histopathological findings in the testes of *Channa punctatus* exposed to a 1.5 mg L⁻¹ concentration of OP fenitrothion for 120 days. It was determined that MP has histopathological effects on *A. tarichi* testes, but it can be said that the spermatogonium groups in the mitotic stage are more sensitive to MP.

5. Conclusion

The histopathological effects of the toxicity of sublethal amounts of MP have been demonstrated. In this way, drawbacks have been identified that may be caused by the unconscious and excessive use of insecticide in agricultural areas near the water environments where *A. tarichi* lives. This study aims to contribute to the preservation of *A. tarichi*, which is an economically and ecologically important species in terms of this region of Turkey, and to ensure the continuity of its population.

The highest concentration of 0.1144 mg L⁻¹ of MP in freshwater environments inhabited by *A. tarichi* appears to be a safe concentration. There should not be MP above this value in the water. It was observed that MP caused histopathologic changes in liver, gill and testicular tissues, but had no pathological effect on ovaries with young oocytes.

As a result, MP is a toxic substance for *A. tarichi*. Therefore, it can be said that MP, which is widely used in the Lake Van basin, should be subject to control.

Acknowledgments

The authors wish to thank Associate Professor Dr. Burak KAPTANER for help during the work.

Conflict of Interest

The authors declare that there is no conflict of interest concerning this work or the preparation of the manuscript.

References

- Abdullah-Al Mamun Md, Nasren S, Rathore SS and Mahbub Alam MM. 2022. Histopathological analysis of striped catfish, *Pangasianodon hypophthalmus* (Sauvage, 1878) spontaneously infected with *Aeromonas hydrophila*. *Jordan Journal of Biological Sciences*, 15(1), 93–100.
- Anonymous 1995. Standard methods for the examination of water and wastewater. 19nd ed. APHA, AWWA, WEF, Washington, USA.
- Audu BS, Wakawa IA, Oyewole OJ and Changdaya PZ. 2021. Histopathological alterations in the gills and liver of *Clarias gariepinus* juveniles exposed to acute concentrations of *Anogeissus leiocarpus*. *Jordan Journal of Biological Sciences*, 14(3), 537–543.
- Balint T, Szegletes T, Szegletes Zs, Halasy K and Nemsok J. 1995. Biochemical and subcellular changes in carp exposed to the organophosphorus methidation and the pyrethroid deltamethrin. *Aquatic Toxicology*, 33(3–4): 279–295.

- Banaee M, Sureda A, Mirvagefei AR and Ahmadi K. 2013. Histopathological alterations induced by diazinon in rainbow trout (*Oncorhynchus mykiss*). *International Journal of Environmental Research*, 7(3): 735–744.
- Çetinkaya O. 2010. Akuatik toksikoloji: balık biyodenyeleri. In: Karataş M (Eds.), *Research Techniques in Fish Biology*, Karaman Bilim ve Araştırma Merkezi Derneği, Türkiye, pp. 139–187.
- De Silva PMCS and Samayawardhena LA. 2002. Low concentrations of lorsban in water result in far reaching behavioral and histological effects in early life stages in guppy. *Ecotoxicology and Environmental Safety*, 53(2): 248–254.
- Dutta HM and Maxwell LB. 2003. Histological examination of sublethal effects of diazinon on ovary of bluegill, *Lepomis macrochirus*. *Environmental Pollution*, 121: 95–102.
- Elp M and Çetinkaya O. 2000. İnci kefalı (*Chalcalburnus tarichi* Pallas, 1811)'nin üreme biyolojisi üzerine bir araştırma. Doğu Anadolu Bölgesi IV. Su Ürünleri Sempozyumu. University of Atatürk, Erzurum, Türkiye.
- Fanta E, Rios FSA, Romao S, Vianna ACC and Freiberger S. 2003. Histopathology of the fish *Corydoras paleatus* contaminated with sublethal levels of organophosphorus in water and food. *Ecotoxicology and Environmental Safety*, 54(2): 119–130.
- Hinton DE. 1990. Histological techniques. In: Schreck CB and Moyle PB (Eds.), *Methods for Fish Biology*, American Fisheries Society, United States, pp. 191–211.
- Kankaya E and Kaptaner B. 2014. Increased apoptosis in the liver of *Chalcalburnus tarichi* exposed to sublethal concentrations of methyl parathion. *Journal of Applied Biological Sciences*, 8(1): 45–48.
- Kankaya E and Kaptaner B. 2017. Sublethal toxicity of formaldehyde in common carp (*Cyprinus carpio* L., 1758). *Yuzuncu Yil University Journal of Agricultural Sciences*, 27(3): 406–415.
- Kankaya E and Ünal G. 2018. Determination of acute and chronic toxic effects of methyl parathion on *Chalcalburnus tarichi* (Pallas, 1811). *Journal of Aquaculture Engineering and Fisheries Research*, 4(1): 35–45.
- Kankaya E, Arslan ÖÇ, Parlak H and Ünal G. 2012. Induction of micronuclei in *Chalcalburnus tarichi* (Pallas, 1811) exposed to sub-lethal concentrations of methyl parathion. *Fresenius Environmental Bulletin*, 21(6): 1417–1421.
- Kwong TC. 2002. Organophosphate pesticides: biochemistry and clinical toxicology. *Therapeutic Drug Monitoring*, 24(1): 144–149.
- Lakshmaiah G. 2016a. Effect of phorate on histopathological changes in the kidney of common carp *Cyprinus carpio* exposed to lethal concentrations. *International Journal of Zoology Studies*, 1(4): 25–28.
- Lakshmaiah G. 2016b. A histopathological study on the liver of common carp *Cyprinus carpio* exposed to sublethal concentrations of phorate. *International Journal of Applied Research*, 2(6): 96–100.
- Lal B. 2007. Pesticide-induced reproductive dysfunction in Indian fishes. *Fish Physiology and Biochemistry*, 33(4): 455–462.
- Lee AC, Idrus FA and Aziz F. 2021. Cadmium and lead concentrations in water, sediment, fish and prawn as indicators of ecological and human health risk in Santubong Estuary, Malaysia. *Jordan Journal of Biological Sciences*, 14(2), 317–325.
- Machado MR and Fanta E. 2003. Effects of the organophosphorous methyl parathion on the branchial epithelium of a freshwater fish *Metynnis roosevelti*. *Brazilian Archives of Biology and Technology*, 46(3): 361–372.
- Murthy KS, Kiran BR and Venkateshwarlu M. 2013. A review on toxicity of pesticides in fish. *International Journal of Open Scientific Research*, 1(1): 15–36.
- Özok N, Oğuz AR, Kankaya E and Yeltekin AÇ. 2018. Hemato-biochemical responses of Van fish (*Alburnus tarichi* Guldenstadt, 1814) during sublethal exposure to cypermethrin. *Human and Ecological Risk Assessment: An International Journal*, 24(8): 2240–2246.
- Pandey A K and Shukla L. 1982. Effect of an organophosphorous insecticide malathion on the testicular histophysiology in *Sarotherodon mossambicus*. *National Academy Science Letters*, 7: 141–143.
- Pawar K R and Katdare M. 1983. Effect of sumithion on the ovaries of freshwater fish *Garra mullya* (Sykes). *Current Science*, 52(16): 784–785.
- Ram RN and Sathyanesan AG. 1987. Effect of long term exposure to cythion on the reproduction of the teleost fish, *Channa punctatus* (Bloch). *Environmental Pollution*, 44(1): 49–60.
- Rico A, Geber-Correa R, Campos PS, Garcia MVB, Waichman AV and Van Den Brink PJ. 2010. Effect of parathion-methyl on amazonian fish and freshwater invertebrates: a comparison of sensitivity with temperate data. *Archives of Environmental Contamination and Toxicology*, 58(3): 765–771.
- Saxena PK and Mani K. 1985. Quantitative study of testicular recrudescence in the freshwater teleost, *Channa punctatus* (bloch) exposed to pesticides. *Bulletin of Environmental Contamination and Toxicology*, 34: 597–607.
- Saxena PK and Mani K. 1987. Effect of safe concentration of some pesticides on testicular recrudescence in the freshwater murrel, *Channa punctatus* (bloch): a morphological study. *Ecotoxicology and Environmental Safety*, 14(1): 56–63.
- Selvi RT and Ilavazhahan M. 2012. Histopathological changes in gill tissue of the fish *Catla catla* exposed to sublethal concentration of pesticide methyl parathion and a heavy metal ferrous sulphate. *Biomedical and Pharmacology Journal*, 5(2): 305–312.
- Sunanda M, Chandra Sekhara Rao J, Neelima P, Govinda Rao K and Simhachalam G. 2016. Effects of chlorpyrifos (an organophosphate pesticide) in fish. *International Journal of Pharmaceutical Sciences Review and Research*, 39(1): 299–305.
- Takashima F and Hibiya T. 1995. An Atlas of Fish Histology: Normal and Pathological Features. Kodansha Ltd, Tokyo.
- Turkish Statistical Institute (Tuik). 2022. Su Ürünleri İstatistikleri. <https://data.tuik.gov.tr/Bulten/Index?p=Su-Urunleri-2021-45745>
- Ünal G. 2010. Balıklarda histolojik teknikler. In: Karataş M (Eds.), *Research Techniques in Fish Biology*, Karaman Bilim ve Araştırma Merkezi Derneği, Türkiye, pp. 303–360.
- Ünsal M. 1998. Kirlilik Deneyleri, Yöntemler ve Sonuçların Değerlendirilmesi. TKB, Su Ürünleri Araştırma Enstitüsü Müdürlüğü, Bodrum.
- Yeltekin AÇ, Oğuz AR, Kankaya E, Özok N and Güneş İ. 2020. Hematological and biochemical response in the blood of *Alburnus tarichi* (Actinopterygii: Cypriniformes: Cyprinidae) exposed to tebuconazole. *Acta Ichthyologica Et Piscatoria*, 50(4): 373–379.

Formulated Hand Sanitizer Utilizing Passion Fruit (*Passiflora edulis*) Leaf Extract as an Active Ingredient

Cabral, Daisy Anne M.¹, Hernandez, Marianne D.¹, Martinez, Leslie Ann B.¹ and Sangalang, Reygan H.^{2*}

¹Department of Chemical and Food Engineering, Batangas State University, Batangas, 4200, Philippines; ²College of Arts and Sciences, Batangas State University, Batangas, 4200, Philippines

Received: October 29, 2022; Revised: February 9, 2023; Accepted: February 23, 2023

Abstract

Passiflora edulis leaf extracts were added as an active ingredient for alcohol-based hand sanitizer (ABHS). Matured leaves were air-dried, powdered, and soaked in methanol (1:10, w/v) for 24 hours. The solvent-free crude extract was used to formulate hand sanitizer utilizing varying amounts of leaf extract (1,3 and 5% w/w). The antimicrobial activities of the leaf extracts and the hand sanitizer formulations were determined by calculating the zone of inhibition against some common pathogenic microorganisms. Physicochemical properties of the formulated hand sanitizers like appearance, odor, color, density, pH, and viscosity were also analyzed. Results show that the crude leaf extract contains alkaloids, flavonoids, and tannins as confirmed by the phytochemical screening and FTIR spectroscopy. Active antimicrobial activity against 3 of 5 microorganisms, namely *Staphylococcus aureus*, *Pseudomonas aeruginosa*, and *Trichophyton mentagrophytes*, was observed in crude leaf extract and formulated hand sanitizer. The formulated hand sanitizers are characterized by gel-to-liquid appearance, yellow-greenish tinge, characteristic citrus scent, and slightly acidic pH. The density and the viscosity of the three formulations were dependent on the concentration of passion fruit extract in the formulation.

Keywords: Antimicrobial Activity, Hand Sanitizer, *P. edulis* Leaf Extract, Phytochemicals

1. Introduction

The emergence of the coronavirus disease 2019 (COVID-19) has become a global health concern which severely affected the economy, livelihood, and overall well-being of people (Golin *et al.*, 2020; Wu *et al.*, 2020; Wang *et al.*, 2021). Among Western Pacific Region countries, the Philippines has faced one of the most severe cases of COVID-19. However, through continued adherence to the minimum health standards, such as appropriate use of face masks, proper hand hygiene, and physical distancing, the probability of COVID transmission per contact was reduced (Caldwell *et al.*, 2021).

The World Health Organization (WHO) has advocated proper hand hygiene to reduce the transmission of pathogenic microorganisms from person-to-person and recommended regular hand washing and the use of sanitizers (WHO, 2009). Proper hand hygiene, particularly hand washing, has been regarded as the cheapest, most effective, and single most important way to prevent and control hand-acquired infection caused by pathogenic microorganisms (Mathur, 2011; Jain *et al.*, 2016; Alsaidan *et al.*, 2020). However, frequent hand washing or continued use of alcohol may cause skin dryness due to the removal of fatty acids or natural oils in the hands, and may result in a microscopic surface crack that will serve as an entry point for microorganisms. Hand sanitizers

formulated with emollients were introduced to be an alternative to hand washing while preventing skin dehydration from occurring (Jain *et al.*, 2016; Alsaidan *et al.*, 2020). Alcohol-based hand sanitizers (ABHS) are more affordable and more predominant in most healthcare settings than its non-alcohol counterpart due to its efficacy in decreasing the transmission of infection (Golin *et al.*, 2020).

Many studies have affirmed the efficacy of many tropical plants in folk medicine due to its excellent antimicrobial activities. An exploration study conducted by Valle *et al.* (2015) validated the potential of twelve (12) Philippine medicinal plants against gram-positive and gram-negative multidrug resistant bacteria. Another study by San Luis *et al.* (2014) verified the presence of many bioactive compounds and confirmed the antibacterial potential of different indigenous plant chosen as revegetation species in landslide scars in Benguet, Philippines. Yellow passion fruit (*Passiflora edulis*) is a tropical fruit commonly consumed to make cakes, juice, jam, jelly, wine and many more (He *et al.*, 2020). In addition, the leaf infusions are commonly used as sedative or tranquilizers in some European countries and in America (Yuan *et al.*, 2017). Recent studies highlighted the antioxidant activity and antimicrobial activity of the compounds identified in the leaves of *P. edulis* (da Silva *et al.*, 2013; Xu *et al.*, 2013; Cazarin *et al.*, 2015). Flavone glycoside conjugates were identified as the major metabolites present in several species of *Passiflora*.

* Corresponding author. e-mail: reygans.sangalang@g.batstate-u.edu.ph.

Cyanogenic glycosides (mandelonitrile-*O*-di-glucoside and mandelonitrile-*O*-rutinoside) were also detected while harman alkaloids were noted at lower quantities than flavonoids (Farag *et al.*, 2016). In addition, the extracts from the fruit pericarp were shown to inhibit the growth of the majority of the bacterial strains examined with the lowest minimum inhibitory concentration (128 µg/mL) was recorded against *E. coli* (Dzotam *et al.*, 2015). *P. edulis* seed extracts exhibited antimicrobial activity against *S. aureus*, *C. albicans*, and *E. coli*, which may be attributed to the alkaloids, flavonoids, tannins, steroids, and saponins present (Kanu *et al.*, 2017). Indeed, the phytochemicals found in *P. edulis* had significant antibacterial properties which qualify it as a good active ingredient for the formulation of hand sanitizer.

The aim of this study was to develop and formulate hand sanitizer with *P. edulis* leaf extract. It also intended to determine the physicochemical and antimicrobial properties of the formulated hand sanitizer. It is envisioned that the outcome of this study will serve as a benchmark for future researchers and entrepreneurs to utilize extracts from underutilized plants and its parts in the production of antimicrobial products.

2. Methodology

2.1. Chemicals

Methanol (GR), HCl (AR), glacial acetic acid (AR), concentrated sulfuric acid, nitric acid, ferric chloride, Dragendorff's reagent were available in the CEFAA Laboratory and were used without further purification. The chemicals (*see Table 1*) used for hand sanitizer formulation were purchased from a local supplier.

2.2. Collection of Passion Fruit Leaves and Preparation of the Plant Extracts

Matured leaves of *P. edulis* with no visible damage or discoloration were collected in a farm at Lucban, Quezon, Philippines. The leaves were rinsed with water to take off the dirt and plant debris followed by final washing with distilled water.

Two hundred grams (200 g) of *P. edulis* leaves were selected and dried for seven (7) days until fully dried and brittle. The dried *P. edulis* leaves were reduced to a powder using a food processor and kept in an air-tight container. Powdered leaves were soaked in 2000 mL methanol (1:10, w/v) and stored in a cool, dry, dark place for 48 hours. Leaf residues were removed by filtration and the extracts were concentrated using rotary evaporator

under reduced pressure at 60 °C. The extracts were collected and stored at 4 °C in an amber bottle.

2.3. Phytochemical Screening of *P. edulis* Leaf Extract

The phytochemical test used for *P. edulis* leaf extracts was based from the method adapted from Guevarra *et al.* (2005). The alkaloids in the leaf extracts were determined by the Munier and Macheboeuf modification test wherein the diluted leaf extract was added with 3 drops of Dragendorff's reagent. Flavonoids in the leaf extract were determined by the Bate-Smith and Metcalf test in which 3 to 5 drops of 12 M HCl was mixed with the extract followed by gentle heating for 15-60 minutes. Fehling's test was done to determine the presence of glycosides in the leaf extract. In this method, one drop of 5% FeCl₃, concentrated H₂SO₄ and glacial acetic acid were added onto 2ml of leaf extract. Froth formation was the basis for the presence of saponins. In this test, leaf extracts were mixed with 2 to 3 mL water and were shaken vigorously afterwards. To test for the presence of tannins, 1% FeCl₃ were added dropwise to 1 mL of the leaf extract.

2.4. FTIR Spectra of Crude Leaf Extract

The functional groups present in the crude *P. edulis* leaf extract were determined using an FTIR (Thermo Scientific Nicolet 6700 FT-IR) spectroscope. Analysis of the FTIR spectra was conducted at the De La Salle University, Manila.

2.5. Formulation of Hand Sanitizer with *P. edulis* Leaf Extract

Formulation of the hand sanitizer with *P. edulis* extract was adopted from the method described by Thombare *et al.* (2015). Three formulations of alcohol-based hand sanitizers (F1, F2, and F3) were prepared as presented in Table 1. In many alcohol-based hand sanitizer formulation, 60-95% (v/v) ethanol, isopropanol, or *n*-propanol was used as hand sanitizer's main ingredient (Hans *et al.*, 2021). Emollients such as glycerin were added to aid in skin moisturization while thickeners were used to enhance the viscosity. Fragrance and dyes are added to increase the product's marketability and safety (Filipe *et al.*, 2021).

Hand sanitizer was formulated by mixing Carbopol 940 to deionized water until it became homogenous. Sodium citrate was then added to the mixture and left undisturbed for 24 hours. *P. edulis* leaf extracts, glycerin, polysorbate 20 were added to ethanol and were mixed with aqueous phase until homogenous. The hand sanitizers were kept in an air-tight HDPE container.

Table 1. Formulation of Hand Sanitizer

COMPONENTS	Quantity given (% w/w)			Uses
	F1	F2	F3	
Deionized water	32.5	30.5	28.5	Vehicle (Solvent)
Ethanol	62	62	62	Antimicrobial agent
<i>P. edulis</i> leaf extract	1	3	5	Antimicrobial agent
Carbopol 940	0.5	0.5	0.5	Thickening agent
Sodium Citrate	0.7	0.7	0.7	Solubilizing agent
Glycerin	2.3	2.3	2.3	Emollient
Polysorbate 20	0.5	0.5	0.5	Emulsifier
Fragrance Oil	0.5	0.5	0.5	Fragrance
Total	100	100	100	

2.6. Antimicrobial Activity of *P. edulis* Leaf Extract and Formulated Hand Sanitizer

The disc-diffusion assay was conducted to determine the antimicrobial activity of *P. edulis* leaf extract, formulated hand sanitizers, and commercial hand sanitizer. Analysis was done at the Microbiological Research and Services Laboratory (MRSL) of the University of the Philippines-Natural Science Research Institute (UP-NSRI). The antimicrobial activities of the aforementioned samples were tested on five (5) microorganisms: *Escherichia coli* (UPCC 1195), *Staphylococcus aureus* (UPCC 1143), *Pseudomonas aeruginosa* (UPCC 1244), *Candida albicans* (UPCC 2168), and *Trichophyton mentagrophytes* (UPCC 4193).

The microbial suspension used in the assay were made from the test organisms subcultured for 24 hours. Culture plates, about 3 mm thick, were prepared by pouring nutrient agar, glucose yeast peptone agar, potato dextrose agar onto the plates, followed by inoculation of the microbial suspension by swabbing the agar surface evenly. Using a sterile cork borer, 3 wells (about 10 mm) were made at equal distance and about 200 µg of samples were placed on each well. Culture plates with nutrient agar and glucose yeast peptone were incubated at 35° C and observed after 24 hours while the potato dextrose agar plates were incubated for 5 to 7 days at room temperature.

The inhibitory activity of the leaf extracts and hand sanitizer samples were determined by obtaining the diameter of the clearing zone (in mm). Ciprofloxacin (1 µg), tetracycline (30 µg), doxycycline (5µg) and Canesten solution (100 µL with 1% clotrimazole) were used as positive control. The antibacterial index was computed using the formula:

$$\text{Antimicrobial Index} = \frac{(\text{Diameter of clearing zone} - \text{Diameter of well})}{\text{Diameter of well}} \quad (1)$$

The following interpretative range of standard zone was adopted from Guevarra *et al.* (2005).

Table 2. Interpretative Range of Standard Zone

Zone of Inhibition, mm	Inhibitory Activity	Interpretation
> 19	+++	Very Active
14 - 19	++	Active
10 - 13	+	Partially Active
< 10	-	Inactive

2.7. Physicochemical Analysis of Hand Sanitizers

The physicochemical properties of the formulated hand sanitizers and commercial hand sanitizer were analyzed at the Chemical Engineering Laboratory of Batangas State University. Sensory analysis was used to evaluate the organoleptic characteristics of the formulated hand sanitizers. Visual test was made to check the appearance and color while an olfactory test was done to determine the odor of the samples. The pH of the samples were analyzed using a pH meter (Eutech, Thermo Scientific), wherein the average of three trials was used to compute the pH. The density was determined by pycnometer method as prescribed in ASTM D854. The average of three trials was used to compute the density. To determine the viscosity, Oswald viscometer was utilized in which the average of the three trials was used to calculate the viscosity.

2.8. Data Analysis

Independent T-test and One-way analysis of variance (ANOVA) were used to analyze the results and were carried out using SPSS version 20.0

3. Results and Discussion

3.1. Antibacterial Activity of *P. edulis* Leaf Extract

Active antibacterial activity was demonstrated by *P. edulis* leaf extract against 3 of 5 pathogenic microorganisms, namely *S. aureus*, *P. aeruginosa*, and *T. mentagrophytes* as depicted by the clearing zone values of 15 mm, 17 mm, and 15 mm, respectively. On the contrary, no growth inhibition against *E. coli* and *C. albicans* was observed (Table 3).

Table 3. Antimicrobial Activity of the *P. edulis* Leaf Extract*

Test Organism	Sample	Clearing zone (mm)	Antimicrobial Index	Inhibitory Activity
<i>E.coli</i>	Leaf Extract	NI	0	-
	Control ^a	28	3.7	+++
<i>S. aureus</i>	Leaf Extract	15.0 ± 0.0	0.5	++
	Control ^b	45	6.5	+++
<i>P. aeruginosa</i>	Leaf Extract	17.0 ± 1.0	0.7	++
	Control ^c	18	2.0	++
<i>C. albicans</i>	Leaf Extract	NI	0	-
	Control ^d	40	3.0	+++
<i>T. mentagrophytes</i>	Leaf Extract	14.67 ± 0.58	0.5	++
	Control ^d	70	6.0	+++

Note: Leaf extract, 3%; NI means no inhibition of growth of the test organism. ^aDisc contains 1 µg Ciprofloxacin, 6 mm diameter. ^b Disc contains 30 µg Tetracycline, 6 mm diameter. ^c Disc contains 5 µg Doxycycline, 6 mm diameter. ^d Canesten solution, 100 µL (contains 1% clotrimazole)

Similar investigations on the antimicrobial activity of the methanolic extract of *P. edulis* leaf revealed its efficacy against *S. aureus*, *P. vulgaris*, *E. coli*, *S. faecalis*, *B. subtilis*, and *S. typhi* (Kanan *et al.*, 2011). In a similar

study, *P. edulis* leaf extract significantly inhibited the growth of *L. monocytogenes*, *S. gallolyticus*, *S. aureus*, *B. subtilis*, and *B. cereus*. Intermediate activity against *B. subtilis*, *S. aureus*, and *L. monocytogenes* were observed in

methanol extracts, while a small zone of inhibition was noted in the petroleum ether and acetone extracts. In addition, partially active antimicrobial activity was observed against *P. aeruginosa* and *E. coli*. Moreover, *S. enteritidis* and *P. vulgaris* was observed to be sensitive towards methanolic extracts (Ramaiya *et al.*, 2014). In the investigation conducted by the group of Ripa (2009), chloroform extracts of *P. edulis* leaf exhibited moderate antibacterial activity, while no activity was determined from petroleum ether extract. The highest growth inhibition was observed against *P. aeruginosa*, *S. boydii*, and *S. dysenteriae*. The abovementioned results of the cited studies validate the antimicrobial action of *P. edulis* extract against pathogenic bacteria.

3.2. Phytochemical Screening of *P. edulis* Leaf Extract

Table 4. Phytochemical Screening of the *P. edulis* Leaf Extract*

Plant Constituent	Chemical Test	Result	Descriptive Result
Alkaloids	Munier and Macheboeuf Modification Test	+	Orange precipitate was formed.
Flavonoids	Bate-Smith and Metcalf Test	+	Generation of magenta color.
Tannins	Ferric Chloride Test	+	Generation of brownish-green color. Brick-red colored precipitate was not observed.
Glycosides	Fehling's Test	-	No formation of froth
Saponins	Froth Test	-	No formation of froth

Note: *Methanolic extract; The notations (+) and (-) indicates presence or absence, respectively.

Analysis of the *P. edulis* leaf extract through phytochemical screening showed that alkaloids, flavonoids, and tannins were present (Table 4). The phytochemicals in the methanolic leaf extract were confirmed by the Bate-Smith and Metcalf test, Munier and Macheboeuf modification test, and Ferric chloride test, respectively, wherein its concentration depends largely on the polarity of the solvent utilized for extraction. The phytochemical screening findings in the present study are comparable to the outcome of the study by the team of Doss (2008) and Johnson (2008).

The presence of flavonoid compounds such as vitexin, isovitexin, isorientin, vicenin-2, and 6,8-di-C-glycosyl chrysin in *P. edulis* leaf extracts was identified and quantified by the team of da Silva (2013), Ayres (2015) and Cazarin (2015). Flavonoid compounds were identified to be present in high quantities in the leaves. In the study of Ferreres and coworkers (2007), sixteen (16) apigenin and luteolin derivatives including *O*-glycosyl-*C*-glycosyl, *O*-glycosyl, and mono-*C*-glycosyl and were identified and characterized to be present in *P. edulis* leaves. In addition, 4 flavones mainly 2,6-dideoxyhexose-*C*-glycosyl were also isolated and identified in the stem and leaves of *P. edulis* Sims (Xu *et al.*, 2013). Solvent partitioning and

chromatographic separation of the methanolic leaf extract led the team of Yuan (2017) to the identification of 12 new compounds such as benzenoids (3), flavonoids (4), quinol (1), amides (2), steroid (1) and lignan (1) in *P. edulis*.

Flavonoids, alkaloids, and tannins are reported to possess antioxidant activity and antibacterial activity by forming a complex with soluble and extracellular proteins, most especially bacterial cell walls, thereby negating their activity (Othman *et al.*, 2019; Pizzi, 2021). Alkaloids, phenols, glycosyl flavonoids and cyanogenic compounds were found mostly throughout the *Passiflora* genus. Other phytoconstituents such as anthocyanins, γ -lactone, carotenoids, and volatile oil constituents were also reported to be isolated in *P. edulis* (Dhawan *et al.*, 2004). The antimicrobial activity exhibited by the passion fruit leaf extracts against *S. aureus*, *P. aeruginosa*, and *T. mentagrophytes* may be due to the presence of these phytochemicals.

3.3. FTIR Spectrum of the Crude Leaf Extract

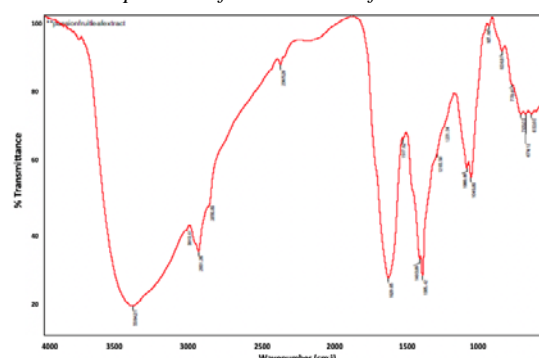


Figure 1. FTIR Spectrum of the *P. edulis* leaf extract

FTIR analysis of the methanolic leaf extract of *P. edulis* (Figure 1) revealed different peaks corresponding to different functional groups (Table 5). The result of FTIR analysis further confirmed that flavonoids, alkaloids, and tannins (Ricci *et al.*, 2015; Ayalew, 2020) were present in the crude leaf extract and were accountable for the antimicrobial activity of the *P. edulis* leaf extract.

Table 5. FTIR Peak Values in *P. edulis* Leaf Extract

Wave Number, cm ⁻¹	Compound Assignment
3342	O-H stretching vibration (presence of OH group in flavonoids)
2931	-CH, CH ₂ asymmetric stretching
2365	CH ₃ asymmetric and symmetric stretching
1620 & 1517	C=C aromatic ring stretching vibration (Presence of aromatic ring)
1403	Ring stretching vibration
1306	CH ₃ and CH ₂ scissoring (CH ₃ and CH ₂ groups in flavonoids and aromatics)
1060 & 1049	C-O stretching of alcohol and hydroxy compounds (phenols in tannins and flavonoids)
836	C-H deformation aromatic ring (attributed to tannins)
770	C-C stretching vibration
705	Ring deformation (attributed to tannins)
674 & 632	Aromatic C-H out of plane bending

3.4. Properties of Formulated Hand Sanitizers with *P. edulis* Leaf Extract (1%, 3% and 5%) and Commercial Hand Sanitizer

Table 6. Properties of Formulated and Commercial Hand Sanitizer

Properties	Formulated Hand Sanitizer			Brand A*
	F1	F2	F3	
Appearance	Gel	Gel-Liquid	Non-gel	Gel
Color	Translucent, light green with yellowish tinge	Translucent, dull green with yellowish tinge	Translucent, dark green with yellowish tinge	Translucent, green with yellowish tinge
Odor	Characteristic citrus scent	Characteristic citrus scent	Characteristic citrus scent	Sweet and Fruit-like Scent
pH	4.92 ± 0.02 ^A	4.59 ± 0.01 ^B	4.42 ± 0.01 ^B	6.18 ± 0.05 ^C
Density	0.8829 ± 0.0001 ^A	0.8830 ± 0.0003 ^A	0.8873 ± 0.0001 ^B	0.8813 ± 0.0015 ^A
Viscosity (Pa-s)	2.27 ± 0.02 ^A	0.07 ± 0.0 ^B	0.0005 ± 0.0 ^C	4.21 ± 0.15 ^D

*Brand A is the commercial hand sanitizer.

Mean values with different superscript within the same row indicate significant difference at 5% level of significance.

The properties of formulated hand sanitizers and commercial hand sanitizers are presented in Table 6. The appearance and color of formulated hand sanitizers varies as the amount of *P. edulis* extract increases (Figure 2). F1 is characterized as a gel with translucent light green, a yellowish tinge, and a characteristic citrus scent. On the other hand, F3 is a non-gel with translucent dull green with a yellowish tinge and characteristic citrus scent.

Compared to commercial hand sanitizer, significant differences in the pH and viscosity ($p < 0.05$) were noted for all the formulated hand sanitizer, while no significant difference in the density ($p > 0.05$) was noted. The formulated hand sanitizer is more acidic and less viscous than commercial hand sanitizer.



Figure 2. Formulated Hand Sanitizer with varying level of *P. edulis* Leaf Extract

The amount of *P. edulis* extract in the formulation greatly impacts the pH and viscosity of the formulated

hand sanitizer. It was observed that when the amount of *P. edulis* extract in the formulation was increased, the density increased while the pH and viscosity decreased. The pH of the formulated hand sanitizer in this study is slightly lower than the pH of the hand sanitizer with *Calendula officinalis* and aloe vera (4.16 to 6.65) formulated by the group of Fallica (2021). Both hand sanitizers are slightly acidic and were within the skin's pH range (4.5 to 6.5), indicating that the skin can tolerate it. In addition, due to addition of aloe vera, xanthan gum, and hydroxyethyl cellulose as viscosity thickener, the viscosity of the hand sanitizer developed by the group of Fallica (2021) was higher than the viscosity in the present study (except for F1 which has gel-like appearance and has a viscosity of 2.27 Pa-s). It is also comparable to the viscosity of the formulated hand sanitizer with zinc-amino clay and *Opuntia humifusa* extract (1.4 to 1.5 Pa-s) formulated by Hoang *et al.* (2021). Hand sanitizer with reasonable viscosity is important since it contributes to skin feel, and spreadability of the product (Hoang *et al.*, 2021). In their study, Binder *et al.* (2019) concluded that penetrability of the active ingredient onto the skin was independent of the dynamic viscosity of the product. Hence, formulation with moderate viscosity is recommended to allow ease of application.

3.5. Antimicrobial Activity of the Formulated Hand Sanitizers with *P. edulis* leaf extract and Commercial Hand Sanitizer**Table 7.** Antimicrobial Properties of Formulated Hand Sanitizer

Test Organism	Sample	Clearing zone, mm	Antimicrobial Index (AI)	Inhibitory Activity
<i>E. coli</i>	F1	NI	0	-
	F2	NI	0	-
	F3	NI	0	-
	Brand A [*]	12.3 ± 0.58	0.2	+
	Ciprofloxacin	38	2.8	+++
<i>S. aureus</i>	F1	21.6 ± 0.53 ^A	1.2	+++
	F2	26.0 ± 0.87 ^B	1.6	+++
	F3	25.9 ± 0.60 ^B	1.6	+++
	Brand A	18.7 ± 1.15 ^D	0.2	+++
	Ciprofloxacin	32	2.2	+++
<i>P. aeruginosa</i>	F1	14.6 ± 0.53 ^A	0.5	++
	F2	16.1 ± 0.60 ^B	0.6	++
	F3	17.4 ± 0.88 ^C	0.8	++
	Brand A	12.3 ± 0.58 ^D	0.9	+
	Ciprofloxacin	33	2.3	+++
<i>C. albicans</i>	F1	NI	0	-
	F2	NI	0	-
	F3	NI	0	-
	Brand A	16.3 ± 2.31	0.6	++
	Canesten ^a	35	2.5	+++
<i>T. mentagrophytes</i>	F1	15.8 ± 0.83 ^A	0.6	++
	F2	20.8 ± 1.72 ^B	1.1	+++
	F3	15.8 ± 0.44 ^A	0.6	++
	Brand A	31.3 ± 0.58 ^D	2.1	+++
	Canesten ^a	80	7.0	+++

NI means no inhibition of growth of the test organism. ^{*}Brand A is the commercial hand sanitizer.

^a Contains 1% clotrimazole

Mean values with different superscript within the same column (per microorganism) indicates significant difference at 5% level of significance.

Results obtained for the antimicrobial activity of the formulated hand sanitizer with *P. edulis* leaf extract against pathogenic food-borne bacteria were presented in Table 7. From the result of the disc diffusion assay (Figure 3), the formulated hand sanitizer exhibited very active antibacterial activity against *S. aureus*, while active activity was noted against *P. aeruginosa* and *T. mentagrophytes* (except for F2, which has very active activity). On the other hand, the formulated hand sanitizer has inactive activity towards *E. coli* and *C. albicans*. Significant differences ($p < 0.05$) in the antimicrobial activity of formulated and commercial hand sanitizer were observed in the *S. aureus*, *P. aeruginosa* and *T. mentagrophytes*. In addition, no significant differences ($p > 0.05$) in the inhibition of *S. aureus* between F2 and F3 and in *T. mentagrophytes* between F1 and F3 were observed.

The antimicrobial activity of the formulated hand sanitizer can be attributed to the combined activity of phytochemicals present in the extracts. The high antibacterial activity of the leaf extracts against the 3 out of 5 pathogenic microorganisms tested in the present study may be due to the alkaloids, tannins, and flavonoids present in the extract. The antimicrobial activity of tannins and flavonoids can be ascribed to its ability to provide stable free radicals and inactivate protein due to complex

formation with nucleophilic amino acids in the microbial cell wall (Suurbaar *et al.*, 2017, Tura *et al.*, 2017). The non-inhibitory activity of formulated hand sanitizers against *Candida albicans* may be due to the absence of glycosides which is the active phytochemical compound responsible for inhibiting the growth of the said microorganism (Park *et al.*, 2010; Klunda *et al.*, 2016). The negative antimicrobial result of passion fruit leaf extract against the aforementioned microorganism further supports this. In the case of commercial hand sanitizers, excellent antimicrobial activity was exhibited by hand sanitizers with ethanol (80 %), isopropanol (75%) or benzalkonium chloride as the main active ingredient. However, significant variation in the efficacy against other pathogens was noted in different commercial hand sanitizers wherein *E. coli* is more susceptible to most of the samples evaluated than *S. aureus* (Chojnacki. *et al.*, 2021). In their study, Manaye *et al.* (2021) evaluated the effectiveness of ABHS marketed in Southwest Ethiopia. Commercially available ABHS with ethanol concentration ranging from 70% to 80% were utilized. Results revealed that the minimum inhibitory concentration (MIC) against the test organisms, *E. coli* and *S. aureus*, was at 45%, 55%, 65% and in undiluted form for Taflen. Five of the seven ABHS brands were successful in inhibiting the growth of test microorganisms.

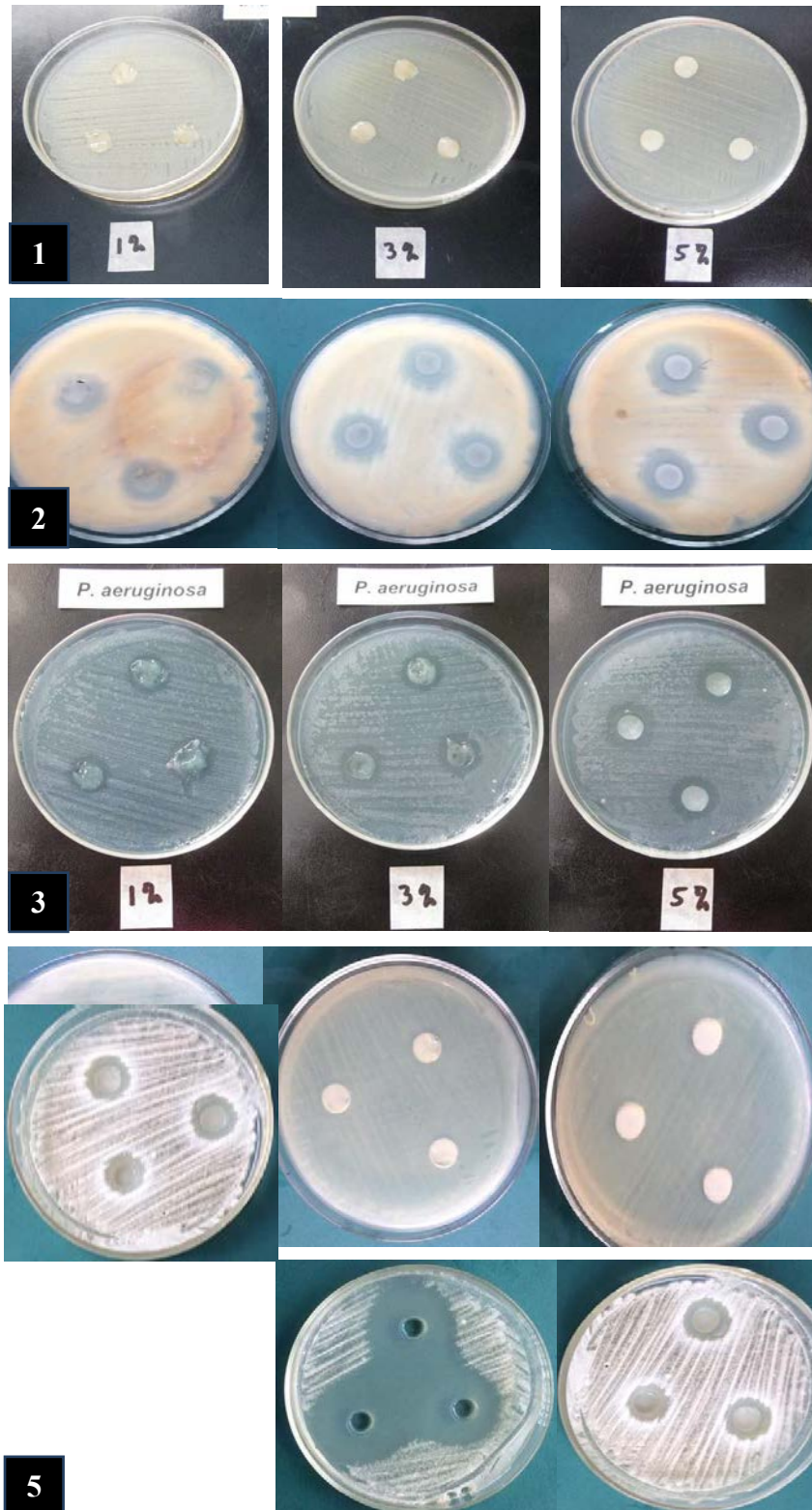


Figure 3. Antibacterial Test of Formulated Hand Sanitizer Samples Against (1) *E. coli* (2) *S. aureus* (3) *P. aeruginosa* (4) *C. albicans* (5) *T. mentagrophytes* (from left to right, F1, F2, and F3)

Nzekwe *et al.* (2021) assessed the effects of various formulation conditions such as pH, electrolyte concentration, and additives such as plant extracts and benzalkonium chloride on the killing rate of ABHS against microorganisms. Addition of plant extracts such as aloe vera, carrots and cucumber led to wider differences in the activities of ethanol and isopropanol against *S. aureus* than *E. coli*. Moreover, inclusion of extracts can confer

additional properties in ABHS such as antioxidant activity, skin brightening effects, and anti-inflammatory effects. Addition of plant-based extracts to current formulation was noted as a possible solution to reduce the toxicity problem posed by alcohol based-hand sanitizers (Alghamdi, 2021).

4. Conclusion

Passiflora edulis leaf extract was added as an active ingredient to formulate a hand sanitizer. The leaf extracts contained alkaloids, flavonoids, and tannins based on the phytochemical screening analysis. The presence of the said compounds was further confirmed, as shown in the FTIR spectra. The leaf extracts were observed to prevent the growth of *P. aeruginosa*, *S. aureus*, and *T. mentagrophytes*. The formulated hand sanitizer had a greenish tinge and characteristic citrus odor. The addition of varying amounts of *P. edulis* leaf extracts was observed to significantly affect the hand sanitizer's physical properties ($p < 0.05$). It was observed that as the amount of *P. edulis* leaf extract in the hand sanitizer is increased, the density increased while the pH and viscosity decreased. The formulated hand sanitizer can prevent the growth of pathogenic organisms such as *S. aureus*, *P. aeruginosa*, and *T. mentagrophytes*.

Acknowledgment

This study would not have been possible without the support and assistance of the CAS and CEFAA administration, the researchers' friends and family. Heartful gratitude is bestowed to Ms. Ivy Fides R. Perez for lending her time in the final checking of the manuscript.

References

Alghamdi, H.A. 2021. A need to combat COVID-19; herbal disinfection techniques, formulations and preparations of human health friendly hand sanitizers. *Saudi J. Biol. Sci.*, **28**(7): 3943–3947.

Alsaidan, M.S., Abuyassin, A.H., Alsaeed, Z.H., Alshmmari, S.H., Bindaaj, T.F., & Alhababi, A.A. 2020. The Prevalence and Determinants of Hand and Face Dermatitis during COVID-19 Pandemic: A Population-Based Survey. *Dermatol Res Pract.*, 2020, 6627472, 8 pp.

Ayalew A.A. 2020. Chromatographic and spectroscopic determination of solvent-extracted *Lantana camara* leaf oil. *J. Int Med Res.*, **48**(10): 1-12.

Ayres, A.S.F.S.J., de Araújo, L.L.S., Soares, T.C., Costa, G.M., Reginatto, F.H., Ramos, F.A., Castellanos, L., Schenkel, E.P., Soares-Rachetti, V.P., Zucolotto, S.M., & Gavioli, E.C. 2015. Comparative central effects of the aqueous leaf extract of two populations of *Passiflora edulis*. *Revista Brasileira de Farmacognosia*, **25**: 499-505.

Binder, L., Mazál, J., Petz, R., Klang, V., & Valenta, C. 2019. The role of viscosity on skin penetration from cellulose ether-based hydrogels. *Skin Res. Technol.*, **25**: 725–734.

Caldwell, J.M., de Lara-Tuprio, E., Teng, T.R., Estuar, M.R.J.E., Sarmiento, R.F.R., Abayawardana, M., Leong, R.N.F., Gray, R.T., Wood, J.G., Le, L.V., McBryde, E.S., Ragonnet, R. & Trauer, J.M. 2021. Understanding COVID-19 dynamics and the effects of interventions in the Philippines: A mathematical modelling study. *Lancet Regl Health West Pac.*, **14**: 100211.

Cazarin, C.B.B., da Silva, J.K., Colomeu, T.C., Batista, Â.G., Meletti, L.M.M., Paschoal, J.A.R., Bogusz Junior, S., Reyes, F.G.R., Augusto, F., de Meirelles, L.R., Zollner, R.L., Maróstica Júnior, M.R. 2015. Intake of *Passiflora edulis* leaf extract improves antioxidant and anti-inflammatory status in rats with 2,4,6-trinitrobenzenesulphonic acid induced colitis. *J. Funct. Foods*, **17**: 575-586.

Chojnacki, M., Dobrotka, C., Osborn, R., Johnson, W., Young, M., Meyer, B., Laskey, E., Wozniak, R., Dewhurst, S., & Dunman, P.M. 2021. Evaluating the Antimicrobial Properties of Commercial Hand Sanitizers. *mSphere*, **6**(2): e00062-2.

da Silva, J.K., Cazarin, C.B.B., Colomeu, T.C., Batista, Â.G., Meletti, L.M.M., Paschoal, J.A.R., Bogusz Júnior, S., Furlan, M.F., Reyes, F.G.R., Augusto, F., Maróstica Júnior, M.R. & Zollner, R.L. 2013. Antioxidant activity of aqueous extract of passion fruit (*Passiflora edulis*) leaves: In vitro and in vivo study. *Food Res. Int.*, **53**(2): 882-890.

Dhawan, K., Dhawan, S., & Sharma, A. 2004. Passiflora: a review update. *J Ethnopharmacol.*, **94**(1): 1-23.

Doss, A., Doss, P.A., & Dhanabalan, R. 2008. In-Vitro Antimicrobial Activity of Extracts of *Passiflora edulis* (Passifloraceae) and *Sphaeranthus indicus* (Asteraceae). *Ethnobotanical Leaflets*, **12**: 728-733.

Dzotam, J.K., Touani, F.K. & Kuete, V. 2015. Antibacterial and antibiotic-modifying activities of three food plants (*Xanthosomamaffa* Lam., *Moringa oleifera* (L.) Schott and *Passiflora edulis* Sims) against multidrug-resistant (MDR) Gram-negative bacteria. *BMC Complement Altern Med.*, **16**(9):1-8.

Fallica, F., Leonardi, C., Toscano, V., Santonocito, D., Leonardi, P., & Puglia, C. 2021. Assessment of Alcohol-Based Hand Sanitizers for Long-Term Use, Formulated with Addition of Natural Ingredients in Comparison to WHO Formulation 1. *Pharmaceutics*, **13**(4): 571.

Farag, M. A., Otify, A., Porzel, A., Michel, C. G., Elsayed, A., & Wessjohann, L. A. 2016. Comparative metabolite profiling and fingerprinting of genus *Passiflora* leaves using a multiplex approach of UPLC-MS and NMR analyzed by chemometric tools. *Anal Bioanal Chem.*, **408**(12): 3125–3143.

Ferreres, F., Sousa, C., Valentão, P., Andrade, P.B., Seabra, R.M. & Gil-Izquierdo, Á. 2007. New C-Deoxyhexosyl Flavones and Antioxidant Properties of *Passiflora edulis* Leaf Extract. *J. Agric. Food Chem.*, **55**(25): 10187–10193.

Filipe, H.A.L., Fiuza, S.M., Henriques, C.A., & Antunes, F.E. 2021. Antiviral and antibacterial activity of hand sanitizer and surface disinfectant formulations. *Int J. Pharm.*, **609**: 121139.

Golin, A.P., Choi, D., & Ghahary, A. 2020. Hand sanitizers: A review of ingredients, mechanisms of action, modes of delivery, and efficacy against coronaviruses. *Am. J. Infect Control*, **48**(9): 1062-1067.

Guevara, B.Q. (Ed.), Quinto A., & Santos M.A. 2005. Microbiology Section, **A guidebook to Plant Screening: Phytochemical and Biological, Revised Edition**, Manila: UST Publishing House.

Hans, M., Lugani, Y., Chandel, A.K., Rai, R., Kumar, S. 2021. Production of first- and second-generation ethanol for use in alcohol-based hand sanitizers and disinfectants in India. *Biomass Convers Biorefin.*, **27**: 1-18.

He, X., Luan, F., Yang, Y., Wang, Z., Zhao, Z., Fang, J., Wang, M., Zuo, M., & Li, Y. 2020. *Passiflora edulis*: An Insight Into Current Researches on Phytochemistry and Pharmacology. *Front pharmacol.*, **11**: 617.

Hoang, H.T., Van Tran, V., Bui, V.K.H., Kwon O.H., Moon, J.Y., & Lee, Y.C. 2021. Novel moisturized and antimicrobial hand gel based on zinc-amino clay and *Opuntia humifusa* extract. *Sci Rep*, **11**: 17821.

Jain, V. M., Karibasappa, G. N., Dodamani, A. S., Prashanth, V. K., & Mali, G. V. 2016. Comparative assessment of antimicrobial efficacy of different hand sanitizers: An *in vitro* study. *Dent Res J (Isfahan)*, **13**(5): 424–431.

- Johnson, M., Maridass, M., & Irudayaraj, V. 2008. Preliminary Phytochemical and Antibacterial Studies on *Passiflora edulis*. *Ethnobotanical Leaflets*, **2008(1)**: Art. 51, 425-432.
- Kannan, S., Devi, B.P., & Jayakar, B. 2011. Antibacterial evaluation of the methanolic extract of *Passiflora edulis*. *Hygeia-J. D. Med.*, **3(1)**, 46-49.
- Kanu, A.M., Okorie, A.C., Uche, C., & Awa, U.N. 2017. Phytochemical Screening and Antimicrobial Activity of Ethanolic Extract of *Passiflora edulis* var. *flavicarpa* Seed on Selected Pathogens. *Univ J. Microbiol Res.*, **5(3)**: 35-39.
- Klunda, T., Machová, E., Čížová, A., Horák, R., Poláková, M., & Bystrický, S. 2016. Alkyl glycosides as potential anti-*Candida albicans* growth agents. *Chem. Pap.*, **70(9)**: 1166-1170
- Manaye, G., Muleta, D., Henok, A., Asres, A., Mamo, Y., Feyissa, D., Ejeta, F., & Niguse, W. 2021. Evaluation of the Efficacy of Alcohol-Based Hand Sanitizers Sold in Southwest Ethiopia. *Infect Drug Resist.*, **14**, 547-554.
- Manuel, J.F., Balangcod, T.D., Laruan, L.A., Patacsil, M.C., Martin, S.P. 2011. Suppression of growth of some medically important bacterial pathogens (*Escherichia coli*, *Staphylococcus aureus*, *Pseudomonas aeruginosa*, and *Salmonella typhimurium*) with plant extracts of selected indigenous semi-temperate medicinal plants in the Philippines. *Tangkoyob Journal*, **6(1)**:1-12.
- Mathur P. 2011. Hand hygiene: back to the basics of infection control. *Indian J Med Res.*, **134(5)**, 611-620.
- Nzekwa, I.T., Agwuka, O.I., Okezie, M.U., Fasheun, D.O., Nnamani, P.O. & Agubata, C.O. 2021. Designing an ideal alcohol-based hand sanitizer: in vitro antibacterial responses of ethanol and isopropyl alcohol solutions to changing composition. *AAPS Open*, **7(5)**.
- Othman, L., Sleiman, A., & Abdel-Massih, R.M. 2019. Antimicrobial Activity of Polyphenols and Alkaloids in Middle Eastern Plants. *Front Microbiol.*, **10(911)**: 1-28.
- Park, C., Woo, E.-R., & Lee, D. G. 2010. Anti-*Candida* property of a lignan glycoside derived from *Styrax japonica* S. et Z. via membrane-active mechanisms. *Mol Cells*, **29(6)**: 581-584.
- Penecilla G.L., & Magno C.P. 2011. Antibacterial activity of extracts of twelve common medicinal plants from the Philippines. *J. Med. Plant. Res.*, **5(6)**: 3975-3981.
- Pizzi, A. 2021. Tannins medical/pharmacological and related applications: A critical review. *Sustain. Chem. Pharm.*, **22**: 100481.
- Ramaiya, S.D., Bujang, J.S., & Zakaria, M.H. 2014. Assessment of Total Phenolic, Antioxidant and Antibacterial Activities of *Passiflora* Species. *ScientificWorldJournal*, **Vol. 2014**, 167309, 10 p.
- Ricci, A. Olejar, K.J., Parpinello, G.P., Kilmartin, P.A., & Versari, A. (2015). Application of Fourier Transform Infrared (FTIR) Spectroscopy in the Characterization of Tannins. *Applied Spectroscopy Reviews*, **50(5)**, 407-442.
- Ripa, F.A., Haque, M., Nahar, L., & Islam, M.M. 2009. Antibacterial, Cytotoxic and Antioxidant Activity of *Passiflora edulis* Sims. *European Journal of Scientific Research*, **31(4)**: 592-598.
- San Luis, G. D., Balangcod, T.D., Abucay, Jose Jr. B., Wong, F.M., Balangcod K. D., Afifi, N.G., & Apostol, O.G. (2014). Phytochemical and antibacterial screening of indigenous species that have potential for revegetation of landslides in Atok, Benguet, Philippines. *Indian Journal of Traditional Knowledge*, **13(1)**: 56-62.
- Suurbaar, J., Mosobil, R. & Donkor, AM. 2017. Antibacterial and antifungal activities and phytochemical profile of leaf extract from different extractants of *Ricinus communis* against selected pathogens. *BMC Res Notes*, **10**: 660.
- Thombare, M.A., Udugade, B.V., Hol, T.P., Mulik, M.B., & Pawade, D.A. 2015. Formulation and Evaluation of Novel Herbal Hand Sanitizer. *Indo American Journal of Pharmaceutical Research*, **5(1)**: 483-488.
- Tura, G.T., Eshete, W.B. & Tucho, G.T. 2017. Antibacterial efficacy of local plants and their contribution to public health in rural Ethiopia. *Antimicrob Resist Infect Control*, **6(76)**.
- Valle, D. L., Andrade, J. I., Puzon, J. J. M., Cabrera, E. C., & Rivera, W. L. 2015. Antibacterial activities of ethanol extracts of Philippine medicinal plants against multidrug-resistant bacteria. *Asian Pac J Trop Biomed.*, **5(7)**: 532-540.
- Wang C, Tee M, Roy AE, Fardin MA, Srichokchatchawan W, Habib HA, et al. 2021. The impact of COVID-19 pandemic on physical and mental health of Asians: A study of seven middle-income countries in Asia. *PLoS ONE*, **16(2)**: e0246824.
- World Health Organization, WHO guidelines on hand hygiene in health care: first global patient safety challenge clean care is safer care. 2009. World Health Organization, Geneva
- Wu, Y. C., Chen, C. S., & Chan, Y. J. (2020). The outbreak of COVID-19: An overview. *J Chin Med Assoc: JCMA*, **83(3)**: 217-220.
- Xu, F., Wang, C., Yang, L., Luo, H., Fan, W., Zi, C., Dong, F., Hu, J. & Zhou, J. (2013). C-dideoxyhexosyl flavones from the stems and leaves of *Passiflora edulis* Sims. *Food Chem.*, **136**: 94-99.
- Yuan, T. Z., Kao, C. L., Li, W. J., Li, H. T., & Chen, C.Y. (2017). Chemical Constituents of Leaves of *Passiflora edulis*. *Chem Nat Compd.*, **53(6)**:1165-1166.

Telmisartan Enhances the Accumulation of Doxorubicin as a Combination Therapy for the Management of Triple Negative Breast Cancer

Wala'a Al.Safadi¹, Belal Omar Al-Najjar^{1,3}, Moath Alqaraleh^{1,*}, Anas Ibrahim Abed¹, Walhan Alshaer², Dana Alqudah², Fadwa Daoud², Razan Mohammad Obeidat¹, Obada Abdulmalek Sibai¹, Zainab Zaki Zakaraya¹

¹Pharmacological and Diagnostic Research Center (PDRC), Faculty of Pharmacy, Al-Ahliyya Amman University, Amman, Jordan; ²Cell Therapy Center, The University of Jordan, Amman, Jordan; ³Department of Pharmaceutical Sciences, Faculty of Pharmacy, Al-Ahliyya Amman University, 19328, Amman, Jordan

Received: December 8, 2022; Revised: February 12, 2023; Accepted: March 2, 2023

Abstract

Background: Triple-negative breast cancer (TNBC) is one of the most aggressive tumours with dismal survival and a high death rate. Chemotherapeutic resistance due to P-gp overexpression was shown in MDA-MB-231 human breast cancer cells. The aim of this study was to re-sensitize of MDA-MB-231 human breast cancer cells to Doxorubicin by suggested P-gp inhibitors.

Methods: Screening of around 100 in-house prepared compounds against the crystal structure of the P-glycoprotein was performed using molecular docking tool. The top ranked hits obtained were Verapamil, Benazepril, and Telmisartan. Accordingly, the anticancer activity of Doxorubicin and in combination with suggested P-gp inhibitors were examined on MDA-MB-231 breast cancer cell line, using the [3-(4,5-dimethyliazol-2-yl)-2,5-diphenyl tetrazolium bromide] MTT assay. Accumulation of Doxorubicin was analyzed by flow cytometry.

Results: Telmisartan showed the lowest binding energy (-9.7 Kcal/mol) followed by Benazepril and Verapamil, with -9.2, -7.3 and -6.4 Kcal/mol, respectively. These compounds were chosen for the next phase of studies to evaluate their in vitro biological effects against TNBC cell line (MDA-231). Doxorubicin in combination with Telmisartan significantly inhibited cell proliferation in the MDA-MB-231 breast cancer cell line (IC₅₀=0.08261 μM for MDA-MB-231) more than Doxorubicin alone (IC₅₀=0.2847 μM for MDA-MB-231). Flow cytometry examined the accumulation of Doxorubicin inside the MDA-MB-231 breast cancer cell line after 24 hours of treating them with Telmisartan.

Conclusion: current findings suggest that Telmisartan re-sensitize MDA-MB-231 breast cancer cells to Doxorubicin by increasing Doxorubicin accumulation.

Keywords: Triple negative breast cancer, Doxorubicin, Chemotherapy resistance, Telmisartan, P-glycoprotein inhibitors, Molecular docking.

1. Introduction

Breast cancer is the most prevalent type of cancers in women with a high mortality rate. Of all subtypes of breast cancer, triple negative breast cancer (TNBC) is considered the most aggressive one and is associated with very poor prognosis (Yin et al., 2020). Despite the revolution in cancer therapy, the conventional chemotherapy using combination of drugs remains the cornerstone when it comes to TNBC treatment (O'Reilly et al., 2021).

Doxorubicin-based chemotherapy is the most commonly used regimens in the treatment of variety of cancers including TNBC (Denard et al., 2018). Doxorubicin is an anthracycline compound that intercalates with the DNA and inhibits topoisomerases leading to cell cycle arrest and eventually apoptosis (Al-

malky et al., 2019). However, regardless its popularity, the emerging resistance to Doxorubicin (also known as chemo-resistance) is a significant issue that has not yet been resolved (Christowitz et al., 2019). When applied at the optimum doses, Doxorubicin can efficiently hamper cancer progression and development. However, following repetitive doses, cancer cells develop chemoresistance towards Doxorubicin leading to diminished antiproliferative effect (Mirzaei et al., 2022). Increasing the concentration of Doxorubicin might not be a wise decision due to the cardiotoxicity of Doxorubicin (Zhang et al., 2020). Therefore, continuous efforts should aim for novel strategies to alleviate Doxorubicin resistance.

Several chemoresistance mechanisms have been proposed in breast cancer with the most extensively being the efflux pumps such as P-glycoprotein (P-gp) (Robey et al., 2018). P-gp (also known as MDR1 or ABCB1) is a

* Corresponding author. e-mail: M.alqaraleh@ammanu.edu.jo.

member of the ATP-binding cassette (ABC) family and a well-known drug transporter presents in the cell membrane that mediate resistance against structurally and functionally different chemotherapeutic drugs (Gottesman et al., 1996). Accordingly, it is not surprising that overexpression of P-gp is associated with poor prognosis and higher incidence of relapse (Waghray & Zhang, 2018). An earlier work conducted by Bao et al. (2011) demonstrated that overexpression on P-gp in breast cancer prevented the internalization of Doxorubicin within the nucleus leading to minimal efficacy and chemoresistance (Bao et al., 2011).

Having its key role in mediating resistance towards chemotherapy, the development of P-gp inhibitors has been a primary focus in the cancer research. The rationale behind combining chemotherapy with P-gp inhibitors is that they can logically enhance the cellular uptake of the chemotherapeutic drugs leading to more prominent effects (Lai et al., 2020). To-date, a large set of small molecules that aim to inhibit the function of P-gp have been developed. The clinical progression of the specific P-gp inhibitors has been rather disappointing due to the failure in clinical trials in addition to the safety issues associated with these small molecules (Chung et al., 2016). Therefore, drug repurposing of the currently FDA approved drugs could be an interesting clinical rationale. This is particularly of huge interest since the FDA approved drugs possess a reasonable safety profile. Moreover, combining these drugs with chemotherapy may result in enhanced anti-cancer effects. For instance, Verapamil, a calcium channel blocker known for its potent P-gp inhibitory effect, has been widely studied in clinical research (Lai et al., 2020). For instance, Bao et al. (2011) reported an increased cellular uptake of Doxorubicin when combined with Verapamil leading to superior anti-cancer effect compared to Doxorubicin alone (Bao et al., 2011). Cyclosporin, an immunosuppressant, is another P-gp inhibitor that was shown to enhance the nuclear contents of Doxorubicin in breast and lung cancer cells (Waghray & Zhang, 2018).

In-silico screening can be used to study and understand the intermolecular interactions between the proposed ligands and the therapeutic target (Al-Najjar 2018, Saqallah et al., 2022). Herein, the current study aims to employ the concept of drug repurposing to investigate the P-gp inhibitory function of a variety of FDA approved drugs and their biological activities. More importantly, the study intends to explore whether combining the potential P-gp candidates with Doxorubicin enhances its cellular uptake and subsequently its anti-cancer effect *in vitro*. This approach has the potential to overcome chemoresistance developed against Doxorubicin leading to better clinical outcomes.

2. Materials and Methods

2.1. Molecular docking

The following software packages were utilized in this project:

- Avogadro 1.2.0 (Hanwell et al., 2012).
- ACD/ChemSketch, (www.acdlabs.com) (ACD/Labs, 2019).
- Autodock 4.2 (Morris et al., 2009).

Around 100 ligands were collected according to the availability of the chemicals in the university. These compounds were subjected to molecular docking simulations against the crystal structure of the p-glycoprotein (PDB code: 7A6F) (Nosol et al., 2020). The chemical compounds were created using the ChemSketch software, saved as mol files. A short steepest descent energy minimization procedure was performed to adjust inaccurate bond lengths and bond angles; at this stage, atom types were assigned using the Universal Force Field, pre-packaged with Avogadro' software and converted to pdb format. Atomic charges were added; all hydrogen atoms were combined, and each compound was opened independently. The grid box was centered at the binding site of the co-crystal inhibitor (Zosuquidar) with the coordinates of 162.15, 160.03, 158.00 as x, y, z, respectively. The box volume was set to 22.5 Å³ with the default grid spacing value of 0.375 Å. Afterward, the default docking parameters were used to conduct the molecular docking of each ligand for 100 Lamarckian genetic algorithm runs using AutoDock 4 (Fuhrmann et al., 2010).

2.2. Cell Culture

MDA-231 breast cancer cell line was obtained from the university of Jordan while the origin is "The European Collection of Authenticated Cell Cultures" (ECACC/UK) (ECACC catalogue no. 92020424). MDA-123 cell line is an epithelial, human breast cancer cell line that was established from a pleural effusion of a 51-year-old Caucasian female with a metastatic mammary adenocarcinoma (Cailleau et al., 1978). MDA-231 cells were maintained in a high glucose Dulbecco's Modified Eagle Medium (DMEM), supplemented with 10% (v/v) fetal bovine serum, 1% penicillin and streptomycin. Unless stated otherwise, all other chemicals, reagents and solvents used in this study were purchased from Invitrogen (USA).

2.3. Colorimetric MTT assay

To measure cell viability, the colorimetric microculture tetrazolium assay (MTT) method was used. The cultured MDA-123 cells were seeded at a density of 1X10⁴ cells per well in 96-well plates (Al-Tawarah et al., 2020). The next day cells were treated at concentrations (10-100 µM) of Verapamil, Benazepril, or Telmisartan as single agent or with Doxorubicin at concentrations (0.001-100 µM), which were purchased from Santa Cruz (USA).

The culture plates were incubated for 72 hours (Lee et al., 2020), then 15 µL of MTT solution was added to each well and for 4 hours. After that 100 µL of DMSO were added to each well. Cell growth was determined by measuring the optical density (OD) at 590/630 nm with Microplate Reader Biotech™ ELx800™.

2.4. Cellular uptakes by Flow Cytometry

Human breast cancer cell line MDA-231 cells were seeded in a 12-well plate at 1x10⁴ cells/well and left over 24 hours to attach. Subsequently, 30 µg/mL of Telmisartan were prepared and directly applied to adhered cells and incubated over 1 hour at 37°C. Subsequently, Doxorubicin was added and incubated for 1, 4 and 24 hours. After that, the culture media was removed, and cells were washed two times with PBS. Cells were then detached gently with 200 mL of StemPro™ Accutase™ Cell Dissociation Reagent (Gibco, USA) for 5 min and transferred into 5 mL flow

tubes (BD, USA). 1×10^4 events were counted by FACS Canto II and analyzed using BD FACS Diva™ software version 8.0 (BD, USA).

3. Results

3.1. In-house database virtual screening

The co-crystallised ligand Zosuquidar (Structure Code: ZQU1301) was successfully docked against 7A6F crystal structure of the P-glycoprotein with a root-mean-square distance (RMSD) of 1.0 Å (Figure 1). RMSD is used to quantitatively measure the similarity between two or more compounds. The smaller the RMSD, the more similar compounds (Kufareva & Abagyan, 2012). Generally, molecular docking simulations that produce an RMSD values of less than 2.0 Å are considered to have performed successfully (Yusuf et al., 2008).



Figure 1. Solid ribbon representation of P-glycoprotein (PDB code: 7A6F). crystal structure bound with the co-crystallized ligand (grey) and the re-docked conformation (green).

Upon screening, around 100 molecules were successfully docked against 7A6F crystal structure of the P-glycoprotein. Eventually, Telmisartan, Verapamil, and Benazepril were amongst top-ranked compounds (Figure 2). Investigation of these compounds in the binding site have shown that Telmisartan participates in two hydrogen bond interactions with Gln990 and Phe983 residues, while Leu339, Ile340, Phe343 and Phe983 amino acids perform hydrophobic and aromatic interactions (Figure 3A). Additionally, Benazepril, on the other hand, was found to interact with Gln725 and Gln990 by hydrogen bond interaction, while both Ile306, Phe343 interact by hydrophobic and aromatic interactions, respectively (Figure 3B). Finally, verapamil mainly performs hydrophobic and aromatic interactions with Leu329, Phe343, Gln725 and Phe728, whereas Trp232 was found to perform hydrogen bond interaction (Figure 3C). If we can assume the importance of the residues involved in the interaction with the co-crystallized ligand (Zosuquidar), it will be significant to find a compound that can successfully interact with these key residues. Telmisartan is the only compound among the top-ranked hits that interact with both key residues Leu339, Gln990. Table 1 shows the top-ranked compounds with their corresponding binding energies, as well as the interacting residues. Telmisartan showed the lowest binding energy (-9.7 Kcal/mol) followed by Benazepril and Verapamil, with -9.2, -7.3 and -6.4 Kcal/mol, respectively. These compounds were chosen for the next phase of studies to evaluate their *in vitro* biological effects against TNBC cell line (MDA-231).

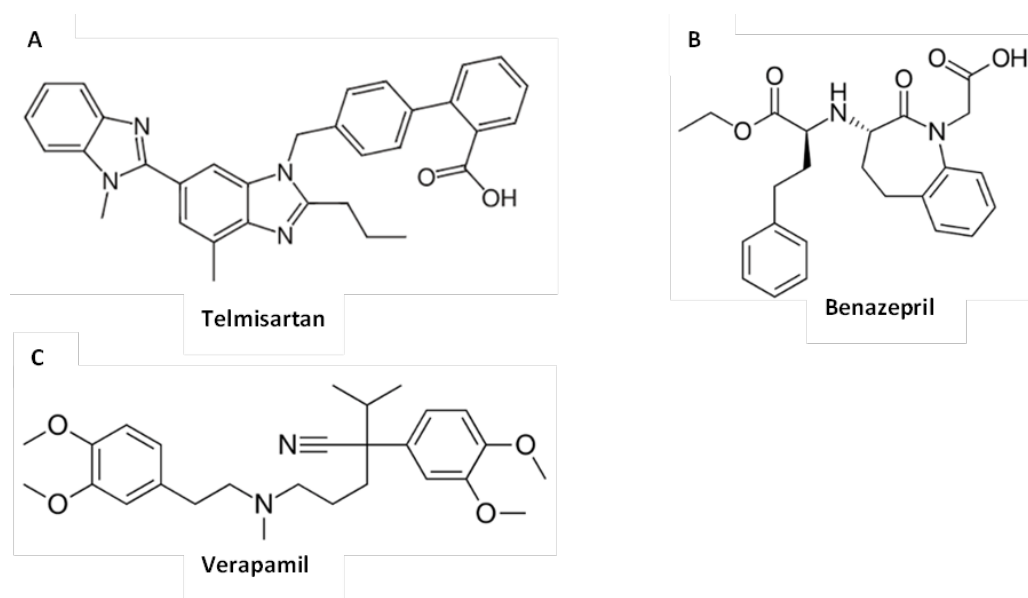


Figure 2: The chemical structure of Telmisartan (A), Benazepril (B), and Verapamil (C).

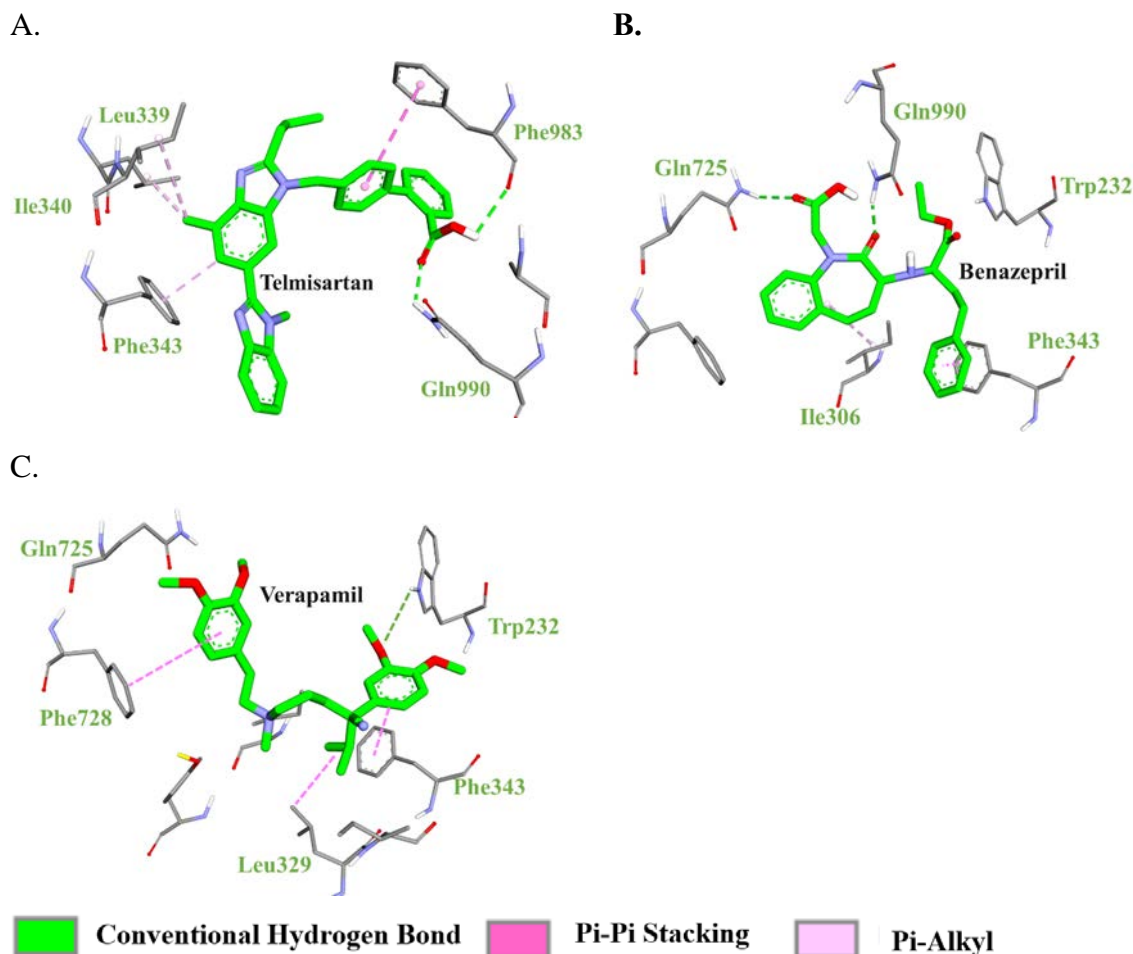


Figure 3. Stick representation of A. Telmisartan, B. Benazepril, and C. Verapamil in the P-gp binding site.

Table 1. The lowest binding energies obtained from AutoDock 4.2 in-house database 7A6F crystal structure and interacting amino acids.

Compound	Lowest Binding Energy (Kcal/mol)	Interacting amino acids
Telmisartan	-9.7	Leu339, Ile340, Phe343, Phe983, Gln990
Benazepril	-7.3	Ile306, Phe343, Gln725, Gln990
Verapamil	-6.4	Trp232, Leu329, Phe343, Phe728
Zosuquidar	-6.5	Phe303, Leu339, Gln990

3.2. Telmisartan enhances the antiproliferative effect of Doxorubicin against MDA-231 TNBC cellline

Following successful docking, it was postulated that the inhibition of P-gp by these compounds may improve the cellular response towards Doxorubicin-induced cell death. Accordingly, the potential synergy between the tested compounds and Doxorubicin against MDA-231 cell line was evaluated using MTT assay. For this purpose, MDA-231 cells were treated with increasing concentrations of

Doxorubicin, Benazepril, Verapamil, as monotherapy or in combination with Doxorubicin for 72 hours prior to viability testing using MTT assay. The results revealed that Doxorubicin treatment resulted in a dose-dependent reduction in cell viability over the period of 72 hours with an IC_{50} of 0.2847 μ M (Figure 4A). On the contrary, monotherapy treatment with Benazepril, Verapamil, and Telmisartan resulted in modest reduction of cell viability (Figure 4B-D).

The combination treatment of Doxorubicin/benazepril had no superior efficacy compared to monotherapy of Doxorubicin illustrated by no significant reduction in the IC_{50} value (Figure 5A). In contrast, Verapamil appeared to enhance the antiproliferative effect of Doxorubicin. However, this synergistic effect was only observed at certain concentrations but not the full panel (Figure 5B). Interestingly, the combination therapy of Doxorubicin/Telmisartan resulted in the strongest synergy demonstrated by significant reduction in the IC_{50} compared to cells treated with either agent alone (Figure 5C) (Table 2).

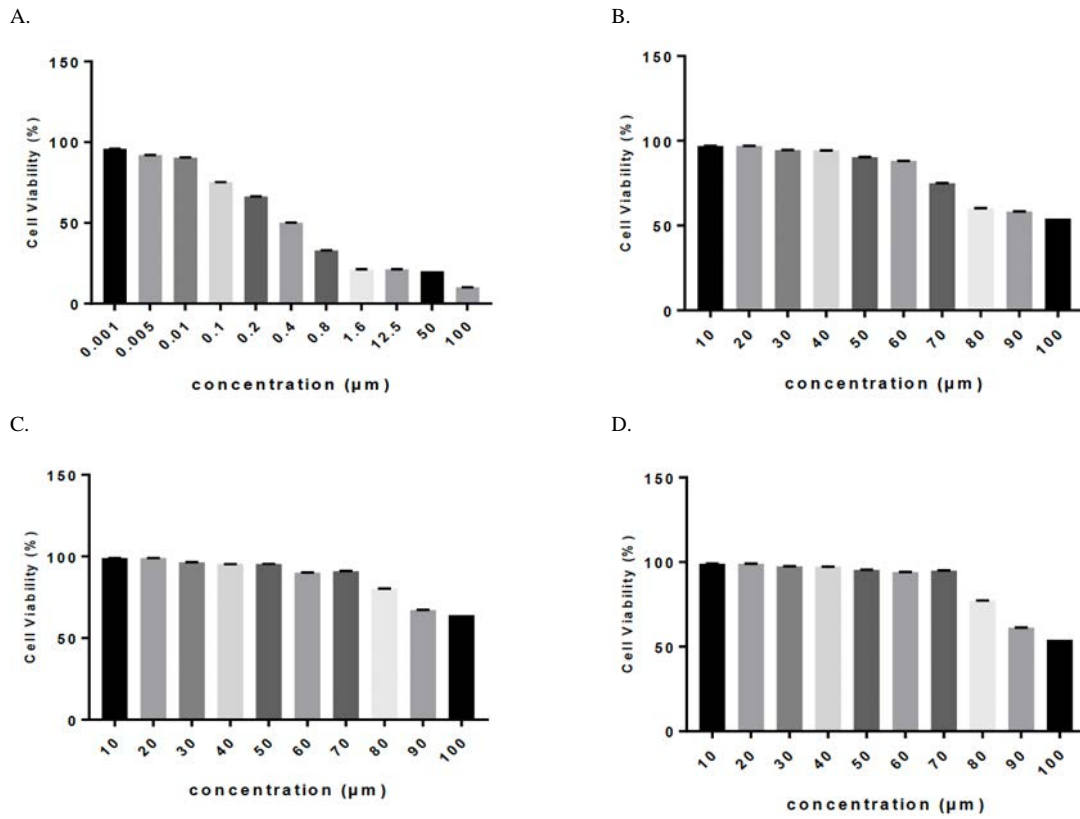


Figure 4. The anti-proliferative effect of Doxorubicin, Benzepiril, Verapamil, and Telmisartan on breast cancer. MDA-231 breast cancer cells were treated with increasing concentrations of Doxorubicin (A), Benzepiril (B), Verapamil (C), or Telmisartan (D) as monotherapy for 72 hours prior to MTT proliferation assay analysis. Data represent mean ± SD (n=3).

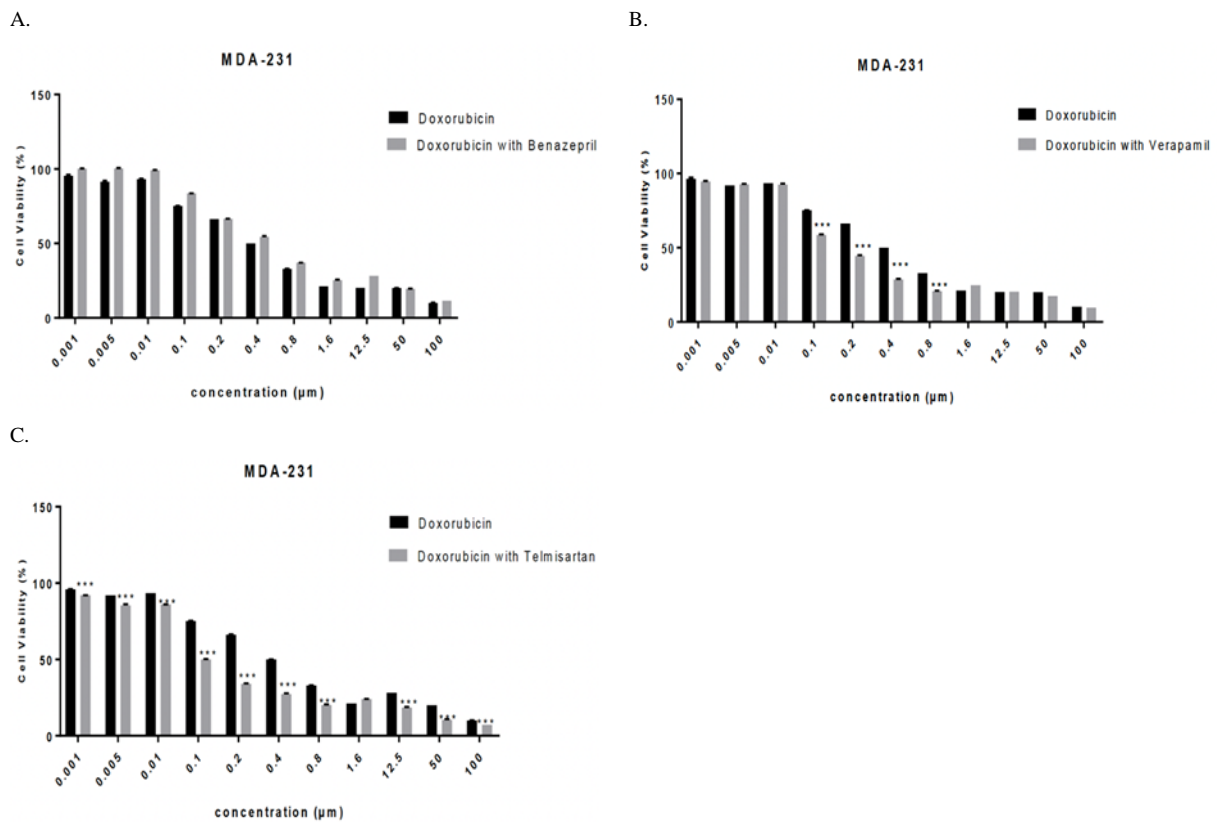


Figure 5. Assessment of the anti-proliferative effect of combination therapy. MDA-231 cells were treated with different concentrations of Doxorubicin (0.001-100 µM) alone or in combination with 70µM Benzepiril (A), 70µM Verapamil (B), or 60µM Telmisartan (C) for 72 hours prior to cell viability testing using MTT assay. Data represent mean ± SD (n=3). P values *: p<0.05, ** p<0.01, ***, p<0.001 calculated using *t-test*.

Table 2. IC₅₀ values (µM) of the *in vitro* antiproliferative activity of Doxorubicin with Verapamil, Doxorubicin with Benazepril, and Doxorubicin with Telmisartan on MDA-231 cell line.

Treatment	IC ₅₀ (µM)	p-value
Doxorubicin	0.2847	
Doxorubicin/Verapamil	0.1175	0.1528
Doxorubicin/Benazepril	0.262	0.8226
Doxorubicin/Telmisartan	0.08261	0.0089***

The results were expressed as mean ± SD (n = 3) and analysed using t-test, *: p<0.05, **: p<0.01, ***: p<0.001 compared to their respective Doxorubicin (control).

3.3. Telmisartan enhances the cellular uptake of Doxorubicin

The significant reduction in IC₅₀ upon dual drug therapy with Doxorubicin and Telmisartan but not with other combinations raised a question whether Telmisartan was more potent P-gp inhibitor than the other compounds which may led to enhanced Doxorubicin accumulation and

therefore improve cytotoxic effect. For this purpose, cellular uptake of Doxorubicin was performed using flow cytometry analysis, thanks to the fluorescent properties of Doxorubicin. MDA-231 cells were exposed to a concentration of 30 µg/mL of Telmisartan for 1 hour prior to the treatment with the IC₅₀ concentration of Doxorubicin for 1, 4, and 24 hours. The analysis revealed no significant uptake of Doxorubicin either alone or in combination with the Telmisartan at 1 and 4 hours' time-point (Figure 6A and B). However, at 24 hours' time-point, while there was a notable cellular uptake of Doxorubicin in cells treated with Doxorubicin alone, the Doxorubicin/Telmisartan co-therapy resulted in superior accumulation indicated by more prominent increase in the fluorescence signal (Figure 6C).

The synergistic effect observed between Telmisartan and Doxorubicin along with the superior cellular uptake of Doxorubicin might be attributed to the potent P-gp inhibitory effect of Telmisartan compared to any other compounds tested.

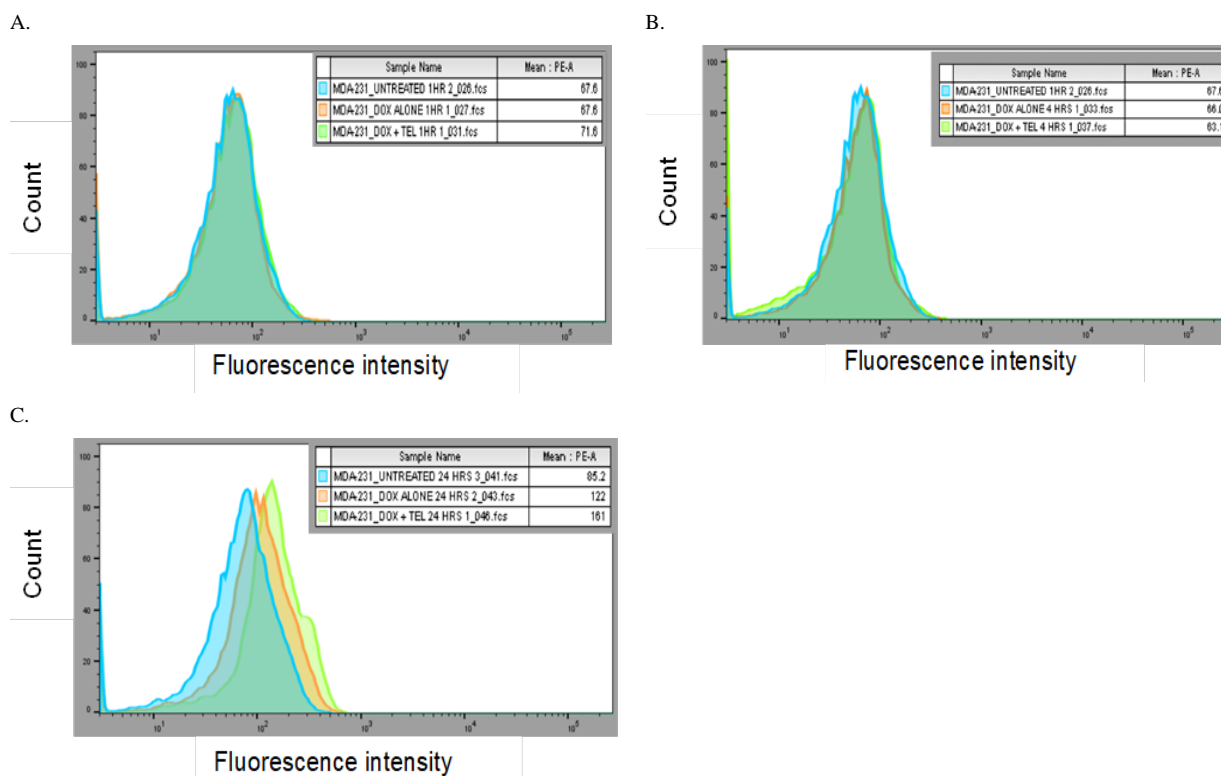


Figure 6. Assessment of cellular uptake of Doxorubicin in combination with Telmisartan. MDA-231 breast cancer cells were treated with 30 µg/mL of Telmisartan for 1 hour prior to the treatment with 0.285 µM of Doxorubicin for 1, 4, and 24 hours (A, B, and C respectively) prior to flow cytometry analysis. The results are summarized by measuring the fluorescence intensity relative to that of untreated (control) cells.

4. Discussion

Regardless the huge ongoing research and efforts, breast cancer continues to be a major health problem. The incidence and mortality rates have dramatically increased during the past few years and are expected to worsen in the future. Recently, breast cancer has been recognized as the most common cancer and the leading cause of cancer-related death especially in young women under 45 years-old of age (Anastasiadi et al., 2017; Karzai et al., 2022).

TNBC counts for almost quarter of newly diagnosed breast cancer cases and relatively to other BC subsets TNBC has higher incidence of metastasis to visceral organs such as brain, lungs, and bones, which usually occurs within 5 years. Also, TNBC has higher incidence of recurrence and relapse that is characterized by chemoresistance and aggressive course (Yin et al., 2020). Accordingly, it is unsurprising that TNBC is the most aggressive type of breast cancer.

Due to the aggressive etiology of TNBC, treatment progression is still a challenge. Systemic chemotherapeutic

agent is the cornerstone treatment for TNBC (Omarini et al., 2018).

Doxorubicin is an anthracycline related chemotherapeutic agent, known to be the most effective cytotoxic agent while using it with adjuvant setting to decrease relapse and mortality in TNBC (Shah & Gradishar, 2018). However, chemoresistance is a major concern. Among variety of proposed mechanisms, the overexpression of a multi-drug resistant (MDR) protein called P-gp represents a major cause of chemoresistance (Trédan et al., 2007). P-gp acts as an efflux pump to efflux the chemotherapeutic agents such as Doxorubicin outside the cancerous cells leading to the development of resistance towards chemotherapeutic drugs (Ughachukwu & Unekwe, 2012). In this context, Bao et al. (2011) have shown that the overexpression of P-gp in breast cancer cells prevented the accumulation of Doxorubicin within the nucleus, and thus the intercalation of Doxorubicin with the DNA was hindered. Therefore, molecules aim to inhibition of P-gp efflux mechanisms represents an attractive clinical concept (Bao et al., 2011).

A plethora of studies were conducted to evaluate the efficacy of P-gp inhibitors in combination with chemotherapeutic agents to re-sensitize the cells to many chemotherapeutic agents. For instance, Kopecka et al. (2020) have shown that Tariquidar (a P-gp inhibitor) re-sensitized TNBC cells towards Doxorubicin-induced apoptosis by inhibiting the efflux pump and increase the accumulation then the cytotoxic effect of Doxorubicin (Kopecka et al., 2020). However, most of the P-gp inhibitors candidates have failed in clinical trials where the combination of chemotherapeutic agents with P-gp inhibitors resulted in no improvements but increased toxicity (Carlson et al., 2006).

Herein, we aimed to explore and investigate potential candidates as P-gp inhibitors that may alleviate the chemoresistance against Doxorubicin in TNBC.

Computational docking studies were done to discover a P-gp inhibitors on cultures of MDR cancerous cells and showed that the inhibitors were not just substrates for P-gp and enhanced the accumulation of chemotherapeutic agents but also some of them activate the immune response, eventually, resulting in enhanced cell death (Nanayakkara et al., 2018).

In this study, we found that many compounds have a high fitting value by the docking study, then Telmisartan, Benazepril, and NCS were selected to bioavailability study on TNBC cells. Amongst all compounds tested, Telmisartan was the only compound found to interact with the key amino acid residues within the P-gp binding site which are Leu339, Gln990. Our findings are supported by data from *in silico* studies where two pharmacophore modelling indicated the exceptional P-gp inhibitory effect of Telmisartan with IC_{50} values of 3.9 and 1.2 μ M (Chang et al., 2006; Weiss et al., 2010). Also, and in agreement with our findings, Telmisartan was shown to exhibit superior potency compared to Verapamil as a P-gp inhibitor rendering it more clinically relevant P-gp inhibitor (Chang et al., 2006).

In cell culture model, the co-treatment of MDA-231 TNBC cells with Doxorubicin and Telmisartan resulted in a significant reduction in the IC_{50} of Doxorubicin suggesting that Telmisartan successfully sensitized the TNBC cells to Doxorubicin potentially through P-gp inhibition (Figure 7). Further studies using flow cytometry analyses demonstrated that the efficacy of Telmisartan is attributed to enhanced accumulation of Doxorubicin in the Doxorubicin/Telmisartan treated cells compared to untreated cells. While the exact mechanism of synergy was not evaluated during the course of this study, Chang et al. (2006) indicated that Telmisartan did not result in reduction in mRNA expression of P-gp. Rather, the inhibition is thought to be a direct interaction between P-gp and Telmisartan (Chang et al., 2006).

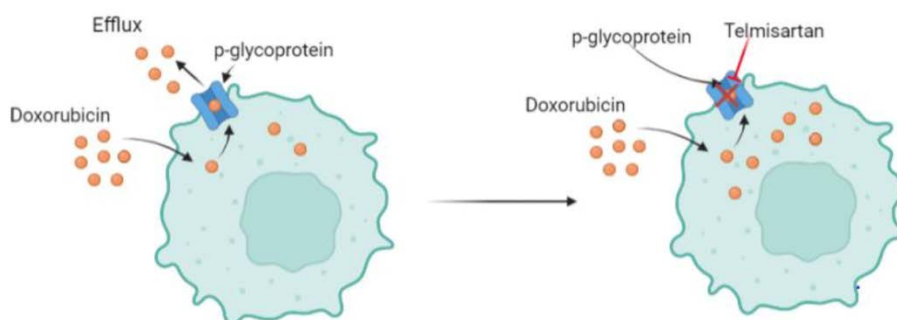


Figure 7. The proposed mechanism of synergy of Doxorubicin and Telmisartan combination therapy.

5. Conclusion

In conclusion, this study shows a potential synergistic effect between Doxorubicin and Telmisartan indicated by a significant reduction in IC_{50} values of combination therapy compared to either agent alone. The mechanism of synergy is proposed to be mediated at least in part by p-glycoprotein inhibition by Telmisartan. This potential mechanism was based on the observation that pre-

treatment with Telmisartan resulted in enhanced Doxorubicin accumulation within breast cancer cells. However, more investigation is still needed to elucidate the exact mechanism of synergy.

Acknowledgment

We would like to acknowledge Al-Ahliyya Amman University for funding and the Pharmacological and

Diagnostic Research Center (PDRC) as well as the Cell Therapy Center (CTC) for their collaboration.

References

- Al-malky, H. S., Al Harthi, S. E., & Osman, A.-M. M. (2019). Major obstacles to doxorubicin therapy: Cardiotoxicity and drug resistance. *J. Oncol. Pharm. Pract.*, **26**(2), 434–444.
- Al-Tawarah, N., Qaralleh, H., Khlaifat, A., Nofal, M., Alqaraleh, M., Khleifat, K., Allimoun, M., Ahmed, M., & Alshhab, M. (2020). Anticancer and Antibacterial Properties of Verthemia Iphonides Essential Oil /Silver Nanoparticles. *Biomed. Pharmacol. J.*, **13**, 1175–1184.
- Anastasiadi, Z., Lianos, G. D., Ignatiadou, E., Harissis, H. V., & Mitsis, M. (2017). Breast cancer in young women: an overview. *Updates Surg.*, **69**(3), 313–317.
- Bao, L., Haque, A., Jackson, K., Hazari, S., Moroz, K., Jetly, R., & Dash, S. (2011). Increased Expression of P-Glycoprotein Is Associated with Doxorubicin Chemoresistance in the Metastatic 4T1 Breast Cancer Model. *Am. J. Pathol.*, **178**(2), 838–852.
- Cailleau, R., Olivé, M., & Cruciger, Q. V. (1978). Long-term human breast carcinoma cell lines of metastatic origin: preliminary characterization. *In Vitro*, **14**(11), 911–915.
- Carlson, R. W., O'Neill, A. M., Goldstein, L. J., Sikic, B. I., Abramson, N., Stewart, J. A., Davidson, N. E., & Wood, W. C. (2006). A Pilot Phase II Trial of Valspodar Modulation of Multidrug Resistance to Paclitaxel in the Treatment of Metastatic Carcinoma of the Breast (E1195): A Trial of the Eastern Cooperative Oncology Group. *Cancer Invest.*, **24**(7), 677–681.
- Chang, C., Bahadduri, P. M., Polli, J. E., Swaan, P. W., & Ekins, S. (2006). Rapid identification of P-glycoprotein substrates and inhibitors. *Drug Metab. Dispos.*, **34**(12), 1976–1984.
- Christowitz, C., Davis, T., Isaacs, A., van Niekerk, G., Hattingh, S., & Engelbrecht, A.-M. (2019). Mechanisms of doxorubicin-induced drug resistance and drug resistant tumour growth in a murine breast tumour model. *BMC Cancer*, **19**(1), 757.
- Chung, F. S., Santiago, J. S., Jesus, M. F. M. De, Trinidad, C. V., & See, M. F. E. (2016). Disrupting P-glycoprotein function in clinical settings: what can we learn from the fundamental aspects of this transporter? *Am. J. Cancer Res.*, **6**(8), 1583–1598.
- Denard, B., Jiang, S., Peng, Y., & Ye, J. (2018). CREB3L1 as a potential biomarker predicting response of triple negative breast cancer to doxorubicin-based chemotherapy. *BMC Cancer*, **18**(1), 813.
- Fuhrmann, J., Rurainski, A., Lenhof, H.-P., & Neumann, D. (2010). A new Lamarckian genetic algorithm for flexible ligand-receptor docking. *J. Comput. Chem.*, **31**, 1911–1918.
- Gottesman, M. M., Pastan, I., & Ambudkar, S. V. (1996). P-glycoprotein and multidrug resistance. *Curr. Opin. Genet. Dev.*, **6**(5), 610–617.
- Hanwell, M. D., Curtis, D. E., Lonie, D. C., Vandermeersch, T., Zurek, E., & Hutchison, G. R. (2012). Avogadro: an advanced semantic chemical editor, visualization, and analysis platform. *J. Cheminform.*, **4**(1), 17.
- Karzai, S., Port, E., Siderides, C., Valente, C., Ahn, S., Moshier, E., Ru, M., Pisapati, K., Couri, R., Margolies, L., Schmidt, H., & Cate, S. (2022). Impact of Screening Mammography on Treatment in Young Women Diagnosed with Breast Cancer. *Ann. Surg. Oncol.*
- Kofareva, I., & Abagyan, R. (2012). Methods of protein structure comparison. *Methods Mol. Biol.*, **857**, 231–257.
- Lai, J.-I., Tseng, Y.-J., Chen, M.-H., Huang, C.-Y. F., & Chang, P. M.-H. (2020). Clinical Perspective of FDA Approved Drugs With P-Glycoprotein Inhibition Activities for Potential Cancer Therapeutics. *Front. Oncol.*, **10**, 561936.
- Lee, K.-S., Lee, M.-G., Kwon, Y.-S., & Nam, K.-S. (2020). Arctigenin Enhances the Cytotoxic Effect of Doxorubicin in MDA-MB-231 Breast Cancer Cells. *Int. J. Mol. Sci.*, **21**(8).
- Mirzaei, S., Gholami, M. H., Hashemi, F., Zabolian, A., Farahani, M. V., Hushmandi, K., Zarrabi, A., Goldman, A., Ashrafizadeh, M., & Orive, G. (2022). Advances in understanding the role of P-gp in doxorubicin resistance: Molecular pathways, therapeutic strategies, and prospects. *Drug Discov. Today*, **27**(2), 436–455.
- Nanayakkara, A. K., Follit, C. A., Chen, G., Williams, N. S., Vogel, P. D., & Wise, J. G. (2018). Targeted inhibitors of P-glycoprotein increase chemotherapeutic-induced mortality of multidrug resistant tumor cells. *Sci. Rep.*, **8**(1), 967.
- O'Reilly, D., Sendi, M. Al, & Kelly, C. M. (2021). Overview of recent advances in metastatic triple negative breast cancer. *World J. Clin. Oncol.*, **12**(3), 164–182.
- Omarini, C., Guaitoli, G., Pipitone, S., Moscetti, L., Cortesi, L., Cascinu, S., & Piacentini, F. (2018). Neoadjuvant treatments in triple-negative breast cancer patients: where we are now and where we are going. *Cancer Manag. Res.*, **10**, 91–103.
- Robey, R. W., Pluchino, K. M., Hall, M. D., Fojo, A. T., Bates, S. E., & Gottesman, M. M. (2018). Revisiting the role of ABC transporters in multidrug-resistant cancer. *Nat. Rev. Cancer*, **18**(7), 452–464.
- Shah, A. N., & Gradishar, W. J. (2018). Adjuvant Anthracyclines in Breast Cancer: What Is Their Role? *Oncologist*, **23**(10), 1153–1161.
- Trédan, O., Galmarini, C. M., Patel, K., & Tannock, I. F. (2007). Drug Resistance and the Solid Tumor Microenvironment. *JNCI J. Natl. Cancer Inst.*, **99**(19), 1441–1454.
- Ughachukwu, P., & Unekwe, P. (2012). Efflux pump-mediated resistance in chemotherapy. *Ann. Med. Health Sci. Res.*, **2**(2), 191–198.
- Waghay, D., & Zhang, Q. (2018). Inhibit or Evade Multidrug Resistance P-Glycoprotein in Cancer Treatment. *J. Med. Chem.*, **61**(12), 5108–5121.
- Weiss, J., Sauer, A., Divac, N., Herzog, M., Schwedhelm, E., Böger, R. H., Haefeli, W. E., & Benndorf, R. A. (2010). Interaction of angiotensin receptor type 1 blockers with ATP-binding cassette transporters. *Biopharm. Drug Dispos.*, **31**(2–3), 150–161.
- Yin, L., Duan, J.-J., Bian, X.-W., & Yu, S. (2020). Triple-negative breast cancer molecular subtyping and treatment progress. *Breast Cancer Res.*, **22**(1), 61.
- Yusuf, D., Davis, A., Kleywegt, G., & Schmitt, S. (2008). An Alternative Method for the Evaluation of Docking Performance: RSR vs RMSD. *J. Chem. Inf. Model.*, **48**, 1411–1422.
- Zhang, X., Hu, C., Kong, C.-Y., Song, P., Wu, H.-M., Xu, S.-C., Yuan, Y.-P., Deng, W., Ma, Z.-G., & Tang, Q.-Z. (2020). FNDC5 alleviates oxidative stress and cardiomyocyte apoptosis in doxorubicin-induced cardiotoxicity via activating AKT. *Cell Death Differ.*, **27**(2), 540–555.

Streptomyces–Alginate Beads Formula Promote Maize Plant Growth and Modify the Rhizosphere Microbiome

Okto Asriatno¹, Abdjad Asih Nawangsih², Rika Indri Astuti¹, Aris Tri Wahyudi^{1,*}

¹Department of Biology, IPB University, Dramaga, Bogor, Indonesia; ²Department of Plant Protection, IPB University, Dramaga, Bogor, Indonesia

Received: December 4, 2022; Revised: February 22, 2023; Accepted: March 8, 2023

Abstract

The present study aimed to formulate *Streptomyces* with alginate as a plant growth promoter and determine its effect on the microbiome of maize rhizosphere. Five *Streptomyces*–alginate beads formulas were produced, namely ARJ14, ARJ16, ARJ28, ARJ32, and ARJ34 formulas using the extrusion technique. The formula morphology was analyzed using scanning electron microscope, and *Streptomyces* viability was tested using the total plate count method. Illumina sequencing was used to investigate rhizosphere microbiome composition. Alpha and Beta diversity analyses were used to determine the effects of the *Streptomyces*–alginate formulas on the maize rhizosphere microbiome. The ARJ28 formula had the lowest water content and the best *Streptomyces* viability after storage at room temperature for 10 weeks. The growth of maize treated with ARJ28 formula was better and significantly different from that of the positive and negative controls 49 days after planting. Specifically, the stem diameter, fresh weight, and dry weight were 1.32 ± 0.02 cm, 71.67 ± 12.58 g, and 9.57 ± 1.07 g, respectively. The rhizosphere from maize treated with ARJ28 formula contained a higher proportion of Acidobacteria, Chloroflexi, Crenarchaeota, Myxococcota, Patescibacteria, and Verrucomicrobiota, as well as *Candidatus-Nitrosotalea*, *Sphingomonas*, and *Bradyrhizobium* genera compared with those in the rhizosphere from ARJ34 formula–treated maize and the controls. Treatment with the ARJ28 formula also resulted in a higher proportion of Actinobacteria in rhizospheres compared with that in rhizospheres of ARJ34 formula–treated maize and negative control. Thus, the ARJ28 formula increased the growth of maize and affected the composition of the maize rhizosphere microbiome.

Keywords: alginate, formulation, microbiome, plant-growth promoter, *Streptomyces*

1. Introduction

Maize is a cereal food crop that belongs to the Poaceae family. It contains various beneficial phytochemical compounds (Rouf Shah *et al.*, 2016) and is a multifunctional commodity used as food, feed, fuel, and industrial raw materials (Panikkai *et al.*, 2017). These important aspects cause higher demand for maize, and one of the tactics implemented to increase maize production is through fertilization. Farmers widely use chemical fertilizers for their low cost and accessibility. Unfortunately, when used for a long time and in high doses, chemical fertilizers destroy the soil's physical and chemical structure, rendering it less fertile (Magdalena and Sumarni 2013). Additionally, frequent use of chemical fertilizers increases the soil density and decreases soil porosity, resulting in soil resistance to plant root penetration (Massah and Azadegan 2016).

The utilization of Plant–Growth Promoter Rhizobacteria (PGPR) allows for reduced chemical fertilizer usage. PGPR are microbes that either directly or indirectly stimulate plant growth, overcome environmental stress, and simultaneously exert a bioremediation function (Prasad *et al.*, 2017). PGPR may comprise a single isolate strain or microbe consortium with many beneficial

properties for plants (Jha and Saraf 2012; Alori *et al.*, 2017; Ahmad *et al.*, 2016). Using PGPR as a biological fertilizer can also increase the activity and diversity of the rhizosphere microbiome, stimulate the secretion of chemical compounds that prevent the growth of pathogens and increase the soil organic content (Liu *et al.*, 2021).

Streptomyces bacteria have been well-studied as effective plant–growth promoters. *Streptomyces* bacteria stimulate plant growth directly by producing growth hormones (Hortsmann *et al.*, 2020; Wahyudi *et al.*, 2019; Niu *et al.*, 2022), contributing to phosphate solubilization, and fixing free nitrogen (Kaur *et al.*, 2013; Wahyudi *et al.*, 2019). However, *Streptomyces* bacteria usage in plants faces many obstacles. Several environmental factors, such as soil type, microbial interactions, and structures on the land, are limiting the use of biofertilizers (Singh 2018). The unprotected inoculated bacteria must compete with the often better-adapted native microflora and withstand predation by soil micro fauna, which may rapidly cause the PGPR population to decline (Bashan 2016). Various formulation techniques such as using liquid formulation (Jha and Saraf 2012), peat with formulated soil amendment (Fitriatin *et al.*, 2021), charcoal (Mäder *et al.*, 2011), clay pellets (Schoebitz *et al.*, 2014), and alginate (Bashan *et al.*, 2012), have been applied to ensure that microbes can survive and colonize the rhizosphere.

* Corresponding author. e-mail: ariswa@apps.ipb.ac.id.

Alginate is the material of choice to encapsulate microorganisms because it is biodegradable and protects bacteria from environmental stress. Additionally, bacterial encapsulation with alginate allows to maintain the optimal concentrations of bacteria for a longer period with the slow-release mechanism (Bashan *et al.*, 2014). However, the application of *Streptomyces*-alginate formulas to maize culture and its effect on maize rhizosphere microbiome remain to be investigated. Therefore, the present study was conducted to determine the formula of *Streptomyces* that can stimulate the growth of maize plants and its effect on the maize rhizosphere microbiome.

2. Materials and Methods

2.1. Culture and Cultivation

Streptomyces bacteria isolated from maize plantation soil samples in East Nusa Tenggara, Indonesia, for previous research were used (Wahyudi *et al.*, 2019). Five isolates (ARJ14, ARJ16, ARJ28, ARJ32, and ARJ34) identified as *Streptomyces* in a previous study using the GenBank database (Table 1) (Deviani, C., IPB University, unpublished observations) were rejuvenated on molasses-yeast extract solid medium (composition: 10 g molasses, 3 g yeast extract, 1 L sterile distilled water, 2% agar) and incubated for 7–14 days. For cultivation, three solid culture plugs were taken, put into molasses-yeast extract liquid medium and stored at $\pm 27^\circ\text{C}$ for 10 days in a shaker (Sari *et al.*, 2021).

Table 1. Identification of the five isolates used in the present study using the GenBank database

No.	Isolate	Homology	Query Cover (%)	E-value	Identity (%)	Accession Number
1.	ARJ14	<i>Streptomyces asenjonii</i> strain KNN 35	79%	0.0	87.31%	NR152642.1
2.	ARJ16	<i>Streptomyces cellulosae</i> strain MF11	100%	0.0	99.84%	MT2114275.1
3.	ARJ28	<i>Streptomyces cellulosae</i> strain F7-7(2)	100%	0.0	100.00%	KR023970.1
4.	ARJ32	<i>Streptomyces tritolerans</i> strain YFP6	100%	0,0	100.00%	MG334130.1
5.	ARJ34	<i>Streptomyces olivaceus</i> strain NRRI-B-3009	100%	0,0	100.00%	MT543222.1

2.2. Alginate Bead Production

A 2% alginate solution was prepared by dissolving 2 g of powdered sodium alginate (Himedia Laboratories, Mumbai, India) into 100 mL of sterile distilled water. The solution was stirred until homogeneous and sterilized using an autoclave for 15 min at 121°C with a pressure of 1 atm. Alginate bead formulation followed that of Shrivastava *et al.* (2008) with modifications. Briefly, 20 mL of *Streptomyces* inoculant suspension dissolved in 60 mL of 2% sodium alginate (1:3 v:v). Then, 1.5% (w/v) skim milk was added and the mixture was vortexed. Then, the mixture was pulled up into a 1-mL syringe and extruded through a 26G" needle into stirred 500 mL of 0.1 M calcium chloride at 40 rpm for 30 min. The beads were filtered and washed using sterile distilled water three times. Then, they were dried in a Petri dish using filter paper and placed inside a laminar air flow for 48 h at $\pm 38^\circ\text{C}$. The filter paper was replaced twice. After that, the formula was stored in a sealed Petri dish, and silica gel was added to it (Bashan *et al.*, 2002). The morphological observations of the formula were conducted in the Central Forensic Laboratory of Indonesian National Police (Pusat Laboratorium Forensik/Puslabfor Polri, Sentul, Indonesia) using a Carl Zeiss EVO MA10 Scanning Electron Microscope (SEM, Carl Zeiss AG, Jena, Germany) with 250 \times , 1000 \times , 2000 \times , and 3000 \times magnifications. The water content of each formula was calculated using the Association of Official Analytical Collaboration (AOAC) equation (1) (Caputi, 1995) as follows:

$$\text{Water content/moisture (\%)} = \frac{W1 - W2}{W1} \times 100 \quad (1)$$

where: W1 = weight of the sample before drying (g)

W2 = weight of the sample after drying (g)

2.3. Analysis of *Streptomyces* Viability in the Formula

Viability analysis was performed as described by Kim *et al.* (2016) with modifications. One gram of alginate bead formula was subjected to serial dilution. The first dilution consisted in transferring 1 g of the *Streptomyces*-alginate beads formula into a 40 mL conical tube containing 10 mL phosphate salt/PBS buffer solution and vortexing for 2 h to dissolve the alginate. The mixture was then shaken for 24 h at room temperature. After that, a series of seven consecutive dilutions was conducted, each consisting of adding 1 mL of the mixture with 9 mL of 0.85% sodium chloride solution. The colony number was determined using the total plate count method on the molasses-yeast extract solid medium after 24 h incubation.

2.4. Application of the *Streptomyces*-Alginate beads formula

Streptomyces-alginate formula applied at a greenhouse scale. Approximately 1 g of formula was added to each maize seed as a seed coating. The BISI-2 variety of maize was used. Maize seeds were successively soaked in sterile distilled water for 6 h, dried, transferred into a 0.5% lecithin solution, and mixed with the alginate bead formula. The maize seeds were planted in polybags containing latosol soil, which had been cleaned and sifted to a depth of ± 5 cm. Each polybag contained 5 kg of soil, which had been mixed with basic N, P, K fertilizer at a dose of 250 kg urea/ha, 100 kg SP36/ha, and 100 kg KCl/ha. The polybags were 15 \times 30 cm in size, and each polybag contained three maize seeds. Fourteen days after planting (14 DAP), the maize with the best growth was maintained, whereas the other two were eliminated.

This study used a one-factor randomized block design (RBD), namely, five *Streptomyces*-alginate formulas (ARJ14, ARJ16, ARJ28, ARJ32, and ARJ34 formulas) with two controls. For negative control, maize was exposed to no biological fertilizer, and maize treated with

a commercial biological fertilizer was used as a positive control. The commercial biological fertilizer consisted of a consortium of bacteria *Pseudomonas* sp., *Azospirillum* sp., *Bacillus* sp., and *Streptomyces* sp. Five replications of each treatment and control were performed. Maize growth data were collected up to 49 days after planting (49 DAP). Growth data included the number of leaves, plant height, and stem diameter. Additionally, measurements of fresh and dry weight were also taken after the plants were harvested.

2.5. Maize Rhizosphere Sampling and DNA Extraction

The rhizosphere microbiome community was analyzed for the maize plants treated with the *Streptomyces*-alginate formula with highest and lowest growth, positive control, and negative control. Rhizosphere soil samples were taken following the method described by Lakshmanan *et al.* (2017) with modifications. Maize plants from each treatment polybag were removed and shaken so that a thin layer of soil remained on the root surface. The roots of the maize plant were cut into 5-cm-long pieces using sterile scissors and transferred into a 50-mL conical tube containing 25 mL PBS. The root pieces subjected to the same treatment were combined and centrifuged (15 min, $6000 \times g$, 4°C) using a VWR 600R Centrifuge (VWR International, LLC., Pennsylvania, USA). The supernatant was discarded, and 5 g of the pellet were subjected to microbiome DNA extraction using a ZymoBIOMICS™ DNA Mini Kit (Zymo Research Corp., Irvine, USA) according to the manufacturer's instructions. DNA quality was checked using a NanoDrop 2000 (Thermo Scientific, Wilmington, DE, USA).

2.6. Illumina Sequencing and Analysis

The isolated metagenomic DNA was submitted to Beijing Novogene Technology Company, Ltd. for 16S rRNA gene sequencing. The sample concentration was first checked using 1%-agarose gel electrophoresis, and samples were dissolved to a final concentration of $1 \text{ ng}/\mu\text{L}$ using sterile distilled water. DNA was amplified by polymerase chain reaction (PCR) using the primers 341F (5'-CCTAYGGRBGCASCAG-3') and 806R (5'-GGACTACNNGGGTATCTAAT-3') with specific adapters targeting the V3-V4 region of the 16S rRNA gene. PCR reactions were performed using Phusion High-Fidelity PCR Master Mix (New England Biolabs, Massachusetts, USA). The gene library was sequenced using Illumina Novaseq 6500 PE250 to produce two-way reads (paired-ends) of 250-bp sequences. The two-way reading data were combined using FLASH software (version 1.2.7, <http://ccb.jhu.edu/software/FLASH>) to produce raw tags, which were then selected using QIIME (version 1.7.0, <http://qiime.org/index.html>). The tags were compared with the SILVA138 database (<https://www.arb-silva.de/>) using the UCHIME algorithm (http://www.drive5.com/usearch/manual/uchime_algo.html). Sequences were analyzed using Uparse software (version 7.0.1090, <http://drive5.com/uparse/>). Representative operational taxonomic unit (OTU) sequence phylogenetic relationships and taxonomic distribution were analyzed using MUSCLE (version 3.8.31, <http://www.drive5.com/muscle/>). Alpha diversity was calculated using QIIME and displayed with the R program. Principal component analysis (PCA) was

conducted using the FactoMineR and ggplot2 packages in the R program (version 2.15.3). Unweighted Pair-Group Method with Arithmetic Means (UPGMA) clustering and beta diversity analysis was performed using QIIME software.

2.7. Statistical Analysis

The maize growth parameters were analyzed using a one-way analysis of the variance (ANOVA). If there was a significant effect of the treatment, Duncan's test (DMRT) with $\alpha = 0.05$ was used. Analyses were performed using IBM SPSS Statistics for Windows version 24.0 (IBM, Armonk, New York, United States).

3. Results

3.1. *Streptomyces*-Alginate Beads Formulation

Five isolates of *Streptomyces* (ARJ14, ARJ16, ARJ28, ARJ32, and ARJ34) were successfully formulated using an alginate carrier (Figure 1). Each formula had a water content of 27.3% (ARJ14 formula), 26.4% (ARJ16), 25.6% (ARJ28 formula), 26.5% (ARJ32 formula), and 26.2% (ARJ34 formula). *Streptomyces*-alginate bead formulas were 500–1000 μm in diameter and slightly round or oval and had a glossy smooth surface and yellow-brown color.

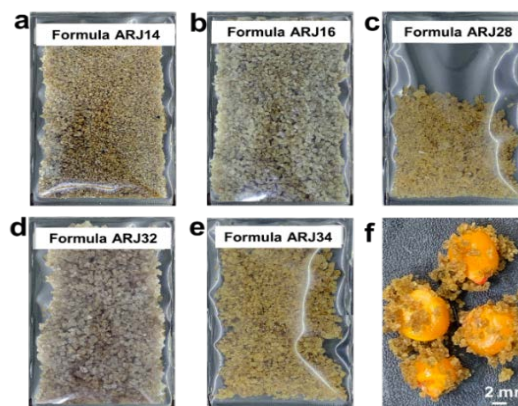


Figure 1. Morphology of *Streptomyces*-alginate bead formula composed of *Streptomyces* ARJ14 (a), ARJ16 (b), ARJ28 (c), ARJ32(d), and ARJ34 (e). Image of formula attached on the maize seed surface (f).

Streptomyces cells were immobilized by the alginate bead matrix. SEM observations confirmed the *Streptomyces* colonies on the surface of the alginate beads (Figure 2).

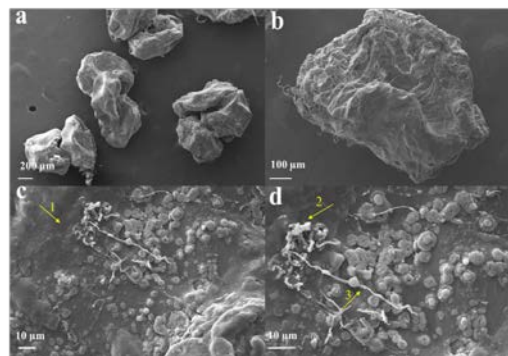


Figure 2. Morphology of the *Streptomyces*-alginate formula analyzed by scanning electron microscopy using (a) 80 \times , (b) 250 \times , (c) 2000 \times , and (d) 3000 \times magnifications. Arrow 1 indicates

the formula surface, arrow 2 shows *Streptomyces* colonies, and arrow 3 indicates *Streptomyces* mycelium.

3.2. *Streptomyces* Viability in the Formula

The viability of the *Streptomyces* in the *Streptomyces*-alginate bead formula was determined using the total plate count method over ten weeks of storage at $\pm 27^\circ\text{C}$. *Streptomyces* ARJ28 showed the best viability. *Streptomyces* ARJ28 viability in the formula was up to 5.1×10^7 cfu/g in the 10th week, whereas the lowest viability (6.2×10^5 cfu/g) was recorded for *Streptomyces* ARJ16. The concentration of cells attached to the maize seedlings was 1.4×10^7 to 2.0×10^7 cfu/g.

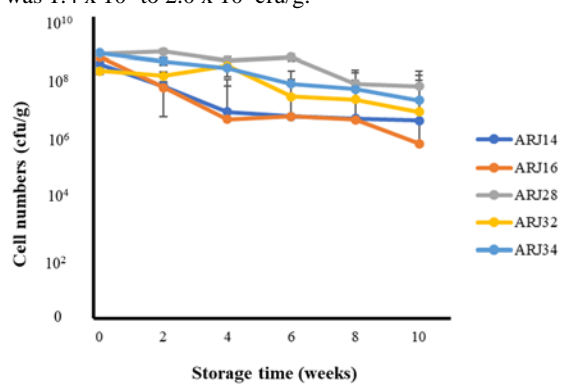


Figure 3. Viability of *Streptomyces* in *Streptomyces*-alginate bead formula quantified using the total plate count method on molasses-yeast extract medium (24 h, $\pm 27^\circ\text{C}$).

3.3. Effects of *Streptomyces*-Alginate Bead Formula on Maize

Table 2 shows that the growth of maize inoculated with the *Streptomyces*-alginate bead formula was better than

Table 2. Effects of the *Streptomyces*-alginate bead formula on maize growth

Formula	Plant Height (cm)*	Number of Leaves*	Stem Diameter (cm)*	Upper Plant Body Fresh Weight (g)*	Upper Plant Body Dry Weight (g)*
Negative control	$92.03^a \pm 5.64$	$7.67^a \pm 0.57$	$0.91^a \pm 0.14$	$20.00^a \pm 5.00$	$2.53^a \pm 0.45$
Positive control	$113.47^b \pm 8.20$	$10.00^b \pm 0.00$	$0.99^a \pm 0.07$	$43.33^b \pm 7.63$	$4.90^{ab} \pm 0.50$
ARJ 14	$115.37^b \pm 3.74$	$10.67^b \pm 1.15$	$1.22^b \pm 0.08$	$65.00^{cd} \pm 5.00$	$7.53^{cd} \pm 2.47$
ARJ 16	$113.20^b \pm 4.35$	$10.33^b \pm 0.57$	$1.18^b \pm 0.12$	$68.33^{cd} \pm 18.92$	$8.13^{cd} \pm 0.96$
ARJ 28	$117.73^b \pm 5.90$	$10.33^b \pm 0.57$	$1.32^b \pm 0.02$	$71.67^d \pm 12.58$	$9.57^d \pm 1.07$
ARJ 32	$115.33^b \pm 2.80$	$10.00^b \pm 0.00$	$1.20^b \pm 0.04$	$63.33^{cd} \pm 2.88$	$8.73^{cd} \pm 0.55$
ARJ 34	$113.97^b \pm 3.91$	$9.67^b \pm 0.57$	$1.19^b \pm 0.06$	$51.67^{bc} \pm 10.40$	$6.37^{bc} \pm 2.17$

Note: *Values are presented as means \pm standard errors.

^{a,b,c,d} Different superscript letters indicate significant differences among treatments (column) with $P < 0.05$.

3.4. Maize Rhizosphere Microbiome Analysis

3.4.1. Alpha Diversity

Streptomyces ARJ28 and ARJ34 formulas induced the highest and lowest growth of maize plants, respectively. Therefore, rhizosphere samples of plants treated with ARJ28 and ARJ34 formulas were analyzed and compared with the samples of the positive and negative controls. Table 3 shows the results of the alpha diversity analysis of four rhizosphere samples performed using Uparse and MUSCLE software. The Shannon index was the highest for rhizospheres of the positive control. It was lower for rhizospheres of maize treated with the ARJ28 formula, even lower for rhizospheres of ARJ34 formula-treated

that of the negative control based on the five growth parameters analyzed. At 49 days after planting, maize plants treated with the ARJ28 formula had an average plant height of 117.73 cm, which was significantly greater than that of the negative control (92.03 cm) but not significantly different from that of the positive control and maize subjected to other treatments. Maize plants treated with the ARJ14 formula had the highest average number of leaves (10.67 leaves). This was not significantly different from the number of leaves in the positive control and maize treated with other formulas, whereas the negative control had significantly fewer leaves (7.67 leaves). The average stem diameter was greater in all maize treated with the *Streptomyces*-alginate formulas compared with that of the positive and negative controls. The stalk average diameter of maize plants treated with the ARJ28 formula was the greatest (1.32 cm) and significantly different from that of the negative and positive controls (0.91 and 0.99 cm, respectively). However, there was no significant difference among treatments. The maize plants treated with the ARJ28 formula had the highest average fresh weight (71.7 g), which was significantly different from that of the negative control (20.00 g), positive control (43.33 g), and ARJ34 formula-treated maize plants (51.67 g). Maize plants treated with the ARJ28 formula had the highest average dry weight (9.57 g), which was significantly different from that of the negative control (2.53 g), positive control (4.9 g), and the ARJ34 formula-treated plants (6.7 g).

maize, and reached the lowest value for the negative control. Thus, the rhizosphere community relative abundance was increased by the inoculation of the ARJ28 and ARJ34 formulas and conventional biofertilizer. Additionally, the range of the rank abundance distribution curve on the horizontal axis was greater for the positive control sample (Figure 4). The Chao1 estimator was the highest for the rhizosphere samples of the positive control and decreased progressively for the samples of maize treated with the ARJ28 formula and the negative control, to reach the lowest value for the rhizospheres of ARJ34 formula-treated maize. These results indicated that the richness of the microbiome community in the rhizospheres of ARJ34 formula-treated maize was lower than that in

rhizospheres of ARJ28 formula-treated maize and both control samples. Thus, there are likely changes in the proportion of the microbiome community.

Table 3. Alpha diversity analysis of the rhizosphere samples

Sample	Shannon
ARJ28	7,196
ARJ34	6,847
Positive Control	7,402
Negative Control	6,721

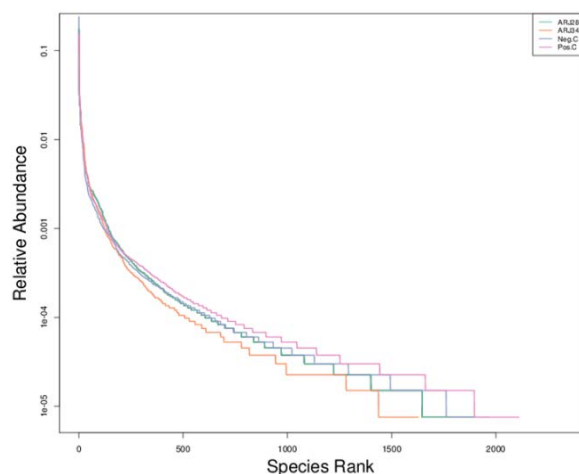


Figure 4. The rank abundance distribution curve of the microbiome community from the rhizosphere samples of maize treated with ARJ28 or ARJ34 formula and of the negative and positive controls.

3.4.2. Beta Diversity of the Bacterial Community in the Maize Rhizospheres

The principal coordinate analysis (PCoA) performed using QIIME software showed a clear separation of the rhizosphere microbiomes of maize treated with the ARJ28 and ARJ34 formulas from those of the positive and negative controls (Figure 5). The rhizosphere microbiomes of the positive and negative controls were clustered, indicating that both microbiomes were quite similar. Additionally, the rhizosphere microbiome of maize treated with formula ARJ28 and that of maize exposed to formula ARJ34 were located in different quadrants and separated by a considerable distance, indicating that there were differences between both microbiomes (Figures 5).

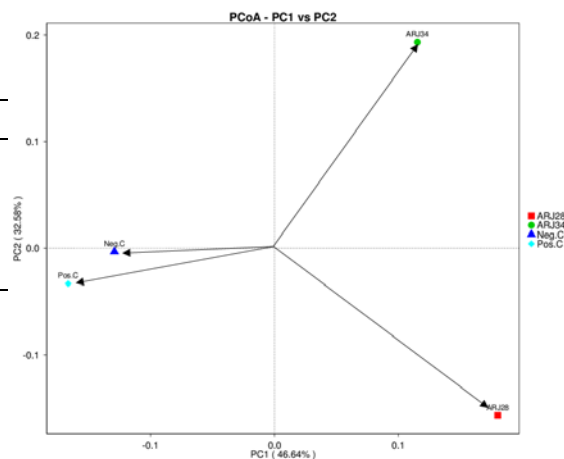


Figure 5. PCoA of the rhizosphere microbiomes of maize treated with ARJ28 or ARJ34 formula, negative control (Neg. C), and positive control (Pos. C). The rhizosphere microbiomes from the positive and negative controls differed from those of maize treated with ARJ28 and ARJ34 formulas.

3.4.3. Taxonomic Distribution of Bacterial Communities between Rhizosphere Samples

The distribution of bacterial community in the maize rhizospheres was determined using the SILVA138 database. The OTU analysis performed using the QIIME software (version 1.7.0) successfully identified 18 phyla from the Bacteria domain and one phylum from the Archaeobacteria domain. There were 10 phyla with more than 1% relative abundance: Proteobacteria, Acidobacteria, Actinobacteria, Chloroflexi, Bacteroidota, Firmicutes, Crenarchaeota, Myxococcota, Patescibacteria, and Verrucomicrobiota (Figure 6). Clusterization of the maize rhizosphere microbiome communities using UPGMA revealed two clusters, namely the treatment cluster (treated with ARJ28 and ARJ34 formulas) and the control cluster (positive and negative controls).

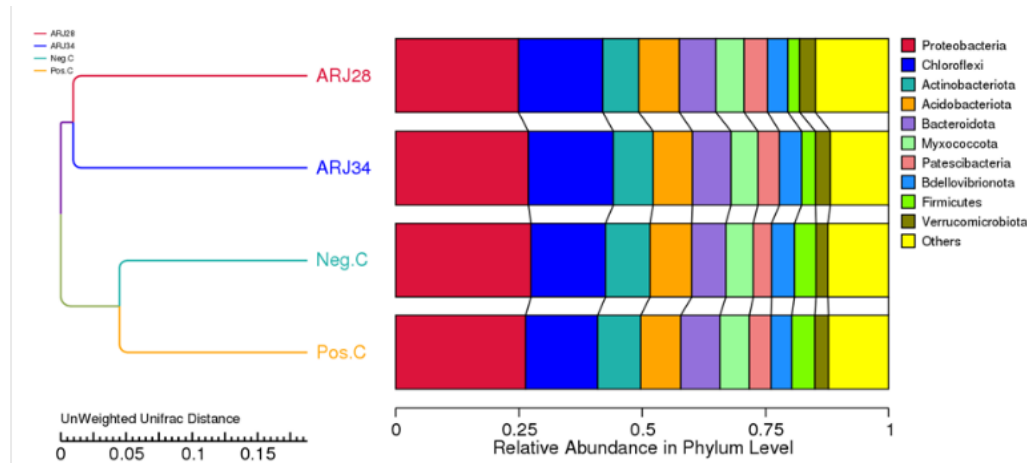


Figure 6. Clusters of bacterial communities in the rhizospheres of maize plants treated with ARJ28 and ARJ34 formulas and that of the positive (Pos. C) and negative (Neg. C) controls.

The rhizosphere analysis of maize plants treated with ARJ28 and ARJ34 formulas and that of the positive and negative controls were different regarding the relative abundance of 10 taxa at the phylum level (Figure 7). The Proteobacteria phylum was the most abundant phylum in rhizospheres of maize treated with ARJ28 (61.51%) and ARJ34 (62.51%) formulas and in those of the positive (64.05%) and negative (70.36%) controls. The Acidobacteriota phylum relative abundance was the highest in the rhizospheres of maize treated with ARJ28 formula (11.91%), whereas it was 8.40%, 11.02%, and 9.31% in rhizospheres of ARJ34 formula-treated maize, the positive control, and the negative control, respectively. The Firmicutes phylum was the most abundant in the rhizospheres of maize treated with ARJ34 formula

(8.07%), whereas its relative abundance was 0.60%, 1.23%, and 1.66% in rhizospheres of ARJ28 formula-treated maize, the positive control, and the negative control, respectively. The phylum Actinobacteriota relative abundance was the highest in the rhizospheres of the positive control (5.48%) and was 4.76% in rhizospheres of maize treated with ARJ28 formula, 4.19% in rhizosphere of the negative control, and 3.45% in rhizospheres of maize treated with ARJ34 formula. The rhizosphere of maize treated with the ARJ28 formula exhibited the highest relative abundance of Chloroflexi, Crenarchaeota, Myxococcota, Patescibacteria, and Verrucomicrobiota, which were 3.96%, 2.49%, 2.21%, 1.51%, and 1.27%, respectively.

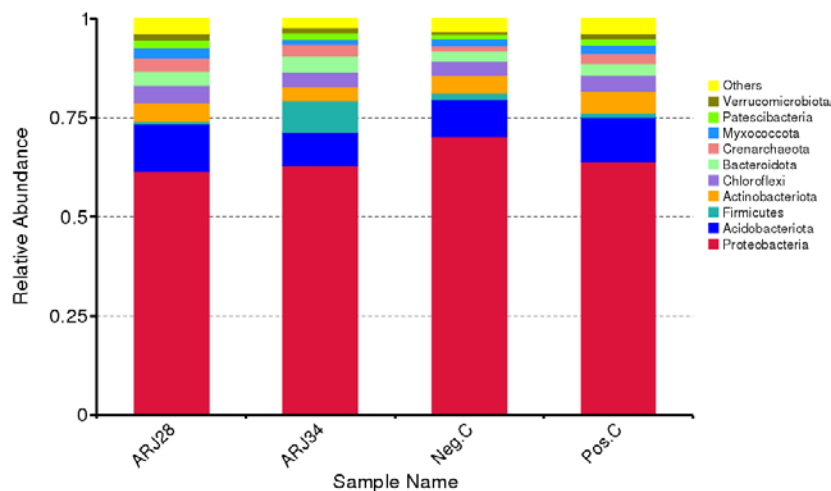


Figure 7. Distribution of the most abundant phyla in the rhizosphere of maize plants treated with ARJ28 and ARJ34 formulas, the negative control (Neg.C), and the positive control (Pos.C).

There were differences in the relative abundance of genera among rhizospheres of maize treated with ARJ28 and ARJ34 formulas, the positive control, and the negative control (Figure 8). *Burkholderia-Caballeronia-Paraburkholderia* was the most abundant genus in rhizospheres of maize treated with the ARJ28 and ARJ34 formulas, positive control, and negative control, with a relative abundance of 19.71%, 18.75%, 18.32%, and 26.83%, respectively. The *Bacillus* genus relative abundance was the lowest in rhizospheres of maize treated with the ARJ28 formula (0.43%), whereas it was 7.81%,

0.77%, and 1.08% in the rhizospheres of maize treated with the ARJ34 formula, positive control, and negative control, respectively. The genus *Dyella* relative abundance was the highest in rhizosphere samples of the negative control (5.85%) and the lowest in the positive control rhizospheres (2.71%). The relative abundances of the genera *Massilia* and *Ralstonia* were the highest in rhizospheres of maize treated with the ARJ34 formula (4.32% and 3.57%, respectively) and the lowest in rhizospheres from the positive controls (2.04%). The relative abundances of the genera *CandidatusNitrosotalea*,

Sphingomonas, and *Bradyrhizobium* were the highest in rhizospheres of maize treated with the ARJ28 formula (3.26%, 2.68%, and 2.33%, respectively). The relative abundances of the genera *Phenylobacter* and *Asticcacaulis* were the highest in the rhizospheres of the positive control (3.05% and 2.78%, respectively). The relative abundance

of other bacterial genera was 60.9% in the positive control rhizospheres and 57.72%, 50.15%, and 50.32% in rhizospheres from maize treated with the ARJ28 and ARJ34 formulas and negative control rhizospheres, respectively.

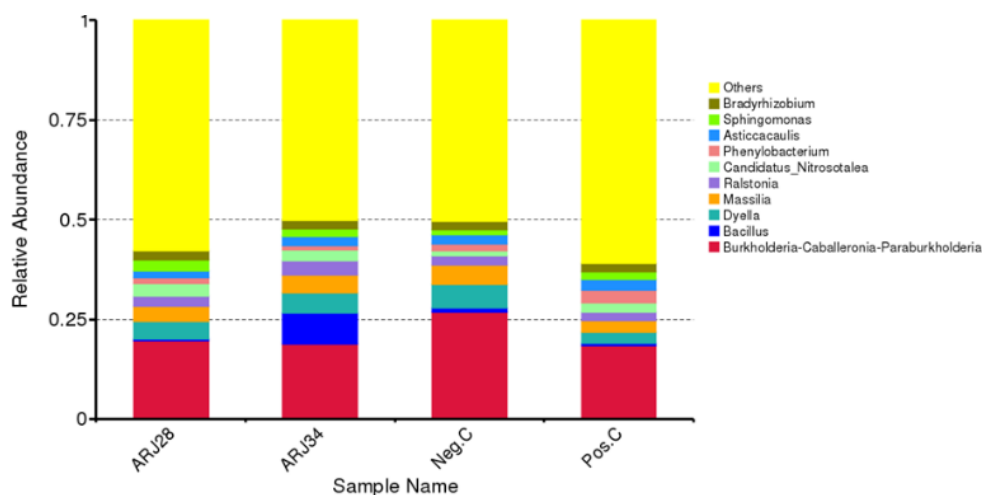


Figure 8. Distribution of bacteria genera in rhizospheres from maize plants treated with ARJ28 and ARJ34 formulas, the negative control, and positive control.

4. Discussion

Here, we successfully formulated five *Streptomyces* isolates using sodium alginate as a carrier. Sodium alginate is a polysaccharide that can be obtained from algae and bacteria. It is environment-friendly, relatively inexpensive to produce, naturally biodegradable, and non-toxic (Puscaselu *et al.*, 2020). *Streptomyces* was encapsulated with alginate using the extrusion method, which consisted in dripping an alginate solution that had been mixed with a *Streptomyces* liquid culture into a calcium chloride solution to generate a reaction between alginate and divalent cations (Malusá *et al.*, 2012). Sodium alginate–divalent cations bonds form a structure that encapsulates bacterial cells and releases these cells slowly over a certain period (Bashan, 2016). Thus, the bacteria are not directly exposed to environmental stress and other microbial contamination (Schoebitz *et al.*, 2013). The diameter of the formula was 400–700 μm , which is categorized as microbeads. Microbeads are large enough to encapsulate some bacteria but too small to attach to seedlings (Bashan *et al.*, 2014). The *Streptomyces*–alginate bead formulas had low water content, the lowest one (25.6%) being in the ARJ28 formula. Therefore, the ARJ28 formula might be better preserved after 10 weeks of storage than the other formulas. Low water content can indeed support microbial survivability in dry formulas for longer storage (Lobo *et al.*, 2019).

The growth of maize treated with the *Streptomyces*–alginate beads formulas was increased at 49 days after planting. Specifically, the plant height, number of leaves, stem diameter, fresh weight, and dry weight were increased by ARJ28 formula treatment compared with those of the negative control. The ARJ28 formula may stimulate the growth of maize plants by excreting plant growth-promoting substances and stimulating the absorption of nutrients important for maize growth. Based

on a previous study, *Streptomyces* ARJ28 can produce indole-3-acetic acid (IAA), grow on a nitrogen-free medium, and significantly increase the growth of maize in the Ragdoll test (Wahyudi *et al.*, 2019). *Streptomyces* bacteria are known to produce growth-promoting substances such as IAA (Goudjal *et al.*, 2013), cytokinins, and gibberellins (Olanrewaju and Babalola 2019), dissolve phosphate (Alori *et al.*, 2017), and fix nitrogen (Dahal *et al.*, 2017). Previous research also found that *Streptomyces* bacteria stimulate maize plant growth as assessed by the plant height, root length, aerial body wet and dry weight, and root fresh weight (Dicko *et al.*, 2018).

The better growth of maize plants treated with the ARJ28 formula might directly result from *Streptomyces* ARJ28. Additionally, the rhizosphere microbiome that is affected by the formula might play a role. Although the ARJ28 formula did not induce the highest microbiome abundance and diversity, the growth of maize treated with the ARJ28 formula was better than that of maize subjected to other treatments or of the positive and negative controls. The ARJ28 formula might attract beneficial microbes in the rhizosphere, resulting in these microbes becoming dominant and in a lower abundance of other microbes. Indeed, PGPR inoculation affects the chemical diversity of root exudates and induces the release of specific compounds involved in the recruitment of beneficial microbes (Kong and Liu, 2022). PGPR inoculation also modifies the functional diversity of the rhizosphere, thereby disrupting plant–soil feedback and modifying the structure of the rhizosphere microbiome (Alzate Zuluaga *et al.*, 2021). In addition, the by-products of PGPR metabolism can be utilized by other rhizosphere microbes as nutrients or energy sources (Kong and Liu, 2022).

The beta diversity analysis showed that *Streptomyces*–alginate bead formulas affected the maize rhizosphere microbiome relative abundance. UPGMA cluster analysis confirmed that the rhizosphere microbiomes of maize treated with the ARJ28 and ARJ34 formulas differ from

those of the positive and negative controls. Particularly, there were differences in the composition and proportion of nine bacteria phyla (Proteobacteria, Acidobacteria, Actinobacteria, Chloroflexi, Bacteroidota, Firmicutes, Myxococcota, Patescibacteria, and Verrucomicrobiota) and one phylum of Archaeobacteria (Crenarchaeota). These results are similar to those of previous studies by Wang *et al.* (2021) and Akinola *et al.* (2021) on maize plant rhizospheres. Differences in the composition and relative abundance of the rhizosphere microbiome community can be influenced by abiotic and biotic factors (Andreote *et al.*, 2014). Microbial inoculation of the soil can affect the activity of native microflora by attaching to the plant roots and competing for space and nutrients released through root exudation. Once the inoculated microbes had enough nutrients and space, they can affect the host plant (Mohanram and Kumar, 2019).

The relative abundance of Actinobacteria in the rhizosphere samples of maize plants treated with the ARJ28 formula was higher than that in the rhizospheres of maize plants treated with the ARJ34 formula and the negative control, but lower than that in the rhizospheres of the positive control. Nevertheless, the inoculation of the ARJ28 formula also increased the relative abundance of Acidobacteria, Chloroflexi, Crenarchaeota, Bacteroidota, Myxococcota, Patescibacteriota, and Verrucomicrobiota. Inoculation of biological fertilizers can enrich, attract, and stimulate the growth of beneficial microbes in plant roots, thereby increasing the availability of nutrients and resistance to pathogenic infections (Dennis *et al.*, 2010). Certain members of Acidobacteria, Chloroflexi, Crenarchaeota, Bacteroidota, Myxococcota, Patescibacteriota, and Verrucomicrobiota are known to promote plant growth through direct or indirect mechanisms. Acidobacteria interact with plants through mechanisms related to auxin production and exhibit growth-promoting effects (Kielak *et al.*, 2016). For example, the growth of tomato and black bean plants increases with the number of Acidobacteria members in the rhizosphere (Kalam *et al.*, 2017). Chloroflexi is a phylum found in a considerable proportion in agricultural soils (Trivedi *et al.*, 2016). It also inhabits other ecosystems and has ecological importance in the habitats of mesophilic, thermophilic, aerobic, anaerobic chemoorganoheterotrophic, and photolithoautotrophic bacteria (Rincón-Molina *et al.*, 2022). The Bacteroidetes phylum is also commonly found on agricultural land, and some members of this phylum produce IAA, dissolve tricalcium phosphate, and break down chitin (Flores-Núñez *et al.*, 2018). The Myxococcota phylum is widely distributed in soil, freshwater, and saltwater and produces a variety of secondary metabolites such as antimicrobial compounds that indirectly act as bioprotectants (Korkar *et al.*, 2022). Crenarchaeota is a phylum from the Archaeobacteria domain known to play an essential role in the oxidation of ammonia as an initial step in the nitrification process (Zhou *et al.*, 2015).

At the genus level, the rhizospheres of maize plants treated with the ARJ28 formula contained the highest levels of *CandidatusNitrosotalea*, *Sphingomonas*, and *Bradyrhizobium*, which play a role in stimulating plant growth. *Candidatus Nitrosotalea* is a member of the Archaeobacteria domain that can oxidize ammonia, which is essential for the rate of steps in the nitrification process

(Maver *et al.*, 2021). *Sphingomonas* is a well-known group of soil bioremediation bacteria and plant-growth promoters in stressed environments (Asaf *et al.*, 2020). *Bradyrhizobium*, which lives freely in the soil and rhizospheres, is involved in carbon metabolism and the degradation of aromatic compounds (Schneiderberg *et al.*, 2018) and fixes nitrogen (Wongdee *et al.*, 2018).

In the present study, the rhizospheres of formula-treated maize plants did not contain a dominant proportion of the *Streptomyces* genus. Even though *Streptomyces* inoculation positively correlated with better maize growth, it was difficult to ensure that the inocula had succeeded in dominating the rhizosphere since the sampling for rhizosphere microbiome analysis was performed in the late vegetative phase. It is important to note that the plant microbiome composition is dynamic and can change throughout the plant life cycle (Edwards *et al.*, 2018). Some microbes may be dominant in the early vegetative phase and be less present in the late developmental stages. The microbial communities can be highly dynamic in the early vegetative phase but start to converge during vegetative growth and become more stable during the reproductive phase (Ferrarezi *et al.*, 2022). In the present study, *Streptomyces* inoculation may promote plant growth during the vegetative stage and may be found in different proportions in each phase. During the vegetative stages, *Streptomyces* may convert plant exudates or macromolecules/supramolecules present in the rhizosphere into a form that can be used by other plant growth-promoting microbes (Sousa and Olivares, 2016). This process may attract other beneficial indigenous microbes. Due to the slow release mediated by alginate encapsulation, the abundance of *Streptomyces* was maintained in the rhizospheres, although not to levels sufficient to dominate the rhizospheres until the end of the vegetative stage.

5. Conclusion

In the present study, the *Streptomyces*-alginate bead ARJ28 formula promoted maize plant growth better than the other treatments and controls. The application of the *Streptomyces* formula increased the relative abundance of Acidobacteria, Chloroflexi, Crenarchaeota, Bacteroidota, Myxococcota, Patescibacteriota, and Verrucomicrobiota as well as the genera *Candidatus Nitrosotalea*, *Sphingomonas*, and *Bradyrhizobium* in rhizospheres. These taxa are known for their plant growth-promoting activity and are thought to play a role in the growth of maize plants. Therefore, the ARJ28 formula might be used as biological fertilizer.

6. Author's Note

The authors declare that there is no conflict of interest regarding this article publication, and the paper was confirmed free of plagiarism.

Acknowledgements

This work was supported by the Ministry of Finance, Indonesia, through the Indonesia Endowment Funds for Education (Lembaga Pengelola Dana Pendidikan/LPDP) scholarship.

References

- Ahmad E, Zaidi A, Khan MS. 2016. Effects of Plant Growth Promoting Rhizobacteria on the Performance of Greengram under Field Conditions. *Jordan J Biol Sci.*, 9(2):79–88.
- Akinola SA, Ayangbenro AS, Babalola OO. 2021. Metagenomic insight into the community structure of maize-rhizosphere bacteria as predicted by different environmental factors and their functioning within plant proximity. *Microorganisms.*, 9(7): 1–24.
- Alori ET, Glick BR, Babalola OO. 2017. Microbial phosphorus solubilization and its potential for use in sustainable agriculture. *Front Microbiol.*,8:971
- Alzate Zuluaga MY, Milani KML, Miras-Moreno MB, Lucini L, Valentinuzzi F, Mimmo T, Pii Y, Cesco S, Rodrigues EP, de Oliveira ALM. 2021. The adaptive metabolomic profile and functional activity of tomato rhizosphere are revealed upon PGPB inoculation under saline stress. *Environ Exp Bot.*,189: 1–14.
- Andreote FD, Gumiére T, Durrer A. 2014. Exploring interactions of plant microbiomes. *Sci Agric.*,71(6):528–539.
- Asaf S, Numan M, Khan AL, Al-Harrasi A. 2020. *Sphingomonas*: from diversity and genomics to functional role in environmental remediation and plant growth. *Crit Rev Biotechnol.*, 40(2):138–152.
- Bashan N. 2016. Inoculant formulations are essential for successful inoculation with plant growth-promoting bacteria and business opportunities. *Indian Phytopath.*,69(4s):739–743.
- Bashan Y, De-Bashan LE, Prabhu SR, Hernandez JP. 2014. Advances in plant growth-promoting bacterial inoculant technology: formulations and practical perspectives (1998-2013). *Plant Soil.*,378(1–2):1–33.
- Bashan Y, Hernandez JP, Leyva LA, Bacilio M. 2002. Alginate microbeads as inoculant carriers for plant growth-promoting bacteria. *Biol Fertil Soils.*,35(5):359–368.
- Bashan Y, Salazar BG, Moreno M, Lopez BR, Linderman RG. 2012. Restoration of eroded soil in the Sonoran Desert with native leguminous trees using plant growth-promoting microorganisms and limited amounts of compost and water. *J Environ Manage.*,102:26–36.
- Bokulich NA, Subramanian S, Faith JJ, Gevers D, Gordon JJ, Knight R, Mills DA, Caporaso JG. 2013. Quality-filtering vastly improves diversity estimates from Illumina amplicon sequencing. *Nat Methods.*,10(1):57–59.
- Caputi AJr (1995). Wines. In: Cunniff P (Ed.), Official Methods of Analysis of AOAC International, 16th Edition. AOAC International. Arlington, Virginia, USA, pp. 28.1–28.6.
- Dahal B, NandaKafle G, Perkins L, Brözel VS. 2017. Diversity of free-living nitrogen fixing *Streptomyces* in soils of the badlands of South Dakota. *Microbiol Res.*,195:31–39
- Dennis PG, Miller AJ, Hirsch PR. 2010. Are root exudates more important than other sources of rhizodeposits in structuring rhizosphere bacterial communities? *FEMS Microbiol Ecol.*,72(3):313–327.
- Dicko AH, Babana AH, Kassogué A, Fané R, Nantoumé D, Ouattara D, Maiga K, Dao S. 2018. A Malian native plant growth promoting actinomycetes based biofertilizer improves maize growth and yield. *Symbiosis.*,75(3):267–275.
- Edwards JA, Santos-Medellín CM, Liechty ZS, Nguyen B, Lurie E, Eason S, Phillips G, Sundaresan V. 2018. Compositional shifts in root-associated bacterial and archaeal microbiota track the plant life cycle in field-grown rice. *PLoS Biol.*,16(2):1–28.
- Ferrarezi JA, Carvalho-Estrada P de A, Batista BD, Aniceto RM, Tschoeke BAP, Andrade PA de M, Lopes B de M, Bonatelli ML, Odisi EJ, Azevedo JL, et al. 2022. Effects of inoculation with plant growth-promoting rhizobacteria from the Brazilian Amazon on the bacterial community associated with maize in field. *Appl Soil Ecol.*,170: 1–14.
- Fitriatin BN, Dellaoceto D, Ambarita M, Rochimi M, Simarmata T. 2021. The role of rhizobacterial inoculum and formulated soil amendment in improving soil chemical-biological properties, chlorophyll content and agronomic efficiency of maize under marginal soils. *Jordan J Biol Sci.*, 14(3):601–605.
- Flores-Núñez VM, Amora-Lazcano E, Rodríguez-Dorantes A, Cruz-Maya JA, Jan-Roblero J. 2018. Comparison of plant growth-promoting rhizobacteria in a pine forest soil and an agricultural soil. *Soil Res.*, 56(4): 1–10.
- Gopalakrishnan S, Humayun P, Vadlamudi S, Vijayabharathi R, Bhimineni RK, Rupela O. 2012. Plant growth-promoting traits of *Streptomyces* with biocontrol potential isolated from herbal vermicompost. *Biocontrol Sci Technol.*,22(10):1199–1210.
- Goudjal Y, Toumatia O, Sabaou N, Barakate M, Mathieu F, Zitouni A. 2013. Endophytic actinomycetes from spontaneous plants of Algerian Sahara: indole-3-acetic acid production and tomato plants growth promoting activity. *World J Microbiol Biotechnol.*,29(10):1821–1829.
- Horstmann JL, Dias MP, Ortolan F, Medina-Silva R, Astarita LV, Santarém ER. 2020) *Streptomyces* sp. CLV45 from Fabaceae rhizosphere benefits growth of soybean plants. *Braz J Microbiol.*,51:1861–1871
- Ivette C, Mart E, Aguirre-noyola JL, Alberto L, Zenteno-rojas A, Rogel MA, Alexander F, Ru M, Rinc R. 2022. Bacterial community with plant growth-promoting potential associated to pioneer plants from an active Mexican volcanic complex. *Microorganisms.*,10(1568):1–22.
- Jha CK, Saraf M. 2012. Evaluation of multispecies plant-growth-promoting consortia for the growth promotion of *Jatropha curcas* L. *J Plant Growth Regul.*,31(4):588–598.
- Kalam S, Das SN, Basu A, Podile AR. 2017. Population densities of indigenous Acidobacteria change in the presence of plant growth promoting rhizobacteria (PGPR) in rhizosphere. *J Basic Microbiol.*,57(5):376–385.
- Kaur T, Sharma D, Kaur A, Manhas RK. 2013. Antagonistic and plant growth promoting activities of endophytic and soil actinomycetes. *Arch Phytopathol Plant Prot.*,46(14):1756–1768.
- Kielak AM, Cipriano MAP, Kuramae EE. 2016. Acidobacteria strains from subdivision 1 act as plant growth-promoting bacteria. *Arch Microbiol.*,198(10):987–993.
- Kong Z, Liu H. 2022. Modification of rhizosphere microbial communities: a possible mechanism of plant growth promoting rhizobacteria enhancing plant growth and fitness. *Front Plant Sci.*,13: 1–11.
- Korkar MH, Magdy M, Rizk SM, Fiteha YG, Atta AH, Rashed MAS. 2022. Rhizosphere-associated microbiome profile of agricultural reclaimed lands in Egypt. *Agronomy.*,12(10):1–17.
- Lakshmanan, V., Ray, P., Craven, K.D. 2017. Rhizosphere Sampling Protocols for Microbiome (16S/18S/ITS rRNA) Library Preparation and Enrichment for the Isolation of Drought Tolerance-Promoting Microbes. In: Sunkar R (Ed.), Plant Stress Tolerance. Methods in Molecular Biology. Humana Press, New York, pp. 349–362.
- Liu Q, Pang Z, Yang Z, Nyumah F, Hu C, Lin W, Yuan Z. 2021. Bio-fertilizer affects structural dynamics, function, and network patterns of the sugarcane rhizospheric microbiota. *Microb Ecol.*, 84: 1195–1211.
- Lobo CB, Juárez Tomás MS, Viruel E, Ferrero MA, Lucca ME. 2019. Development of low-cost formulations of plant growth-promoting bacteria to be used as inoculants in beneficial agricultural technologies. *Microbiol Res.*,219:12–25.
- Mäder P, Kaiser F, Adholeya A, Singh R, Uppal HS, Sharma AK, Srivastava R, Sahai V, Aragno M, Wiemken A. 2011. Inoculation of root microorganisms for sustainable wheat-rice and wheat-black gram rotations in India. *Soil Biol Biochem.*, 43(3):609–619.
- Magdalena F, Sumarni T. 2013. Penggunaan pupuk kandang dan pupuk hijau *Crotalaria juncea* L. untuk mengurangi penggunaan pupuk anorganik pada tanaman jagung (*Zea mays* L.). *J Prod Tanam.*,1(2):61–71.
- Malusá E, Sas-Paszt L, Ciesielska J. 2012. Technologies for beneficial microorganisms inocula used as biofertilizers. *Sci World J.*,2012:1–12.

- Massah J, Azadegan B. 2016. Effect of chemical fertilizers on soil compaction and degradation. *AMA, Agric Mech Asia, Africa Lat Am.*,47(1):44–50.
- Maver M, Escudero-Martinez C, Abbott J, Morris J, Hedley PE, Mimmo T, Bulgarelli D. 2021. Applications of the indole-alkaloid gramine modulate the assembly of individual members of the barley rhizosphere microbiota. *PeerJ.*, 9: 1–24.
- Meier MA, Lopez-Guerrero MG, Guo M, Schmer MR, Herr JR, Schnable JC, Alfano JR, Yang J. 2021. Rhizosphere microbiomes in a historical maize-soybean rotation system respond to host species and nitrogen fertilization at the genus and subgenus levels. *Appl Environ Microbiol.*,87(12):1–13.
- Mohanram S, Kumar P. 2019. Rhizosphere microbiome: revisiting the synergy of plant-microbe interactions. *Ann Microbiol.*,69(4):307–320.
- Niu Z, Yue Y, Su D, Ma S, Hu L, Hou X, Zhang T, Dong D, Zhang D, Lu C. 2022. The characterization of *Streptomyces alfalfae* strain 11F and its effect on seed germination and growth promotion in switchgrass. *Biomass Bioenerg.*, 158:106360
- Olanrewaju OS, Babalola OO. 2019. *Streptomyces*: implications and interactions in plant growth promotion. *Appl Microbiol Biot.*,103:1179–1188
- Panikkai S, Nurmalina R, Mulatsih S, Purwati H. 2017. Analisis ketersediaan jagung nasional menuju swasembada dengan pendekatan model dinamik. *J Inf Pertan.*,26(1):41–48.
- Prasad H, Parmar YS, Sajwan P, Kumari M, Solanki S. 2017. Effect of organic manures and biofertilizer on plant growth, yield and quality of horticultural crop: a review. *Int J Chem Stud.*,5(1):217–221.
- Puscaselu RG, Lobiuc A, Dimian M, Covasa M. 2020. Alginate: from food industry to biomedical applications and management of metabolic disorders. *Polymers (Basel)*. 12(10):1–30.
- Rouf Shah T, Prasad K, Kumar P. 2016. Maize—A potential source of human nutrition and health: a review. *Cogent Food Agric.*,2(1):1–9.
- Sari M, Nawangsih AA, Wahyudi AT. 2021. Rhizosphere *Streptomyces* formulas as the biological control agent of phytopathogenic fungi *Fusarium oxysporum* and plant growth promoter of soybean. *Biodiversitas.*,22(6):3015–3023.
- Schneijderberg M, Schmitz L, Cheng X, Polman S, Franken C, Geurts R, Bisseling T. 2018. A genetically and functionally diverse group of non-diazotrophic *Bradyrhizobium* spp. colonizes the root endophytic compartment of *Arabidopsis thaliana*. *BMC Plant Biol.*,18(1):1–9.
- Schoebitz M, López MD, Roldán A. 2013. Bioencapsulation of microbial inoculants for better soil-plant fertilization. A review. *Agron Sustain Dev.*,33(4):751–765.
- Schoebitz M, Mengual C, Roldán A. 2014. Combined effects of clay immobilized *Azospirillum brasilense* and *Pantoea dispersa* and organic olive residue on plant performance and soil properties in the revegetation of a semiarid area. *Sci Total Environ.*,466:67–73.
- Shrivastava S, D'Souza SF, Desai PD. 2008. Production of indole-3-acetic acid by immobilized actinomycete (*Kitasatospora* sp.) for soil applications. *Curr Sci.*,94(12):1595–1604.
- Singh I. 2018. Plant growth promoting rhizobacteria (PGPR) and their various mechanisms for plant growth enhancement in stressful conditions: a review. *Eur J Biol Res.*, 8(4):191–213.
- Sousa JA de J, Olivares FL. 2016. Plant growth promotion by streptomycetes: Ecophysiology, mechanisms and applications. *Chem Biol Technol Agric.*,3(1):1–12.
- Trivedi P, Delgado-Baquerizo M, Anderson IC, Singh BK. 2016. Response of soil properties and microbial communities to agriculture: Implications for primary productivity and soil health indicators. *Front Plant Sci.*, 7:1–13.
- Wahyudi AT, Priyanto JA, Fijrina HN, Mariastuti HD, Nawangsih AA. 2019. *Streptomyces* spp. from rhizosphere soil of maize with potential as plant growth promoter. *Biodiversitas.*,20(9):2547–2553.
- Wang J, Liu L, Gao X, Hao J, Wang M. 2021. Elucidating the effect of biofertilizers on bacterial diversity in maize rhizosphere soil. *PLoS One.*,16(4):1–15.
- Wongdee J, Boonkerd N, Teamroong N, Tittabutr P, Giraud E. 2018. Regulation of nitrogen fixation in *Bradyrhizobium* sp. strain DOA9 involves two distinct NifA regulatory proteins that are functionally redundant during symbiosis but not during free-living growth. *Front Microbiol.*,9:1–11.
- Zhou L, Wang S, Zou Y, Xia C, Zhu G. 2015. Species, abundance and function of ammonia-oxidizing Archaea in inland waters across China. *Nat Sci Rep.*5: 1–13.

Jordan Journal of Biological Sciences

An International Peer – Reviewed Research Journal

Published by the Deanship of Scientific Research, The Hashemite University, Zarqa, Jordan



Name: الاسم:
 Specialty: التخصص:
 Address: العنوان:
 P.O. Box: صندوق البريد:
 City & Postal Code: المدينة: الرمز البريدي:
 Country: الدولة:
 Phone: رقم الهاتف:
 Fax No.: رقم الفاكس:
 E-mail: البريد الإلكتروني:
 Method of payment: طريقة الدفع:
 Amount Enclosed: المبلغ المرفق:
 Signature: التوقيع:
 Cheque should be paid to Deanship of Research and Graduate Studies – The Hashemite University.

I would like to subscribe to the Journal

For

- One year
 Two years
 Three years

One Year Subscription Rates

	Inside Jordan	Outside Jordan
Individuals	JD10	\$70
Students	JD5	\$35
Institutions	JD 20	\$90

Correspondence

Subscriptions and sales:

The Hashemite University
 P.O. Box 330127-Zarqa 13115 – Jordan
 Telephone: 00 962 5 3903333
 Fax no. : 0096253903349
 E. mail: jjbs@hu.edu.jo

المجلة الأردنية للعلوم الحياتية Jordan Journal of Biological Sciences (JJBS)

<http://jjbs.hu.edu.jo>

المجلة الأردنية للعلوم الحياتية: مجلة علمية عالمية محكمة ومفهرسة ومصنفة، تصدر عن الجامعة الهاشمية وبدعم من صندوق دعم البحث العلمي والإبتكار – وزارة التعليم العالي والبحث العلمي.

هيئة التحرير

رئيس التحرير

الأستاذ الدكتور محمد علي وديان
الجامعة الهاشمية، الزرقاء، الأردن

مساعد رئيس التحرير

الأستاذ الدكتور مهند عليان مساعدة
الجامعة الهاشمية، الزرقاء، الأردن

الأعضاء:

الأستاذ الدكتور خالد محمد خليفات
جامعة مؤتة

الاستاذ الدكتور ليث ناصر العيطان
جامعة العلوم و التكنولوجيا الأردنية

الأستاذ الدكتورة طارق حسن النجار
الجامعة الأردنية / العقبة

الأستاذ الدكتور وسام محمد هادي الخطيب
الجامعة اليرموك

الاستاذ الدكتور عبد اللطيف علي الغزاوي
الجامعة الهاشمية

الاستاذ الدكتور نضال احمد عودات
جامعة البلقاء التطبيقية

فريق الدعم:

المحرر اللغوي

الأستاذ الدكتور شادي نعمانة

تنفيذ وإخراج

م. مهند عقده

ترسل البحوث الى العنوان التالي:

رئيس تحرير المجلة الأردنية للعلوم الحياتية
الجامعة الهاشمية

ص.ب , 330127 , الزرقاء, 13115 , الأردن

هاتف: 0096253903333

E-mail: jjbs@hu.edu.jo, Website: www.jjbs.hu.edu.jo



المملكة الأردنية الهاشمية



المجلة الأردنية



للعلوم الحياتية

مجلة علمية عالمية محكمة

تصدر بدعم من صندوق دعم البحث العلمي و الابتكار



<http://jjbs.hu.edu.jo/>